Supporting Information

Bianthryl-Based Organocatalyst for Asymmetric Henry Reaction of Fluoroketones

Jan Otevrel,*§ David Svestka,§ Pavel Bobal*

Department of Chemical Drugs, Faculty of Pharmacy
University of Veterinary and Pharmaceutical Sciences (UVPS) Brno, Palackeho 1946/1, 612 42 Brno, Czech Republic

*bobalp@vfu.cz, *otevrelj@vfu.cz
§Both authors contributed equally to this work and appear here in alphabetical order

TABLE OF CONTENTS

1. General Information

Solvents and reagents: Purchased from commercial suppliers and used as received, if not stated otherwise. Compounds (S_a)-6,6'-dimethyl-1,1'-biphenyl-2,2'-diamine (S_a-BIPHAM), (S_a)-1,1'-(6,6'-dimethyl-[1,1'-biphenyl]-2,2'-diyl)bis(3-(3,5-bis(trifluoromethyl)phenyl)thiourea (**1b**), (S_a)-1,1'-(6,6'-bis((dimethylamino)methyl)-[1,1'-biphenyl]-2,2'-diyl)bis(3-(3,5-bis(trifluoromethyl)phenyl)thiourea) (**1c**), (S_a)-1,1'-(6,6'-bis(dimethylamino)-[1,1'-biphenyl]-2,2'-diyl)bis(3-(3,5-bis(trifluoromethyl)phenyl)thiourea) (**1t**), (S_a)-1-(3,5-bis(trifluoromethyl)phenyl)-3-(2'-(dimethylamino)-6,6'-dimethyl-[1,1'-biphenyl]-2-yl)thiourea (**1u**) were prepared according to the literature.[1–3] (–)-*N*-Benzylcinchonidium chloride (BCDC) was azeotropically dehydrated by repetitive evaporation of its dichloromethane solution. Anhydrous dichloromethane (DCM) and diethyl ether (Et_2O) were distilled from calcium hydride (CaH_2), tetrahydrofuran (THF) from potassium/benzophenone ketyl, toluene (MePh) from sodium/benzophenone ketyl, dry methanol (MeOH) from magnesium turnings, dry *N,N*-dimethylformamide (DMF), dry 1,2-dimethoxyethane (DME), and dry acetonitrile (MeCN) were purchased.

Special equipment and operating procedures: If not stated otherwise, all experiments were performed standardly under open-vessel conditions. Moisture and air-sensitive reactions were done in oven-dried glassware (140 °C) under argon atmosphere in anhydrous solvents. Small-scale low-temperature experiments were done in an aluminum heat-transfer block with centrally placed stirring rotor. Preparative separations were performed with a Büchi Sepacore flash system X10 (BÜCHI Labortechnik). Catalytic hydrogenations over Pd were conducted with a Parr 3910 Shaker Hydrogenation Apparatus (Parr Instrument Co.).

Analytical data: Specific rotation was determined by an automatic polarimeter AA-5 (Optical Activity). Melting points were measured by Böetius apparatus (Franz Küstner Nachf.) and are uncorrected. HPLC data were recorded on a Dionex UltiMate 3000 LC System (Thermo Fisher Scientific), edited with *Chromeleon Dionex*, software ver. 7.2.0.3765 (Thermo Fisher Scientific) and a Spectra-System (Thermo Separation Products), edited with *Chromatography Data System N2000*, software ver. 3.5 (Baseline ChromTech Research Centre).
IR spectra were collected on a SmartMIRacle ATR (diamond) for Nicolet Impact 410 FT-IR (Thermo Scientific Corp.) and edited with *Omnic* software ver. 7.4 (Thermo Scientific). NMR spectra were obtained from a JEOL ECZR-400 MHz (Jeol Corp.). Experiments were standardly performed at 25 °C, chemical shifts are reported in δ parts per million (ppm) and *J* values in Hz, the signal of TMS or the residual solvent signals of $CDCl_3$, acetone-d_6 or DMSO-d_6 were used as a reference. Spectra were edited with *ACD/NMR processor* software ver. 12.01 (Advanced Chemistry Development).
HRMS measurements were performed using a LTQ Orbitrap XL high-resolution mass spectrometer (Thermo Fisher Scientific) and a Bruker Impact II Q-TOF high-resolution mass spectrometer (Bruker Daltonics).

Diffraction data: Collected on a Rigaku Saturn724+ four-circle CCD X-ray diffractometer at 120 K using monochromated Mo-Kα radiation from MicroMax-007HF DW 1.2 kW rotating anode (Rigaku Corp.). *CrystalClear–SM Expert* ver. 2.1 b32 software package was used for data collection and data reduction (Rigaku Corp.). The structure was solved and refined (full matrix least-squares refinement on F^2) using a *SHELXL* program.[4] All non-hydrogen atoms were refined anisotropically.

2. Syntheses of Catalysts

2.1 Synthesis of 1a

2.1.1 (S_a)-1,1'-([1,1'-Binaphthalene]-2,2'-diyl)bis(3-(3,5-bis(trifluoromethyl)phenyl)thiourea) (**1a**)[5]

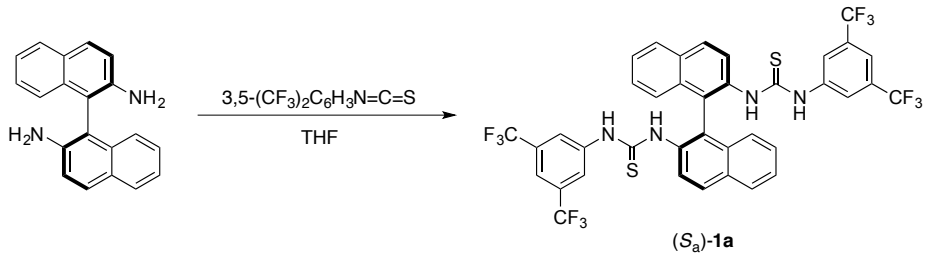

(S_a)-**1a**

To a solution of (S_a)-BINAM (114 mg, 400 μmol) in anhydrous THF (1 mL), 3,5-bis(trifluoromethyl)-phenylisothiocyanate (150 μL, 2.05 equiv) was added dropwise at room temperature. The reaction mixture was stirred 48 h at rt under Ar and then evaporated in vacuo. The resulting glassy residue was triturated with *n*-hexane and sonicated. The white precipitate was filtered off, washed with *n*-hexane, and subjected to flash chromatography (SiO_2) EtOAc–*n*-hexane (1:4).

Physical state: white powder.
Isolated yield: 250 mg (89%).

mp 119–121 °C, lit.[5] 137–138 °C.
$[\alpha]^{25}_D$ +88 (*c* 0.5, $CHCl_3$).
^{1}H NMR (400 MHz, $CDCl_3$) δ/ppm: 8.21 (br s, 2H), 8.05 (d, *J* = 8.8 Hz, 2H), 7.92 (d, *J* = 8.2 Hz, 2H), 7.83 (d, *J* = 8.8 Hz, 2H), 7.62 (s, 2H), 7.60 (s, 4H), 7.54 (s, 2H), 7.46 (t, *J* = 7.5 Hz, 2H), 7.25 (t, *J* = 7.7 Hz, 2H), 7.08 (d, *J* = 8.5 Hz, 2H) [**Fig. S113**].
^{13}C NMR (100 MHz, $CDCl_3$) δ/ppm: 179.9, 138.6, 133.5, 132.7, 132.2, 131.9 (q, $^2J_{CF}$ = 34.0 Hz), 130.6, 128.8, 128.1, 127.4, 127.0, 125.3, 124.8, 124.3, 122.7 (q, $^1J_{CF}$ = 272.9 Hz), 119.7 [**Fig. S114**].
^{19}F NMR (376 MHz, $CDCl_3$) δ/ppm: −62.94 (s) [**Fig. S115**].
IR (neat) $\tilde{\nu}$/cm^{-1}: 3209*w*, 1505*m*, 1471*m*, 1376*m*, 1274*s*, 1171*m*, 1129*s*, 990*w*, 945*w*, 886*m*, 849*w*, 819*w*, 756*m*, 700*m*, 682*m*.
HRMS (ESI-Orbitrap) calcd for $C_{38}H_{23}F_{12}N_4S_2$ $[M+H]^+$ 827.1167 *m*/*z*, found 827.1155 *m*/*z* [**Fig. S44**].

Stereochemical assignment: The absolute configuration of **1a** was established by chemical correlation with (S_a)-BINAM.

2.2 Synthesis of 1d

2.2.1 (S_a)-*N*,*N*'-(6,6'-Dimethyl-[1,1'-biphenyl]-2,2'-diyl)diacetamide (**9**)[6]

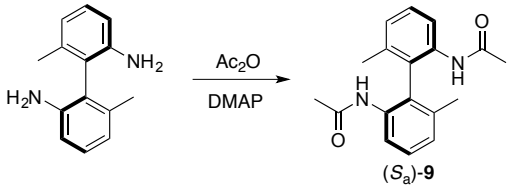

(S_a)-**9**

(S_a)-**9** was prepared from (S_a)-BIPHAM (330 mg, 1.56 mmol) and Ac_2O (1.8 mL, 18.81 mmol) with DMAP (18.8 mg, 0.1 equiv) according to the literature.[6]

Physical state: white solid.
Isolated yield: 453 mg (98%).

mp 239–240 °C.
$[\alpha]^{25}_D$ +23 (*c* 1.0, $CHCl_3$).
^{1}H NMR (400 MHz, DMSO-d_6): 8.72 (br s, 2H), 7.38–7.16 (m, 6H), 1.80 (s, 6H), 1.74 (s, 6H) [**Fig. S116**].
^{13}C NMR (100 MHz, DMSO-d_6): 168.9, 136.7, 136.0, 132.6, 127.7, 127.4, 123.6, 23.0, 19.5 [**Fig. S117**].
IR (neat) $\tilde{\nu}$/cm^{-1}: 3219*m*, 2985*m*, 1656*s*, 1600*w*, 1514*s*, 1465*m*, 1412*m*, 1336*m*, 1294*m*, 1165*w*, 1038*w*, 976*w*, 804*m*, 776*w*, 759*w*, 605*w*.
HRMS (ESI-Orbitrap) calcd for $C_{18}H_{21}N_2O_2$ $[M+H]^+$ 297.1598 *m*/*z*, found 297.1606 *m*/*z* [**Fig. S45**].

Stereochemical assignment: The absolute configuration of **9** was established by chemical correlation with (S_a)-BIPHAM.

2.2.2 (S_a)-*N*,*N*'-(4',6''-Dimethyl-[1,1':3',1'':3'',1'''-quaterphenyl]-2',2''-diyl)diacetamide (**10**)[6]

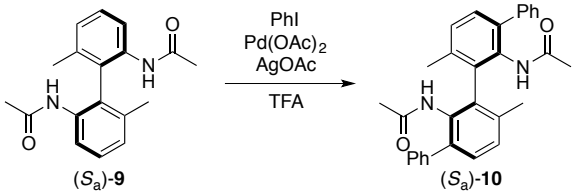

(S_a)-**9** (S_a)-**10**

(S_a)-**10** was prepared from (S_a)-**9** (300 mg, 1.0 mmol), $Pd(OAc)_2$ (34 mg, 0.15 mmol), AgOAc (384 mg, 2.3 mmol), and PhI (0.56 mL, 5.0 mmol) in CF_3CO_2H (3 mL) according to the literature.[6] The crude product was purified by a column chromatography (SiO_2) Et_2O–MePh (1:1).

Physical state: white solid.
Isolated yield: 395 mg (88%).

mp 144–146 °C.
$[\alpha]^{25}_D$ +340 (*c* 0.5, $CHCl_3$).
^{1}H NMR (400 MHz, DMSO-d_6) δ/ppm: 7.37–7.14 (m, 16H), 2.34 (s, 2H), 1.87 (s, 3H), 1.50 (s, 6H) [**Fig. S118**].
^{13}C NMR (100 MHz, DMSO-d_6) δ/ppm: 139.8, 138.5, 132.5, 129.5, 129.3, 129.0, 128.6, 128.2, 128.1, 127.0, 125.3, 22.4, 19.8 [**Fig. S119**].
IR (neat) $\tilde{\nu}$/cm^{-1}: 3352*w*, 3029*w*, 1660*m*, 1465*m*, 1426*m*, 1368*w*, 1288*w*, 1167*w*, 976*w*, 874*w*, 825*w*, 758*s*, 700*s*.
HRMS (ESI-Orbitrap) calcd for $C_{30}H_{29}N_2O_2$ $[M+H]^+$ 449.2224 *m*/*z*, found 449.2237 *m*/*z* [**Fig. S46**].

Stereochemical assignment: The absolute configuration of **10** was established by chemical correlation with (S_a)-BIPHAM.

2.2.3 (S_a)-4',6"-Dimethyl-[1,1':3',1":3",1"'-quaterphenyl]-2',2"-diamine (**11**)[6]

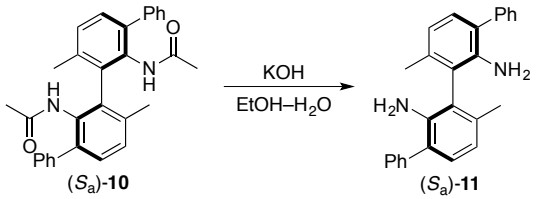

(S_a)-**10** (S_a)-**11**

(S_a)-**11** was prepared from (S_a)-**10** (200 mg, 0.45 mmol) in a mixture of 50% aqueous KOH and 96% ethanol (1:1, 15 mL) according to the literature.[6]

Physical state: brownish solid.
Isolated yield: 150 mg (93%).

mp 135–138 °C.
$[\alpha]^{25}_D$ +284 (*c* 0.5, $CHCl_3$).
^{1}H NMR (400 MHz, $CDCl_3$): 7.54–7.51 (m, 4H), 7.47–7.44 (m, 4H), 7.37–7.33 (m, 2H), 7.11 (d, *J* = 7.7 Hz, 2H), 6.83 (d, *J* = 7.7 Hz, 2H), 3.68 (br s, 4H), 2.07 (s, 6H) [**Fig. S120**].
^{13}C NMR (100 MHz, $CDCl_3$): 141.3, 140.0, 137.1, 129.5, 129.2, 128.7, 126.9, 125.3, 122.5, 119.9, 19.7 [**Fig. S121**].
IR (neat) $\tilde{\nu}$/cm^{-1}: 3370*w*, 1600*s*, 1404*m*, 1283*w*, 1073*w*, 1011*w*, 808*m*, 775*m*, 758*s*, 700*s*.
HRMS (ESI-Orbitrap) calcd for $C_{26}H_{25}N_2$ $[M+H]^+$ 365.2012 *m*/*z*, found 365.2022 *m*/*z* [**Fig. S47**].

Stereochemical assignment: The absolute configuration of **11** was established by chemical correlation with (S_a)-BIPHAM.

2.2.4 (S_a)-1,1'-(4',6"-Dimethyl-[1,1':3',1":3",1"'-quaterphenyl]-2',2"-diyl)bis(3-(3,5-bis(trifluoromethyl)-phenyl)thiourea) (**1d**)

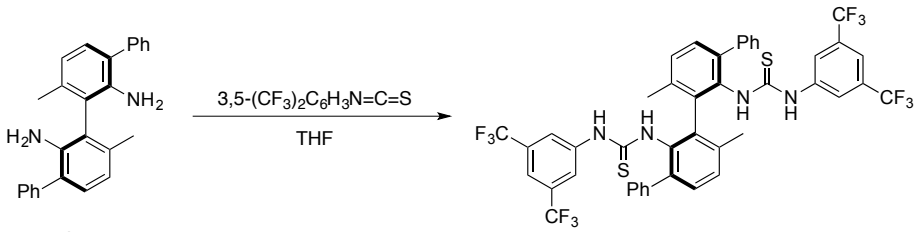

(S_a)-**11** (S_a)-**1d**

A solution of (S_a)-**11** (50 mg, 150 μmol) in dry THF (0.5 mL), was treated with 3,5-bis(trifluoromethyl)-phenylisothiocyanate (56 μL, 2.05 equiv) analogously to the compound **1a**.

Physical state: white powder.
Isolated yield: 70 mg (52%).

mp 157–159 °C.
$[\alpha]^{29}_D$ +11 (*c* 0.6, $CHCl_3$).
^{1}H NMR (400 MHz, $CDCl_3$) δ/ppm: 7.77 (br s, 2H), 7.48 (s, 2H), 7.44–7.36 (m, 16H), 7.10 (s, 4H), 2.14 (s, 6H) [**Fig. S122**].
^{13}C NMR (100 MHz, $CDCl_3$) δ/ppm: 179.5, 139.0, 138.3, 137.8, 136.2, 134.0, 132.0, 131.3, 130.9, 130.5, 129.1, 128.4, 128.2, 126.7, 122.7 (q, $^1J_{CF}$ = 272.9 Hz), 119.7, 19.9 [**Fig. S123**].
^{19}F NMR (376 MHz, $CDCl_3$) δ/ppm: −62.99 (s) [**Fig. S124**].
IR (neat) $\tilde{\nu}$/cm^{-1}: 1468*w*, 1383*w*, 1276*s*, 1179*m*, 1128*s*, 985*w*, 891*w*, 826*w*, 757*w*, 700*m*, 681*m*.
HRMS (ESI-Orbitrap) calcd for $C_{44}H_{31}F_{12}N_4S_2$ $[M+H]^+$ 907.1793 *m*/*z*, found 907.1774 *m*/*z* [**Fig. S48**].

Stereochemical assignment: The absolute configuration of **1d** was established by chemical correlation with (S_a)-BIPHAM.

2.3 Synthesis of 1e

2.3.1 (*S*)-1-(3,5-Bis(trifluoromethyl)phenyl)-3-(1-hydroxy-3-phenylpropan-2-yl)thiourea (**1e**)[7]

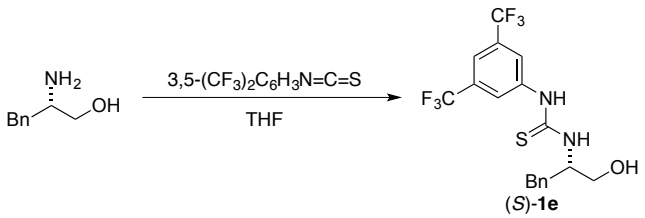

To a solution of (*S*)-2-amino-3-phenylpropan-1-ol (50 mg, 330 μmol) in anhydrous THF (1 mL), 3,5-bis-(trifluoromethyl)phenylisothiocyanate (63 μL, 1.05 equiv) was added dropwise at room temperature. The reaction mixture was stirred 48 h at rt under Ar and then evaporated in vacuo. The resulting glassy residue was subjected to a column chromatography (SiO_2) EtOAc–*n*-hexane (1:4).

Physical state: colorless glassy solid.
Isolated yield: 105 mg (75%).

mp 83–86 °C, lit.[7] 97–99 °C.
$[\alpha]^{25}_{D}$ –54 (*c* 0.5, $CHCl_3$).
^{1}H NMR (400 MHz, $CDCl_3$) δ/ppm: 8.58 (br s, 1H), 7.74 (s, 2H), 7.67 (s, 1H), 7.34–7.23 (m, 6H), 6.82 (br s, 1H), 4.77 (br s, 1H), 3.84 (dd, *J* = 10.8, 3.0 Hz, 1H), 3.68 (dd, *J* = 10.8, 5.4 Hz, 1H), 3.02 (dd, *J* = 13.7, 7.7 Hz, 1H), 2.89 (dd, *J* = 13.7, 6.4 Hz, 1H) [**Fig. S125**].
^{13}C NMR (100 MHz, $CDCl_3$) δ/ppm: 180.6, 139.0, 136.8, 132.6 (q, $^2J_{CF}$ = 35.0 Hz), 129.1, 128.9, 127.1, 123.7, 122.8 (q, $^1J_{CF}$ = 272.9 Hz), 119.1, 63.3, 57.5, 36.8 [**Fig. S126**].
^{19}F NMR (376 MHz, $CDCl_3$) δ/ppm: −62.92 (s) [**Fig. S127**].
IR (neat) $\tilde{\nu}$/cm^{-1}: 3579*w*, 3028*w*, 3057*w*, 1656*w*, 1533*m*, 1471*w*, 1382*m*, 1431*w*, 1273*s*, 1170s, 1127*s*, 1043*w*, 983*w*, 892*w*, 752*w*, 700*m*, 681*m*.
HRMS (ESI-Orbitrap) calcd for $C_{18}H_{17}F_6N_2OS$ $[M+H]^+$ 423.0960 *m*/*z*, found 423.0964 *m*/*z* [**Fig. S49**].

Stereochemical assignment: The absolute configuration of **1e** was established by chemical correlation with (*S*)-2-amino-3-phenylpropan-1-ol and by comparison of the sign of specific rotation with the literature value.[7]

2.4 Synthesis of 1f

2.4.1 (*S*)-1-(3,5-Bis(trifluoromethyl)phenyl)-3-(1-hydroxy-3-methylbutan-2-yl)thiourea (**1f**)[8]

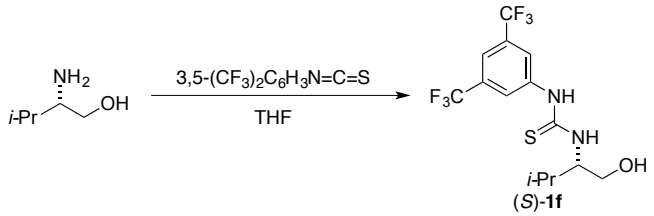

A solution of (*S*)-2-amino-3-methylbutan-1-ol (50 mg, 480 µmol) in dry THF (1 mL), was treated with 3,5-bis(trifluoromethyl)phenylisothiocyanate (93 µL, 1.05 equiv) analogously to the compound **1a**.

Physical state: white powder.
Isolated yield: 118 mg (66%).

mp 122–124 °C, lit.[8] 121 °C.
$[\alpha]^{29}_{D}$ −42 (*c* 0.5, $CHCl_3$).
^{1}H NMR (400 MHz, $CDCl_3$) δ/ppm: 8.82 (br s, 1H), 7.89 (s, 2H), 7.64 (s, 1H), 6.78 (br s, 1H), 4.48 (br s, 1H), 3.89 (d, *J* = 9.0 Hz, 1H), 3.69 (dd, *J* = 11.0, 7.3 Hz, 1H), 1.90 (dq, *J* = 13.4, 6.6 Hz, 1H), 0.98 (d, *J* = 6.8 Hz, 3H), 0.97 (d, *J* = 5.4, 3H) [**Fig. S128**].
^{13}C NMR (100 MHz, $CDCl_3$) δ/ppm: 181.2, 139.1, 132.5, 123.4, 122.8 (q, $^1J_{CF}$ = 272.6 Hz), 118.8, 63.0, 61.7, 29.6, 19.2, 18.9 [**Fig. S129**].
^{19}F NMR (376 MHz, $CDCl_3$) δ/ppm: −63.00 (s) [**Fig. S130**].
IR (neat) ṽ/cm^{-1}: 1537*m*, 1468*w*, 1384*m*, 1273*s*, 1174*m*, 1132*s*, 1063*w*, 983*w*, 889*m*, 847*w*, 708*m*, 680*m*.
HRMS (ESI-Orbitrap) calcd for $C_{14}H_{17}F_6N_2OS$ $[M+H]^+$ 375.0960 *m*/*z*, found 375.0960 *m*/*z* [**Fig. S50**].

Stereochemical assignment: The absolute configuration of **1f** was established by chemical correlation with (*S*)-2-amino-3-methylbutan-1-ol and by comparison of the sign of specific rotation with the literature value.[8]

2.5 Synthesis of 1g

2.5.1 *rac*-[1,1'-Bianthracene]-2,2'-diamine (*rac*-**12,** *rac*-BIANAM)[9]

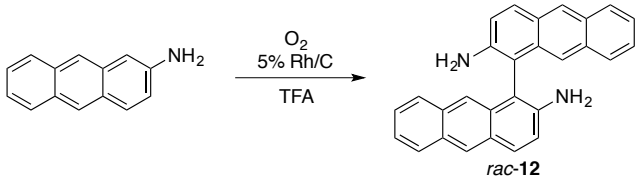

rac-**12** was prepared by a slightly modified literature procedure.[9]

A solution of 2-anthramine (500 mg, 2.6 mmol) in CF_3CO_2H (25 mL) was treated with 5% Rh/C (275 mg, 5 mol%) and left to stir vigorously at rt for 48 h under O_2 atmosphere from a thin-walled rubber balloon. After a TLC monitoring (SiO_2) CH_2Cl_2 revealed complete consumption of the starting material (middle yellow-colored spot), the reaction mixture was carefully poured into ice-cold 2.5 M NaOH (150 mL), extracted with EtOAc, washed with brine, dried with anhydrous Na_2SO_4, filtered through Celite pad, and evaporated in vacuo.

The crude product was further purified by a short column chromatography (SiO_2) CH_2Cl_2.

Physical state: yellow to brownish glassy solid.

Isolated yield: 451 mg (90%).

mp 158–160 °C, lit.[10] 160–163 °C.

^{1}H NMR (400 MHz, DMSO-d_6) δ/ppm: 8.44 (s, 2H), 8.03 (d, J = 9.2 Hz, 2H), 7.93 (d, J = 8.2 Hz, 2H), 7.49 (d, J = 8.4 Hz, 2H), 7.39–7.37 (m, 4H), 7.27–7.18 (m, 4H), 4.89 (br s, 4H) [**Fig. S131**].

^{13}C NMR (100 MHz, DMSO-d_6) δ/ppm: 143.7, 132.4, 131.9, 129.2, 128.5, 128.0, 127.7, 127.3, 126.7, 125.2, 123.3, 121.0, 119.4, 107.4 [**Fig. S132**].

IR (neat) $\tilde{\nu}$/cm^{-1}: 3353*w*, 1616*s*, 1476*m*, 1458*m*, 1426*m*, 1406*m*, 1340*m*, 1279*w*, 1167*w*, 1135*w*, 878*m*, 801*w*, 739*m*.

HRMS (ESI-Orbitrap) calcd for $C_{28}H_{21}N_2$ $[M+H]^+$ 385.1699 *m*/*z*, found 385.1709 *m*/*z* [**Fig. S51**].

2.5.2 (R_a)-(–)-[1,1'-Bianthracene]-2,2'-diamine (R_a-**12,** R_a-BIANAM)[10]

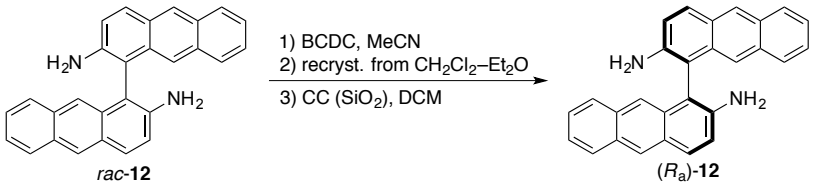

rac-**12** (384 mg, 1.0 mmol) was resolved with (–)-*N*-benzylcinchonidium chloride (210 mg, 0.5 mmol) in dry acetonitrile (5 mL) according to the literature. The diastereomeric purity of the inclusion complex (250 mg) was further refined by dissolving the complex in a minimum amount of CH_2Cl_2 and covering this solution with five volume equivalents of diethyl ether. The resulting mixture was allowed to crystallize slowly in dark for 1 week and then worked up as described in the above literature.[10]

Figure S1: Layering of the solution of BCDC and (R_a)-**12** in CH_2Cl_2 with Et_2O.

Isolated yield: 95 mg (24%).
Physical state: golden yellow solid.

mp 250–252 °C, lit.[10] 235–255 °C.
$[\alpha]^{29}_D$ –305 (*c* 4.0, $CHCl_3$).

Chiral HPLC conditions: a Hypersil silica column (3 µm, 100 × 4.6 mm) used as a precolumn, which was connected via the standard blue PEEK capillary tubing (L 300 mm, ID 0.01", OD 1/16") to a Daicel Chiralpak IA column (5 µm, 250 × 4.6 mm), *i*-PrOH–MeOH–*n*-heptane, 22:10:68, 0.5 mL/min, 25 °C (λ = 230 nm).

rac-**12** [**Fig. S2**].
(R_a)-**12** (>99% ee): t_R = 20.12 min (major) [**Fig. S3**].

Stereochemical assignment: The absolute configuration of (R_a)-**12** was established by comparison of the sign of specific rotation and the relative elution order of the resolved peaks with the literature data.[10]

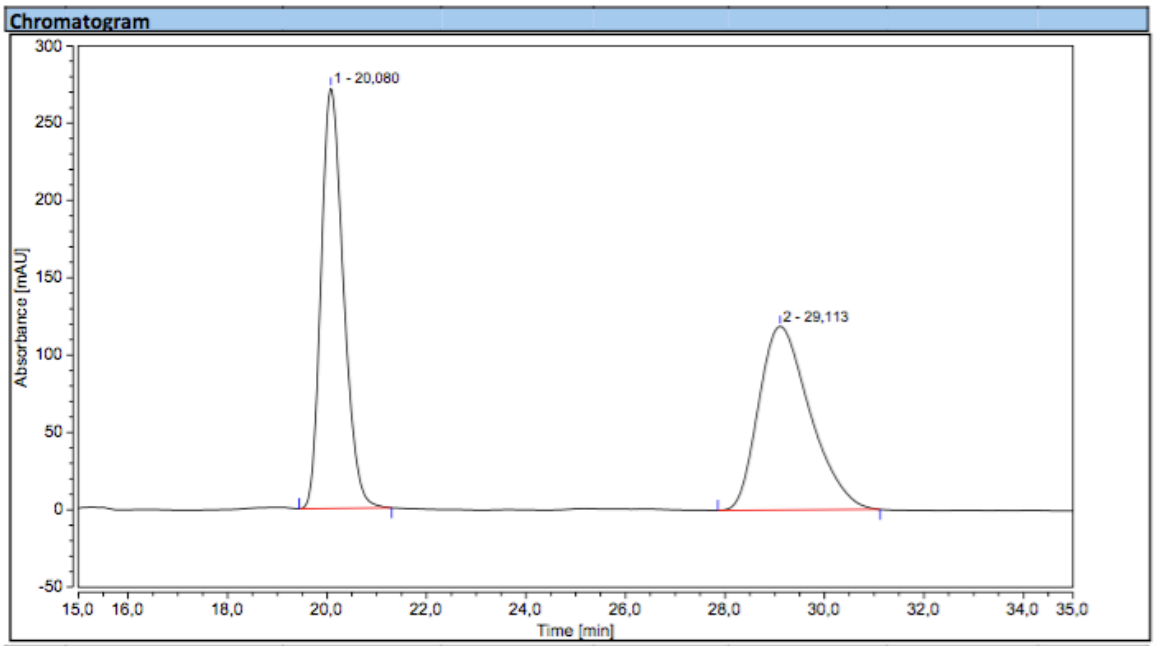

Integration Results

No.	Peak Name	Retention Time min	Area mAU*min	Height mAU	Relative Area %	Relative Height %	Amount n.a.
1		20,080	141,006	271,812	49,80	69,59	n.a.
2		29,113	142,149	118,804	50,20	30,41	n.a.
Total:			**283,155**	**390,616**	**100,00**	**100,00**	

Figure S2: *rac*-**12**.

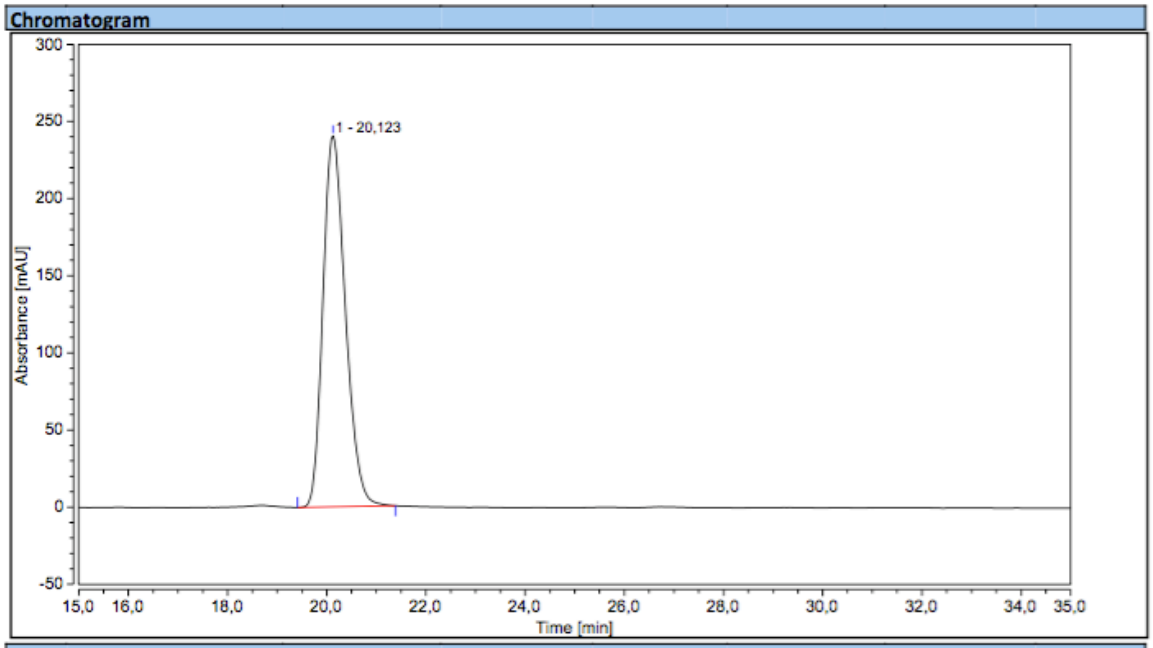

Integration Results

No.	Peak Name	Retention Time min	Area mAU*min	Height mAU	Relative Area %	Relative Height %	Amount n.a.
1		20,123	125,388	240,517	100,00	100,00	n.a.
Total:			**125,388**	**240,517**	**100,00**	**100,00**	

Figure S3: (R_a)-(–)-**12**.

2.5.3 (R_a)-1,1'-([1,1'-Bianthracene]-2,2'-diyl)bis(3-(3,5-bis(trifluoromethyl)phenyl)thiourea) (**1g**)

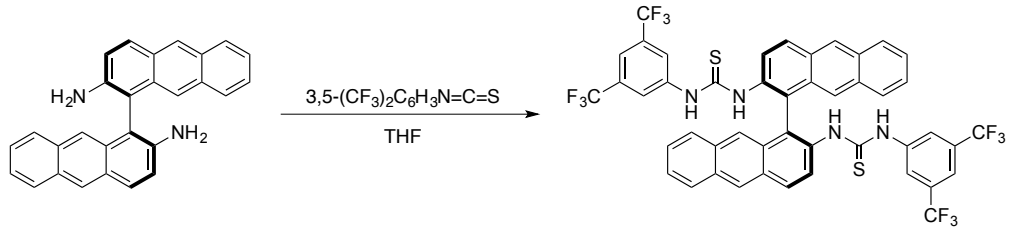

(R_a)-**12** (R_a)-**1g**

A solution of (R_a)-(–)-**12** (100 mg, 260 µmol) in dry THF (1 mL), was treated with 3,5-bis(trifluoromethyl)-phenylisothiocyanate (106 µL, 2.2 equiv) analogously to the compound **1a**.

Physical state: yellow to brown solid.
Isolated yield: 200 mg (83%).

mp 145–147 °C.
$[\alpha]^{25}_D$ +240 (*c* 0.5, $CHCl_3$).
^{1}H NMR (400 MHz, $CDCl_3$): 8.52 (s, 2H), 8.33 (br s, 2H), 8.23 (d, *J* = 8.9 Hz, 2H), 8.09 (br s, 2H), 7.97 (d, *J* = 8.6 Hz, 2H), 7.81–7.74 (m, 4H), 7.53–7.48 (m, 6H), 7.44–7.41 (m, 4H), 7.32–7.28 (m, 2H) [**Fig. S133**].
^{13}C NMR (100 MHz, $CDCl_3$): 179.3, 138.4, 133.3, 132.3, 131.9, 131.8 (q, $^2J_{CF}$ = 33.7 Hz), 130.9, 130.4, 130.2, 128.0, 127.9, 127.7, 126.5, 126.4, 124.5, 124.3, 122.6 (q, $^1J_{CF}$ = 272.9 Hz), 119.5 [**Fig. S134**].
^{19}F NMR (376 MHz, $CDCl_3$): −62.97 (s) [**Fig. S135**].
IR (neat) $\tilde{\nu}$/cm^{-1}: 1471*m*, 1377*m*, 1275*s*, 1173*m*, 1129*s*, 882*m*, 739*w*, 699*w*, 681*m*.
HRMS (ESI-Orbitrap) calcd for $C_{46}H_{27}N_4F_{12}S_2$ $[M+H]^+$ 927.1480 *m*/*z*, found 927.1514 *m*/*z* [**Fig. S52**].

Stereochemical assignment: The absolute configuration of **1g** was established by chemical correlation with (R_a)-(–)-BIANAM.

2.6 Synthesis of 1h

2.6.1 (S_a)-5,5'-Dibromo-6,6'-dimethyl-[1,1'-biphenyl]-2,2'-diamine (**13**)[11]

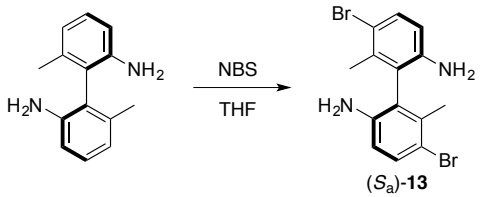

(S_a)-**13**

(S_a)-**13** was prepared from (S_a)-BIPHAM (200 mg, 0.94 mmol) and NBS (340 mg, 1.88 mmol) in dry THF (2 mL) according to the literature.[11] The crude product was purified by a column chromatography (SiO_2) EtOAc–*n*-hexane (1:4).

Physical state: white solid.
Isolated yield: 300 mg (86%).

mp 204–206 °C, lit.[11b] 200–201 °C.
$[\alpha]^{25}_D$ −42 (*c* 1.0, MeOH).
^{1}H NMR (400 MHz, $CDCl_3$) δ/ppm: 7.36 (d, *J* = 8.6 Hz, 2H), 6.57 (d, *J* = 8.6 Hz, 2H), 3.43 (s, 4H), 2.04 (s, 6H) [**Fig. S136**].
^{13}C NMR (100 MHz, $CDCl_3$) δ/ppm: 143.4, 137.0, 132.5, 123.4, 114.5, 113.6, 19.8 [**Fig. S137**].
IR (neat) $\tilde{\nu}$/cm^{-1}: 3474*w*, 3426*w*, 3343*m*, 1614*m*, 1568*m*, 1454*m*, 1434*m*, 1377*w*, 1304*m*, 1249*w*, 1141*w*, 1027*w*, 806*s*, 624*m*.
HRMS (ESI-Orbitrap) calcd for $C_{14}H_{15}N_2Br_2$ $[M+H]^+$ 368.9597 *m*/*z*, found 368.9605 *m*/*z* [**Fig. S53**].

Stereochemical assignment: The absolute configuration of **13** was established by chemical correlation with (S_a)-BIPHAM.

2.6.2 (S_a)-1,1'-(5,5'-Dibromo-6,6'-dimethyl-[1,1'-biphenyl]-2,2'-diyl)bis(3-(3,5-bis(trifluoromethyl)phenyl)-thiourea) (**1h**)

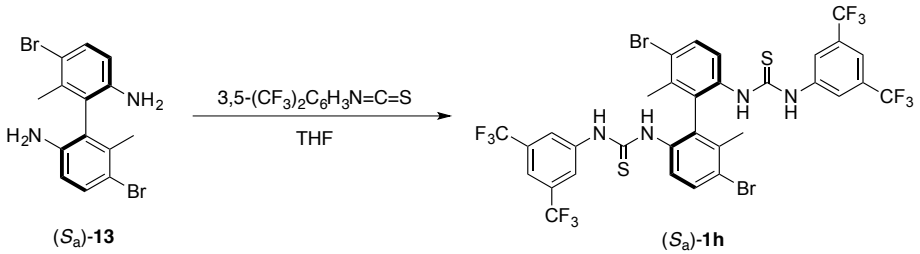

(S_a)-**13** (S_a)-**1h**

A solution of (S_a)-**13** (80 mg, 216 μmol) in dry THF (1 mL), was treated with 3,5-bis(trifluoromethyl)-phenylisothiocyanate (83 μL, 2.1 equiv) analogously to the compound **1a**.

Physical state: white solid.
Isolated yield: 85 mg (43%).

mp 122–125 °C.
$[\alpha]^{25}_{D}$ −124 (*c* 0.5, $CHCl_3$).
^{1}H NMR (400 MHz, $CDCl_3$) δ/ppm: 8.91 (br s, 2H), 7.81–7.45 (m, 12H), 2.02 (s, 6H) [**Fig. S138**].
^{13}C NMR (100 MHz, $CDCl_3$) δ/ppm: 181.3, 138.3, 137.9, 134.6, 132.9, 132.4 (q, $^2J_{CF}$ = 32.8 Hz), 125.2, 124.2, 122.7 (q, $^1J_{CF}$ = 272.6 Hz), 120.1, 20.6 [**Fig. S139**].
^{19}F NMR (376 MHz, $CDCl_3$) δ/ppm: –62.88 (s) [**Fig. S140**].
IR (neat) $\tilde{\nu}$/cm^{-1}: 1519*w*, 1379*m*, 1276*s*, 1177*m*, 1131*s*, 1036*w*, 987*w*, 887*w*, 702*w*, 682*m*.
HRMS (ESI-Orbitrap) calcd for $C_{32}H_{19}N_4F_{12}S_2Br_2$ $[M-H]^-$ 908.9232 *m*/*z*, found 908.9257 *m*/*z* [**Fig. S54**].

Stereochemical assignment: The absolute configuration of **1h** was established by chemical correlation with (S_a)-BIPHAM.

2.7 Synthesis of 1i

2.7.1 Dibenzyl ((2*S*,2'*S*)-(((*S*$_a$)-[1,1'-binaphthalene]-2,2'-diyl)bis(azanediyl))bis(3-methyl-1-oxobutane-1,2-diyl))dicarbamate (**14**)

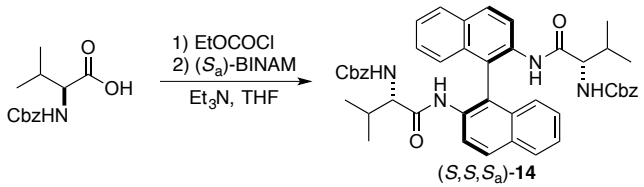

A solution of *N*-carbobenzyloxy-L-valine (389 mg, 1.55 mmol) and anhydrous Et_3N (0.22 mL, 1.58 mmol) in anhydrous THF (5 mL) was treated dropwise over 15 min with a solution of ethyl chloroformate (0.15 mL, 1.55 mmol) in anhydrous THF (0.5 mL) at 0 °C. The resulting mixture was stirred for 30 min at the same temperature. Then a solution of (S_a)-BINAM (200 mg, 0.70 mmol) in anhydrous THF (5 mL) was added over 30 min at 0 °C. The reaction mass was left to stir and warm to ambient temperature overnight. The precipitate of $Et_3N{\cdot}HCl$ was filtered off and the filtrate was evaporated under reduced pressure. The residue was purified by a column chromatography (SiO_2) EtOAc–*n*-hexane (1:3).

Physical state: beige solid.
Isolated yield: 65 mg (12%).

mp 54–55 °C.
$[\alpha]^{25}_D$ −158 (*c* 0.5, $CHCl_3$).
^{1}H NMR (400 MHz, $CDCl_3$): 8.23 (d, *J* = 8.5 Hz, 2H), 7.97 (d, *J* = 8.9 Hz, 2H), 7.91 (d, *J* = 8.1 Hz, 2H), 7.67 (br s, 2H), 7.47–7.43 (m, 2H), 7.36–7.26 (m, 12H), 7.09 (d, *J* = 8.4 Hz, 2H), 5.01–4.90 (m, 6H), 3.82–3.79 (m, 2H), 1.82–1.79 (m, 2H), 0.61 (d, *J* = 6.2 Hz, 6H), 0.46 (d, *J* = 6.6 Hz, 2H) [**Fig. S141**].
^{13}C NMR (100 MHz, $CDCl_3$): 170.1, 160.0, 136.1, 134.2, 132.3, 131.6, 129.8, 128.5, 128.3, 128.2, 128.1, 127.3, 125.8, 125.0, 123.4, 122.4, 67.1, 60.7, 30.3, 18.6, 17.0 [**Fig. S142**].
IR (neat) $\tilde{\nu}$/cm^{-1}: 3292*br*, 2915*s*, 2849*m*, 1729*s*, 1497*m*, 1469*w*, 1215*w*, 1179*w*, 1047*w*, 744*w*, 697*w*.
HRMS (ESI-Orbitrap) calcd for $C_{46}H_{47}N_4O_6$ $[M+H]^+$ 751.3490 *m*/*z*, found 751.3513 *m*/*z* [**Fig. S55**].

Stereochemical assignment: The absolute configuration of **14** was established by chemical correlation with (S_a)-BINAM and *N*-carbobenzyloxy-L-valine.

2.7.2 (2*S*,2'*S*)-*N*,*N*'-((*S*$_a$)-[1,1'-Binaphthalene]-2,2'-diyl)bis(2-amino-3-methylbutanamide) (**15**)

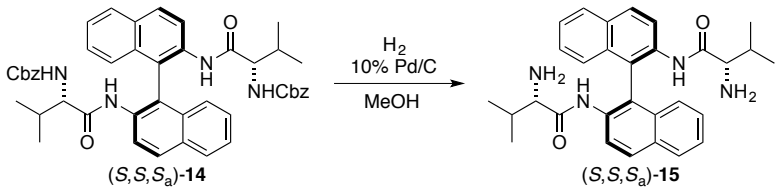

(*S*,*S*,*S*$_a$)-**14** (*S*,*S*,*S*$_a$)-**15**

(*S*,*S*,*S*$_a$)-**14** (120 mg, 0.16 mmol) was dissolved in anhydrous MeOH (25 mL) and hydrogenated over 10% Pd/C (50 mg) under atmosphere of H_2 (45 psi) for 2 hours. The mixture was filtered through a Celite pad and evaporated in vacuo.

Physical state: white solid.
Isolated yield: 42 mg (54%).

mp 49–50 °C.
$[\alpha]^{25}_D$ +82 (*c* 0.5, $CHCl_3$).
^{1}H NMR (400 MHz, $CDCl_3$) δ/ppm: 9.29 (s, 2H), 8.48 (d, *J* = 8.9 Hz, 2H), 8.02 (d, *J* = 9.0 Hz, 2H), 7.94 (d, *J* = 8.1 Hz, 2H), 7.45–7.41 (m, 2H), 7.29–7.24 (m, 2H), 7.17 (d, *J* = 8.4 Hz, 2H), 3.13 (d, *J* = 3.4 Hz, 2H), 2.12–2.05 (m, 2H), 1.57 (br s, 4H), 0.79 (d, *J* = 6.9 Hz, 6H), 0.55 (d, *J* = 6.9 Hz, 6H) [**Fig. S143**].
^{13}C NMR (100 MHz, $CDCl_3$) δ/ppm: 173.2, 134.8, 132.6, 131.1, 129.3, 128.2, 126.8, 125.5, 125.1, 121.6, 121.0, 60.3, 30.7, 19.4, 16.1 [**Fig. S144**].
IR (neat) $\tilde{\nu}$/cm^{-1}: 3320*w*, 2953*m*, 2915*s*, 2849*m*, 1729*m*, 1671*w*, 1590*w*, 1493*m*, 1424*w*, 1178*w*, 826*w*, 753*w*.
HRMS (ESI-Orbitrap) calcd for $C_{30}H_{33}N_4O_2$ $[M-H]^-$ 481.2609 *m*/*z*, found 481.2610 *m*/*z* [**Fig. S56**].

Stereochemical assignment: The absolute configuration of **15** was established by chemical correlation with (*S*$_a$)-BINAM and *N*-carbobenzyloxy-L-valine.

2.7.3 (2*S*,2'*S*)-*N*,*N*'-((*S*$_a$)-[1,1'-Binaphthalene]-2,2'-diyl)bis(2-(3-(3,5-bis(trifluoromethyl)phenyl)thioureido)-3-methylbutanamide) (**1i**)

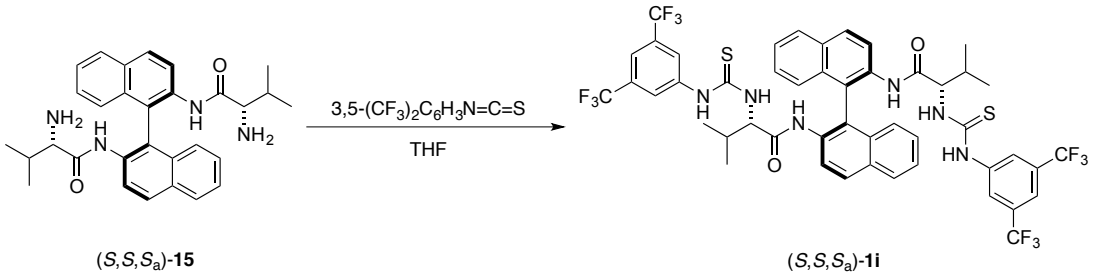

(*S*,*S*,*S*$_a$)-**15** (*S*,*S*,*S*$_a$)-**1i**

A solution of (*S*,*S*,*S*$_a$)-**15** (32 mg, 66 μmol) in dry THF (0.5 mL), was treated with 3,5-bis(trifluoromethyl)-phenylisothiocyanate (26 μL, 2.1 equiv) analogously to the compound **1a**. The crude product was purified by a column chromatography (SiO_2) EtOAc–*n*-hexane (1:3).

Physical state: beige solid.
Isolated yield: 50 mg (74%).

mp 148–150 °C.
$[\alpha]^{25}_D$ −116 (*c* 1.0, $CHCl_3$).
^{1}H NMR (400 MHz, $CDCl_3$) δ/ppm: 8.66 (br s, 2H), 8.02–6.96 (m, 22H), 4.35 (br s, 2H), 1.80 (br s, 2H), 0.66 (s, 6H), 0.52 (s, 6H) [**Fig. S145**].
^{13}C NMR (100 MHz, $CDCl_3$) δ/ppm: 181.2, 139.6, 133.1, 132.5, 131.5 (q, $^2J_{CF}$ = 32.7 Hz), 130.0, 128.3, 127.5, 126.4, 124.9, 123.6, 122.9 (q, $^1J_{CF}$ = 272.9 Hz), 118.4, 30.2, 18.6, 18.3 [**Fig. S146**].
^{19}F NMR (376 MHz, $CDCl_3$) δ/ppm: −62.82 (s) [**Fig. S147**].
IR (neat) $\tilde{\nu}$/cm^{-1}: 3278*w*, 2966*w*, 1660*w*, 1501*m*, 1471*m*, 1381*m*, 1275*s*, 1175*m*, 1128*s*, 965*w*, 885*w*, 701*w*, 681*w*
HRMS (ESI-Q-TOF) calcd for $C_{48}H_{39}F_{12}N_6O_2S_2$ $[M–H]^-$ 1023.2379 *m*/*z*, found 1023.2327 *m*/*z* [**Fig. S57**].

Stereochemical assignment: The absolute configuration of **1i** was established by chemical correlation with (*S*$_a$)-BINAM and *N*-carbobenzyloxy-L-valine.

2.8 Synthesis of 1j

2.8.1 (S_a)-2',2''-Dimethyl-3,3''',5,5'''-tetrakis(trifluoromethyl)-[1,1':3',1'':3'',1'''-quaterphenyl]-4',6''-diamine (**16**)

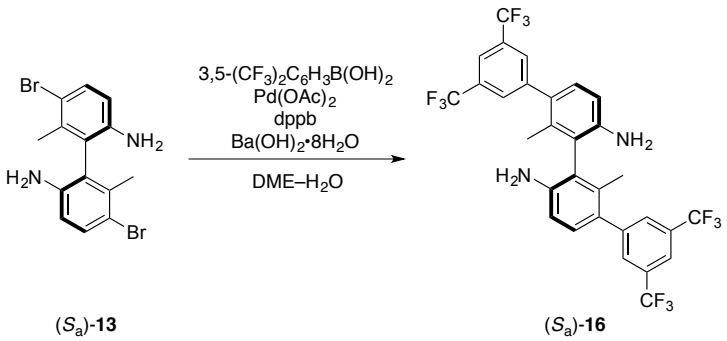

(S_a)-**13** (S_a)-**16**

A mixture of (S_a)-**13** (100 mg, 0.27 mmol), $Pd(OAc)_2$ (6 mg, 270 μmol), 1,4-bis(diphenylphosphino)butane (23 mg, 540 μmol), $Ba(OH)_2{\cdot}8H_2O$ (341 mg, 1.08 mmol), and 3,5-bis(trifluoromethyl)phenylboronic acid (209 mg, 0.81 mmol) in degassed dimethoxyethanol (1.1 mL) and water (110 μL) was refluxed under Ar atmosphere for 48 h. After cooling to room temperature, the mixture was poured into water and repetitively extracted with EtOAc. The combined organic extracts were washed with water and brine, dried over anhydrous Na_2SO_4, filtered and evaporated in vacuo. The crude product was purified by a column chromatography (SiO_2) EtOAc–*n*-hexane (1:9).

Physical state: brown solid.
Isolated yield: 60 mg (35%).

mp 122–123 °C.
$[\alpha]^{25}_D$ +32 (*c* 0.5, $CHCl_3$).
^{1}H NMR (400 MHz, $CDCl_3$) δ/ppm: 7.83 (s, 2H), 7.80 (s, 4H), 7.12 (d, J = 8.1 Hz, 2H), 6.83 (d, J = 8.1 Hz, 2H), 3.74 (br s, 4H), 1.95 (s, 6H) [**Fig. S148**].
^{13}C NMR (100 MHz, $CDCl_3$) δ/ppm: 144.3, 135.1, 131.3 (q, $^2J_{CF}$ = 32.7 Hz), 130.5, 129.7, 123.4 (q, $^1J_{CF}$ = 272.6 Hz), 122.7, 120.1, 113.5, 17.3 [**Fig. S149**].
^{19}F NMR (376 MHz, $CDCl_3$) δ/ppm: −62.59 (s) [**Fig. S150**].
IR (neat) $\tilde{\nu}$/cm^{-1}: 3348*w*, 2973*w*, 1593*m*, 1462*w*, 1374*s*, 1276*s*, 1166*m*, 1124*s*, 1047*w*, 897*w*, 847*w*, 816*w*, 709*w*, 683*w*.
HRMS (ESI-Orbitrap) calcd for $C_{30}H_{21}N_2F_{12}$ $[M+H]^+$ 637.1508 *m*/*z*, found 637.1491 *m*/*z* [**Fig. S58**].

Stereochemical assignment: The absolute configuration of **16** was established by chemical correlation with (S_a)-BIPHAM.

2.8.2 (S_a)-1,1'-(2',2''-Dimethyl-3,3''',5,5'''-tetrakis(trifluoromethyl)-[1,1':3',1'':3'',1'''-quaterphenyl]-4',6''-diyl)bis(3-(3,5-bis(trifluoromethyl)phenyl)thiourea) (**1j**)

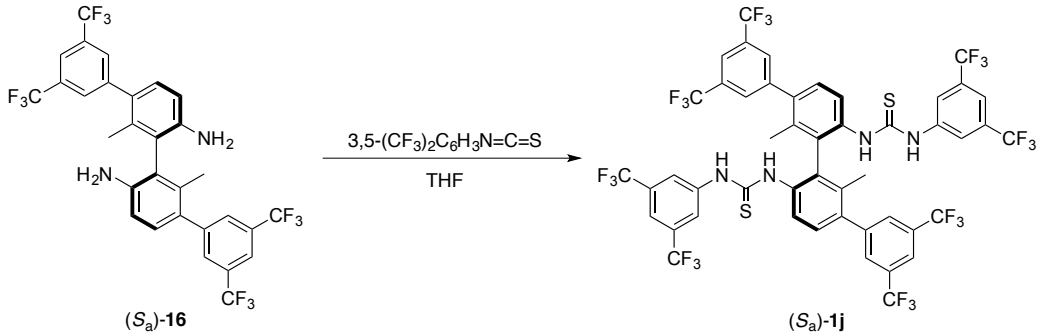

(S_a)-**16** (S_a)-**1j**

To a solution of (S_a)-**16** (30 mg, 47 μmol) in dry THF (0.5 mL), 3,5-bis(trifluoromethyl)-phenylisothiocyanate (18 μL, 2.05 equiv) was added dropwise at room temperature. The reaction mixture was stirred 48 h at rt under Ar and then evaporated in vacuo. The resulting glassy residue was subjected to flash chromatography (SiO_2) EtOAc–*n*-hexane (1:9).

Physical state: white powder.
Isolated yield: 35 mg (65%).

mp 115–117 °C.
$[\alpha]^{25}_D$ −80 (*c* 0.5, $CHCl_3$).
^{1}H NMR (400 MHz, acetone-d_6) δ/ppm: 9.66 (br s, 2H), 8.94 (br s, 2H), 8.18 (br s, 4H), 8.10–8.06 (m, 6H), 7.89–7.87 (m, 2H), 7.73 (br s, 2H), 7.54–7.51 (m, 2H), 2.08 (br s, 6H) [**Fig. S151**].
^{13}C NMR (100 MHz, acetone-d_6) δ/ppm: 182.1, 182.0, 181.9, 145.0, 142.3, 142.2, 139.0, 138.4, 138.3, 136.8, 134.9, 132.2 (q, $^2J_{CF}$ = 33.1 Hz), 131.9 (q, $^2J_{CF}$ = 33.1 Hz), 130.9, 127.2, 125.3, 125.2, 124.5 (q, $^1J_{CF}$ = 272.3 Hz), 124.3 (q, $^1J_{CF}$ = 272.0 Hz), 121.9, 118.7, 18.7 (a mixture of conformers) [**Fig. S152**].
^{19}F NMR (376 MHz, acetone-d_6) δ/ppm: −63.13 (s, 12F), −63.43 (s, 12F) [**Fig. S153**].
IR (neat) $\tilde{\nu}$/cm^{-1}: 1522*w*, 1377*m*, 1275*s*, 1171*m*, 1126*s*, 1052*w*, 900*m*, 826*w*, 709*w*, 682*m*.
HRMS (ESI-Q-TOF) calcd for $C_{48}H_{25}F_{24}N_4S_2$ $[M–H]^-$ 1177.1132 *m*/*z*, found 1177.1094 *m*/*z* [**Fig. S59**].

Stereochemical assignment: The absolute configuration of **1j** was established by chemical correlation with (S_a)-BIPHAM.

2.9 Synthesis of 1k

2.9.1 1-((*R*)-Phenyl(((*R*)-1-phenylethyl)amino)methyl)naphthalen-2-ol (**17**)[12]

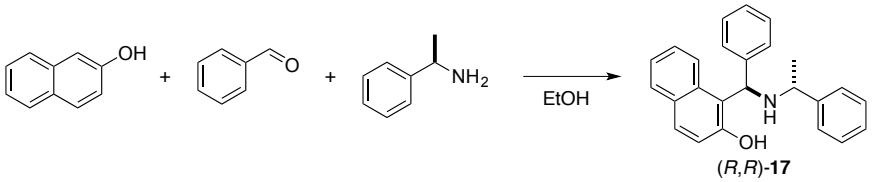

(*R*,*R*)-**17**

(*R*,*R*)-**17** was prepared from 2-naphthol (1.0 g, 7.0 mmol), benzaldehyde (0.85 mL, 1.20 equiv) and (*R*)-(+)-phenylethylamine (0.94 mL, 1.05 equiv) according to the literature.[12] The crude product was triturated with 96% ethanol, filtered, and then recrystallized from a mixture of EtOAc–*n*-hexane (3:1, 20 mL).

Physical state: white solid.
Isolated yield: 1.86 g (75%).

mp 153–155 °C, lit.[12] 154–156 °C.
$[\alpha]^{25}_{D}$ –221 (*c* 1.0, $CHCl_3$).
^{1}H NMR (400 MHz, $CDCl_3$) δ/ppm: 7.77–7.73 (m, 2H), 7.44–7.37 (m, 4H), 7.26–7.19 (m, 10H), 5.48 (s, 1H), 3.92 (q, *J* = 6.6 Hz, 1H), 1.52 (d, *J* = 6.9 Hz, 3H) [**Fig. S154**].
^{13}C NMR (100 MHz, $CDCl_3$) δ/ppm: 157.2, 142.9, 141.3, 132.6, 129.7, 129.0, 128.9, 128.73, 128.68, 126.7, 126.4, 122.4, 121.1, 120.0 [**Fig. S155**].
IR (neat) $\tilde{\nu}$/cm^{-1}: 3372*w*, 1622*m*, 1602*w*, 1517*w*, 1494*w*, 1469*w*, 1415*w*, 1318*w*, 1270*w*, 1238*m*, 1161*w*, 1077*w*, 947*w*, 875*w*, 813*m*, 765*m*, 743*s*, 696*s*, 651*w*.
HRMS (ESI-Orbitrap) calcd for $C_{25}H_{24}NO$ $[M+H]^+$ 354.1852 *m*/*z*, found 354.1843 *m*/*z* [**Fig. S60**].

Stereochemical assignment: The absolute configuration of **17** was established by chemical correlation with (*R*)-(+)-phenylethylamine and by comparison of the sign of specific rotation with the literature value.[12] The diastereomeric ratio 98:2 was determined by integration of the ^{1}H NMR signals 5.63 (s, 0.02H) and 5.48 (s, 1H) corresponding to the minor (*S*,*R*) and major (*R*,*R*)-diastereomer respectively.

2.9.2 1-Benzylnaphthalen-2-ol (**18**)[13]

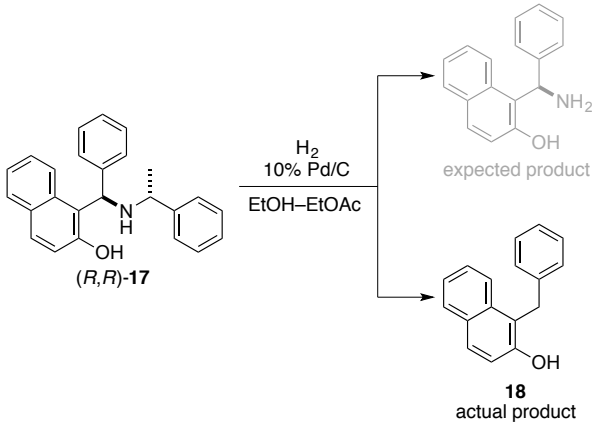

The compound **18** was unexpectedly formed by a catalytic hydrogenation of (*R*,*R*)-**17** over Pd/C.

(*R*,*R*)-**17** (1.0 g, 2.8 mmol) dissolved in anhydrous EtOH–EtOAc, 1:1 (50 mL) was hydrogenated over 10% Pd/C (0.5 g) under atmosphere of H_2 (75 psi).
After the TLC analysis (SiO_2) EtOAc–*n*-hexane (1:5) revealed a complete disappearance of the starting material (48 h), the mixture was filtered through a Celite pad and evaporated in vacuo.

Physical state: brownish solid
Isolated yield: 0.5 g (76%).

mp 99–100 °C, lit.[13b] 110–111 °C.
^{1}H NMR (400 MHz, $CDCl_3$) δ/ppm: 7.94 (d, *J* = 8.5 Hz, 1H), 7.82 (d, *J* = 8.0 Hz, 1H), 7.73 (d, *J* = 8.8 Hz, 1H), 7.47 (ddd, *J* = 7.7, 7.7, 1.0 Hz, 1H), 7.38–7.34 (ddd, *J* = 7.5, 7.5, 0.8 Hz, 1H), 7.29–7.18 (m, 5H), 7.13 (d, *J* = 8.8 Hz, 1H), 5.08 (br s, 1H), 4.48 (s, 2H) [**Fig. S156**].
^{13}C NMR (100 MHz, $CDCl_3$) δ/ppm: 151.2, 140.0, 133.6, 129.5, 128.6, 128.52, 128.49, 128.2, 126.7, 126.1, 123.3, 123.2, 118.1, 117.9, 30.7 [**Fig. S157**].
IR (neat) $\tilde{\nu}$/cm^{-1}: 3420*w*, 2938*w*, 1630*w*, 1603*w*, 1493*m*, 1438*m*, 1357*w*, 1266*m*, 1229*m*, 1060*w*, 988*m*, 859*w*, 813*m*, 747*m*, 717*s*, 692*m*.
HRMS (ESI-Orbitrap) calcd for $C_{17}H_{13}O$ $[M-H]^-$ 233.0972 *m*/*z*, found 233.0971 *m*/*z* [**Fig. S61**].

2.9.3 *rac*-1-(Amino(phenyl)methyl)naphthalen-2-ol (*rac*-**19**)[14]

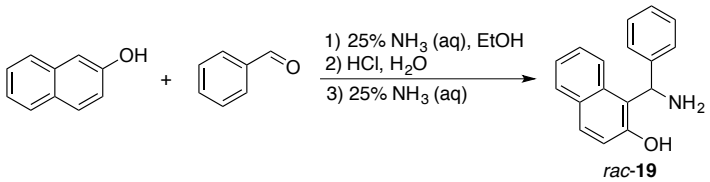

rac-**19**

rac-**19** was prepared from 2-naphthol (2.9 g, 20.0 mmol), benzaldehyde (4.0 mL, 2.0 equiv) and 25% aqueous ammonia (4.0 mL) in 96% ethanol (4.0 mL) according to the literature.[14] The reaction conversion was monitored by TLC (SiO_2) EtOAc–*n*-hexane (1:5).

Physical state: beige solid.
Isolated yield: 2.0 g (43%).

mp 121–122 °C, lit.[14b] 120–122 °C.
^{1}H NMR (400 MHz, DMSO-d_6) δ/ppm: 7.86 (d, J = 8.6 Hz, 1H), 7.75 (d, J = 7.9 Hz, 1H), 7.71 (d, J = 8.8 Hz, 1H), 7.50 (d, J = 7.3 Hz, 1H), 7.37–7.19 (m, 6H), 7.05 (d, J = 8.8 Hz, 1H), 6.08 (s, 1H), 3.39 (br s, 2H) [**Fig. S158**].
^{13}C NMR (100 MHz, DMSO-d_6) δ/ppm: 143.6, 131.8, 128.9, 128.5, 127.7, 127.3, 127.2, 126.2, 122.0, 121.5, 120.3, 116.9, 54.6 [**Fig. S159**].
IR (neat) $\tilde{\nu}$/cm^{-1}: 3364*w*, 3291*w*, 1622*m*, 1601*m*, 1518*w*, 1470*m*, 1415*m*, 1378*w*, 1267*m*, 1237*s*, 1155*m*, 1019*m*, 927*m*, 907*m*, 822*s*, 799*m*, 761*s*, 744*s*, 698*s*.
HRMS (ESI-Orbitrap) calcd for $C_{17}H_{16}NO$ $[M+H]^+$ 250.1232 *m*/*z*, found 250.1215 *m*/*z* [**Fig. S62–63**].

2.9.4 (*S*)-(+)-1-(Amino(phenyl)methyl)naphthalen-2-ol (*S*-**19**)[15]

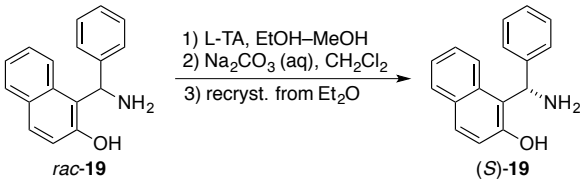

rac-**19** (*S*)-**19**

rac-**19** (2.0 g, 8.0 mmol) was resolved with (2*R*,3*R*)-tartaric acid (1.2 g, 8.0 mmol) in a mixture of 96% ethanol (5.3 mL) and methanol (2.7 mL) according to the literature.[15] The enantiomeric purity of (*S*)-**19** (750 mg) was further improved by triturating the sample with a small amount of diethyl ether.

Physical state: white solid.
Isolated yield: 450 mg (45%).

mp 124–126 °C, lit.[15b] 132–133 °C.
$[\alpha]^{25}_{D}$ +58 (*c* 5.0, C_6H_6).

Chiral HPLC conditions: a Hypersil silica column (3 μm, 100 × 4.6 mm) used as a precolumn, which was connected via the standard blue PEEK capillary tubing (L 300 mm, ID 0.01", OD 1/16") to a Daicel Chiralpak IB column (5 μm, 250 × 4.6 mm), *i*-PrOH–*n*-heptane, 20:80, 0.5 mL/min, 25 °C (λ = 230 nm).

rac-**19** [**Fig. S4**].
(*S*)-**19** (98% ee): t_S = 17.24 min (major), t_R = 26.96 min (minor) [**Fig. S5**].

2.2.1 Stereochemical assignment
The absolute configuration of (*S*)-**19** was established by comparison of the sign of specific rotation and the relative elution order of the resolved peaks with the literature data.[15]

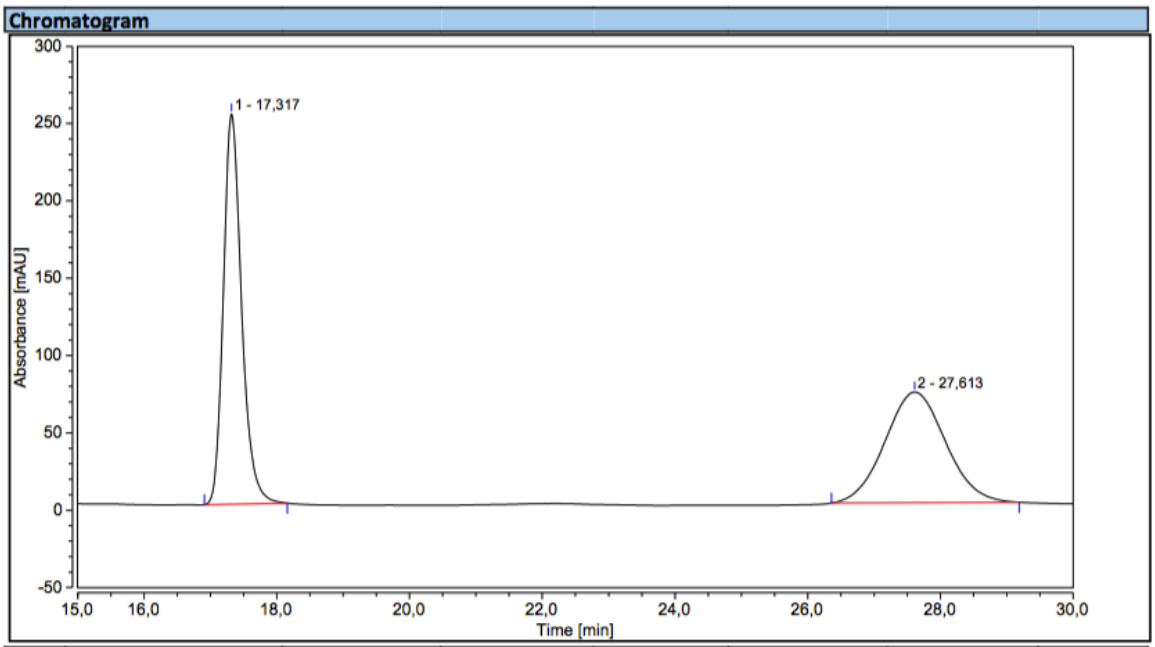

Integration Results

No.	Peak Name	Retention Time min	Area mAU*min	Height mAU	Relative Area %	Relative Height %	Amount n.a.
1		17,317	80,225	252,381	51,40	77,91	n.a.
2		27,613	75,858	71,551	48,60	22,09	n.a.
Total:			**156,083**	**323,932**	**100,00**	**100,00**	

Figure S4: *rac*-**19**.

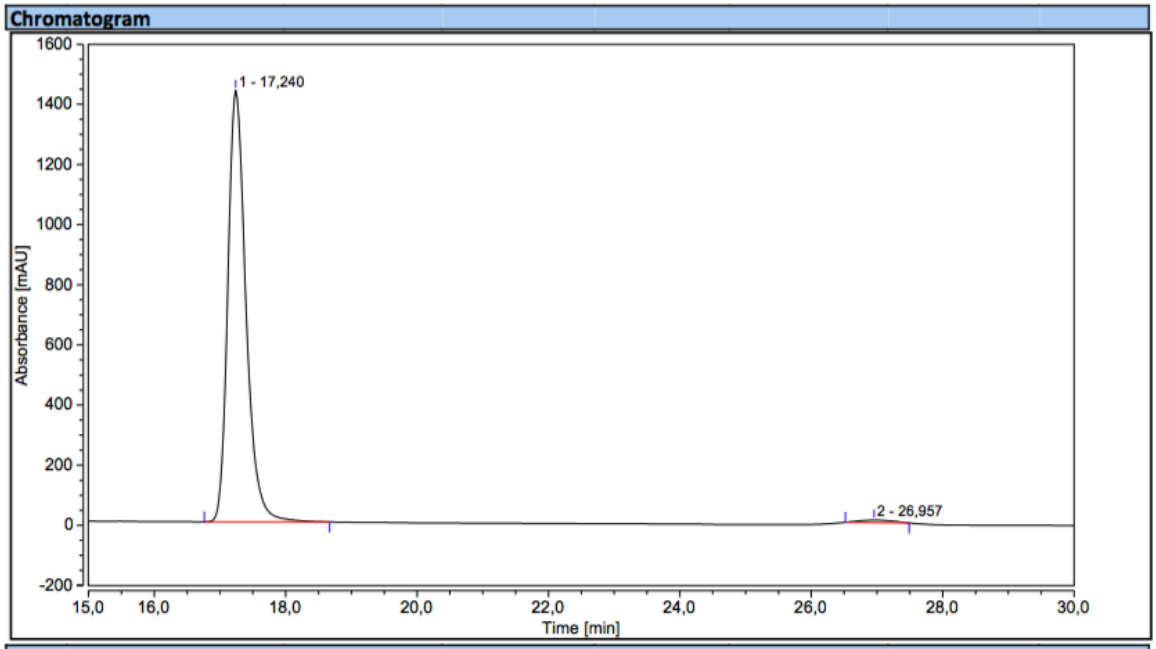

Integration Results

No.	Peak Name	Retention Time min	Area mAU*min	Height mAU	Relative Area %	Relative Height %	Amount n.a.
1		17,240	458,897	1434,841	98,92	99,42	n.a.
2		26,957	5,021	8,312	1,08	0,58	n.a.
Total:			**463,918**	**1443,153**	**100,00**	**100,00**	

Figure S5: (*S*)-**19**.

2.9.5 (*S*)-1-(3,5-Bis(trifluoromethyl)phenyl)-3-((2-hydroxynaphthalen-1-yl)(phenyl)methyl)thiourea (**1k**)[16]

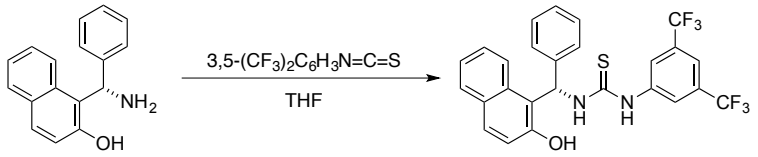

(*S*)-**19** (*S*)-**1k**

A solution of (*S*)-(+)-**19** (150 mg, 0.51 mmol) in dry THF (2 mL), was treated with 3,5-bis-(trifluoromethyl)phenylisothiocyanate (98 µL, 1.05 equiv) analogously to the compound **1a**.

Physical state: white solid.
Isolated yield: 160 mg (82%).

mp 112–114 °C, lit.[16] 139–140 °C.
$[\alpha]^{25}_{D}$ +8 (*c* 0.7, $CHCl_3$).
^{1}H NMR (400 MHz, $CDCl_3$) δ/ppm: 8.81 (br s, 1H), 8.44 (br s, 1H), 8.17 (br s, 1H), 8.01–7.91 (m, 1H), 7.80 (d, *J* = 8.1 Hz, 1H), 7.73 (d, *J* = 8.5 Hz, 1H), 7.71 (s, 2H), 7.66 (s, 1H), 7.50 (t, *J* = 7.6 Hz, 1H), 7.37 (t, *J* = 7.5, 1H), 7.24–7.16 (m, 5H), 7.07 (d, *J* = 8.8 Hz, 1H), 6.14 (br s, 1H) [**Fig. S160**].
^{13}C NMR (100 MHz, $CDCl_3$) δ/ppm: 179.9, 151.1, 140.0, 138.5, 132.8 (q, $^2J_{CF}$ = 33.7 Hz), 132.4, 129.6, 128.7, 128.5, 127.7, 127.3, 126.1, 124.1, 123.6, 123.0, 122.8 (q, $^1J_{CF}$ = 272.6 Hz), 119.2 (q, $^3J_{CF}$ = 3.9 Hz), 118.8, 118.2, 55.5 [**Fig. S161**].
^{19}F NMR (376 MHz, $CDCl_3$) δ/ppm: –62.88 (s) [**Fig. S162**].
IR (neat) ṽ/cm^{-1}: 1516*m*, 1471*w*, 1376*m*, 1276*s*, 1175*m*, 1132*s*, 952*w*, 888*w*, 810*w*, 741*w*, 697*w*, 682*m*.
HRMS (ESI-Orbitrap) calcd for $C_{26}H_{17}F_6N_2OS$ $[M–H]^–$ 519.0966 *m*/*z*, found 519.0980 *m*/*z* [**Fig. S64**].

Stereochemical assignment: The absolute configuration of **1k** was established by chemical correlation with (*S*)-(+)-1-(amino(phenyl)methyl)naphthalen-2-ol and by comparison of the sign of specific rotation with the literature value.[16]

2.10 Synthesis of 1l

2.10.1 *rac*-2'-Amino-[1,1'-binaphthalen]-2-ol (*rac*-**20,** *rac*-NOBIN)[17]

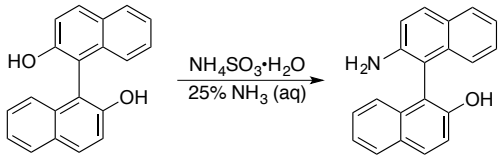

rac-**20**

rac-**20** was prepared from *rac*-BINOL (5.0 g, 17.5 mmol), $(NH_4)SO_3 \cdot H_2O$ (23.5 g, 175 mmol) and 25% aqueous ammonia (65 mL) according to the literature.[17a] Based on a TLC analysis (SiO_2) CH_2Cl_2–MeOH (99:1) the crude product contaminated with a large amount of BINOL was further purified by extraction of its ethanol–aqueous HCl solution with toluene according to the literature.[17b]

Physical state: white powder.
Isolated yield: 0.6 g (12%).

mp 249–250 °C, lit.[17c] 240 °C.
^{1}H NMR (400 MHz, DMSO-d_6) δ/ppm: 9.33 (s, 1H), 7.90–7.86 (m, 2H), 7.74–7.72(m, 2H), 7.37 (d, J = 8.9 Hz, 1H), 7.27–7.23 (m, 1H), 7.21–7.17 (m, 2H), 7.11–7.05 (m, 2H), 6.95 (d, J = 8.3 Hz, 1H), 6.77–6.74 (m, 1H), 4.56 (s, 2H) [**Fig. S163**].
^{13}C NMR (100 MHz, DMSO-d_6) δ/ppm: 153.4, 144.0, 134.1, 133.7, 129.2, 128.5, 128.2, 128.1, 127.9, 127.1, 126.2, 125.8, 124.2, 123.5, 122.6, 120.8, 118.9, 118.5, 115.0, 111.3 [**Fig. S164**].
IR (neat) $\tilde{\nu}$/cm^{-1}: 3397*s*, 3321*m*, 1616*s*, 1595*m*, 1508*m*, 1463*m*, 1432*w*, 1311*w*, 1274*m*,1248*w*, 1214*s*, 1174*s*, 1145*s*, 956*w*, 817*s*, 751*s*, 661*m*.
HRMS (ESI-Orbitrap) calcd for $C_{20}H_{16}NO$ $[M+H]^+$ 286.1226 *m*/*z*, found 286.1231 *m*/*z* [**Fig. S65**].

2.10.2 (R_a)-(+)-2'-Amino-[1,1'-binaphthalen]-2-ol (R_a-**20,** R_a-NOBIN)[18]

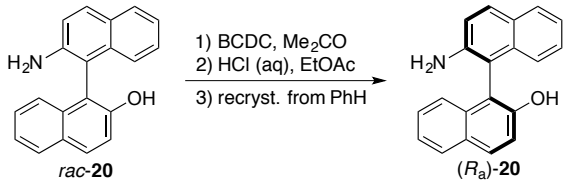

rac-**20** (Ra)-**20**

rac-**20** (500 mg, 1.8 mmol) was resolved with (–)-*N*-benzylcinchonidium chloride (470 mg, 1.3 mmol) in dry acetone (9 mL) according to the literature.[18] The enantiomeric purity of (R_a)-(+)-**20** (280 mg) was further improved by recrystallization from benzene (4 mL).

Physical state: white solid.
Isolated yield: 130 mg (52%).

mp 167–169 °C, lit.[18b] 167–169 °C.
$[\alpha]^{29}_{D}$ +123 (*c* 1.0, THF).

Chiral HPLC conditions: a Hypersil silica column (3 μm, 100 × 4.6 mm) used as a precolumn, which was connected via the standard blue PEEK capillary tubing (L 300 mm, ID 0.01", OD 1/16") to a Daicel Chiralpak IB column (5 μm, 250 × 4.6 mm), *i*-PrOH–*n*-heptane, 10:90, 0.5 mL/min, 25 °C (λ = 230 nm).

rac-**20** [**Fig. S6**].
(R_a)-**20** (>99% ee): t_S = 26.40 min (minor), t_R = 27.48 min (major) [**Fig. S7**].

Stereochemical assignment: The absolute configuration of (R_a)-**20** was established by comparison of the sign of specific rotation and the relative elution order of the resolved peaks with the literature data.[18a]

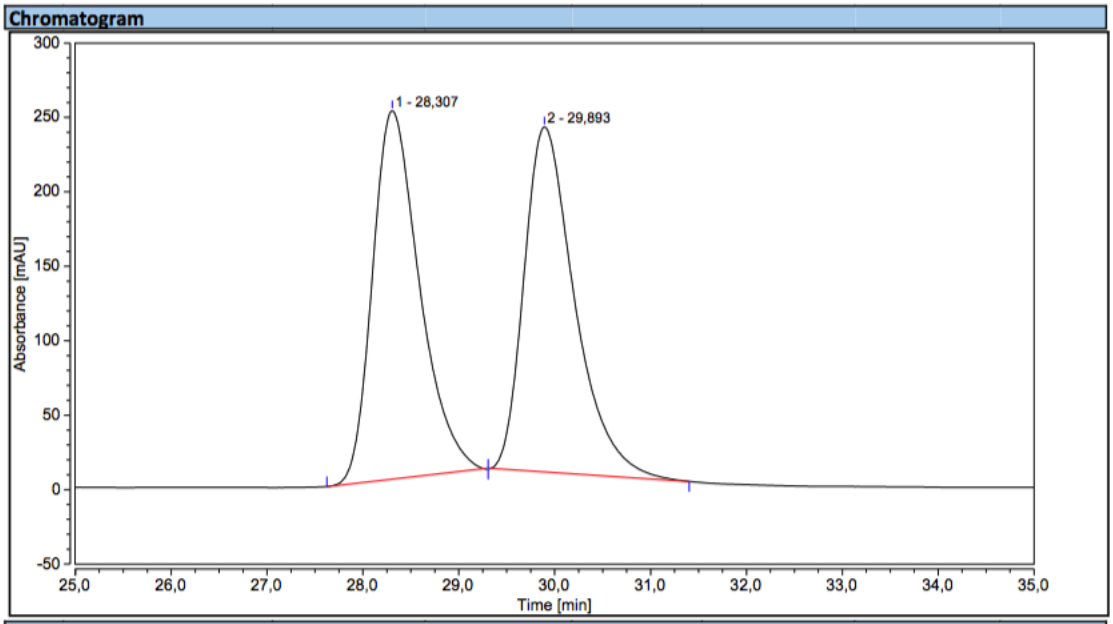

Integration Results

No.	Peak Name	Retention Time min	Area mAU*min	Height mAU	Relative Area %	Relative Height %	Amount n.a.
1		28,307	140,593	247,513	49,81	51,64	n.a.
2		29,893	141,675	231,808	50,19	48,36	n.a.
Total:			**282,267**	**479,321**	**100,00**	**100,00**	

Figure S6: *rac*-**20**.

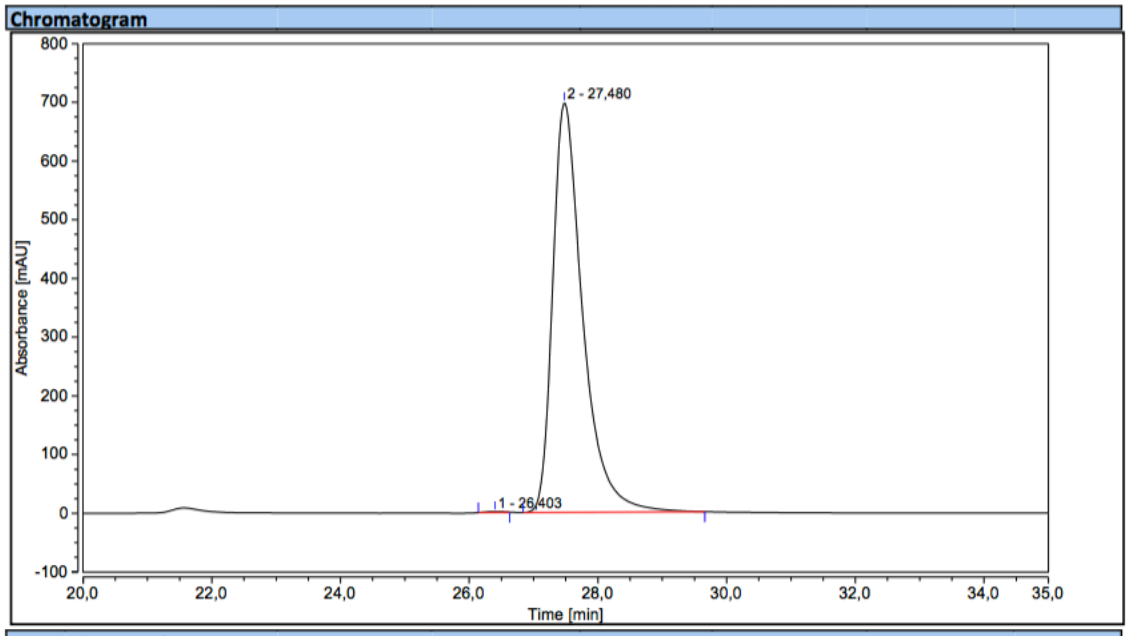

Integration Results

No.	Peak Name	Retention Time min	Area mAU*min	Height mAU	Relative Area %	Relative Height %	Amount n.a.
1		26,403	0,383	1,282	0,10	0,18	n.a.
2		27,480	377,249	697,670	99,90	99,82	n.a.
Total:			**377,632**	**698,951**	**100,00**	**100,00**	

Figure S7: (R_a)-(–)-**20**.

2.10.3 (R_a)-1-(3,5-Bis(trifluoromethyl)phenyl)-3-(2'-hydroxy-[1,1'-binaphthalen]-2-yl)thiourea (**1l**)[19]

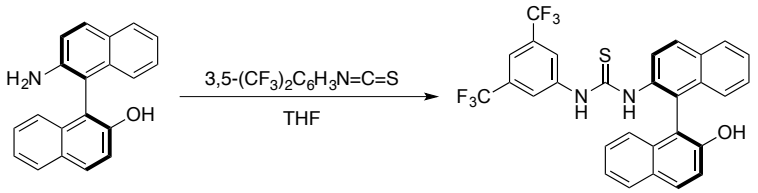

(R_a)-**20** (R_a)-**1l**

A solution of (R_a)-(+)-**20** (50 mg, 175 μmol) in dry THF (0.5 mL), was treated with 3,5-bis-(trifluoromethyl)phenylisothiocyanate (34 μL, 1.05 equiv) analogously to the compound **1a**.

Physical state: white powder.
Isolated yield: 76 mg (78%).

mp 108–109 °C, lit.[19] 103–107 °C.
$[\alpha]^{25}_{D}$ −153 (*c* 0.5, $CHCl_3$).
^{1}H NMR (400 MHz, $CDCl_3$) δ/ppm: 8.05 (d, *J* = 8.8 Hz, 1H), 7.95 (d, *J* = 8.2 Hz, 1H), 7.83–7.78 (m, 4H), 7.63 (s, 1H), 7.54–7.51 (m, 2H), 7.45 (s, 2H), 7.35–7.31 (m, 1H), 7.27–7.24 (m, 2H), 7.18–7.13 (m, 2H), 6.89 (d, *J* = 8.4 Hz, 1H), 5.75 (br s, 1H) [**Fig. S165**].
^{13}C NMR (100 MHz, $CDCl_3$) δ/ppm: 180.0, 151.4, 138.5, 133.9, 133.1, 133.0, 132.9, 132.1 (q, $^2J_{CF}$ = 33.7 Hz), 131.0, 130.3, 129.0, 128.7, 128.4, 128.1, 127.6, 127.5, 127.1, 126.3, 124.8, 124.6, 123.9, 123.5, 122.6 (q, $^1J_{CF}$ = 272.9 Hz), 119.7, 118.1, 113.8 [**Fig. S166**].
^{19}F NMR (376 MHz, $CDCl_3$) δ/ppm: −62.82 (s) [**Fig. S167**].
IR (neat) ṽ/cm^{-1}: 1506*m*, 1471*m*, 1381*m*, 1346*w*, 1276*s*, 1172*m*, 1124*s*, 887*w*, 817*m*, 750*m*, 701*m*, 682*m*.
HRMS (ESI-Orbitrap) calcd for $C_{29}H_{19}F_6N_2OS$ $[M+H]^+$ 557.1117 *m*/*z*, found 557.1135 *m*/*z* [**Fig. S66**].

Stereochemical assignment: The absolute configuration of **1l** was established by chemical correlation with (R_a)-(+)-NOBIN.[19]

2.11 Synthesis of 2m

2.11.1 (*S*)-2-(6-Methoxynaphthalen-2-yl)propanamide (**21**)[20]

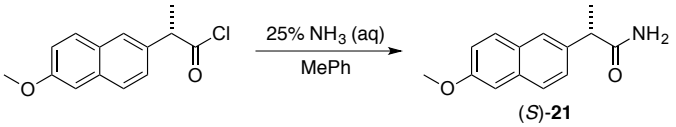

(*S*)-**21**

(*S*)-**21** was prepared from (*S*)-(+)-naproxen chloride (1.30 g, 5.2 mmol) according to the literature.[20]

Physical state: white solid.
Isolated yield: 1.0 g (86%).

mp 166–167 °C, lit.[20b] 177–178 °C.
$[\alpha]^{25}_{D}$ +20 (*c* 0.5, MeOH).
^{1}H NMR (400 MHz, DMSO-d_6) δ/ppm: 7.78–7.72(m, 3H), 7.47–7.42 (m, 2 H), 7.27 (br s, 1H), 7.15–7.13 (m, 1H), 6.83 (br s, 1H), 3.86 (s, 3H), 3.72 (q, J = 6.8 Hz, 1H), 1.40 (d, J = 7.0 Hz, 3H) [**Fig. S168**].
^{13}C NMR (100 MHz, DMSO-d_6) δ/ppm: 176.0, 157.5, 138.1, 133.7, 129.6, 128.9, 127.1, 127.0, 125.8, 119.1, 106.3, 55.7, 45.4, 19.0 [**Fig. S169**].
IR (neat) $\tilde{\nu}$/cm^{-1}: 3339*w*, 3194*w*, 1636*s*, 1605*m*, 1485*w*, 1461*m*, 1402*m*, 1267*m*, 1217*m*, 1174*w*, 1113*w*, 1026*m*, 926*m*, 893*w*, 852*s*, 813*s*, 673*m.*
HRMS (ESI-Orbitrap) calcd for $C_{14}H_{16}NO_2$ $[M+H]^+$ 230.1176 *m*/*z*, found 230.1180 *m*/*z* [**Fig. S67**].

Stereochemical assignment: The absolute configuration of **21** was established by chemical correlation with (*S*)-(+)-naproxen and by comparison of the sign of specific rotation with the literature value.[20]

2.11.2 (*S*)-1-(6-Methoxynaphthalen-2-yl)ethan-1-amine (**22**)[21]

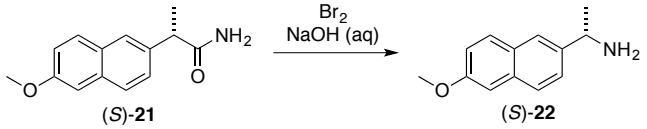

(*S*)-**21** (*S*)-**22**

(*S*)-**22** was prepared by a slightly modified literature procedure.[21]
Br_2 (0.25 mL, 5 mmol) was added dropwise to 1M aqueous NaOH (25 mL) at 0 °C under vigorous stirring. After 15 min (*S*)-**21** (1.0 g, 4.4 mmol) was added in one portion. The resulting suspension was stirred at 60 °C for 2 h, TLC monitoring (SiO_2) CH_2Cl_2–MeOH (9:1). Then the reaction mixture was quenched by saturated aqueous $Na_2S_2O_3$ (2 mL). The mixture was repetitively extracted with Et_2O. The combined organic phase was dried over anhydrous Na_2SO_4, filtered, and evaporated in vacuo.
The crude yellowish residue was dissolved in a mixture of Et_2O and MeOH (4:1, 10 mL) and the solution of anhydrous oxalic acid (0.5 g, 1.1 equiv) in Et_2O–MeOH (4:1, 10 mL) was added dropwise. The resulting precipitate was filtered off, washed several times with Et_2O–MeOH (4:1) then Et_2O, and dried in vacuo.
The free base was released by addition of aqueous 5M NaOH, back-extracted to toluene, dried over anhydrous Na_2SO_4, filtered and evaporated in vacuo.

Physical state: yellow waxy solid.
Isolated yield: 270 mg (31%).

$[\alpha]^{25}_D$ −31 (*c* 1.0, $CHCl_3$).
^{1}H NMR (400 MHz, $CDCl_3$): 7.74–7.71 (m, 3H), 7.46 (dd, *J* = 8.5, 1.8 Hz, 1H), 7.17–7.13 (m, 2H), 4.26 (q, *J* = 6.6 Hz, 1H), 3.92 (s, 3H), 1.64 (br s, 2H), 1.47 (d, *J* = 6.6 Hz, 3H) [**Fig. S170**].
^{13}C NMR (100 MHz, $CDCl_3$): 157.3, 142.8, 133.6, 129.2, 128.8, 127.0, 125.0, 123.6, 118.7, 105.6, 55.2, 51.2, 25.6 [**Fig. S171**].
IR (neat) $\tilde{\nu}$/cm^{-1}: 3342*w*, 2969*m*, 1605*s*, 1504*m*, 1448*m*, 1434*w*, 1390*m*, 1312*w*, 1268*m*, 1248*m*, 1216*m*, 1169*m*, 1093*w*, 1024*m*, 948*w*, 879*w*, 857*s*, 817*m*, 750*w*, 674*w*.
HRMS (ESI-Orbitrap) calcd for $C_{13}H_{13}O$ $[M–NH_3+H]^+$ 185.0961 *m*/*z*, found 185.0956 *m*/*z* [**Fig. S68**].

Stereochemical assignment: The absolute configuration of **22** was established by chemical correlation with (*S*)-(+)-naproxen and by comparison of the sign of specific rotation with the literature value.[21]

2.11.3 *tert*-Butyl (*S*)-(1-(6-hydroxynaphthalen-2-yl)ethyl)carbamate (**23**)

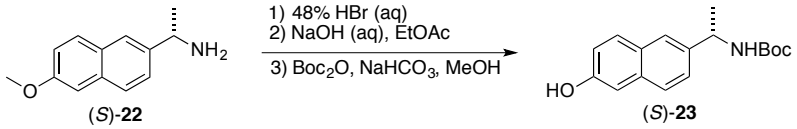

(*S*)-**22** (*S*)-**23**

Step 1: A mixture of (*S*)-**22** (1.0 g, 5.0 mmol) and 48% aqueous HBr (10 mL) was stirred and refluxed under Ar atmosphere for 6 h. Then the solvent was removed under reduced pressure. The residue was dissolved in water, alkalized with 2.5M NaOH and repetitively extracted with EtOAc. The combined organic extracts were washed with water, brine, dried over Na_2SO_4, filtered, and evaporated in vacuo to provide crude (*S*)-6-(1-aminoethyl)naphthalen-2-ol as yellowish solid, which was used directly in the following step.

Step 2: Di-*tert*-butyl dicarbonate (1.2 g, 5.5 mmol) was added portionwise to the stirring suspension of crude (*S*)-6-(1-aminoethyl)naphthalen-2-ol and $NaHCO_3$ (1.7 g, 20.2 mmol) in dry MeOH (25 ml). The reaction mixture was stirred at ambient temperature for 24 h under Ar. Then the solvent was removed under reduced pressure. The crude product was loaded on SiO_2 and purified by a column chromatografy (SiO_2) CH_2Cl_2–MeOH (99:1).

Physical state: beige solid.
Isolated yield: 770 mg (51% over two steps).

mp 183–185 °C.
$[\alpha]^{25}_D$ −72 (*c* 1.0, acetone).
^{1}H NMR (400 MHz, DMSO-d_6) δ/ppm: 9.66 (s, 1H), 7.70 (d, *J* = 8.7 Hz, 1H), 7.64–7.60 (m, 2H), 7.43–7.36 (m, 2H), 7.08–7.05 (m, 2H), 4.73–4.69 (m, 1H), 1.36 (s, 12H) [**Fig. S172**].
^{13}C NMR (100 MHz, DMSO-d_6) δ/ppm: 155.0, 154.9, 139.6, 133.6, 129.2, 127.5, 126.1, 125.0, 123.8, 118.7, 108.6, 77.7, 49.6, 28.3, 22.8 [**Fig. S173**].
IR (neat) ṽ/cm^{-1}:3353*m*, 3286*m*, 2981*w*, 2934*w*, 1672*s*, 1613*w*, 1522*s*, 1445*w*, 1364*m*, 1282*s*, 1240*m*, 1159*s*, 1106*w*, 1057*m*, 991*w*,890*w*, 863*m*, 825*m*, 673*w*.
HRMS (ESI-Orbitrap) calcd for $C_{17}H_{22}NO_3$ $[M+H]^+$ 288.1594 *m*/*z*, found 288.1602 *m*/*z* [**Fig. S69**].

Stereochemical assignment: The absolute configuration of **23** was established by chemical correlation with (*S*)-(+)-naproxen.

2.11.4 Di-*tert*-butyl ((1*S*,1'*S*)-((ethane-1,2-diylbis(oxy))bis(naphthalene-6,2-diyl))bis(ethane-1,1-diyl))di-carbamate (**24**)

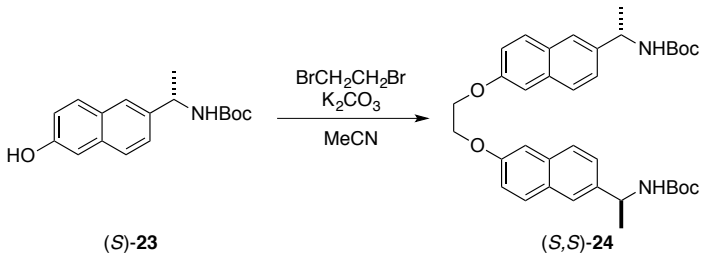

(*S*)-**23** (*S*,*S*)-**24**

A suspension of (*S*)-**23** (250 mg, 0.87 mmol) and anhydrous K_2CO_3 (240 mg, 1.74 mmol) in dry MeCN (5 mL) was treated with 1,2-dibromoethane (45 μL, 0.52 mmol). The reaction mixture was heated to 65 °C and left to stir for 24 h under Ar atmosphere. The solvent was removed in vacuo. The residue was suspended in water (15 mL) and repetitively extracted with EtOAc. The combined organic extracts were washed with water, brine, dried over anhydrous Na_2SO_4, filtered and evaporated in vacuo. The crude product was purified by a column chromatography (SiO_2) EtOAc–*n*-hexane (1:2).

Physical state: white solid.
Isolated yield: 150 mg (57%).

mp 181–184 °C.
$[\alpha]^{25}_D$ −86 (*c* 0.5, acetone).
^{1}H NMR (400 MHz, acetone-d_6) δ/ppm: 8.70 (s, 2H), 7.73–7.70 (m, 4H), 6.63 (d, *J* = 8.5 Hz, 2H), 7.43 (dd, *J* = 8.6 Hz, 1.6 Hz, 2H), 7.17 (d, *J* = 2.2 Hz, 2H), 7.12 (dd, *J* = 8.8 Hz, 2.4 Hz, 2H), 6.39 (br s, 4H), 4.87 (m, 2H), 1.49 (d, *J* = 7.1 Hz, 6H), 1.38 (br s, 18H) [**Fig. S174**].
^{13}C NMR (100 MHz, acetone-d_6) δ/ppm: 156.2, 156.1, 140.6, 135.1, 130.3, 129.3, 127.3, 126.1, 125.0, 119.4, 119.3, 109.8, 109.7, 78.8, 51.0, 28.7, 23.1 [**Fig. S175**].
IR (neat) $\tilde{\nu}$/cm^{-1}: 3354*m*, 3286*m*, 2981*w*, 2934*w*, 1673*s*, 1613*w*, 1552*s*, 1484*w*, 1445*w*, 1364*m*, 1283*s*, 1240*m*, 1160*s*, 1106*w*, 1057*m*, 991*w*, 863*m*, 825*w*, 669*w*.
HRMS (ESI-Orbitrap) calcd for $C_{35}H_{46}N_2O_6$ $[M+H]^+$ 601.3272 *m*/*z*, found 601.3300 *m*/*z* [**Fig. S70**].

Stereochemical assignment: The absolute configuration of **24** was established by chemical correlation with (*S*)-(+)-naproxen.

2.11.5 1,1'-((1*S*,1'*S*)-((Ethane-1,2-diylbis(oxy))bis(naphthalene-6,2-diyl))bis(ethane-1,1-diyl))bis-(3-(3,5-bis(trifluoromethyl)phenyl)thiourea) (**1m**)

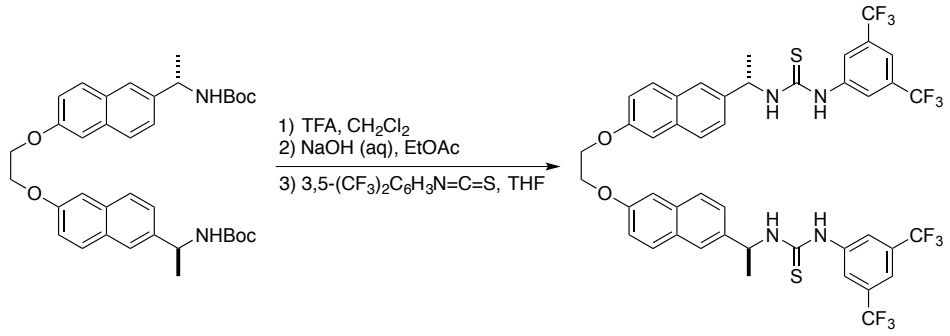

(*S*,*S*)-**24** (*S*,*S*)-**1m**

Step 1: (*S*,*S*)-**24** (125 mg, 0.21 mmol) was dissolved in dry CH_2Cl_2 (0.6 mL) and trifluoroacetic acid (0.6 mL) was added dropwise under Ar atmosphere. The reaction mixture was left to stir overnight at ambient temperature. Then the mixture was cooled to 0 °C and alkalized with 5M NaOH. The reaction mixture was repetitively extracted with EtOAc, the combined organic extracts were dried over anhydrous Na_2SO_4, filtered and evaporated in vacuo to give the crude (1*S*,1'*S*)-1,1'-((ethane-1,2-diylbis(oxy))-bis(naphthalene-6,2-diyl))bis(ethan-1-amine) as brownish solid, which was used directly in the following step.

Step 2: A solution of crude (1*S*,1'*S*)-1,1'-((ethane-1,2-diylbis(oxy))bis(naphthalene-6,2-diyl))bis(ethan-1-amine) (80 mg, 200 μmol) in dry THF (1 mL), was treated with 3,5-bis(trifluoromethyl)phenyl-isothiocyanate (80 μL, 2.2 equiv) analogously to the compound **1a**.

Physical state: beige solid.
Isolated yield: 81 mg (35% over two steps).

mp 85–88 °C.
$[\alpha]^{25}_{D}$ –30 (*c* 0.5, acetone).
^{1}H NMR (400 MHz, acetone-d_6) δ/ppm: 9.45 (br s, 2H), 8,86 (br s, 2H), 8.34–8.32 (m, 4H), 8.13 (br d, J = 7.9 Hz, 2H), 7.80 (s, 2H), 7.75 (d, J = 8.8 Hz, 2H), 7.69–7.67 (m, 2H), 7.49 (dd, J = 8.5, 1.3 Hz, 2H), 7.19 (d, J = 1.8 Hz, 2H), 7.14 (dd, J = 8.8, 2.3 Hz, 2H), 5.83 (m, 4H), 1.65 (d, J = 7.0 Hz, 6H), [**Fig. S176**].
^{13}C NMR (100 MHz, acetone-d_6) δ/ppm: 181.5, 181.4, 181.3, 181.2, 156.4, 156.3, 143.1, 143.0, 138.5, 135.3, 131.9 (q, $^2J_{CF}$ = 32.8 Hz), 130.4, 129.2, 127.5, 126.3, 125.6, 124.4 (q, $^1J_{CF}$ = 271.7 Hz), 123.4, 123.3, 119.6, 119.5, 117.41, 117.38, 109.7, 109.6, 54.22, 54.19, 54.11, 54.09, 21.8 (a mixture of conformers) [**Fig. S177**].
^{19}F NMR (376 MHz, acetone-d_6) δ/ppm: –63.42 (s) [**Fig. S178**].
IR (neat) $\tilde{\nu}$/cm^{-1}: 3362*m*, 1610*m*, 1518*m*, 1474*m*, 1381*m*, 1275*s*, 1173*s*, 1126*s*, 977*w*, 885*m*, 861*m*, 808*w*, 700*w*, 678*m*.
HRMS (ESI-Q-TOF) calc for $[M–C_{23}H_{18}F_6N_2OS–H]^-$ 457.0809 *m*/*z*, found 457.0809 *m*/*z* [**Fig. S71**].

Stereochemical assignment: The absolute configuration of **1m** was established by chemical correlation with (*S*)-(+)-naproxen.

2.12 Synthesis of 1n

2.12.1 L-Phenylalaninamide (**25**)[22]

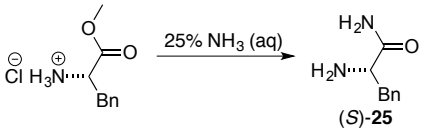

(*S*)-**25**

L-Phenylalanine methyl ester hydrochloride (1.2 g, 5.6 mmol) was added in one portion to ice-cold solution of 25% aqueous ammonia (12 mL) and left to stir at rt for 24 h. After TLC analysis (SiO_2) CH_2Cl_2–MeOH (85:15) revealed a complete consumption of the starting material, the mixture was evaporated to dryness and the residue was dissolved in 5 M NaOH (10 mL) and repetitively extracted with CH_2Cl_2. The combined organic extracts were washed with brine, dried with anhydrous Na_2SO_4, filtered, and evaporated in vacuo.

Physical state: beige solid.
Isolated yield: 0.65 g (71%).

mp 94–95 °C, lit.[22b] 94.5–95.5 °C.
$[\alpha]^{25}_D$ +11 (*c* 1.0, MeOH).
^{1}H NMR (400 MHz, $CDCl_3$) δ/ppm: 7.27–7.23 (m, 2H), 7.20–7.15 (m, 3H), 7.04 (s, 1H), 5.97 (s, 1H), 3.54 (dd, *J* = 9.5, 4.1 Hz, 1H), 3.20 (dd, *J* = 13.7, 4.1 Hz, 1H), 2.64 (dd, *J* = 13.7, 9.5 Hz, 1H), 1.29 (s, 2H) [**Fig. S179**].
^{13}C NMR (100 MHz, $CDCl_3$) δ/ppm: 177.5, 137.8, 129.2, 128.7, 126.8, 56.5, 40.9 [**Fig. S180**].
IR (neat) $\tilde{\nu}$/cm^{-1}: 3338*s*, 3028*s*, 1661*s*, 1604*m*, 1494*m*, 1446*m*, 1410*w*, 1299*w*, 1076*w*, 991*w*, 896*w*, 777*w*, 731*w*, 699*m*.
HRMS (ESI-Orbitrap) calcd for $C_9H_{13}N_2O$ $[M+H]^+$ 165.1022 *m*/*z*, found 165.1024 *m*/*z* [**Fig. S72**].

Stereochemical assignment: The absolute configuration of **25** was established by chemical correlation with L-phenylalanine methyl ester hydrochloride and by comparison of the sign of specific rotation with the literature value.[22]

2.12.2 (*S*)-3-Phenylpropane-1,2-diamine (**26**)[23]

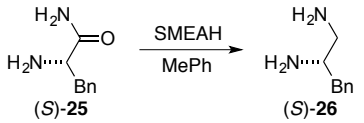

(*S*)-**25** (*S*)-**26**

To a suspension of (*S*)-**25** (1.0 g, 6.9 mmol) in dry toluene (15 mL), 60% SMEAH in toluene (29.8 mL, 15 equiv) was added dropwise at 20 °C. The resulting mixture was stirred under Ar at rt for 48 h. After TLC (SiO_2) CH_2Cl_2–MeOH (9:1) revealed the complete consumption of the starting material. The mixture was cooled and quenched by a dropwise addition of 5M aqueous NaOH (25 mL). Aqueous phase was repetitively extracted with toluene and the combined organic extracts were dried over anhydrous Na_2SO_4, filtered and evaporated in vacuo.
The crude yellow oily residue was dissolved in a mixture of Et_2O and MeOH (4:1, 10 mL) and the solution of anhydrous oxalic acid (1.2 g, 2.2 equiv) in Et_2O–MeOH (4:1, 15 mL) was added dropwise. The resulting precipitate was filtered off, washed several times with Et_2O–MeOH (4:1) then Et_2O, and dried in vacuo.
The free base was released by addition of aqueous 5M NaOH, back-extracted to toluene, dried over anhydrous Na_2SO_4, filtered and evaporated in vacuo.

Physical state: yellow oil.
Isolated yield: 301 mg (33%).

$[\alpha]^{25}_D$ –14 (*c* 1.0, $CHCl_3$).
^{1}H NMR (400 MHz, $CDCl_3$) δ/ppm: 7.29–7.25 (m, 2H), 7.21–7.14 (m, 3H), 2.96–2.90 (m, 1H), 2.79–2.73 (m, 2H), 2.53–2.43 (m, 2H), 1.35 (br s, 4H) [**Fig. S181**].
^{13}C NMR (100 MHz, $CDCl_3$) δ/ppm: 139.1, 129.1, 128.4, 126.2, 55.0, 48.1, 42.2 [**Fig. S182**].
IR (neat) ṽ/cm^{-1}: 2915*w*, 1662*m*, 1494*m*, 1081*w*, 746*m*, 698*s*.
HRMS (ESI-Orbitrap) calcd for $C_9H_{15}N_2$ $[M+H]^+$ 151.1230 *m*/*z*, found 151.1231 *m*/*z* [**Fig. S73**].

Stereochemical assignment: The absolute configuration of **26** was established by chemical correlation with L-phenylalanine methyl ester hydrochloride.

2.12.3 (*S*)-1,1'-(3-Phenylpropane-1,2-diyl)bis(3-(3,5-bis(trifluoromethyl)phenyl)thiourea) (**1n**)[24]

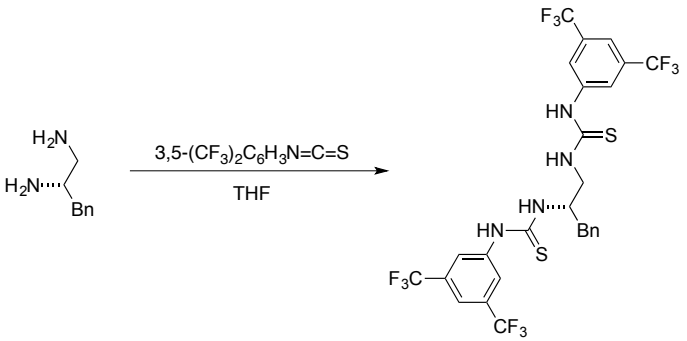

(*S*)-**26** (*S*)-**1n**

A solution of (*S*)-**26** (50 mg, 330 µmol) in dry THF (0.5 mL), was treated with 3,5-bis(trifluoromethyl)-phenylisothiocyanate (125 µL, 2.05 equiv) analogously to the compound **1a**.

Physical state: white powder.
Isolated yield: 190 mg (83%).

mp 79–81 °C.
$[\alpha]^{25}_{D}$ –60 (*c* 1.0, $CHCl_3$).
^{1}H NMR (400 MHz, $CDCl_3$) δ/ppm: 8.31 (br s, 1H), 7.73–7.64 (m, 5H), 7.27–7.13 (m, 6H), 6.85 (br s, 1H), 4.93 (br s, 1H), 4.14–4.06 (m, 1H), 3.57 (br s, 1H), 2.96 (br s, 2H) [**Fig. S183**].
^{13}C NMR (100 MHz, $CDCl_3$) δ/ppm: 181.5, 180.9, 138.3, 135.9, 133.0 (q, $^2J_{CF}$ = 30.8 Hz), 129.1, 128.9, 127.5, 125.1, 124.8, 122.8 (q, $^1J_{CF}$ = 272.6 Hz), 122.7 (q, $^1J_{CF}$ = 272.6 Hz), 120.2, 56.2, 49.3, 38.7 [**Fig. S184**].
^{19}F NMR (376 MHz, $CDCl_3$) δ/ppm: −62.94 (s, 6F), −62.95 (s, 6F) [**Fig. S185**].
IR (neat) $\tilde{\nu}$/cm^{-1}: 1532*m*, 1471*w*, 1375*m*, 1275*s*, 1170*m*,1127*s*, 886*m*, 846*w*, 700*m*, 681*m*.
HRMS (ESI-Orbitrap) calcd for $C_{27}H_{21}F_{12}N_4S_2$ $[M+H]^+$ 693.1011 *m*/*z*, found 693.0997 *m*/*z* [**Fig. S74**].

The absolute configuration of **1n** was established by chemical correlation with L-phenylalanine methyl ester hydrochloride and by comparison of the sign of specific rotation with the literature value.[24]

2.13 Synthesis of 1o

2.13.1 L-Leucinamide (**27**)[25]

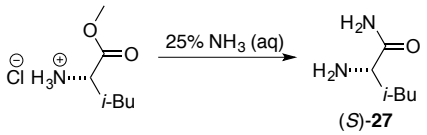

(*S*)-**27**

L-Leucine methyl ester hydrochloride (1.0 g, 6.0 mmol) was treated with 25% aqueous ammonia (10 mL) analogously to the compound **25**.

Physical state: colorless solid.
Isolated yield: 0.56 g (72%).

mp 101–103 °C, lit.[25b] 101–102 °C.
$[\alpha]^{25}_{D}$ +9 (*c* 1.0, MeOH).
^{1}H NMR (400 MHz, DMSO-d_6) δ/ppm: 7.28 (br s, 1H), 6.86 (br s, 1H), 3.07 (dd, *J* = 8.9, 5.3 Hz, 1H), 1.74–1.65 (m, 1H), 1.61 (br s, 2H), 1.36 (ddd, *J* = 13.4, 8.3, 5.3 Hz, 1H), 1.19 (ddd, *J* = 13.4, 8.9, 5.7 Hz, 1H), 0.87 (d, *J* = 8.7 Hz, 3H), 0.84 (d, *J* = 8.7 Hz, 3H) [**Fig. S186**].
^{13}C NMR (100 MHz, DMSO-d_6) δ/ppm: 178.2, 53.1, 44.5, 24.2, 23.2, 21.8 [**Fig. S187**].
IR (neat) $\tilde{\nu}$/cm^{-1}: 3284*s*, 2956*s*, 1598*s*, 1442*m*, 1384*m*, 1315*m*, 1244*w*, 1101*w*, 971*m*, 906*m*, 803*w*, 664*w*.
HRMS (ESI-Orbitrap) calcd for $C_6H_{15}N_2O$ $[M+H]^+$ 131.1179 *m*/*z*, found 131.1177 *m*/*z* [**Fig. S75**].

Stereochemical assignment: The absolute configuration of **27** was established by chemical correlation with L-leucine methyl ester hydrochloride.

2.13.2 (*S*)-4-Methylpentane-1,2-diamine (**28**)[25]

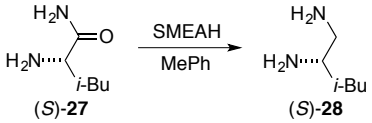

(*S*)-**27** (*S*)-**28**

A suspension of (*S*)-**27** (1.0 g, 7.7 mmol) in toluene (15 mL) was treated with 60% SMEAH in toluene (37.5 mL, 15 equiv) analogously to the compound **26**. The crude oily product was purified by Kugelrohr distillation under the reduced pressure (60 °C, 2.0 torr) to provide (*S*)-**28** slightly contaminated with 2-methoxyethanol, which was enough pure for the next step.

Physical state: colorless oil.
Isolated yield: 354 mg (39%).

$[\alpha]^{25}_{D}$ –15 (*c* 0.2, $CHCl_3$).
^{1}H NMR (400 MHz, $CDCl_3$) δ/ppm: 2.73–2.65 (m, 2H), 2.41–2.36 (m, 1H), 1.73–1.63 (m, 1H), 1.43 (br s, 4H), 1.16–1.12 (M, 2H), 0.88 (d, *J* = 6.6 Hz), 0.85 (d, *J* = 6.6 Hz) [**Fig. S188**].
^{13}C NMR (100 MHz, $CDCl_3$) δ/ppm: 51.2, 49.0, 44.9, 24.6, 23.4, 22.0 [**Fig. S189**].
IR (neat) ṽ/cm^{-1}: 1537*m*, 1468*w*, 1384*m*, 1273*s*, 1174*m*, 1132*s*, 1063*m*, 983*m*, 889*m*, 847*w*, 708*s*, 680*s*.
HRMS (ESI-Orbitrap) calcd for $C_6H_{17}N_2$ $[M+H]^+$ 117.1386 *m*/*z*, found 117.1385 *m*/*z* [**Fig. S76**].

Stereochemical assignment: The absolute configuration of **28** was established by chemical correlation with L-leucine methyl ester hydrochloride**.**

2.13.3 (*S*)-1,1'-(4-Methylpentane-1,2-diyl)bis(3-(3,5-bis(trifluoromethyl)phenyl)thiourea) (**1o**)

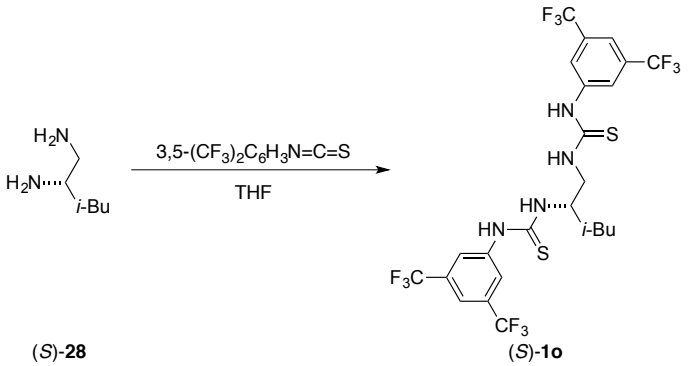

(*S*)-**28** (*S*)-**1o**

A solution of (*S*)-**28** (30 mg, 260 μmol) in dry THF (0.5 mL), was treated with 3,5-bis(trifluoromethyl)-phenylisothiocyanate (97 μL, 2.05 equiv) analogously to the compound **1a**.

Physical state: white powder.
Isolated yield: 153 mg (79%).

mp 153–154 °C.
$[\alpha]^{25}_{D}$ −33 (*c* 1.0, $CHCl_3$).
^{1}H NMR (400 MHz, $CDCl_3$) δ/ppm: 8.38 (br s, 1H), 7.82–7.70 (m, 6H), 7.42 (br s, 1H), 6.40 (br s, 1H), 4.85 (br s, 1H), 4.02 (br s, 2H), 3.54 (br s, 1H), 1.72–1.62 (m, 1H), 1.49–1.40 (m, 2H), 0.95 (d, J = 6.5 Hz, 6H) [**Fig. S190**].
^{13}C NMR (100 MHz, $CDCl_3$) δ/ppm: 181.1, 138.4, 132.8 (q, $^2J_{CF}$ = 33.7 Hz), 124.7, 122.7 (q, $^1J_{CF}$ = 272.6 Hz), 120.0, 119.8, 118.6, 53.5, 51.1, 41.7, 25.2, 22.9, 21.9 [**Fig. S191**].
^{19}F NMR (376 MHz, $CDCl_3$) δ/ppm: –62.98 (s, 6F), –63.08 (s, 6F) [**Fig. S192**].
IR (neat) $\tilde{\nu}$/cm^{-1}: 1559*w*, 1470*w*, 1379*m*, 1276*s*, 1173*m*, 1130*s*, 892*m*, 701*m*, 681*m*.
HRMS (ESI-Orbitrap) calcd for $C_{24}H_{23}F_{12}N_4S_2$ $[M+H]^+$ 659.1167 *m*/*z*, found 659.1186 *m*/*z* [**Fig. S77**].

Stereochemical assignment: The absolute configuration of **1o** was established by chemical correlation with L-leucine methyl ester hydrochloride.

2.14 Synthesis of 1p

2.14.1 1,1'-((1*R*,2*R*)-Cyclohexane-1,2-diyl)bis(3-(3,5-bis(trifluoromethyl)phenyl)thiourea) (**1p**)[26]

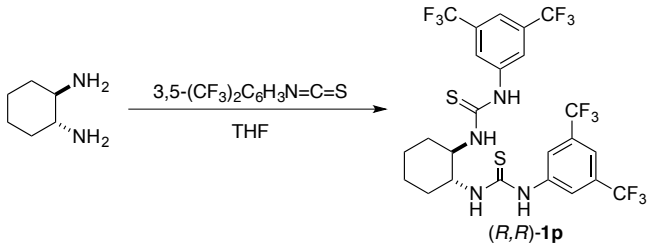

(*R*,*R*)-**1p**

A solution of (*R*,*R*)-(−)-cyclohexane-1,2-diamine (31 µL, 400 µmol) in dry THF (1 mL), was treated with 3,5-bis(trifluoromethyl)phenylisothiocyanate (150 µL, 2.05 equiv) analogously to the compound **1a**.

Physical state: white powder.
Isolated yield: 200 mg (76%).

mp 101–102 °C, lit.[26b] 132–134 °C.
$[\alpha]^{25}_{D}$ +40 (*c* 1.0, $CHCl_3$).
^{1}H NMR (400 MHz, DMSO-d_6) δ/ppm: 10.14 (s, 2H), 8.17 (s, 6H), 7.69 (s, 2H), 4.34 (br s, 2H), 2.19 (br s, 2H), 1.72 (br s, 2H), 1.30 (br s, 4H) [**Fig. S193**].
^{13}C NMR (100 MHz, DMSO-d_6) δ/ppm: 180.1, 141.6, 130.2 (q, $^2J_{CF}$ = 33.1 Hz), 123.2 (q, $^1J_{CF}$ = 272.6 Hz), 122.0, 116.2, 56.8, 31.2, 24.2 [**Fig. S194**].
^{19}F NMR (376 MHz, DMSO-d_6) δ/ppm: −61.69 (s) [**Fig. S195**].
IR (neat) $\tilde{\nu}$/cm^{-1}: 3198*w*, 1530*m*, 1472*m*, 1383*m*, 1276*s*, 1172*m*, 1128*s*, 1048*w*, 977*w*, 957*w*, 885*m*, 848*w*, 720*w*, 700*w*, 681*m*.
HRMS (ESI-Orbitrap) calcd for $C_{24}H_{21}F_{12}N_4S_2$ $[M+H]^+$ 657.1011 *m*/*z*, found 657.0999 *m*/*z* [**Fig. S78**].

Stereochemical assignment: The absolute configuration of **1p** was established by chemical correlation with (*R*,*R*)-(−)-cyclohexane-1,2-diamine and by comparison of the sign of specific rotation with the literature value.[26]

2.15 Synthesis of 1q

2.15.1 1-(3,5-Bis(trifluoromethyl)phenyl)-3-((3*R*)-quinuclidin-3-yl)thiourea (**1q**)[27]

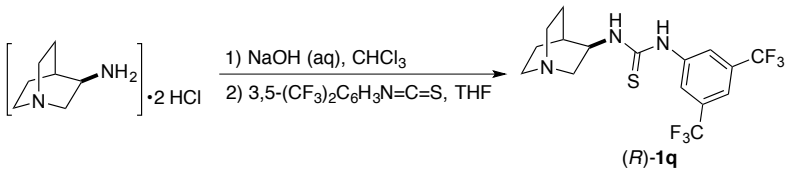

(*R*)-**1q**

Step 1: A suspension of (3*R*)-quinuclidin-3-amine dihydrochloride (100 mg, 0.5 mmol) in $CHCl_3$ (10 mL) was treated with 2M aqueous solution of NaOH (0.51 mL, 2.05 equiv). The resulting mixture was stirred well for 30 min and then anhydrous Na_2SO_4 was added, stirred for 30 min, filtered, and the filtrate was evaporated in vacuo to provide (3*R*)-quinuclidin-3-amine, which was used directly in the following step.

Step 2: A solution of (3*R*)-quinuclidin-3-amine (50 mg, 400 μmol) in dry THF (0.5 mL), was treated with 3,5-bis(trifluoromethyl)phenylisothiocyanate (76 μL, 1.05 equiv) analogously to the compound **1a**. The crude product was triturated with *n*-hexane and sonicated. The precipitated product was filtered off, washed with *n*-hexane, and used without further chromatographic purification.

Physical state: white hygroscopic powder.
Isolated yield: 108 mg (68%).

mp 109–111 °C.
$[\alpha]^{25}_D$ +40 (*c* 0.5, $CHCl_3$).
^{1}H NMR (400 MHz, DMSO-d_6) δ/ppm: 10.55 (br s, 1H), 8.82 (br s, 1H), 8.32 (s, 2H), 7.71 (s, 1H), 4.36–4.29 (m, 1H), 3.40–3.33 (m, 1H), 2.96–2.82 (m, 4H), 2.72–2.69 (m, 1H), 2.09–2.04 (m, 1H), 1.89–1.82 (m, 1H), 1.68–1.66 (m, 2H), 1.55–1.48 (m, 1H) [**Fig. S196**].
^{13}C NMR (100 MHz, DMSO-d_6) δ/ppm: 180.9, 142.5, 130.7 (q, $^2J_{CF}$ = 32.8 Hz), 123.8 (q, $^1J_{CF}$ = 272.6 Hz), 121.8, 116.4, 54.7, 50.5, 46.9, 46.3, 25.3, 24.8, 19.7 [**Fig. S197**].
^{19}F NMR (376 MHz, DMSO-d_6) δ/ppm: −61.56 (s) [**Fig. S198**].
IR (neat) $\tilde{\nu}$/cm^{-1}: 1539*w*, 1472*w*, 1383*m*, 1274*s*, 1169*m*, 1123*s*, 960*w*, 884*w*, 701*w*, 680*m*.
HRMS (ESI-Orbitrap) calcd for $C_{16}H_{18}F_6N_3S$ $[M+H]^+$ 398.1120 *m*/*z*, found 398.1122 *m*/*z* [**Fig. S79**].

Stereochemical assignment: The absolute configuration of **1q** was established by chemical correlation with (3*R*)-quinuclidin-3-amine dihydrochloride and by comparison of the sign of specific rotation with the literature value.[27]

2.16 Synthesis of 1r

2.16.1 1,1'-((1*R*,2*R*)-2,3-Dihydro-1*H*-indene-1,2-diyl)bis(3-(3,5-bis(trifluoromethyl)phenyl)thiourea) (**1r**)

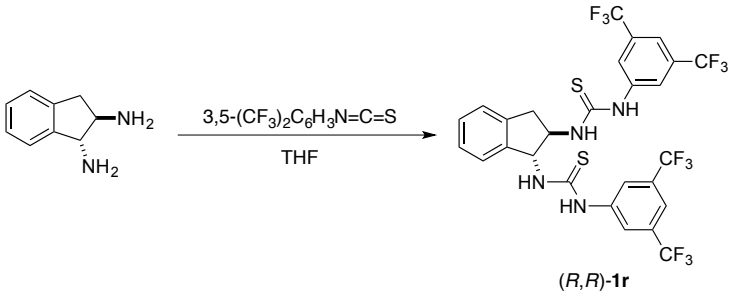

(*R*,*R*)-**1r**

A solution of (1*R*,2*R*)-2,3-dihydro-1*H*-indene-1,2-diamine (20 mg, 140 μmol) in dry THF (0.25 mL), was treated with 3,5-bis(trifluoromethyl)phenylisothiocyanate (51 μL, 2.05 equiv) analogously to the compound **1a**.

Physical state: white powder.
Isolated yield: 83 mg (89%).

mp 110–113 °C.
$[\alpha]^{25}_{D}$ +12 (*c* 1.0, $CHCl_3$).
^{1}H NMR (400 MHz, $CDCl_3$) δ/ppm: 10.62 (br s, 1H), 8.45 (br s, 1H), 8.21–7.69 (m, 8H), 7.26–7.06 (m, 2H), 6.43 (br s, 1H), 6.03 (br s, 1H), 4.74 (br s, 1H), 3.59 (br s, 1H), 2.76 (d, J = 12.6 Hz, 1H), 1.86 (br s, 1H). [**Fig. S199**].
^{13}C NMR (100 MHz, $CDCl_3$) δ/ppm: 180.9, 138.3, 137.9, 132.8 (q, $^2J_{CF}$ = 37.6 Hz), 127.8, 126.8, 125.7, 125.1, 124.3, 122.7 (q, $^1J_{CF}$ = 273.6 Hz), 120.0, 65.0, 63.8, 36.5 [**Fig. S200**].
^{19}F NMR (376 MHz, $CDCl_3$) δ/ppm: –62.95 (s), –63.01 (s) [**Fig. S201**].
IR (neat) ṽ/cm^{-1}: 1526*w*, 1472*w*, 1379*m*, 1275*s*, 1172*m*, 1128*s*, 959*w*, 887*w*, 701*m*, 681*m*.
HRMS (ESI-Orbitrap) calcd for $C_{27}H_{19}F_{12}N_4S_2$ $[M+H]^+$ 691.0854 *m*/*z*, found 691.0846 *m*/*z* [**Fig. S80**].

Stereochemical assignment: The absolute configuration of **1r** was established by chemical correlation with (1*R*,2*R*)-2,3-dihydro-1*H*-indene-1,2-diamine.

2.17 Synthesis of 1s

2.17.1 1,1'-((11*R*,12*R*)-9,10-Dihydro-9,10-ethanoanthracene-11,12-diyl)bis(3-(3,5-bis(trifluoromethyl)phenyl)thiourea) (**1s**)

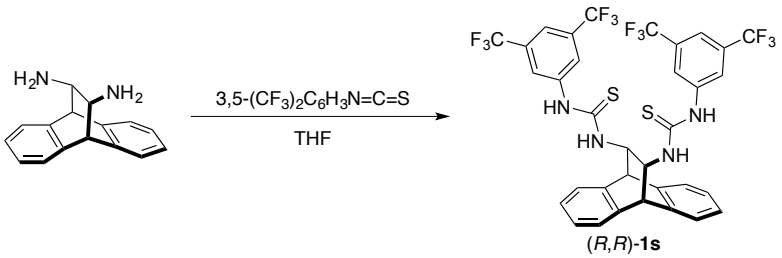

(*R*,*R*)-**1s**

A solution of (11*R*,12*R*)-9,10-dihydro-9,10-ethanoanthracene-11,12-diamine (50 mg, 210 μmol) in dry THF (0.5 mL), was treated with 3,5-bis(trifluoromethyl)phenylisothiocyanate (81 μL, 2.05 equiv) analogously to the compound **1a**.

Physical state: white powder.
Isolated yield: 142 mg (87%).

mp 130–133 °C.
$[\alpha]^{25}_{D}$ +118 (*c* 0.5, $CHCl_3$).
^{1}H NMR (400 MHz, DMSO-d_6) δ/ppm: 9.87 (br s, 2H), 8.29 (s, 4H), 8.16 (d, J = 6.5 Hz, 2H), 7.74 (s, 2H), 7.46–7.41 (m, 4H), 7.26–7.19 (m, 4H), 4.69 (br s, 2H), 4.54 (d, J = 7.0 Hz, 2H) [**Fig. S202**].
^{13}C NMR (100 MHz, DMSO-d_6) δ/ppm: 180.4, 141.8, 141.6, 139.0, 130.1 (q, $^{2}J_{CF}$ = 32.8 Hz), 126.6, 126.5, 126.2, 124.1, 123.2 (q, $^{1}J_{CF}$ = 272.9 Hz), 122.0, 116.5, 60.1, 48.2 [**Fig. S203**].
^{19}F NMR (376 MHz, DMSO-d_6) δ/ppm: −61.47 (s) [**Fig. S204**].
IR (neat) $\tilde{\nu}$/cm^{-1}: 1517*m*, 1496*w*, 1379*m*, 1275*s*, 1173*s*, 1128*s*, 957*w*, 886*m*, 763*w*, 702*m*, 681*m*.
HRMS (ESI-Orbitrap) calcd for $C_{34}H_{23}F_{12}N_4S_2$ $[M+H]^+$ 779.1167 *m*/*z*, found 779.1160 *m*/*z* [**Fig. S81**].

Stereochemical assignment: The absolute configuration of **1s** was established by chemical correlation with (11*R*,12*R*)-9,10-dihydro-9,10-ethanoanthracene-11,12-diamine.

2.18 Synthesis of 1v

2.18.1 1,1'-((1*R*,2*R*)-1,2-Diphenylethane-1,2-diyl)bis(3-(3,5-bis(trifluoromethyl)phenyl)thiourea) (**1v**)[28]

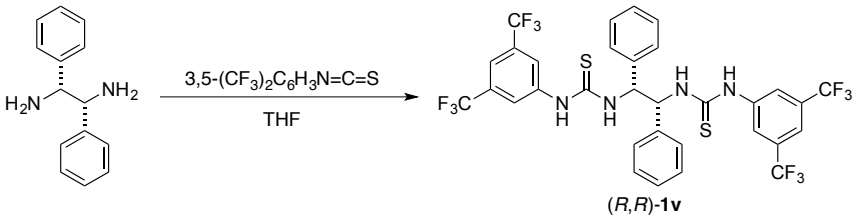

A solution of (*R*,*R*)-(+)-1,2-diphenylethane-1,2-diamine (50 mg, 240 µmol) in dry THF (0.5 mL), was treated with 3,5-bis(trifluoromethyl)phenylisothiocyanate (90 µL, 2.05 equiv) analogously to the compound **1a**.

Physical state: white powder.
Isolated yield: 110 mg (61%).

mp 174–175 °C, lit.[26b] 192–194 °C.
$[\alpha]^{25}_{D}$ −28 (*c* 0.4, $CHCl_3$).
^{1}H NMR (400 MHz, DMSO-d_6) δ/ppm: 10.35 (s, 2H), 8.72 (br s, 2H), 8.16 (s, 4H), 7.69 (s, 2H), 7.28–7.19 (m, 10H), 5.97 (br s, 2H) [**Fig. S205**].
^{13}C NMR (100 MHz, DMSO-d_6) δ/ppm: 180.4, 141.5, 138.5, 130.2 (q, $^{2}J_{CF}$ = 33.1 Hz), 128.3, 128.0, 127.6, 123.1 (q, $^{1}J_{CF}$ = 272.9 Hz), 121.9, 116.4, 62.6 [**Fig. S206**].
^{19}F NMR (376 MHz, DMSO-d_6) δ/ppm: −61.74 (s) [**Fig. S207**].
IR (neat) $\tilde{\nu}$/cm^{-1}: 3276*w*, 1541*m*, 1472*w*, 1374*m*, 1275*s*, 1174*m*, 1125*s*, 956*w*, 884*w*, 850*w*, 750*w*, 698*m*, 681*w*.
HRMS (ESI-Orbitrap) calcd for $C_{32}H_{23}F_{12}N_4S_2$ $[M+H]^+$ 755.1167 *m*/*z*, found 755.1157 *m*/*z* [**Fig. S82**].

Stereochemical assignment: The absolute configuration of **1v** was established by chemical correlation with (*R*,*R*)-(+)-1,2-diphenylethane-1,2-diamine and by comparison of the sign of specific rotation with the literature value.[28]

2.19 Synthesis of 1w

2.19.1 (*S*)-1-(3,5-Bis(trifluoromethyl)phenyl)-3-(1-phenylethyl)thiourea (**1w**)[29]

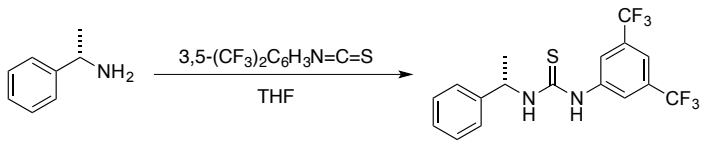

(*S*)-**1w**

A solution of (*S*)-(–)-phenylethylamine (200 µL, 1.6 mmol) in dry THF (4 mL), was treated with 3,5-bis(trifluoromethyl)phenylisothiocyanate (311 µL, 1.05 equiv) analogously to the compound **1a**.

Physical state: white powder.
Isolated yield: 580 mg (93%).

mp 141–143 °C, lit.[29b] 137–140 °C.
$[\alpha]^{29}_{D}$ +46 (*c* 0.7, $CHCl_3$).
^{1}H NMR (400 MHz, $CDCl_3$) δ/ppm: 7.67 (s, 3H), 7.42–7.32 (m, 5H), 6.63 (br s, 1H), 5.41 (br s, 1H), 1.60 (d, J = 6.8 Hz, 3H) [**Fig. S208**].
^{13}C NMR (100 MHz, $CDCl_3$) δ/ppm: 179.8, 141.2, 139.0, 132.7 (q, $^2J_{CF}$ = 34.0 Hz), 129.3, 128.3, 126.0, 123.9, 122.7 (q, $^1J_{CF}$ = 273.1 Hz), 119.3 (q, $^3J_{CF}$ = 3.4 Hz), 54.7, 22.0 [**Fig. S209**].
^{19}F NMR (376 MHz, $CDCl_3$) δ/ppm: −63.02 (s) [**Fig. S210**].
IR (neat) $\tilde{\nu}$/cm^{-1}: 3226*w*, 1542*m*, 1469*w*, 1382*m*, 1340*w*, 1278*s*, 1173*m*, 1132*s*, 1023*w*, 976*w*, 892*w*, 848*w*, 699*m*, 681*m*.
HRMS (ESI-Orbitrap) calcd for $C_{17}H_{15}F_6N_2S$ $[M+H]^+$ 393.0855 *m*/*z*, found 393.0848 *m*/*z* [**Fig. S83**].

Stereochemical assignment: The absolute configuration of **1w** was established by chemical correlation with (*S*)-(–)-phenylethylamine and by comparison of the sign of specific rotation with the literature value.[29]

2.20 Synthesis of 1x

2.20.1 (*S*)-1-(3,5-Bis(trifluoromethyl)phenyl)-3-(1-(6-methoxynaphthalen-2-yl)ethyl)thiourea (**1x**)

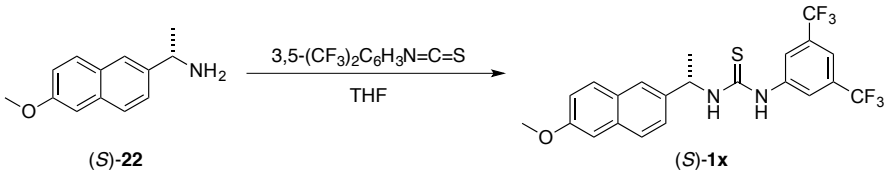

(*S*)-**22** (*S*)-**1x**

A solution of (*S*)-**22** (50 mg, 250 μmol) in dry THF (0.5 mL), was treated with 3,5-bis(trifluoromethyl)-phenylisothiocyanate (48 μL, 1.05 equiv) analogously to the compound **1a**.

Physical state: white powder.
Isolated yield: 103 mg (87%).

mp 136–138 °C.
$[\alpha]^{29}_{D}$ −74 (*c* 1.0, $CHCl_3$).
^{1}H NMR (400 MHz, $CDCl_3$) δ/ppm: 7.76–7.63 (m, 6H), 7.41 (d, *J* = 7.8 Hz, 1H), 7.18–7.12 (m, 2H), 6.73 (br s, 1H), 5.55 (br s, 1H), 3.92 (s, 3H), 1.66 (d, *J* = 6.8 Hz, 3H) [**Fig. S211**].
^{13}C NMR (100 MHz, $CDCl_3$) δ/ppm: 179.9, 158.1, 139.0, 136.2, 134.3, 132.6 (q, $^2J_{CF}$ = 35.3 Hz), 129.3, 128.7, 128.1, 124.7, 124.5, 123.9, 122.7 (q, $^1J_{CF}$ = 272.9 Hz), 119.6, 119.2, 105.7, 55.3, 54.7, 21.9 [**Fig. S212**].
^{19}F NMR (376 MHz, $CDCl_3$) δ/ppm: −62.98 (s) [**Fig. S213**].
IR (neat) $\tilde{\nu}$/cm^{-1}: 1607*w*, 1541*m*, 1382*m*, 1273*s*, 1174*m*, 1131*s*, 1030*m*, 978*w*, 889*m*, 849*w*, 710*w*, 681*m*.
HRMS (ESI-Orbitrap) calcd for $C_{22}H_{19}F_6N_2OS$ $[M+H]^+$ 473.1117 *m*/*z*, found 473.1112 *m*/*z* [**Fig. S84**].

Stereochemical assignment: The absolute configuration of **1x** was established by chemical correlation with (*S*)-(+)-naproxen.

2.21 Synthesis of 2a

2.21.1 (S_a)-1,1'-([1,1'-Binaphthalene]-2,2'-diyl)bis(3-(3,5-bis(trifluoromethyl)phenyl)urea) (**2a**)[30]

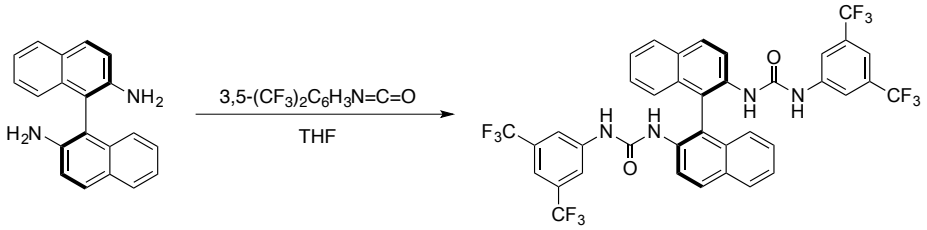

(S_a)-**2a**

A solution of (*S*)-[1,1'-binaphthy]-2,2'-diamine (50 mg, 176 μmol) in dry THF (1 mL), was treated with 3,5-bis(trifluoromethyl)phenylisocyanate (64 μL, 2.05 equiv) analogously to the compound **1a**.

Physical state: white powder.
Isolated yield: 120 mg (86%).

mp 150–152 °C, lit.[30a] 128–130 °C (for the opposite enantiomer).
$[\alpha]^{25}_{D}$ −110 (*c* 0.5, $CHCl_3$).
^{1}H NMR (400 MHz, $CDCl_3$) δ/ppm: 8.05 (d, *J* = 8.9 Hz, 2H), 7.96 (d, *J* = 8.9 Hz, 2H), 7.86 (d, *J* = 8.2 Hz, 2H), 7.50 (s, 4H), 7.43–7.39 (m, 4H), 7.34 (s, 2H), 7.23–7.19 (m, 2H), 6.98 (d, *J* = 8.5 Hz, 2H), 6.87 (s, 2H) [**Fig. S214**].
^{13}C NMR (100 MHz, $CDCl_3$) δ/ppm: 153.3, 139.3, 134.3, 132.8, 132.1 (q, $^2J_{CF}$ = 33.4 Hz), 131.3, 129.9, 128.3, 127.4, 125.8, 125.3, 122.83 (q, $^1J_{CF}$ = 272.9 Hz), 122.80, 122.7, 118.6, 116.5 [**Fig. S215**].
^{19}F NMR (376 MHz, $CDCl_3$) δ/ppm: −63.20 (s) [**Fig. S216**].
IR (neat) ṽ/cm^{-1}: 1668*w*, 1504*m*, 1473*m*, 1384*m*, 1275*s*, 1175*m*, 1127*s*, 883*w*, 701*m*, 682*m*.
HRMS (ESI-Orbitrap) calcd for $C_{38}H_{21}N_4F_{12}O_2$ $[M-H]^-$ 793.1478 *m*/*z*, found 793.1491 *m*/*z* [**Fig. S85**].

Stereochemical assignment: The absolute configuration of **2a** was established by chemical correlation with (S_a)-BINAM and by comparison of the sign of specific rotation with the literature value.[30b]

2.22 Synthesis of 2b

2.22.1 (R_a)-1,1'-([1,1'-Bianthracene]-2,2'-diyl)bis(3-(3,5-bis(trifluoromethyl)phenyl)urea) (**2b**)

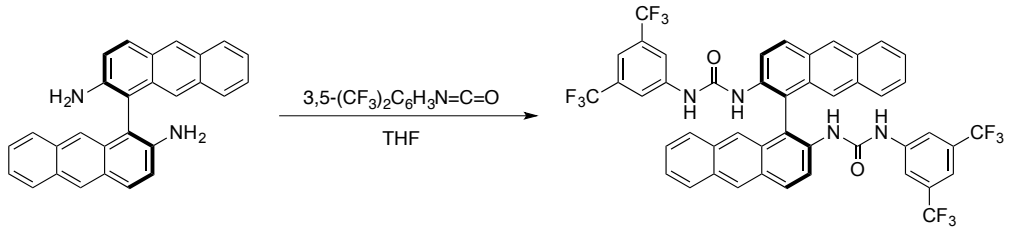

(R_a)-**12** (R_a)-**2b**

A solution of (R_a)-(–)-**12** (25 mg, 65 µmol) in dry THF (0.5 mL), was treated with 3,5-bis(trifluoromethyl)-phenylisocyanate (23 µL, 2.05 equiv) analogously to the compound **1a**. The crude product was purified by preparative TLC (SiO_2) EtOAc–*n*-hexane (1:2).

Physical state: yellow solid.
Isolated yield: 26 mg (45%).

mp 156–159 °C.
$[\alpha]^{25}_D$ +72 (*c* 0.5, $CHCl_3$).
^{1}H NMR (400 MHz, $CDCl_3$) δ/ppm: 8.50 (s, 2H), 8.20–8.14 (m, 4H), 7.95 (d. *J* = 8.7 Hz, 2H), 7.62 (s, 2H), 7.57 (s, 4H), 7.52 (d, *J* = 8.6 Hz, 2H), 7.43–7.39 (m, 4H), 7.32–7.29 (m, 2H), 7.14 (br s, 2H), 6.82 (br s, 2H) [**Fig. S217**].
^{13}C NMR (100 MHz, $CDCl_3$) δ/ppm: 153.0, 139.4, 134.3, 132.3, 132.1 (q, $^2J_{CF}$ = 33.4 Hz), 131.4, 130.7, 130.4, 129.6, 128.2, 127.9, 127.2, 126.1, 125.9, 123.9, 122.9 (q, $^1J_{CF}$ = 272.9 Hz), 122.5, 120.9, 118.5, 116.4 [**Fig. S218**].
^{19}F NMR (376 MHz, $CDCl_3$) δ/ppm: −63.15 (s) [**Fig. S219**].
IR (neat) $\tilde{\nu}$/cm^{-1}: 3349*w*, 1690*w*, 1568*m*, 1471*m*, 1379*m*, 1273*s*, 1171*m*, 1123*s*, 880*m*, 741*w*, 701*w*, 681*w*.
HRMS (ESI-Orbitrap) calcd for $C_{46}H_{27}F_{12}N_4O_2$ $[M+H]^+$ 895.1942 *m*/*z*, found 895.1927 *m*/*z* [**Fig. S86**].

Stereochemical assignment: The absolute configuration of **2b** was established by chemical correlation with (R_a)-(–)-BIANAM.

2.23 Synthesis of 2c

2.23.1 (S_a)-1,1'-(2',2"-Dimethyl-3,3'",5,5'"-tetrakis(trifluoromethyl)-[1,1':3',1":3",1'"-quaterphenyl]-4',6"-diyl)bis(3-(3,5-bis(trifluoromethyl)phenyl)urea) (**2c**)

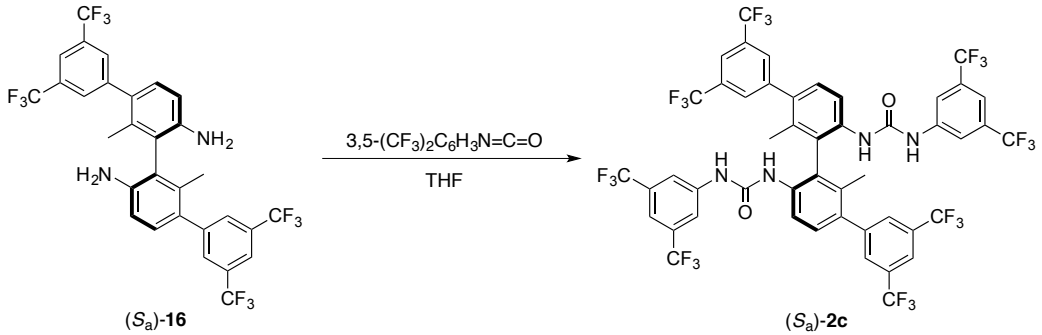

(S_a)-**16** (S_a)-**2c**

A solution of (S_a)-**16** (30 mg, 47 μmol) in dry THF (0.5 mL), was treated with 3,5-bis(trifluoromethyl)-phenylisocyanate (17 μL, 2.05 equiv) analogously to the compound **1a**.

Physical state: white solid.
Isolated yield: 40 mg (75%).

mp 126–129 °C.
$[\alpha]^{25}_{D}$ –54 (*c* 0.5, $CHCl_3$).
^{1}H NMR (400 MHz, acetone-d_6) δ/ppm: 9.30 (br s, 2H), 8.28–8.25 (m, 2H), 8.07–8.02 (m, 10H), 7.55–7.52 (m, 4H), 7.46 (br s, 2H), 2.00 (s, 6H) [**Fig. S220**].
^{13}C NMR (100 MHz, acetone-d_6) δ/ppm: 153.7, 145.3, 142.6, 138.4, 136.3, 136.1, 132.5 (q, $^2J_{CF}$ = 32.8 Hz), 132.1 (q, $^2J_{CF}$ = 33.1 Hz), 131.6, 131.0, 124.6 (q, $^1J_{CF}$ = 272.3 Hz), 124.4 (q, $^1J_{CF}$ = 272.0 Hz), 121.6, 121.0, 118.9, 115.8, 18.1 [**Fig. S221**].
^{19}F NMR (376 MHz, acetone-d_6) δ/ppm: −61.10 (s, 12F), −63.63 (s, 12F) [**Fig. S222**].
IR (neat) $\tilde{\nu}$/cm^{-1}: 2970*w*, 1678*w*, 1574*w*, 1474*w*, 1377*m*, 1275*s*, 1172*m*, 1125*s*, 900*w*, 683*m*.
HRMS (ESI-Q-TOF) calcd for $C_{48}H_{25}F_{24}N_4O_2$ $[M–H]^-$ 1145.1589 *m*/*z*, found 1145.1548 *m*/*z* [**Fig. S87**].

Stereochemical assignment: The absolute configuration of **2c** was established by chemical correlation with (S_a)-BIPHAM.

2.24 Synthesis of 3a

2.24.1 4,4'-((1*R*,2*R*)-Cyclohexane-1,2-diylbis(azanediyl))bis(3-((3,5-bis(trifluoromethyl)benzyl)amino)-cyclobut-3-ene-1,2-dione) (**3a**)

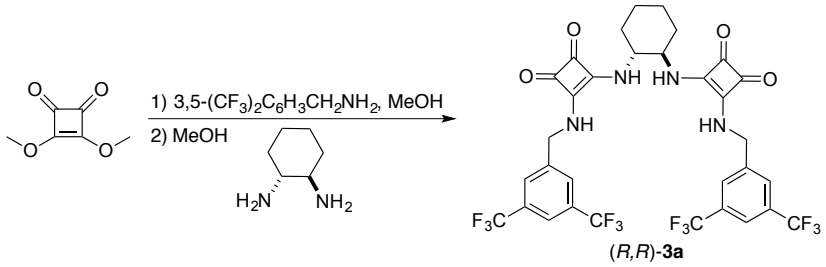

(*R,R*)-**3a**

3,4-Dimethoxycyclobut-3-ene-1,2-dione (50 mg, 0.35 mmol) and 3,5-bis(trifluoromethyl)benzylamine (90 mg, 0.35 mmol) were dissolved in anhydrous MeOH (1 mL) and left to stir at room temperature for 4 days. Then a solution of (1*R*,2*R*)-(−)-1,2-diaminocyclohexane (20 mg, 0.18 mmol) in dry MeOH (2 mL) was added. The mixture was stirred at room temperature for 18 hours. The resulting precipitate was filtered off, washed with MeOH and dried.

Physical state: white powder.
Isolated yield: 60 mg (46 %).

mp >300 °C.
$[\alpha]^{25}_{D}$ +34 (*c* 0.5, DMSO).
^{1}H NMR (400 MHz, DMSO-d_6) δ/ppm: 8.04 (s, 4H), 7.99 (s, 2H), 7.77 (br s, 2H), 7.41 (br s, 2H), 4.84 (d, J = 6.0 Hz, 4H), 3.80 (br s, 2H), 2.00 (d, J = 10.6 Hz, 2H), 1.72 (d, J = 6.4 Hz, 2H), 1.42–1.28 (m, 4H) [**Fig. S223**].
^{13}C NMR (100 MHz, DMSO-d_6) δ/ppm 182.5, 182.2, 167.7, 167.2, 142.2, 130.4 (q, $^{2}J_{CF}$ = 32.8 Hz), 128.4, 123.1 (q, $^{1}J_{CF}$ = 272.6 Hz), 121.0, 57.2, 45.7, 32.8, 23.9 [**Fig. S224**].
^{19}F NMR (376 MHz, DMSO-d_6) δ/ppm: −61.33 (s) [**Fig. S225**].
IR (neat) ṽ/cm^{-1}: 2938*w*, 1795*w*, 1671*w*, 1556*s*, 1445*s*, 1375*s*, 1276*s*, 1180*m*, 1127*s*, 940*w*, 884*w*, 684*m*.
HRMS (ESI-Q-TOF) calcd for $C_{32}H_{23}F_{12}N_4O_4$ $[M–H]^-$ 755.1522 *m*/*z*, found 755.1490 *m*/*z* [**Fig. S88**–**89**].

Stereochemical assignment: The absolute configuration of **3a** was established by chemical correlation with (1*R*,2*R*)-(−)-1,2-diaminocyclohexane.

2.25 Synthesis of 3b

2.25.1 4,4'-((((11*R*,12*R*)-9,10-Dihydro-9,10-ethanoanthracene-11,12-diyl)bis(methylene))bis(azanediyl))-bis(3-((3,5-bis(trifluoromethyl)phenyl)amino)cyclobut-3-ene-1,2-dione) (**3b**)

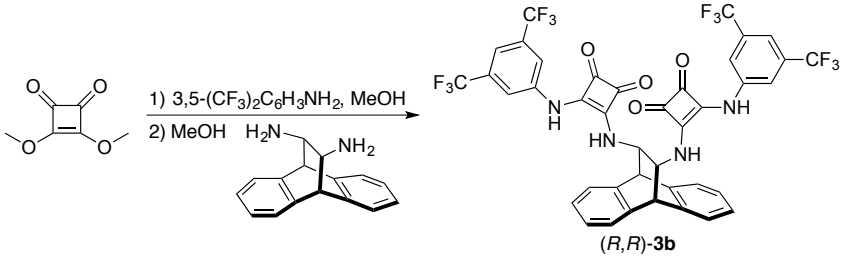

3,4-Dimethoxycyclobut-3-ene-1,2-dione (50 mg, 0.35 mmol) and 3,5-bis(trifluoromethyl)aniline (55 μL, 0.35 mmol) were were dissolved in anhydrous MeOH (1 mL) and left to stir at room temperature for 4 days. Then a solution of (11*R*,12*R*)-9,10-dihydro-9,10-ethanoanthracene-11,12-diamine (42 mg, 0.18 mmol) in dry MeOH (2 mL) was added. The mixture was stirred at room temperature for 18 hours. The resulting precipitate was filtered off, washed with MeOH and dried.

Physical state: white powder.
Isolated yield: 50 mg (32%).

mp 263–265 °C.
$[\alpha]^{25}_{D}$ +174 (*c* 0.5, acetone).
^{1}H NMR (400 MHz, DMSO-d_6) δ/ppm: 10.09 (br s, 2H), 8.01 (s, 4H), 7.75 (d, J = 6.7 Hz, 4H), 7.65 (s, 4H), 7.54–7.49 (m, 4H), 7.33–7.27 (m, 4H), 4.62 (s, 2H), 4.34 (d, J = 5.8 Hz, 2H) [**Fig. S226**].
^{13}C NMR (100 MHz, DMSO-d_6) δ/ppm: 184.4, 180.6, 166.7, 163.1, 141.3, 140.7, 137.6, 131.3 (q, $^{2}J_{CF}$ = 32.8 Hz), 127.0, 126.6, 124.3, 123.1 (q, $^{1}J_{CF}$ = 272.9 Hz), 118.1, 115.0, 61.2, 50.2, 48.6 [**Fig. S227**].
^{19}F NMR (376 MHz, DMSO-d_6) δ/ppm: −61.69 (s) [**Fig. S228**].
IR (neat) $\tilde{\nu}$/cm^{-1}: 3265*w*, 1769*w*, 1674*w*, 1597*m*, 1556*m*, 1432*m*, 1374*s*, 1276*s*, 1172*m*, 1126*s*, 1024*w*, 936*w*, 884*w*, 766*w*, 700*w*.
HRMS (ESI-Q-TOF) calcd for $C_{40}H_{21}F_{12}N_4O_4$ $[M–H]^-$ 849.1366 *m*/*z*, found 849.1352 *m*/*z* [**Fig. S90**].

Stereochemical assignment: The absolute configuration of **3b** was established by chemical correlation with (11*R*,12*R*)-9,10-dihydro-9,10-ethanoanthracene-11,12-diamine**.**

2.26 Synthesis of 3c

2.26.1 (*S*)-3-((3,5-Bis(trifluoromethyl)benzyl)amino)-4-((1-phenylethyl)amino)cyclobut-3-ene-1,2-dione (**3c**)[31]

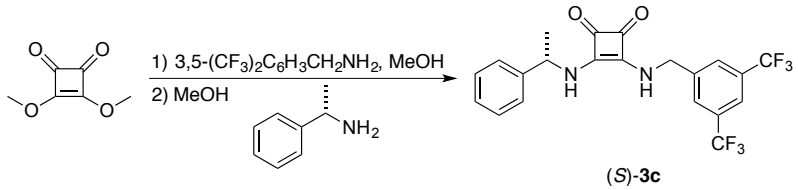

(*S*)-**3c**

3,4-Dimethoxycyclobut-3-ene-1,2-dione (50 mg, 0.35 mmol) and 3,5-bis(trifluoromethyl)benzylamine (90 mg, 0.35 mmol) were were dissolved in anhydrous MeOH (1 mL) and left to stir at room temperature for 4 days. Then a solution of (*S*)-1-phenylethanamine (45 µL, 0.35 mmol) in dry MeOH (2 mL) was added. The mixture was stirred at room temperature for 18 hours. The resulting precipitate was filtered off, washed with MeOH and dried.

Physical state: white powder.
Isolated yield: 95 mg (61%).

mp 231–233 °C, lit.[31] 244–247 °C.
$[\alpha]^{25}_{D}$ –60 (*c* 0.25, acetone).
^{1}H NMR (400 MHz, DMSO-d_6) δ/ppm: 8.04–8.02 (m, 3H), 7.84 (br s, 1H), 7.36–7.25 (m, 5H), 5.21 (br s, 1H), 4.95–4.84 (m, 2H), 1.53 (d, J = 6.9 Hz, 3H) [**Fig. S229**].
^{13}C NMR (100 MHz, DMSO-d_6) δ/ppm: 182.6, 167.3, 143.6, 124.6, 130.5 (q, $^{2}J_{CF}$ = 32.8 Hz), 128.6, 127.3, 125.9, 123.3 (q, $^{1}J_{CF}$ = 272.6 Hz), 121.2, 52.8, 45.8, 22.9 [**Fig. S230**].
^{19}F NMR (376 MHz, DMSO-d_6) δ/ppm: −61.24 (s) [**Fig. S231**].
IR (neat) $\tilde{\nu}$/cm^{-1}: 3161*w*, 1650*m*, 1562*s*, 1380*w*, 1346*m*, 1278*s*, 1173*s*, 1117*s*, 906*w*, 876*m*, 750*w*, 695*m*, 682*m*.
HRMS (ESI-Q-TOF) calcd for $C_{21}H_{15}F_6N_2O_2$ $[M–H]^-$ 441.1032 *m*/*z*, found 441.1033 *m*/*z* [**Fig. S91**].

Stereochemical assignment: The absolute configuration of **3c** was established by chemical correlation with (*S*)-(–)-phenylethylamine.

2.27 Synthesis of 3d

2.27.1 (*S*)-3-((3,5-Bis(trifluoromethyl)benzyl)amino)-4-((1-(6-methoxynaphthalen-2-yl)ethyl)amino)cyclobut-3-ene-1,2-dione (**3d**)

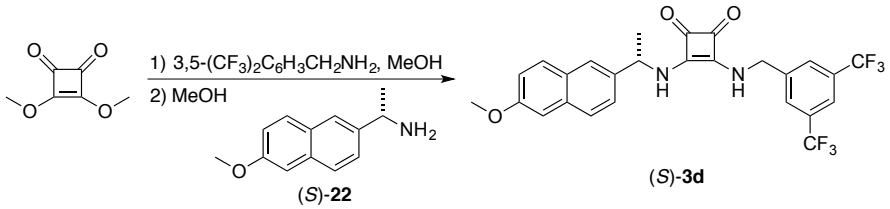

3,4-Dimethoxycyclobut-3-ene-1,2-dione (50 mg, 0.35 mmol) and 3,5-bis(trifluoromethyl)benzylamine (90 mg, 0.35 mmol) were dissolved in anhydrous MeOH (1 mL) and left to stir at room temperature for 4 days. Then a solution of (*S*)-**22** (71 mg, 0.35 mmol) in dry MeOH (2 mL) was added. The mixture was stirred at room temperature for 18 hours. The resulting precipitate was filtered off, washed with MeOH and dried.

Physical state: white powder.
Isolated yield: 72 mg (39%).

mp 255–257 °C.
$[\alpha]^{25}_{D}$ –40 (*c* 0.5, acetone).
^{1}H NMR (400 MHz, DMSO-d_6) δ/ppm: 8.06 (s, 2H), 8.04 (s, 1H), 7.82–7.77 (m, 3H), 7.47 (d, J = 7.7 Hz, 1H), 7.30 (s, 1H), 7.16 (dd, J = 8.8, 2.2 Hz, 1H), 5.36 (br s, 1H), 4.95–4.85 (m, 2H), 3.86 (s, 3H), 1.61 (d, J = 6.7 Hz, 3H) [**Fig. S232**].
^{13}C NMR (100 MHz, DMSO-d_6) δ/ppm: 182.7, 182.6, 167.3, 157.3, 142.5, 138.5, 133.6, 130.4 (q, $^{2}J_{CF}$ = 33.1 Hz), 129.3, 128.6, 128.2, 127.3, 127.2, 125.0, 124.1, 123.3 (q, $^{1}J_{CF}$ = 272.9 Hz), 121.2, 118.9, 105.8, 55.2, 52.8, 45.8, 22.8 [**Fig. S233**].
^{19}F NMR (376 MHz, DMSO-d_6) δ/ppm: −61.24 (s) [**Fig. S234**].
IR (neat) $\tilde{\nu}$/cm^{-1}: 3151*m*, 1798*w*, 1653*m*, 1570*s*, 1381*w*, 1347*m*, 1278*s*, 1173*s*, 1127*s*, 1031*w*, 851*w*, 682*w*, 669*w*.
HRMS (ESI-Q-TOF) calcd for $C_{26}H_{19}F_6N_2O_3$ $[M–H]^-$ 521.1294 *m*/*z*, found 521.1281 *m*/*z* [**Fig. S92**].

Stereochemical assignment: The absolute configuration of **3d** was established by chemical correlation with (*S*)-(+)-naproxen.

3. Optimization of Asymmetric Henry Reaction

3.1 Catalyst Screening Protocol

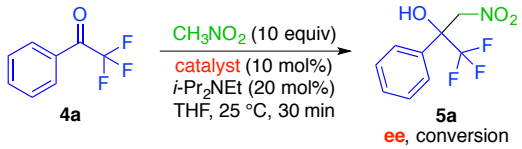

Experiments were performed with **4a** (14 μL, 0.1 mmol), nitromethane (53.5 μL, 1.0 mmol), a Hünig's base (3.4 μL, 20 μmol) and an appropriate catalyst (10.0 μmol) in anhydrous THF (100 μL) at ambient temperature under air (**Fig. S8**, **Tab. S1**). After 30 min, the reactions were quenched by a saturated aqueous solution of NH_4Cl and then repetitively extracted with Et_2O. Combined organic extracts were dried with anhydrous Na_2SO_4, filtered through a silica plug, and evaporated in vacuo (30 °C). The resulting samples were diluted with a mobile phase (1 mL) and directly subjected to an HPLC analysis:

Injection volume: 1 μL.
Precolumn: Thermo Hypersil Silica (3 μm, 100 × 4.6 mm).
Connection: standard blue PEEK capillary tubing (L 300 mm, ID 0.01", OD 1/16").
CSP column: Daicel Chiralpak IB (5 μm, 250 × 4.6 mm).
Mobile phase: *i*-PrOH–*n*-heptane, 20:80.
Flow rate: 0.5 mL/min.
Temperature: 25 °C.
Detection wavelength: 230 nm.

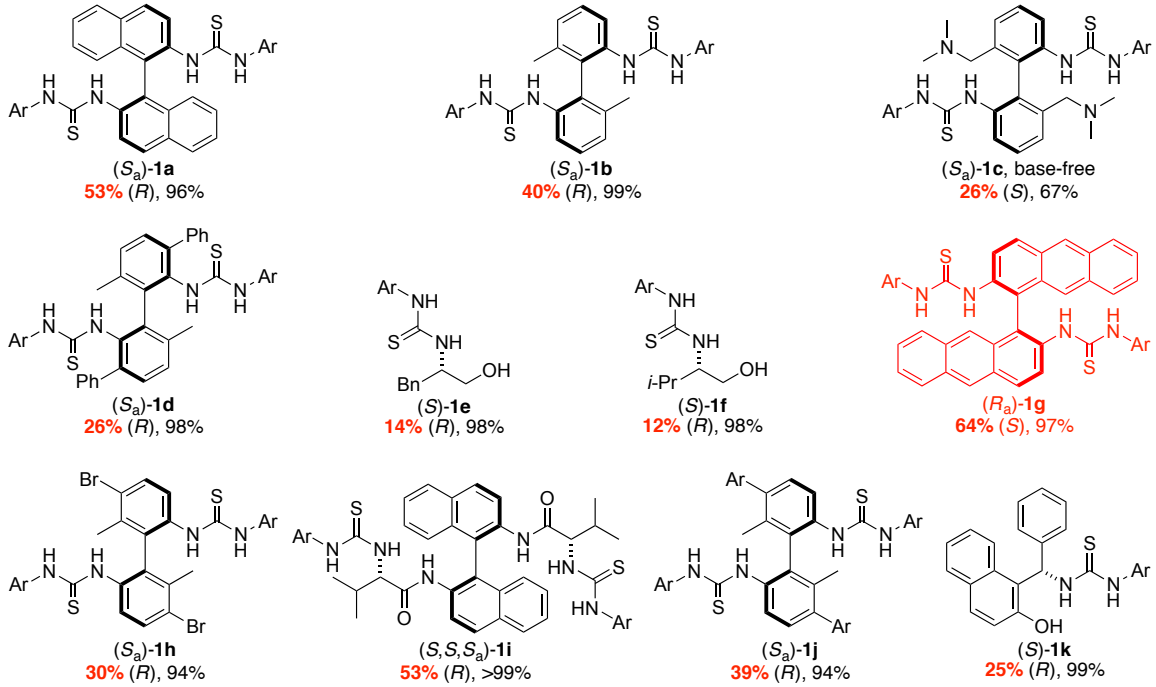

Figure S8. Catalyst Screening Protocol. Note: Ar = 3,5-$(CF_3)_2C_6H_3$.

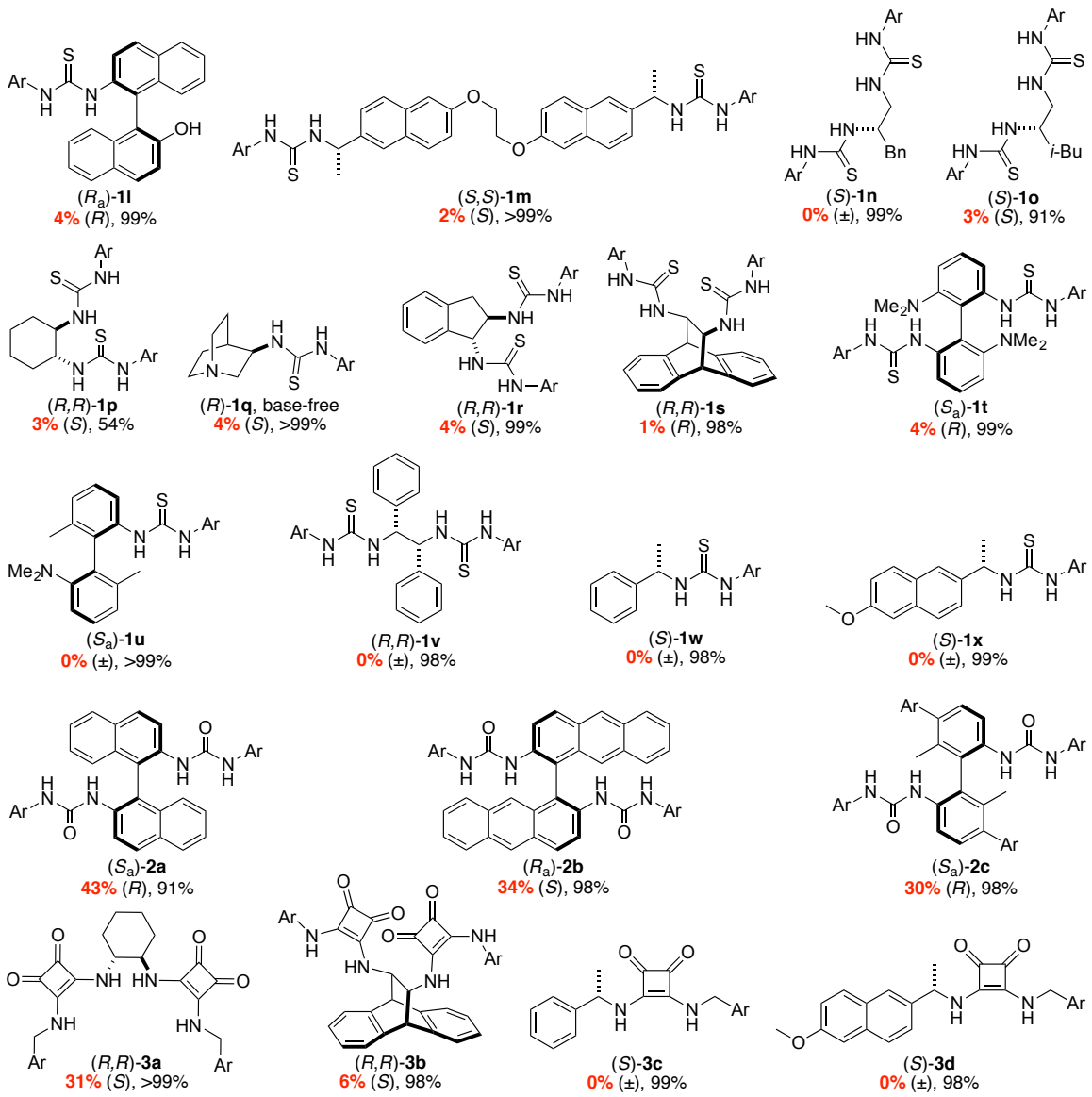

Figure S8. Cont'd.

Table S1. Catalyst Screening Steps.

entry	cat.	base	$MeNO_2$	solvent	t	time	conv. [1]	ee [2]	variable
1	**1a** [10 mol%]	*i*-Pr_2NEt [20 mol%]	10 equiv [54 µl]	THF [100 µL]	25 °C	0.5 h	96%	53% (*R*)	Catalyst Type
2	**1b** [10 mol%]	*i*-Pr_2NEt [20 mol%]	10 equiv [54 µl]	THF [100 µL]	25 °C	0.5 h	99%	40% (*R*)	
3	**1c** [10 mol%]	–	10 equiv [54 µl]	THF [100 µL]	25 °C	0.5 h	67%	26% (*S*)	
4	**1d** [10 mol%]	*i*-Pr_2NEt [20 mol%]	10 equiv [54 µl]	THF [100 µL]	25 °C	0.5 h	98%	26% (*R*)	
5	**1e** [10 mol%]	*i*-Pr_2NEt [20 mol%]	10 equiv [54 µl]	THF [100 µL]	25 °C	0.5 h	98%	14% (*R*)	
6	**1f** [10 mol%]	*i*-Pr_2NEt [20 mol%]	10 equiv [54 µl]	THF [100 µL]	25 °C	0.5 h	98%	12% (*R*)	
7	**1g** [10 mol%]	*i*-Pr_2NEt [20 mol%]	10 equiv [54 µL]	THF [100 µL]	25 °C	0.5 h	97%	64% (*S*)	
8	**1h** [10 mol%]	*i*-Pr_2NEt [20 mol%]	10 equiv [54 µl]	THF [100 µL]	25 °C	0.5 h	94%	30% (*R*)	
9	**1i** [10 mol%]	*i*-Pr_2NEt [20 mol%]	10 equiv [54 µl]	THF [100 µL]	25 °C	0.5 h	>99%	46% (*R*)	
10	**1j** [10 mol%]	*i*-Pr_2NEt [20 mol%]	10 equiv [54 µl]	THF [100 µL]	25 °C	0.5 h	94%	39% (*R*)	
11	**1k** [10 mol%]	*i*-Pr_2NEt [20 mol%]	10 equiv [54 µl]	THF [100 µL]	25 °C	0.5 h	99%	25% (*R*)	
12	**1l** [10 mol%]	*i*-Pr_2NEt [20 mol%]	10 equiv [54 µl]	THF [100 µL]	25 °C	0.5 h	99%	4% (*R*)	
13	**1m** [10 mol%]	*i*-Pr_2NEt [20 mol%]	10 equiv [54 µl]	THF [100 µL]	25 °C	0.5 h	>99%	2% (*R*)	
14	**1n** [10 mol%]	*i*-Pr_2NEt [20 mol%]	10 equiv [54 µl]	THF [100 µL]	25 °C	0.5 h	99%	0% (*rac*)	
15	**1o** [10 mol%]	*i*-Pr_2NEt [20 mol%]	10 equiv [54 µl]	THF [100 µL]	25 °C	0.5 h	91%	3% (*S*)	
16	**1p** [10 mol%]	*i*-Pr_2NEt [20 mol%]	10 equiv [54 µl]	THF [100 µL]	25 °C	0.5 h	54%	3% (*S*)	
17	**1q** [10 mol%]	–	10 equiv [54 µl]	THF [100 µL]	25 °C	0.5 h	>99%	4% (*S*)	
18	**1r** [10 mol%]	*i*-Pr_2NEt [20 mol%]	10 equiv [54 µl]	THF [100 µL]	25 °C	0.5 h	99%	4% (*S*)	
19	**1s** [10 mol%]	*i*-Pr_2NEt [20 mol%]	10 equiv [54 µl]	THF [100 µL]	25 °C	0.5 h	98%	1% (*R*)	
20	**1t** [10 mol%]	*i*-Pr_2NEt [20 mol%]	10 equiv [54 µl]	THF [100 µL]	25 °C	0.5 h	99%	4% (*R*)	
21	**1u** [10 mol%]	*i*-Pr_2NEt [20 mol%]	10 equiv [54 µl]	THF [100 µL]	25 °C	0.5 h	>99%	0% (*rac*)	
22	**1v** [10 mol%]	*i*-Pr_2NEt [20 mol%]	10 equiv [54 µl]	THF [100 µL]	25 °C	0.5 h	98%	0% (*rac*)	
23	**1w** [10 mol%]	*i*-Pr_2NEt [20 mol%]	10 equiv [54 µl]	THF [100 µL]	25 °C	0.5 h	98%	0% (*rac*)	
24	**1x** [10 mol%]	*i*-Pr_2NEt [20 mol%]	10 equiv [54 µl]	THF [100 µL]	25 °C	0.5 h	99%	0% (*rac*)	
25	**2a** [10 mol%]	*i*-Pr_2NEt [20 mol%]	10 equiv [54 µl]	THF [100 µL]	25 °C	0.5 h	91%	43% (*R*)	
26	**2b** [10 mol%]	*i*-Pr_2NEt [20 mol%]	10 equiv [54 µl]	THF [100 µL]	25 °C	0.5 h	98%	34% (*S*)	
27	**2c** [10 mol%]	*i*-Pr_2NEt [20 mol%]	10 equiv [54 µl]	THF [100 µL]	25 °C	0.5 h	98%	30% (*R*)	
28	**3a** [10 mol%]	*i*-Pr_2NEt [20 mol%]	10 equiv [54 µl]	THF [100 µL]	25 °C	0.5 h	>99%	31% (*S*)	
29	**3b** [10 mol%]	*i*-Pr_2NEt [20 mol%]	10 equiv [54 µl]	THF [100 µL]	25 °C	0.5 h	98%	6% (*S*)	
30	**3c** [10 mol%]	*i*-Pr_2NEt [20 mol%]	10 equiv [54 µl]	THF [100 µL]	25 °C	0.5 h	99%	0% (*rac*)	
31	**3d** [10 mol%]	*i*-Pr_2NEt [20 mol%]	10 equiv [54 µl]	THF [100 µL]	25 °C	0.5 h	99%	0% (*rac*)	

Footnotes: Experiments were performed at the 0.1 mmol scale. Notes: [1] based on HPLC analyses of the crude reaction mixtures, calibration curves were constructed separately for both standards of analyzed compounds **4a** and **5a** by a linear regression analysis of the peak areas (mAU·min) versus the corresponding known concentrations within the expected analyzed concentration range (1.000–0.001 M). Accordingly, the corresponding calibration factors for **4a** (CF = 356.4; λ = 230 nm; R^2 = 0.9829) and **5a** (CF = 217.9; λ = 230 nm; R^2 = 0.9947) were determined. **4a**/**5a** RRF = 1.64 (λ = 230 nm), [2] measured by chiral HPLC analyses of the crude reaction mixtures.

3.2 Base and Solvent Screening Protocol

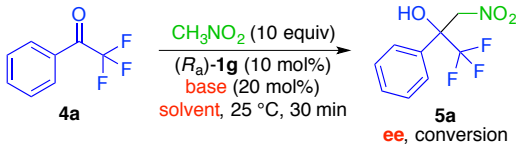

Experiments were performed with **4a** (14 µL, 0.1 mmol), nitromethane (53.5 µL, 1.0 mmol), catalyst (R_a)-**1g** (9.3 mg, 10.0 µmol), a corresponding base (20 µmol) in an appropriate anhydrous solvent (100 µL) at ambient temperature under air (**Tab. S2**). After 30 min, the reactions were quenched by a saturated aqueous solution of NH_4Cl and then repetitively extracted with Et_2O. Combined organic extracts were dried with anhydrous Na_2SO_4, filtered through a silica plug, and evaporated in vacuo (30 °C). The resulting samples were diluted with a mobile phase (1 mL) and directly subjected to the abovementioned HPLC analysis.

Table S2. Base and Solvent Screening Steps.

entry	cat.	base	$MeNO_2$	solvent	t	time	conv.[1]	ee[2]	variable
32	**1g** [10 mol%]	TMEDA [20 mol%]	10 equiv [54 µl]	THF [100 µL]	25 °C	0.5 h	98%	79% (*S*)	Base Type
33	**1g** [10 mol%]	DMAP [20 mol%]	10 equiv [54 µl]	THF [100 µL]	25 °C	0.5 h	99%	83% (*S*)	
34	**1g** [10 mol%]	Et_3N [20 mol%]	10 equiv [54 µl]	THF [100 µL]	25 °C	0.5 h	99%	48% (*S*)	
35	**1g** [10 mol%]	NMP [20 mol%]	10 equiv [54 µl]	THF [100 µL]	25 °C	0.5 h	>99%	30% (*S*)	
36	**1g** [10 mol%]	*n*-Bu_3N [20 mol%]	10 equiv [54 µl]	THF [100 µL]	25 °C	0.5 h	93%	29% (*S*)	
37	**1g** [10 mol%]	DMAP [20 mol%]	10 equiv [54 µl]	Et_2O [100 µL]	25 °C	0.5 h	>99%	80% (*S*)	Solvent Type
38	**1g** [10 mol%]	DMAP [20 mol%]	10 equiv [54 µl]	MePh [100 µL]	25 °C	0.5 h	98%	52% (*S*)	
39	**1g** [10 mol%]	DMAP [20 mol%]	–	$MeNO_2$ [100 µL]	25 °C	0.5 h	98%	53% (*S*)	
40	**1g** [10 mol%]	DMAP [20 mol%]	10 equiv [54 µl]	CH_2Cl_2 [100 µL]	25 °C	0.5 h	95%	31% (*S*)	
41	**1g** [10 mol%]	DMAP [20 mol%]	10 equiv [54 µl]	DME [100 µL]	25 °C	0.5 h	97%	77% (*S*)	
42	**1g** [10 mol%]	DMAP [20 mol%]	10 equiv [54 µl]	*t*-BuOMe [100 µL]	25 °C	0.5 h	95%	72% (*S*)	

Footnotes: Experiments were performed at the 0.1 mmol scale. Notes: [1] based on HPLC analyses of the crude reaction mixtures, calibration curves were constructed separately for both standards of analyzed compounds **4a** and **5a** by a linear regression analysis of the peak areas (mAU·min) versus the corresponding known concentrations within the expected analyzed concentration range (1.000–0.001 M). Accordingly, the corresponding calibration factors for **4a** (CF = 356.4; λ = 230 nm; R^2 = 0.9829) and **5a** (CF = 217.9; λ = 230 nm; R^2 = 0.9947) were determined. **4a**/**5a** RRF = 1.64 (λ = 230 nm), [2] measured by chiral HPLC analyses of the crude reaction mixtures.

3.3 Catalyst and Base Load Screening Protocol

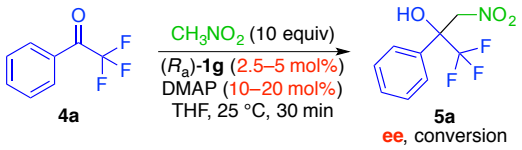

Experiments were performed with **4a** (14 µL, 0.1 mmol), nitromethane (53.5 µL, 1.0 mmol), catalyst (R_a)-**1g** (2.5–5.0 µmol), DMAP (10–20 µmol) in THF (100 µL) at ambient temperature under air (**Tab. S3**). After 30 min, the reactions were quenched by a saturated aqueous solution of NH_4Cl and then repetitively extracted with Et_2O. Combined organic extracts were dried with anhydrous Na_2SO_4, filtered through a silica plug, and evaporated in vacuo (30 °C). The resulting samples were diluted with a mobile phase (1 mL) and directly subjected to the abovementioned HPLC analysis.

Table S3. Catalyst and Base Load Screening Steps.

entry	cat.	base	$MeNO_2$	solvent	t	time	conv.[1]	ee[2]	variable
43	**1g** [5 mol%]	DMAP [20 mol%]	10 equiv [54 µl]	THF [100 µL]	25 °C	0.5 h	>99%	83% (*S*)	Catalyst & Base Load
44	**1g** [2.5 mol%]	DMAP [20 mol%]	10 equiv [54 µl]	THF [100 µL]	25 °C	0.5 h	97%	79% (*S*)	
45	**1g** [5 mol%]	DMAP [10 mol%]	10 equiv [54 µl]	THF [100 µL]	25 °C	0.5 h	98%	82% (*S*)	

Footnotes: Experiments were performed at the 0.1 mmol scale. Notes: [1] based on HPLC analyses of the crude reaction mixtures, calibration curves were constructed separately for both standards of analyzed compounds **4a** and **5a** by a linear regression analysis of the peak areas (mAU·min) versus the corresponding known concentrations within the expected analyzed concentration range (1.000–0.001 M). Accordingly, the corresponding calibration factors for **4a** (CF = 356.4; λ = 230 nm; R^2 = 0.9829) and **5a** (CF = 217.9; λ = 230 nm; R^2 = 0.9947) were determined. **4a**/**5a** RRF = 1.64 (λ = 230 nm), [2] measured by chiral HPLC analyses of the crude reaction mixtures.

3.4 Temperature Screening Protocol

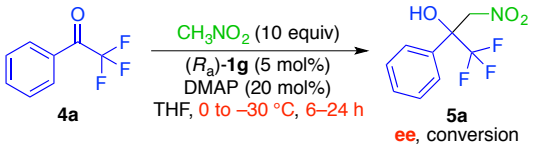

Experiments were performed with **4a** (14 µL, 0.1 mmol), nitromethane (53.5 µL, 1.0 mmol), catalyst (R_a)-**1g** (4.6 mg, 5.0 µmol), DMAP (2.4 mg, 20 µmol) in THF (100 µL) at 0 to –30 °C under argon (**Tab. S4**). After the depicted time, the reactions were quenched by a saturated aqueous solution of NH_4Cl and then repetitively extracted with Et_2O. Combined organic extracts were dried with anhydrous Na_2SO_4, filtered through a silica plug, and evaporated in vacuo (30 °C). The resulting samples were diluted with a mobile phase (1 mL) and directly subjected to the abovementioned HPLC analysis.

Table S4. Temperature Screening Steps.

entry	cat.	base	$MeNO_2$	solvent	t	time	conv.[1]	ee[2]	variable
46	**1g** [5 mol%]	DMAP [20 mol%]	10 equiv [54 µl]	THF [100 µL]	0 °C	6 h	99%	91% (*S*)	Temperature
47	**1g** [5 mol%]	DMAP [20 mol%]	10 equiv [54 µl]	THF [100 µL]	–20 °C	8 h	95%	94% (*S*)	
48	**1g** [5 mol%]	DMAP [20 mol%]	10 equiv [54 µl]	THF [100 µL]	–20 °C	12 h	>99%	95% (*S*)	
49	**1g** [5 mol%]	DMAP [20 mol%]	10 equiv [54 µl]	THF [100 µL]	–30 °C	24 h	97%	95% (*S*)	

Footnotes: Experiments were performed at the 0.1 mmol scale. Notes: [1] based on HPLC analyses of the crude reaction mixtures, calibration curves were constructed separately for both standards of analyzed compounds **4a** and **5a** by a linear regression analysis of the peak areas (mAU·min) versus the corresponding known concentrations within the expected analyzed concentration range (1.000–0.001 M). Accordingly, the corresponding calibration factors for **4a** (CF = 356.4; λ = 230 nm; R^2 = 0.9829) and **5a** (CF = 217.9; λ = 230 nm; R^2 = 0.9947) were determined. **4a**/**5a** RRF = 1.64 (λ = 230 nm), [2] measured by chiral HPLC analyses of the crude reaction mixtures.

4. Syntheses of α,α,α-Trifluoroketones

4.1 2,2,2-Trifluoro-1-(3-nitrophenyl)ethan-1-one (4f)[32]

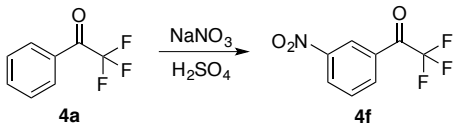

4a **4f**

4f was prepared by a slightly modified literature procedure.
A solution of 2,2,2-trifluoroacetophenone (0.5 mL, 3.68 mmol) in 96% sulfuric acid (3 mL) was treated with $NaNO_3$ (0.33 g, 3.86 mmol) at −10 °C. The temperature during addition should not exceed −5°C. Then the reaction mixtrure was left to stir 1 h at 0 °C. After the TLC analysis (SiO_2) *n*-hexane–EtOAc (4:1) revealed a complete conversion, the reaction mixture was poured into water (50 mL), alkalinized to pH 8–9 by 5M aqueous solution of NaOH and repetitively extracted by a mixture of $CHCl_3$–*i*-PrOH (4:1). The combined organic extracts were washed with brine, dried over anhydrous Na_2SO_4 and evaporated in vacuo. The crude product was purified by a column chromatography (SiO_2) *n*-hexane–EtOAc (5:1).

Physical state: white solid.
Isolated yield: 700 mg (87 %).

mp 44–46 °C, lit.[32b] 50–51 °C.
^{1}H NMR (400 MHz, $CDCl_3$) δ/ppm: 8.92 (s, 1H), 8.59 (dd, *J* = 8.0, 1.1 Hz, 1H), 8.41 (d, *J* = 8.0 Hz, 1H), 7.83 (app t, *J* = 8.0 Hz, 1H) [**Fig. S235**].
^{13}C NMR (100 MHz, $CDCl_3$) δ/ppm: 178.8 (q, $^2J_{CF}$ = 36.6 Hz), 148.6, 135.3, 131.1, 130.6, 129.6, 124.9, 116.2 (q, $^1J_{CF}$ = 290.6 Hz) [**Fig. S236**].
^{19}F NMR (376 MHz, $CDCl_3$) δ/ppm: −71.71 (s) [**Fig. S237**].
IR (neat) $\tilde{\nu}$/cm^{-1}: 3092*w*, 1725*s*, 1611*m*, 1577*w*, 1537*m*, 1442*w*, 1348*s*, 1221*m*, 1189*m*, 1143*m*, 1086*m*, 988*m*, 859*w*, 829*w*, 722*w*, 697*m*.
HRMS (ESI-Q-TOF) calcd for $C_8H_5F_3NO_4$ $[M+H_2O–H]^-$ 236.0176 *m*/*z*, found 236.0176 *m*/*z* [**Fig. S93**].

4.2 Methyl 4-(2,2,2-trifluoroacetyl)benzoate (4i)[33]

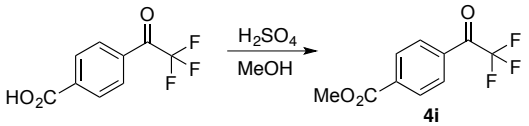

4i

A solution of 4-(2,2,2-trifluoroacetyl)benzoic acid (218 mg, 1 mmol) in absolute MeOH (5 mL) was treated with 96% sulfuric acid (100 μL, 1.8 mmol), the resulting solution was left to stir at 60 °C for 12 h. After the TLC analysis (SiO_2) *n*-hexane–EtOAc (5:1) revealed a complete conversion, the reaction was quenched by a dropwise addition of saturated aqueous solution of $NaHCO_3$ and repetitively extracted with Et_2O. The combined organic extracts were washed with saturated aqueous solution of $NaHCO_3$ and brine, dried over anhydrous Na_2SO_4 and evaporated in vacuo. The obtained product was used without further purification.

Physical state: colorless solid.
Isolated yield: 209 mg (90 %).

mp 37–38 °C, lit.[33b] 37–39 °C.
^{1}H NMR (400 MHz, $CDCl_3$) δ/ppm: 8.21–8.19 (m, 2H), 8.15–8.13 (m, 2H), 3.98 (s, 3H) [**Fig. S238**].
^{13}C NMR (100 MHz, $CDCl_3$) δ/ppm: 180.1 (q, $^2J_{CF}$ = 35.6 Hz), 165.6, 135.9, 132.9, 130.1, 130.0, 116.4 (q, $^1J_{CF}$ = 291.2 Hz), 52.7 [**Fig. S239**].
^{19}F NMR (376 MHz, $CDCl_3$) δ/ppm: −71.61 (s) [**Fig. S240**].
IR (neat) ṽ/cm^{-1}: 3295*m*, 1694*s*, 1440*m*, 1411*m*, 1287*s*, 1205*w*, 1168*s*, 1125*s*, 1098*m*, 1043*m*, 1016*m*, 963*w*, 917*m*, 859*m*, 775*m*, 755*w*, 714*m*.
HRMS (ESI-Q-TOF) calcd for $C_{10}H_8F_3O_3$ $[M+H]^+$ 233.0420 *m*/*z*, found 233.0398 *m*/*z* [**Fig. S94**].

5. Syntheses of Nitroaldol Adducts

5.1 General Procedure for Synthesis of Racemic Adducts

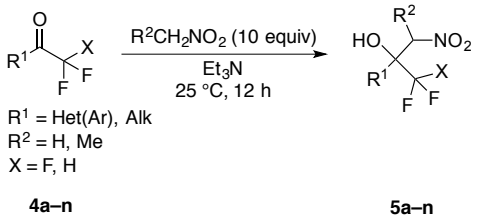

4a–n **5a–n**

A solution of the corresponding fluoroketone **4a**–**n** (0.5 mmol), triethylamine (209 μL, 3 equiv) in nitromethane (271 μL, 10 equiv) or nitroethane (358 μL, 10 equiv) was left to stir for 12 h at ambient temperature.

Then the reaction mixture was quenched by saturated aqueous solution of NH_4Cl and repetitively extracted with Et_2O. The combined extracts were dried over anhydrous Na_2SO_4, filtered through a plug of SiO_2 and evaporated in vacuo (30 °C). The crude Henry adducts **5a–n** were further purified by a preparative TLC (SiO_2) *n*-hexane–EtOAc 5:1 (**5a**–**e**, **g–k**, **n**), 9:1 (**5l**, **m, o**), or 2:1 (**5f**).

5.2 General Procedure for Synthesis of Enantioenriched Adducts

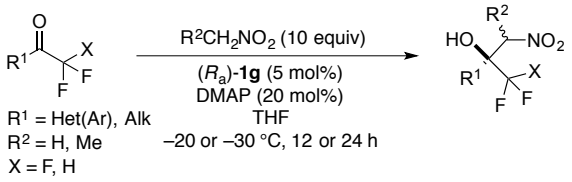

Solutions of the corresponding ketones (0.1 mmol), catalyst (R_a)-**1g** (4.6 mg, 5.0 μmol), and DMAP (2.4 mg, 20 μmol) in THF (100 μL) were left to stir under argon for 10 min at –20 or –30 °C. Then nitromethane (53.5 μL, 1.0 mmol) or nitroethane (71.5 μL, 1.0 mmol) was added dropwise and the resulting mixtures were left to stir at the above temperature for 12 or 24 h. After the depicted time, the reactions were quenched by a saturated aqueous solution of NH_4Cl and then repetitively extracted with Et_2O. Combined organic extracts were dried with anhydrous Na_2SO_4, filtered through a silica plug, and evaporated in vacuo (30 °C). The resulting crude samples were diluted with a mobile phase (1 mL) and directly subjected to the abovementioned CSP-HPLC analysis. For other purposes, the adducts were isolated by a column chromatography (SiO_2), *n*-hexane–EtOAc 5:1.

Stereochemical assignments: The absolute configurations of nitroaldol adducts **5a**, **5e**, **5l**, and **5m** were determined by comparison of the sign of specific rotation and relative elution order of the resolved peaks with the literature data.[34] The absolute configurations of nitroaldol adducts **5b**, **5g**, **5h**, and **5l–o** were determined by comparison of the relative elution order of the resolved peaks with the literature data.[34] The absolute configurations of **5c, 5d, 5f**, and **5i–k** were assigned by analogy with other nitroaldol adducts.

5.2.1 1,1,1-Trifluoro-2-phenyl-3-nitropropan-2-ol (**5a**)[34a]

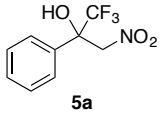

5a

Chiral HPLC conditions: a Hypersil silica column (3 μm, 100 × 4.6 mm) used as a precolumn, which was connected via the standard blue PEEK capillary tubing (L 300 mm, ID 0.01", OD 1/16") to a Daicel Chiralpak IB column (5 μm, 250 × 4.6 mm), *i*-PrOH–*n*-heptane, 20:80, 0.5 mL/min, 25 °C (λ = 230 nm).

Physical state: colorless oil.
Isolated yield: 21.6 mg (92%) at the 0.1 mmol scale, 285 mg (81%) at the 1.5 mmol scale.

$[\alpha]^{20}_{D}$ +42 (*c* 1.0, MeOH).
^{1}H NMR (400 MHz, $CDCl_3$) δ/ppm: 7.62–7.59 (m, 2H), 7.48–7.44 (m, 3H), 5.10, 5.03 (q, AB, J_{AB} = 13.7 Hz, 2H), 4.63 (br s, 1H) [**Fig. S241**].
^{13}C NMR (100 MHz, $CDCl_3$) δ/ppm 133.1, 130.0, 129.1, 126.2, 123.5 (q, $^{1}J_{CF}$ =285.6 Hz), 77.6, 76.3 (q, $^{2}J_{CF}$ =29.9 Hz) [**Fig. S242**].
^{19}F NMR (376 MHz, $CDCl_3$) δ/ppm: −78.58 (s) [**Fig. S243**].
HRMS (ESI-Orbitrap) calcd for $C_9H_7F_3NO_3$ $[M–H]^-$ 234.0384 *m*/*z*, found 234.0386 *m*/*z* [**Fig. S95**].

rac-**5a** [**Fig. S9**].
(*S*)-**5a** (95% ee): t_S = 15.95 min (major), t_R = 18.36 min (minor) [**Fig. S10**].

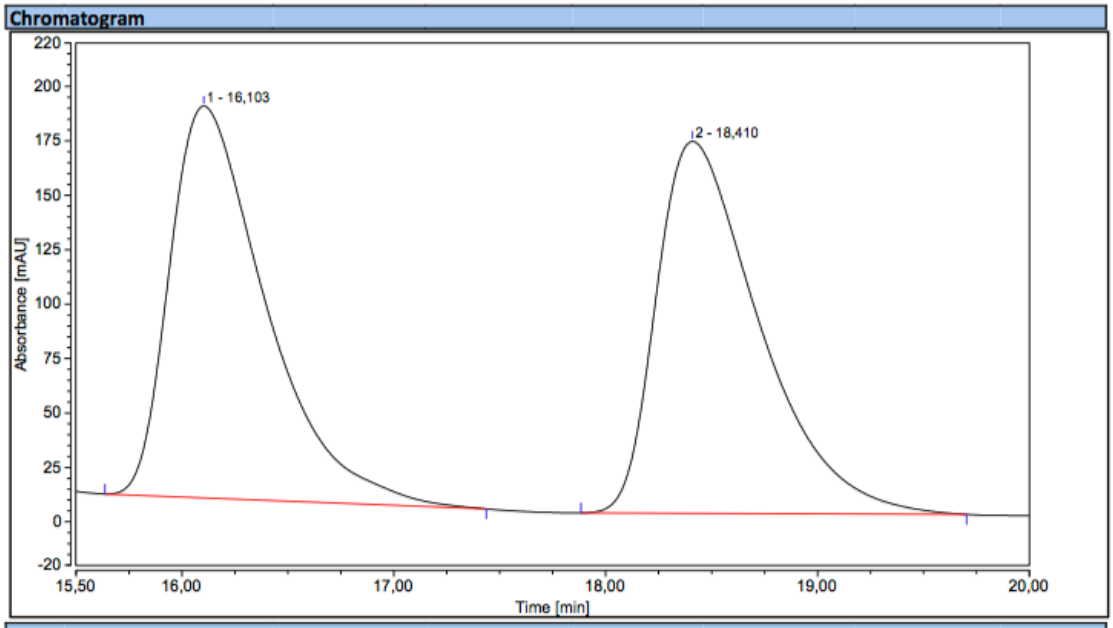

Integration Results

No.	Peak Name	Retention Time min	Area mAU*min	Height mAU	Relative Area %	Relative Height %	Amount n.a.
1		16,103	94,859	179,971	49,62	51,30	n.a.
2		18,410	96,314	170,871	50,38	48,70	n.a.
Total:			**191,172**	**350,842**	**100,00**	**100,00**	

Figure S9. Chiral HPLC chromatogram of *rac*-**5a**.

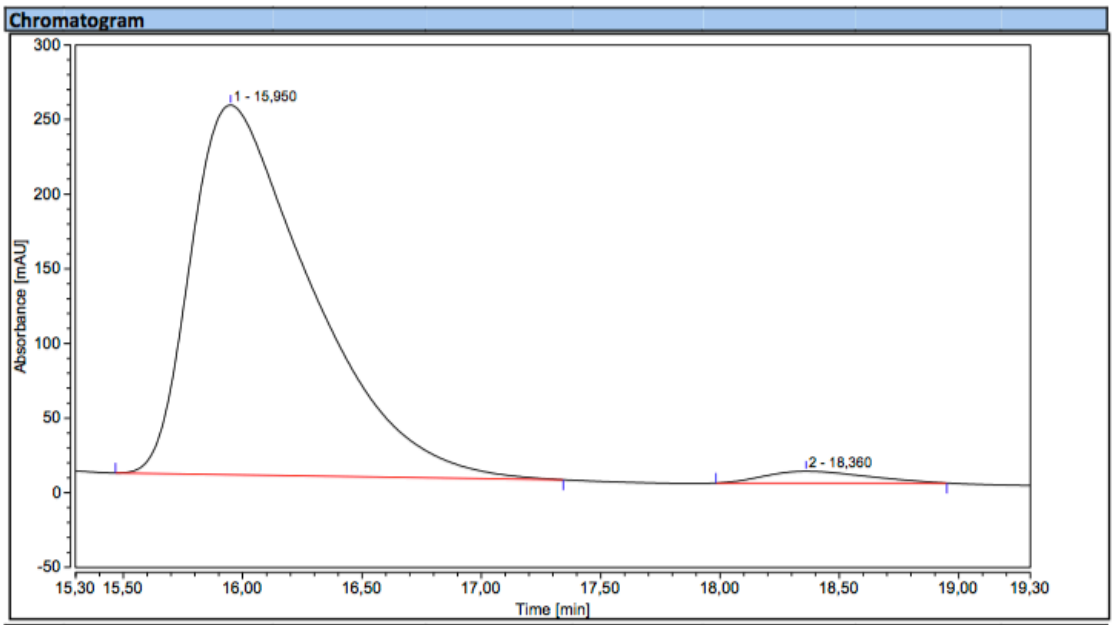

Integration Results

No.	Peak Name	Retention Time min	Area mAU*min	Height mAU	Relative Area %	Relative Height %	Amount n.a.
1		15,950	145,066	247,561	97,38	96,91	n.a.
2		18,360	3,902	7,898	2,62	3,09	n.a.
Total:			**148,968**	**255,460**	**100,00**	**100,00**	

Figure S10. Chiral HPLC chromatogram of (*S*)-**5a** (95% ee).

5.2.2 1,1,1-Trifluoro-3-nitro-2-(thiophen-2-yl)propan-2-ol (**5b**)[34a]

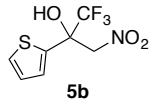

5b

Chiral HPLC conditions: a Hypersil silica column (3 μm, 100 × 4.6 mm) used as a precolumn, which was connected via the standard blue PEEK capillary tubing (L 300 mm, ID 0.01", OD 1/16") to a Daicel Chiralpak IB column (5 μm, 250 × 4.6 mm), *i*-PrOH–*n*-heptane, 10:90, 0.5 mL/min, 25 °C (λ = 230 nm).

Physical state: colorless oil.
Isolated yield: 21.7 mg (90%).

^{1}H NMR (400 MHz, $CDCl_3$) δ/ppm: 7.45 (dd, *J* = 5.1, 1.2 Hz, 1H), 7.18–7.17 (m, 1H), 7.08 (dd, *J* = 5.1, 3.8 Hz, 1H), 5.01 (s, 1H), 5.00 (s, 2H) [**Fig. S244**].
^{13}C NMR (100 MHz, $CDCl_3$) δ/ppm: 136.5, 128.1, 127.8, 126.8, 123.0 (q, $^{1}J_{CF}$ = 285.5 Hz), 77.7, 75.5 (q, $^{2}J_{CF}$ = 31.5 Hz) [**Fig. S245**].
^{19}F NMR (376 MHz, $CDCl_3$) δ/ppm: −79.57 (s) [**Fig. S246**].
HRMS (ESI-Orbitrap) calcd for $C_7H_6NF_3O_3S$ $[M-H]^-$ 239.9948 *m*/*z*, found 239.9947 *m*/*z* [**Fig. S96**].

rac-**5b** [**Fig. S11**].
(*S*)-**5b** (85% ee): t_R = 25.13 min (minor), t_S = 27.32 min (major) [**Fig. S12**].

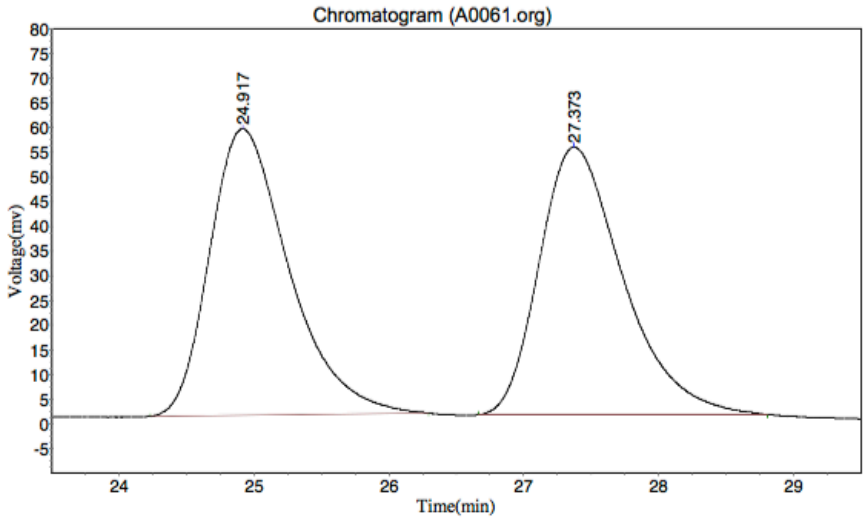

Results

Peak No.	Peak ID	Ret Time	Height	Area	Conc.
1		24.917	58063.063	2377453.750	50.3298
2		27.373	54230.188	2346297.750	49.6702
Total			112293.250	4723751.500	100.0000

Figure S11. Chiral HPLC chromatogram of *rac*-**5b**.

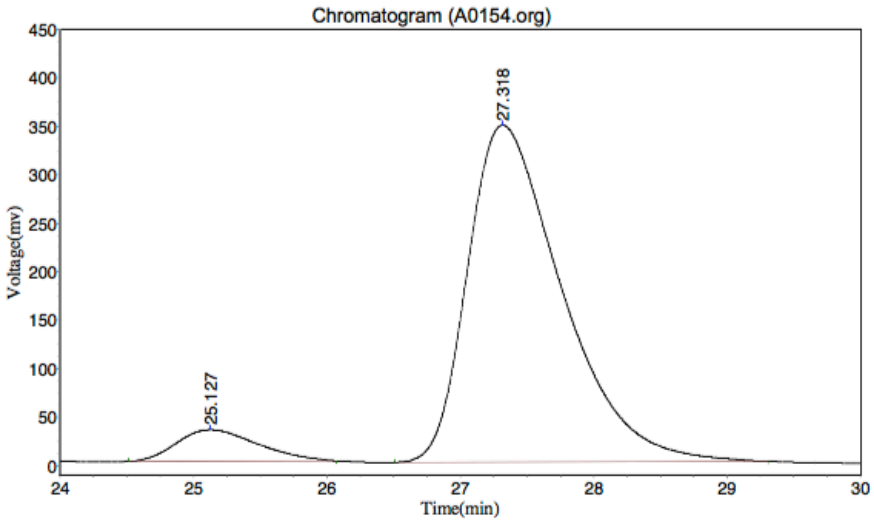

Results

Peak No.	Peak ID	Ret Time	Height	Area	Conc.
1		25.127	32491.557	1355389.625	7.3649
2		27.318	347874.281	17048064.000	92.6351
Total			380365.838	18403453.625	100.0000

Figure S12. Chiral HPLC chromatogram of (*S*)-**5b** (85% ee).

5.2.3 2-(2-Bromophenyl)-1,1,1-trifluoro-3-nitropropan-2-ol (**5c**)

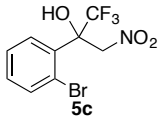

5c

Chiral HPLC conditions: a Hypersil silica column (3 μm, 100 × 4.6 mm) used as a precolumn, which was connected via the standard blue PEEK capillary tubing (L 300 mm, ID 0.01", OD 1/16") to a Daicel Chiralcel OJ-3 column (3 μm, 150 × 4.6 mm), *i*-PrOH–*n*-heptane, 10:90, 0.5 mL/min, 25 °C (λ = 230 nm).

Physical state: colorless oil.
Isolated yield: 26.7 mg (85%).

^{1}H NMR (400 MHz, $CDCl_3$) δ/ppm: 7.91 (d, *J* = 8.0 Hz, 1H), 7.68 (dd, *J* = 8.0, 1.2 Hz, 1H), 7.46–7.42 (m, 1H), 7.31–7.28 (m, 1H), 6.08 (d, *J* = 14.6 Hz, 1H), 5.08 (d, *J* = 14.6 Hz, 1H), 4.80 (s, 1H) [**Fig. S247**].
^{13}C NMR (100 MHz, $CDCl_3$) δ/ppm: 136.2, 132.3, 131.5, 130.8, 128.0, 123.4 (q, $^{1}J_{CF}$ = 286.7 Hz), 120.3, 76.5 [**Fig. S248**].
^{19}F NMR (376 MHz, $CDCl_3$) δ/ppm: −76.51 (s) [**Fig. S249**].
HRMS (ESI-Orbitrap) calcd for $C_9H_6NF_3O_3Br$ $[M-H]^-$ 311.9489 *m*/*z*, found 311.9491 *m*/*z* [**Fig. S97**].

rac-**5c** [**Fig. S13**].
(*S*)-**5c** (67% ee): t_R = 24.01 min (minor), t_S = 27.12 min (major) [**Fig. S14**].

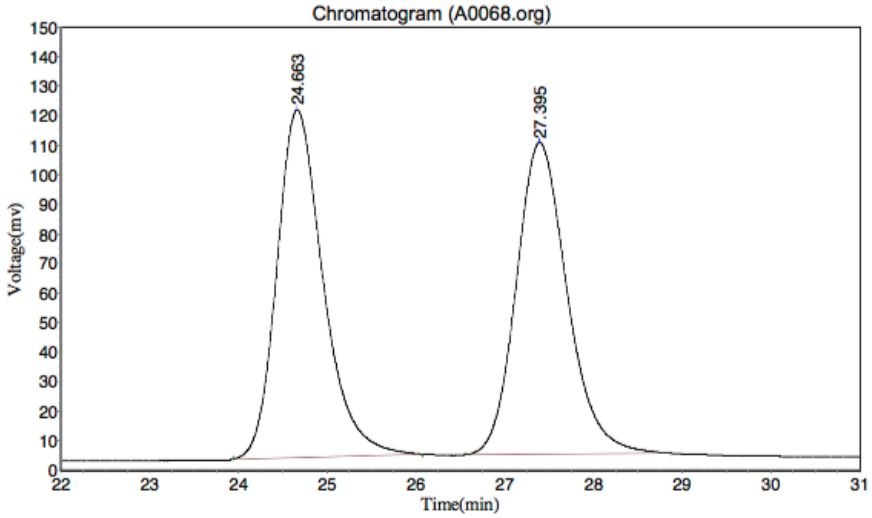

Results

Peak No.	Peak ID	Ret Time	Height	Area	Conc.
1		24.663	117565.211	4252147.000	50.3152
2		27.395	105389.023	4198873.500	49.6848
Total			222954.234	8451020.500	100.0000

Figure S13. Chiral HPLC chromatogram of *rac*-**5c**.

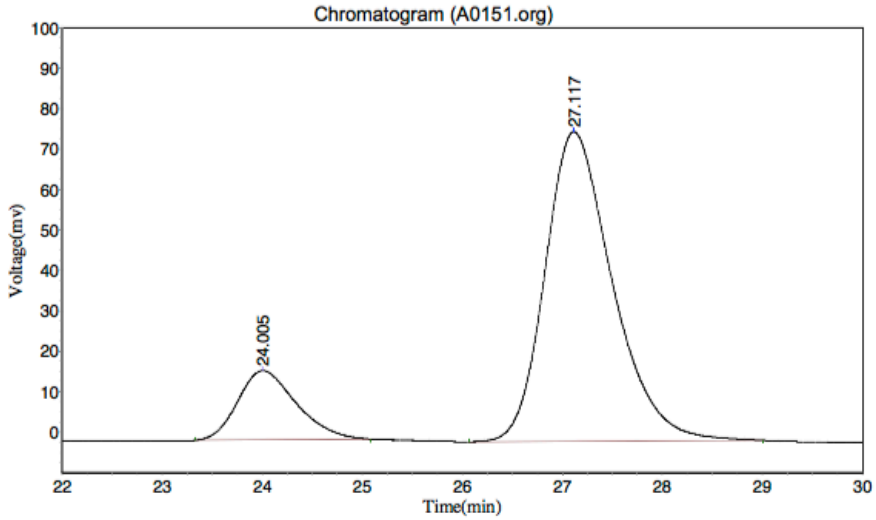

Results

Peak No.	Peak ID	Ret Time	Height	Area	Conc.
1		24.005	17113.600	695324.125	16.2946
2		27.117	76446.383	3571872.250	83.7054
Total			93559.982	4267196.375	100.0000

Figure S14. Chiral HPLC chromatogram of (*S*)-**5c** (67% ee).

5.2.4 2-(3-Bromophenyl)-1,1,1-trifluoro-3-nitropropan-2-ol (**5d**)

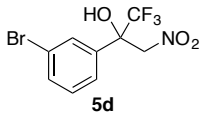

5d

Chiral HPLC conditions: a Hypersil silica column (3 μm, 100 × 4.6 mm) used as a precolumn, which was connected via the standard blue PEEK capillary tubing (L 300 mm, ID 0.01", OD 1/16") to a Daicel Chiralpak IB column (5 μm, 250 × 4.6 mm), *i*-PrOH–*n*-heptane, 20:80, 0.5 mL/min, 25 °C (λ = 230 nm).

Physical state: yellowish oil.
Isolated yield: 28.6 mg (91%).

$[\alpha]^{25}_{D}$ +22 (*c* 0.3, $CHCl_3$).
^{1}H NMR (400 MHz, $CDCl_3$) δ/ppm: 7.80 (s, 1H), 7.60 (ddd, *J* = 8.0, 1.9, 1.0 Hz, 1H), 7.51–7.49 (m, 1H), 7.33 (dd, *J* = 8.0, 7.9 Hz, 1H), 5.05, 5.01 (q, AB, J_{AB} = 13.7 Hz), 4.72 (br s, 1H) [**Fig. S250**].
^{13}C NMR (100 MHz, $CDCl_3$) δ/ppm: 135.1, 133.3, 130.4, 129.6, 124.7, 123.3, 123.1 (q, $^1J_{CF}$ = 286.1 Hz), 77.2, 75.8 (q, $^2J_{CF}$ = 29.9 Hz) [**Fig. S251**].
^{19}F NMR (376 MHz, $CDCl_3$) δ/ppm: −78.43 (s) [**Fig. S252**].
HRMS (ESI-Orbitrap) calcd for $C_9H_6NF_3O_3Br$ $[M-H]^-$ 311.9489 *m*/*z*, found 311.9490 *m*/*z* [**Fig. S98**].

rac-**5d** [**Fig. S15**].
(*S*)-**5d** (92% ee): t_S = 14.62 min (major), t_R = 18.99 min (minor) [**Fig. S16**].

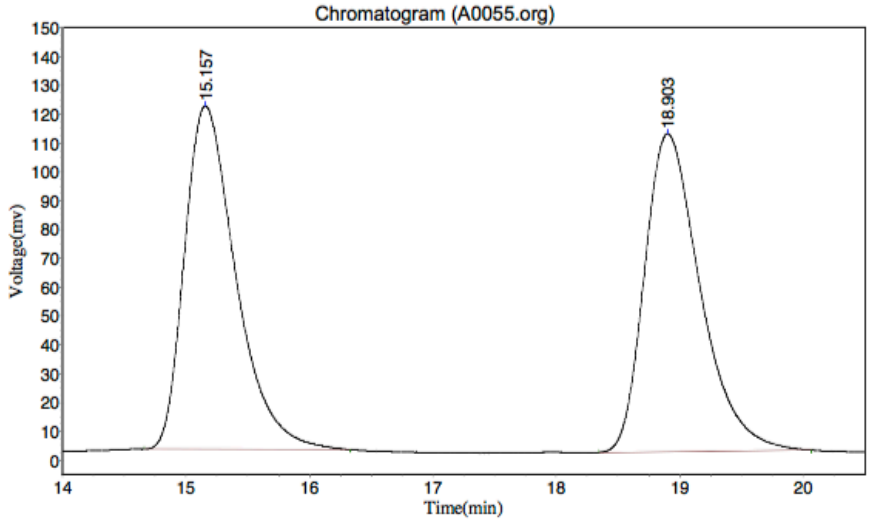

Results

Peak No.	Peak ID	Ret Time	Height	Area	Conc.
1		15.157	119132.656	3442374.000	49.8684
2		18.903	110326.898	3460548.000	50.1316
Total			229459.555	6902922.000	100.0000

Figure S15. Chiral HPLC chromatogram of *rac*-**5d**.

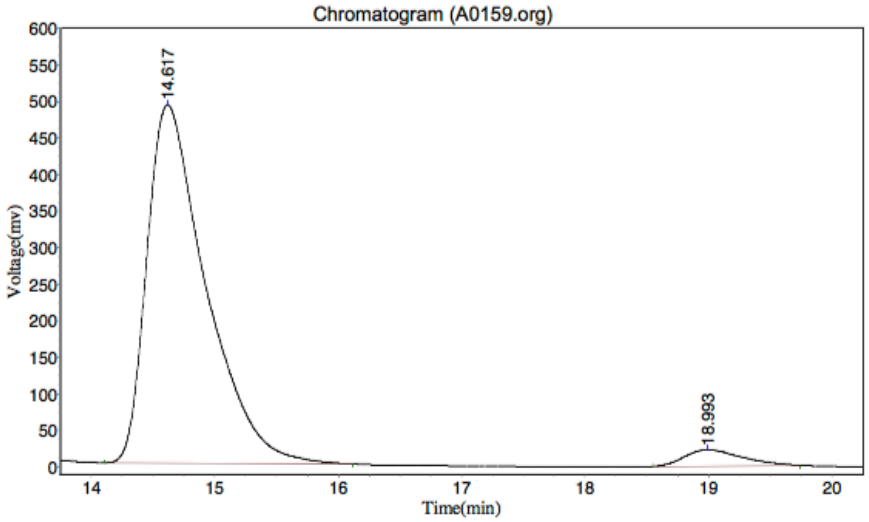

Results

Peak No.	Peak ID	Ret Time	Height	Area	Conc.
1		14.617	489631.656	16227080.000	95.8136
2		18.993	22110.361	709019.375	4.1864
Total			511742.018	16936099.375	100.0000

Figure S16. Chiral HPLC chromatogram of (*S*)-**5d** (92% ee).

5.2.5 1,1,1-Trifluoro-3-nitro-2-(3-(trifluoromethyl)phenyl)propan-2-ol (**5e**)[34b]

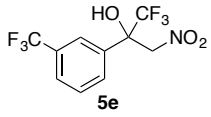

5e

Chiral HPLC conditions: a Hypersil silica column (3 μm, 100 × 4.6 mm) used as a precolumn, which was connected via the standard blue PEEK capillary tubing (L 300 mm, ID 0.01", OD 1/16") to a Daicel Chiralcel OJ-3 column (3 μm, 150 × 4.6 mm), *i*-PrOH–*n*-heptane, 10:90, 0.5 mL/min, 25 °C (λ = 230 nm).

Physical state: colorless oil.
Isolated yield: 27.3 mg (90%).

$[\alpha]^{25}_{D}$ –28 (*c* 0.2, $CHCl_3$).
^{1}H NMR (400 MHz, $CDCl_3$) δ/ppm: 7.92 (s, 1H), 7.79–7.73 (m, 2H), 7.61 (dd, *J* = 7.9, 7.9 Hz, 1H), 5.10, 5.06 (q, AB, J_{AB} = 13.7 Hz, 2H), 4.78 (s, 1H) [**Fig. S253**].
^{13}C NMR (100 MHz, $CDCl_3$) δ/ppm: 134.2, 131.7 (q, $^2J_{CF}$ = 32.8 Hz), 129.6, 129.5, 127.0, 123.6, (q, $^1J_{CF}$ = 272.6 Hz), 123.4, 123.1 (q, $^1J_{CF}$ = 285.8 Hz), 77.2, 76.0 (q, $^2J_{CF}$ = 30.2 Hz) [**Fig. S254**].
^{19}F NMR (376 MHz, $CDCl_3$) δ/ppm: −62.72 (s, 3F), −78.51 (s, 3F) [**Fig. S255**].
HRMS (ESI-Orbitrap) calcd for $C_{10}H_6NF_6O_3$ $[M-H]^-$ 302.0257 *m*/*z*, found 302.0254 *m*/*z* [**Fig. S99**].

rac-**5e** [**Fig. S17**].
(*S*)-**5e** (89% ee): t_S = 18.34 min (major), t_R = 21.11 min (minor) [**Fig. S18**].

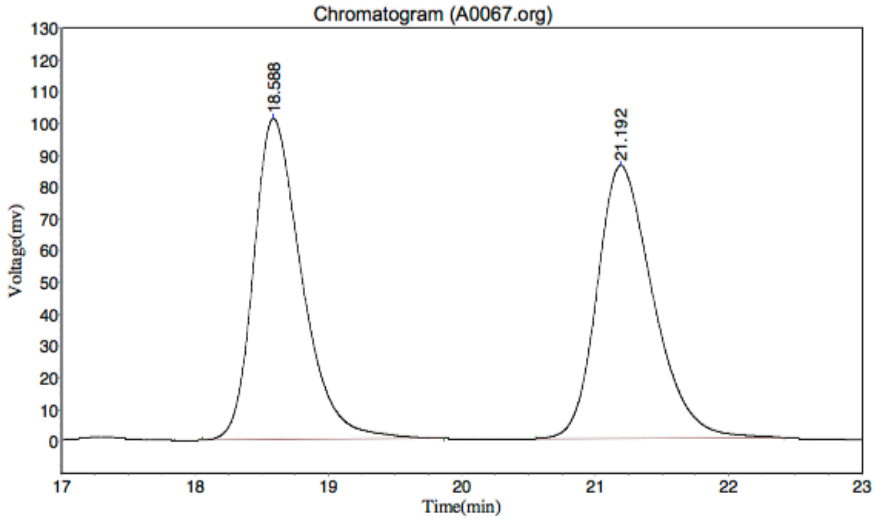

Results

Peak No.	Peak ID	Ret Time	Height	Area	Conc.
1		18.588	100949.906	2529422.750	50.3203
2		21.192	85757.344	2497225.500	49.6797
Total			186707.250	5026648.250	100.0000

Figure S17. Chiral HPLC chromatogram of *rac*-**5e**.

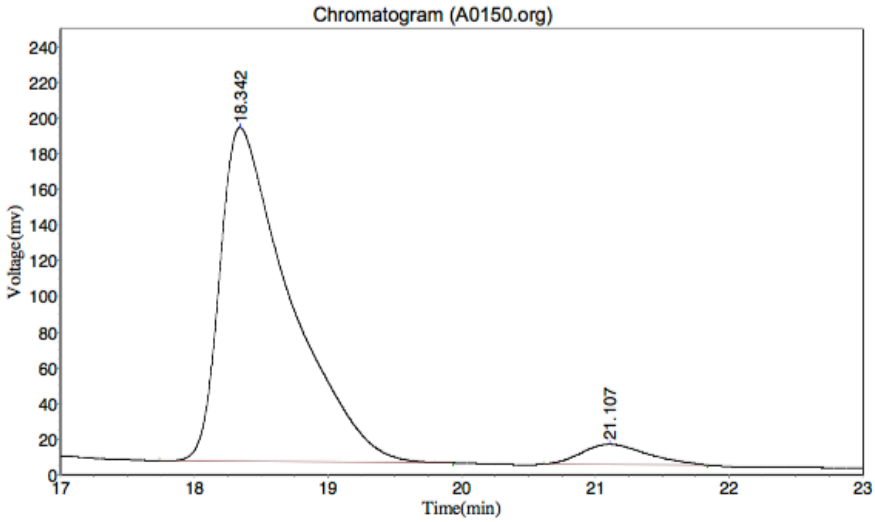

Results

Peak No.	Peak ID	Ret Time	Height	Area	Conc.
1		18.342	186923.766	6824568.000	94.6220
2		21.107	11334.257	387883.125	5.3780
Total			198258.022	7212451.125	100.0000

Figure S18. Chiral HPLC chromatogram of (*S*)-**5e** (89% ee).

5.2.6 1,1,1-Trifluoro-3-nitro-2-(3-nitrophenyl)propan-2-ol (**5f**)

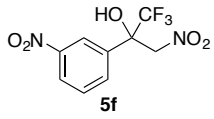

5f

Chiral HPLC conditions: a Hypersil silica column (3 μm, 100 × 4.6 mm) used as a precolumn, which was connected via the standard blue PEEK capillary tubing (L 300 mm, ID 0.01", OD 1/16") to a Daicel Chiralpak IB column (5 μm, 250 × 4.6 mm), *i*-PrOH–*n*-heptane, 10:90, 0.5 mL/min, 25 °C (λ = 230 nm).

Physical state: yellowish oil.
Isolated yield: 25.5 mg (91%).

^{1}H NMR (400 MHz, $CDCl_3$) δ/ppm: 8.54 (s, 1H), 8.34 (ddd, J = 8.2, 2.2, 0.9 Hz, 1H), 7.96–7.94 (m, 1H), 7.69 (dd, J = 8.2, 8.0 Hz, 1H), 5.15, 5.11 (q, AB, J_{AB} = 13.7 Hz, 2H), 4.86 (s, 1H) [**Fig. S256**].
^{13}C NMR (100 MHz, $CDCl_3$) δ/ppm: 148.6, 135.2, 132.1, 130.2, 125.1, 123.0 (q, $^{1}J_{CF}$ = 286.1 Hz), 121.8, 77.1, 75.8 (q, $^{2}J_{CF}$ = 30.5 Hz) [**Fig. S257**].
^{19}F NMR (376 MHz, $CDCl_3$) δ/ppm: −78.44 (s) [**Fig. S258**].
HRMS (ESI-Orbitrap) calcd for $C_9H_6N_2F_3O_5$ $[M-H]^-$ 279.0234 *m*/*z*, found 279.0232 *m*/*z* [**Fig. S100**].

rac-**5f** [**Fig. S19**].
(*S*)-**5f** (80% ee): t_S = 34.54 min (major), t_R = 39.20 min (minor) [**Fig. S20**].

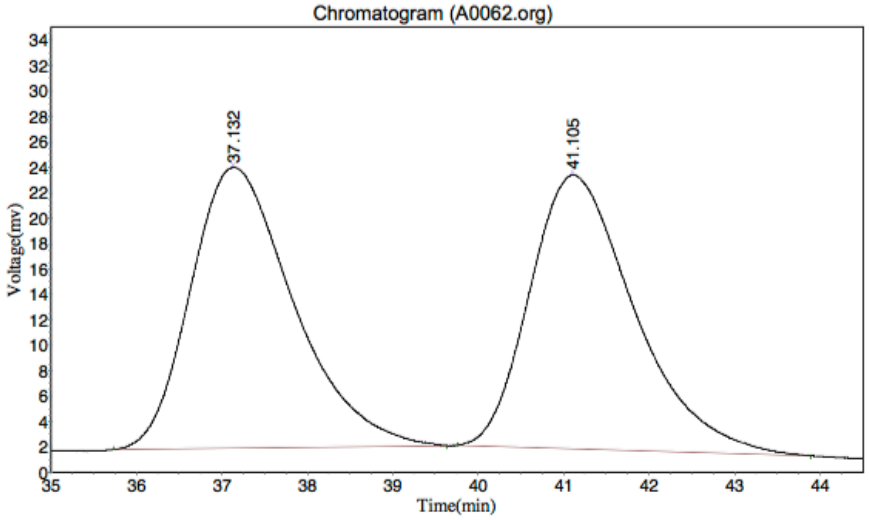

Results

Peak No.	Peak ID	Ret Time	Height	Area	Conc.
1		37.132	22086.422	1843991.875	50.2058
2		41.105	21522.354	1828872.375	49.7942
Total			43608.775	3672864.250	100.0000

Figure S19. Chiral HPLC chromatogram of *rac*-**5f**.

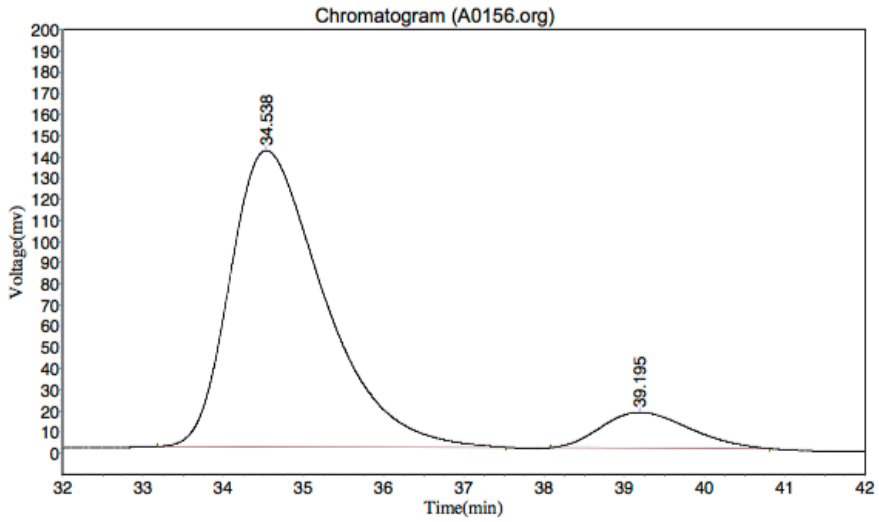

Results

Peak No.	Peak ID	Ret Time	Height	Area	Conc.
1		34.538	139975.531	11366665.000	89.8705
2		39.195	16871.836	1281162.250	10.1295
Total			156847.367	12647827.250	100.0000

Figure S20. Chiral HPLC chromatogram of (*S*)-**5f** (80% ee).

5.2.7 1,1,1-Trifluoro-2-(4-fluorophenyl)-3-nitropropan-2-ol (**5g**)[34b]

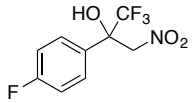

5g

Chiral HPLC conditions: a Hypersil silica column (3 μm, 100 × 4.6 mm) used as a precolumn, which was connected via the standard blue PEEK capillary tubing (L 300 mm, ID 0.01", OD 1/16") to a Daicel Chiralcel OJ-3 column (3 μm, 150 × 4.6 mm), *i*-PrOH–*n*-heptane, 10:90, 0.5 mL/min, 25 °C (λ = 230 nm).

Physical state: colorless oil.
Isolated yield: 22.5 mg (89%).

^{1}H NMR (400 MHz, $CDCl_3$) δ/ppm: 7.61–7.58 (m, 2H), 7.18–7.12 (m, 2H), 5.07, 5.01 (q, AB, J_{AB} = 13.6 Hz, 2H), 4.67 (br s, 1H) [**Fig. S259**].
^{13}C NMR (100 MHz, $CDCl_3$) δ/ppm: 163.6 (d, $^{1}J_{CF}$ = 250.5 Hz), 128.7, 128.3 (d, $^{3}J_{CF}$ = 8.7 Hz), 123.2 (q, $^{1}J_{CF}$ = 285.8 Hz), 116.1 (d, $^{2}J_{CF}$ = 22.2 Hz), 77.4, 75.9 (q, $^{2}J_{CF}$ = 29.9 Hz) [**Fig. S260**].
^{19}F NMR (376 MHz, $CDCl_3$) δ/ppm: −78.81 (s, 3F), −110.79 (br s, 1F) [**Fig. S261**].
HRMS (ESI-Orbitrap) calcd for $C_9H_6NF_4O_3$ $[M-H]^-$ 252.0289 *m*/*z*, found 252.0286 *m*/*z* [**Fig. S101**].

rac-**5g** [**Fig. S21**].
(*S*)-**5g** (97% ee): t_S = 30.17 min (major), t_R = 32.01 min (minor) [**Fig. S22**].

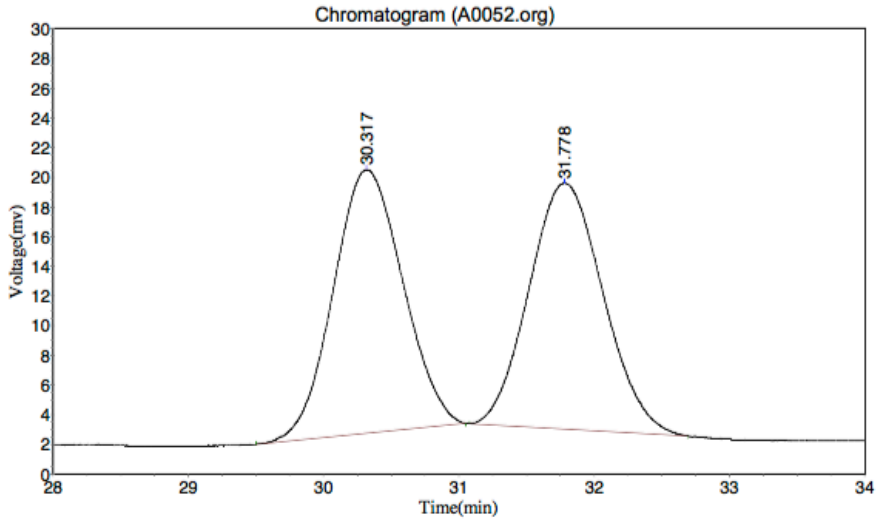

Results

Peak No.	Peak ID	Ret Time	Height	Area	Conc.
1		30.317	17752.010	633155.313	50.0252
2		31.778	16570.043	632518.625	49.9748
Total			34322.053	1265673.938	100.0000

Figure S21. Chiral HPLC chromatogram of *rac*-**5g**.

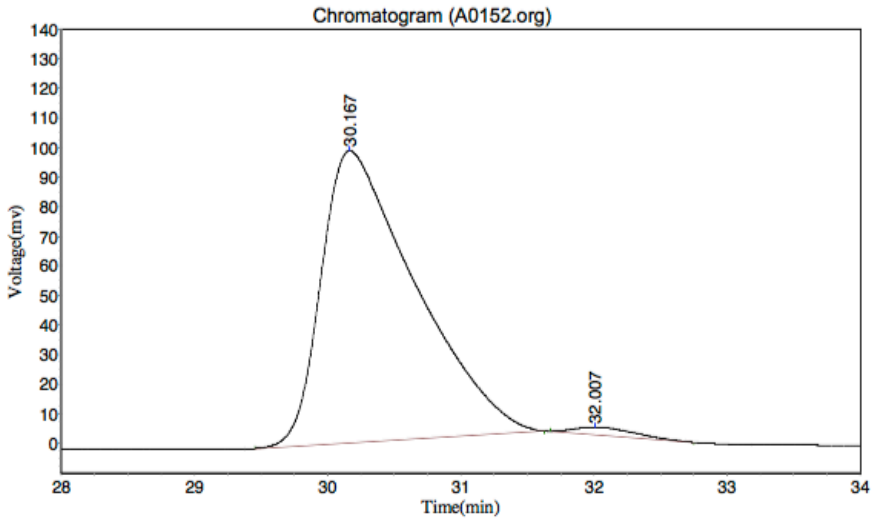

Results

Peak No.	Peak ID	Ret Time	Height	Area	Conc.
1		30.167	98621.461	4841872.000	98.3785
2		32.007	2390.243	79806.945	1.6215
Total			101011.704	4921678.945	100.0000

Figure S22. Chiral HPLC chromatogram of (*S*)-**5g** (97% ee).

5.2.8 2-(4-Chlorophenyl)-1,1,1-trifluoro-3-nitropropan-2-ol (**5h**)[34c]

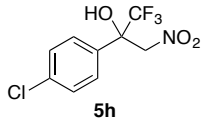

5h

Chiral HPLC conditions: a Hypersil silica column (3 μm, 100 × 4.6 mm) used as a precolumn, which was connected via the standard blue PEEK capillary tubing (L 300 mm, ID 0.01", OD 1/16") to a Daicel Chiralcel OJ-3 column (3 μm, 150 × 4.6 mm), *i*-PrOH–*n*-heptane, 10:90, 0.5 mL/min, 25 °C (λ = 230 nm).

Physical state: colorless oil.
Isolated yield: 25.1 mg (93%).

^{1}H NMR (400 MHz, $CDCl_3$) δ/ppm: 7.56–7.53 (m, 2H), 7.45–7.43 (m, 2H), 5.07, 5.01 (q, AB, J_{AB} = 13.7 Hz, 2H), 4.65 (s, 1H) [**Fig. S262**].
^{13}C NMR (100 MHz, $CDCl_3$) δ/ppm: 136.4, 131.4, 129.3, 127.7, 123.2 (q, $^{1}J_{CF}$ = 285.8 Hz), 77.3, 76.0 (q, $^{2}J_{CF}$ = 29.9 Hz) [**Fig. S263**].
^{19}F NMR (376 MHz, $CDCl_3$) δ/ppm: −78.68 (s) [**Fig. S264**].
HRMS (ESI-Orbitrap) calcd for $C_9H_6NF_3O_3Cl$ $[M-H]^-$ 267.9994 *m*/*z*, found 267.9993 *m*/*z* [**Fig. S102**].

rac-**5h** [**Fig. S23**].
(*S*)-**5h** (90% ee): t_S = 24.17 min (major), t_R = 29.16 min (minor) [**Fig. S24**].

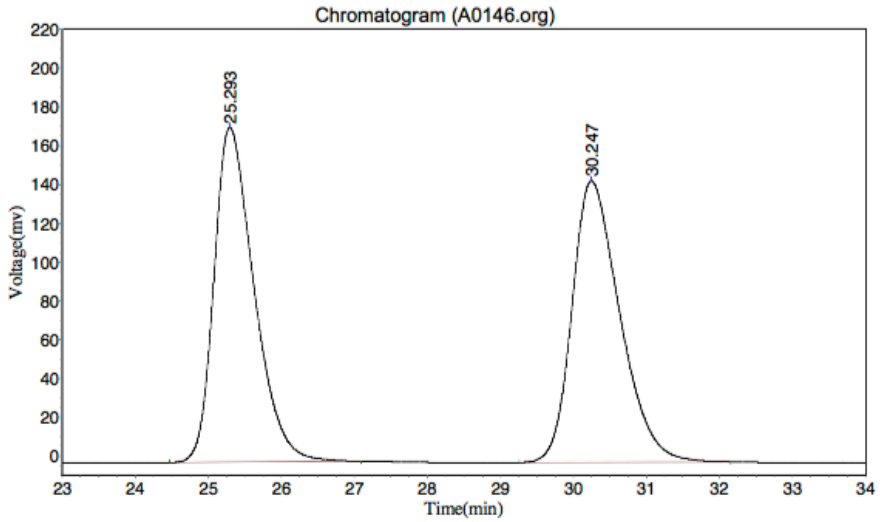

Results

Peak No.	Peak ID	Ret Time	Height	Area	Conc.
1		25.293	172626.797	6560400.500	49.8645
2		30.247	145151.344	6596066.000	50.1355
Total			317778.141	13156466.500	100.0000

Figure S23. Chiral HPLC chromatogram of *rac*-**5h**.

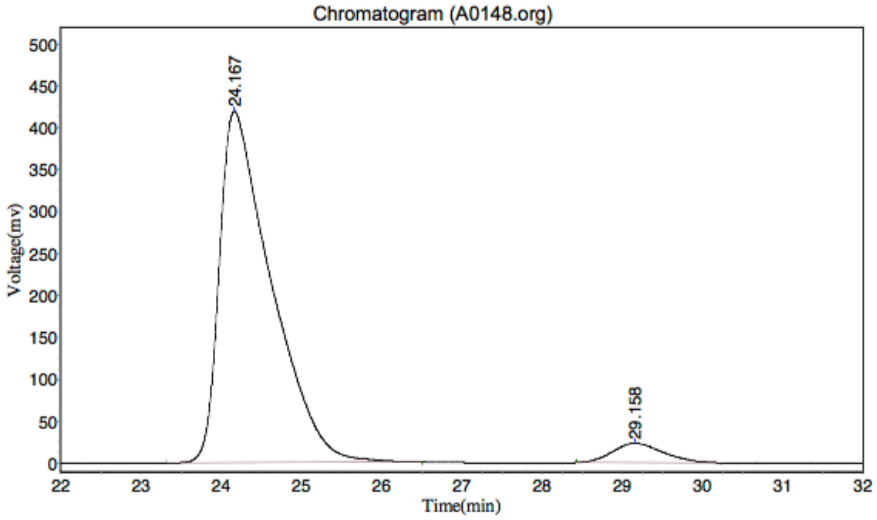

Results

Peak No.	Peak ID	Ret Time	Height	Area	Conc.
1		24.167	418657.625	18765764.000	94.9605
2		29.158	22804.549	995886.125	5.0395
Total			441462.174	19761650.125	100.0000

Figure S24. Chiral HPLC chromatogram of (*S*)-**5h** (90% ee).

5.2.9 1,1,1-Trifluoro-2-(4-fluorophenyl)-3-nitropropan-2-ol (**5i**)

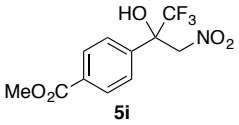

5i

Chiral HPLC conditions: a Hypersil silica column (3 μm, 100 × 4.6 mm) used as a precolumn, which was connected via the standard blue PEEK capillary tubing (L 300 mm, ID 0.01", OD 1/16") to a Daicel Chiralcel IB column (5 μm, 250 × 4.6 mm), *i*-PrOH–*n*-heptane, 10:90, 0.5 mL/min, 25 °C (λ = 230 nm).

Physical state: colorless oil.
Isolated yield: 26.4 mg (90%).

^{1}H NMR (400 MHz, $CDCl_3$) δ/ppm: 8.16–8.07 (m, 2H), 7.70 (d, J = 8.4 Hz, 2H), 5.11, 5.05 (q, AB, J_{AB} = 13.7 Hz, 2H), 4.75 (s, 1H), 3.94 (s, 3H) [**Fig. S265**].
^{13}C NMR (100 MHz, $CDCl_3$) δ/ppm: 166.2, 137.6, 131.8, 130.1, 126.4, 123.2 (q, $^{1}J_{CF}$ = 286.1 Hz), 77.3, 76.2 (q, $^{2}J_{CF}$ = 30.3 Hz), 52.4 [**Fig. S266**].
^{19}F NMR (376 MHz, $CDCl_3$) δ/ppm: −78.32 (s) [**Fig. S267**].
HRMS (ESI-Orbitrap) calcd for $C_{11}H_9NF_3O_5$ $[M-H]^-$ 292.0438 *m*/*z*, found 292.0436 *m*/*z* [**Fig. S103**].

rac-**5i** [**Fig. S25**].
(*S*)-**5i** (92% ee): t_S = 33.80 min (major), t_R = 36.55 min (minor) [**Fig. S26**].

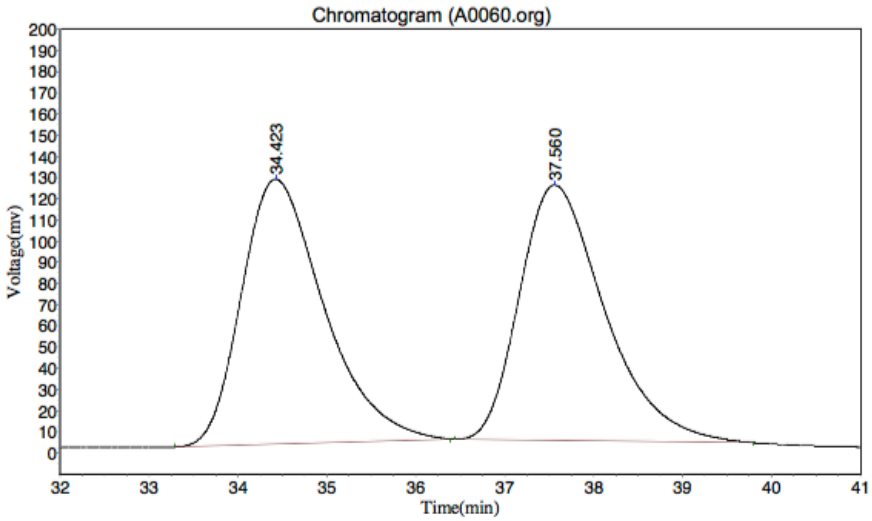

Results

Peak No.	Peak ID	Ret Time	Height	Area	Conc.
1		34.423	124990.063	8045167.500	50.1051
2		37.560	120502.992	8011416.000	49.8949
Total			245493.055	16056583.500	100.0000

Figure S25. Chiral HPLC chromatogram of *rac*-**5i**.

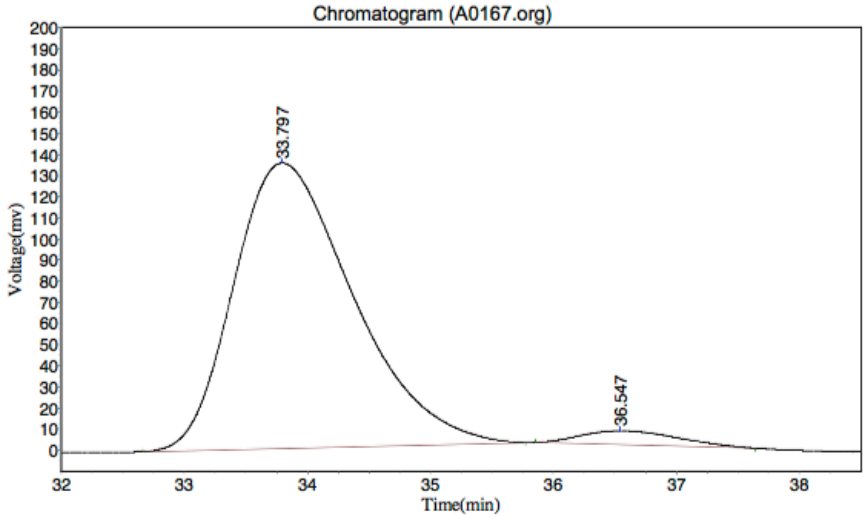

Results

Peak No.	Peak ID	Ret Time	Height	Area	Conc.
1		33.797	135038.594	9106674.000	96.1519
2		36.547	6598.775	364454.125	3.8481
Total			141637.369	9471128.125	100.0000

Figure S26. Chiral HPLC chromatogram of (*S*)-**5i** (92% ee).

5.2.10 2-(2,4-Dimethoxyphenyl)-1,1,1-trifluoro-3-nitropropan-2-ol (**5j**)[35]

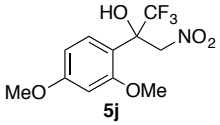

5j

Chiral HPLC conditions: a Hypersil silica column (3 μm, 100 × 4.6 mm) used as a precolumn, which was connected via the standard blue PEEK capillary tubing (L 300 mm, ID 0.01", OD 1/16") to a Phenomenex Lux Amylose-1 column (3 μm, 250 × 4.6 mm), *i*-PrOH–*n*-heptane, 2:98, 0.5 mL/min, 25 °C (λ = 230 nm).

Physical state: yellowish oil.
Isolated yield: 26.6 mg (90%).

^{1}H NMR (400 MHz, $CDCl_3$) δ/ppm: 7.56 (d, *J* = 8.8 Hz, 1H), 6.59 (dd, *J* = 8.8, 2.4 Hz, 1H), 6.51 (d, *J* = 2.4 Hz, 1H), 5.55 (d, *J* = 13.5 Hz, 1H), 4.91 (d, *J* = 13.5 Hz, 1H), 3.91 (d, *J* = 4.3 Hz, 1H), 3.85 (s, 3H), 3.83 (s, 3H) [**Fig. S268**].
^{13}C NMR (100 MHz, $CDCl_3$) δ/ppm: 162.1, 158.2, 130.6, 123.8 (q, $^{1}J_{CF}$ = 286.7 Hz), 112.9, 105.4, 99.7, 77.5, 76.5 (q, $^{2}J_{CF}$ = 30.8 Hz), 55.9, 55.4 [**Fig. S269**].
^{19}F NMR (376 MHz, $CDCl_3$) δ/ppm: −79.37 (s) [**Fig. S270**].
HRMS (ESI-Orbitrap) calcd for $C_{11}H_{11}NF_3O_5$ $[M-H]^-$ 294.0595 *m*/*z*, found 294.0593 *m*/*z* [**Fig. S104**].

rac-**5j** [**Fig. S27**].
(*S*)-**5j** (91% ee): t_S = 54.98 min (major), t_R = 59.23 min (minor) [**Fig. S28**].

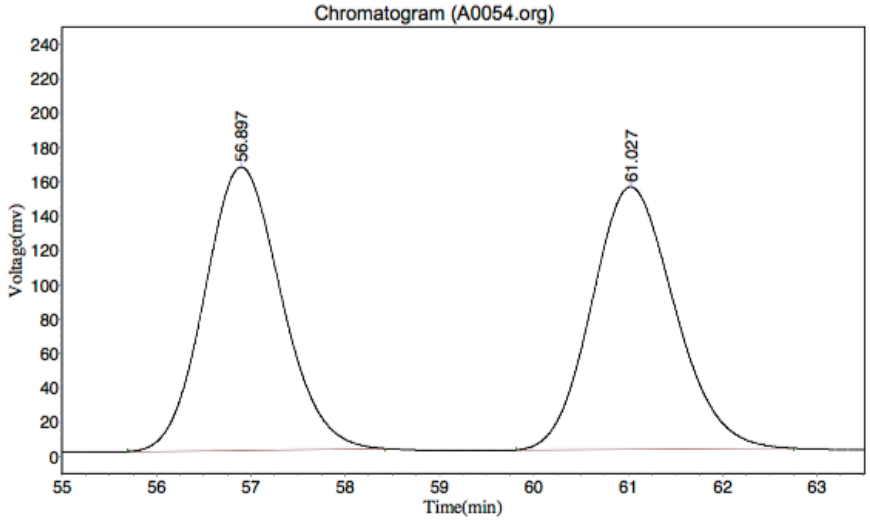

Results

Peak No.	Peak ID	Ret Time	Height	Area	Conc.
1		56.897	165013.609	9301982.000	49.9384
2		61.027	152847.047	9324944.000	50.0616
Total			317860.656	18626926.000	100.0000

Figure S27. Chiral HPLC chromatogram of *rac*-**5j**.

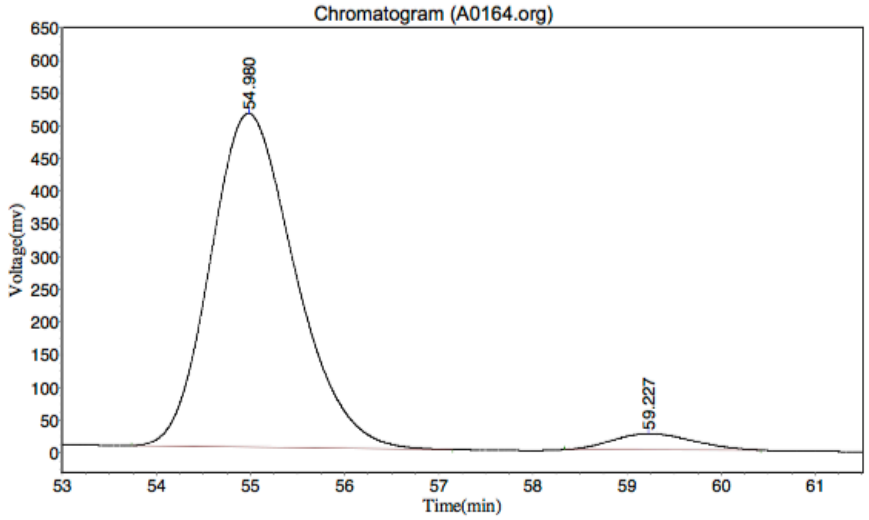

Results

Peak No.	Peak ID	Ret Time	Height	Area	Conc.
1		54.980	509937.188	31799148.000	95.5398
2		59.227	24783.467	1484518.375	4.4602
Total			534720.654	33283666.375	100.0000

Figure S28. Chiral HPLC chromatogram of (*S*)-**5j** (91% ee).

5.2.11. 2-(3,4-Difluorophenyl)-1,1,1-trifluoro-3-nitropropan-2-ol (**5k**)

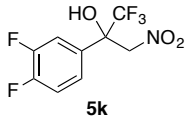

5k

Chiral HPLC conditions: a Hypersil silica column (3 μm, 100 × 4.6 mm) used as a precolumn, which was connected via the standard blue PEEK capillary tubing (L 300 mm, ID 0.01", OD 1/16") to a Daicel Chiralpak OJ-3 column (3 μm, 150 × 4.6 mm), *i*-PrOH–*n*-heptane, 10:90, 0.5 mL/min, 25 °C (λ = 230 nm).

Physical state: yellowish oil.
Isolated yield: 24.7 mg (91%).

^{1}H NMR (400 MHz, $CDCl_3$) δ/ppm: 7.53–7.48 (m, 1H), 7.33–7.23 (m, 2H), 5.03, 5.01 (q, AB, J_{AB} = 13.7 Hz, 2H), 4.72 (s, 1H) [**Fig. S271**].
^{13}C NMR (100 MHz, $CDCl_3$) δ/ppm: 151.3 (dd, J_{CF} = 254.8, 14.0 Hz), 150.5 (dd, J_{CF} = 252.4, 15.4 Hz), 129.9, 123.1 (q, $^{1}J_{CF}$ = 285.5 Hz), 122.6, 118.0 (dd, J_{CF} = 12.5, 5.8 Hz), 116.4 (d, J_{CF} = 19.3 Hz), 77.2, 75.6 (q, $^{2}J_{CF}$ = 30.2 Hz) [**Fig. S272**].
^{19}F NMR (376 MHz, $CDCl_3$) δ/ppm: −78.72 (s, 3F), −134.64 to −134.83 (m, 2F) [**Fig. S273**].
HRMS (ESI-Orbitrap) calcd for $C_9H_5NF_5O_3$ $[M-H]^-$ 270.0195 *m*/*z*, found 270.0195 *m*/*z* [**Fig. S105**].

rac-**5k** [**Fig. S29**].
(*S*)-**5k** (93% ee): t_S = 20.66 min (major), t_R = 23.64 (minor) [**Fig. S30**].

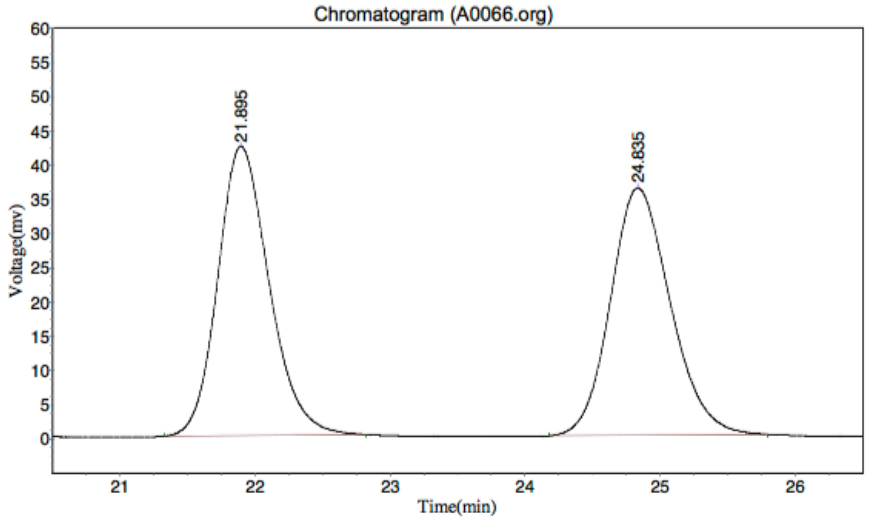

Results

Peak No.	Peak ID	Ret Time	Height	Area	Conc.
1		21.895	42253.316	1117902.750	50.1263
2		24.835	36094.688	1112269.500	49.8737
Total			78348.004	2230172.250	100.0000

Figure S29. Chiral HPLC chromatogram of *rac*-**5k**.

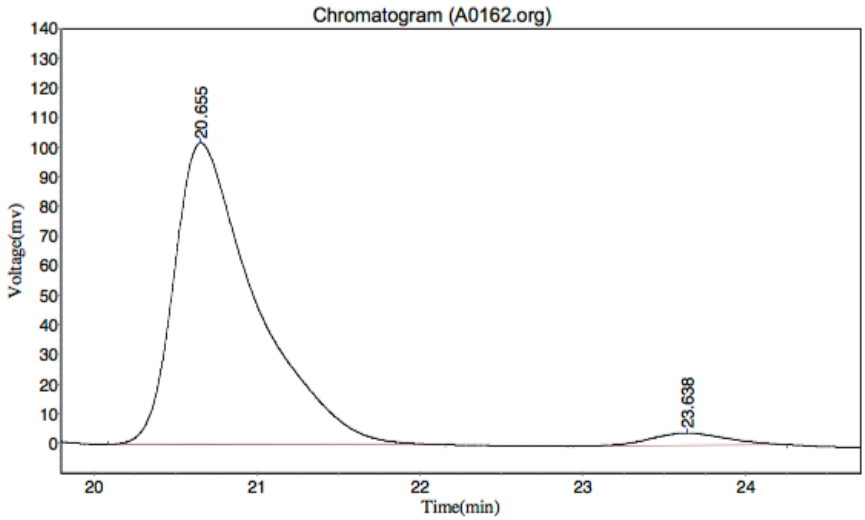

Results

Peak No.	Peak ID	Ret Time	Height	Area	Conc.
1		20.655	101770.352	3549237.000	96.4159
2		23.638	4138.143	131935.859	3.5841
Total			105908.495	3681172.859	100.0000

Figure S30. Chiral HPLC chromatogram of (*S*)-**5k** (93% ee).

5.2.12 2-Benzyl-1,1,1-trifluoro-3-nitropropan-2-ol (**5l**)[34b]

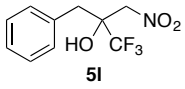

5l

Chiral HPLC conditions: a Hypersil silica column (3 μm, 100 × 4.6 mm) used as a precolumn, which was connected via the standard blue PEEK capillary tubing (L 300 mm, ID 0.01", OD 1/16") to a Daicel Chiralcel OJ-3 column (3 μm, 150 × 4.6 mm), *i*-PrOH–*n*-heptane, 10:90, 0.5 mL/min, 25 °C (λ = 230 nm).

Physical state: colorless oil.
Isolated yield: 23.4 mg (94%).

$[\alpha]^{25}_{D}$ −10 (*c* 0.2, $CHCl_3$).
^{1}H NMR (400 MHz, $CDCl_3$) δ/ppm: 7.40–7.29 (m, 5H), 4.65 (d, *J* = 13.2 Hz, 1H), 4.34 (br s, 1H), 4.24 (dd, *J* = 13.2, 1.0 Hz, 1H), 3.32 (d, *J* = 14.4 Hz, 1H), 2.93 (d, *J* = 14.5 Hz, 1H) [**Fig. S274**].
^{13}C NMR (100 MHz, $CDCl_3$) δ/ppm: 131.9, 130.8, 128.9, 128.1, 124.5 (q, $^1J_{CF}$ = 287.1 Hz), 75.8, 74.8 (q, $^2J_{CF}$ = 28.6 Hz), 38.3 [**Fig. S275**].
^{19}F NMR (376 MHz, $CDCl_3$) δ/ppm: −79.70 (s) [**Fig. S276**].
HRMS (ESI-Orbitrap) calcd for $C_{10}H_9NF_3O_3$ $[M-H]^-$ 248.0540 *m*/*z*, found 248.0539 *m*/*z* [**Fig. S106**].

rac-**5l** [**Fig. S31**].
(*S*)-**5l** (75% ee): t_S = 14.77 min (major), t_R = 16.74 (minor) [**Fig. S32**].

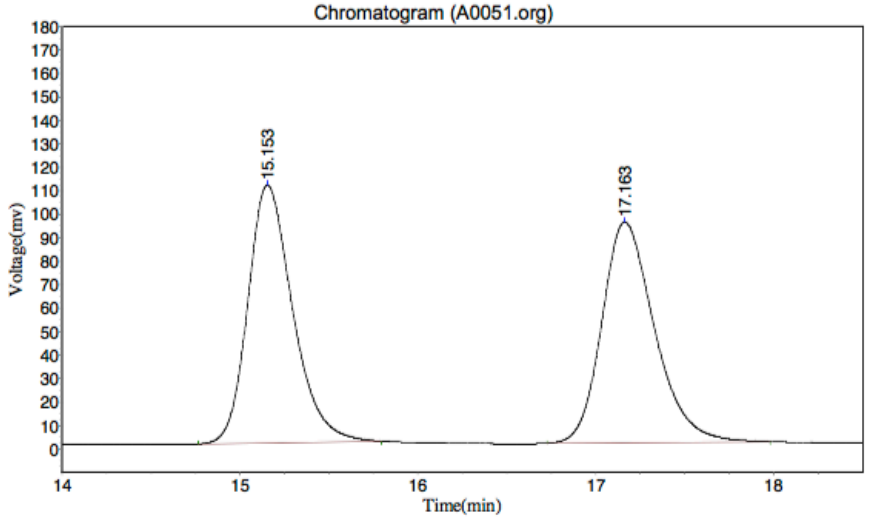

Results

Peak No.	Peak ID	Ret Time	Height	Area	Conc.
1		15.153	110147.727	1926344.125	49.8408
2		17.163	94191.266	1938647.125	50.1592
Total			204338.992	3864991.250	100.0000

Figure S31. Chiral HPLC chromatogram of *rac*-**5l**.

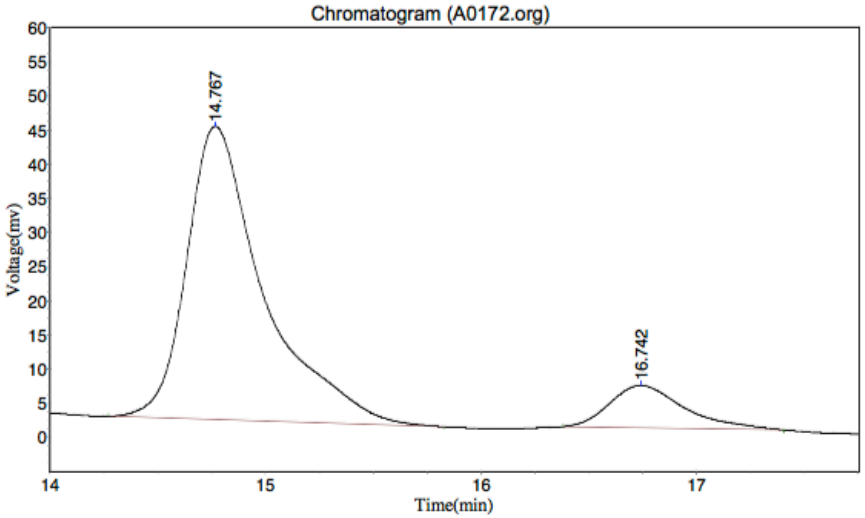

Results

Peak No.	Peak ID	Ret Time	Height	Area	Conc.
1		14.767	42932.996	1061602.500	87.7194
2		16.742	6183.124	148623.000	12.2806
Total			49116.120	1210225.500	100.0000

Figure S32. Chiral HPLC chromatogram of (*S*)-**5l** (75% ee).

5.2.13 1,1,1-Trifluoro-2-(nitromethyl)butan-2-ol (**5m**)[34c]

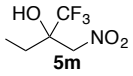

Chiral HPLC conditions: a Hypersil silica column (3 μm, 100 × 4.6 mm) used as a precolumn, which was connected via the standard blue PEEK capillary tubing (L 300 mm, ID 0.01", OD 1/16") to a Daicel Chiralpak OJ-3 column (3 μm, 150 × 4.6 mm), *i*-PrOH–*n*-heptane, 5:95, 0.5 mL/min, 25 °C (λ = 210 nm).

Physical state: colorless oil.
Isolated yield: 15.3 mg (82%).

$[\alpha]^{25}_{D}$ –20 (*c* 0.2, $CHCl_3$).
^{1}H NMR (400 MHz, $CDCl_3$) δ/ppm: 4.68, 4.58 (q, AB, J_{AB} = 13.6 Hz, 2H), 3.97 (s,1H), 1.96 (dq, J = 14.8, 7.4 Hz, 1H), 1.82 (dq, J = 14.8, 7.4 Hz, 1H), 1.08 (t, J = 7.4 Hz, 3H) [**Fig. S277**].
^{13}C NMR (100 MHz, $CDCl_3$) δ/ppm: 124.6 (q, $^1J_{CF}$ = 286.7 Hz), 76.0, 74.8 (q, $^2J_{CF}$ = 28.9 Hz), 26.0, 6.9 [**Fig. S278**].
^{19}F NMR (376 MHz, $CDCl_3$) δ/ppm: −79.29 (s) [**Fig. S279**].
HRMS (ESI-Orbitrap) calcd for $C_5H_7NF_3O_3$ $[M-H]^-$ 186.0384 *m*/*z*, found 186.0384 *m*/*z* [**Fig. S107**].

rac-**5m** [**Fig. S33**].
(*S*)-**5m** (90% ee): t_S = 20.23 min (major), t_R = 21.65 min (minor) [**Fig. S34**].

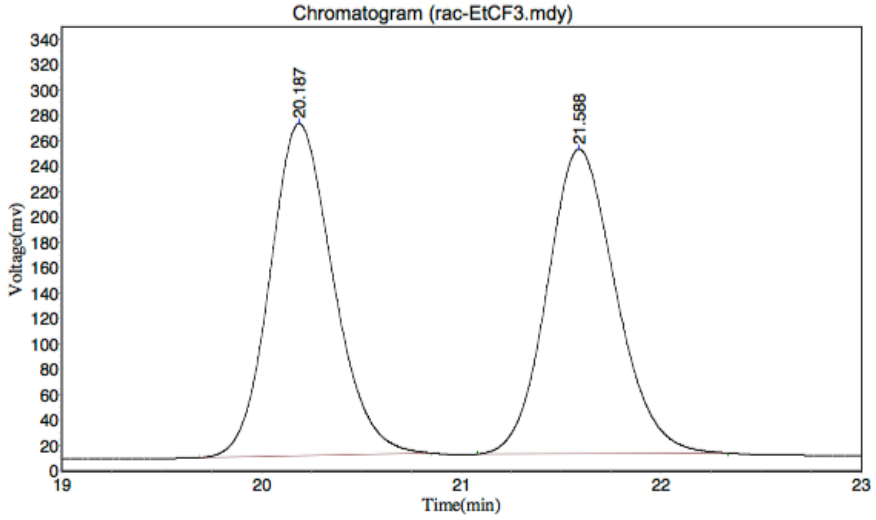

Results

Peak No.	Peak ID	Ret Time	Height	Area	Conc.
1		20.187	261768.156	5729224.000	50.0585
2		21.588	239777.125	5715823.500	49.9415
Total			501545.281	11445047.500	100.0000

Figure S33. Chiral HPLC chromatogram of *rac*-**5m**.

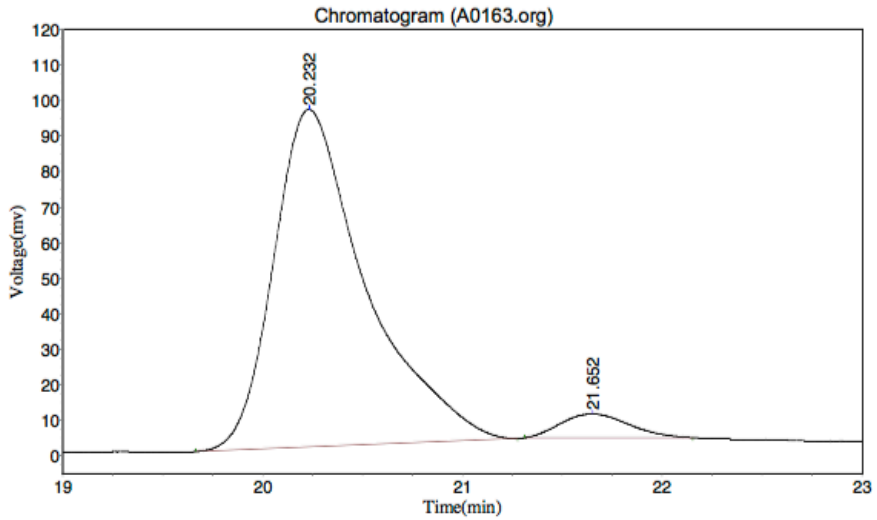

Results

Peak No.	Peak ID	Ret Time	Height	Area	Conc.
1		20.232	95010.531	3048450.750	95.0181
2		21.652	6758.528	159834.891	4.9819
Total			101769.059	3208285.641	100.0000

Figure S34. Chiral HPLC chromatogram of (*S*)-**5m** (90% ee)**.**

5.2.14 (*S*)-1,1-Difluoro-3-nitro-2-phenylpropan-2-ol (**5n**)[34c]

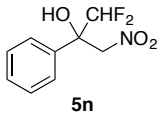

5n

Chiral HPLC conditions: a Hypersil silica column (3 μm, 100 × 4.6 mm) used as a precolumn, which was connected via the standard blue PEEK capillary tubing (L 300 mm, ID 0.01", OD 1/16") to a Daicel Chiralpak IB column (5 μm, 250 × 4.6 mm), *i*-PrOH–*n*-heptane, 20:80, 0.5 mL/min, 25 °C (λ = 230 nm).

Physical state: colorless oil.
Isolated yield: 20.2 mg (93%).

^{1}H NMR (400 MHz, $CDCl_3$) δ/ppm: 7.56–7.53 (m, 2H), 7.48–7.40 (m, 3H), 5.83 (t, $^{2}J_{HF}$ = 55.3 Hz, 1H), 5.06, 4.99 (q, AB, J_{AB} = 13.6 Hz, 2H), 4.20 (s, 1H) [**Fig. S280**].
^{13}C NMR (100 MHz, $CDCl_3$) δ/ppm: 134.8, 129.5, 129.0, 125.9, 115.2 (t, $^{1}J_{CF}$ = 251.4 Hz), 77.3, 75.6 (t, $^{2}J_{CF}$ = 22.2 Hz) [**Fig. S281**].
^{19}F NMR (376 MHz, $CDCl_3$) δ/ppm: −128.34 (dd, $^{2}J_{FF}$ = 280.3 Hz, $^{2}J_{HF}$ = 55.6 Hz, 1F), −130.0 (dd, $^{2}J_{FF}$ = 280.3 Hz, $^{2}J_{HF}$ = 54.9 Hz, 1F) [**Fig. S282**].
HRMS (ESI-Orbitrap) calcd for $C_9H_8NF_2O_3$ $[M-H]^-$ 216.0478 *m*/*z*, found 216.0477 *m*/*z* [**Fig. S108**].

rac-**5n** [**Fig. S35**].
(*S*)-**5n** (97% ee): t_S = 17.78 min (major), t_R = 22.46 (minor) [**Fig. S36**].

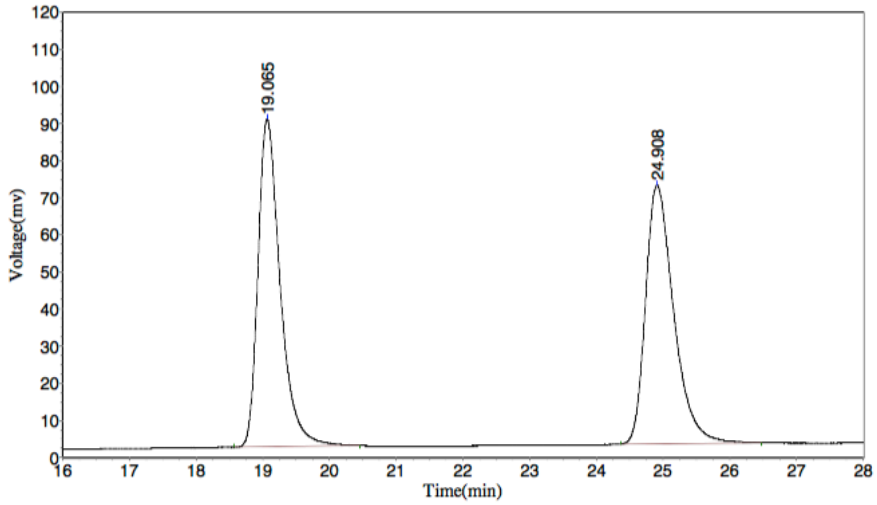

Results

Peak No.	Peak ID	Ret Time	Height	Area	Conc.
1		19.065	88327.977	2042526.125	49.9607
2		24.908	69676.055	2045738.500	50.0393
Total			158004.031	4088264.625	100.0000

Figure S35. Chiral HPLC chromatogram of *rac*-**5n**.

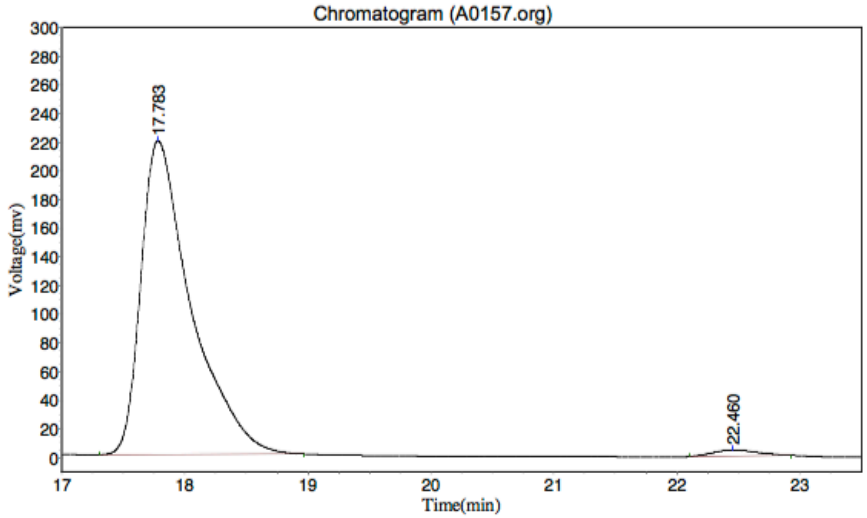

Results

Peak No.	Peak ID	Ret Time	Height	Area	Conc.
1		17.783	218981.859	6204643.500	98.3270
2		22.460	4274.122	105569.305	1.6730
Total			223255.981	6310212.805	100.0000

Figure S36. Chiral HPLC chromatogram of (*S*)-**5n** (97% ee).

5.2.15 (2*S*,3*R*)- and (2*S*,3*S*)-1,1,1-trifluoro-3-nitro-2-phenylbutan-2-ol (**5o**)[34d]

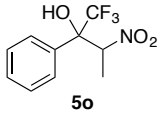

5o

Chiral HPLC conditions: a Hypersil silica column (3 μm, 100 × 4.6 mm) used as a precolumn, which was connected via the standard blue PEEK capillary tubing (L 300 mm, ID 0.01", OD 1/16") to a Daicel Chiralpak IA column (5 μm, 250 × 4.6 mm), *i*-PrOH–*n*-heptane, 1:99, 0.5 mL/min, 25 °C (λ = 230 nm).

Physical state: colorless oil.
Isolated yield: 22.7 mg (91%).

^{1}H NMR (2:3 diastereomeric ratio, 400 MHz, $CDCl_3$) δ/ppm: 7.62–7.57 (m, 3.1H, minor), 7.49–7.42 (m, 5.0H, major), 5.52 (q, *J* = 6.9 Hz, 0.6H, minor), 5.32 (q, *J* = 6.9 Hz, 1.0H, major), 4.73 (br s, 0.9H, major), 4.16 (br s, 0.5H, minor), 1.92 (d, *J* = 6.6 Hz, 1.8H, minor), 1.38 (d, *J* = 6.9 Hz, 3.0H, major) [**Fig. S283**].
^{13}C NMR (2:3 diastereomeric ratio, 100 MHz, $CDCl_3$) δ/ppm: 134.8 (minor), 132.7 (major), 129.8 (minor), 129.6 (major), 129.0 (major), 128.8 (minor), 125.8 (minor), 125.6 (major), 124.2 (q, $^{1}J_{CF}$ = 287.1 Hz, major), 123.3 (q, $^{1}J_{CF}$ = 286.1 Hz, minor), 85.5 (minor), 83.7 (major), 77.8 (q, $^{2}J_{CF}$ = 28.9 Hz, minor), 77.7 (q, $^{2}J_{CF}$ = 28.9 Hz, major), 15.4 (minor), 14.8 (major) [**Fig. S284**].
^{19}F NMR (2:3 diastereomeric ratio, 376 MHz, $CDCl_3$) δ/ppm: –74.84 (s, 3.0F, major), –76.77 (s, 1.8F, minor) [**Fig. S285**].
HRMS (ESI-Q-TOF) calcd for $C_{10}H_9F_3NO_3$ $[M–H]^-$ 248.0540 *m*/*z*, found 248.0509 *m*/*z* [**Fig. S109**].

rac-**5o** (a mixture of diastereomers) [**Fig. S37**].
(2*S*,3*R*)-**5o** (77% ee) and (2*S*,3*S*)-**5o** (90% ee): t_{SR} = 21.09 min (major), t_{RS} = 22.93 min (minor), t_{RR} = 44.61 min (minor), t_{SS} = 79.86 min (major) [**Fig. S38**].

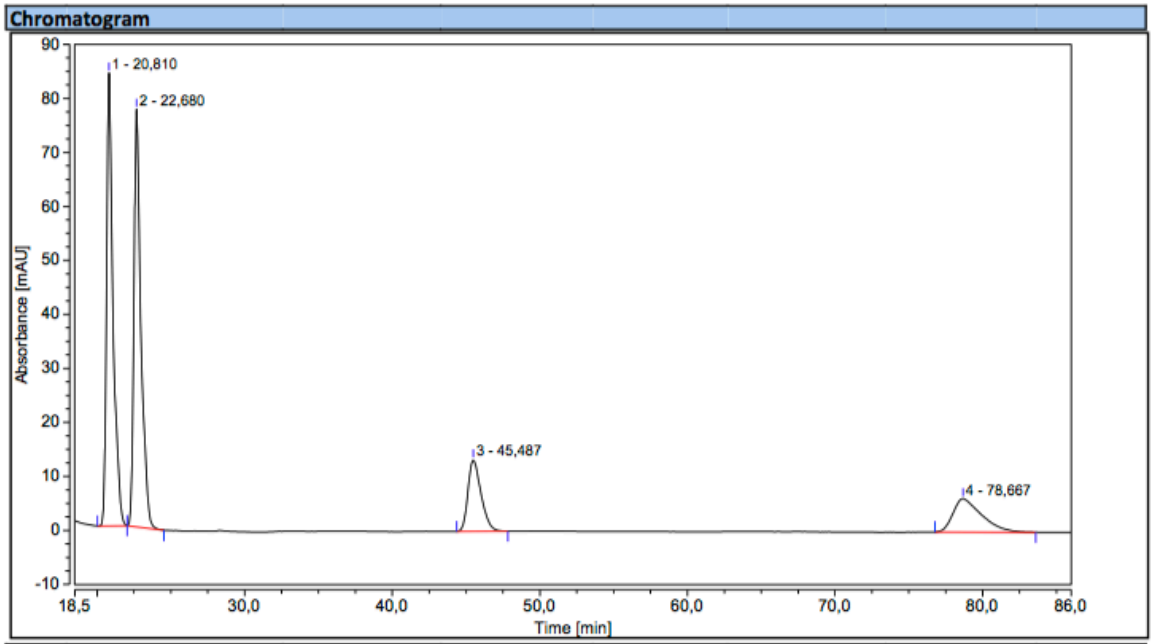

Integration Results

No.	Peak Name	Retention Time min	Area mAU*min	Height mAU	Relative Area %	Relative Height %	Amount n.a.
1		20,810	42,388	83,836	37,86	46,43	n.a.
2		22,680	42,186	77,308	37,68	42,82	n.a.
3		45,487	13,633	13,231	12,18	7,33	n.a.
4		78,667	13,741	6,171	12,27	3,42	n.a.
Total:			**111,948**	**180,547**	**100,00**	**100,00**	

Figure S37. Chiral HPLC chromatogram of (2*S*,3*R*)-**5o**, (2*R*,3*S*)-**5o** and (2*R*,3*R*)-**5o**, (2*S*,3*S*)-**5o**.

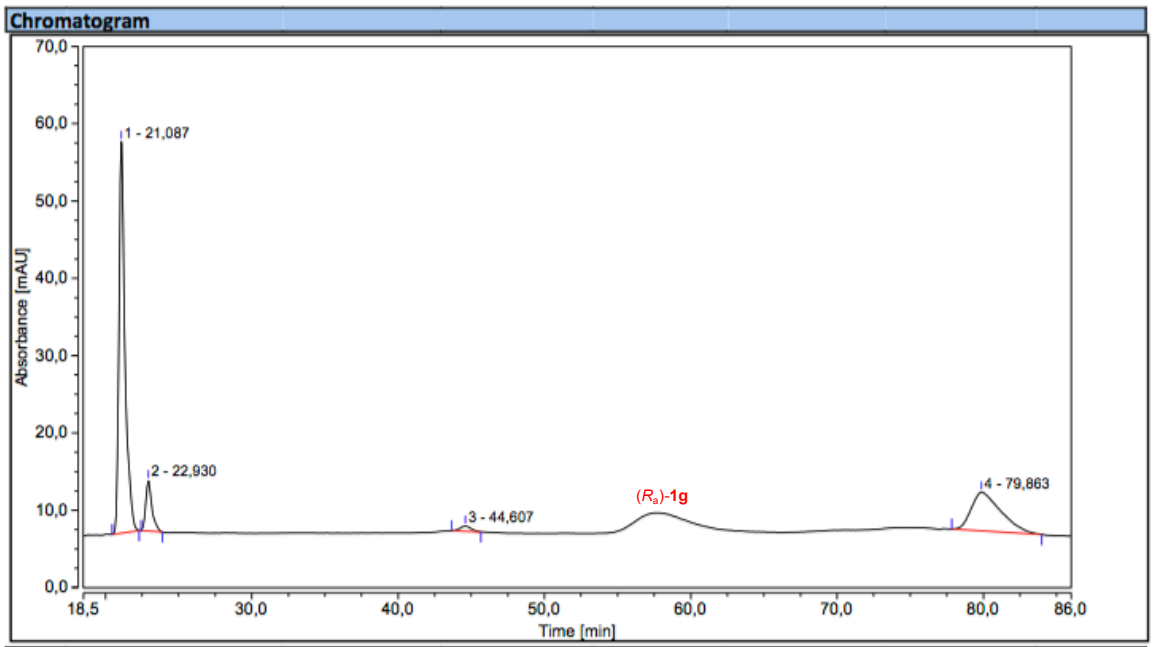

Integration Results

No.	Peak Name	Retention Time min	Area mAU*min	Height mAU	Relative Area %	Relative Height %	Amount n.a.
1		21,087	24,055	50,649	60,67	80,52	n.a.
2		22,930	3,198	6,552	8,07	10,42	n.a.
3		44,607	0,604	0,679	1,52	1,08	n.a.
4		79,863	11,793	5,026	29,74	7,99	n.a.
Total:			**39,650**	**62,905**	**100,00**	**100,00**	

Figure S38. Chiral HPLC chromatogram of the crude mixture of (2*S*,3*R*)-**5o** (77% ee) and (2*S*,3*S*)-**5o** (90% ee).

6. Synthesis of CF_3-Tethered (*S*)-Halostachine

6.1 (*S*)-3-Amino-1,1,1-trifluoro-2-phenylpropan-2-ol (6)[34b]

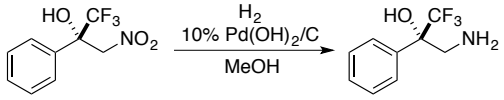

(*S*)-**5a** (*S*)-**6**

(*S*)-**5a** (280 mg, 1.2 mmol) dissolved in MeOH (12 mL) was hydrogenated over 10% $Pd(OH)_2/C$ (72 mg) under atmosphere of H_2 (15 psi).
After the TLC analysis (SiO_2) EtOAc–*n*-hexane (1:5) revealed a complete disappearance of the starting material (3 h), the mixture was filtered through a Celite pad and evaporated in vacuo.

Physical state: white solid.
Isolated yield: 210 mg (86%).

mp 66–68 °C, lit.[36] 63–66 °C.
$[\alpha]^{25}_D$ +40 (*c* 0.2, $CHCl_3$).
^{1}H NMR (400 MHz, $CDCl_3$) δ/ppm: 7.60–7.58 (m, 2H), 7.43–7.35 (m, 3H), 3.57 (d, J = 10.6 Hz, 1H), 3.06 (d, J = 10.6 Hz, 1H), 2.72 (br s, 2H) [**Fig. S286**].
^{13}C NMR (100 MHz, $CDCl_3$) δ/ppm: 137.4, 128.5, 128.3, 126.2, 125.8 (q, $^1J_{CF}$ = 286.1 Hz), 73.9 (q, $^2J_{CF}$ = 27.3 Hz), 45.4 [**Fig. S287**].
^{19}F NMR (376 MHz, $CDCl_3$) δ/ppm: −78.25 (s) [**Fig. S288**].
IR (neat) $\tilde{\nu}$/cm^{-1}: 3361*w*, 2983*w*, 1604*w*, 1454*m*, 1272*m*, 1190*m*, 1150*s*, 1073*m*, 952*m*, 916*w*, 762*m*, 733*w*, 698*m*.
HRMS (ESI-Orbitrap) calcd for $C_9H_{11}F_3NO$ $[M+H]^+$ 206.0787 *m*/*z*, found 206.0790 *m*/*z* [**Fig. S110**].

Stereochemical assignment: The absolute configuration of (*S*)-**6** was established by chemical correlation with (*S*)-**5a** and by comparison of the sign of specific rotation with the literature value.[34b]

6.2 (*S*)-*N*-(3,3,3-Trifluoro-2-hydroxy-2-phenylpropyl)formamide (7)

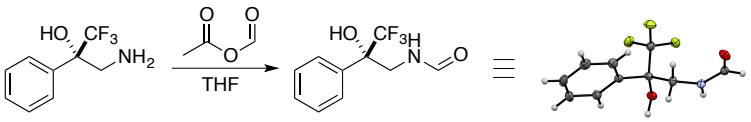

(*S*)-**6** (*S*)-**7** **CCDC 1904739**

Step 1. Acetic acid anhydride (0.2 mL, 2.1 mmol) was treated dropwise with 98% formic acid (2.5 mmol, 0.1 mL) at 0 °C under Ar atmosphere. The resulting solution was left to reach the ambient temperature and then heated and stirred at 50–60 °C for 2h.[37]

Step 2. A solution of (*S*)-**6** (200 mg, 0.1 mmol) in THF (2 mL) was added dropwise to the above acetic formic anhydride at 0 °C under atmosphere of Ar and the resulting mixture was left to stir overnight at ambient temperature.

After the TLC analysis (SiO_2) EtOAc–*n*-hexane (1:2) revealed a complete disappearance of the starting material, the volatiles were evaporated and the residue was dissolved in CH_2Cl_2 and repetitively extracted with saturated aqueous solution of $NaHCO_3$, brine, dried over anhydrous Na_2SO_4, filtered and evaporated in vacuo. The crude product was further purified by a column chromatography (SiO_2) EtOAc–*n*-hexane (1:1).

Physical state: colorless crystalline solid.
Isolated yield: 143 mg (63%).

mp 95–97 °C.
$[\alpha]^{25}_D$ +64 (*c* 0.2, $CHCl_3$).
^{1}H NMR (400 MHz, $CDCl_3$) δ/ppm: 8.08 (s, 1H), 7.61–7.59 (m, 2H), 7.45–7.40 (m, 3H), 5.98 (br s, 1H), 5.09 (s, 1H), 4.15 (dd, *J* = 14.7, 6.4 Hz, 1H), 3.87 (dd, *J* = 14.7, 6.1 Hz, 1H) [**Fig. S289**].
^{13}C NMR (15:1 rotamer ratio, signals correspond to major rotamer, 100 MHz, $CDCl_3$) δ/ppm: 163.7, 135.2, 129.0, 128.6, 126.5, 124.8 (q, $^1J_{CF}$ = 286.1 Hz), 77.6 (q, $^2J_{CF}$ = 27.6 Hz), 44.2 [**Fig. S290**].
^{19}F NMR (15:1 rotamer ratio, signal corresponds to major rotamer, 376 MHz, $CDCl_3$) δ/ppm: −78.22 (s). [**Fig. S291**].
IR (neat) $\tilde{\nu}$/cm^{-1}: 3342*w*, 3129*m*, 2890*m*, 1650*s*, 1542*m*, 1445*w*, 1375*m*, 1283*m*, 1236*m*, 1159*s*, 1138*s*, 1087*m*, 1012*w*, 963*m*, 757*m*, 698*s*, 633*s*.
HRMS (ESI-Q-TOF) calcd for $C_{10}H_9F_3NO_2$ $[M–H]^-$ 232.0591 *m*/*z*, found 232.0598 *m*/*z* [**Fig. S111**].

Stereochemical assignment: The absolute configuration of (*S*)-**7** was established by chemical correlation with (*S*)-**5a** and (*S*)-**6**.

6.3 (*S*)-3,3,3-Trifluoro-2-hydroxy-*N*-methyl-2-phenylpropan-1-aminium chloride (8·HCl)

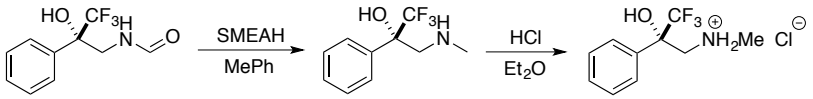

(*S*)-**7** (*S*)-**8** (*S*)-**8**·HCl

To a solution of (*S*)-**7** (130 mg, 0.56 mmol) in dry toluene (3 mL), 60% SMEAH in toluene (2.7 mL, 15 equiv) was added dropwise at 20 °C. The resulting mixture was stirred under Ar at rt for 48 h. After TLC (SiO_2) EtOAc–*n*-hexane–Et_2NH (1:9:0.1) revealed the complete consumption of the starting material, the mixture was cooled and quenched by a dropwise addition of 5M aqueous NaOH (10 mL). Aqueous phase was repetitively extracted with toluene and the combined organic extracts were dried over anhydrous Na_2SO_4, filtered and evaporated in vacuo. The resulting yellow oil was treated with saturated solution of HCl in Et_2O and isolated as hydrochloride (*S*)-**8**·HCl.

Physical state: white hygroscopic solid.
Isolated yield: 80 mg (56%).

$[\alpha]^{25}_D$ +25 (*c* 0.6, MeOH).
mp 112–115 °C.
^{1}H NMR (400 MHz, DMSO-d_6) δ/ppm: 8.77 (br s, 1H), 8.41 (br s, 1H), 7.68 (br s, 1H), 7.63–7.60 (m, 2H), 7.45–7.42 (m, 3H), 3.85–3.81 (m, 1H), 3.66–3.64 (m, 1H), 2.46 (s, 3H) [**Fig. S292**].
^{13}C NMR (100 MHz, DMSO-d_6) δ/ppm: 134.1, 129.3, 128.5, 126.8, 124.6 (q, $^1J_{CF}$ = 287.1 Hz), 74.4 (q, $^2J_{CF}$ = 28.9 Hz), 51.3, 34.6 [**Fig. S293**].
^{19}F NMR (376 MHz, DMSO-d_6) δ/ppm: –77.38 (s) [**Fig. S294**].
IR (neat) $\tilde{\nu}$/cm^{-1}: 3226*w*, 2965*w*, 2762*w*, 1467*w*, 1453*w*, 1276*m*, 1199*m*, 1150*s*, 1019*m*, 937*w*, 897*w*, 764*m*, 701*s*, 632*m*.
HRMS (ESI-Q-TOF) calcd for $C_{10}H_{13}F_3NO$ $[M–HCl+H]^+$ 220.0944 *m*/*z*, found 220.0918 *m*/*z* [**Fig. S112**].

Stereochemical assignment: The absolute configuration of (*S*)-**8**·HCl was established by chemical correlation with (*S*)-**5a** and (*S*)-**6**.

7. Non-Linear Effect

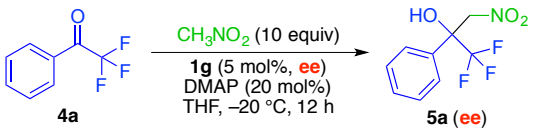

A nonlinear effect was surveyed using 1,1,1-trifluoroacetophenone (**4a**) as a model substrate under the following reaction conditions: **4a** (14 µL, 0.1 mmol), nitromethane (53.5 µL, 1.0 mmol), catalyst **1g** (4.6 mg, 5.0 µmol), DMAP (2.4 mg, 20 µmol) in THF (100 µL) at –20 °C (12 h). Catalyst **1g** of the corresponding enantiomeric excess (0%, 23%, 47%, 71%, and >99% ee) was prepared by mixing the racemic form of **1g** with the (R_a)-enantiomer in the proper weight ratio. The obtained results are summarized in **Tab. S5** (for chromatograms of **Entries 1** and **5**, please see **Fig. S9–10**).

entry	ee of 1g (R_a)	ee of 5a (S)	Figure
1	0 (±)	0 (±)	**S9**
2	23.2	20.0	**S40**
3	47.4	45.8	**S41**
4	70.5	66.3	**S42**
5	99.9	94.8	**S10**

Table S5. Experimental data used to generate **Fig. S39**.

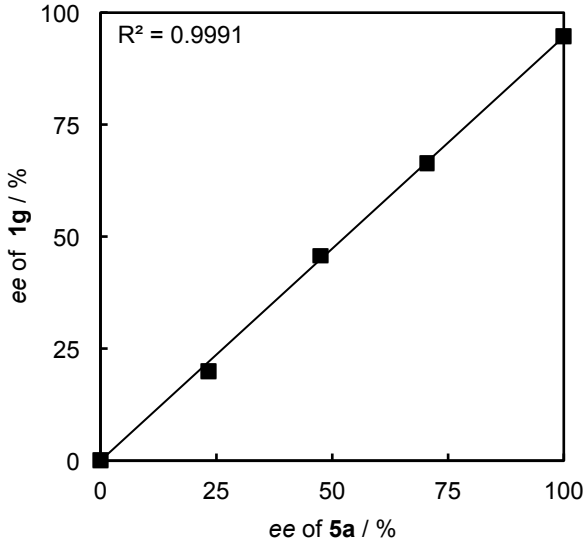

Figure S39. A relationship between catalyst ee (**1g**) and product ee (**5a**) for the asymmetric Henry reaction of nitromethane and 1,1,1-trifluoroacetophenone (**4a**).

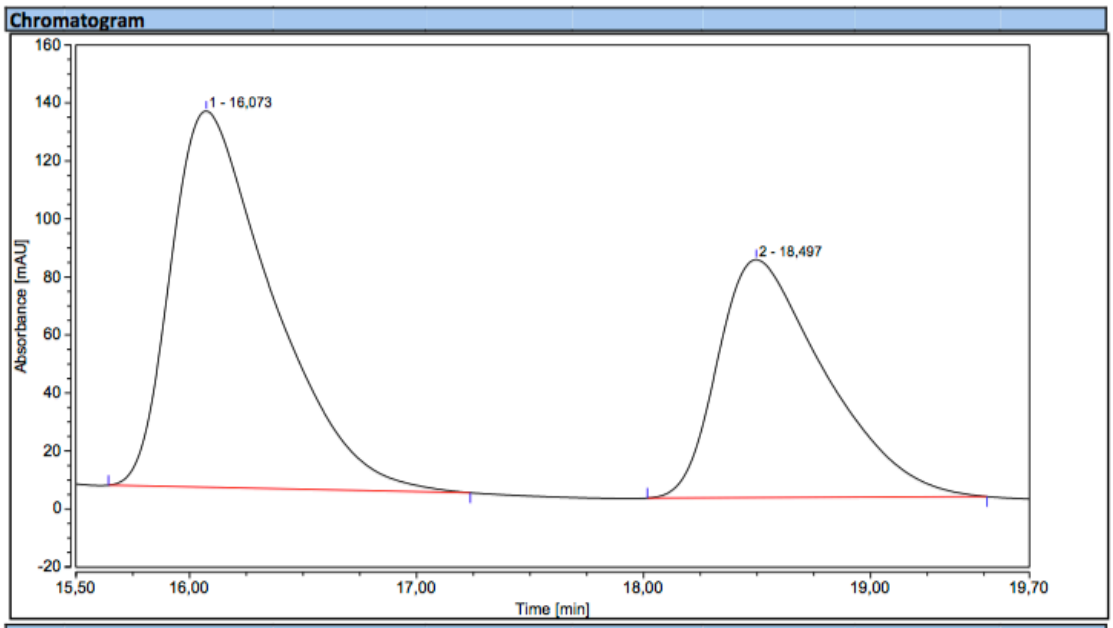

Integration Results

No.	Peak Name	Retention Time min	Area mAU*min	Height mAU	Relative Area %	Relative Height %	Amount n.a.
1		16,073	67,480	129,674	59,98	61,27	n.a.
2		18,497	45,033	81,985	40,02	38,73	n.a.
Total:			**112,513**	**211,659**	**100,00**	**100,00**	

Figure S40. Product (*S*)-**5a** (ee = 20%) of the asymmetric Henry reaction catalyzed by (R_a)-**1g** (ee = 23%).

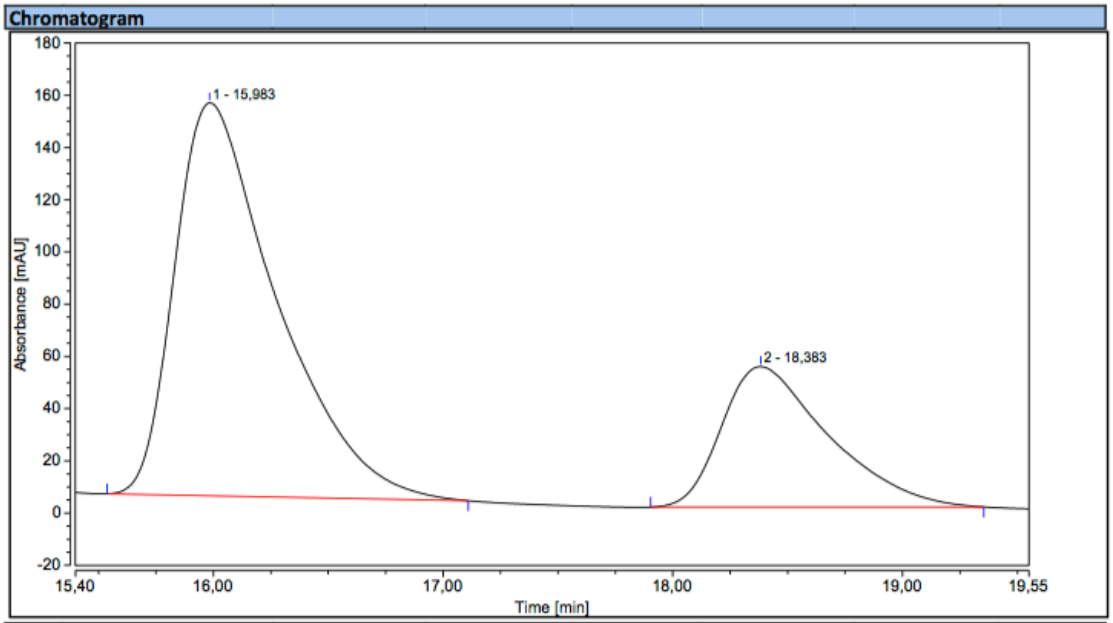

Integration Results

No.	Peak Name	Retention Time min	Area mAU*min	Height mAU	Relative Area %	Relative Height %	Amount n.a.
1		15,983	77,423	150,434	72,86	73,67	n.a.
2		18,383	28,837	53,765	27,14	26,33	n.a.
Total:			**106,260**	**204,199**	**100,00**	**100,00**	

Figure S41. Product (*S*)-**5a** (ee = 46%) of the asymmetric Henry reaction catalyzed by (R_a)-**1g** (ee = 47%).

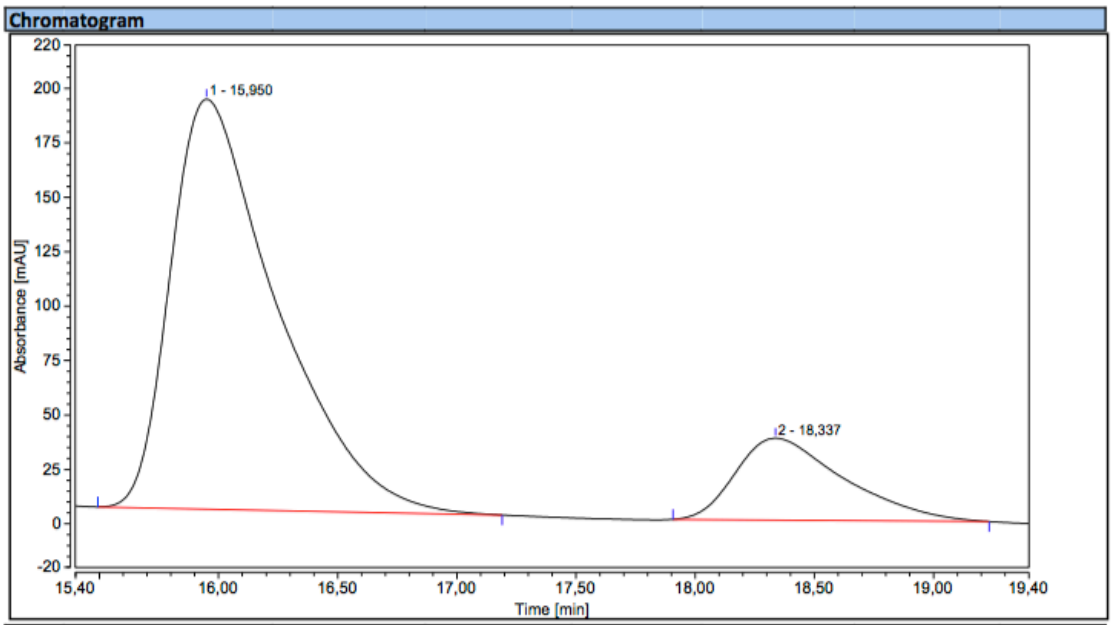

Integration Results

No.	Peak Name	Retention Time min	Area mAU*min	Height mAU	Relative Area %	Relative Height %	Amount n.a.
1		15,950	97,411	188,272	83,15	83,35	n.a.
2		18,337	19,745	37,600	16,85	16,65	n.a.
Total:			**117,156**	**225,873**	**100,00**	**100,00**	

Figure S42. Product (*S*)-**5a** (ee = 66%) of the asymmetric Henry reaction catalyzed by (R_a)-**1g** (ee = 71%).

8. References

1. Kudoh, T.; Ishikawa, T.; Shimizu, Y.; Saito, S. *Org. Lett.* **2003**, *5*, 3875–3878.
2. Otevrel, J.; Bobal, P. *Synthesis.* **2017**, *49*, 593–603.
3. Otevrel, J.; Bobal, P. *J. Org. Chem.* **2017**, *82*, 8342–8358.
4. Sheldrick, G. M. *Acta Crystallogr. Sect. A.* **2008**, *64*, 112–122.
5. Fleming, E. M.; McCabe, T.; Connon, J. S. *Tetrahedron Lett.* **2006**, *47*, 7037–7042.
6. Scarborough, C. C.; McDonald, R. I.; Hartmann, C.; Sazama, G. T.; Bergant, A.; Stahl, S. S. *J. Org. Chem.* **2009**, *74*, 2613–2615.
7. Herrera, R. P.; Monge, D.; Martin-Zamora, E.; Fernandez, R.; Lassaletta, J. M. *Org. Lett.* **2007**, *9*, 3303–3306.
8. Schneider, J. F.; Lauber, M. B.; Muhr, V.; Kratzer, D.; Paradies, J. *Org. Biomol. Chem.* **2011**, *9*, 4323–4327.
9. Matsumoto, K.; Dougomori, K.; Tachikawa, S.; Ishii, T.; Shindo, M. *Org. Lett.* **2014**, *16*, 4754−4757.
10. Vyskocil, S.; Smrcina, M.; Lorenc, M.; Tislerova, I.; Brooks, R. D.; Kulagowski, J. J.; Langer, V.; Farrugia, L. J.; Kocovsky, P. *J. Org. Chem* . **2001,** *66,* 1359–1365.
11. (a) Yonson, N.; Yim, J. C.-H.; Schafer, L. L. *Inorg. Chim. Acta.* **2014**, *422*, 14–20; (b) Kanoh, S.; Goka, S.; Murose, N.; Kubo, H.; Kondo, M.; Sugino, T.; Motoi, M.; Suda, H. *Polym. J.* **1987**, *19*, 1047–1065.
12. Periasamy, M.; Anwar, S.; Reddy, M. R. *Indian J. Chem.* **2009**, *48B*, 1261–1273.
13. (a) Kito, T.; Ota, K. *Chem. Lett.* **1975**, *10*, 1019–1020; (b) Dada, R.; Singh, G.; Pareek, A.; Kausar, S.; Yaragorla, S. *Tetrahedron Lett.* **2016**, *57*, 3739–3742.
14. (a) Carswell, E. L.; Kerra, W. J.; McArthur, D.; Pazicky, M.; Watson, A. J. B. *Tetrahedron.* **2014**, *70*, 7344–7349; (b) Smith, H. E.; Cooper, N. E. *J. Org. Chem.* **1970**, *35*, 2212–2215.
15. (a) Cardellicchio, C.; Ciccarella, G.; Naso, F.; Schingaro, E.; Scordari, F. *Tetrahedron: Asymmetry.* **1998**, *9*, 3667–3675; (b) Bian, G.; Yang, S.; Huang, H.; Song, L. *Synthesis.* **2013**, 45, 899–902.
16. Kanemitsu, T.; Toyoshima, E.; Miyazaki, M.; Nagata, K.; Itoh, T. *Heterocycles.* **2010**, *81*, 2781–2792.
17. (a) Korber, K.; Tang, W.; Hu, X.; Zhang, X. *Tetrahedron Lett.* **2002**, *43*, 7163–7165; (b) Smrcina, M.; Vyskocil, S. Polivkova, J.; Polakova, J.; Kocovsky, P. *Collect. Czech Chem. Commun.* **1996**, *61*, 1520–1524; (c) Bhor, M. D.; Nandurkar, N. S.; Bhanushali, M. J.; Bhanage, B. M. *Catal. Lett.* **2006**, *112*, 45–50.
18. (a) Hassan, F.; Kawamoto, M.; Salikolimi, K.; Hashizume, D.; Hirose, T.; Ito, Y. *Tetrahedron Lett.* **2018**, *59*, 99–102; (b) Ding, K.; Wang, Y.; Yun, H.; Liu, J.; Wu, Y.; Terada, M.; Okubo, Y.; Mikami, K. *Chem. Eur. J.* **1999**, 5, 1734–1737.
19. Marques‐Lopez, E.; Alcaine, A.; Tejero, T. Herrera, R. P. *Eur. J. Org. Chem.* **2011**, 3700–3705.
20. (a) Mukhlall, J. A:; Noll, B. C.; Hersh, W. H. *J. Sulfur Chem*. **2011**, *32*, 199–212; (b) Kerdesky, F. A. J.; Brooks, C. D. W.; Hulkower, K. I.; Bouska, J. B.; Bell, R. L. *Bioorg. Med. Chem.* **1997**, *5*, 393–396.
21. Scheidt, T.; Land, H.; Anderson, M.; Chen, Y.; Berglund, P.; Yi, D.; Fessner, W.-D. *Adv. Synth. Catal.* **2015**, *357*, 1721–1731.
22. (a) Tsukano, C.; Yokouchi, S.; Girard, A.-L.; Kuribayashi, T; Sakamoto, S. Enomoto, T.; Takemoto, Y. *Org. Biomol. Chem.* **2012**, *10*, 6074–6086; (b) Pande, C. S; Rudick, J.; Ornstein, L.; Schwartz, I. L.; Walter, R. *Mol. Pharmacol.* **1969**, *5*, 227–235.
23. Robertson, M. J.; De Iuliis, G. N.; Maeder, M.; Lawrance, G. A. *Inorg. Chim. Acta.* **2004**, *357*, 557–570.
24. Sohtome, Y.; Takemura, N.; Takagi, R.; Hashimoto, Y.; Nagasawa, K. *Tetrahedron.* **2008**, *64*, 9423–9429.
25. (a) Dales, N.; Zhang, Z.; Fu, J.; Hou, D.; Sun, S.; Kodumuru, V.; Pokrovskaia, N. (Novartis AG, Switz.; Xenon Pharmaceuticals Inc.) *Patent* WO2009156484A2, **2009**; *Chem. Abstr.* **2009**, *152*, 119439; (b) Kato; T.; Tsuchiya, Y. *Agric. Biol. Chem.* **1962**, *26*, 467–472.
26. (a) Mittal, N.; Lippert, K. M.; Kanta De, C.; Klauber, E. G.; Emge, T. J.; Schreiner, P. R.; Seidel, D. *J. Am. Chem. Soc.* **2015**, *137*, 5748–5758; (b) Lu, A.; Wang, Z.; Zhou, Z.; Chen, J.; Wang, Q. *J. Agric. Food Chem.* **2015**, *63*, 1378–1384.
27. Wang, W.; Miyamoto, T.; Miki, T.; Ikemoto, T. (Sumitomo Chemical Company, Ltd., Japan) *Patent* WO 2014192841, **2014**; *Chem. Abstr.* **2014**, *162*, 37328.
28. Wu, M. Y.; He, W. W.; Liu, X. Y.; Tan, B. *Angew. Chem. Int. Ed.* **2015**, *54*, 9409–9413.

29. (a) Sibi, M. P.; Itoh, K. *J. Am. Chem. Soc.* **2007**, *129*, 8064–8065; (b) Brase, S.; Volz, N.; Glaser, F.; Nieger, M. *Beilstein J. Org. Chem.* **2012**, *8*, 1385–1392.
30. (a) Stibor, I.; Holakovsky, R.; Mustafina, A. R.; Lhotak, P. *Coll. Czech. Chem. Commun.* **2004**, *69*, 365–383; (b) Curinova, P.; Dracinsky, M.; Jakubec, M.; Tlusty, M.; Janku, K.; Izak, P.; Holakovsky, R. *Chirality* **2018**, *30*, 1–9.
31. Specklin, D.; Hild, F.; Chen, L.; Thevenin, L.; Munch, M.; Dumas, F.; Le Bideau, F.; Dagorne, S. *ChemCatChem* **2017**, *9*, 3041–3046.
32. (a) Bae, I. H.; Son, J. B.; Han, S. M.; Kwak, E. J.; Kim, H. S.; Song, J. Y.; Byun, E. Y.; Jun, S. A.; Ahn, Y. G.; Suh, K. H. (Hanmi Pharm Co., Ltd., S. Korea) *Patent* WO 2013100632A1, **2013**; *Chem. Abstr.* **2013**, *159*, 197000; (b) Kelly, C. B.; Mercadante, M. A.; Hamlin, T. A.; Fletcher, M. H.; Leadbeater, N. E. *J. Org. Chem.* **2012**, *77*, 8131–8141.
33. Emer, E; Twilton, J.; Tredwell, M.; Calderwood, S.; Collier, T. L.; Liegault, B.; Taillefer, M; Gouverneur, V. *Org. Lett.* **2014**, *16*, 6004–6007; (b) Uno, H.; Nibu, N.; Misobe, N. *Bull. Chem. Soc. Jpn.* **1999**, *72*, 1365–1375.
34. (a) Palacio, C.; Connon, S. J. *Org. Lett.* **2011**, *13*, 1298–1301; (b) Tur, F.; Saa, J. M. *Org. Lett.* **2007**, *9*, 5079–5082; (c) Bandini, M.; Sinisi, R.; Umani-Ronchi, A. *Chem. Commun.* **2008**, 4360–4362; (d) Karasawa, T.; Kumagai, N.; Shibasaki, M. *Org. Lett.* **2018**, *20*, 308−311.
35. Das, A.; Choudhary, M. K.; Kureshy, R. I.; Jana, K.; Verma, S.; Khan, N. H.; Abdi, S. H. R.; Bajaj, H. C.; Ganguly, B. *Tetrahedron.* **2015**, *71*, 5229–5237.
36. Tur, F.; Mansilla, J.; Lillo, V. J.; Saa, J. M. *Synthesis*. **2010**, 11, 1909–1923.
37. Krishnamurthy, S. *Tetrahedron Lett.* **1982,** *23*, 3315–3318.

9. Crystallographic, HRMS, and NMR Data

Compound: 7.
Crystal description: colorless prism.
Crystallization technique: vapor diffusion, a solution of **7** (20 mg) in chloroform (1 mL) in a loosely capped vial was placed into a sealed container filled with light petroleum (bp 40–65 °C) as an anti-solvent and left undisturbed at ambient temperature for 3 weeks.
CCDC-1904739 contains the supplementary crystallographic data [**Fig. S43**].
These data can be obtained free of charge from The Cambridge Crystallographic Data Centre via: www.ccdc.cam.ac.uk/data_request/cif.

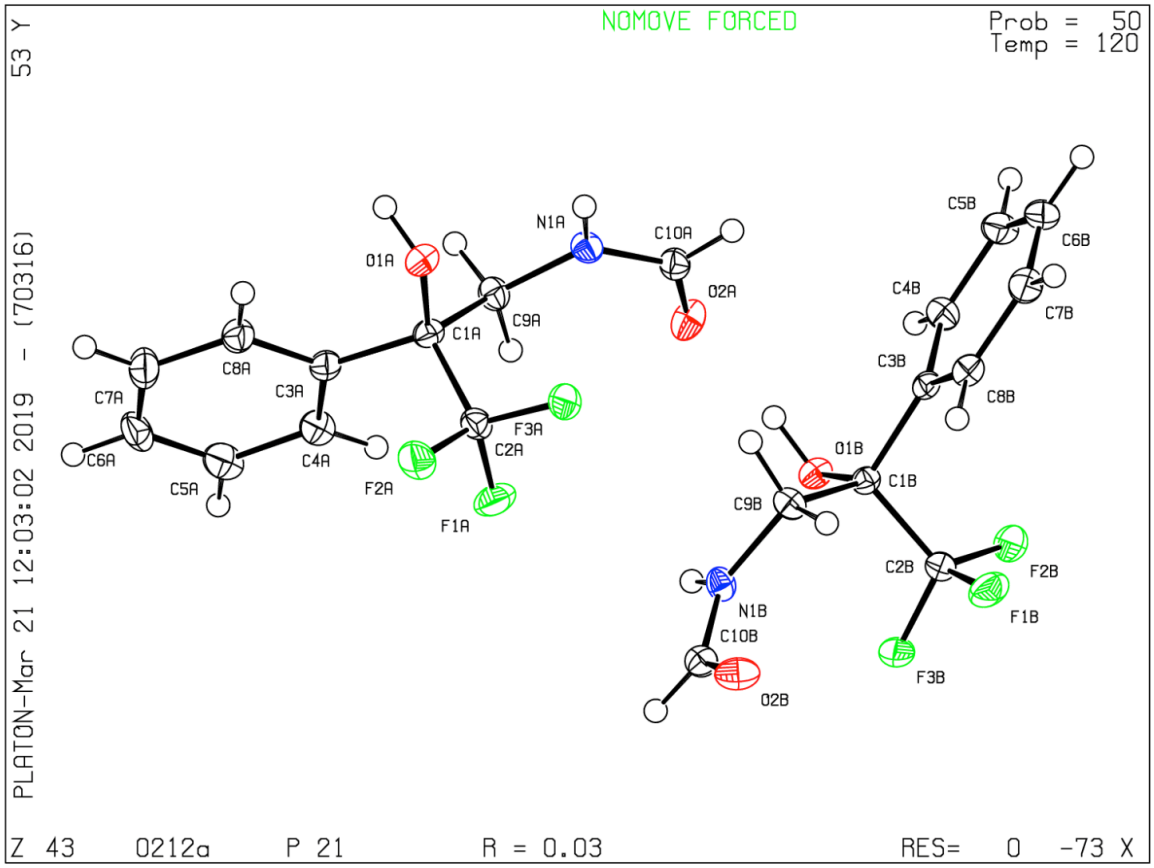

Figure S43. ORTEP representation of **7** (thermal ellipsoids are set at 50% probability level).

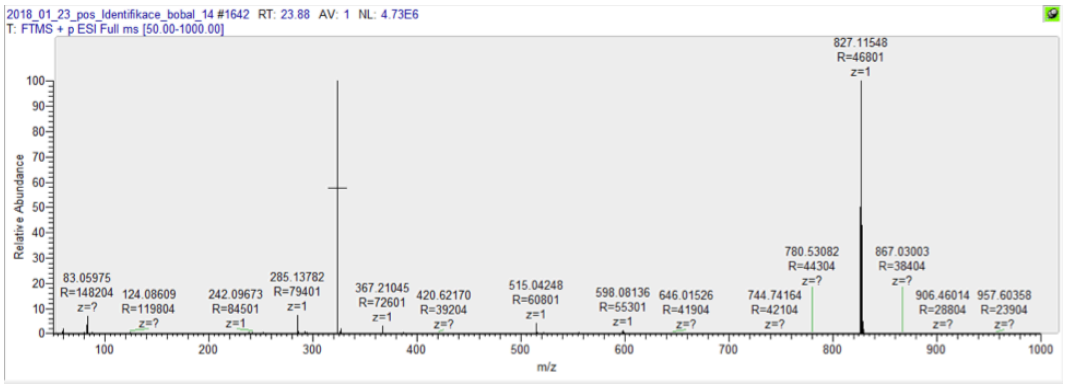

Figure S44. HRMS (ESI-Orbitrap) spectrum of **1a** $[M+H]^+$.

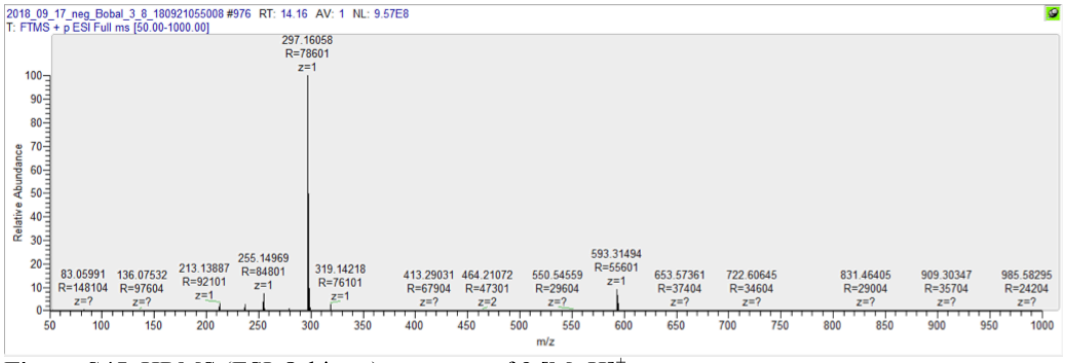

Figure S45. HRMS (ESI-Orbitrap) spectrum of **9** $[M+H]^+$.

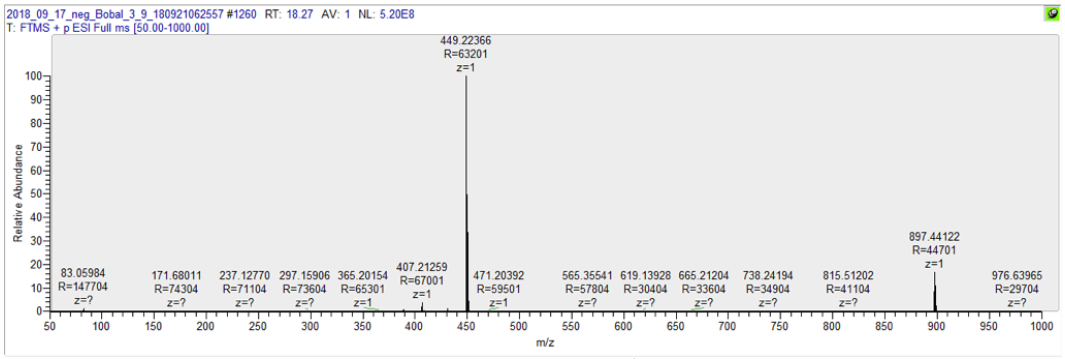

Figure S46. HRMS (ESI-Orbitrap) spectrum of **10** $[M+H]^+$.

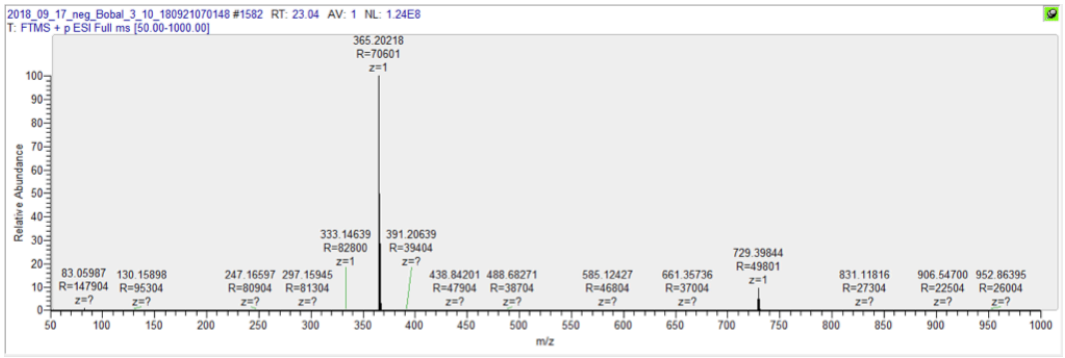

Figure S47. HRMS (ESI-Orbitrap) spectrum of **11** $[M+H]^+$.

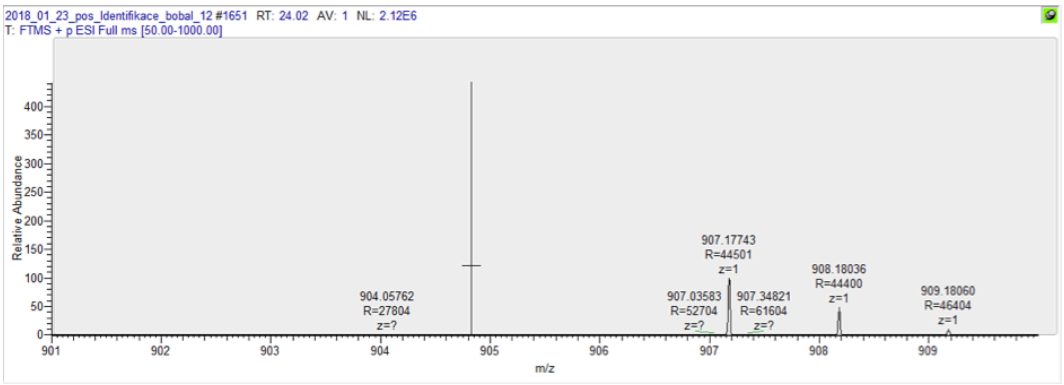

Figure S48. HRMS (ESI-Orbitrap) spectrum of **1d** $[M+H]^+$.

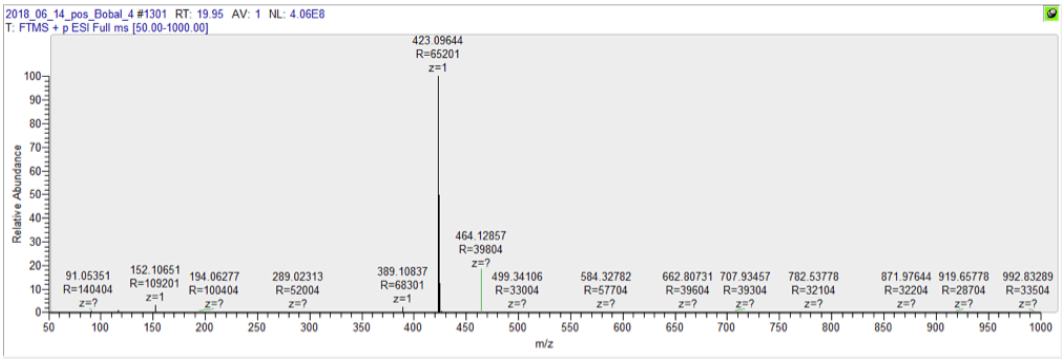

Figure S49. HRMS (ESI-Orbitrap) spectrum of **1e** $[M+H]^+$.

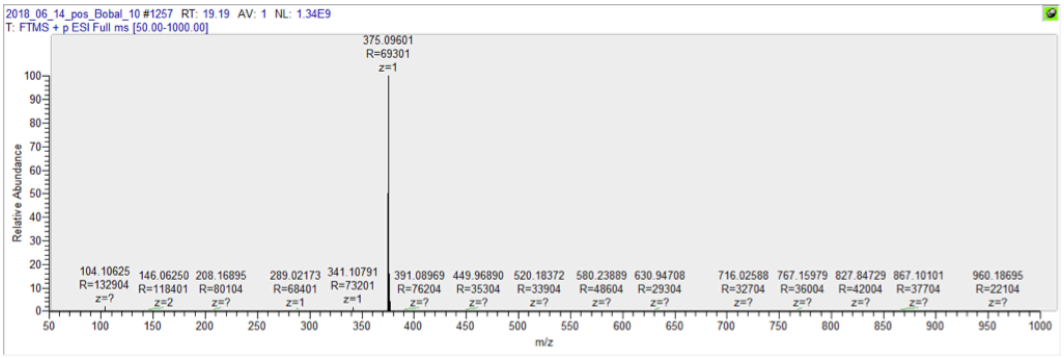

Figure S50. HRMS (ESI-Orbitrap) spectrum of **1f** $[M+H]^+$.

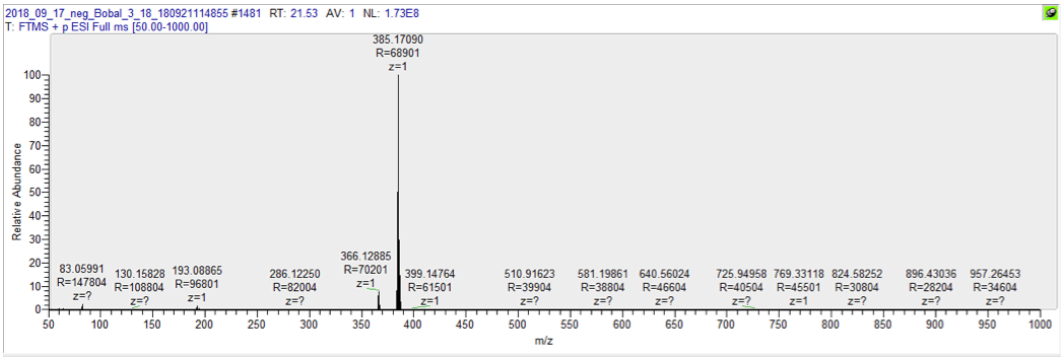

Figure S51. HRMS (ESI-Orbitrap) spectrum of **12** $[M+H]^+$.

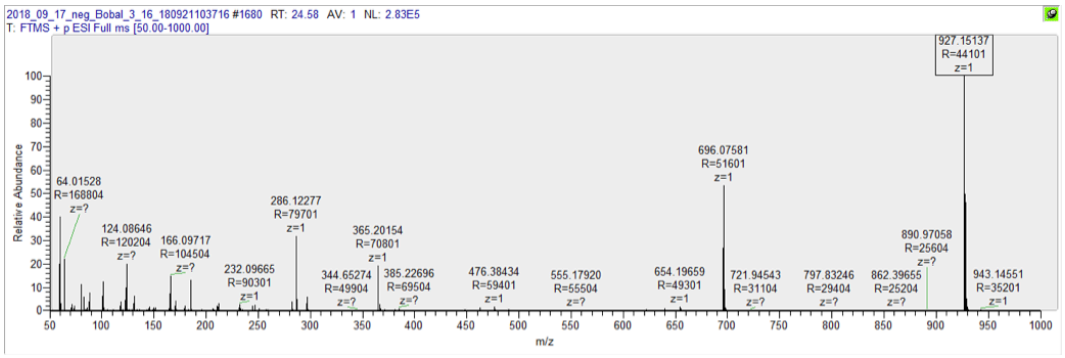

Figure S52. HRMS (ESI-Orbitrap) spectrum of **1g** $[M+H]^+$.

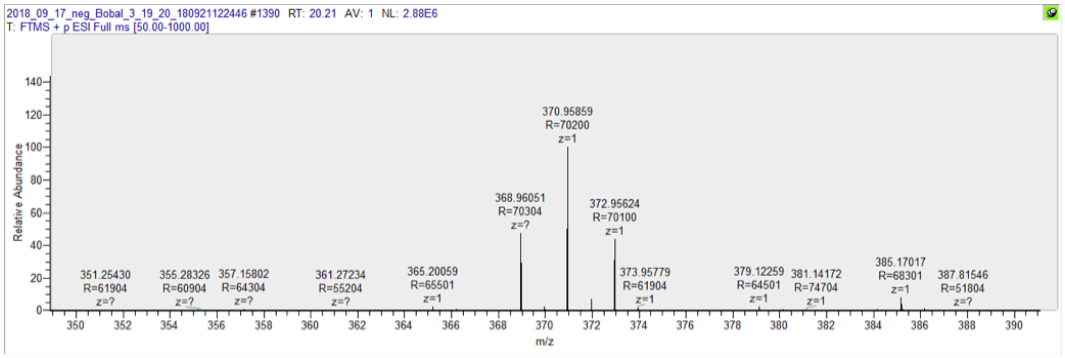

Figure S53. HRMS (ESI-Orbitrap) spectrum of **13** $[M+H]^+$.

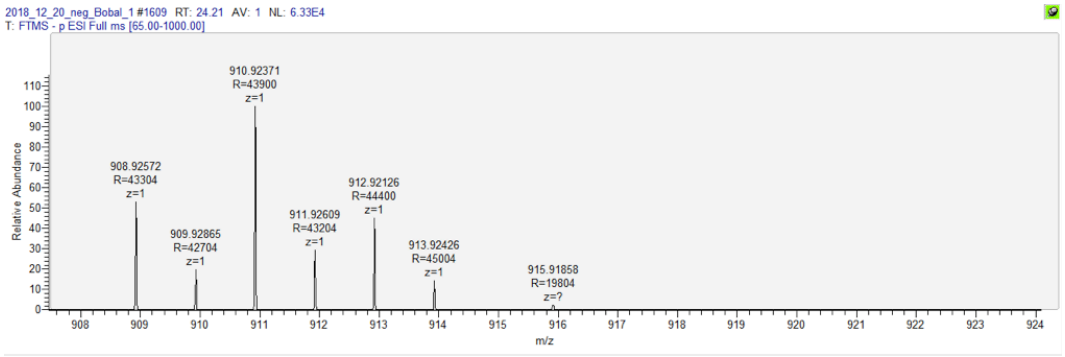

Figure S54. HRMS (ESI-Orbitrap) spectrum of **1h** $[M–H]^-$.

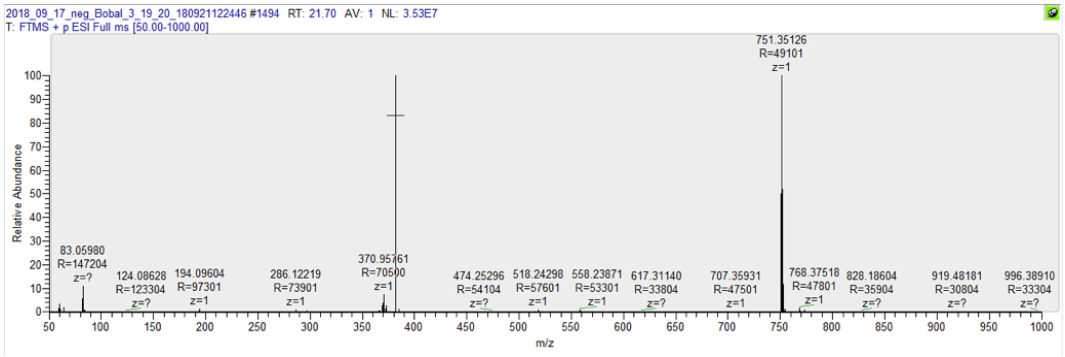

Figure S55. HRMS (ESI-Orbitrap) spectrum of **14** $[M+H]^+$.

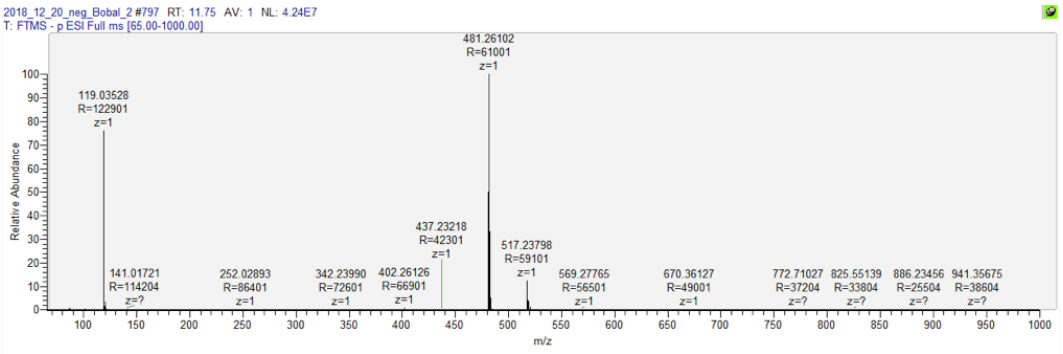

Figure S56. HRMS (ESI-Orbitrap) spectrum of **15** $[M–H]^-$.

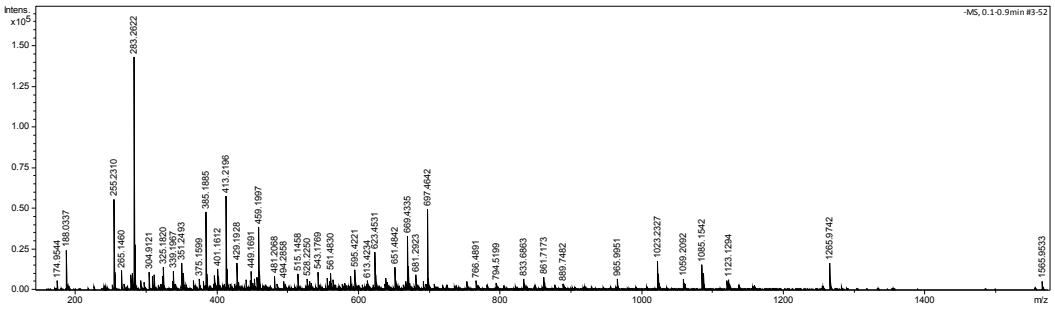

Figure S57. HRMS (ESI-Q-TOF) spectrum of **1i** $[M–H]^-$.

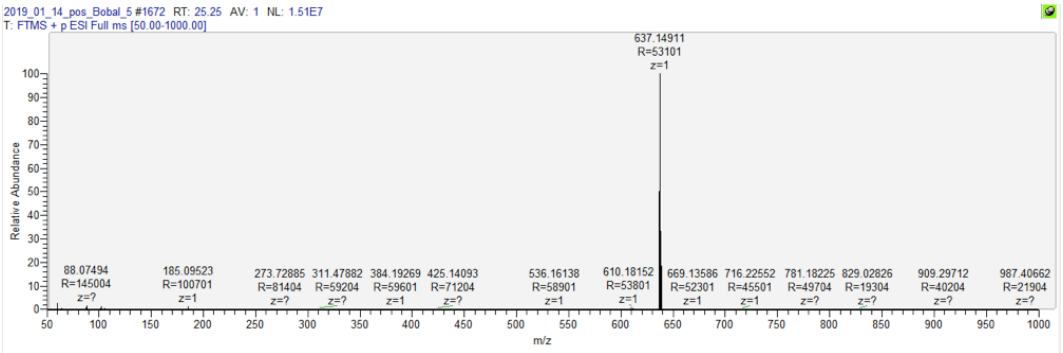

Figure S58. HRMS (ESI-Orbitrap) spectrum of **16** $[M+H]^+$.

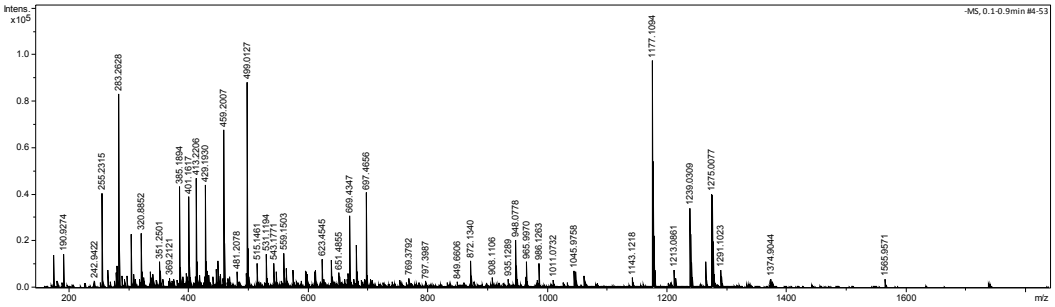

Figure S59. HRMS (ESI-Q-TOF) spectrum of **1j** $[M–H]^-$.

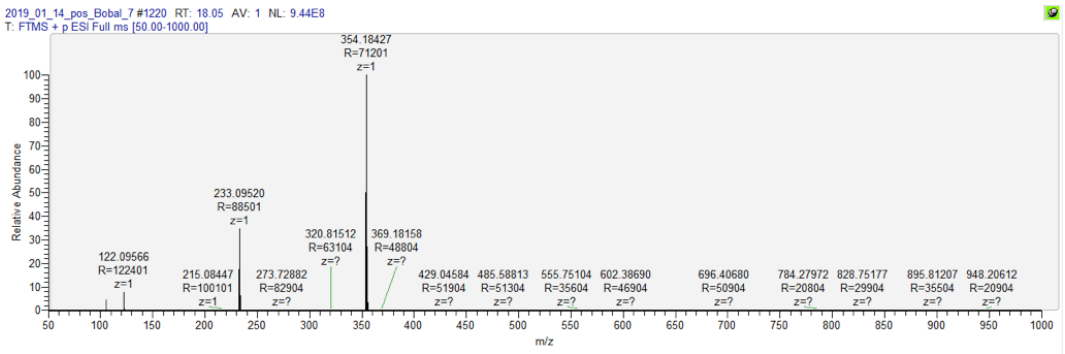

Figure S60. HRMS (ESI-Orbitrap) spectrum of **17** $[M+H]^+$.

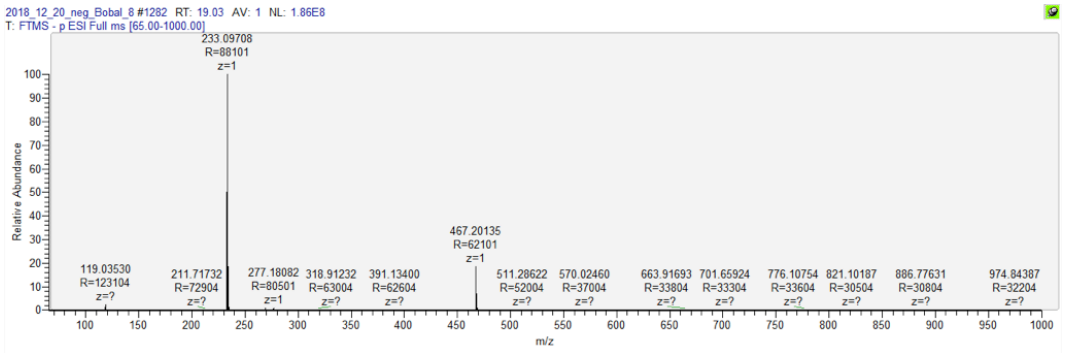

Figure S61. HRMS (ESI-Orbitrap) spectrum of **18** $[M-H]^-$.

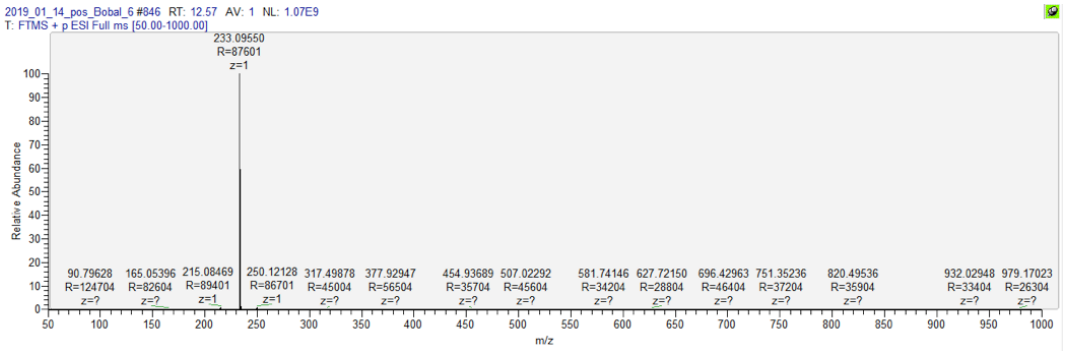

Figure S62. HRMS (ESI-Orbitrap) spectrum of **19** $[M-NH_3+H]^+$.

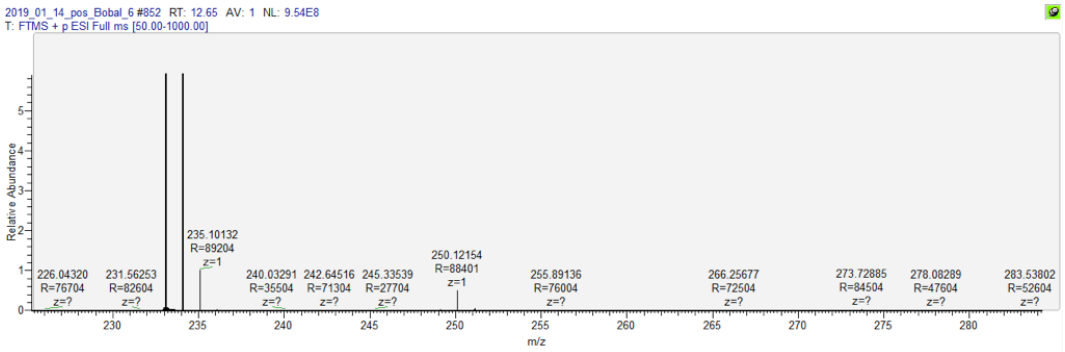

Figure S63. HRMS (ESI-Orbitrap) spectrum of **19** $[M+H]^+$ (detail).

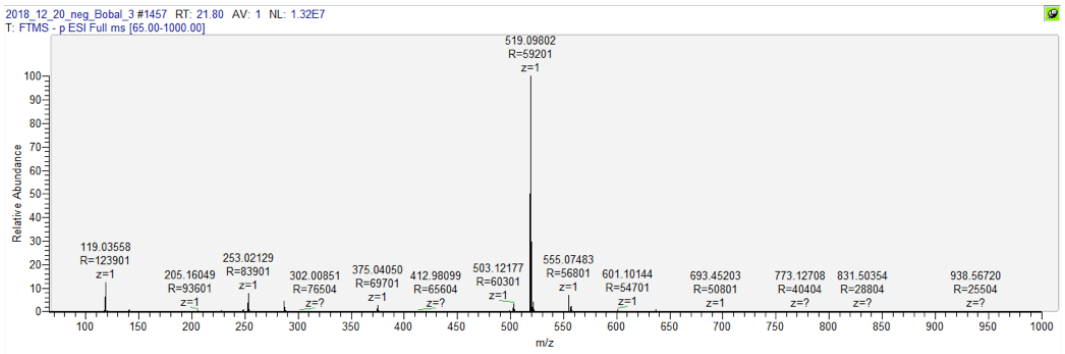

Figure S64. HRMS (ESI-Orbitrap) spectrum of **1k** $[M–H]^-$.

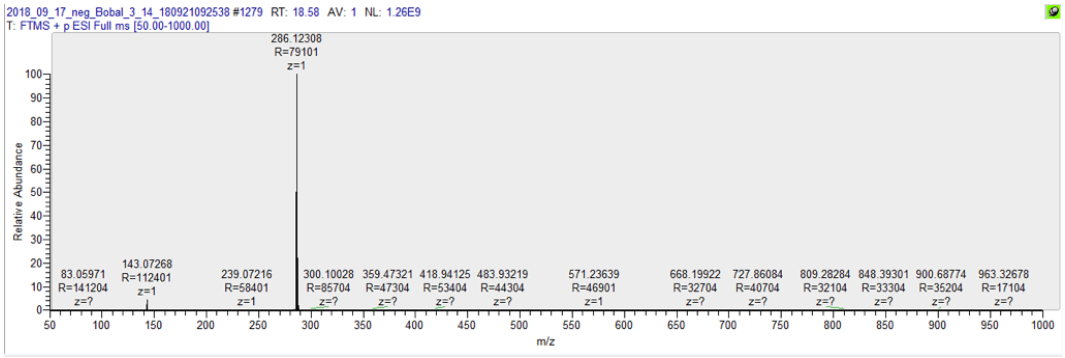

Figure S65. HRMS (ESI-Orbitrap) spectrum of **20** $[M+H]^+$.

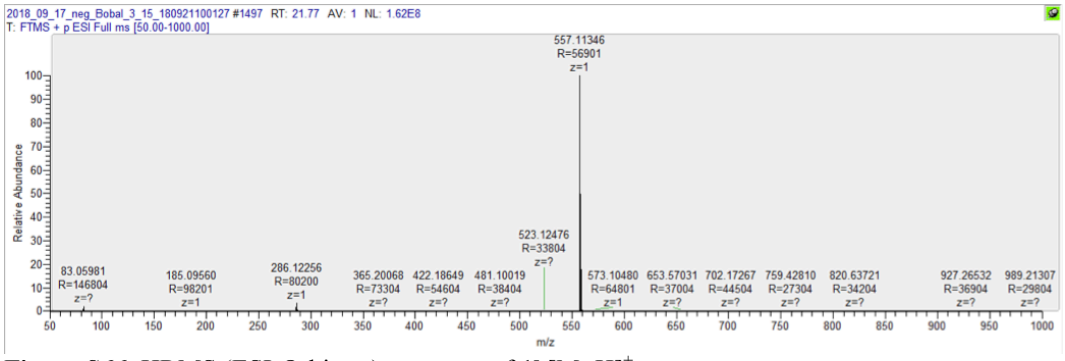

Figure S66. HRMS (ESI-Orbitrap) spectrum of **1l** $[M+H]^+$.

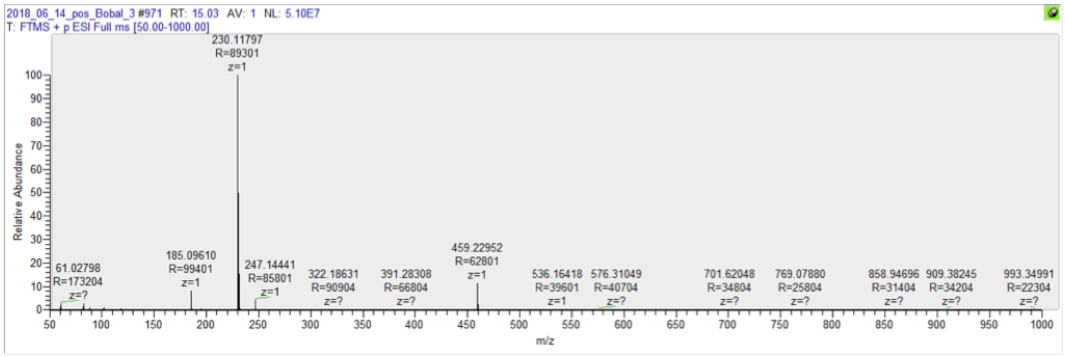

Figure S67. HRMS (ESI-Orbitrap) spectrum of **21** $[M+H]^+$.

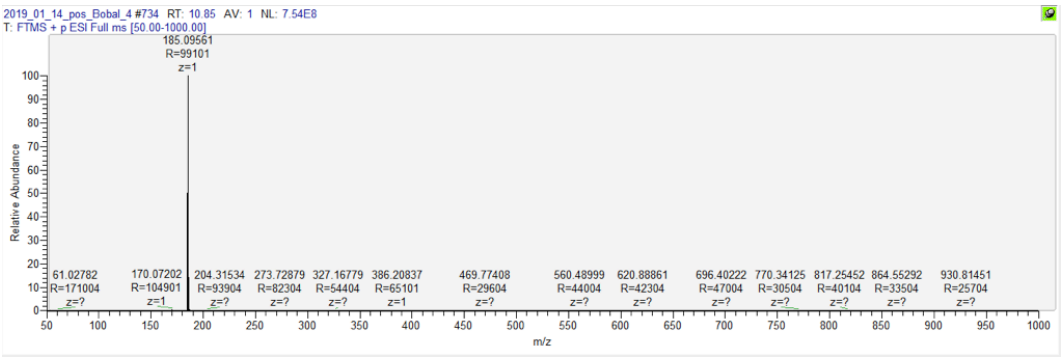

Figure S68. HRMS (ESI-Orbitrap) spectrum of **22** $[M–NH_3+H]^+$.

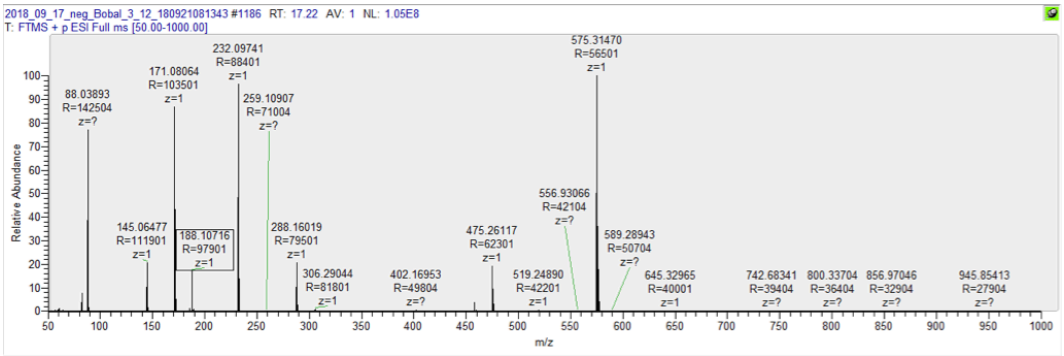

Figure S69. HRMS (ESI-Orbitrap) spectrum of **23** $[M+H]^+$.

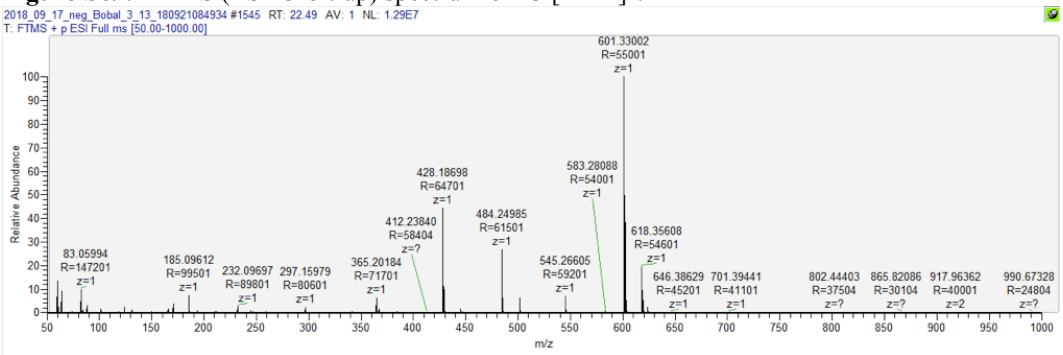

Figure S70. HRMS (ESI-Orbitrap) spectrum of **24** $[M+H]^+$.

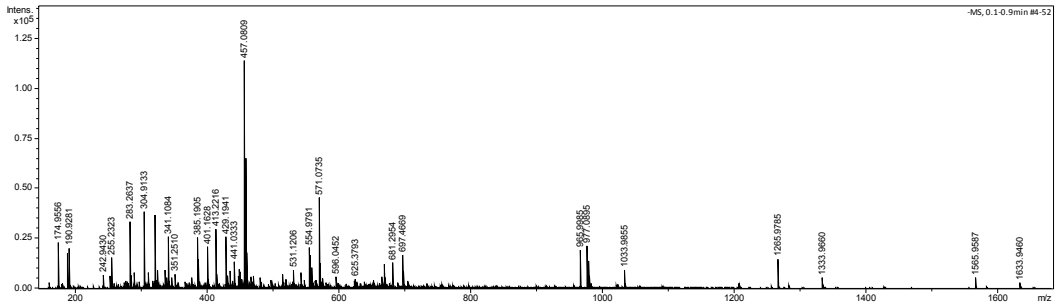

Figure S71. HRMS (ESI-Q-TOF) spectrum of **1m** $[M–C_{23}H_{18}F_6N_2OS–H]^-$.

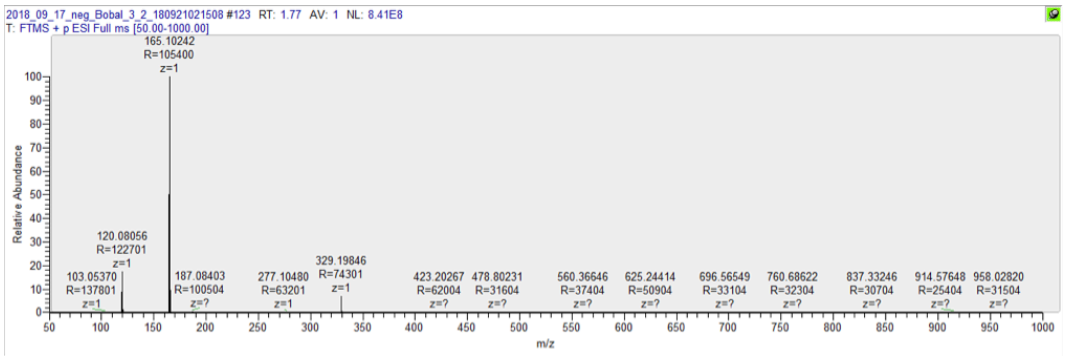

Figure S72. HRMS (ESI-Orbitrap) spectrum of **25** $[M+H]^+$.

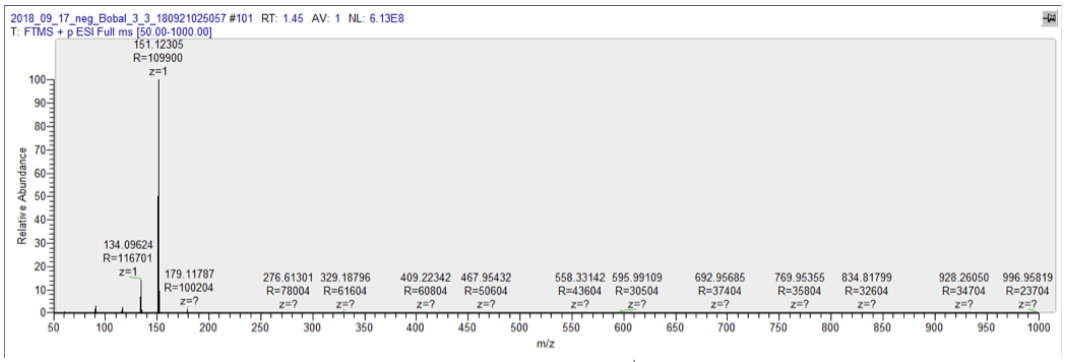

Figure S73. HRMS (ESI-Orbitrap) spectrum of **26** $[M+H]^+$.

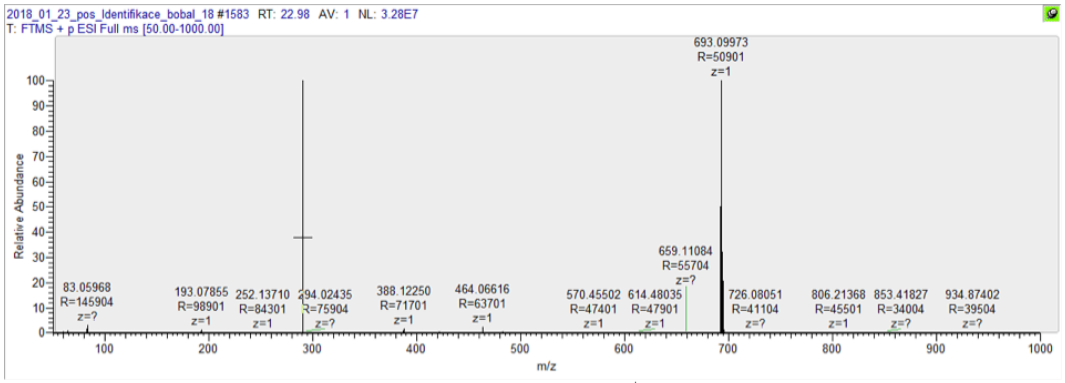

Figure S74. HRMS (ESI-Orbitrap) spectrum of **1n** $[M+H]^+$.

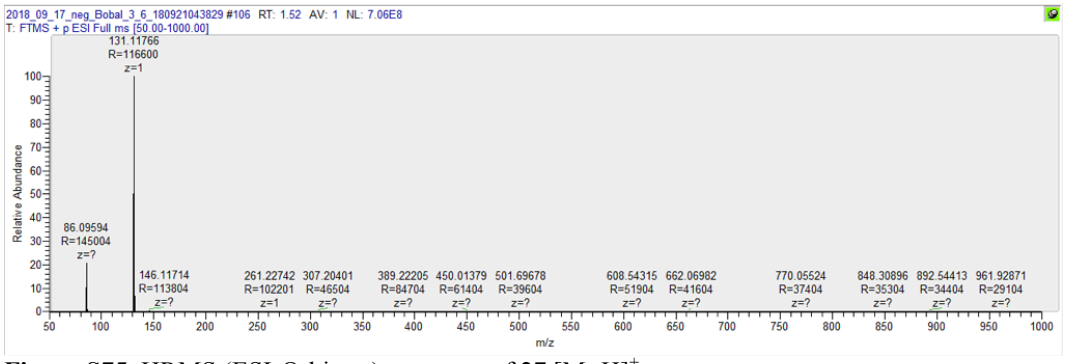

Figure S75. HRMS (ESI-Orbitrap) spectrum of **27** $[M+H]^+$.

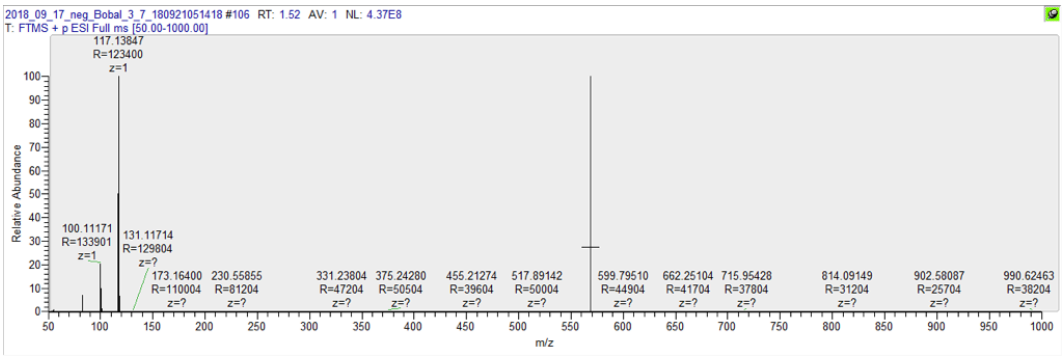

Figure S76. HRMS (ESI-Orbitrap) spectrum of **28** $[M+H]^+$.

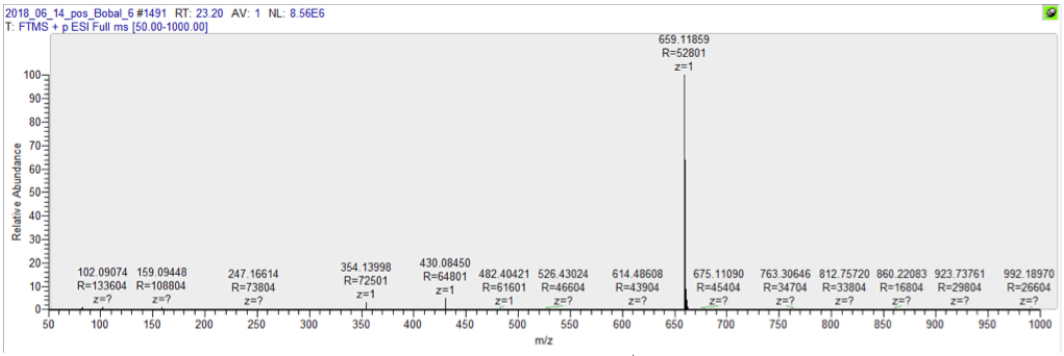

Figure S77. HRMS (ESI-Orbitrap) spectrum of **1o** $[M+H]^+$.

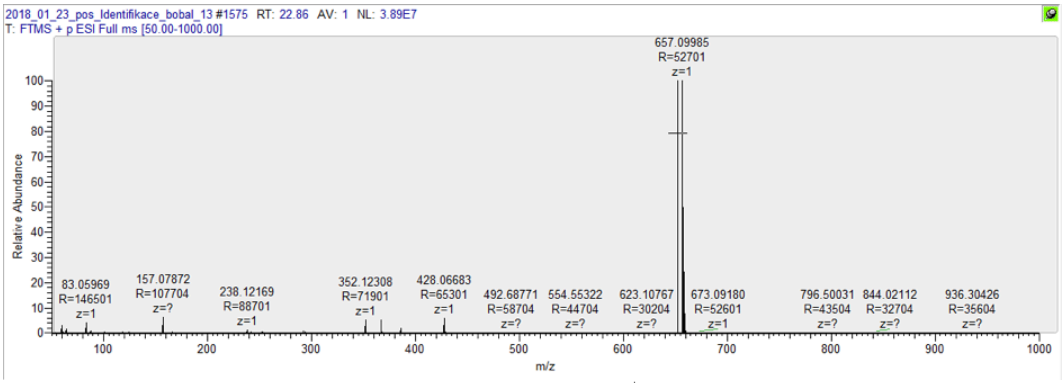

Figure S78. HRMS (ESI-Orbitrap) spectrum of **1p** $[M+H]^+$.

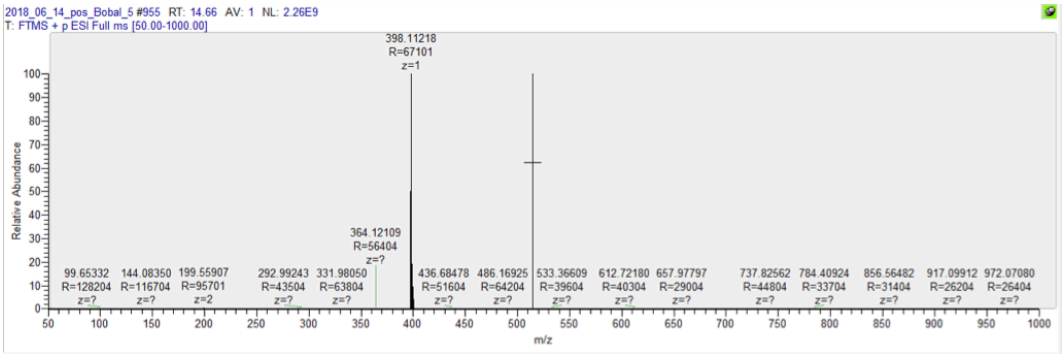

Figure S79. HRMS (ESI-Orbitrap) spectrum of **1q** $[M+H]^+$.

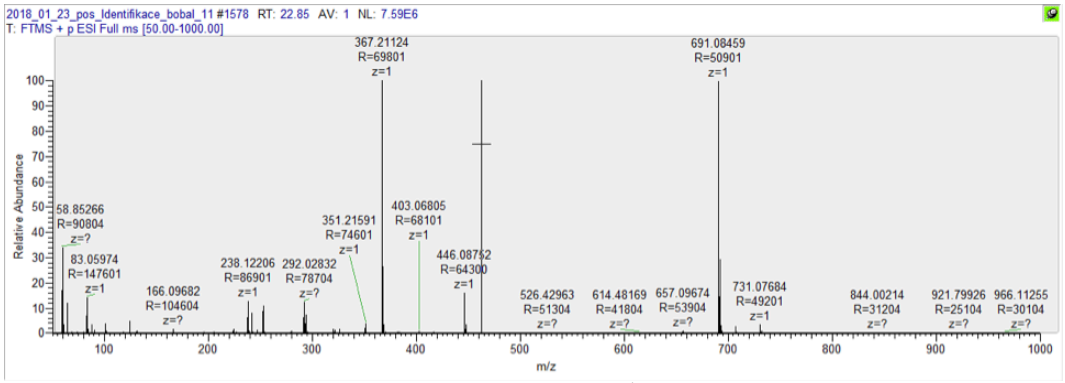

Figure S80. HRMS (ESI-Orbitrap) spectrum of **1r** $[M+H]^+$.

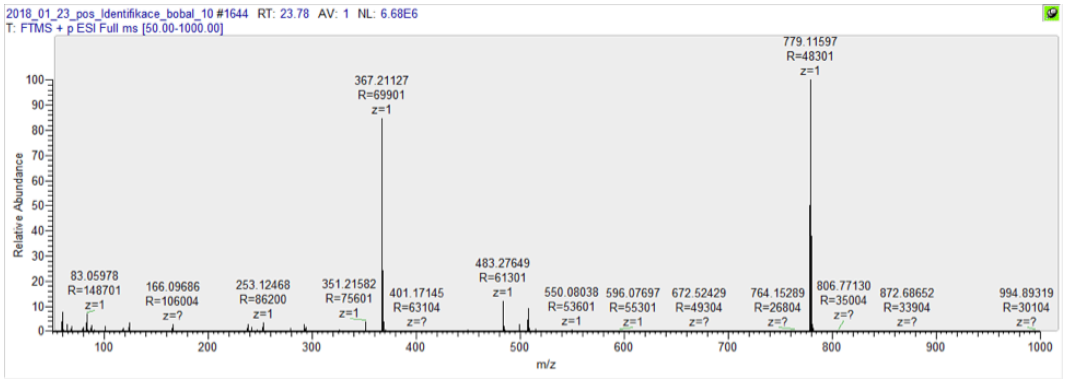

Figure S81. HRMS (ESI-Orbitrap) spectrum of **1s** $[M+H]^+$.

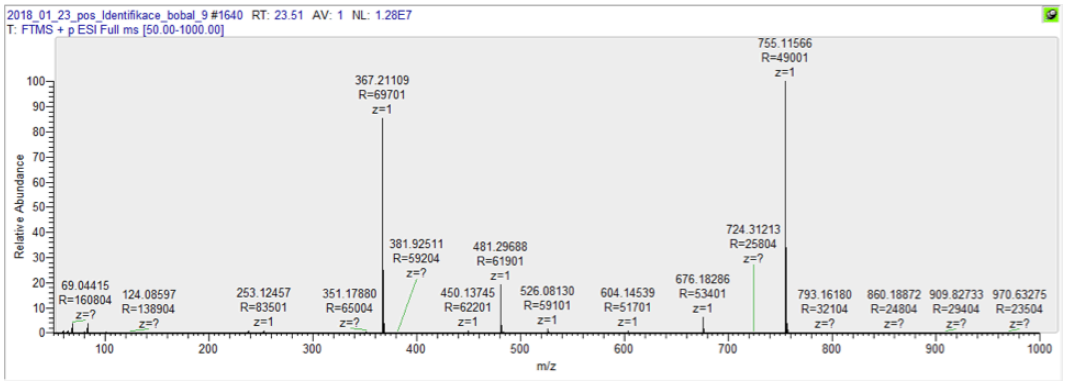

Figure S82. HRMS (ESI-Orbitrap) spectrum of **1v** $[M+H]^+$.

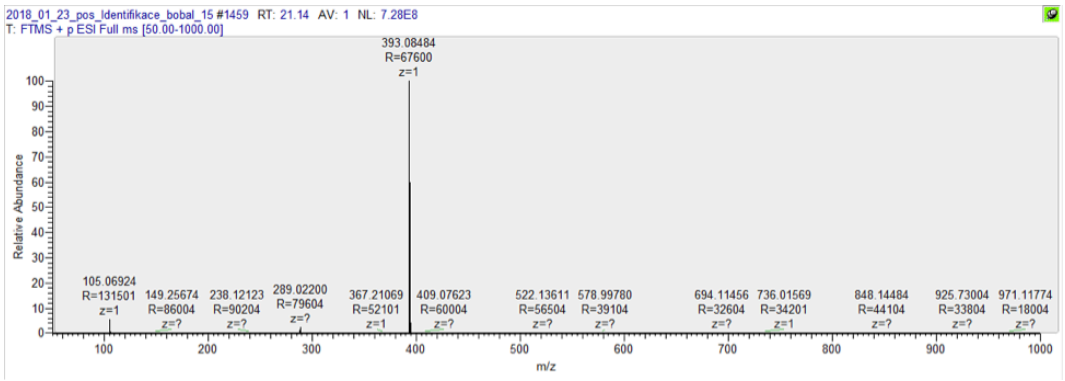

Figure S83. HRMS (ESI-Orbitrap) spectrum of **1w** $[M+H]^+$.

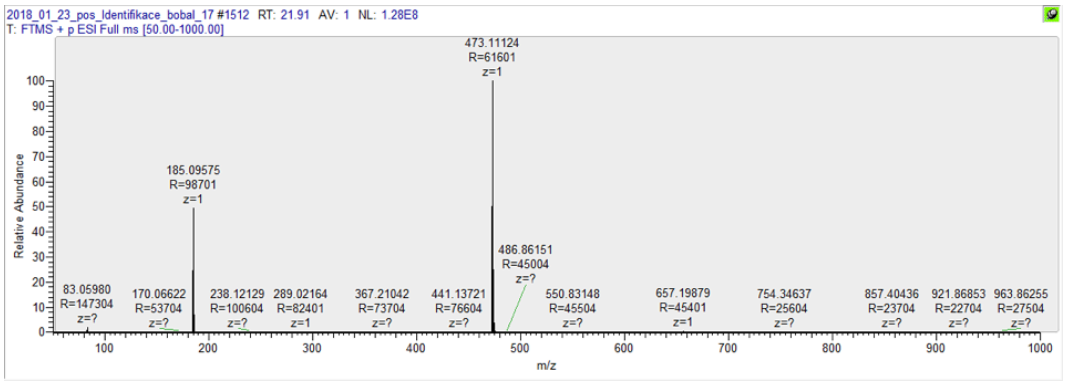

Figure S84. HRMS (ESI-Orbitrap) spectrum of **1x** $[M+H]^+$.

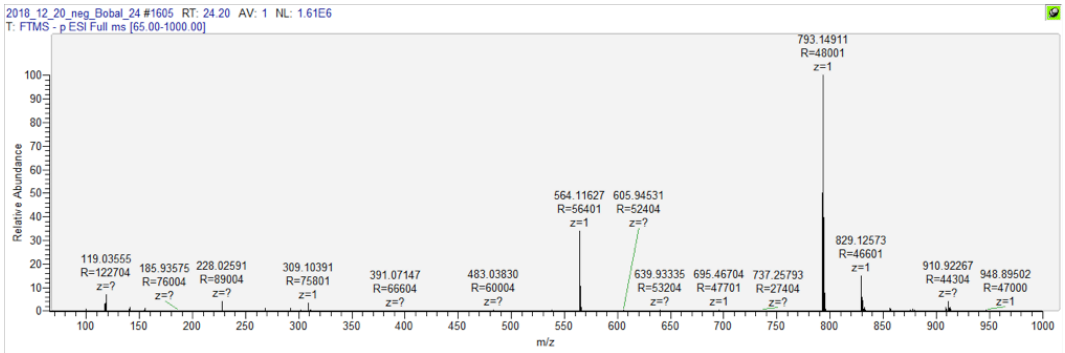

Figure S85. HRMS (ESI-Orbitrap) spectrum of **2a** $[M–H]^-$.

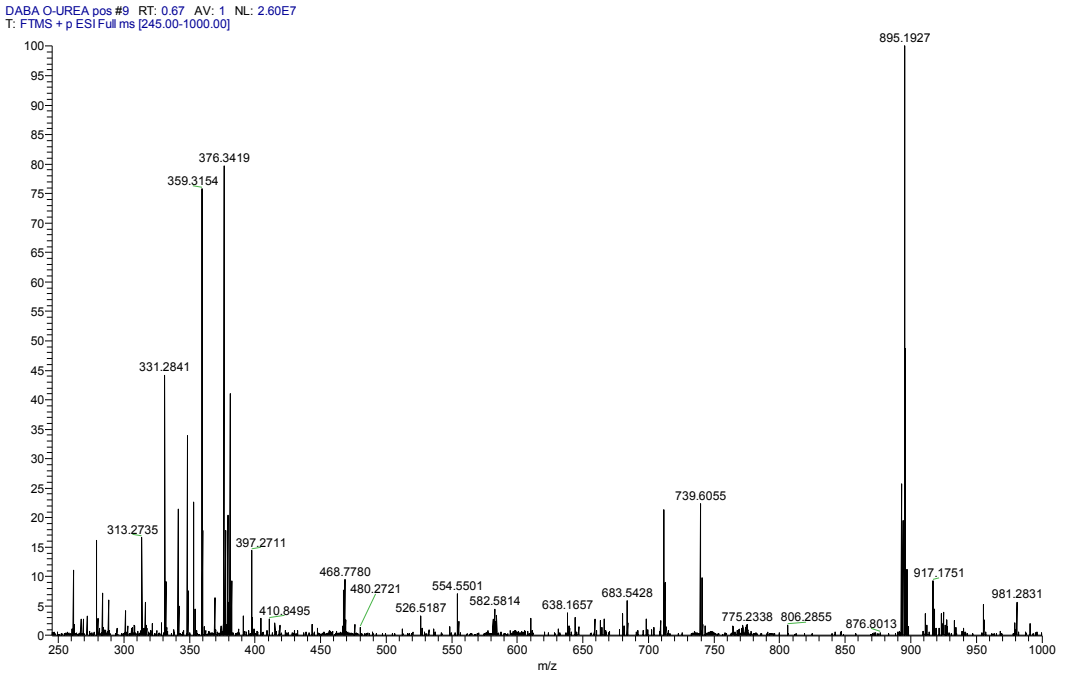

Figure S86. HRMS (ESI) spectrum of **2b** $[M+H]^+$.

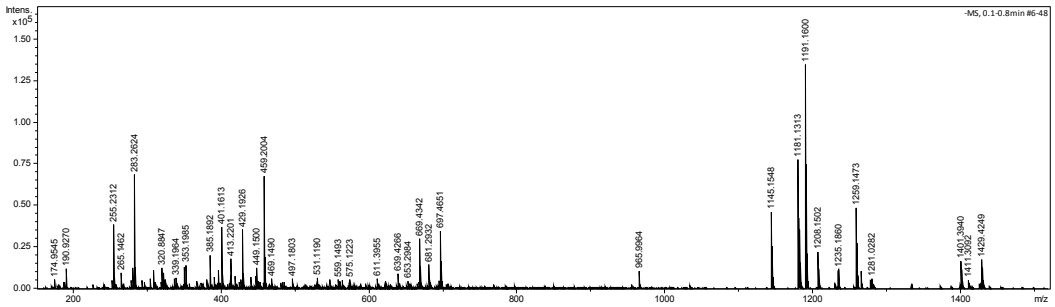

Figure S87. HRMS (ESI-Q-TOF) spectrum of **2c** $[M–H]^-$.

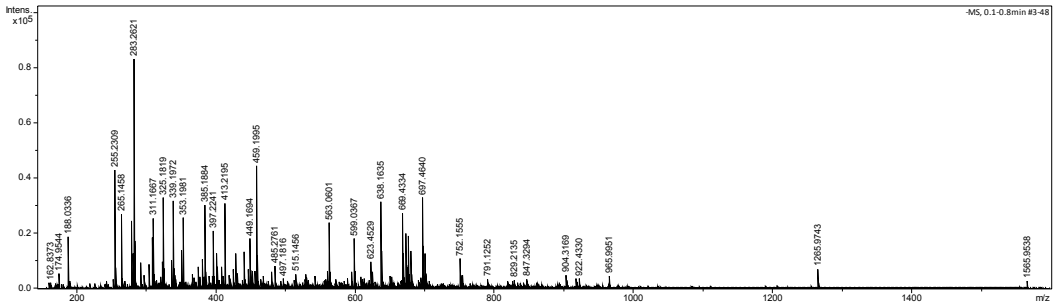

Figure S88. HRMS (ESI-Q-TOF) spectrum of **3a** $[M–H]^-$.

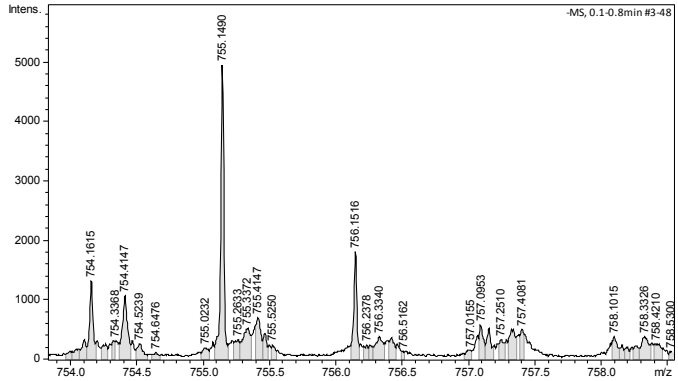

Figure S89. HRMS (ESI-Q-TOF) spectrum of **3a** $[M–H]^-$ (detail).

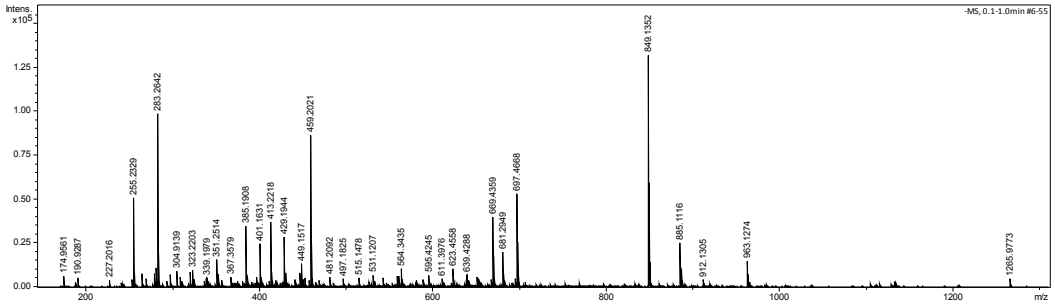

Figure S90. HRMS (ESI-Q-TOF) spectrum of **3b** $[M–H]^-$.

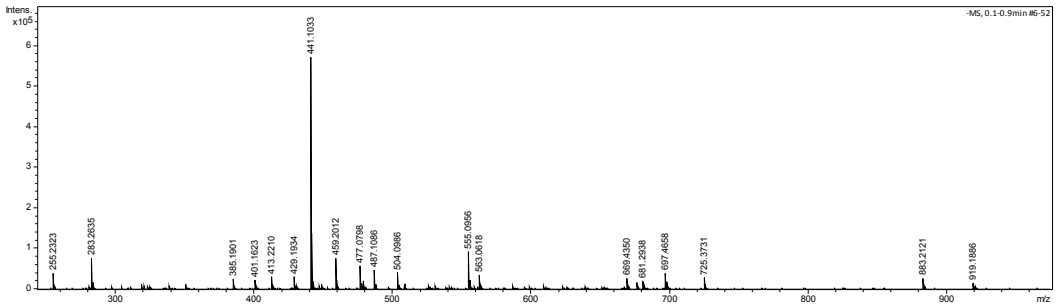

Figure S91. HRMS (ESI-Q-TOF) spectrum of **3c** $[M–H]^-$.

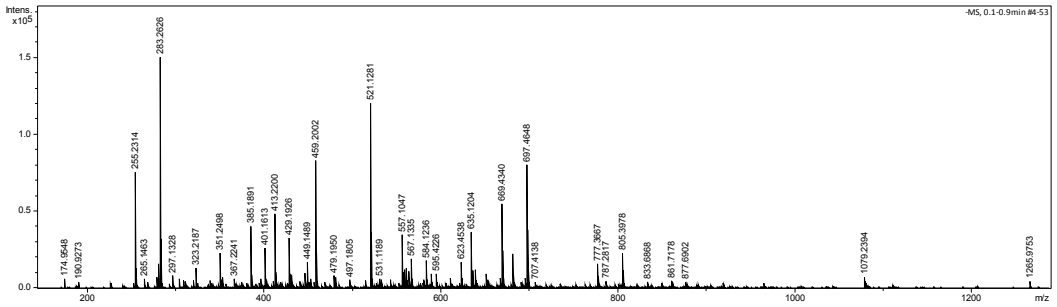

Figure S92. HRMS (ESI-Q-TOF) spectrum of **3d** $[M–H]^-$.

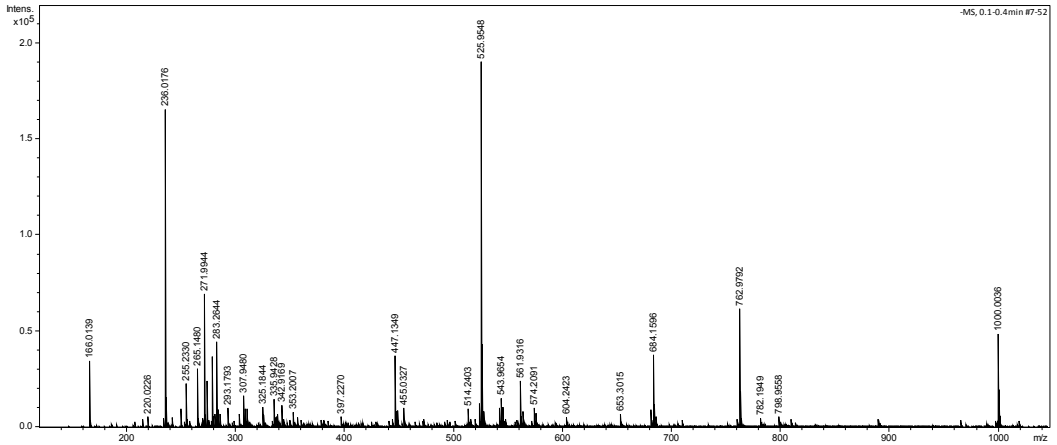

Figure S93. HRMS (ESI-Q-TOF) spectrum of **4f** $[M+H_2O–H]^-$.

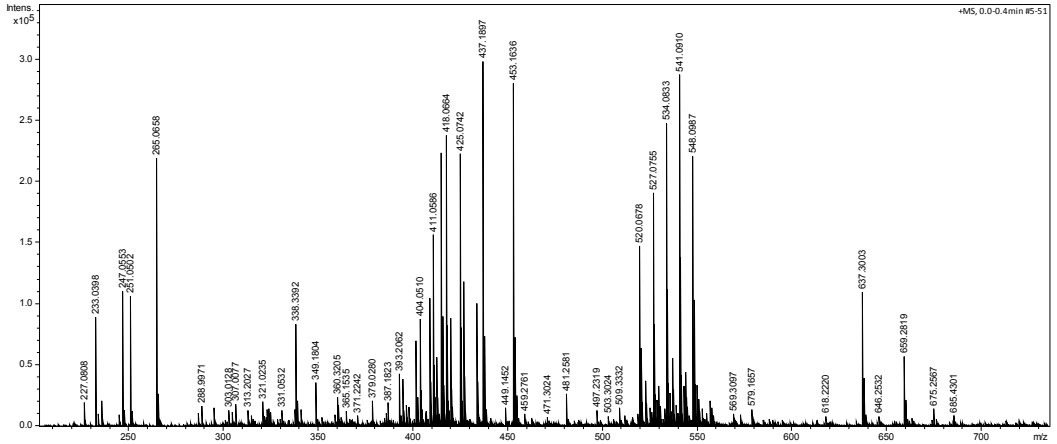

Figure S94. HRMS (ESI-Q-TOF) spectrum of **4i** $[M+H]^+$.

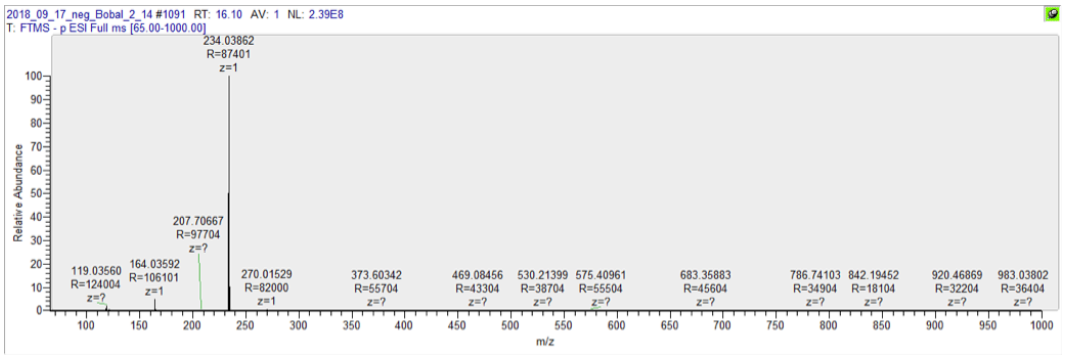

Figure S95. HRMS (ESI-Orbitrap) spectrum of **5a** [M–H]⁻.

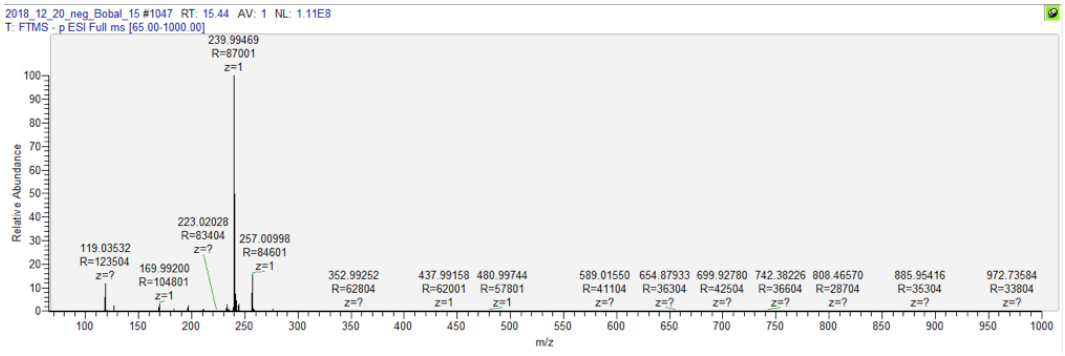

Figure S96. HRMS (ESI-Orbitrap) spectrum of **5b** [M–H]⁻.

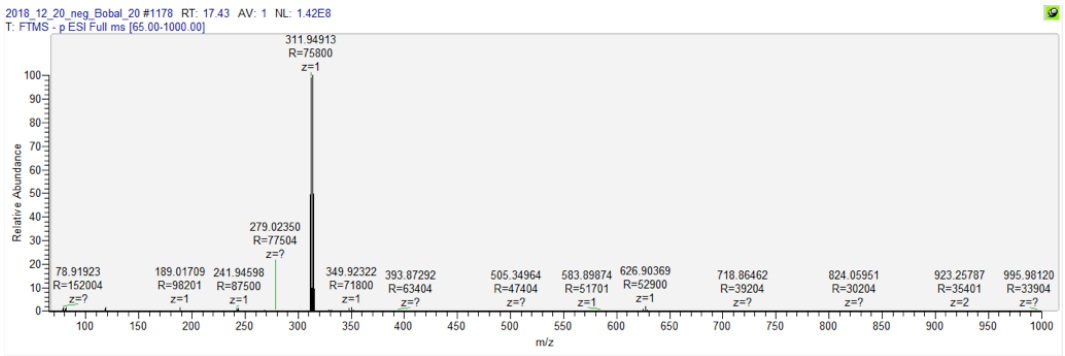

Figure S97. HRMS (ESI-Orbitrap) spectrum of **5c** [M–H]⁻.

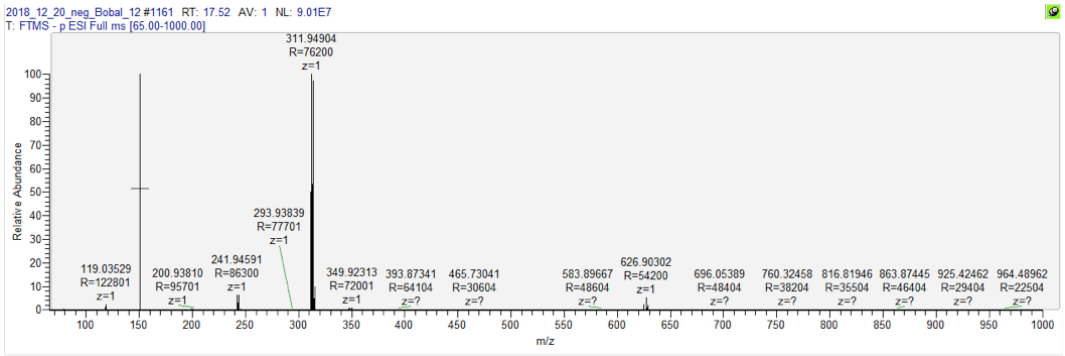

Figure S98. HRMS (ESI-Orbitrap) spectrum of **5d** [M–H]⁻.

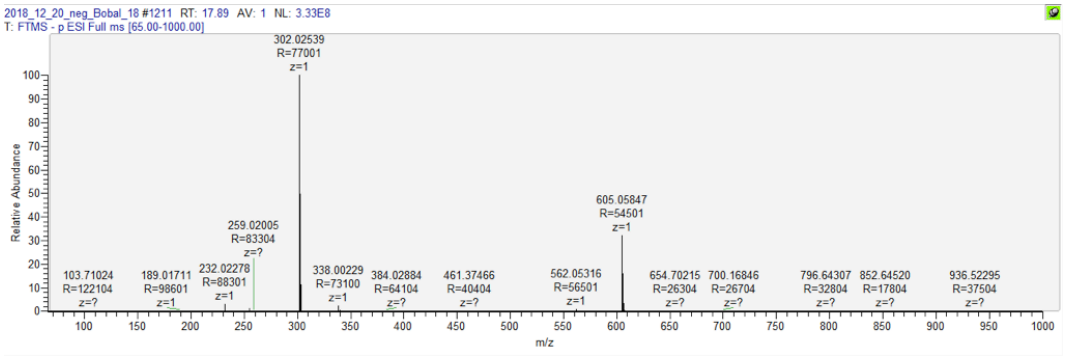

Figure S99. HRMS (ESI-Orbitrap) spectrum of **5e** [M–H]$^-$.

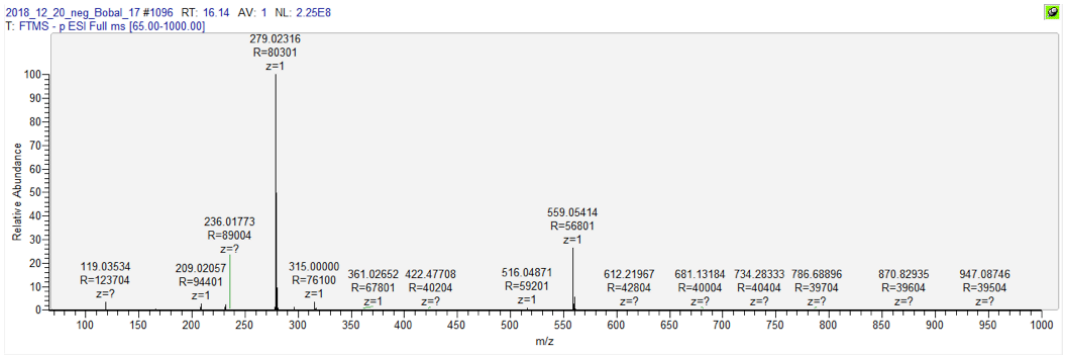

Figure S100. HRMS (ESI-Orbitrap) spectrum of **5f** [M–H]$^-$.

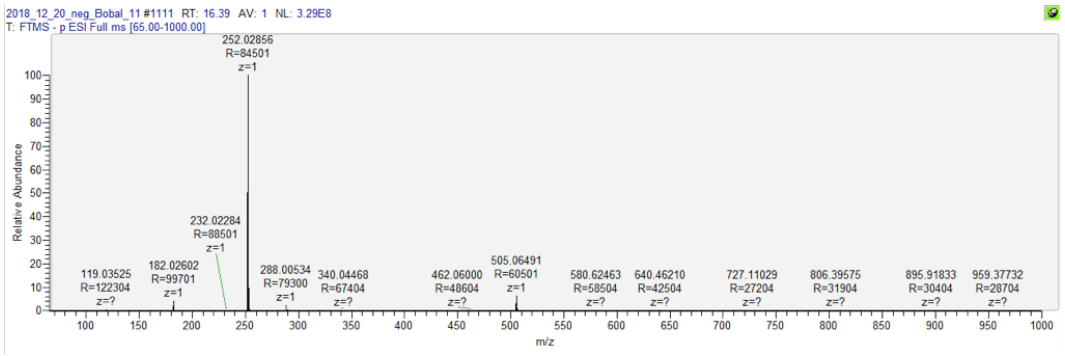

Figure S101. HRMS (ESI-Orbitrap) spectrum of **5g** [M–H]$^-$.

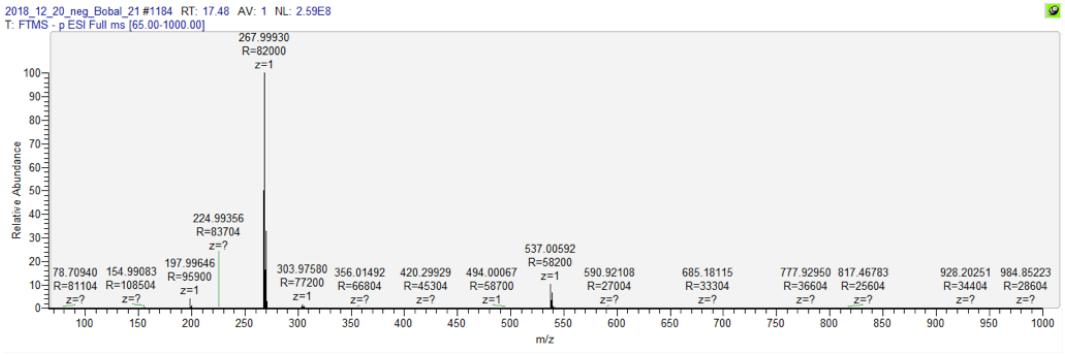

Figure S102. HRMS (ESI-Orbitrap) spectrum of **5h** [M–H]$^-$.

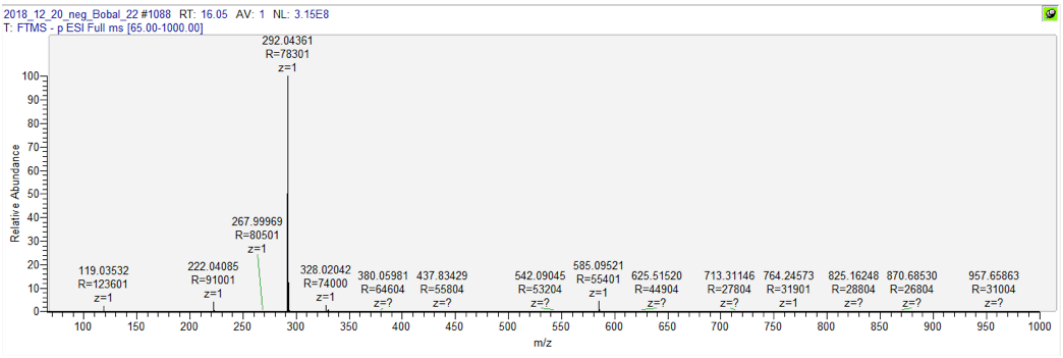

Figure S103. HRMS (ESI-Orbitrap) spectrum of **5i** [M–H]⁻.

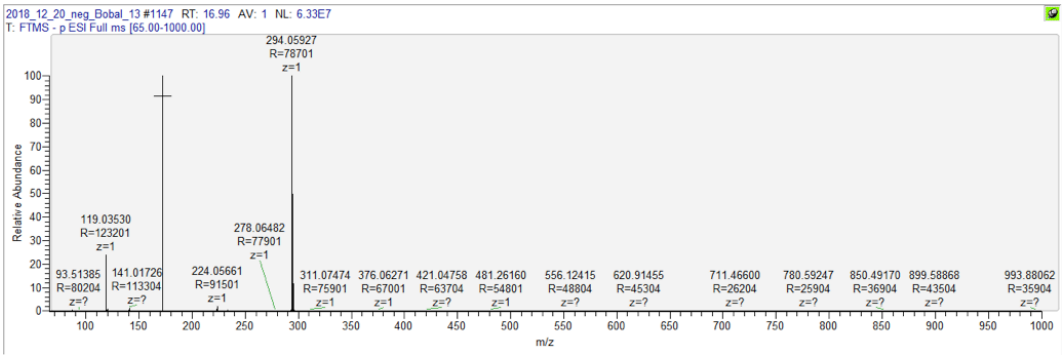

Figure S104. HRMS (ESI-Orbitrap) spectrum of **5j** [M–H]⁻.

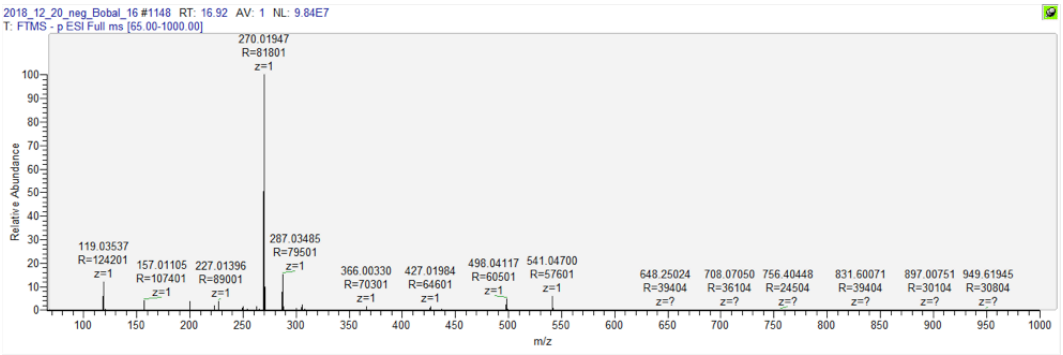

Figure S105. HRMS (ESI-Orbitrap) spectrum of **5k** [M–H]⁻.

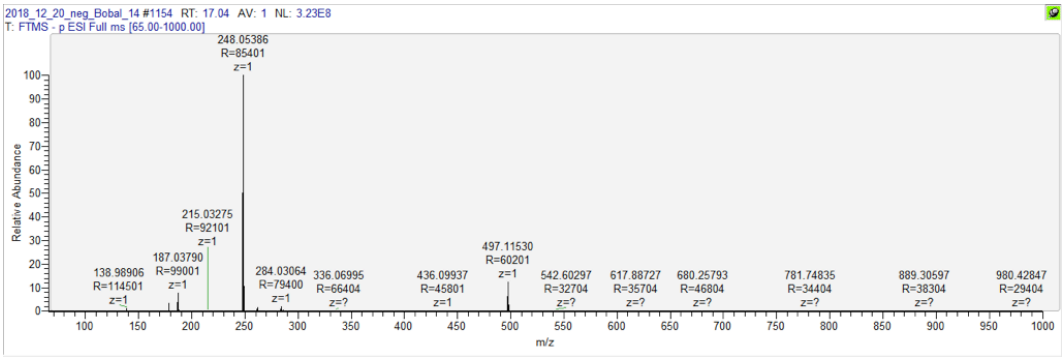

Figure S106. HRMS (ESI-Orbitrap) spectrum of **5l** [M–H]⁻.

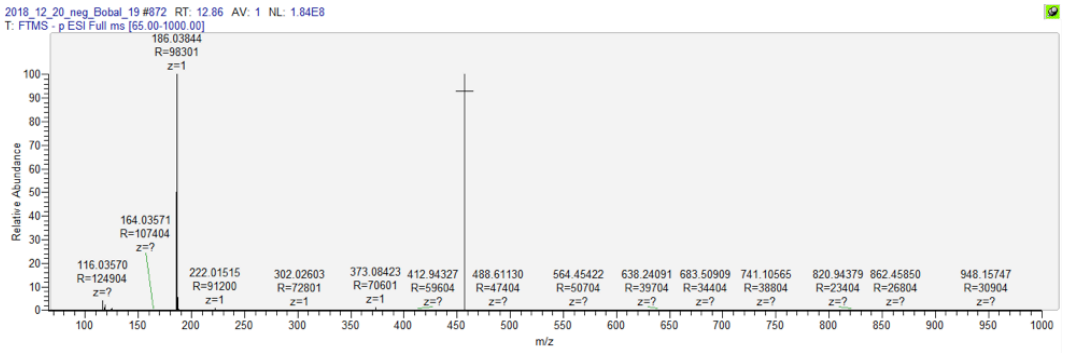

Figure S107. HRMS (ESI-Orbitrap) spectrum of **5m** $[M–H]^-$.

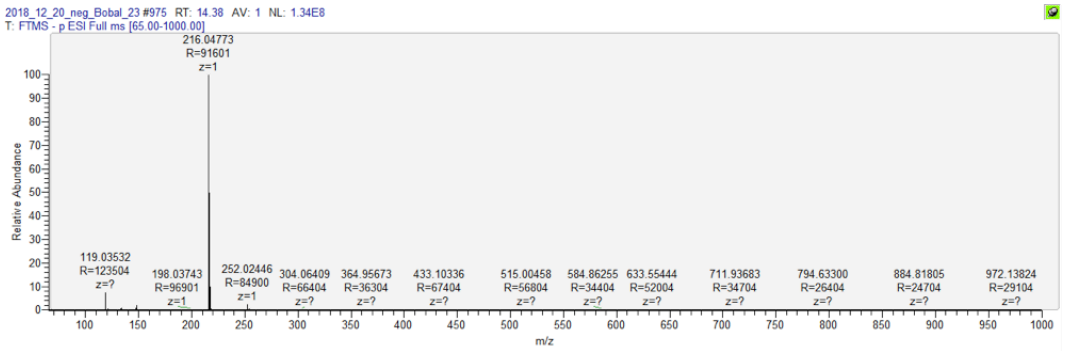

Figure S108. HRMS (ESI-Orbitrap) spectrum of **5n** $[M–H]^-$.

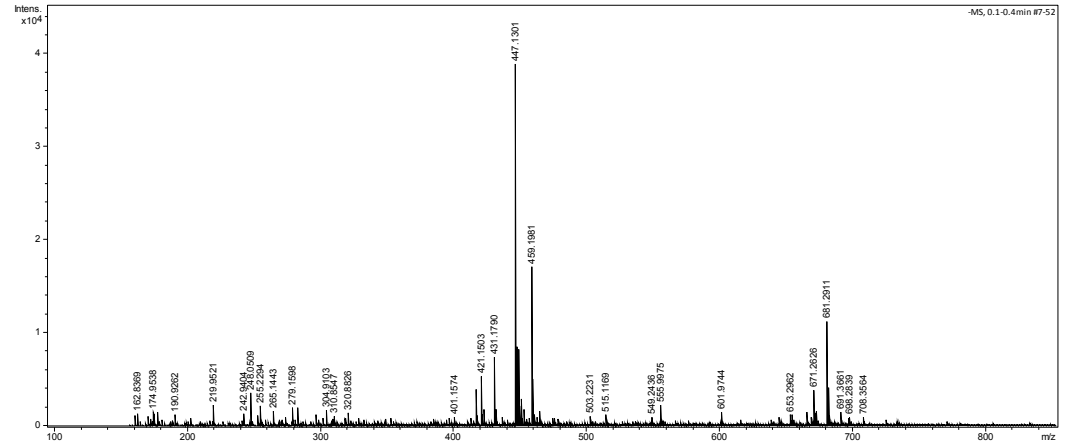

Figure S109. HRMS (ESI-Q-TOF) spectrum of **5o** $[M–H]^-$.

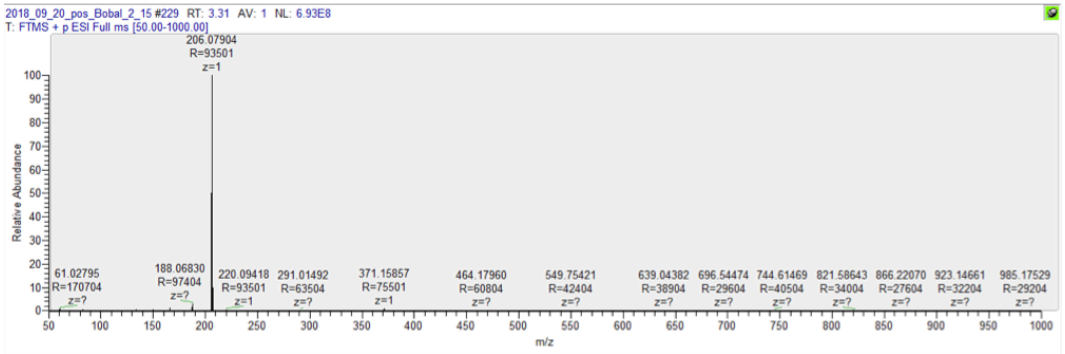

Figure S110. HRMS (ESI-Orbitrap) spectrum of **6** $[M+H]^+$.

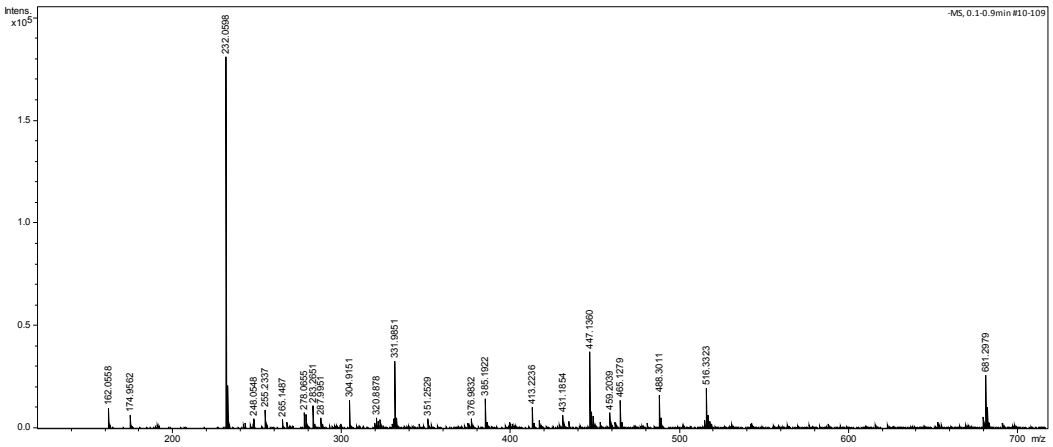

Figure S111. HRMS (ESI-Q-TOF) spectrum of **7** $[M–H]^-$.

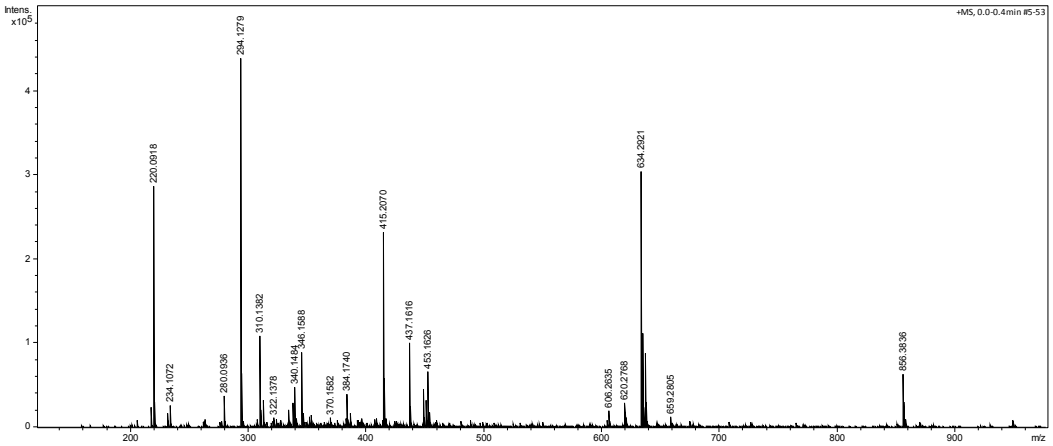

Figure S112. HRMS (ESI-Q-TOF) spectrum of **8** $[M+H]^+$.

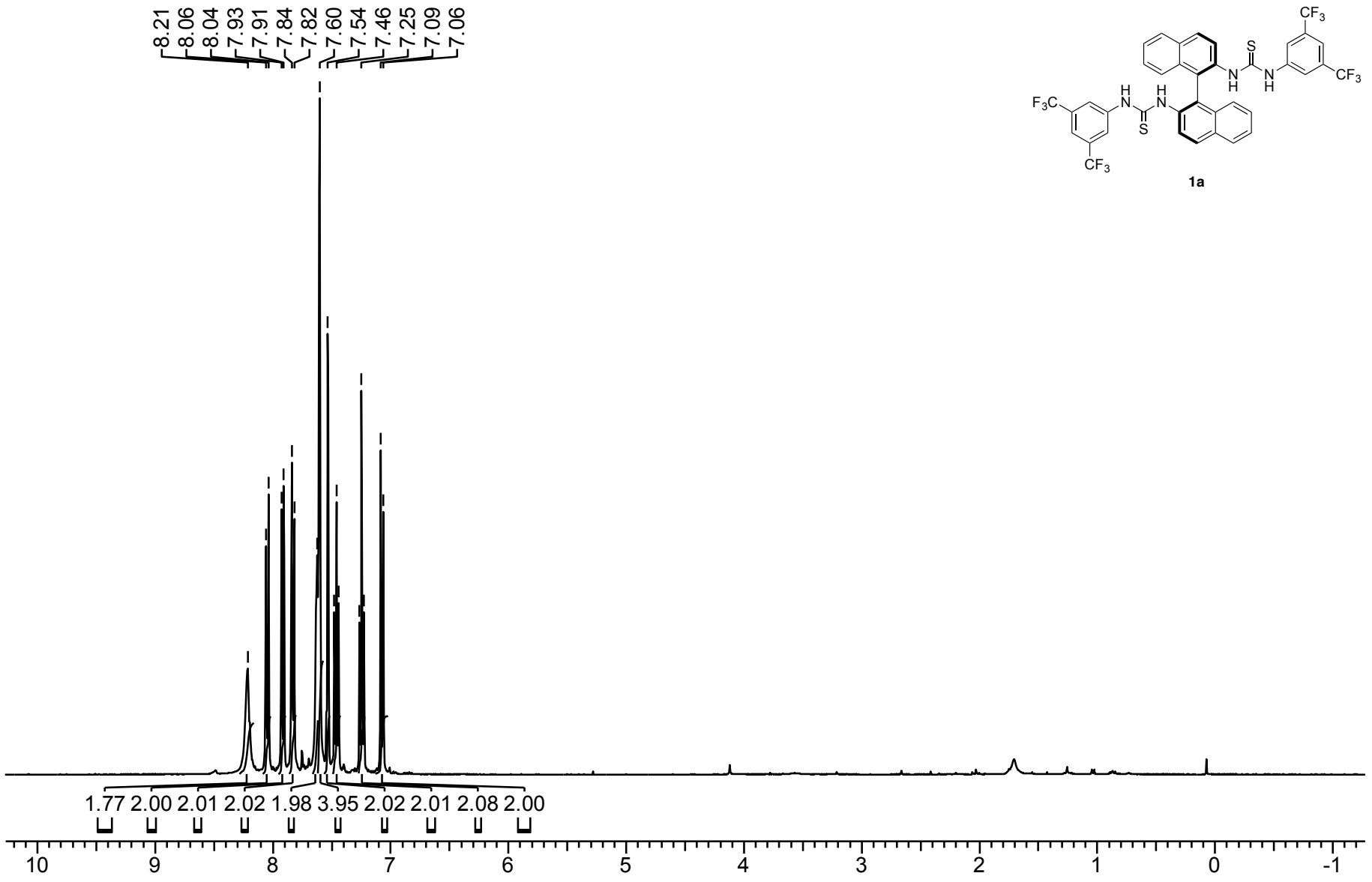

Figure S113. ^{1}H NMR (400 MHz, $CDCl_3$) spectrum of **1a**.

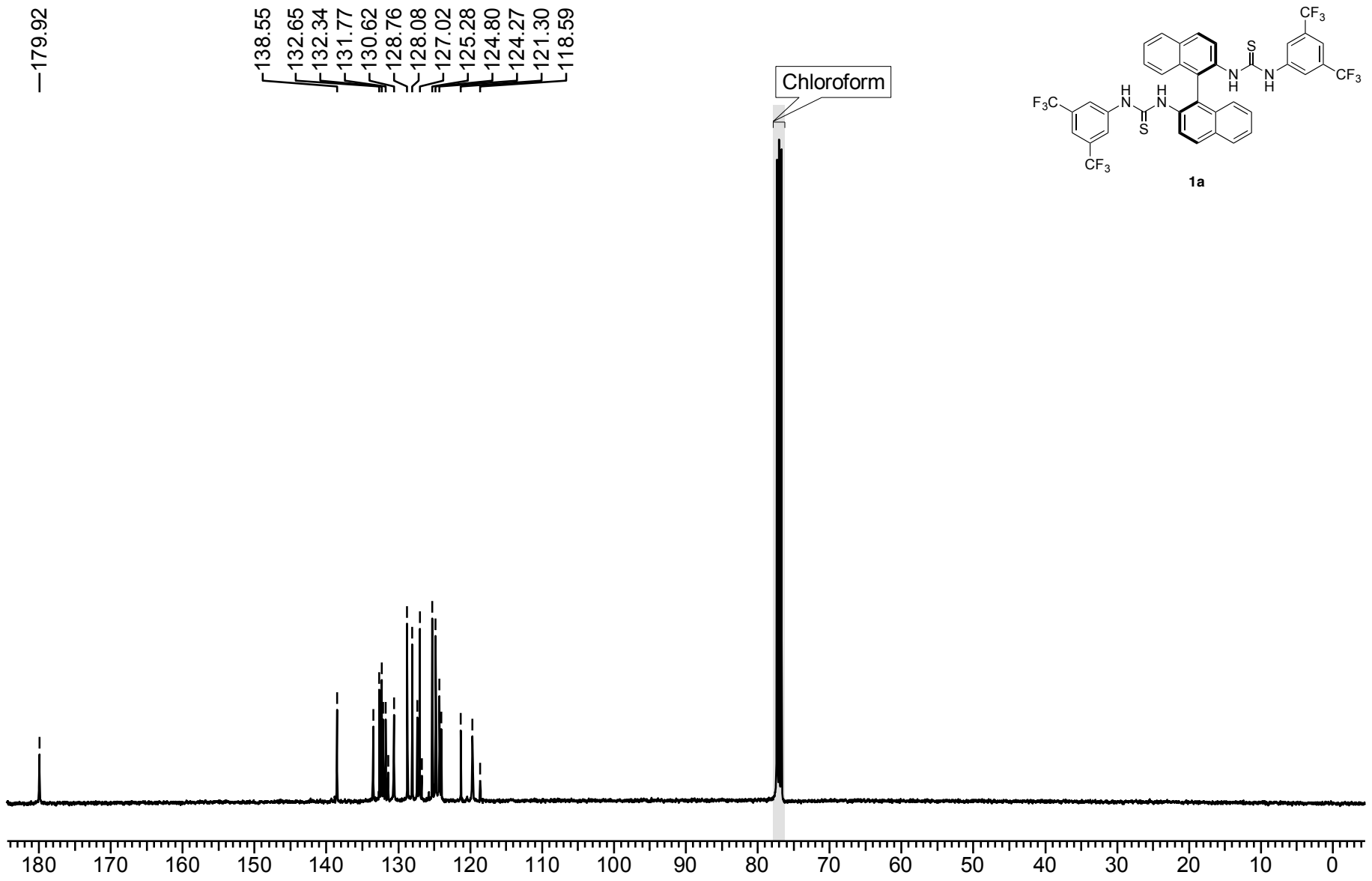

Figure S114. ^{13}C NMR (100 MHz, $CDCl_3$) spectrum of **1a**.

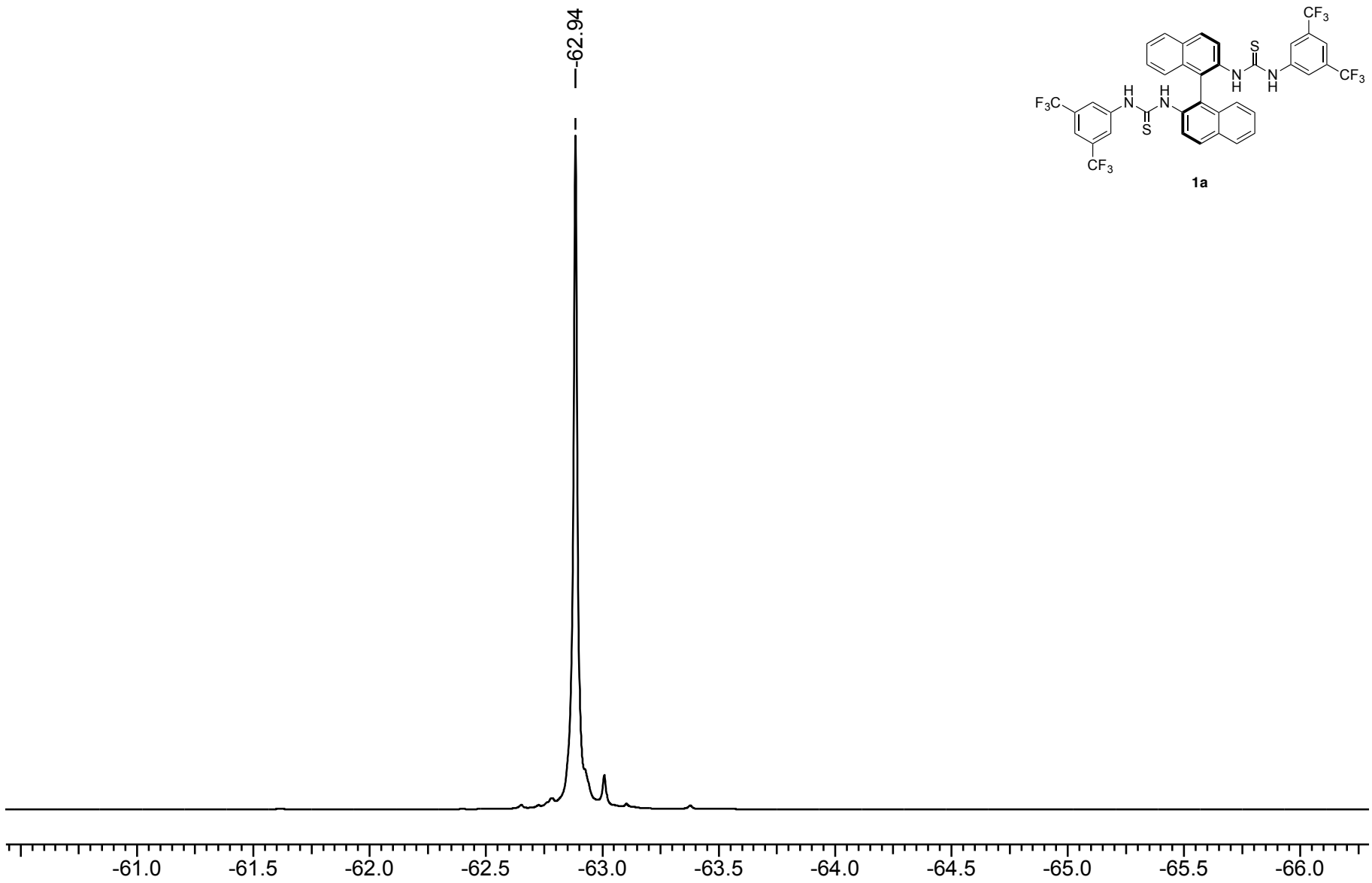

Figure S115. ^{19}F NMR (376 MHz, $CDCl_3$) spectrum of **1a**.

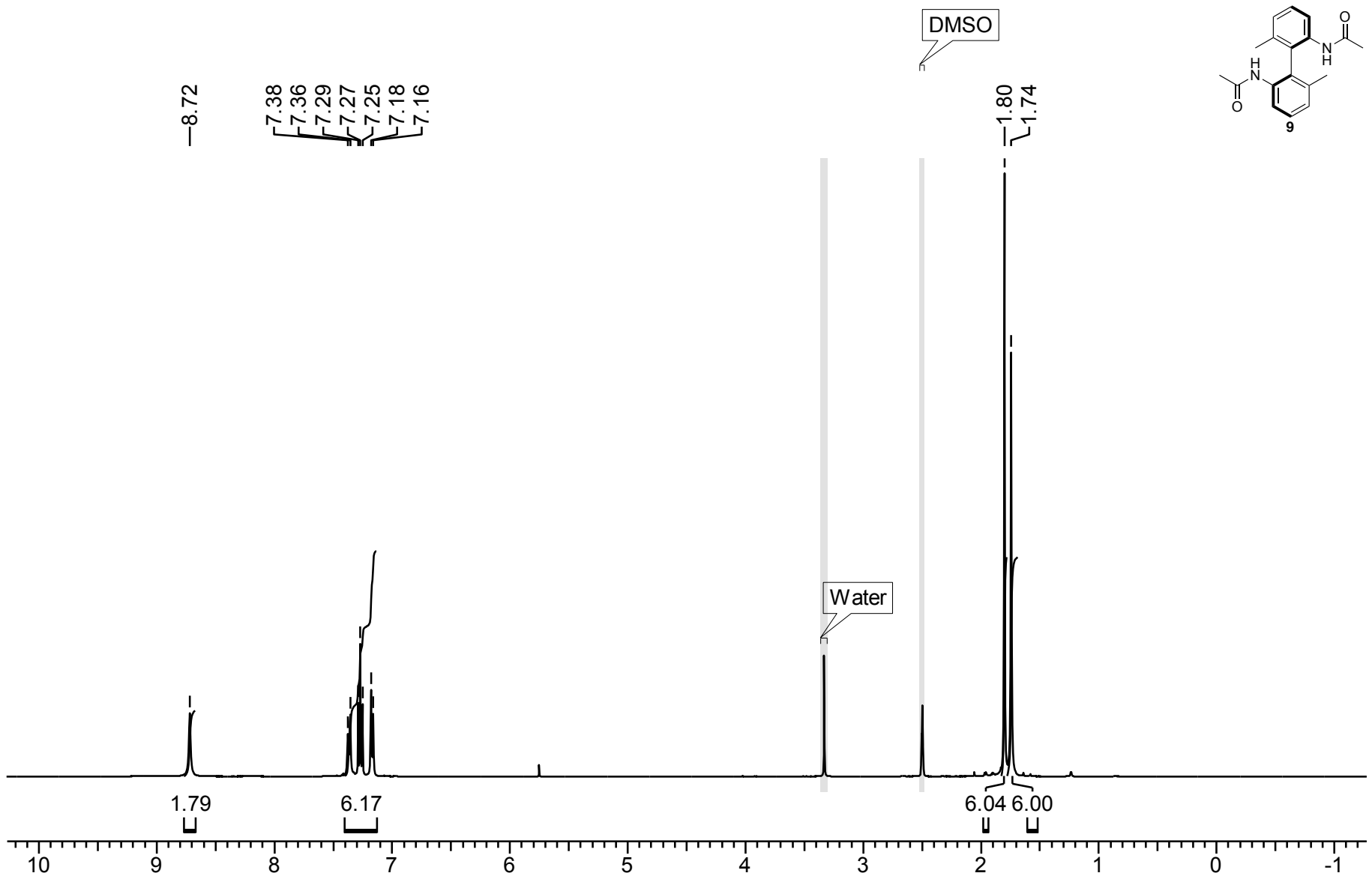

Figure S116. ^{1}H NMR (400 MHz, DMSO-d_6) spectrum of **9**.

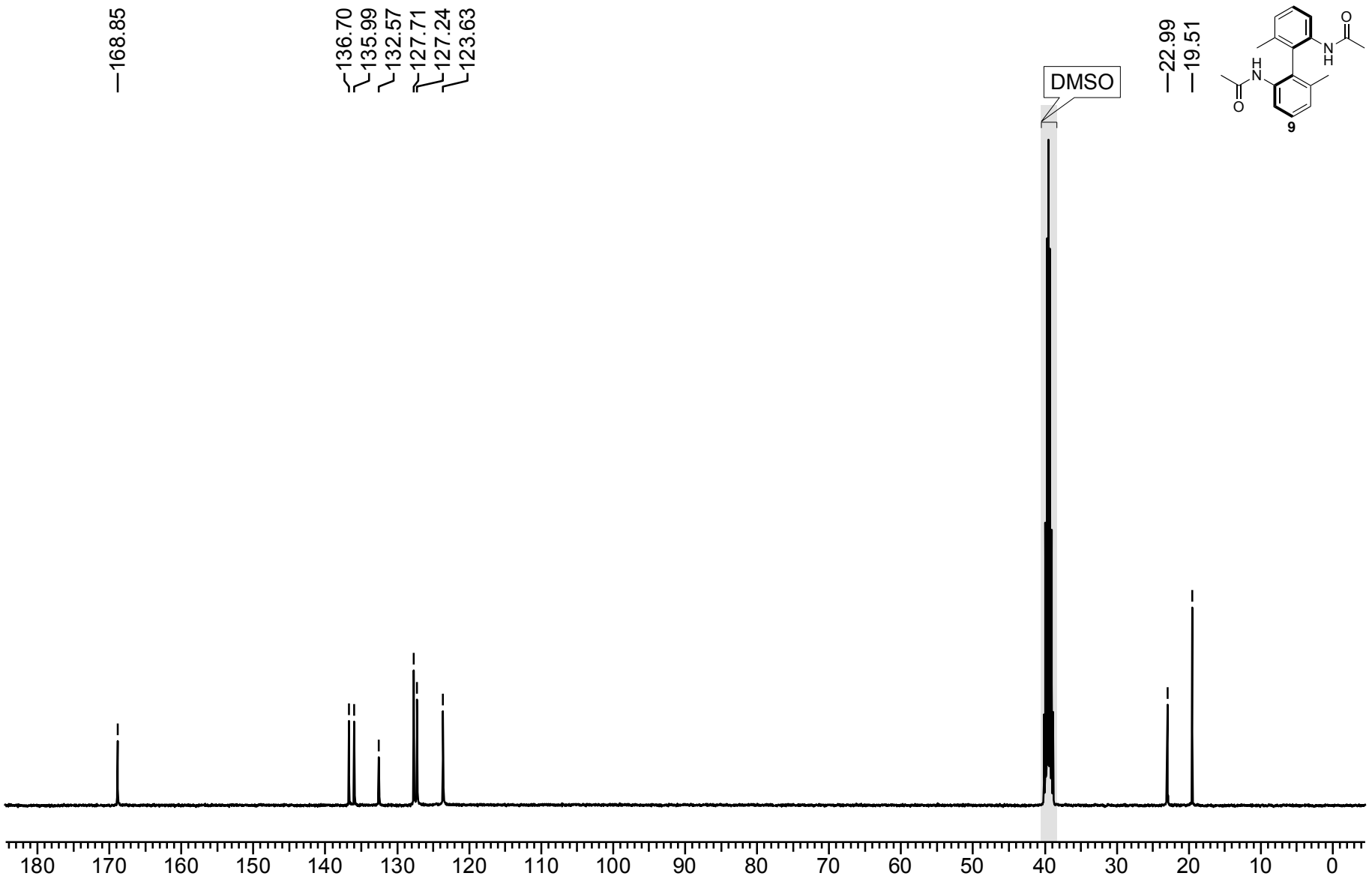

Figure S117. ^{13}C NMR (100 MHz, DMSO-d_6) spectrum of **9**.

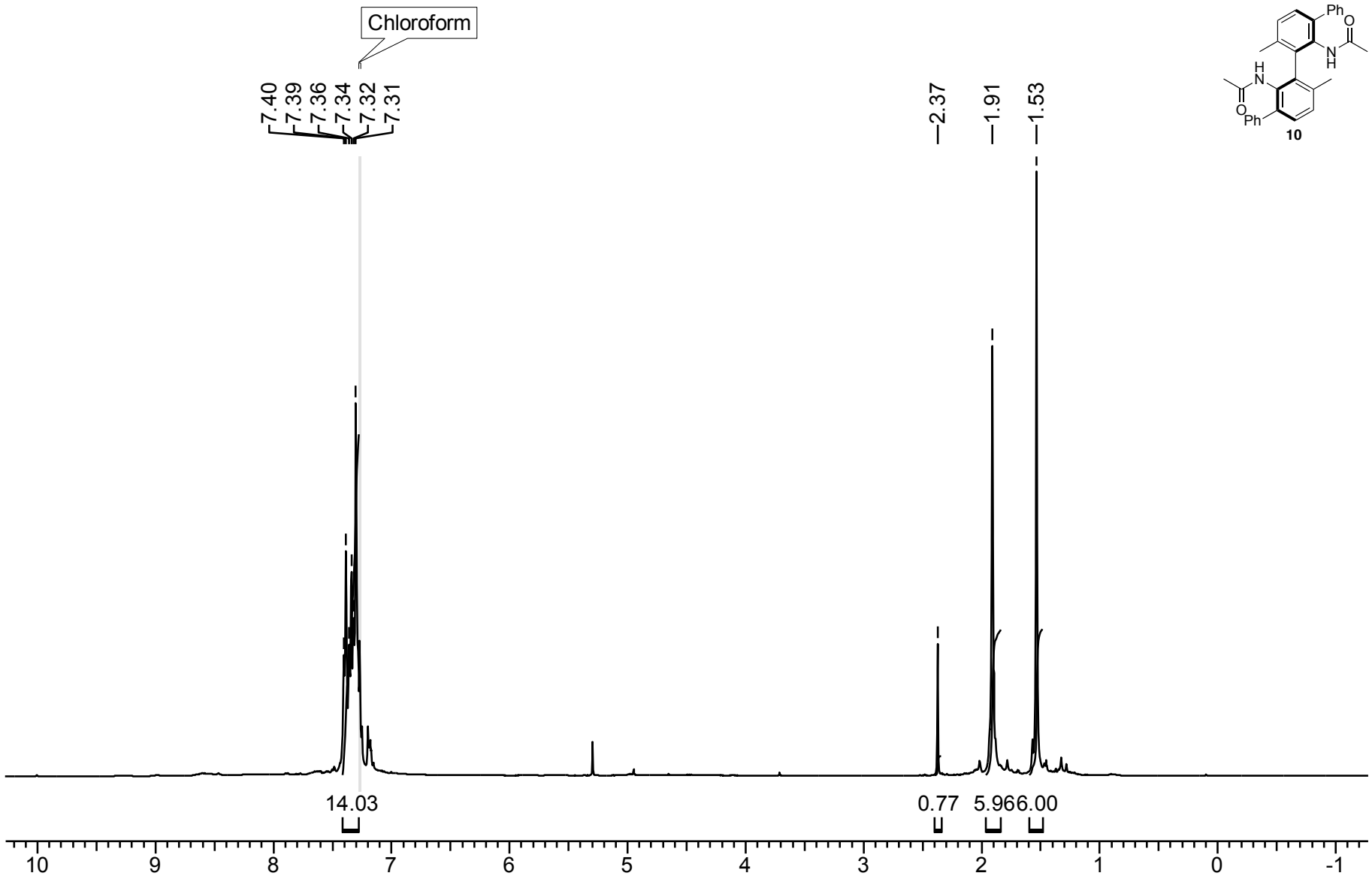

Figure S118. ^{1}H NMR (400 MHz, $CDCl_3$) spectrum of **10**.

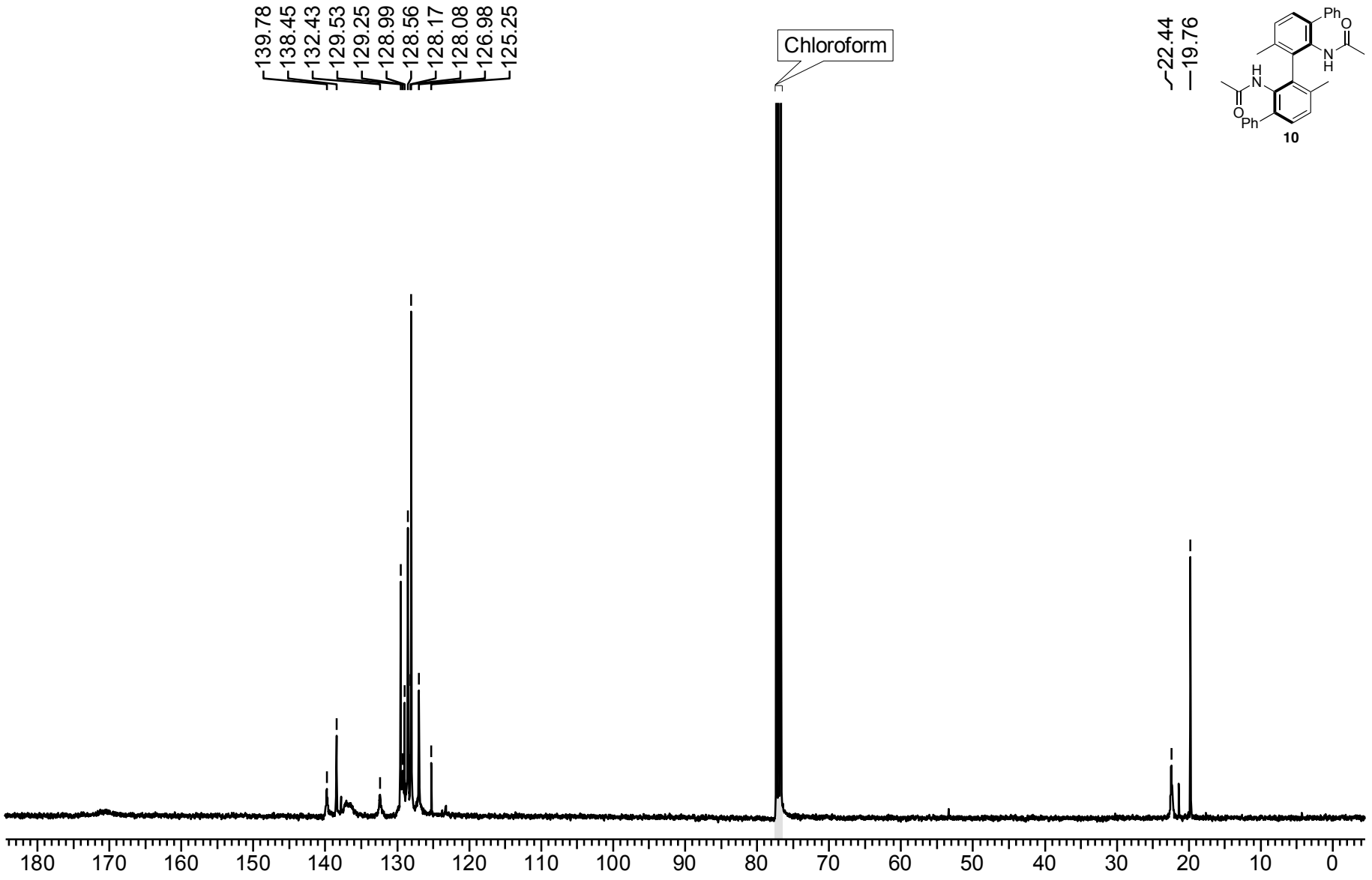

Figure S119. ^{13}C NMR (100 MHz, $CDCl_3$) spectrum of **10**.

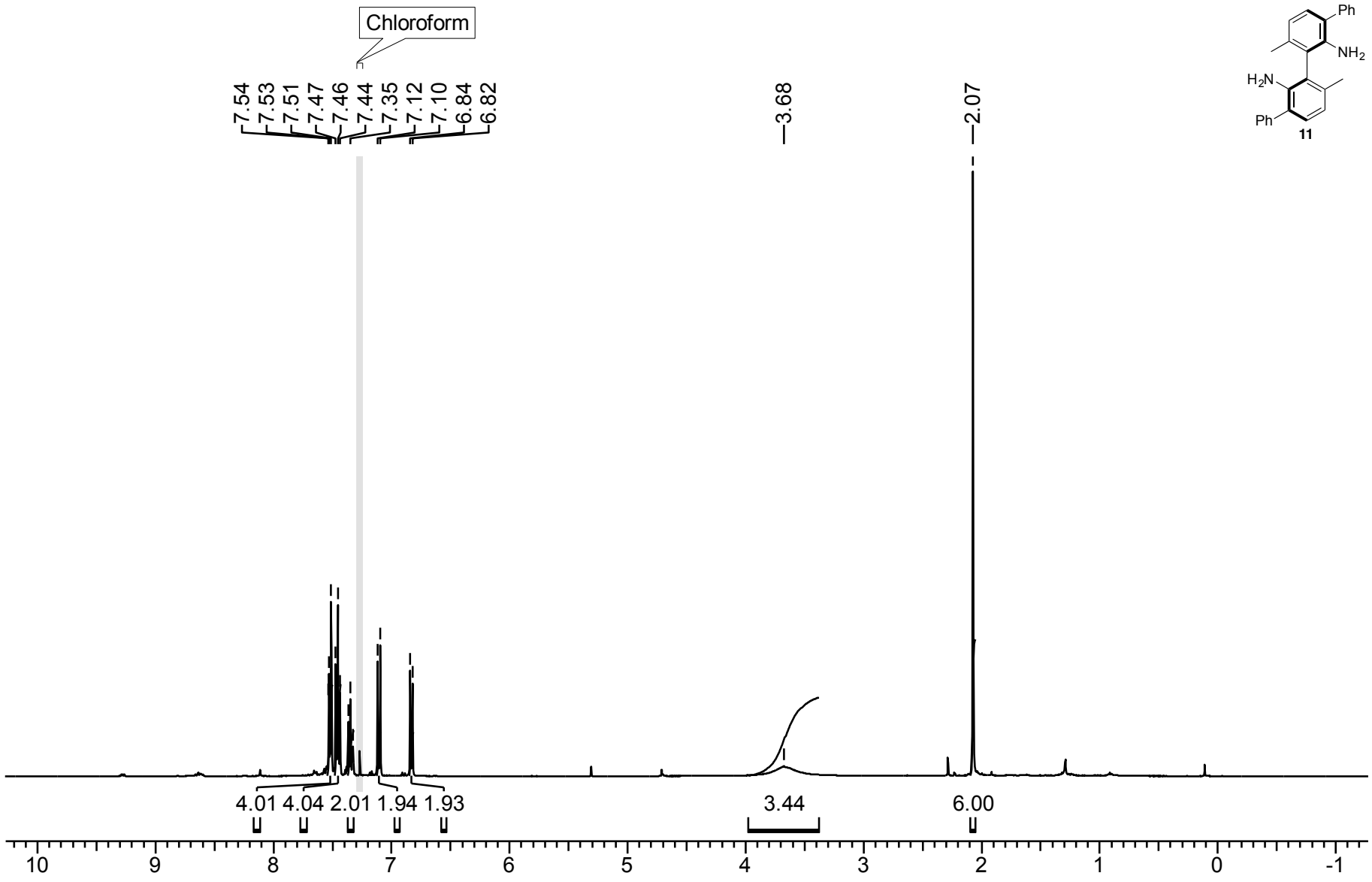

Figure S120. ^{1}H NMR (400 MHz, $CDCl_3$) spectrum of **11**.

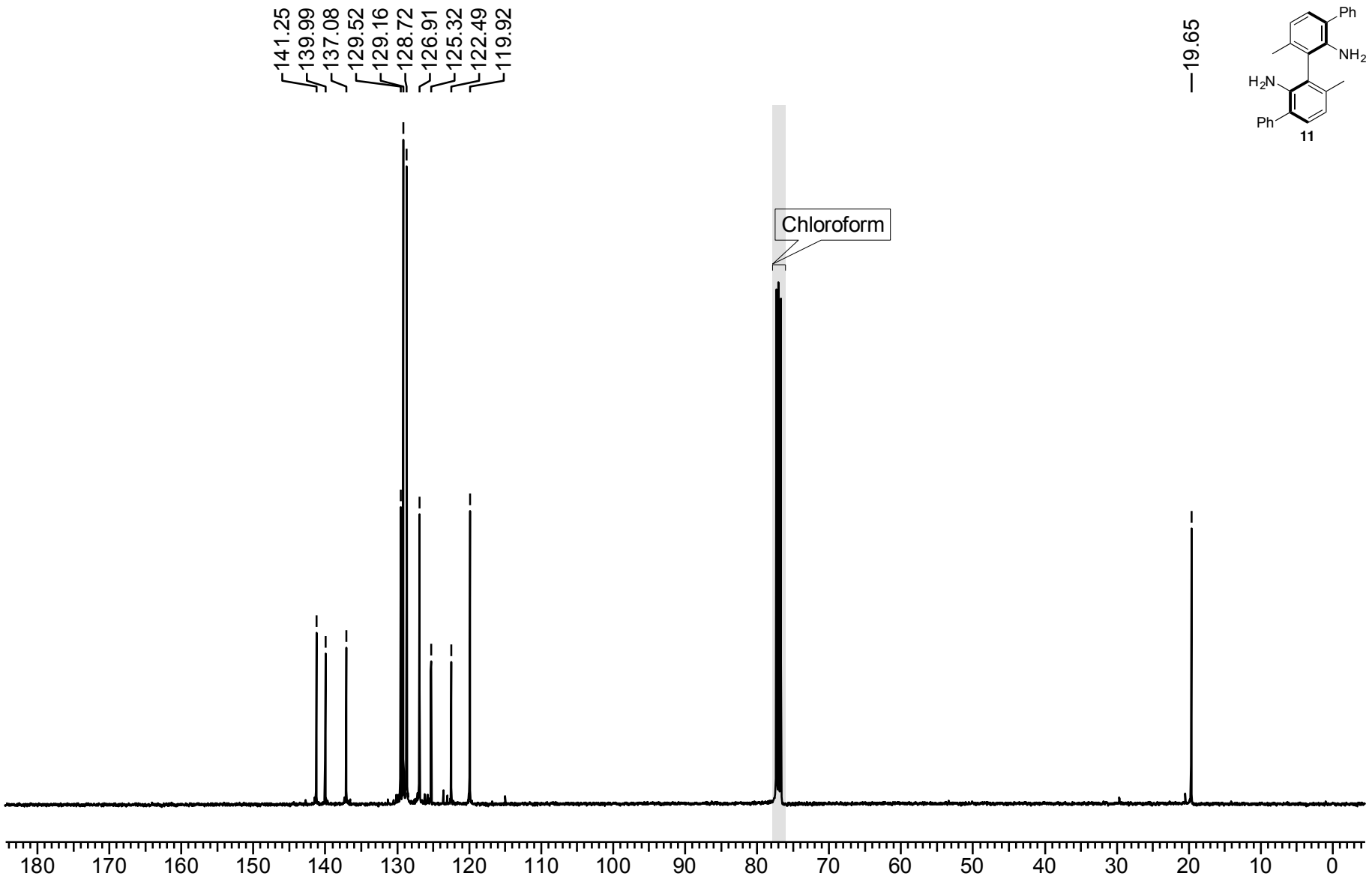

Figure S121. ^{13}C NMR (100 MHz, $CDCl_3$) spectrum of **11**.

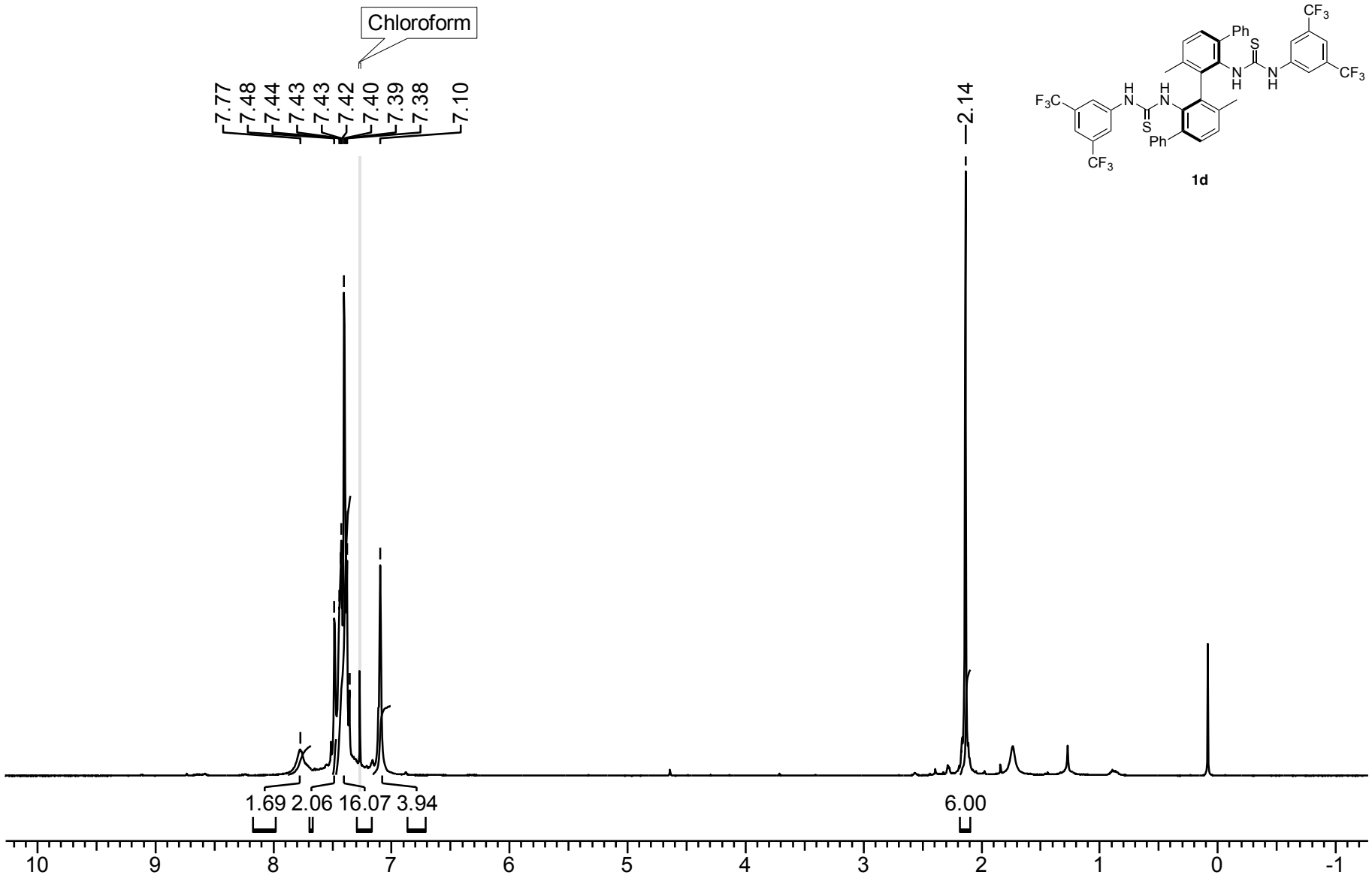

Figure S122. ^{1}H NMR (400 MHz, $CDCl_3$) spectrum of **1d**.

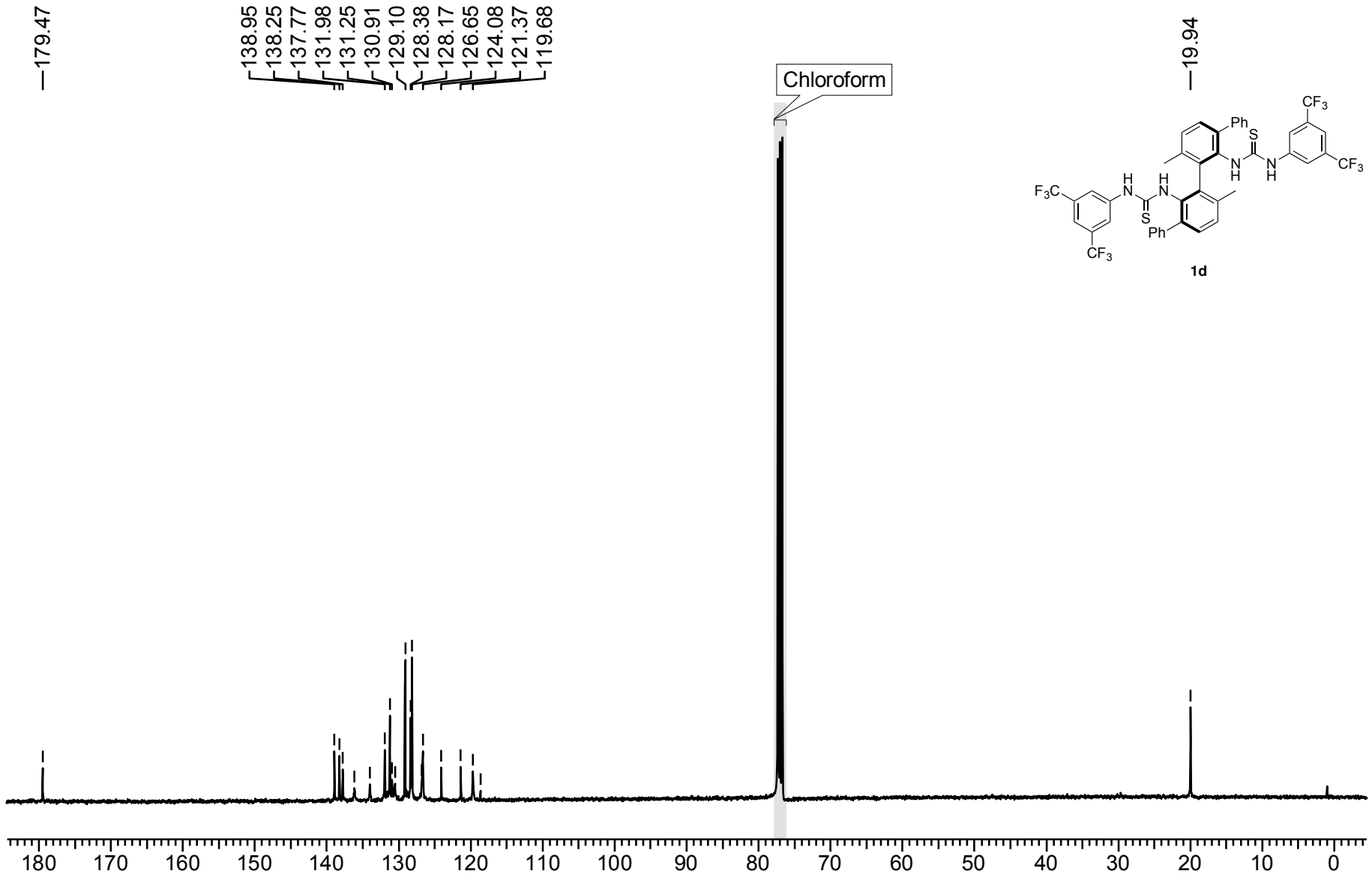

Figure S123. ^{13}C NMR (100 MHz, $CDCl_3$) spectrum of **1d**.

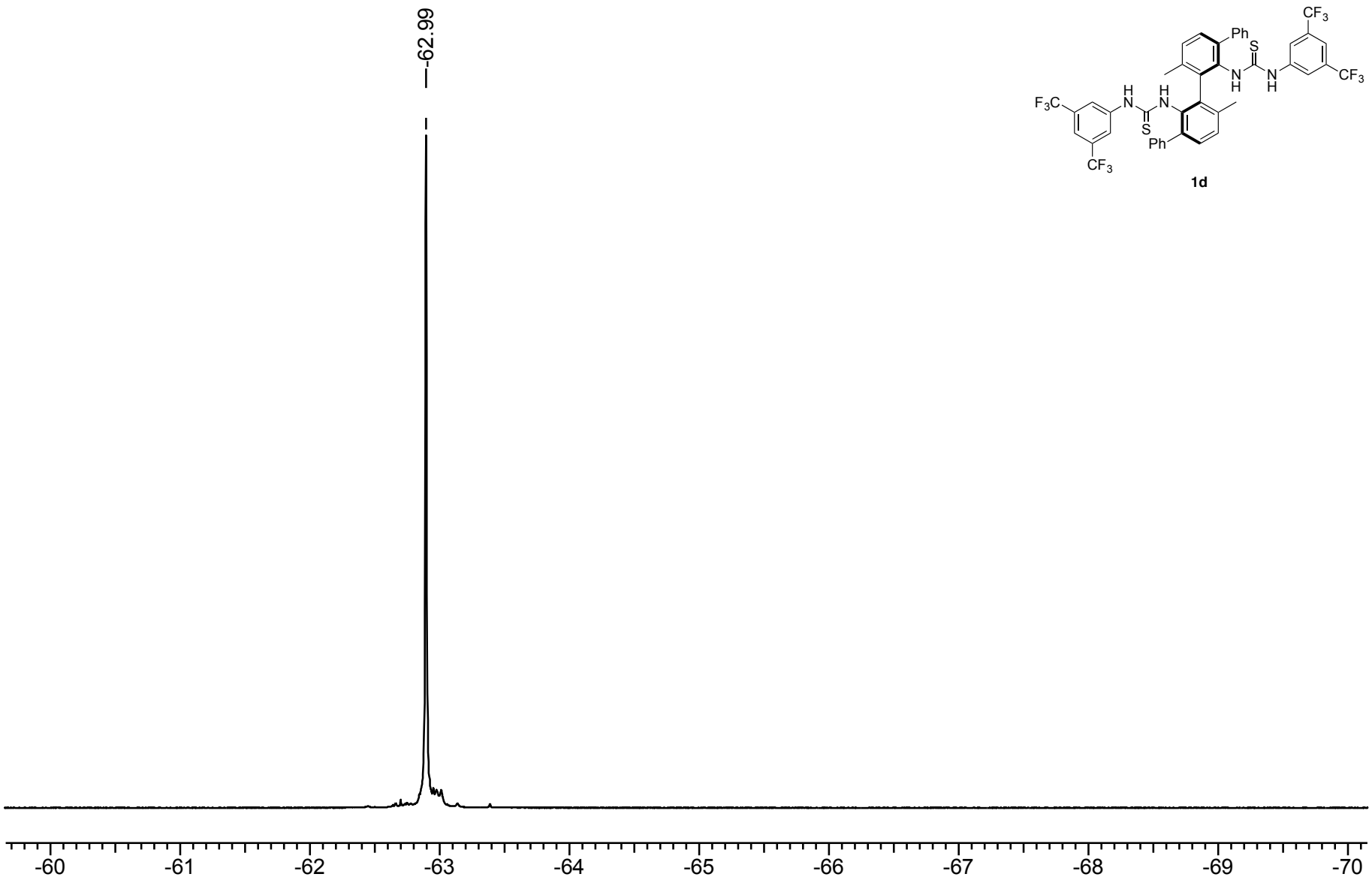

Figure S124. ^{19}F NMR (376 MHz, $CDCl_3$) spectrum of **1d**.

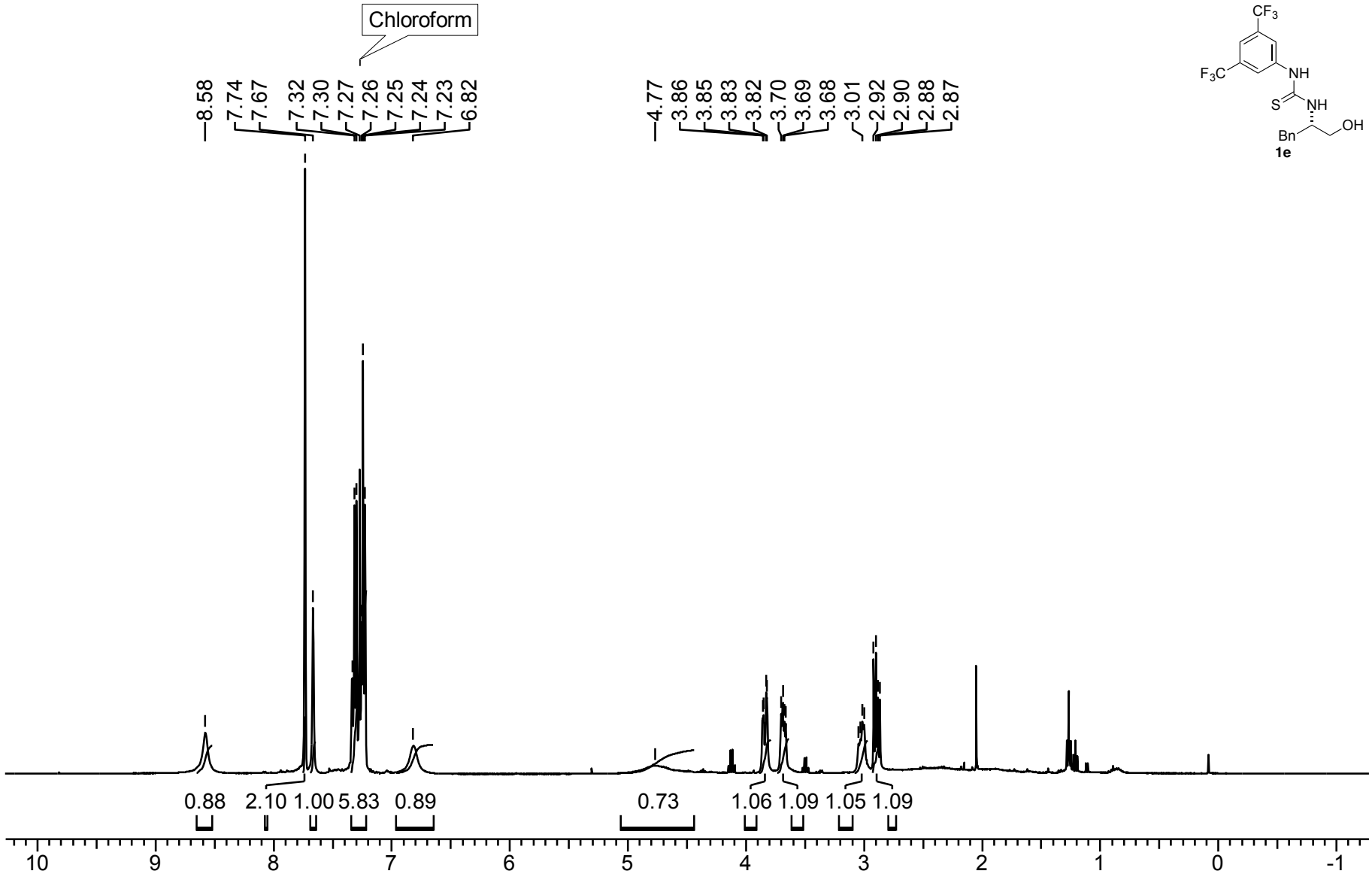

Figure S125. ^{1}H NMR (400 MHz, $CDCl_3$) spectrum of **1e**.

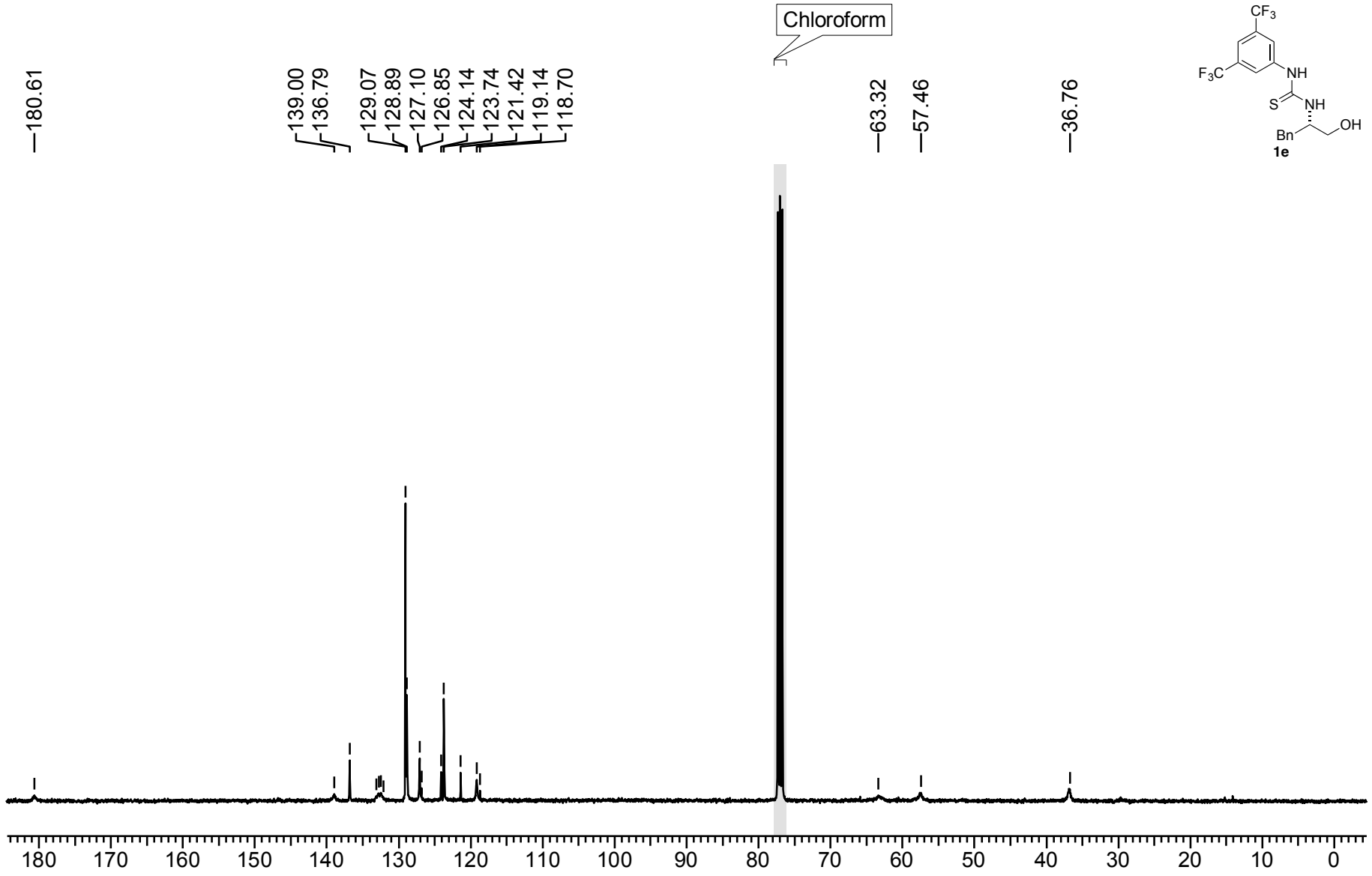

Figure S126. ^{13}C NMR (100 MHz, $CDCl_3$) spectrum of **1e**.

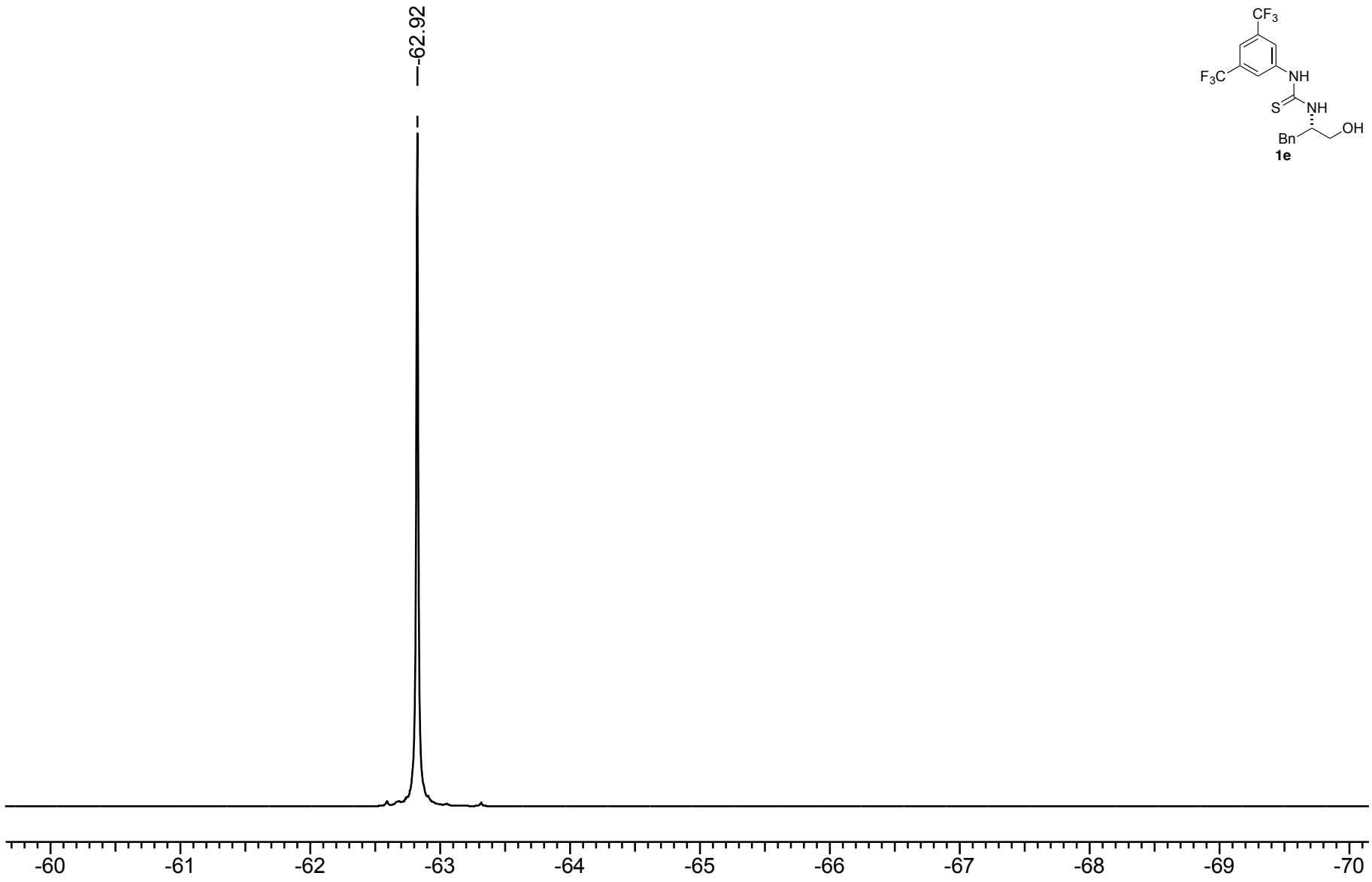

Figure S127. ^{19}F NMR (376 MHz, $CDCl_3$) spectrum of **1e**.

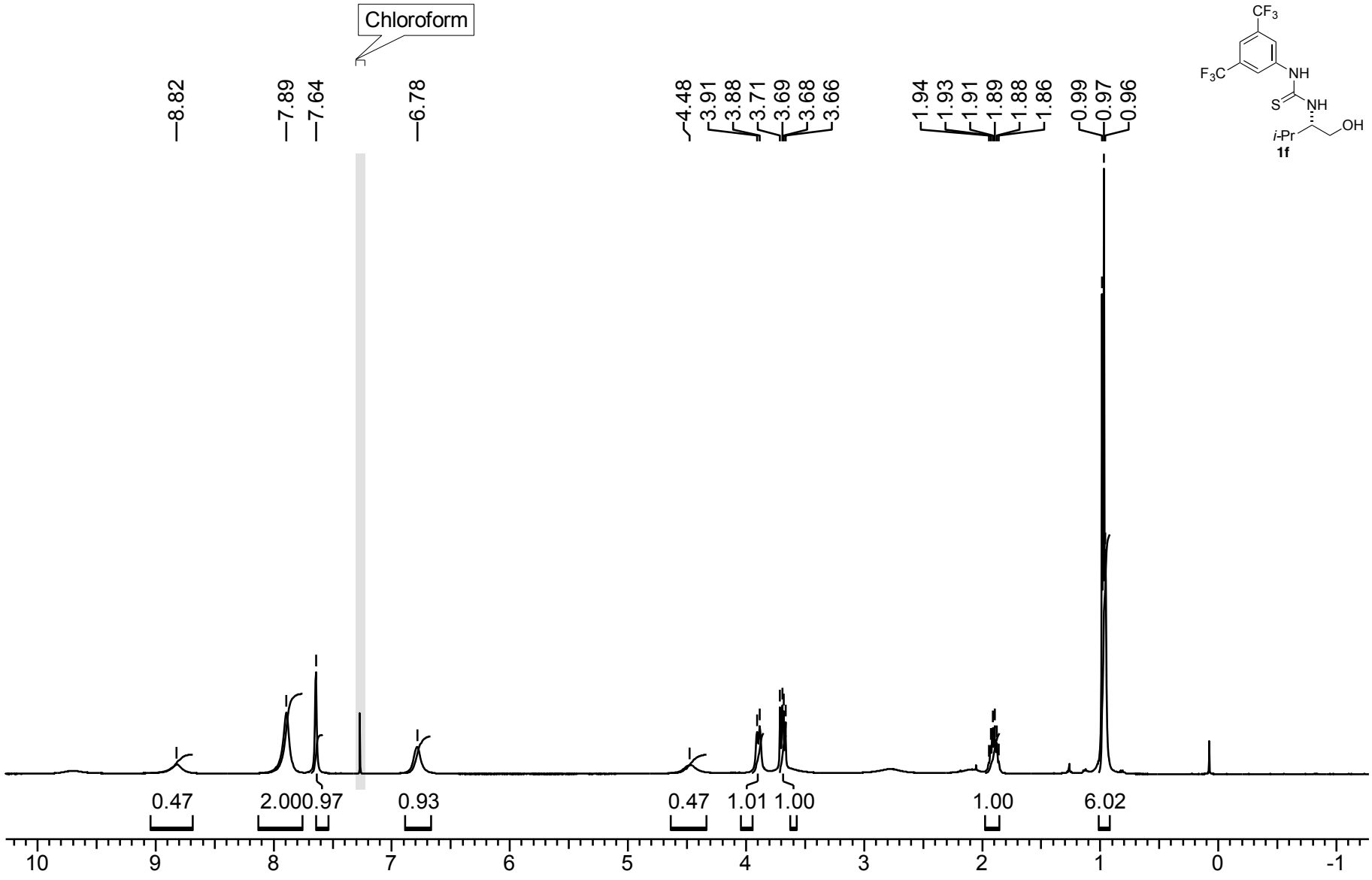

Figure S128. ^{1}H NMR (400 MHz, $CDCl_3$) spectrum of **1f**.

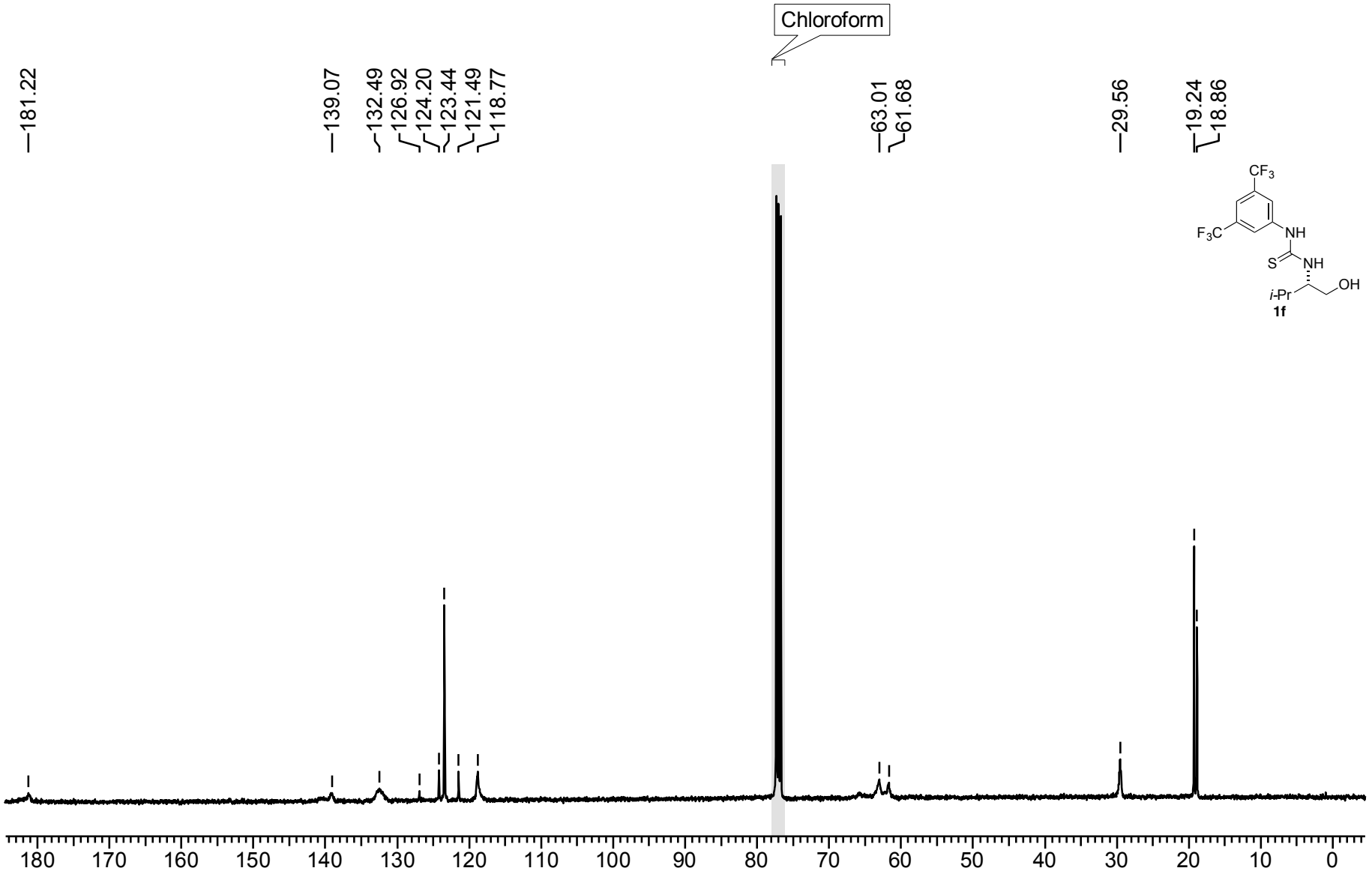

Figure S129. ^{13}C NMR (100 MHz, $CDCl_3$) spectrum of **1f**.

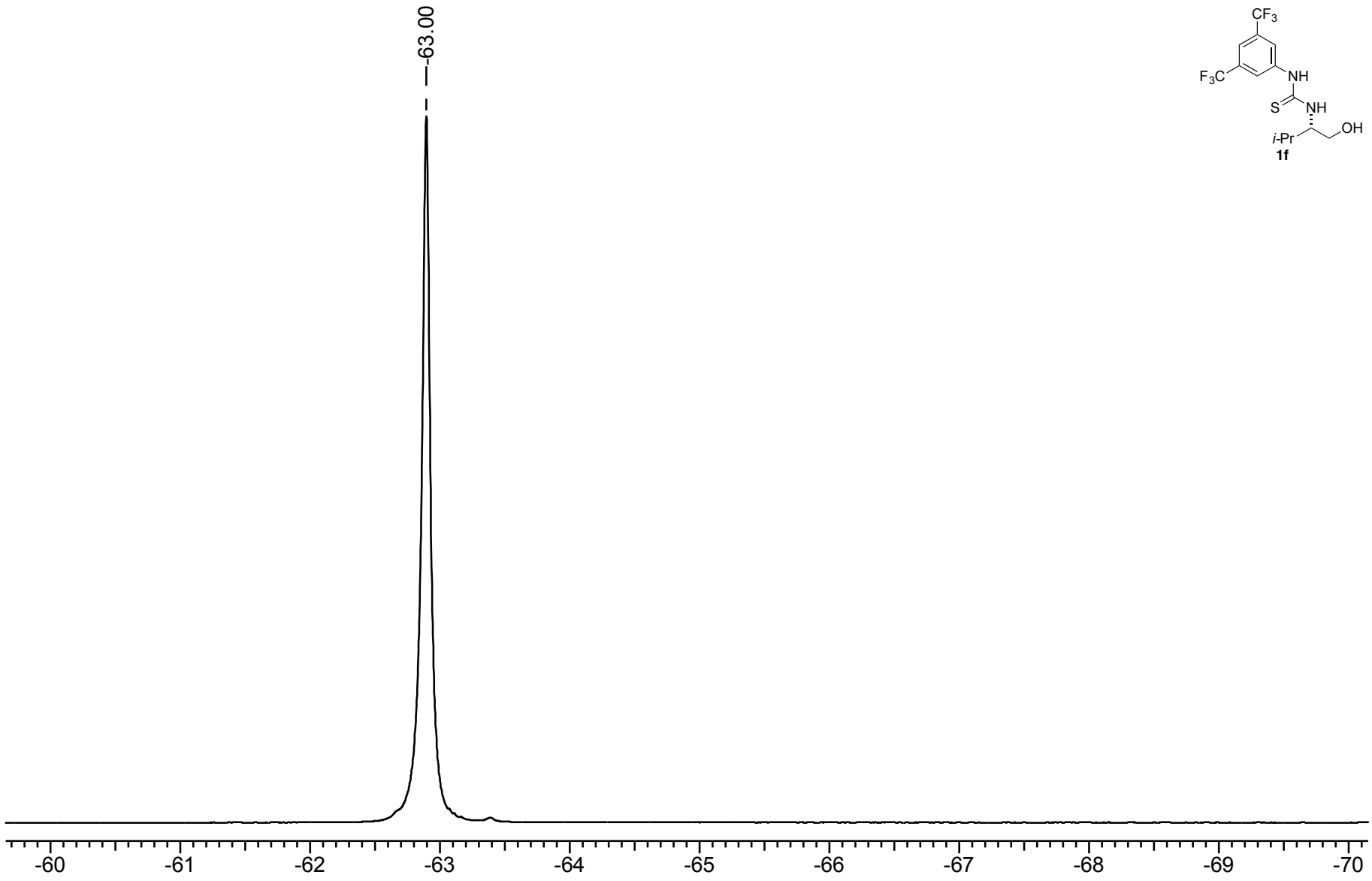

Figure S130. ^{19}F NMR (376 MHz, $CDCl_3$) spectrum of **1f**.

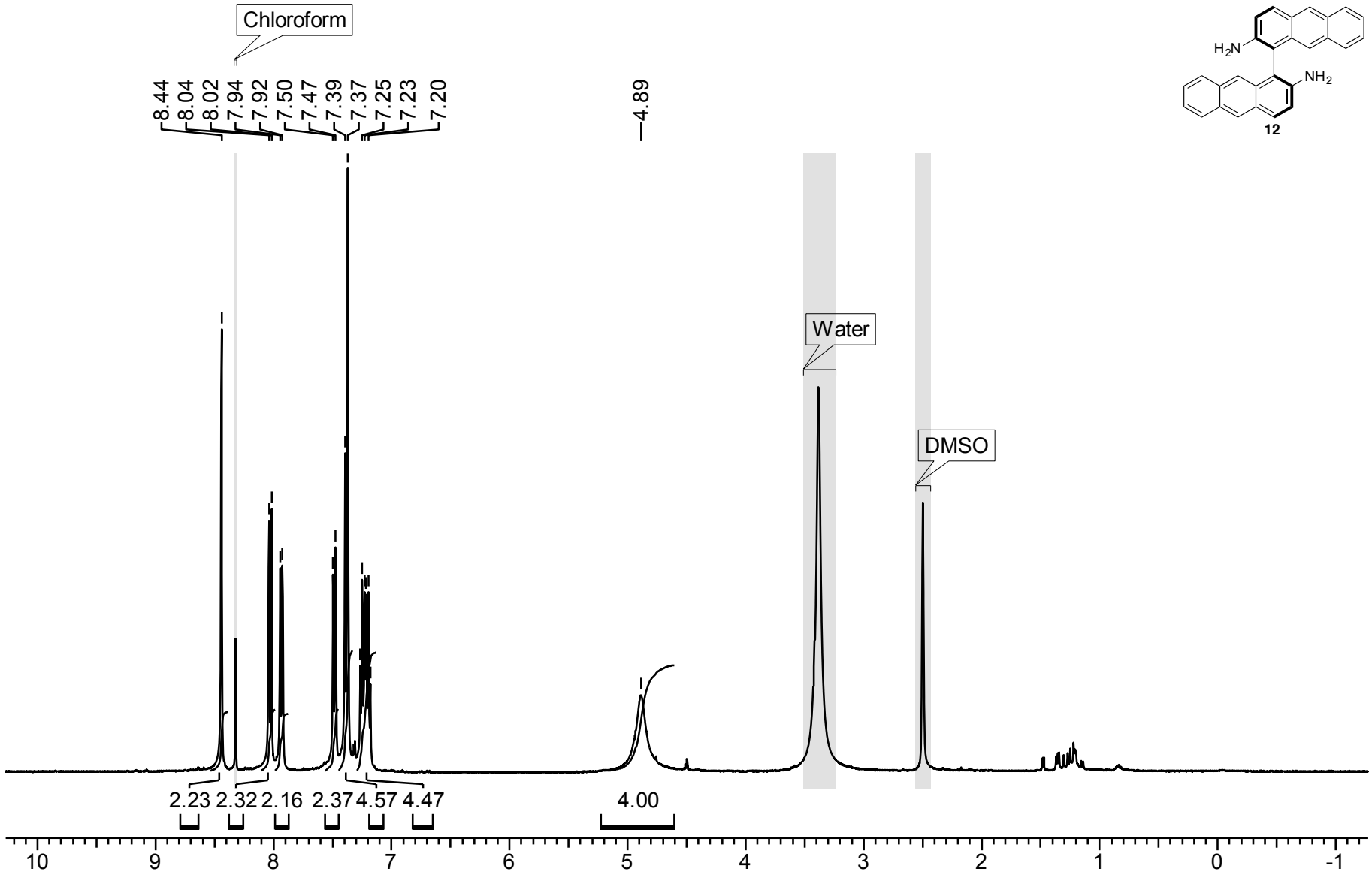

Figure S131. ^{1}H NMR (400 MHz, DMSO-d_6) spectrum of **12**.

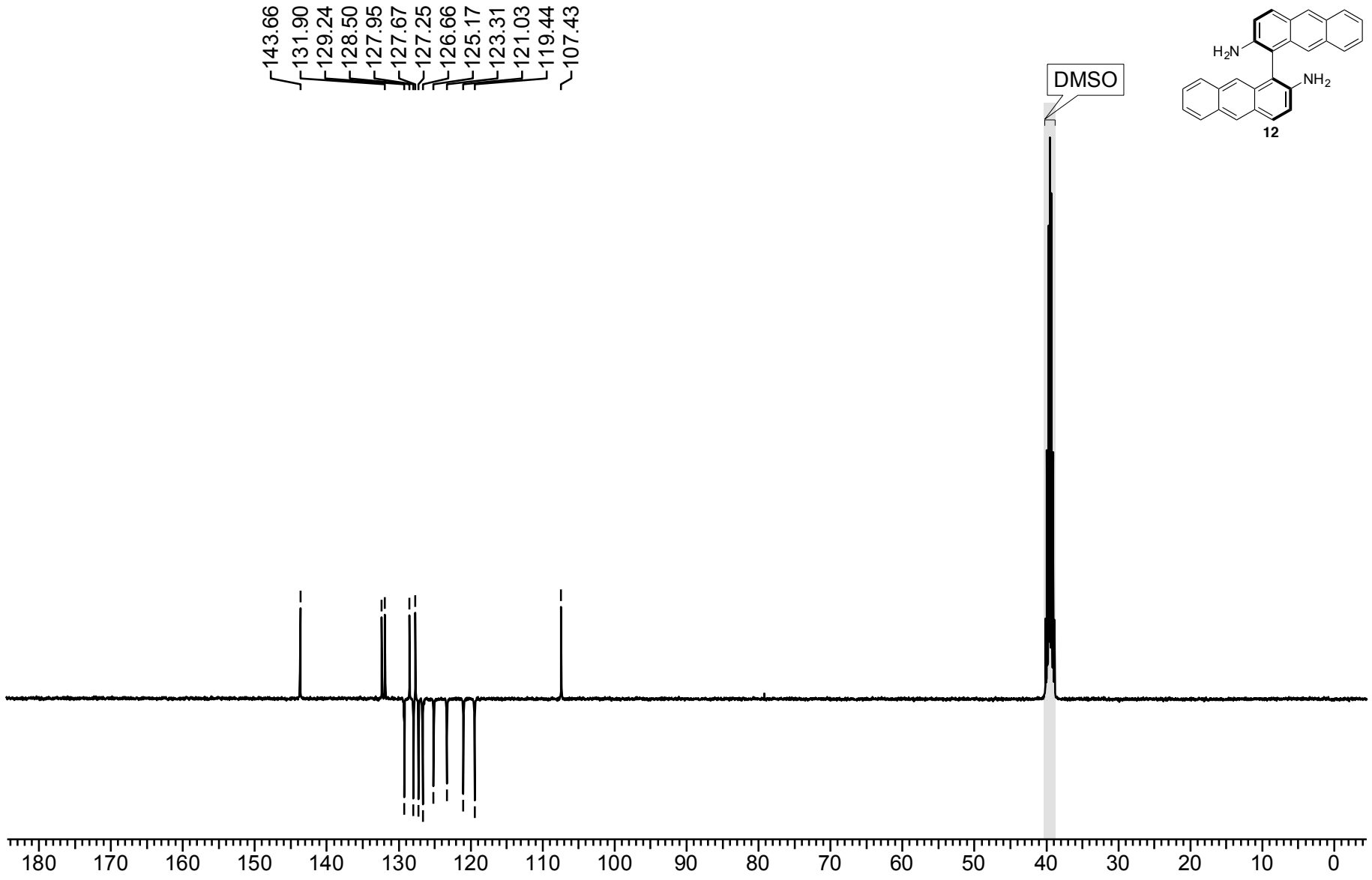

Figure S132. ^{13}C NMR APT (100 MHz, DMSO-d_6) spectrum of **12**.

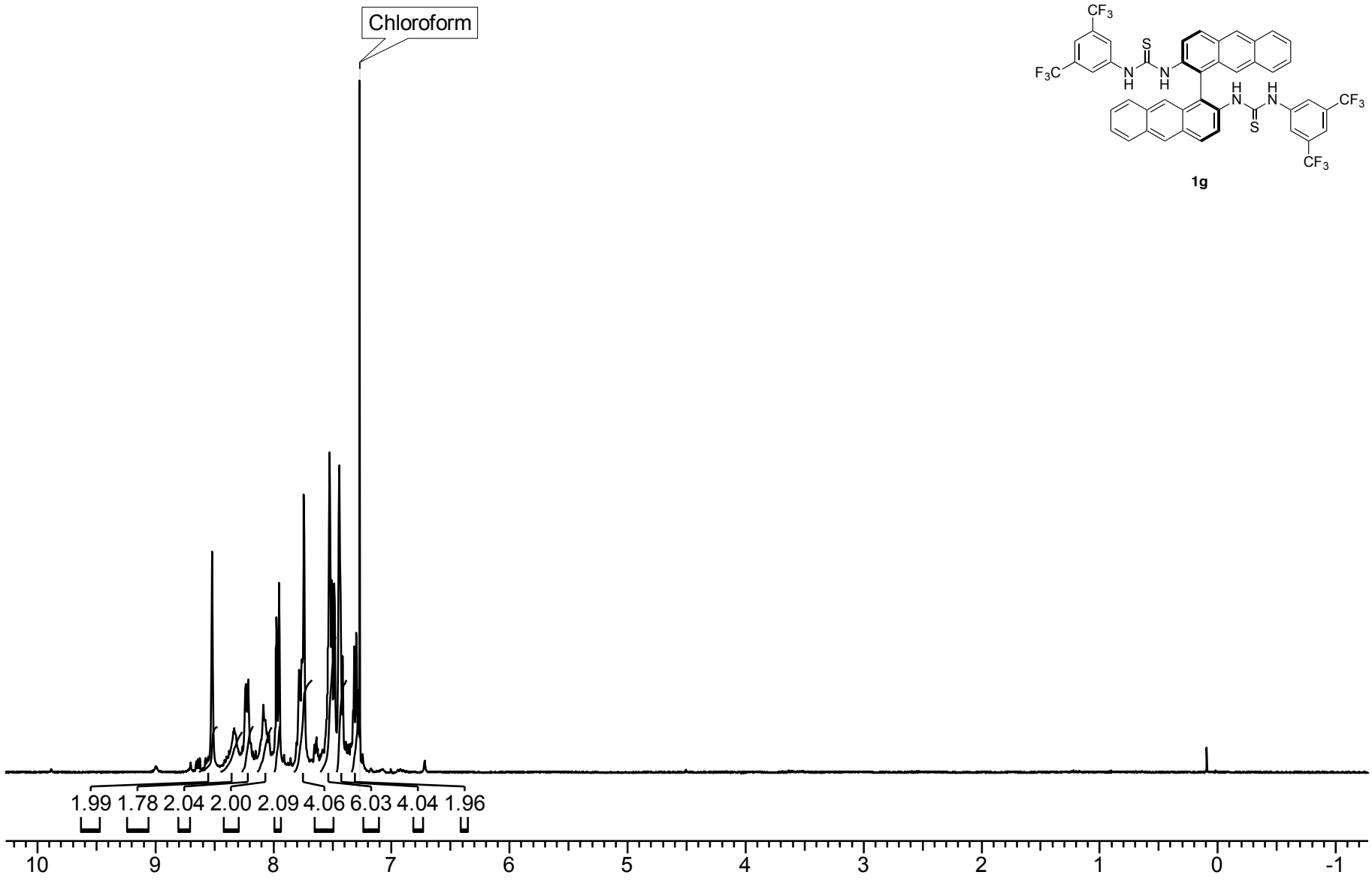

1g

Figure S133. ^{1}H NMR (400 MHz, $CDCl_3$) spectrum of **1g**.

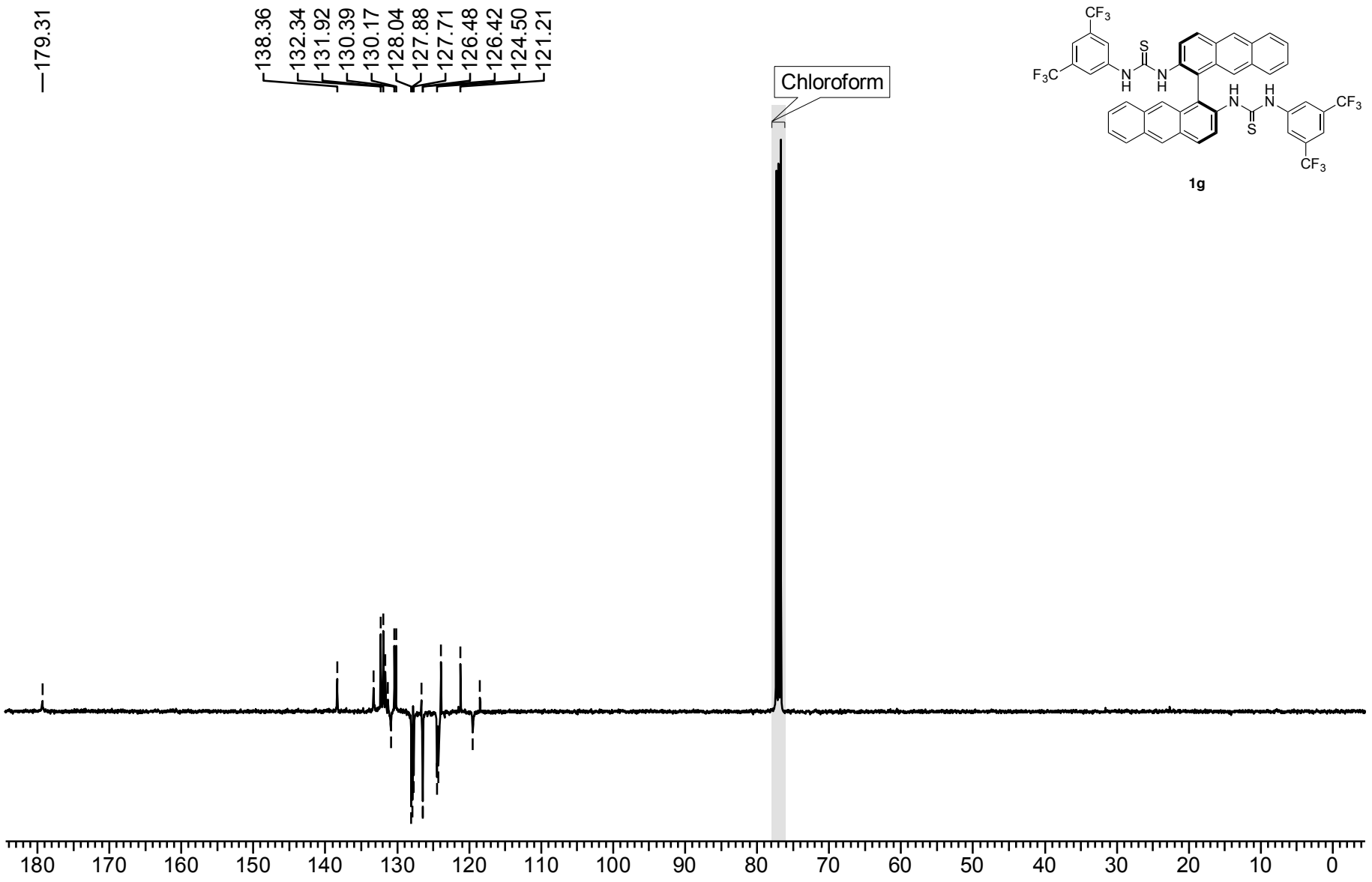

Figure S134. ^{13}C NMR APT (100 MHz, $CDCl_3$) spectrum of **1g**.

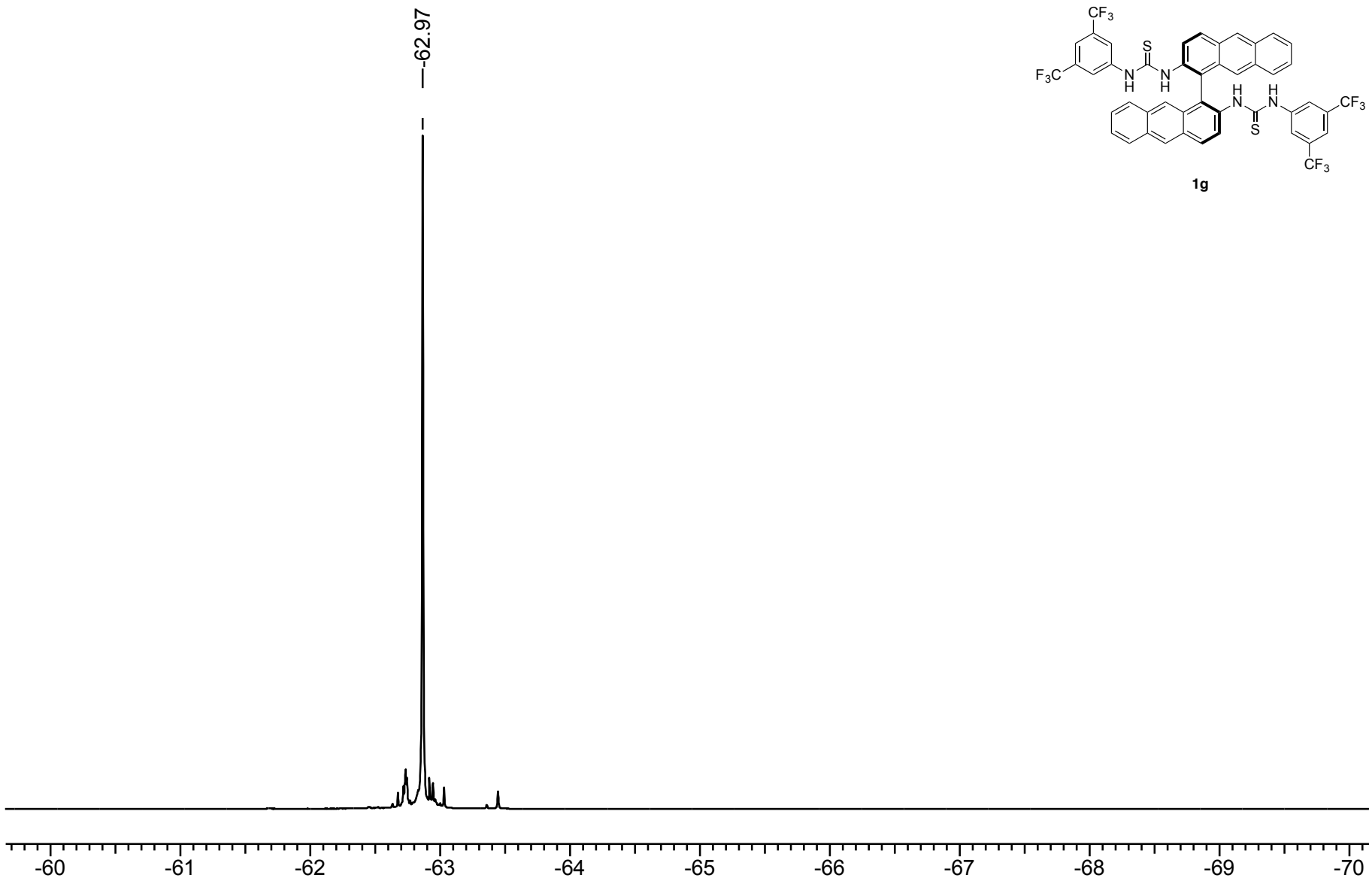

1g

Figure S135. ^{19}F NMR (376 MHz, $CDCl_3$) spectrum of **1g**.

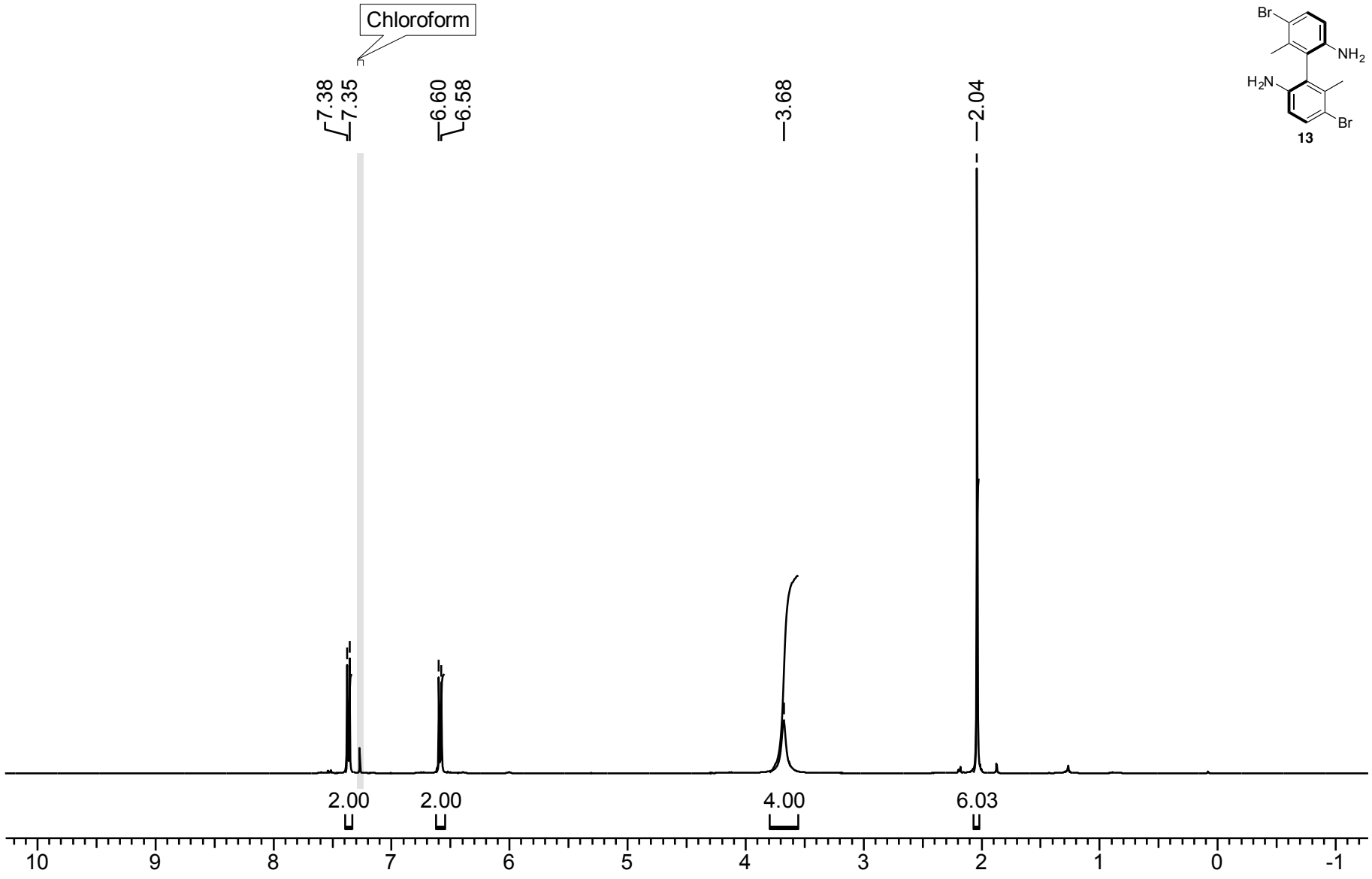

Figure S136. ^{1}H NMR (400 MHz, $CDCl_3$) spectrum of **13**.

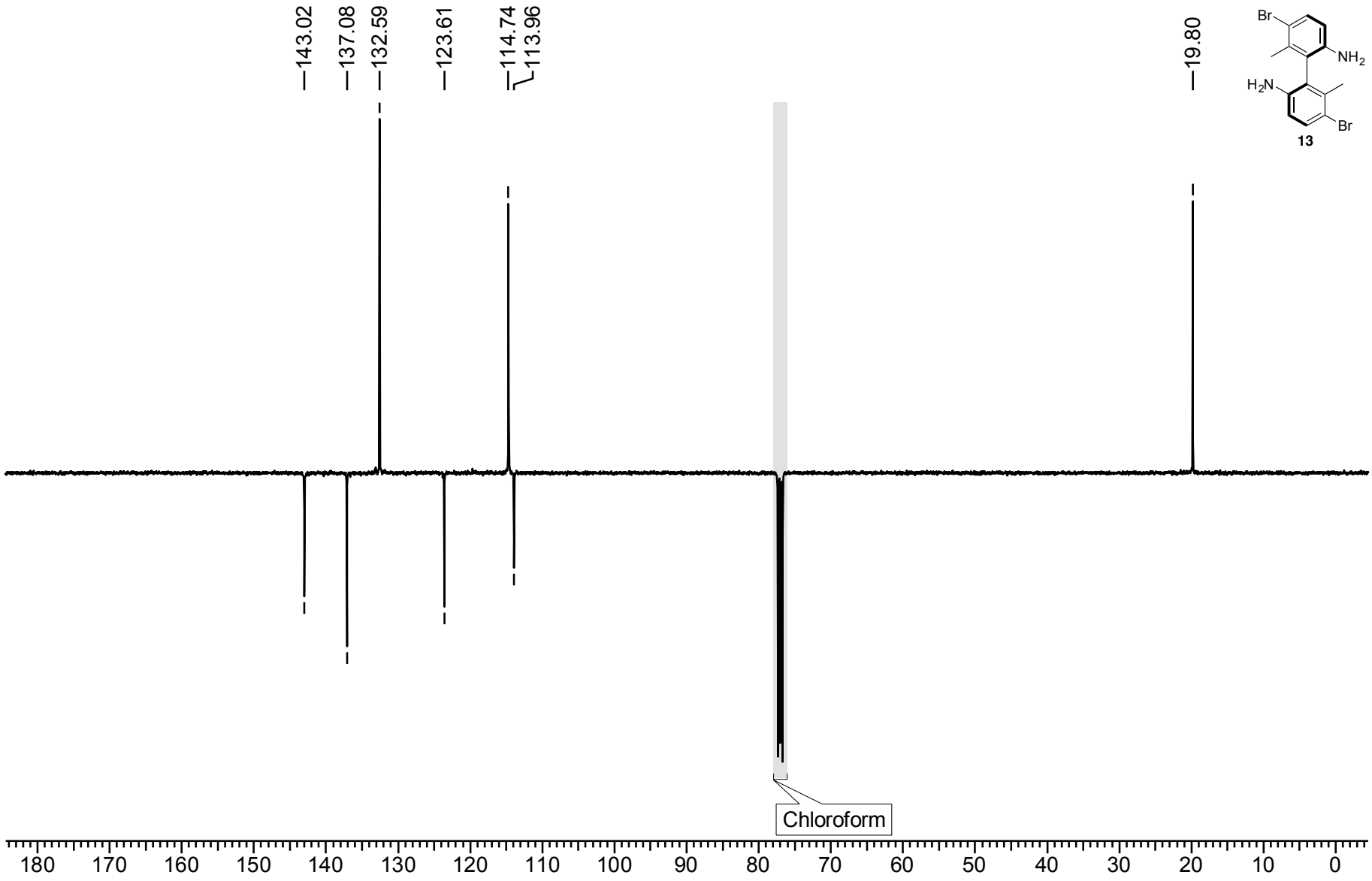

Figure S137. ^{13}C NMR APT (100 MHz, $CDCl_3$) spectrum of **13**.

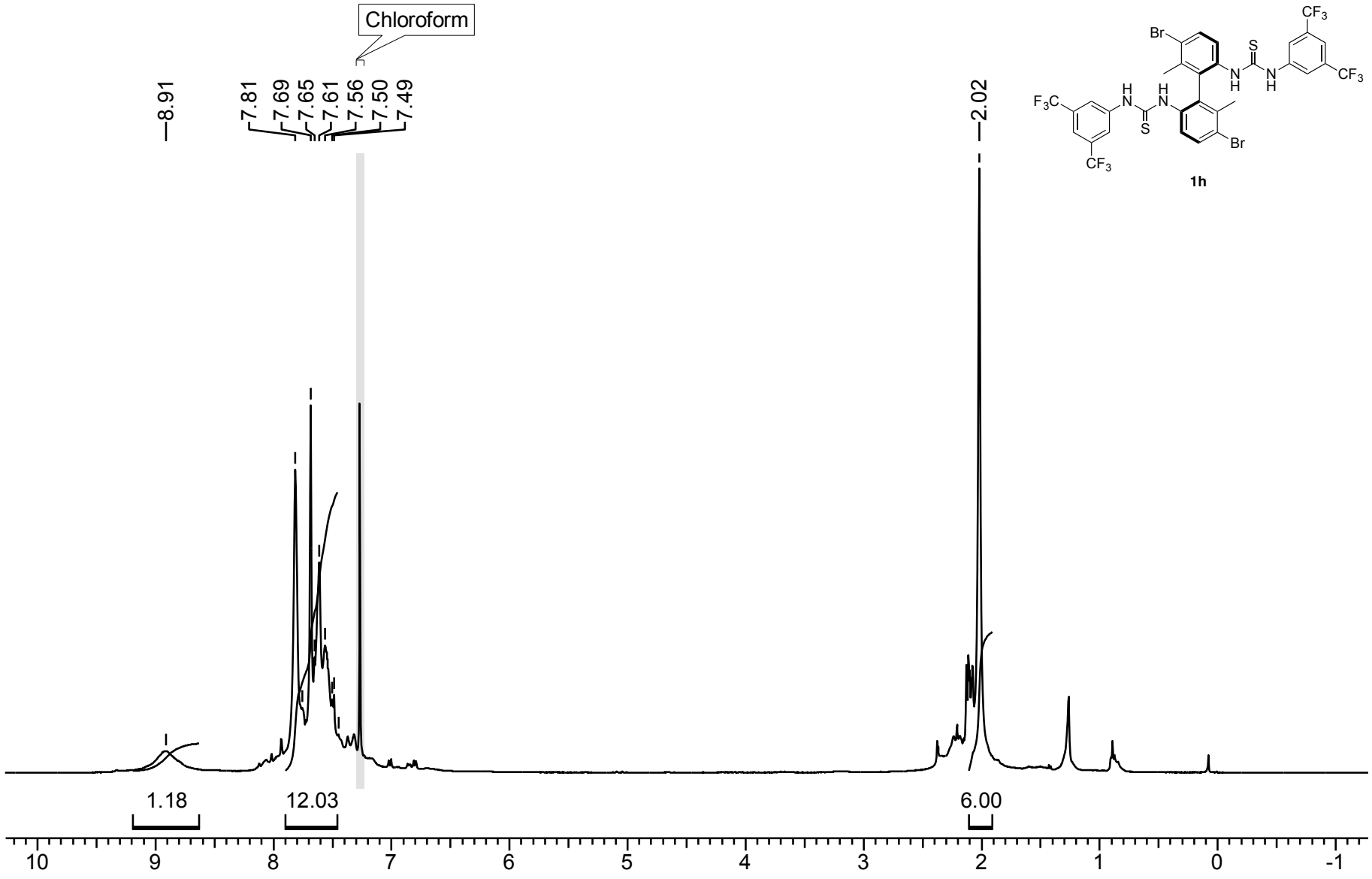

Figure S138. ^{1}H NMR (400 MHz, $CDCl_3$) spectrum of **1h**.

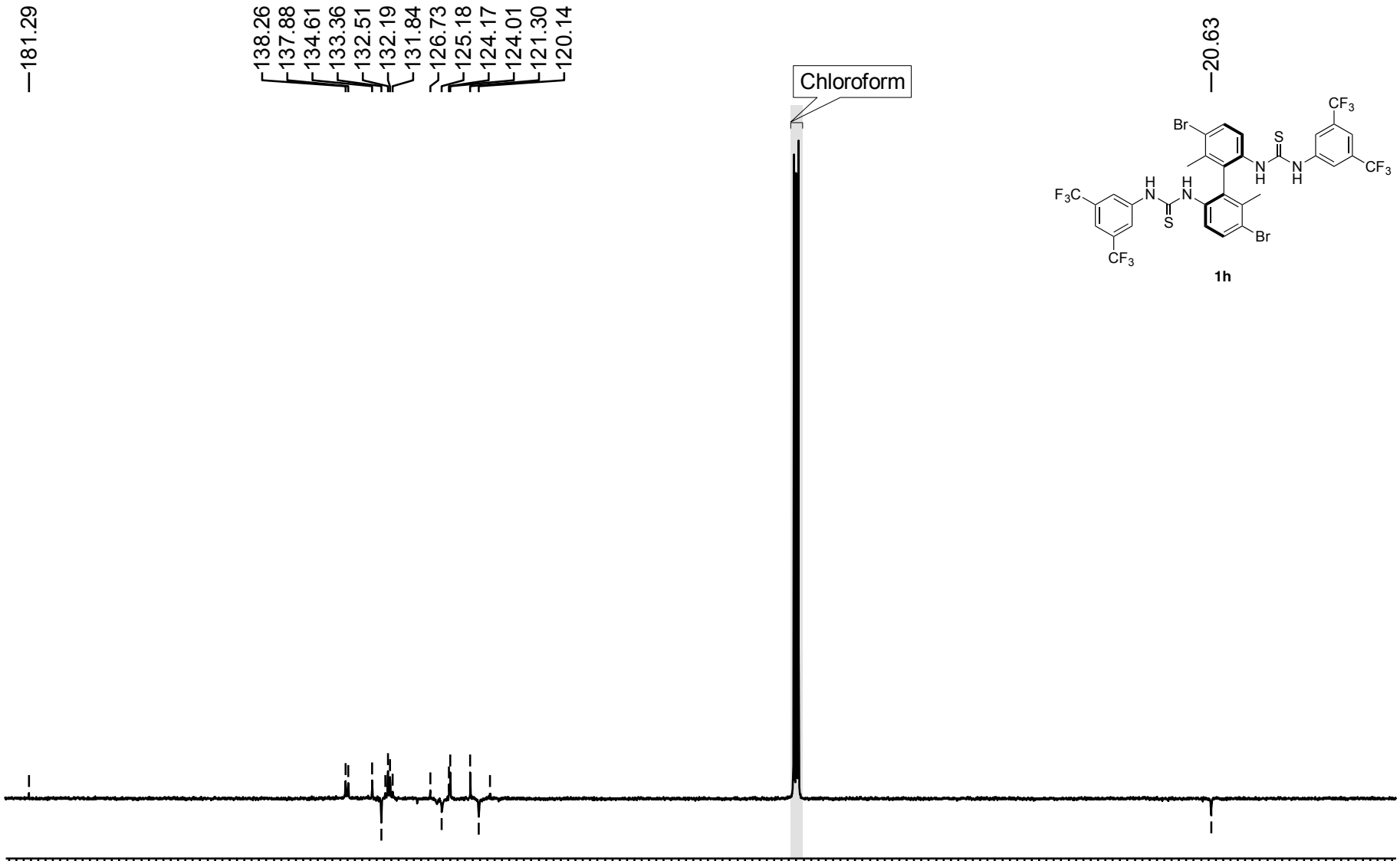

Figure S139. ^{13}C NMR (100 MHz, $CDCl_3$) spectrum of **1h**.

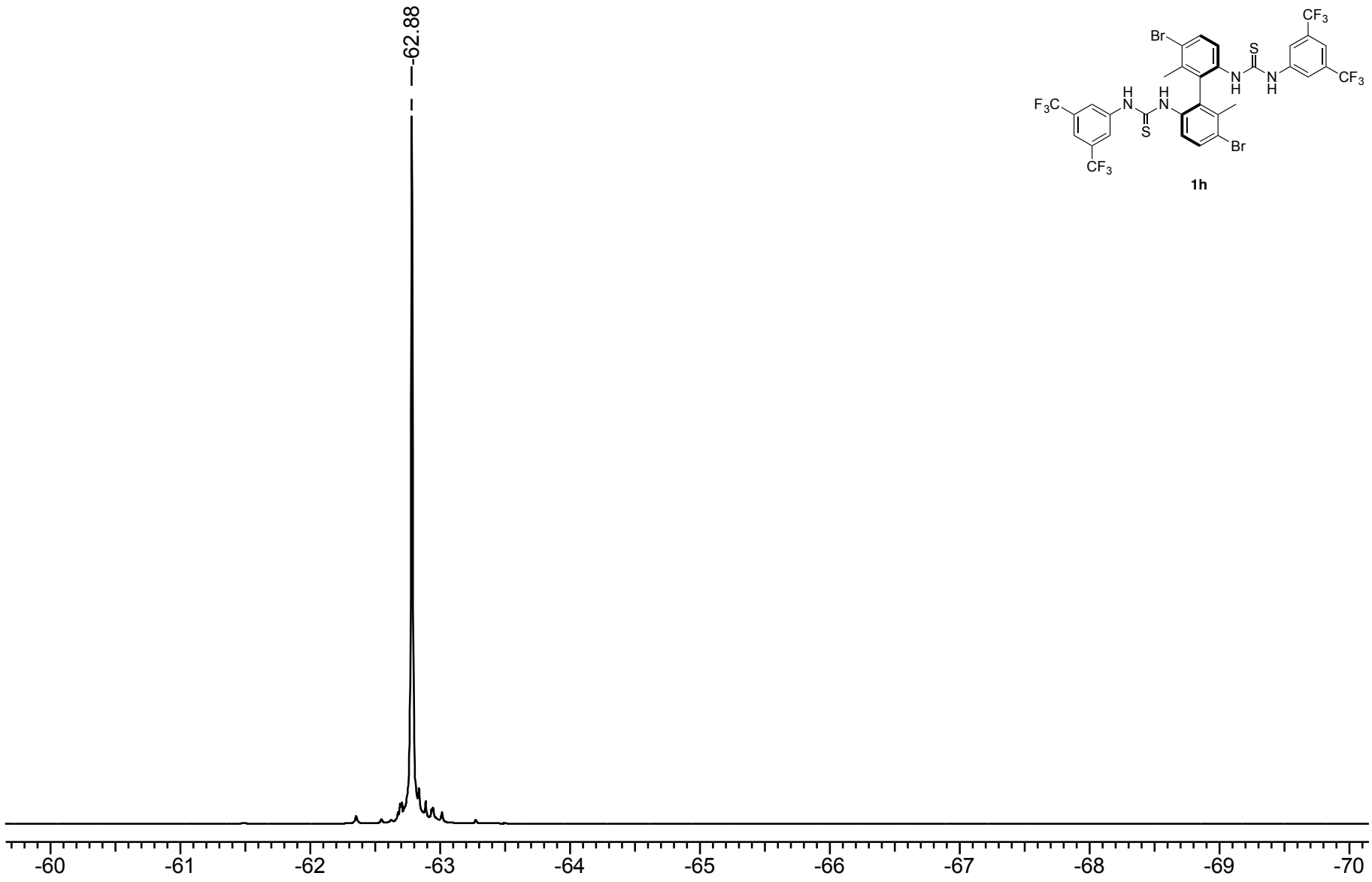

1h

Figure S140. ^{19}F NMR (376 MHz, $CDCl_3$) spectrum of **1h**.

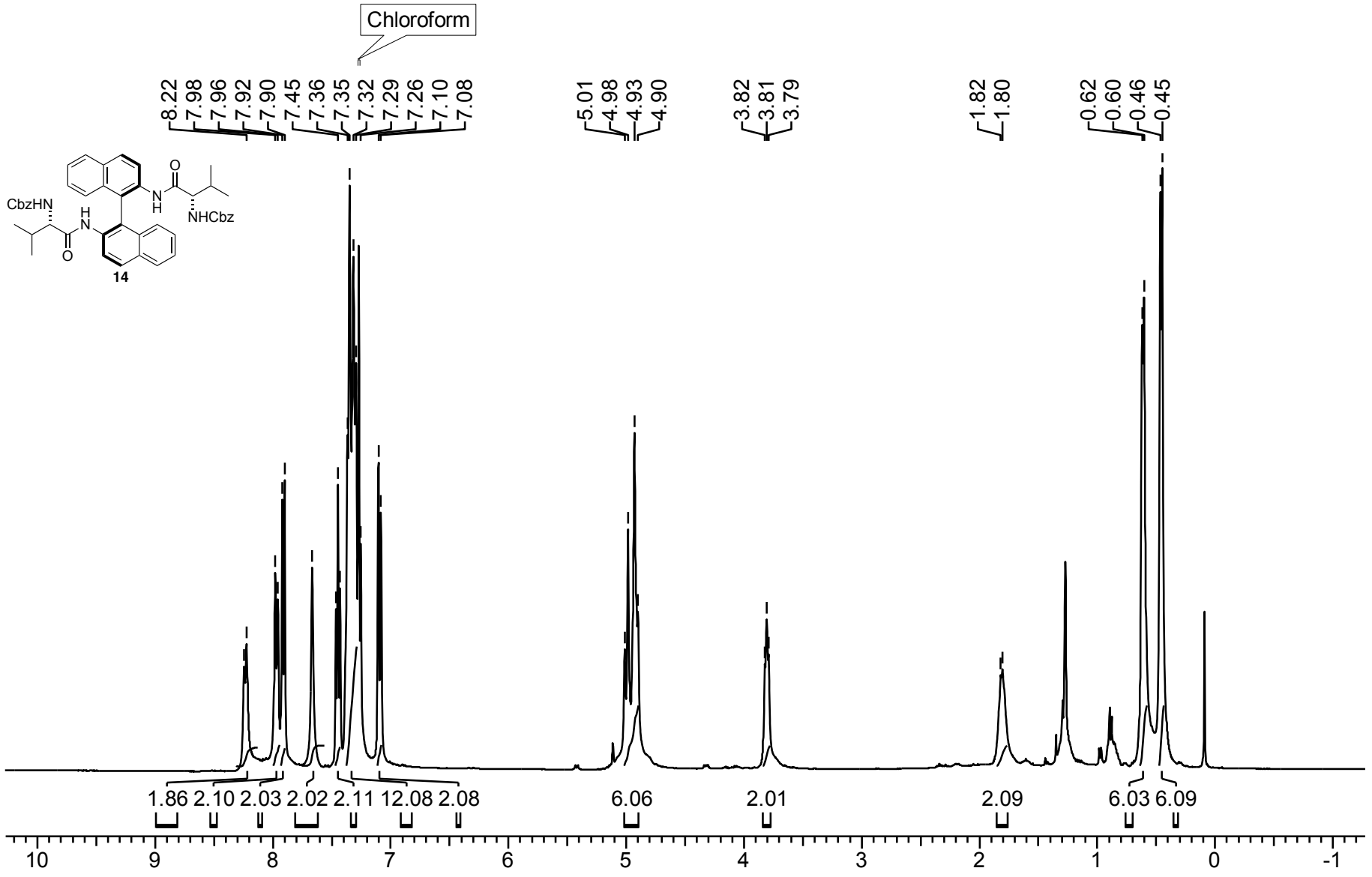

Figure S141. ^{1}H NMR (400 MHz, $CDCl_3$) spectrum of **14**.

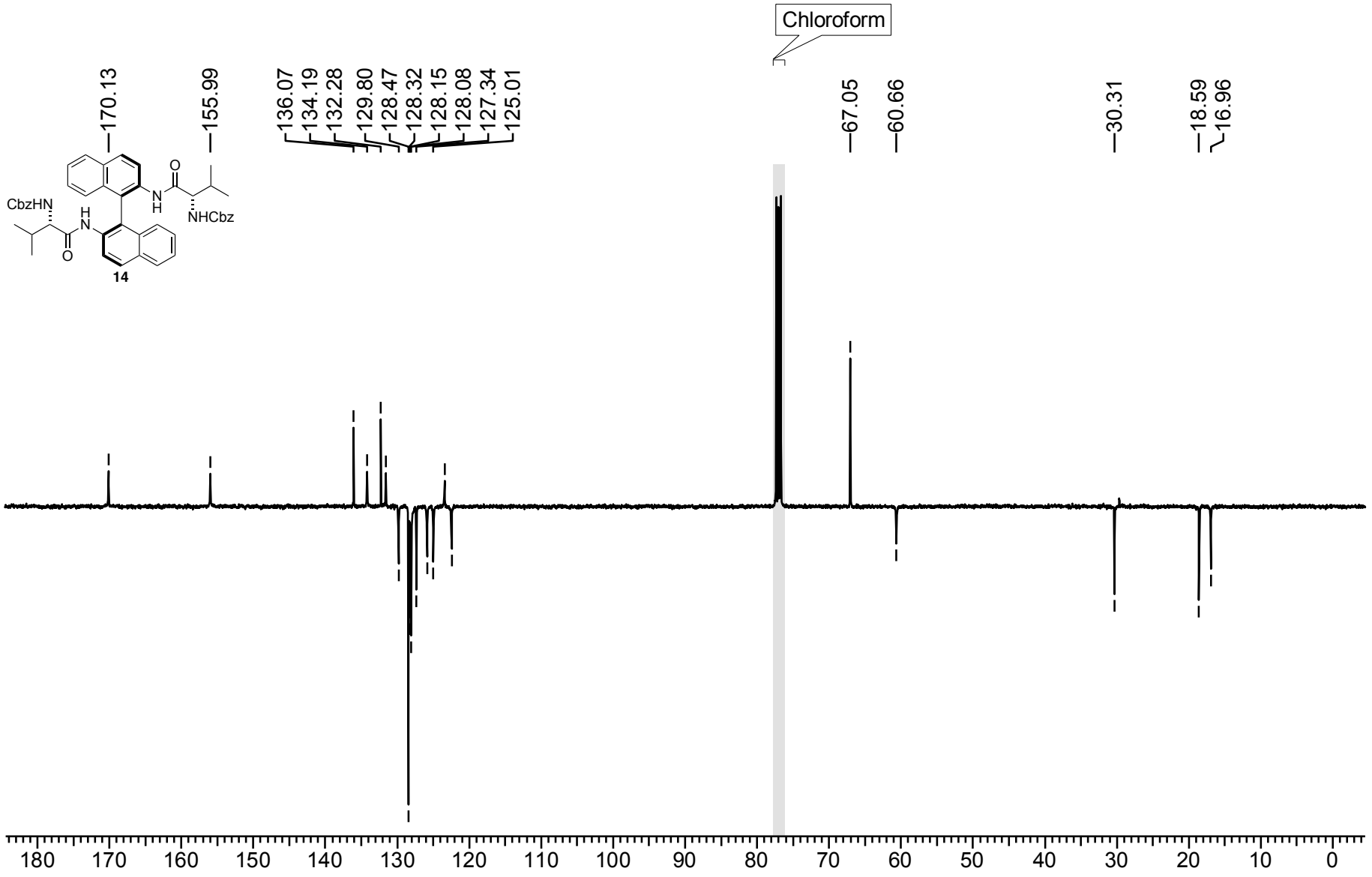

Figure S142. ^{13}C NMR APT (100 MHz, $CDCl_3$) spectrum of **14**.

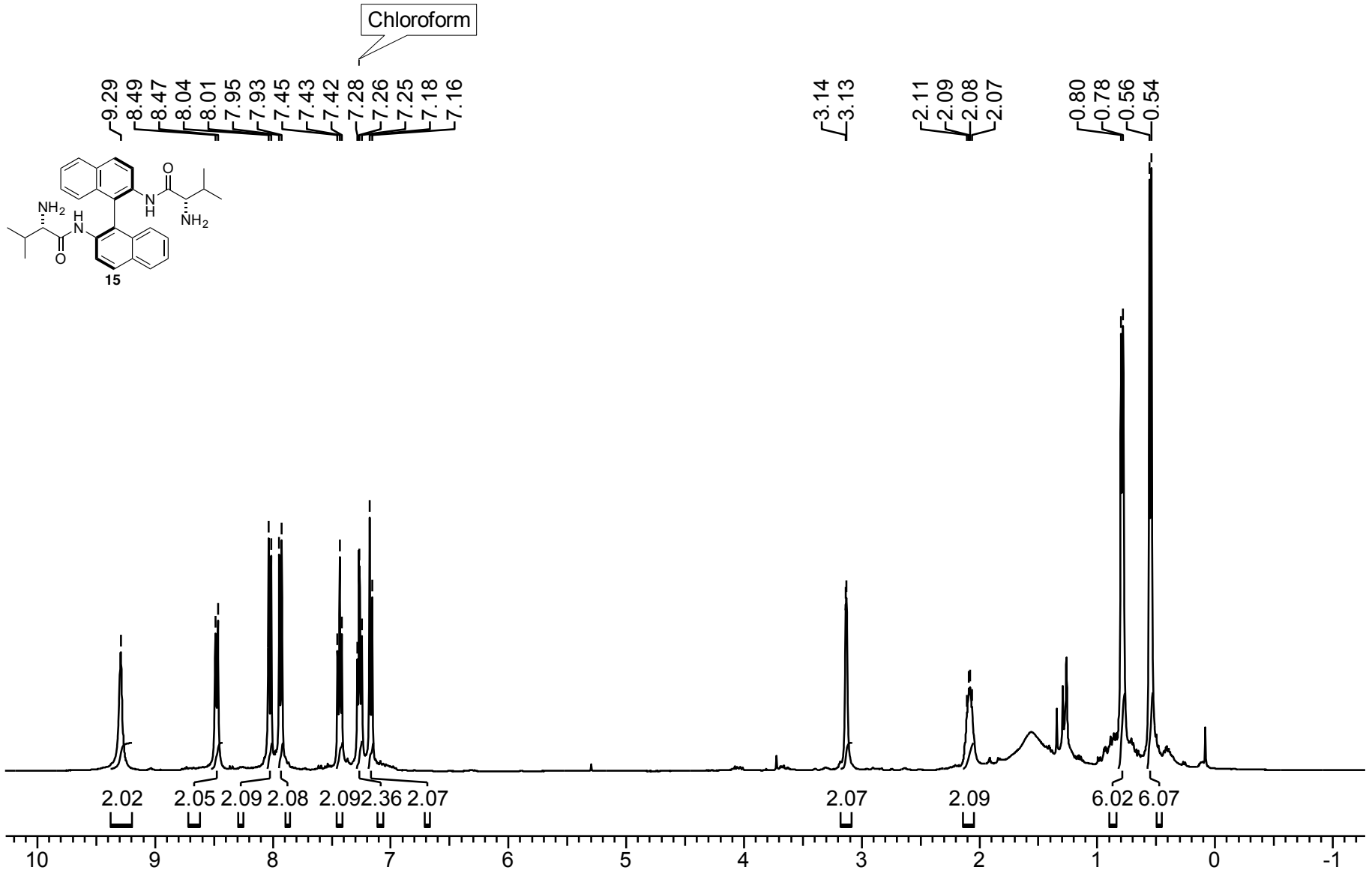

Figure S143. ^{1}H NMR (400 MHz, $CDCl_3$) spectrum of **15**.

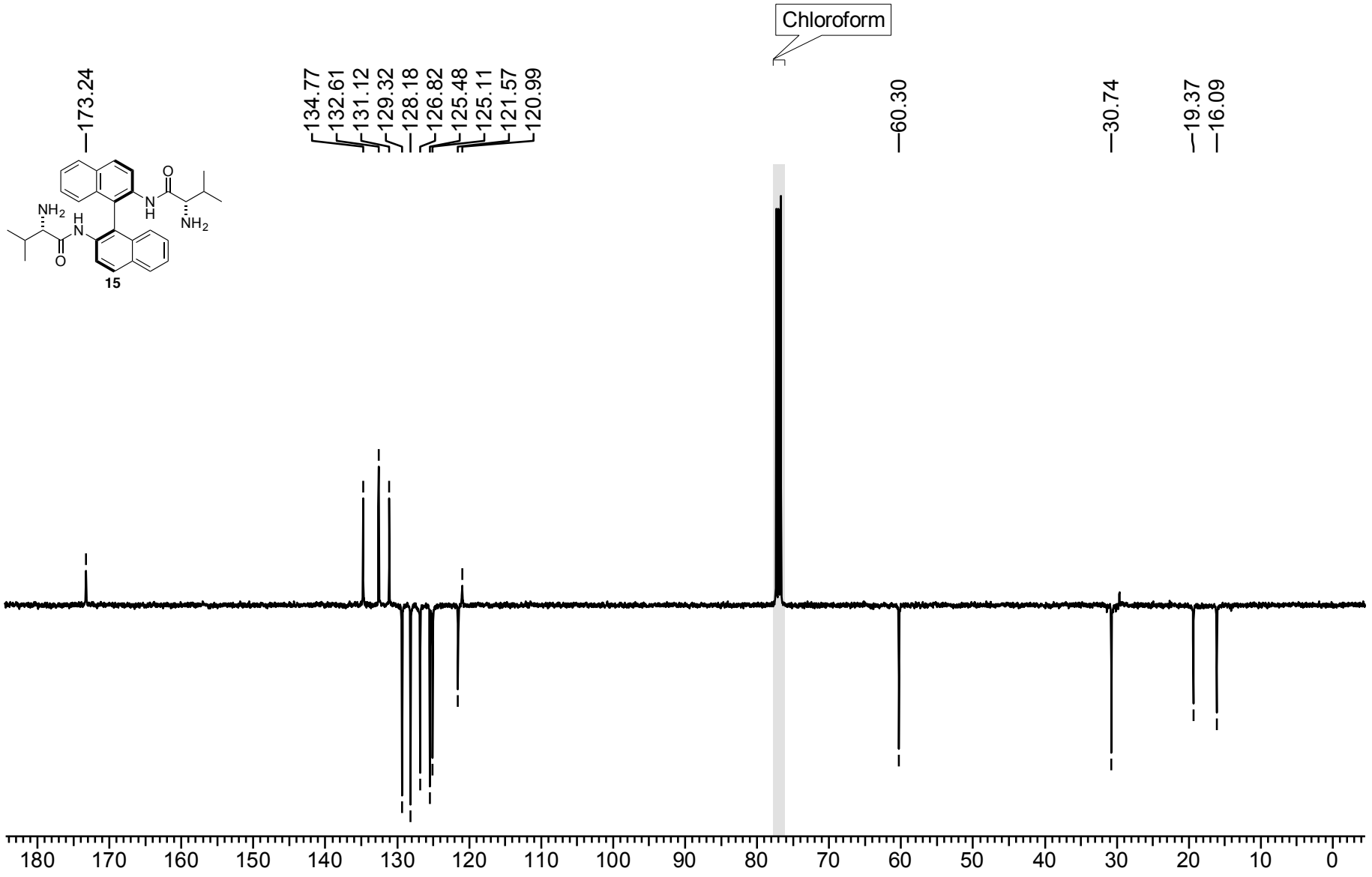

Figure S144. ^{13}C NMR APT (100 MHz, $CDCl_3$) spectrum of **15**.

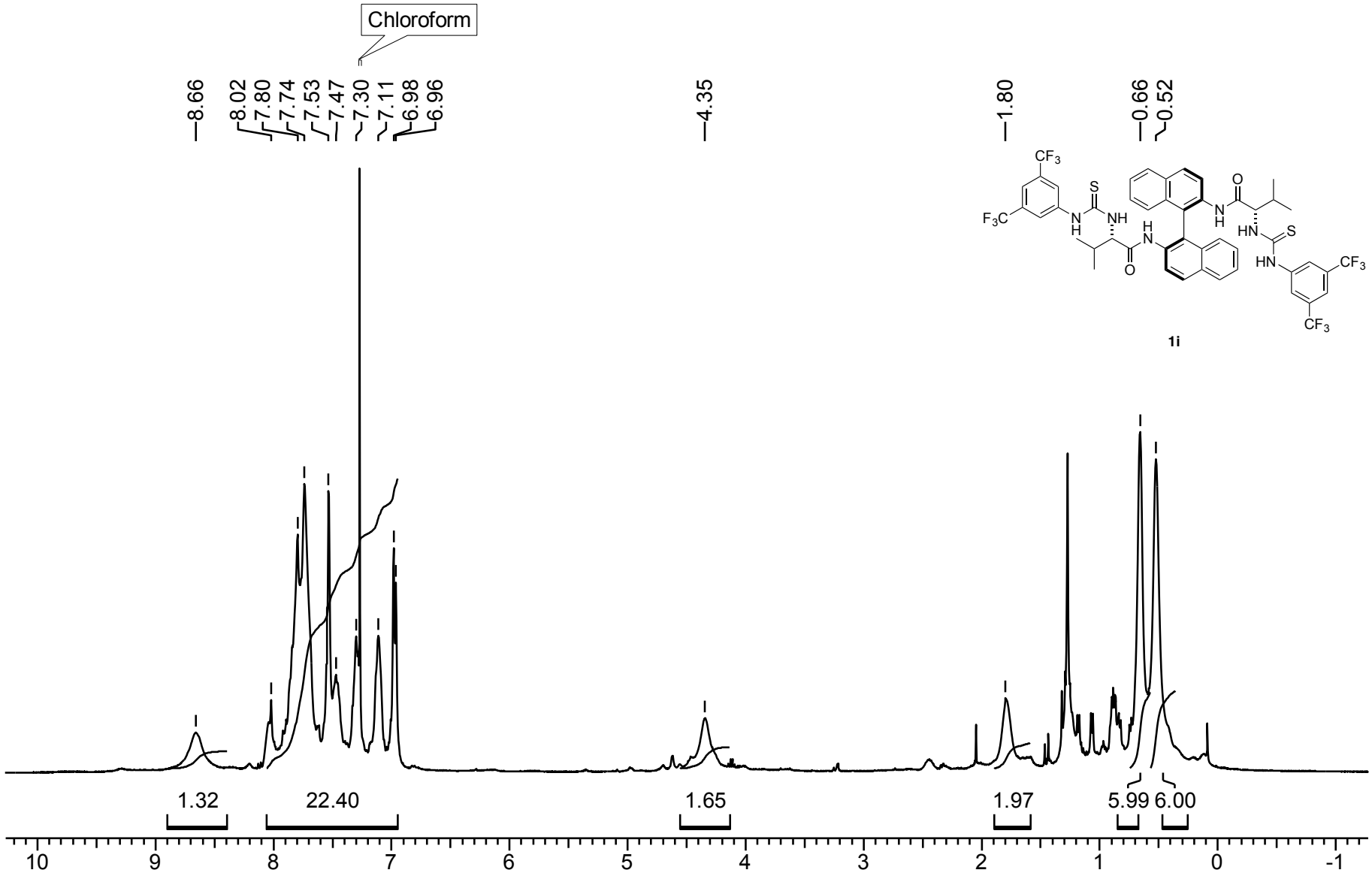

Figure S145. ^{1}H NMR (400 MHz, $CDCl_3$) spectrum of **1i**.

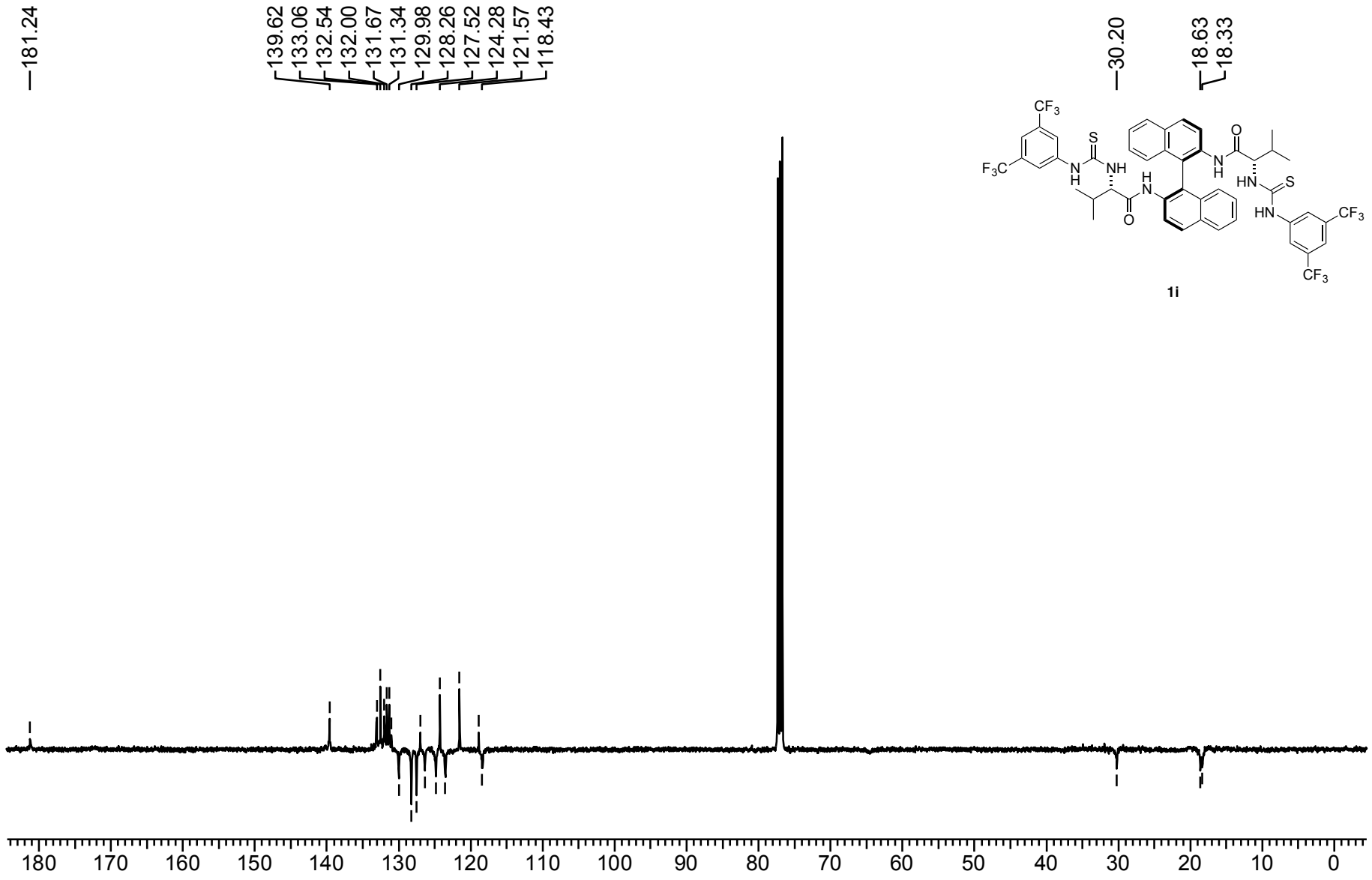

Figure S146. ^{13}C NMR APT (100 MHz, $CDCl_3$) spectrum of **1i**.

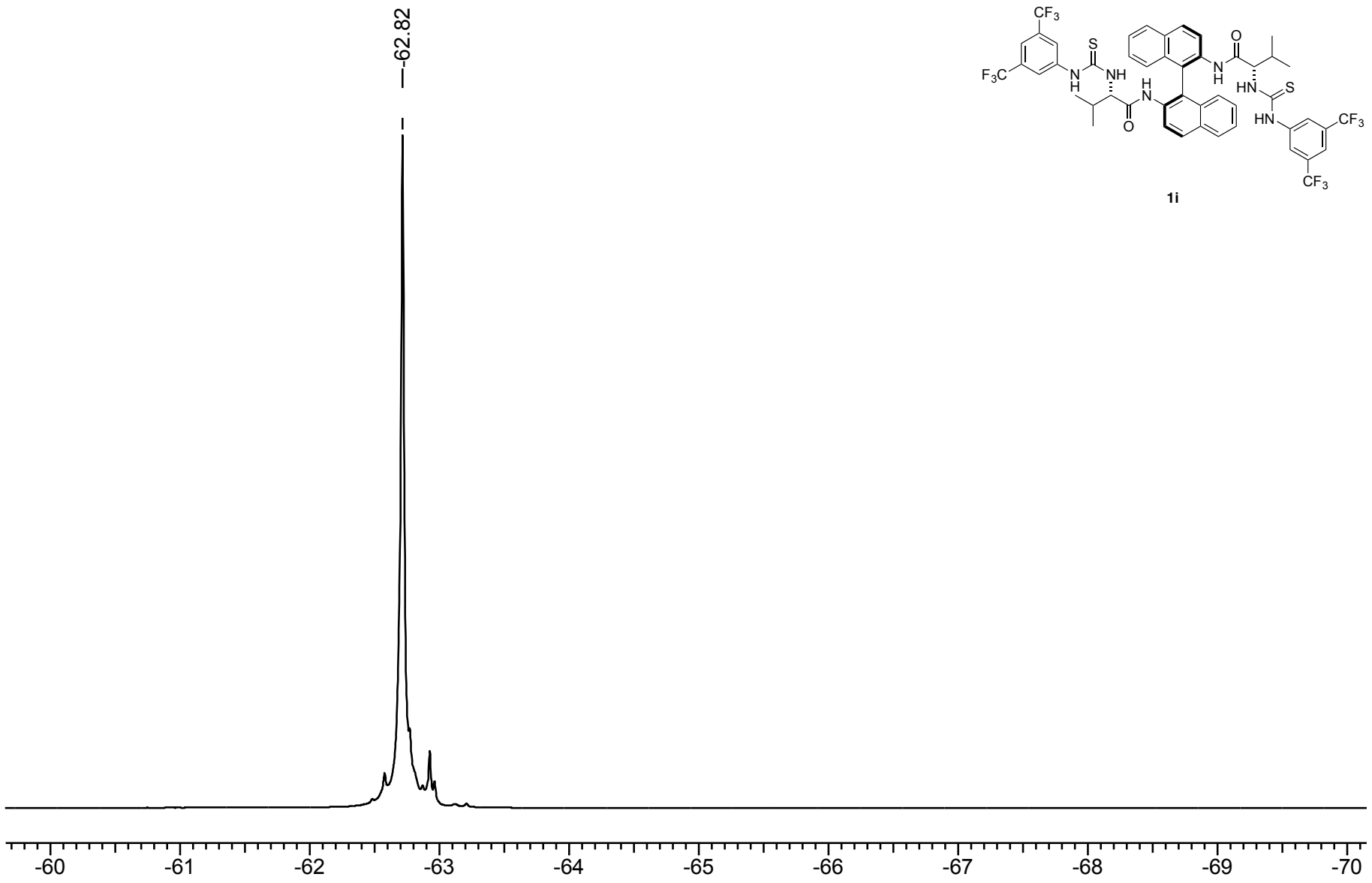

1i

Figure S147. ^{19}F NMR (376 MHz, $CDCl_3$) spectrum of **1i**.

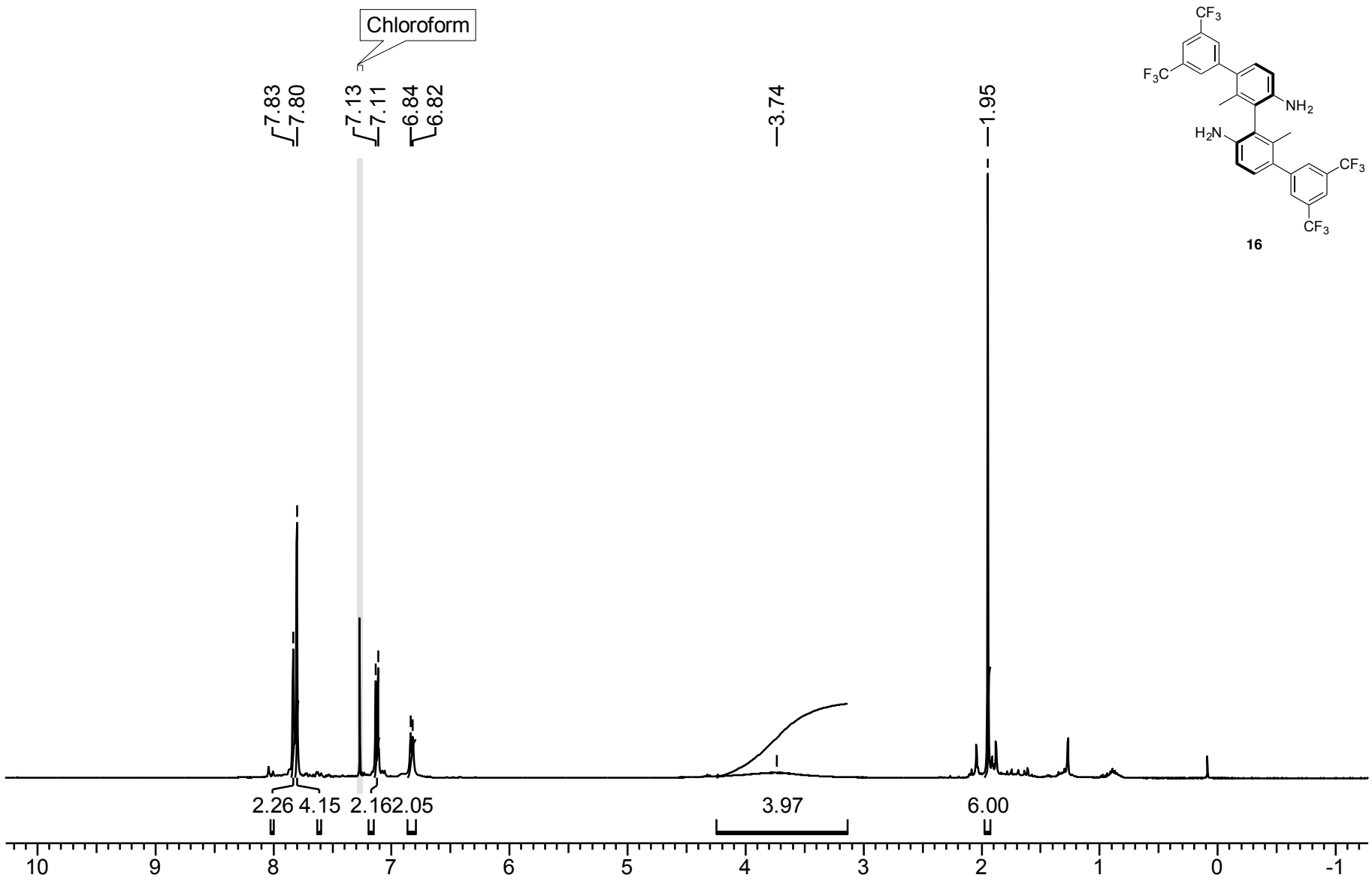

Figure S148. ^{1}H NMR (400 MHz, $CDCl_3$) spectrum of **16**.

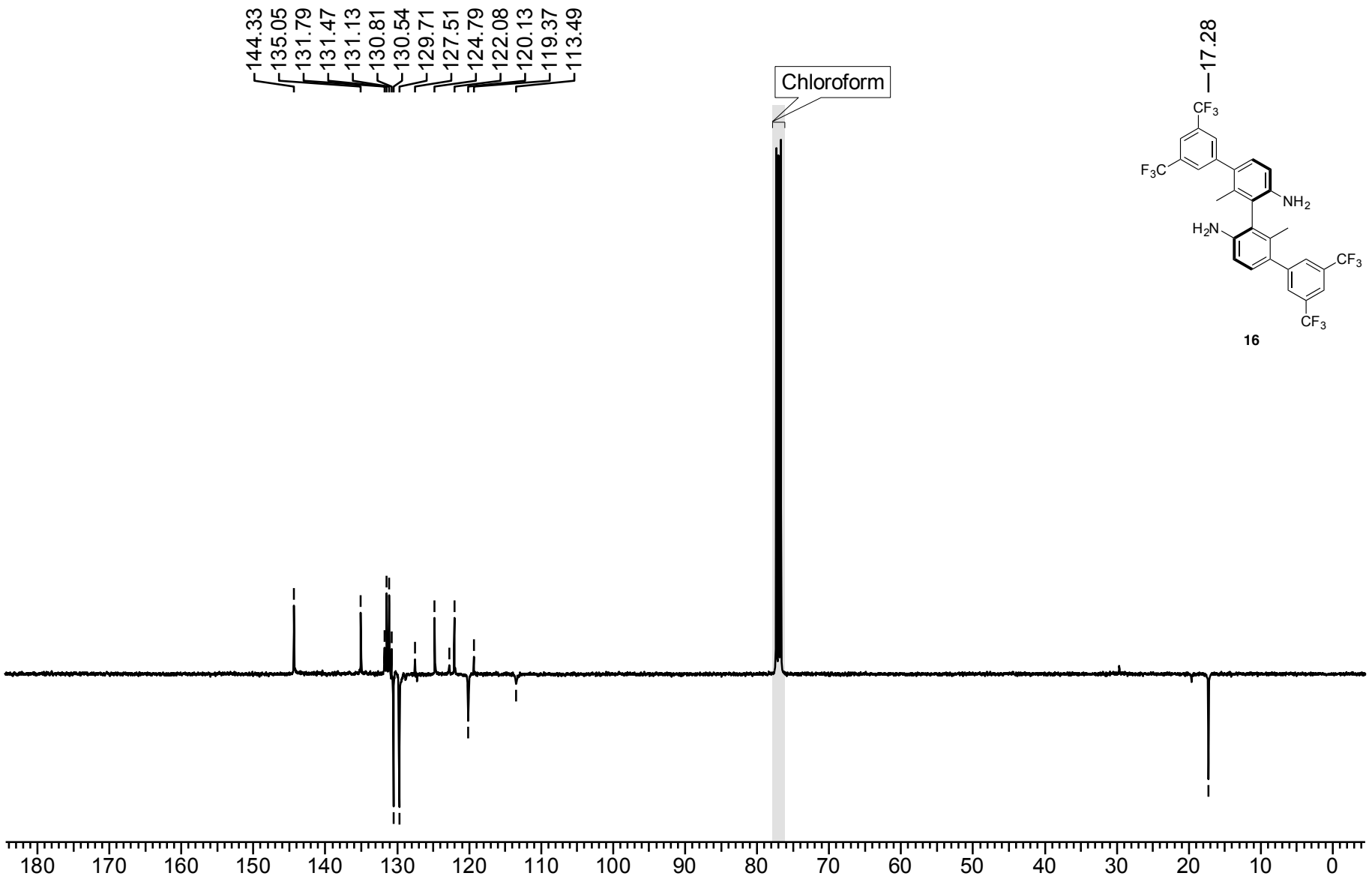

Figure S149. ^{13}C NMR APT (100 MHz, $CDCl_3$) spectrum of **16**.

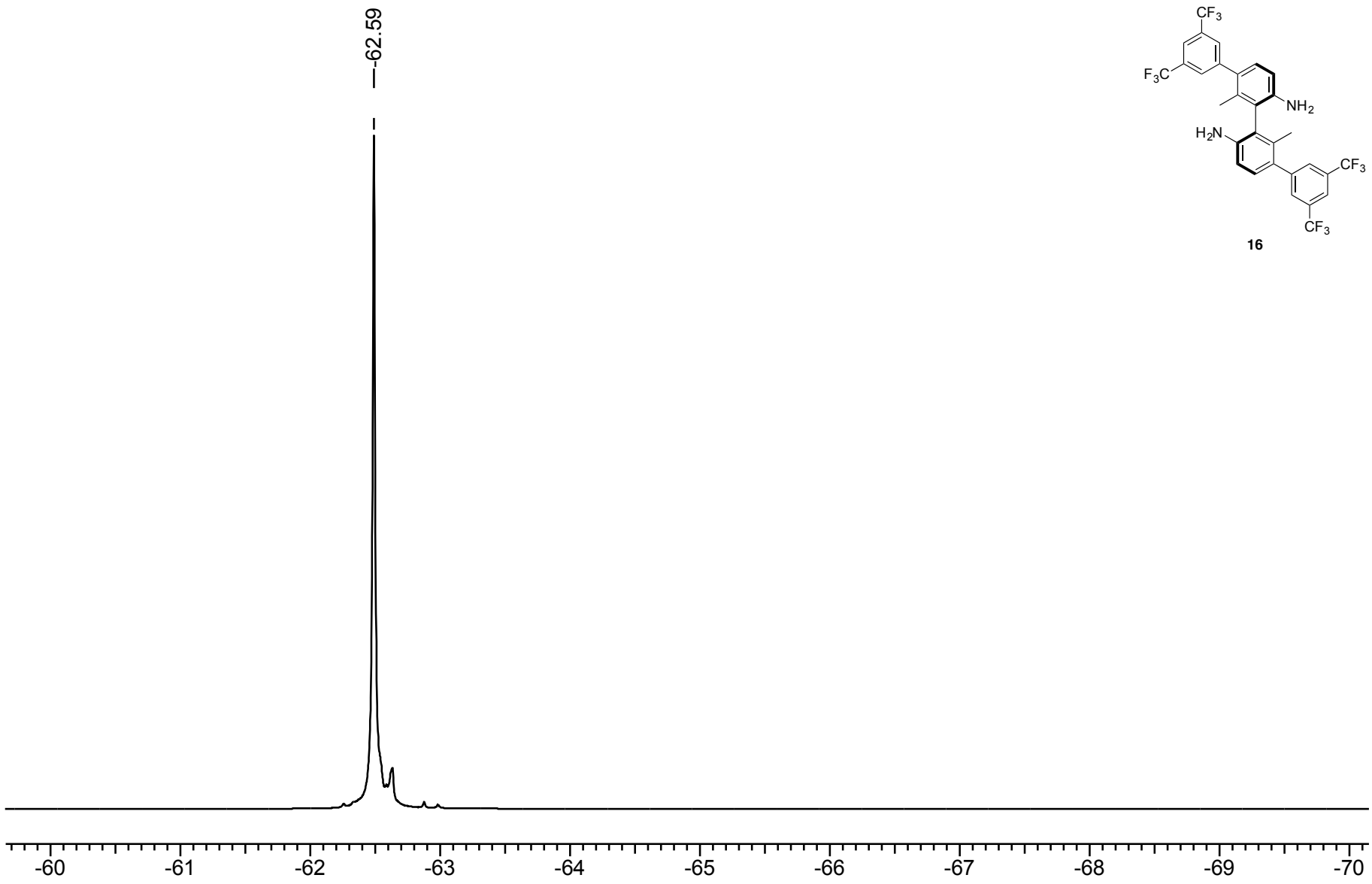

16

Figure S150. ^{19}F NMR (376 MHz, $CDCl_3$) spectrum of **16**.

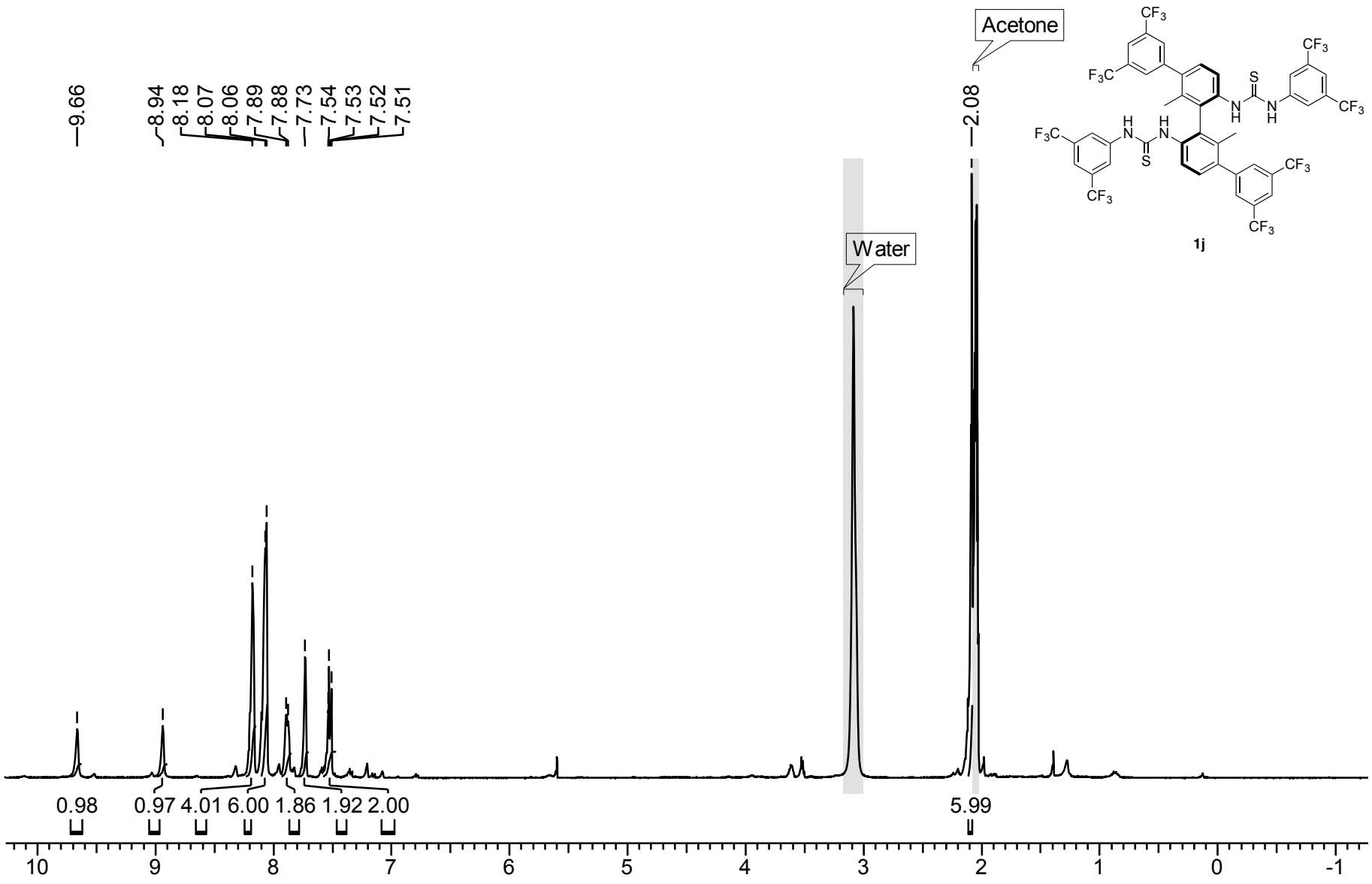

Figure S151. ^{1}H NMR (400 MHz, acetone-d_6) spectrum of **1j**.

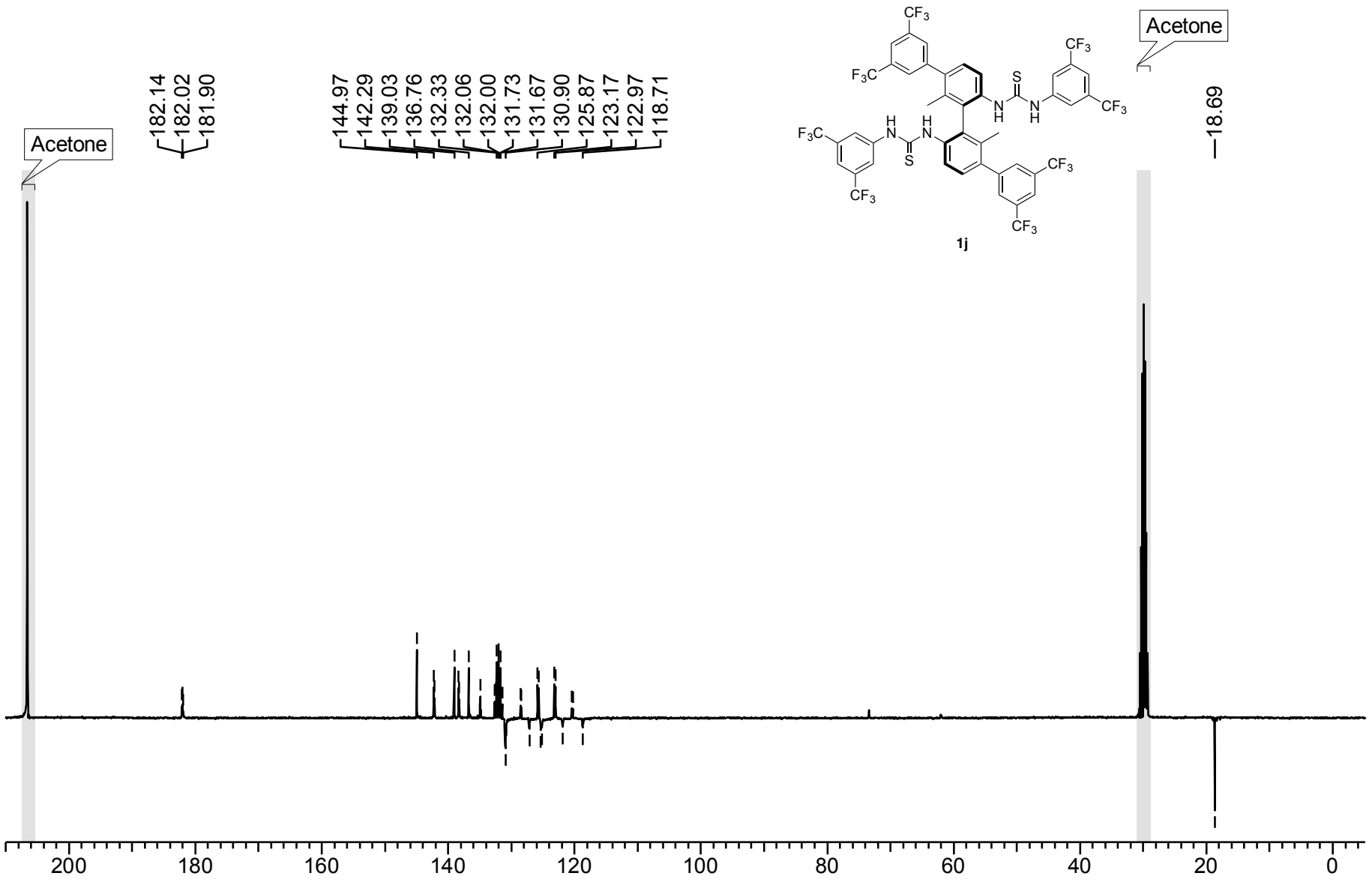

Figure S152. ^{13}C NMR APT (100 MHz, acetone-d_6) spectrum of **1j**.

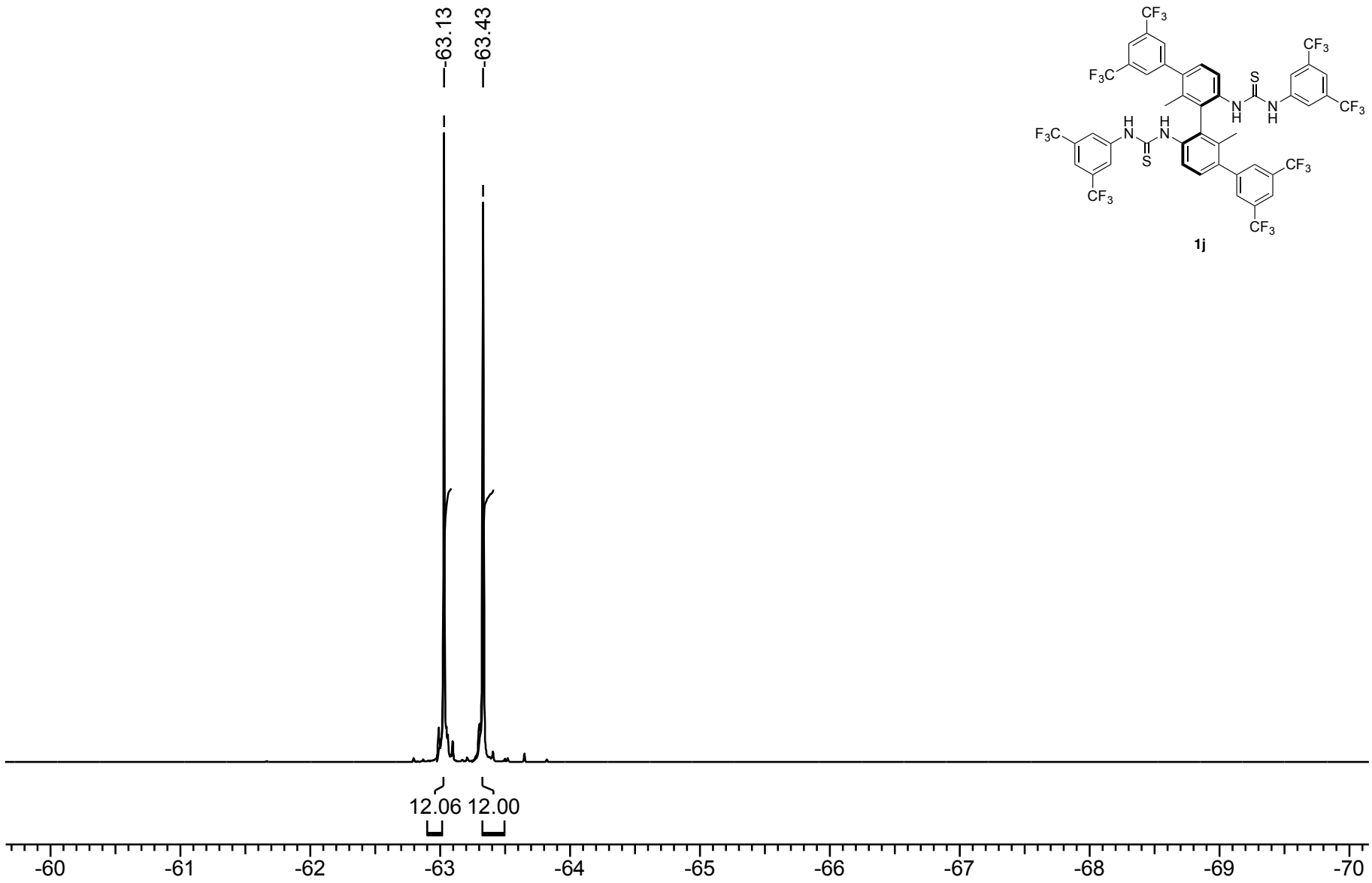

1j

Figure S153. ^{19}F NMR (376 MHz, acetone-d_6) spectrum of **1j**.

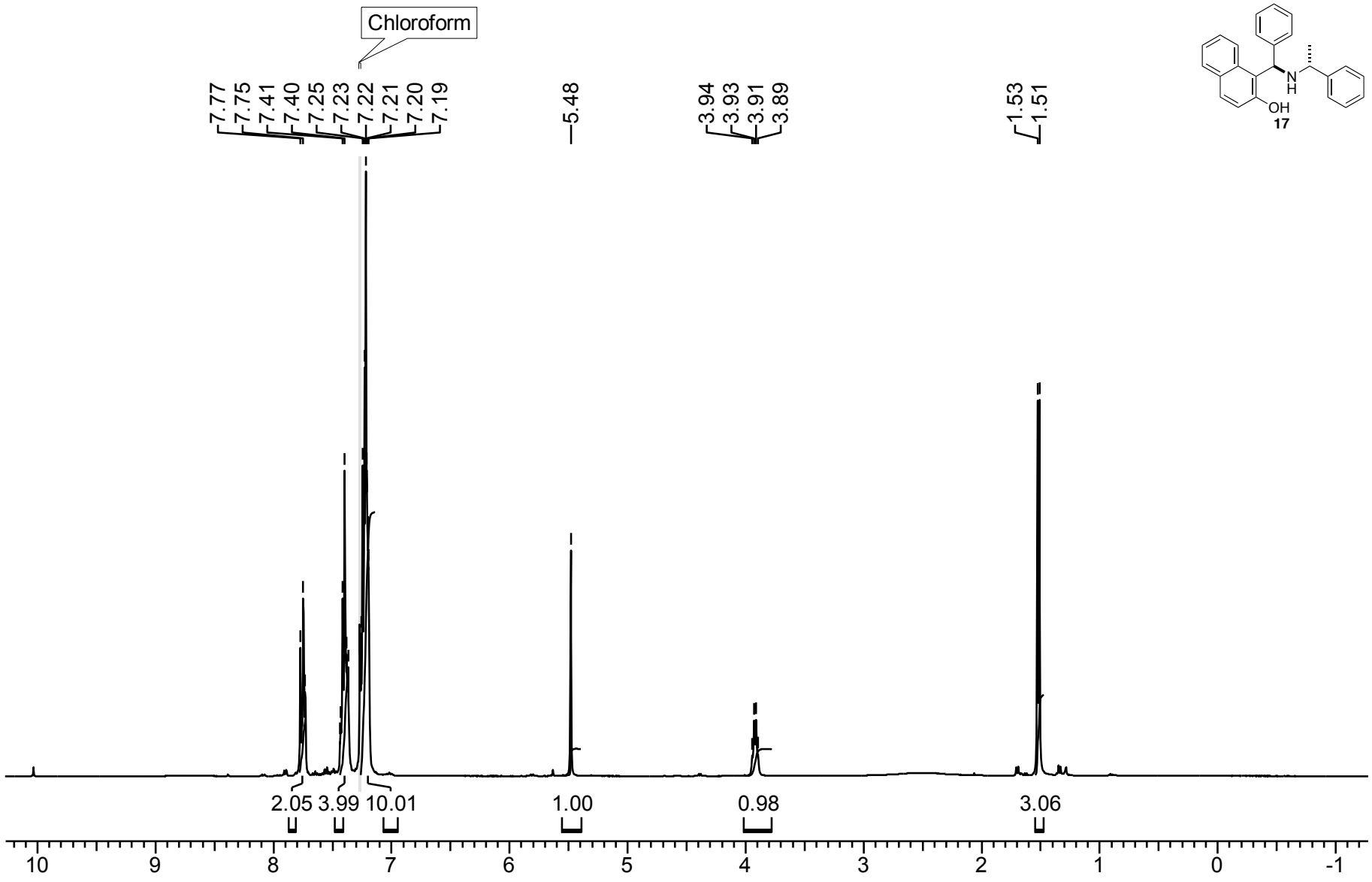

Figure S154. ^{1}H NMR (400 MHz, $CDCl_3$) spectrum of **17**.

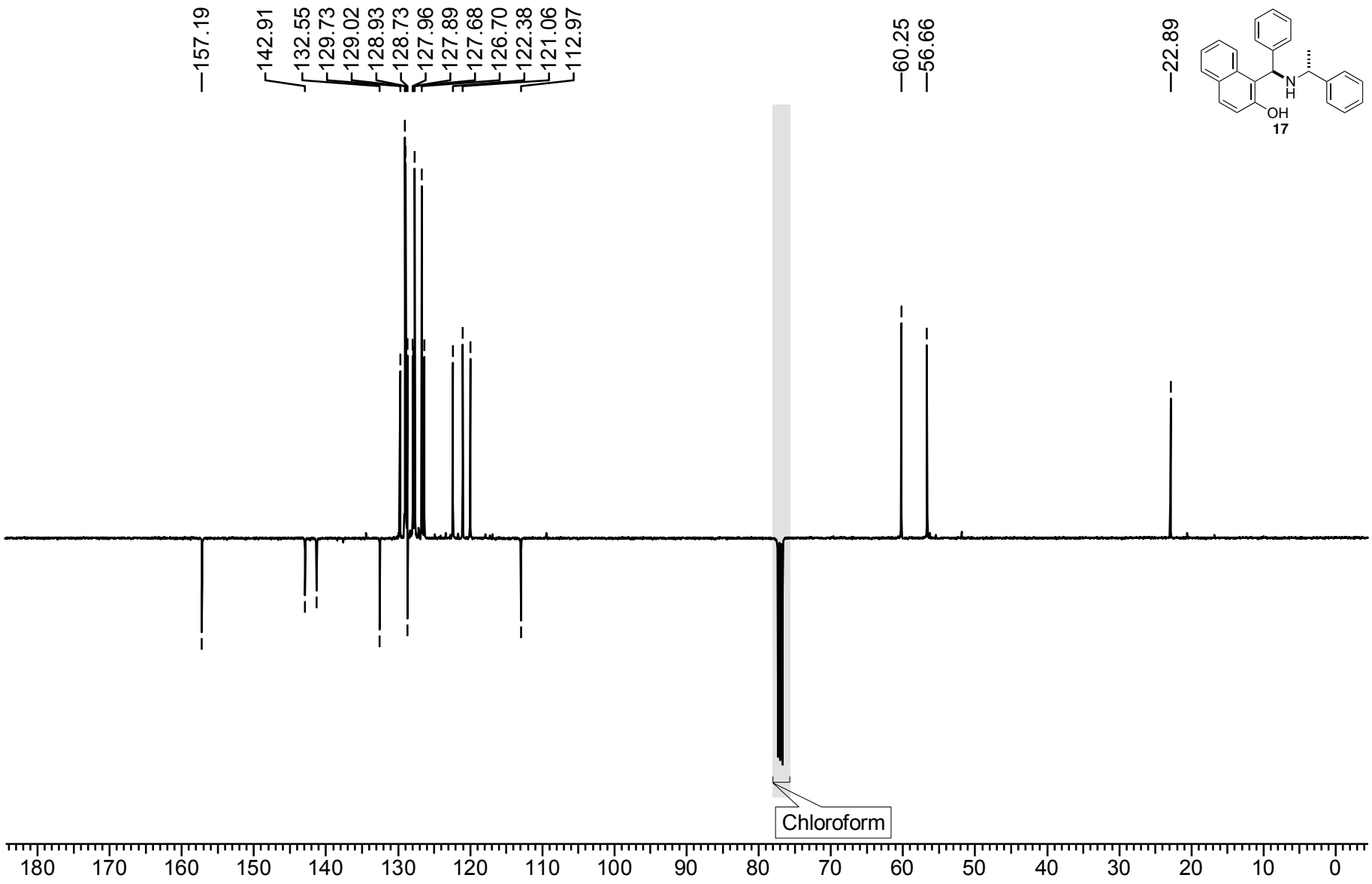

Figure S155. ^{13}C NMR APT (100 MHz, $CDCl_3$) spectrum of **17**.

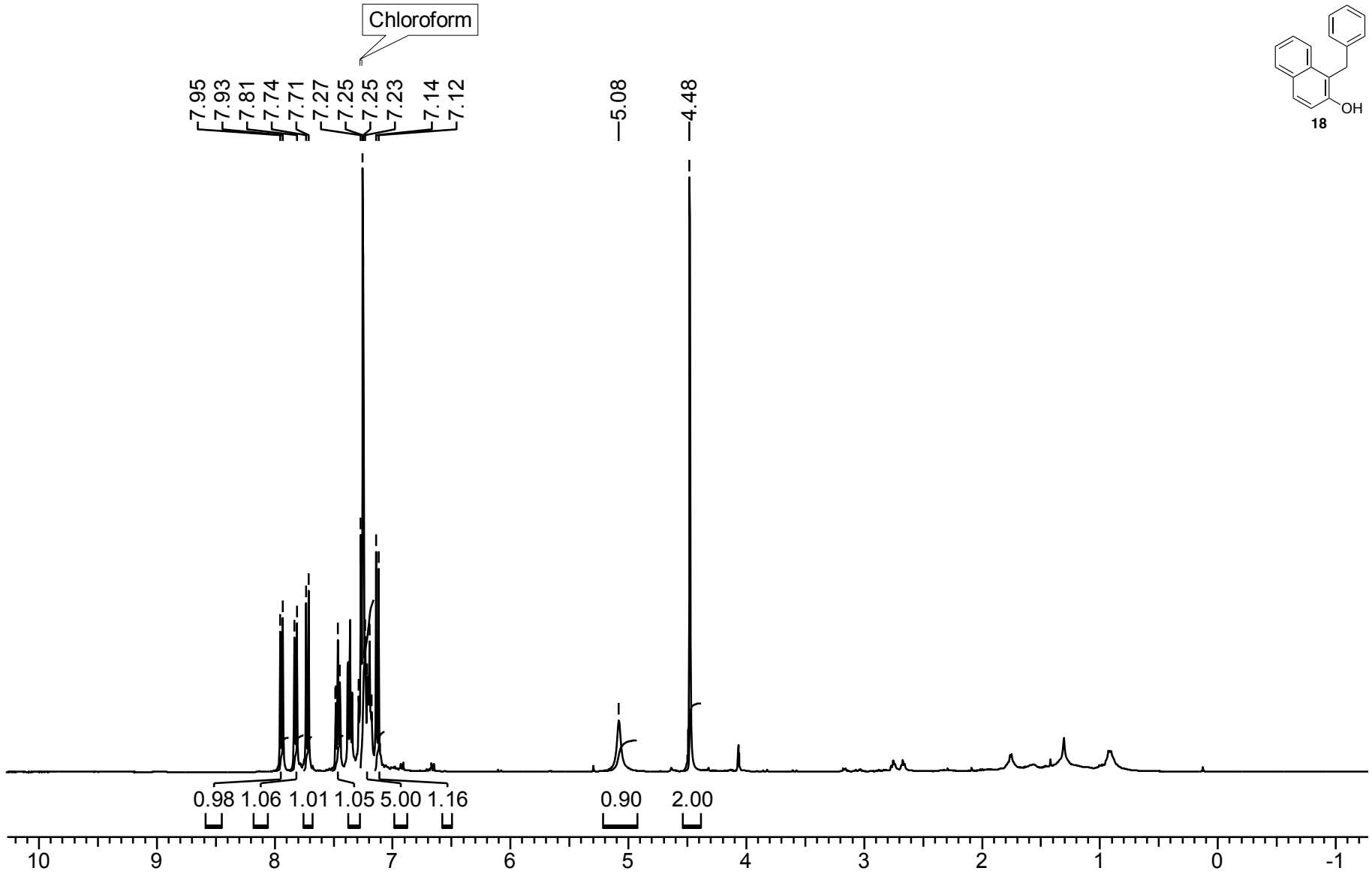

Figure S156. ^{1}H NMR (400 MHz, $CDCl_3$) spectrum of **18**.

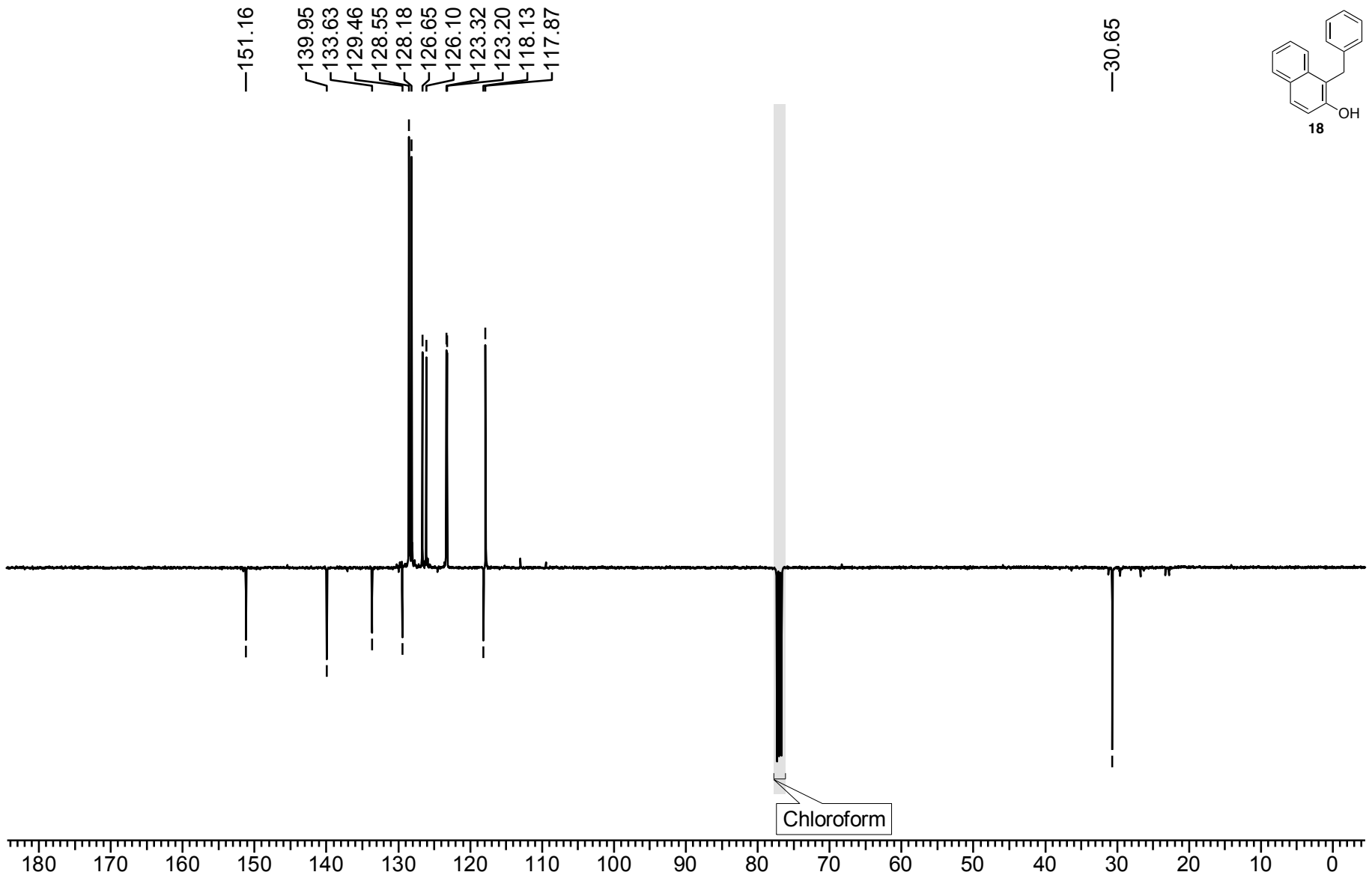

Figure S157. ^{13}C NMR APT (100 MHz, $CDCl_3$) spectrum of **18**.

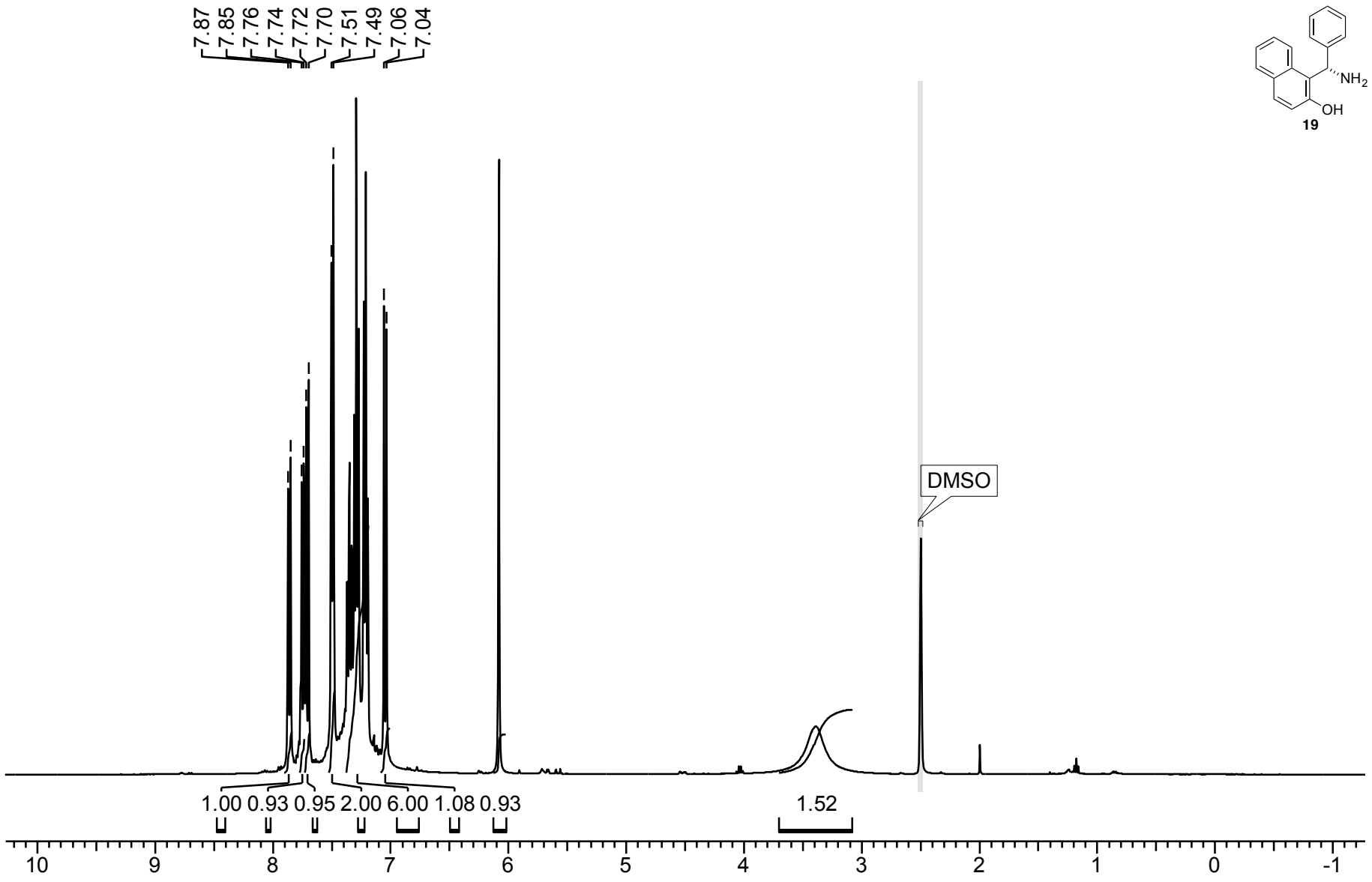

Figure S158. ^{1}H NMR (400 MHz, DMSO-d_6) spectrum of **19**.

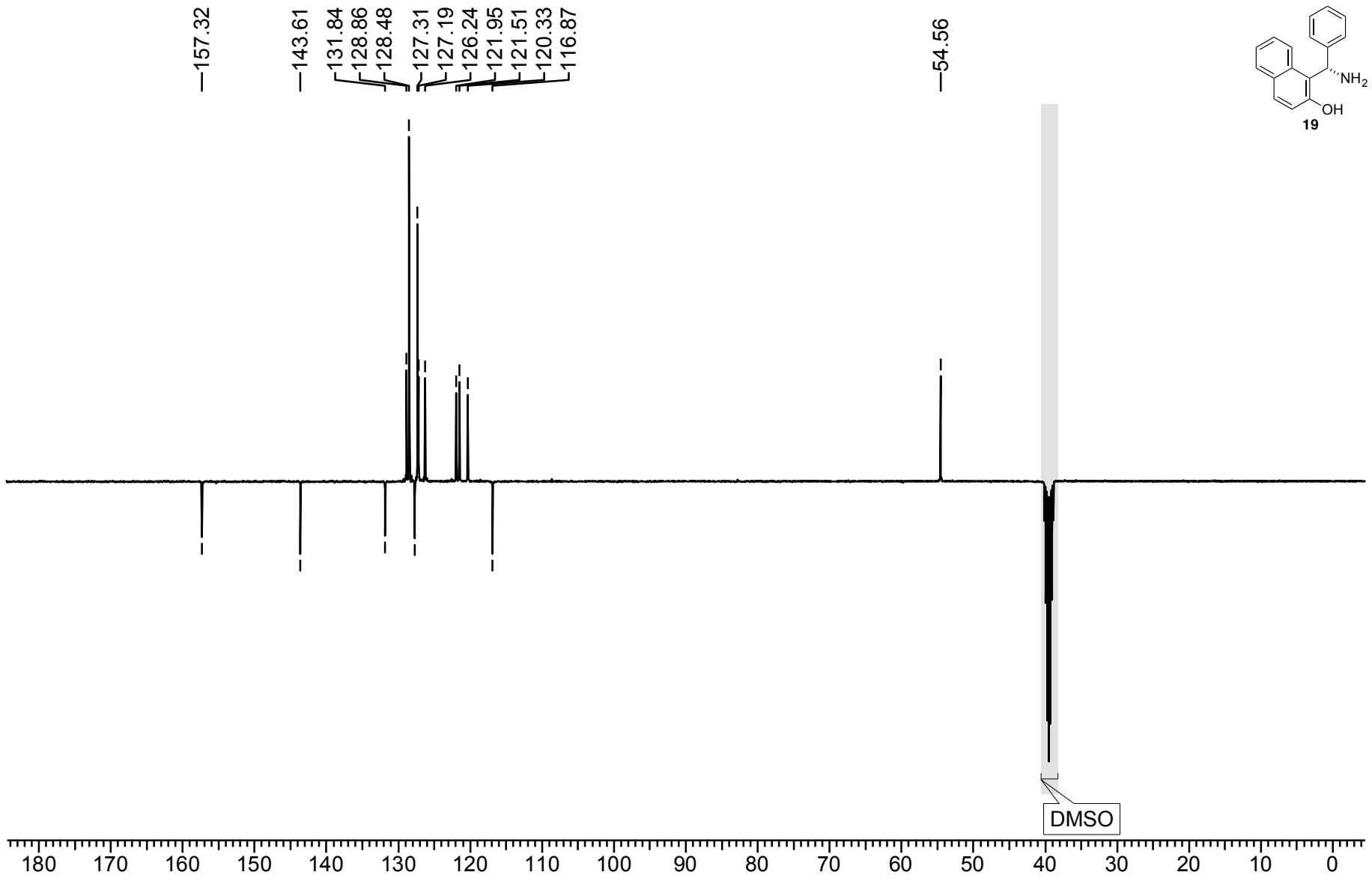

Figure S159. ^{13}C NMR APT (100 MHz, DMSO-d_6) spectrum of **19**.

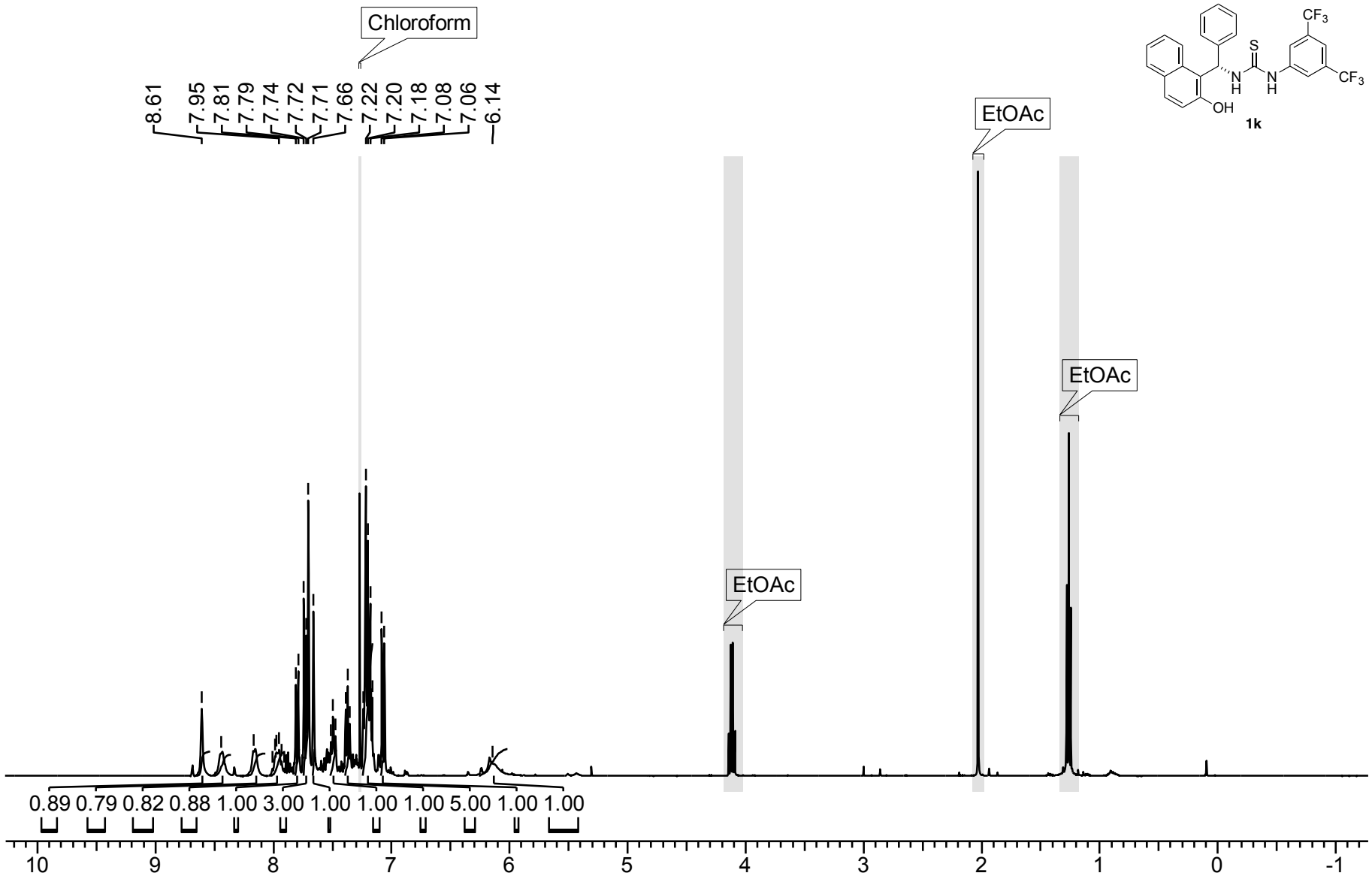

Figure S160. ^{1}H NMR (400 MHz, $CDCl_3$) spectrum of **1k**.

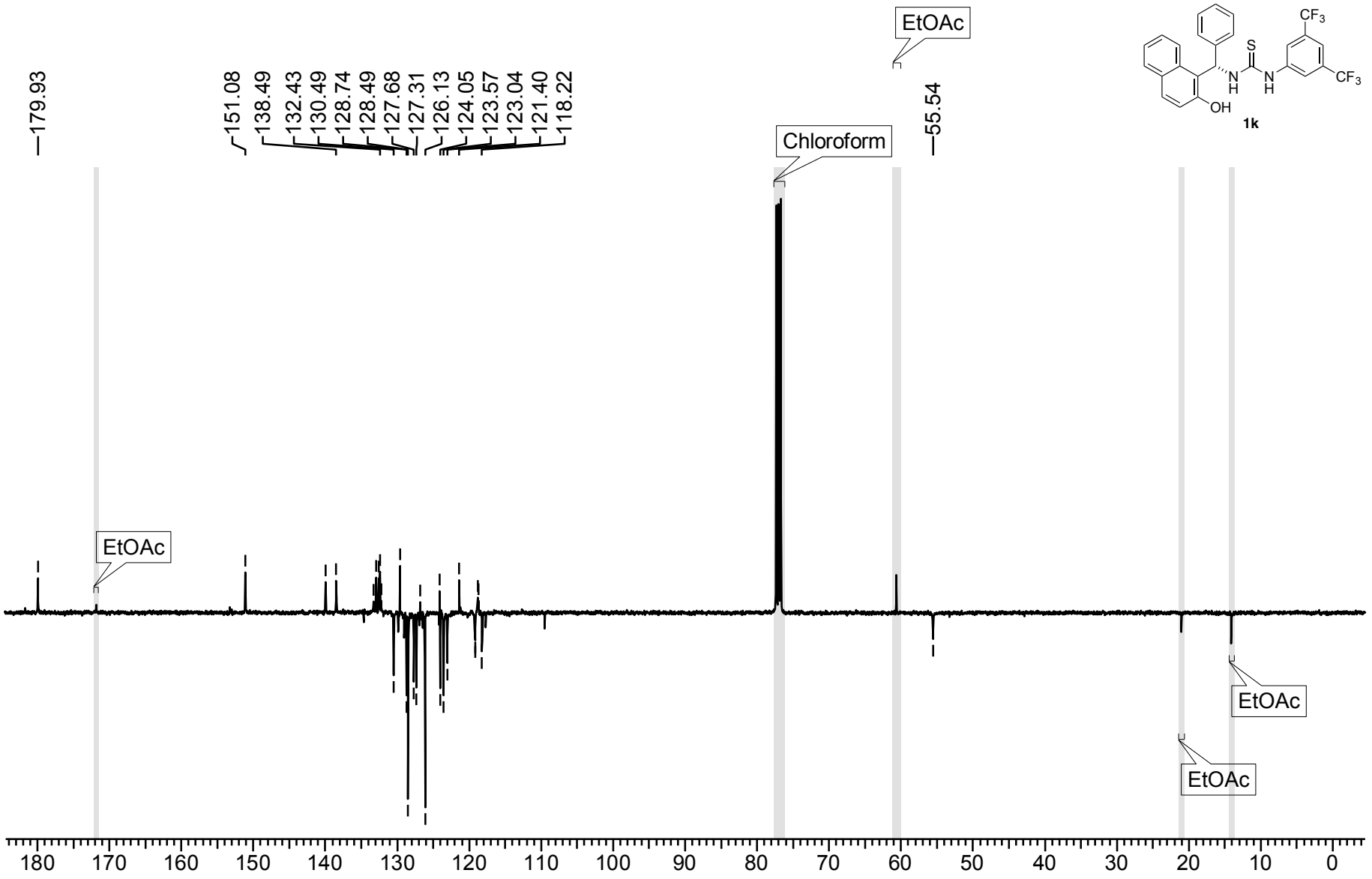

Figure S161. ^{13}C NMR APT (100 MHz, $CDCl_3$) spectrum of **1k**.

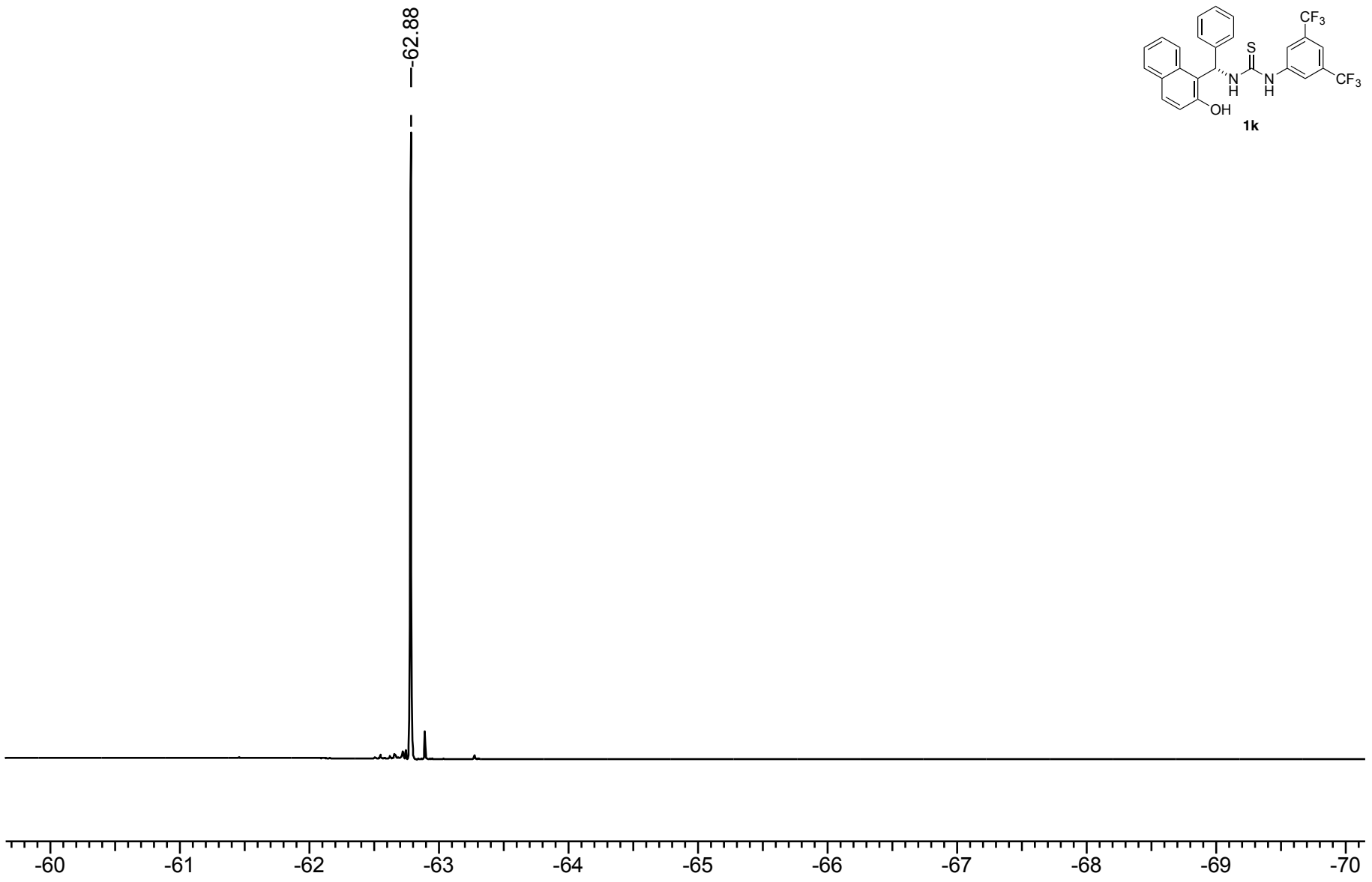

Figure S162. ^{19}F NMR (376 MHz, $CDCl_3$) spectrum of **1k**.

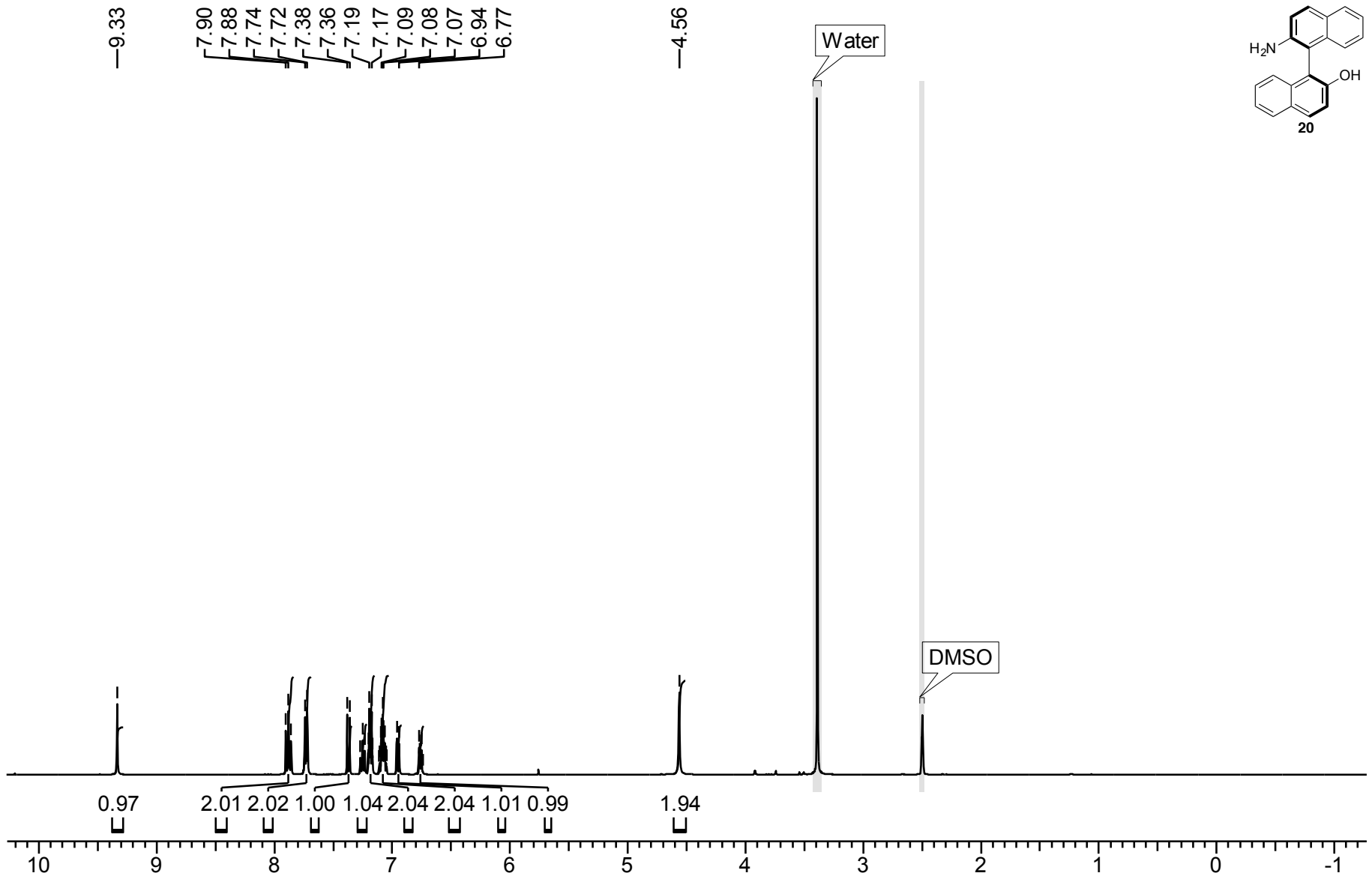

Figure S163. ^{1}H NMR (400 MHz, DMSO-d_6) spectrum of **20**.

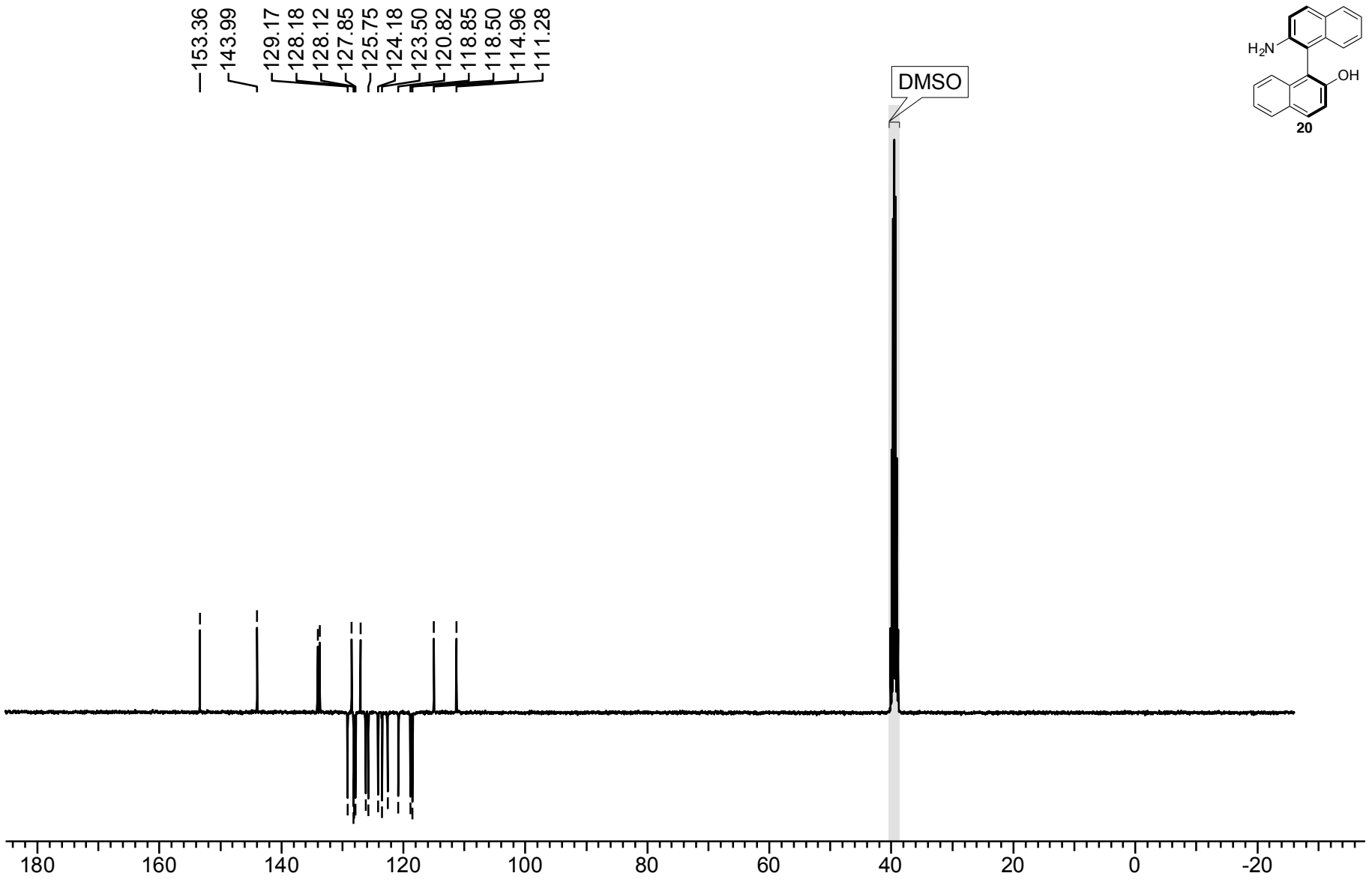

Figure S164. ^{13}C APT NMR (100 MHz, DMSO-d_6) spectrum of **20**.

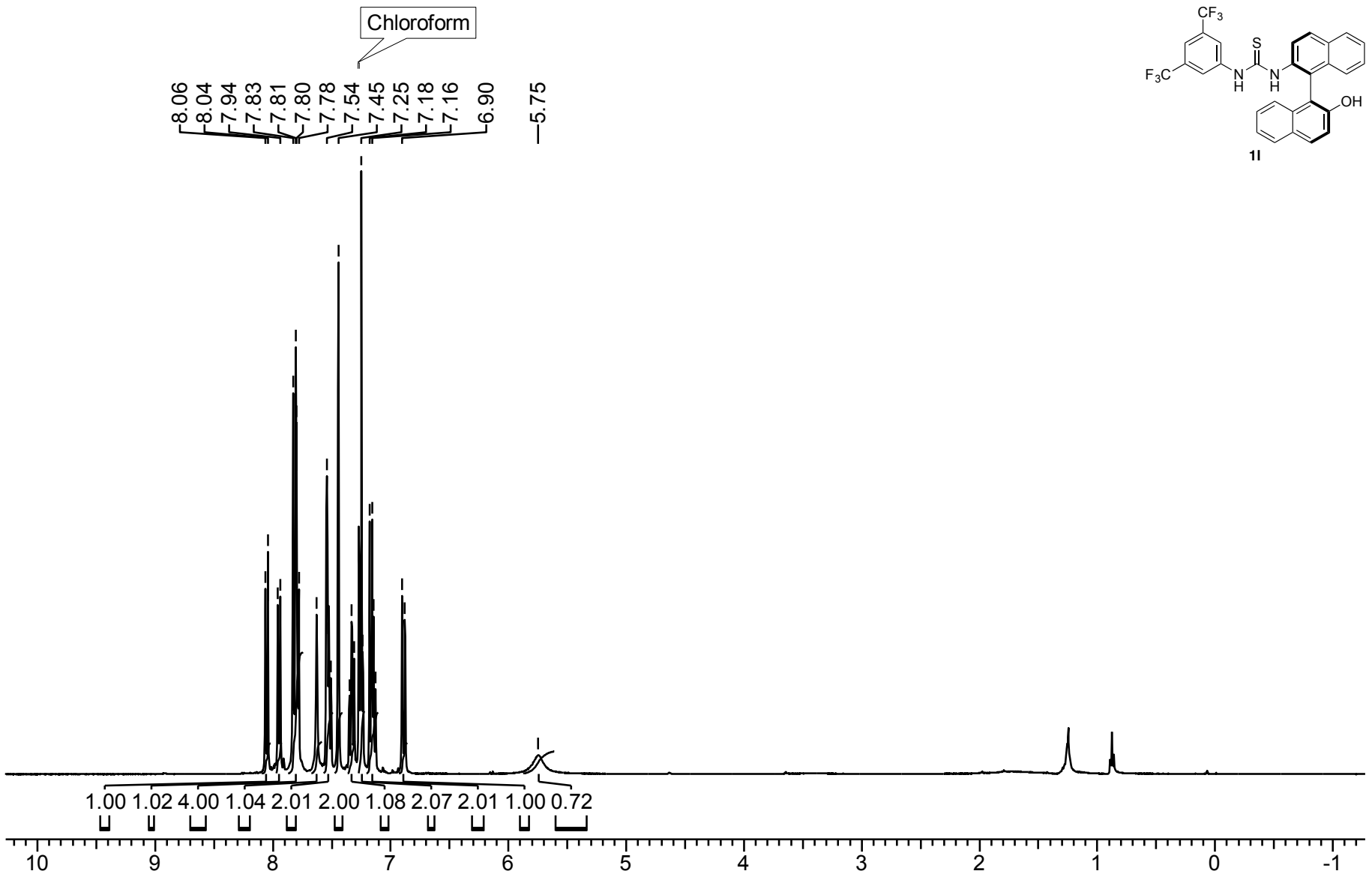

Figure S165. ^{1}H NMR (400 MHz, $CDCl_3$) spectrum of **1l**.

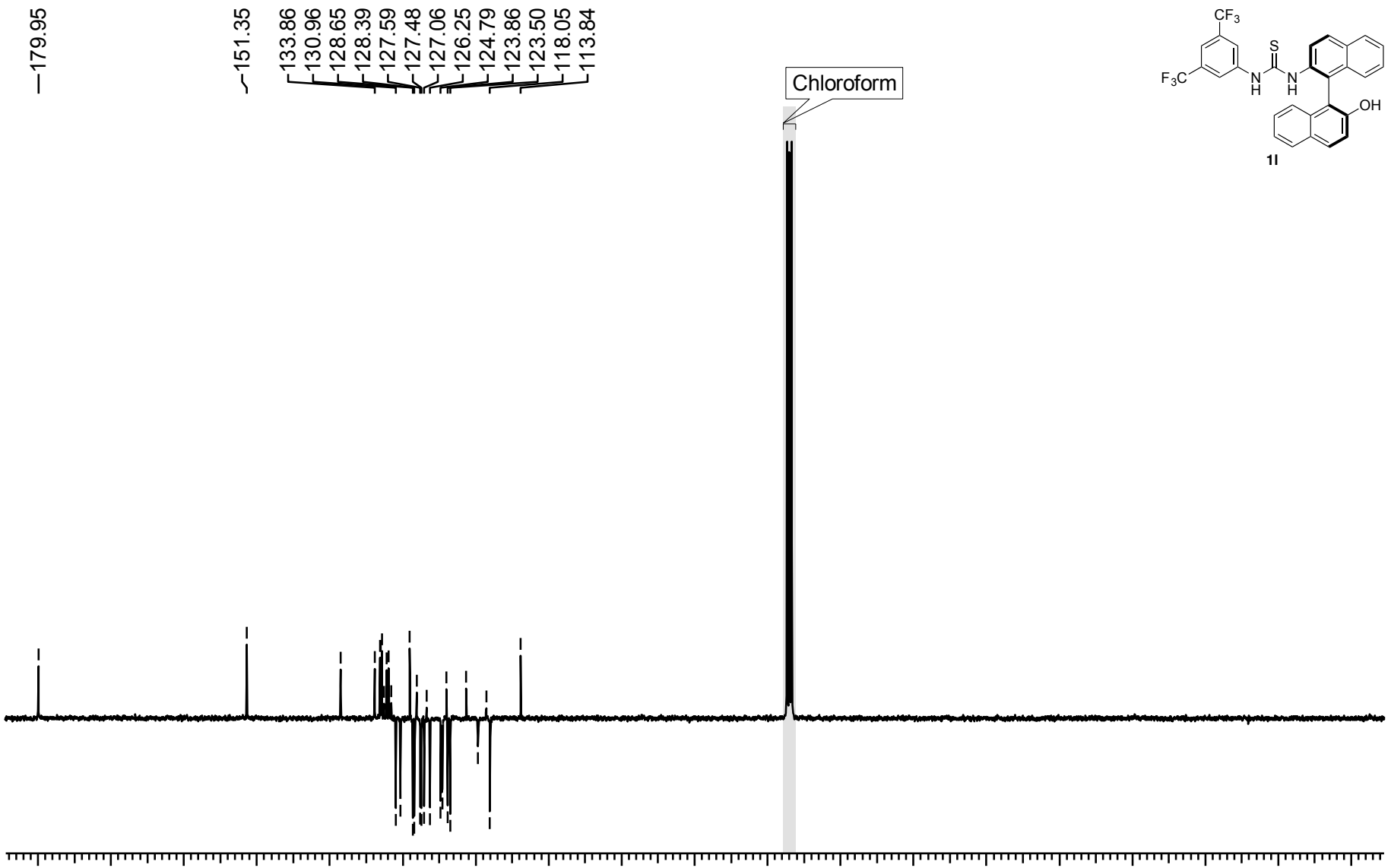

Figure S166. ^{13}C NMR APT (100 MHz, $CDCl_3$) spectrum of **1l**.

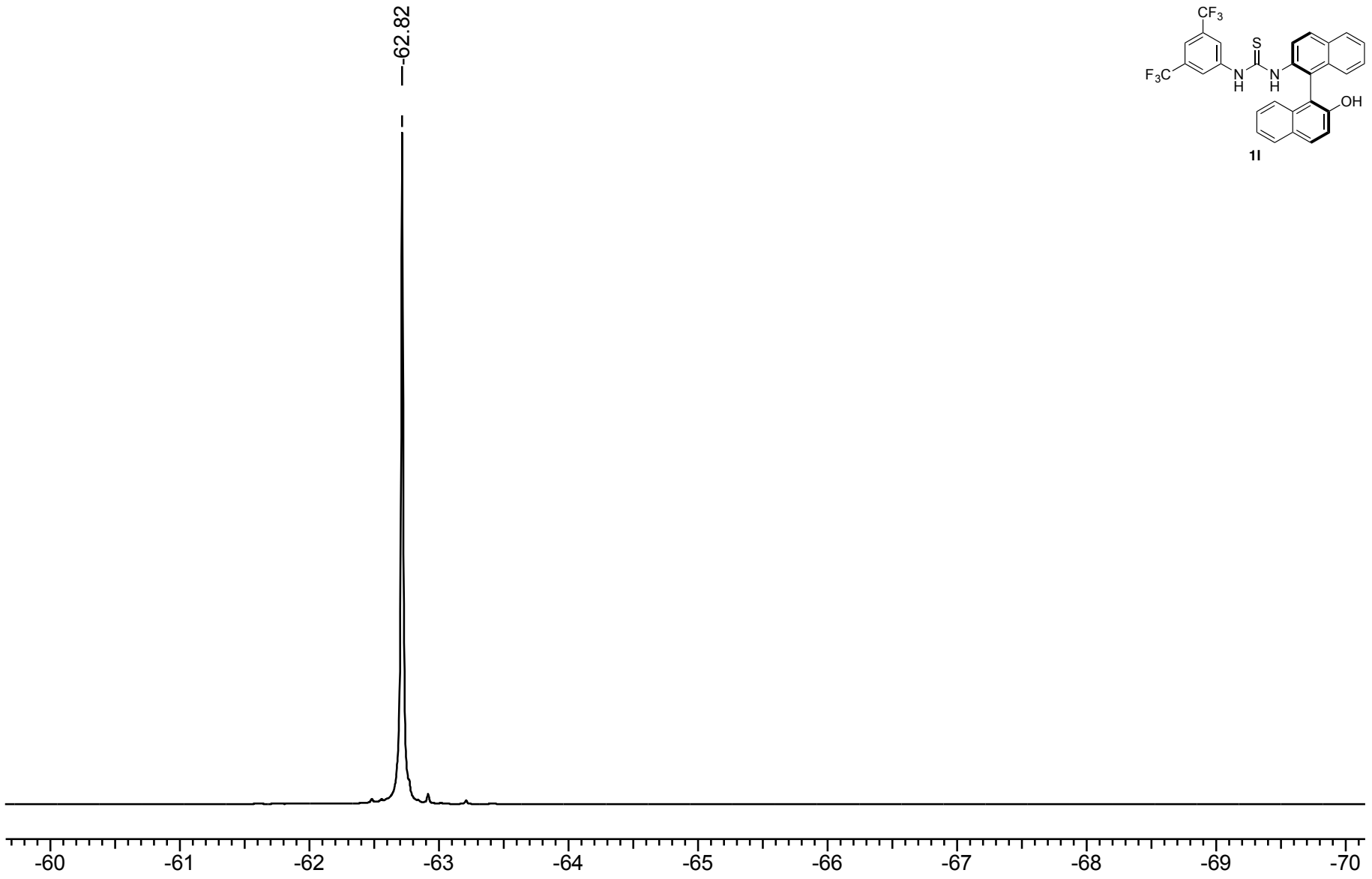

Figure S167. ^{19}F NMR (376 MHz, $CDCl_3$) spectrum of **1l**.

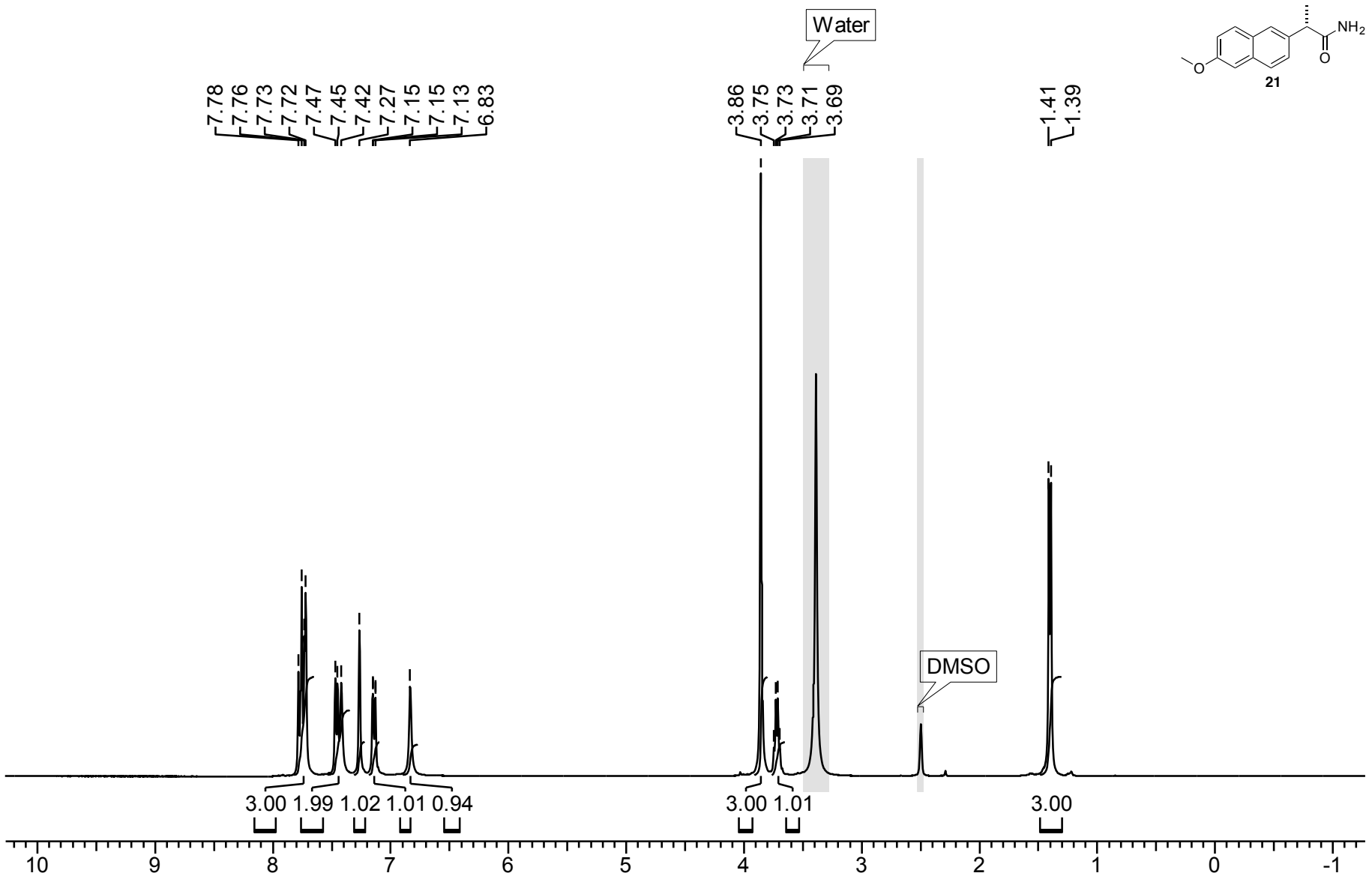

Figure S168. ^{1}H NMR (400 MHz, DMSO-d_6) spectrum of **21**.

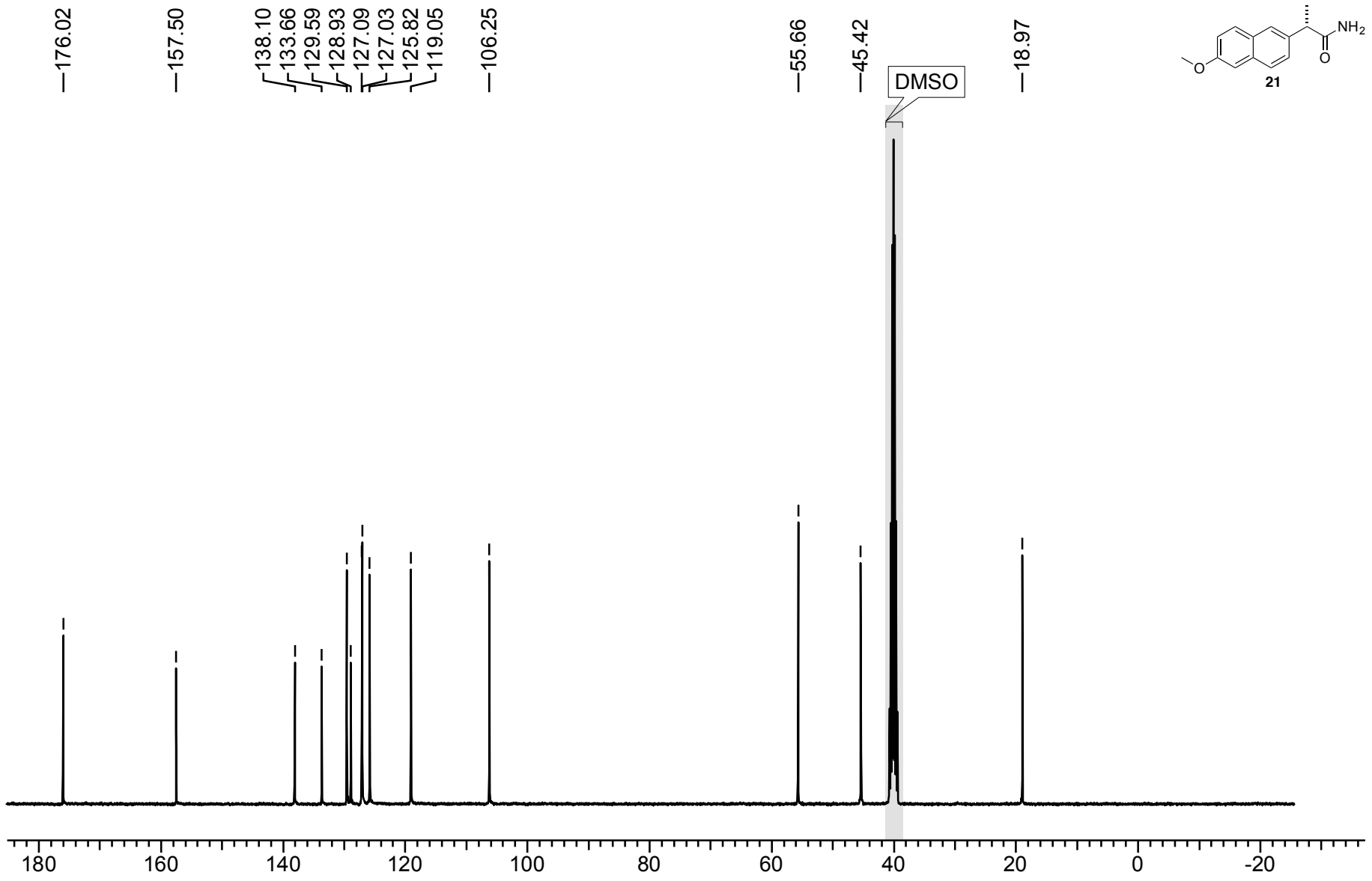

Figure S169. ^{13}C NMR (100 MHz, DMSO-d_6) spectrum of **21**.

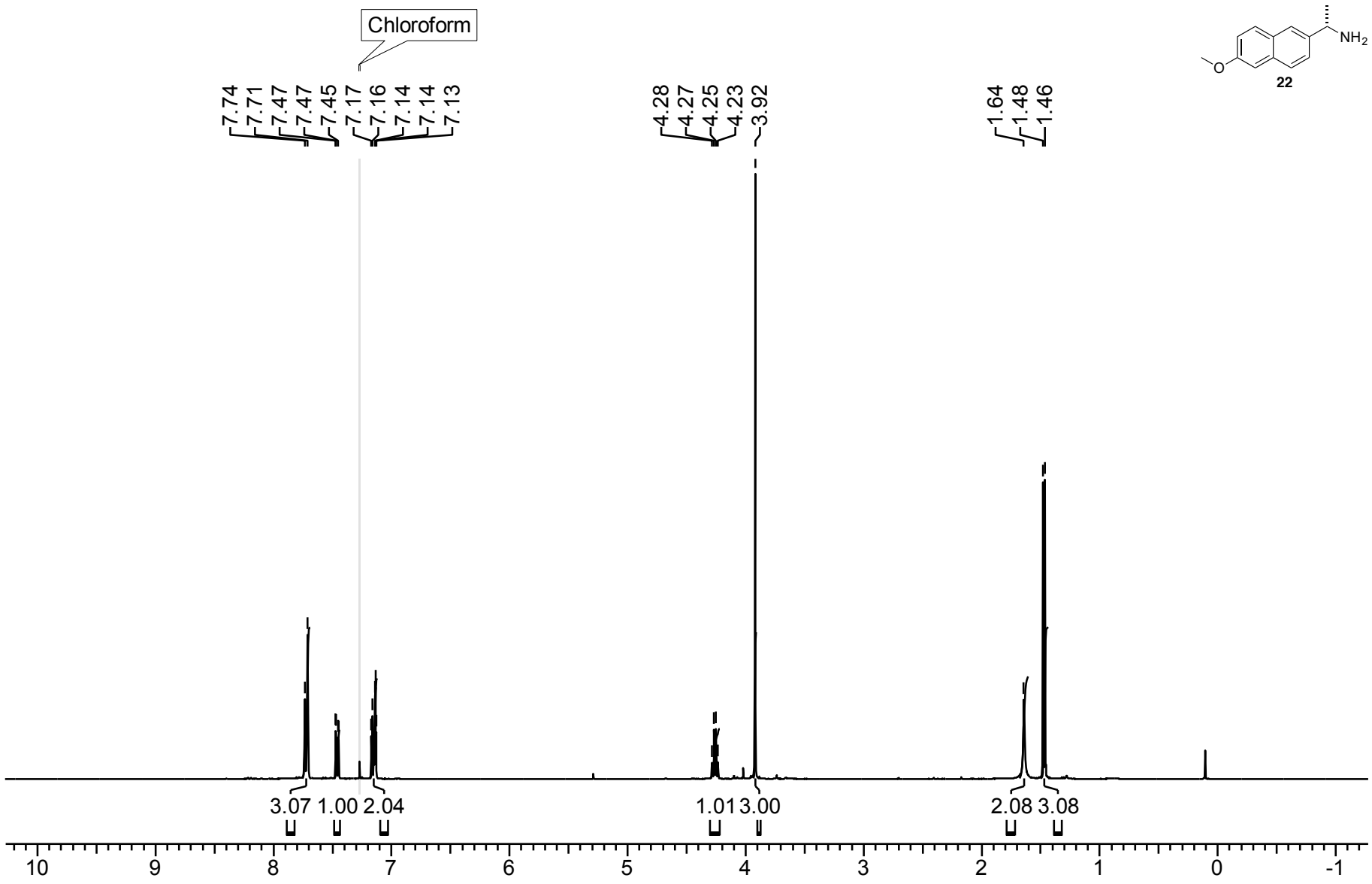

Figure S170. ^{1}H NMR (400 MHz, $CDCl_3$) spectrum of **22**.

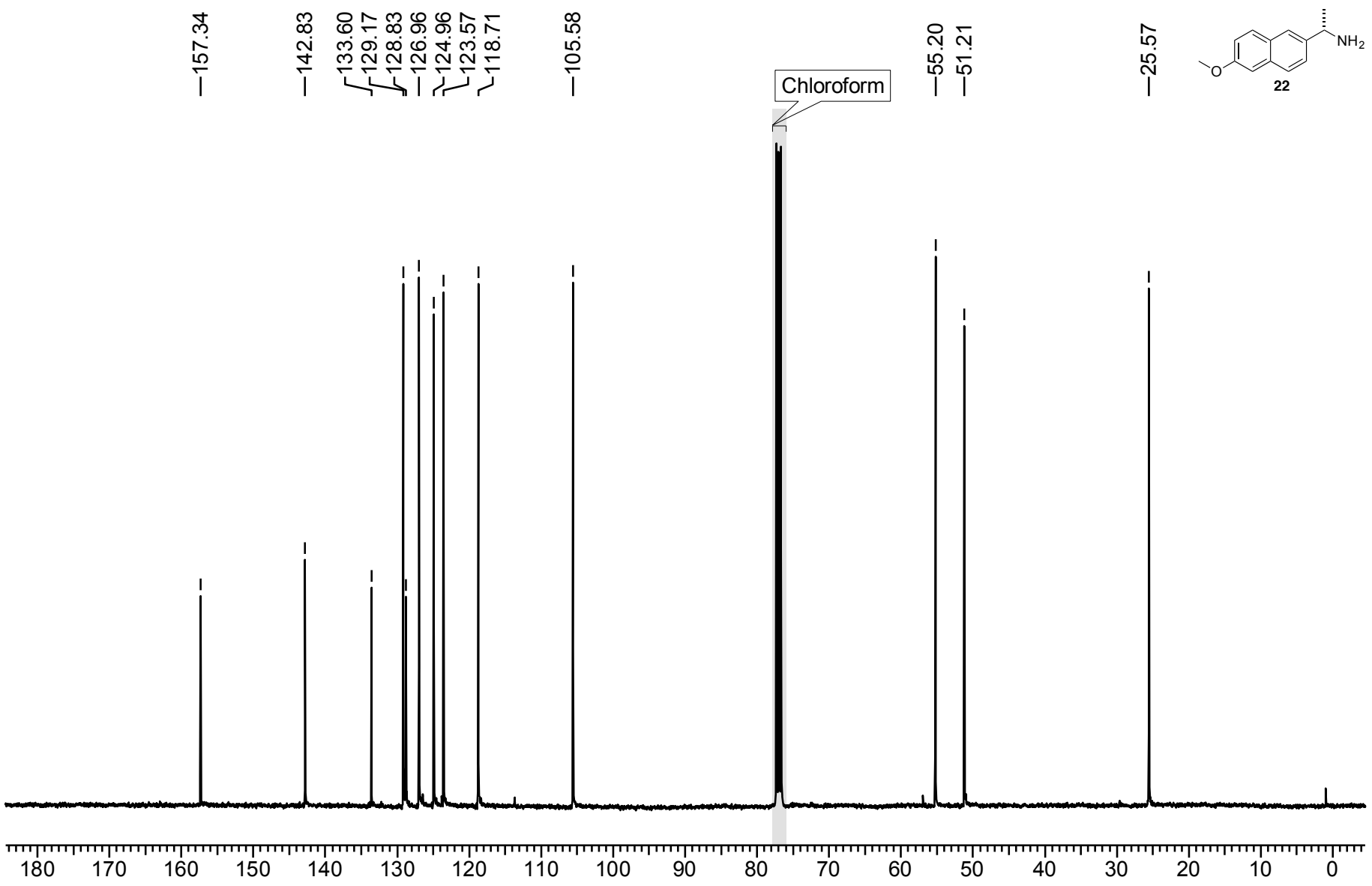

Figure S171. ^{13}C NMR (100 MHz, $CDCl_3$) spectrum of **22**.

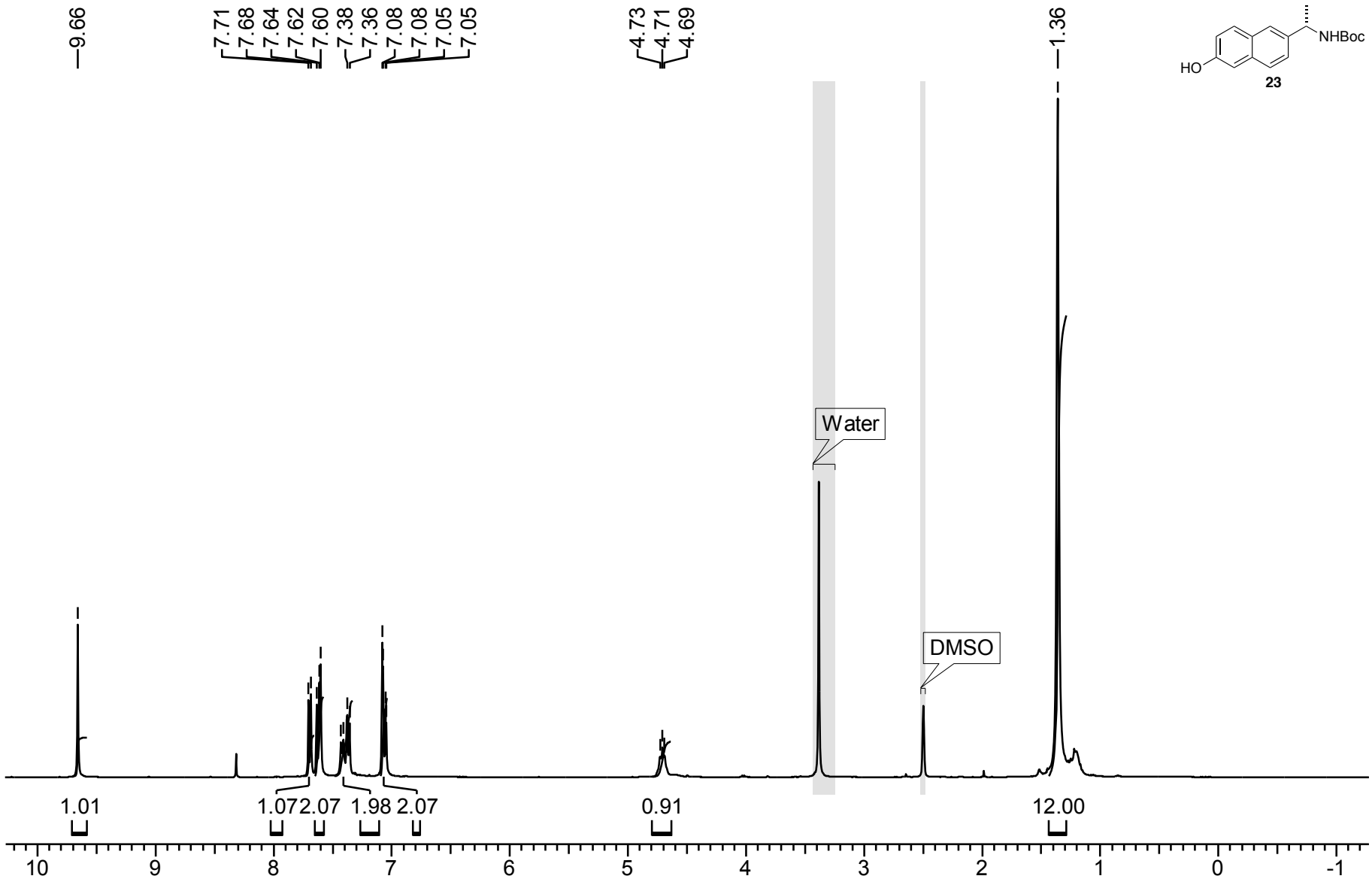

Figure S172. ^{1}H NMR (400 MHz, DMSO-d_6) spectrum of **23**.

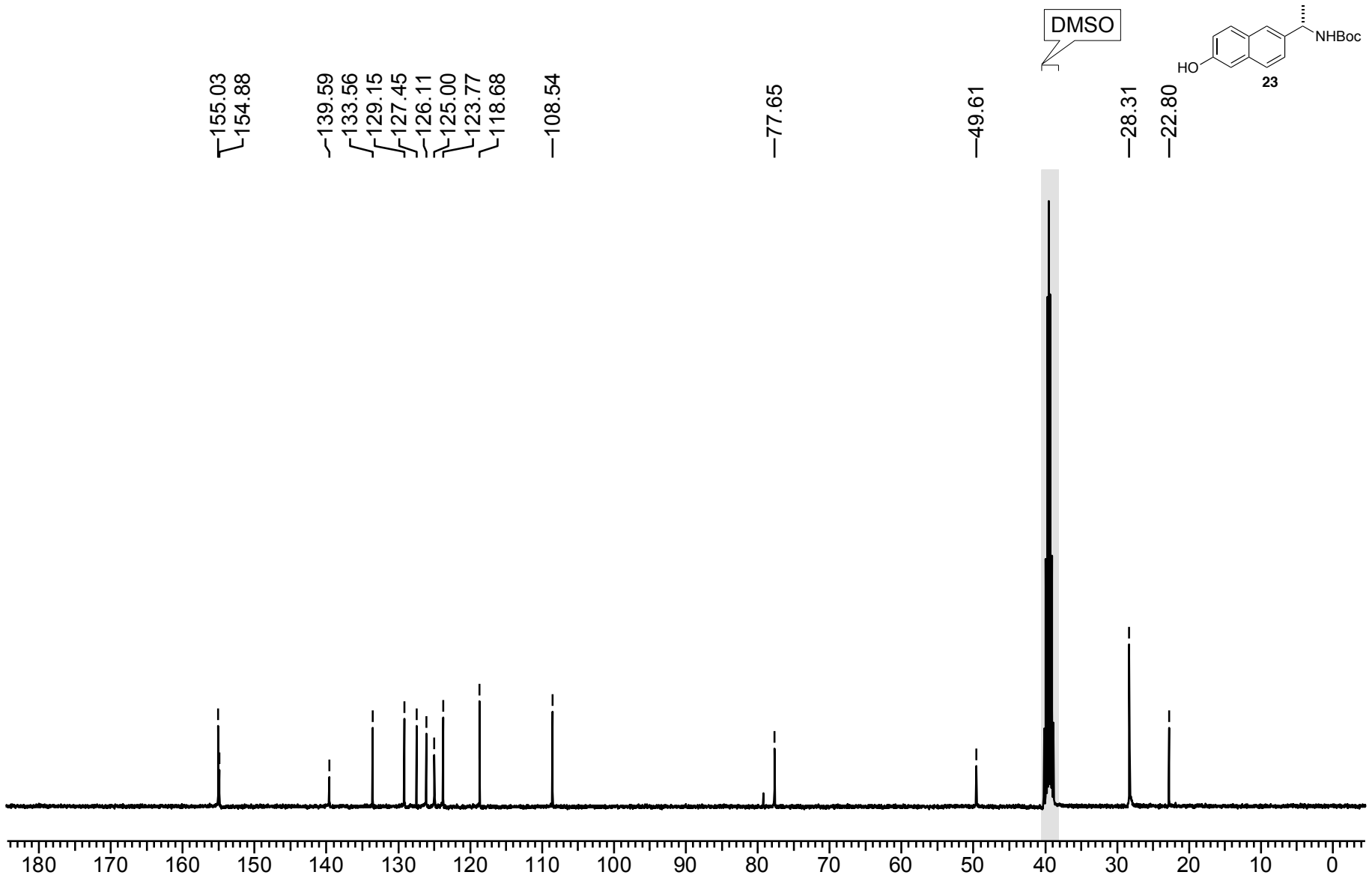

Figure S173. ^{13}C NMR (100 MHz, DMSO-d_6) spectrum of **23**.

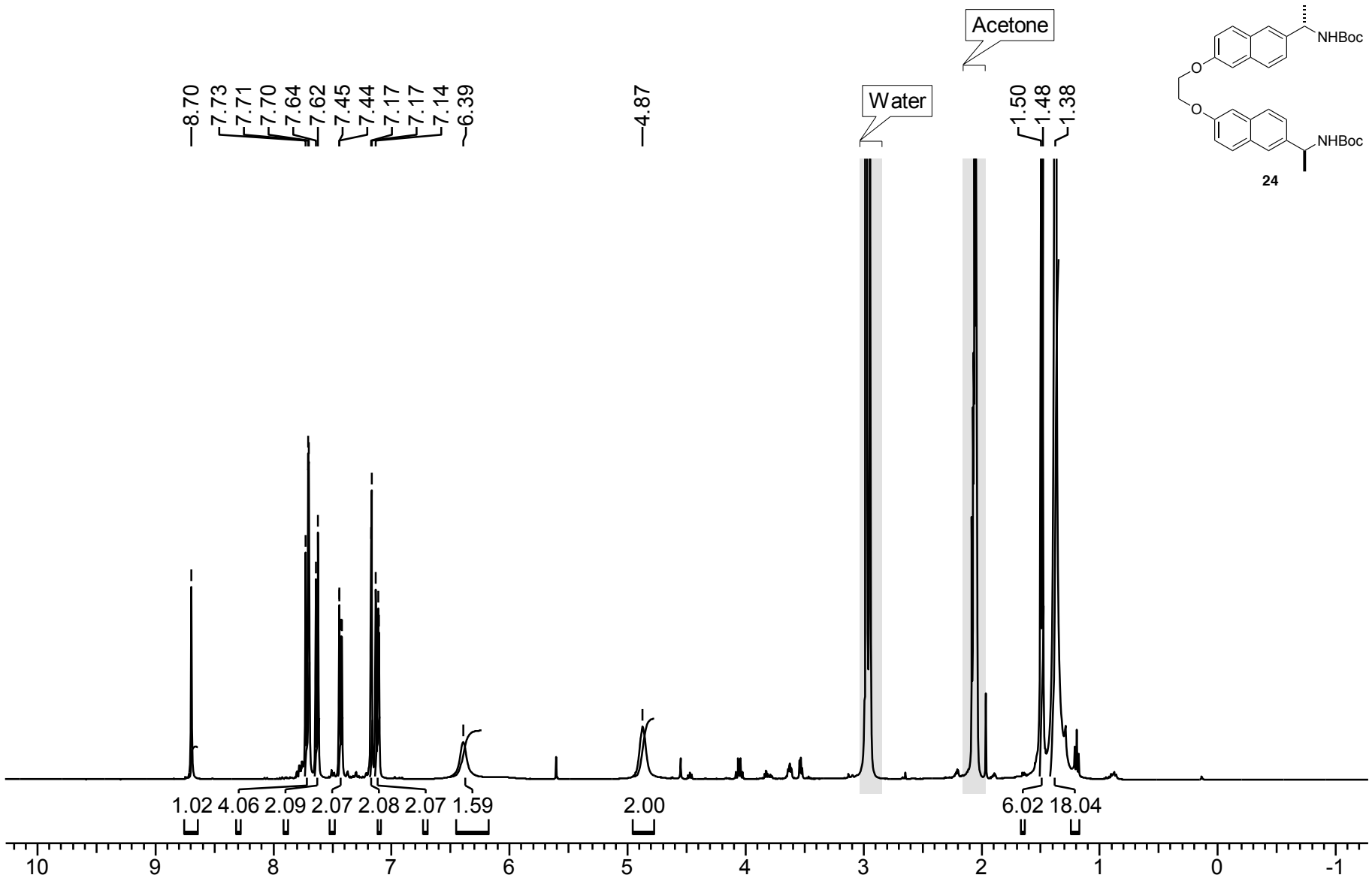

Figure S174. ^{1}H NMR (400 MHz, acetone-d_6) spectrum of **24**.

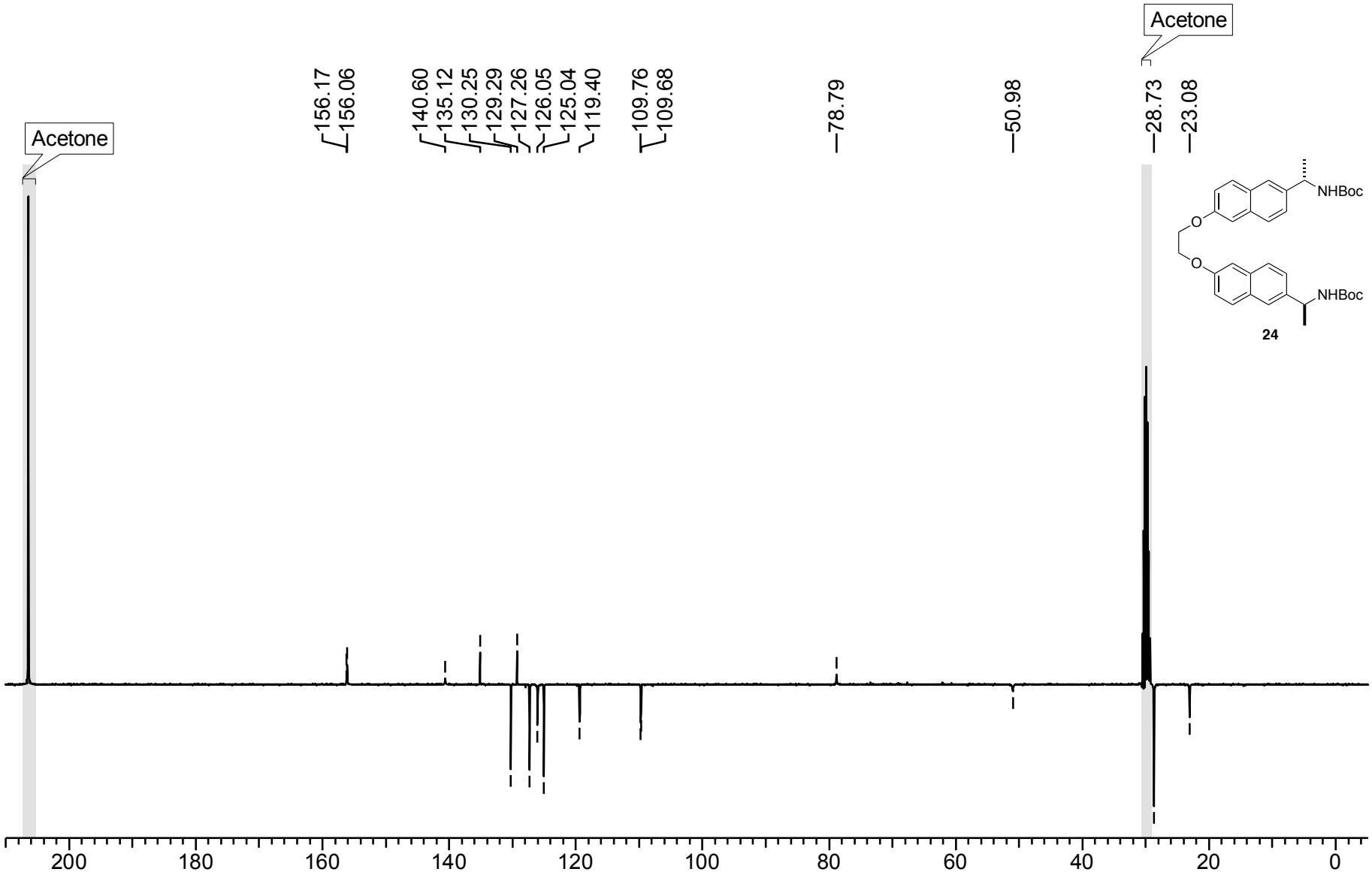

Figure S175. ^{13}C NMR APT (100 MHz, acetone-d_6) spectrum of **24**.

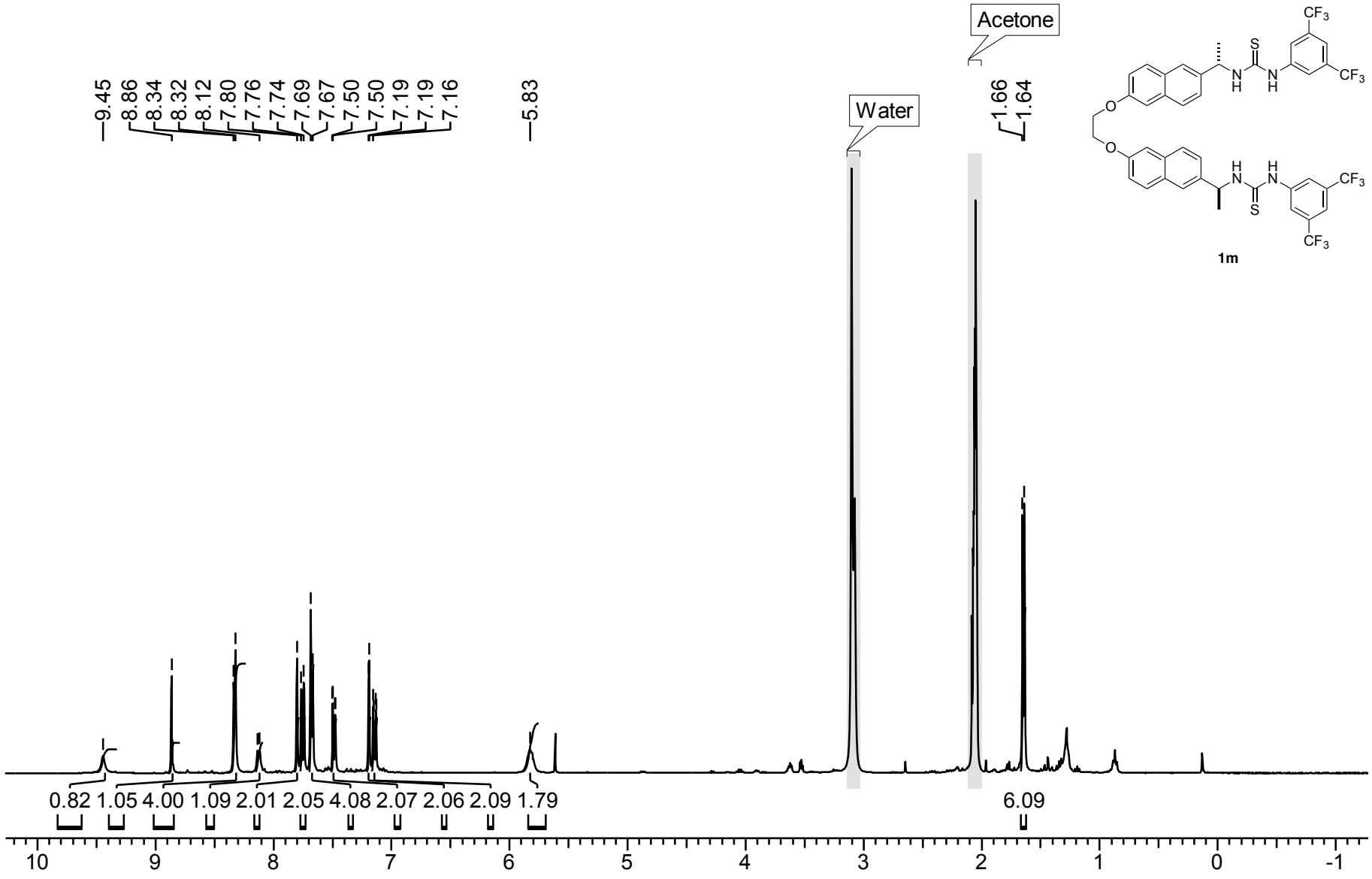

Figure S176. ^{1}H NMR (400 MHz, acetone-d_6) spectrum of **1m**.

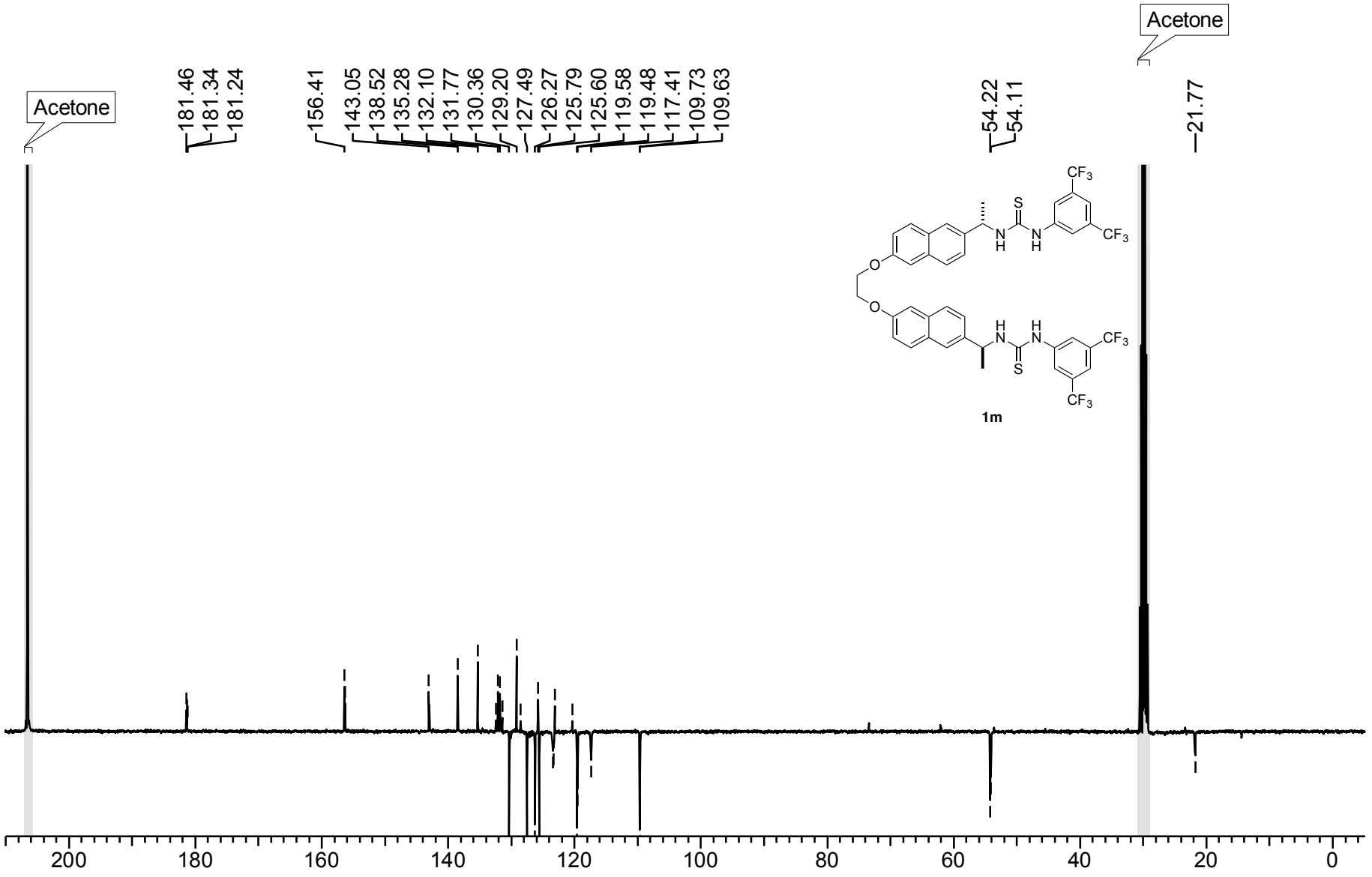

Figure S177. ^{13}C NMR APT (100 MHz, acetone-d_6) spectrum of **1m**.

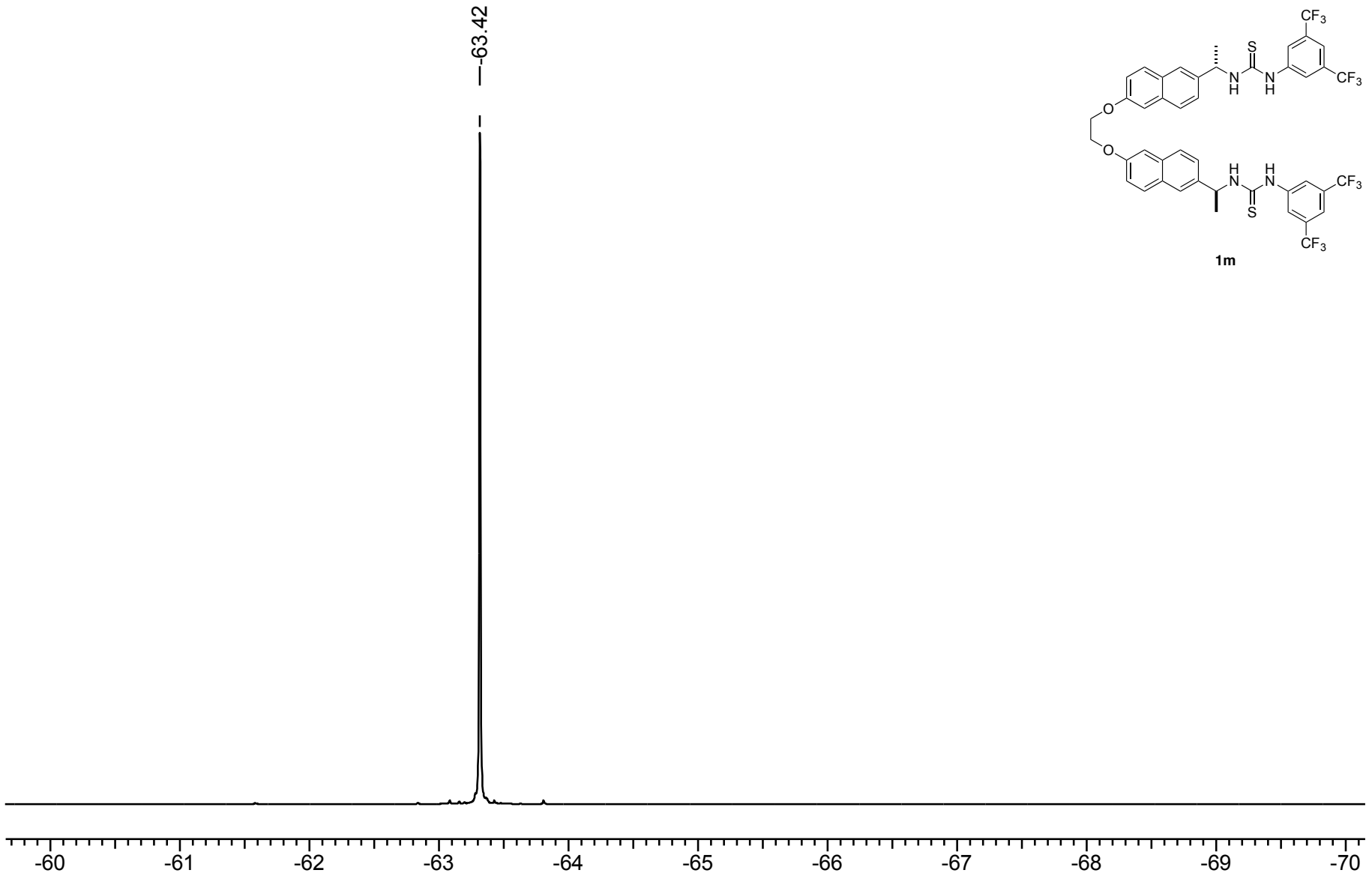

Figure S178. ^{19}F NMR (376 MHz, acetone-d_6) spectrum of **1m**.

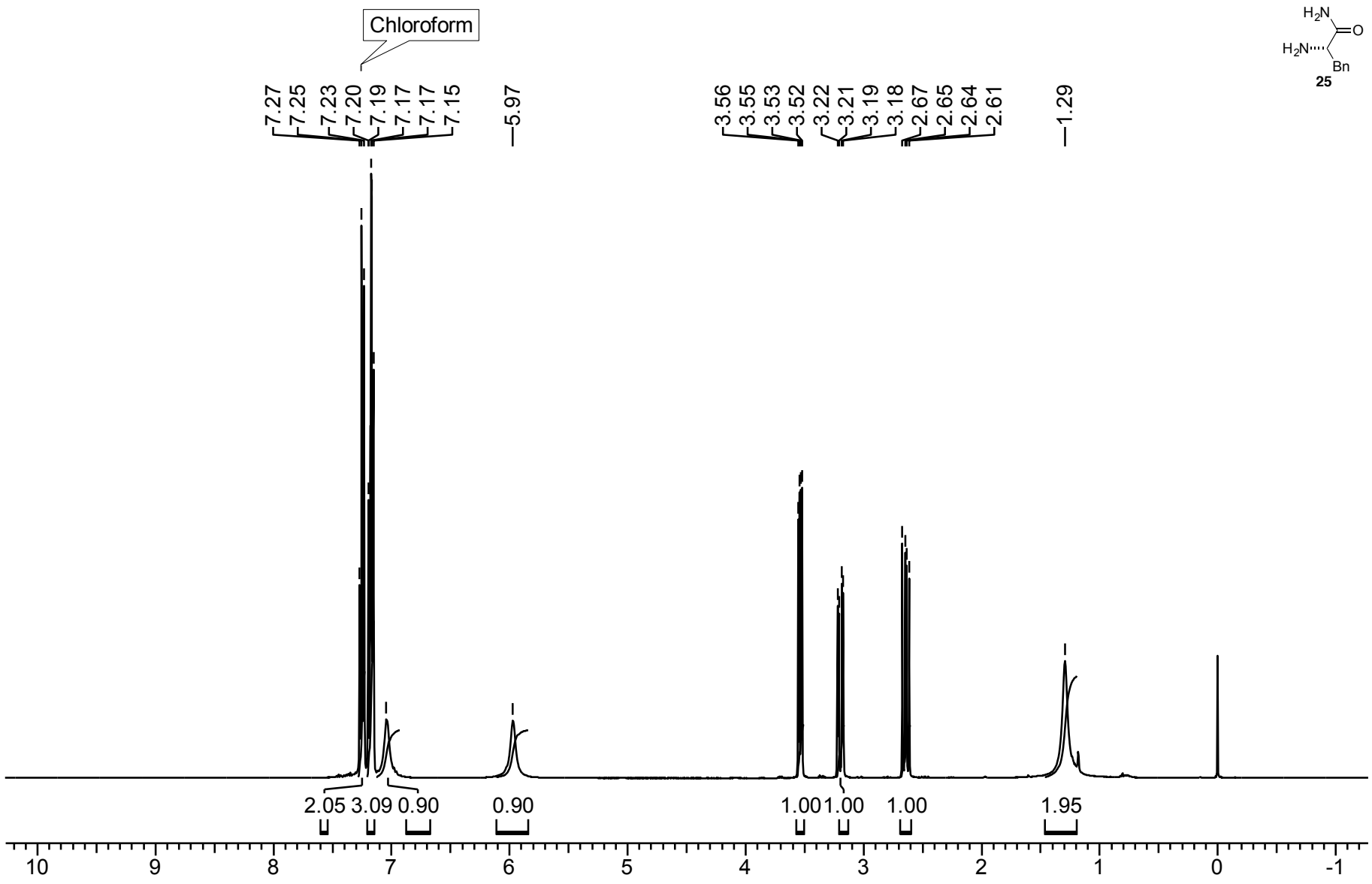

Figure S179. ^{1}H NMR (400 MHz, $CDCl_3$) spectrum of **25**.

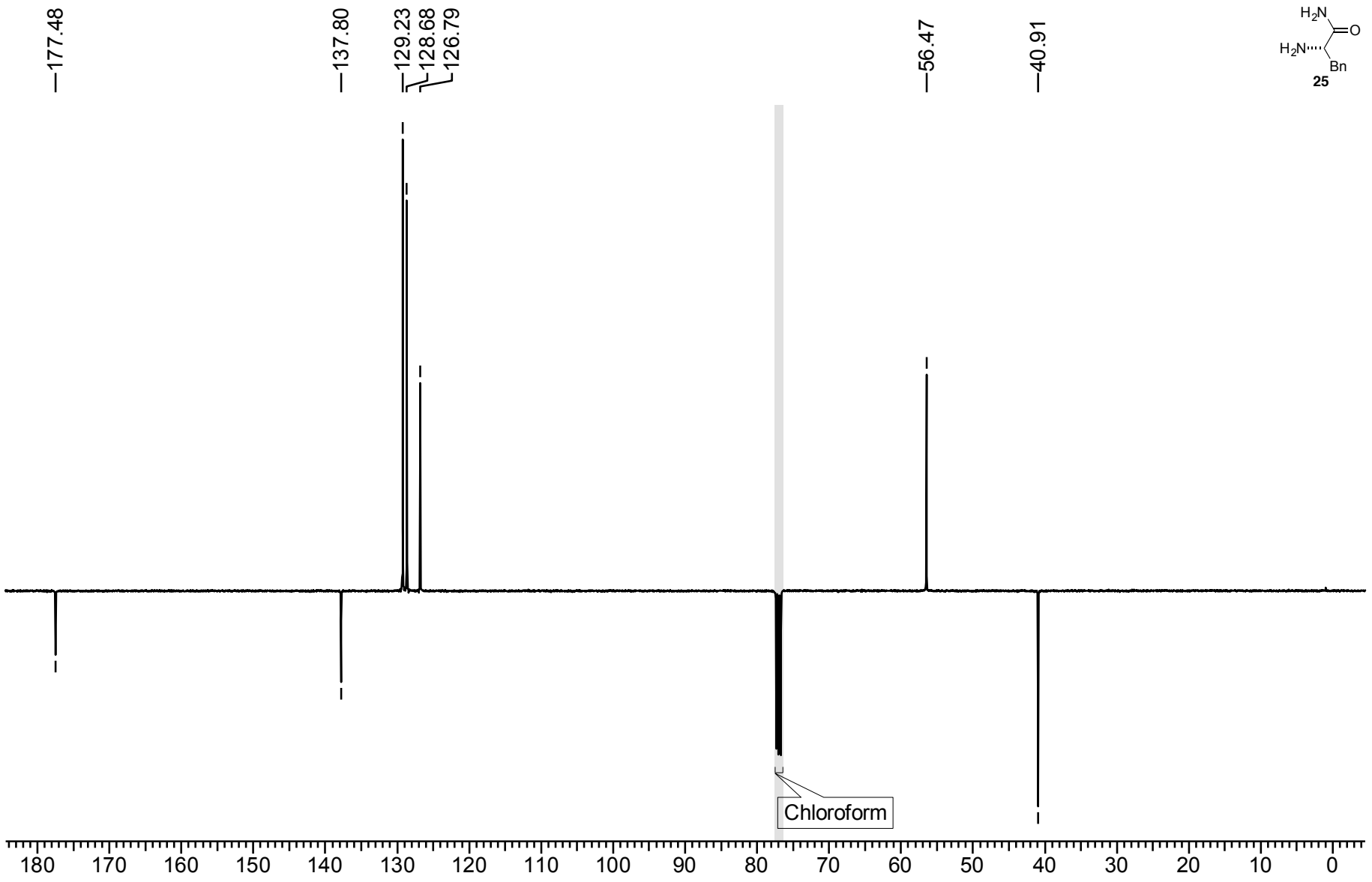

Figure S180. ^{13}C NMR APT (100 MHz, $CDCl_3$) spectrum of **25**.

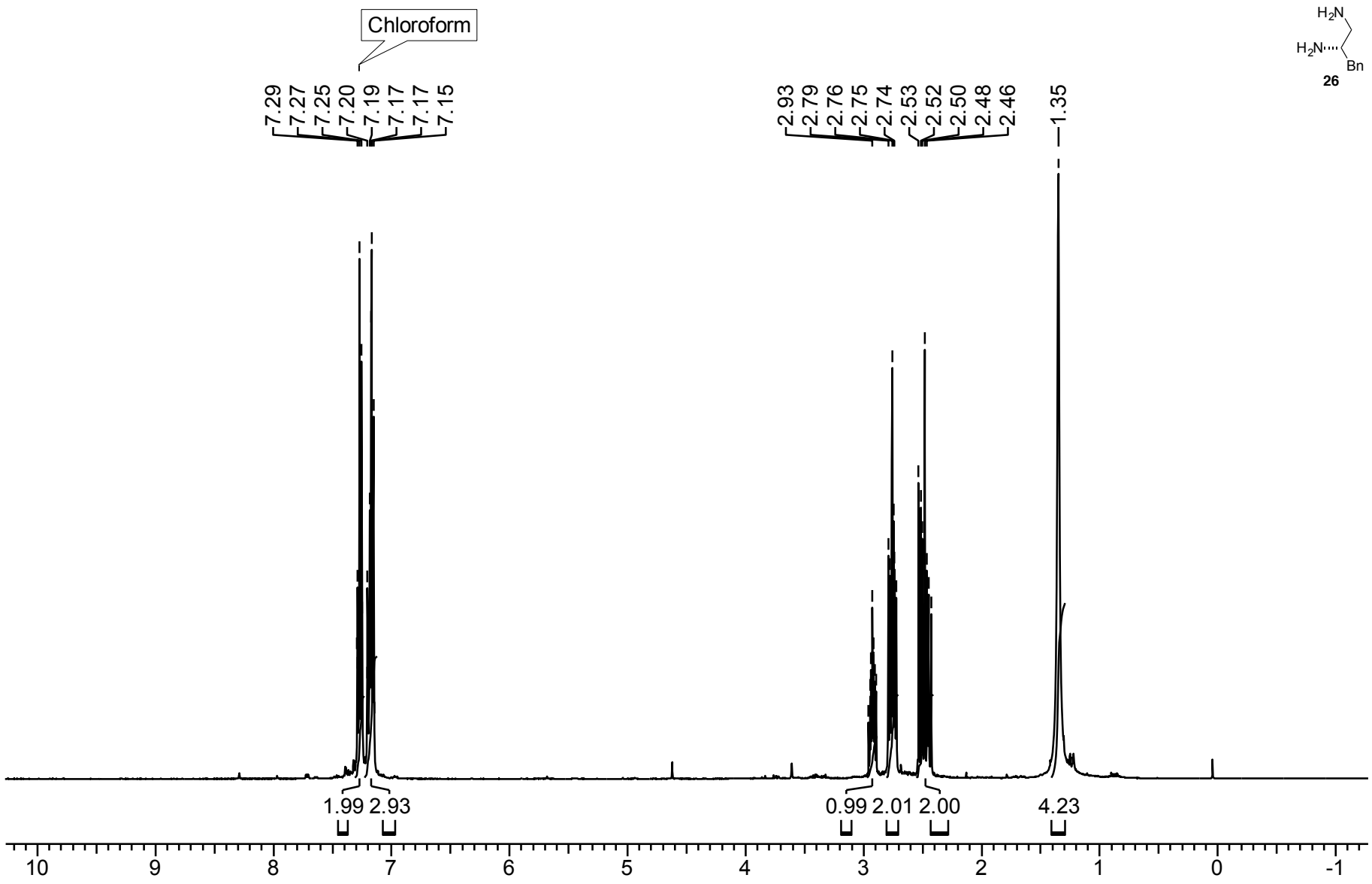

Figure S181. ^{1}H NMR (400 MHz, $CDCl_3$) spectrum of **26**.

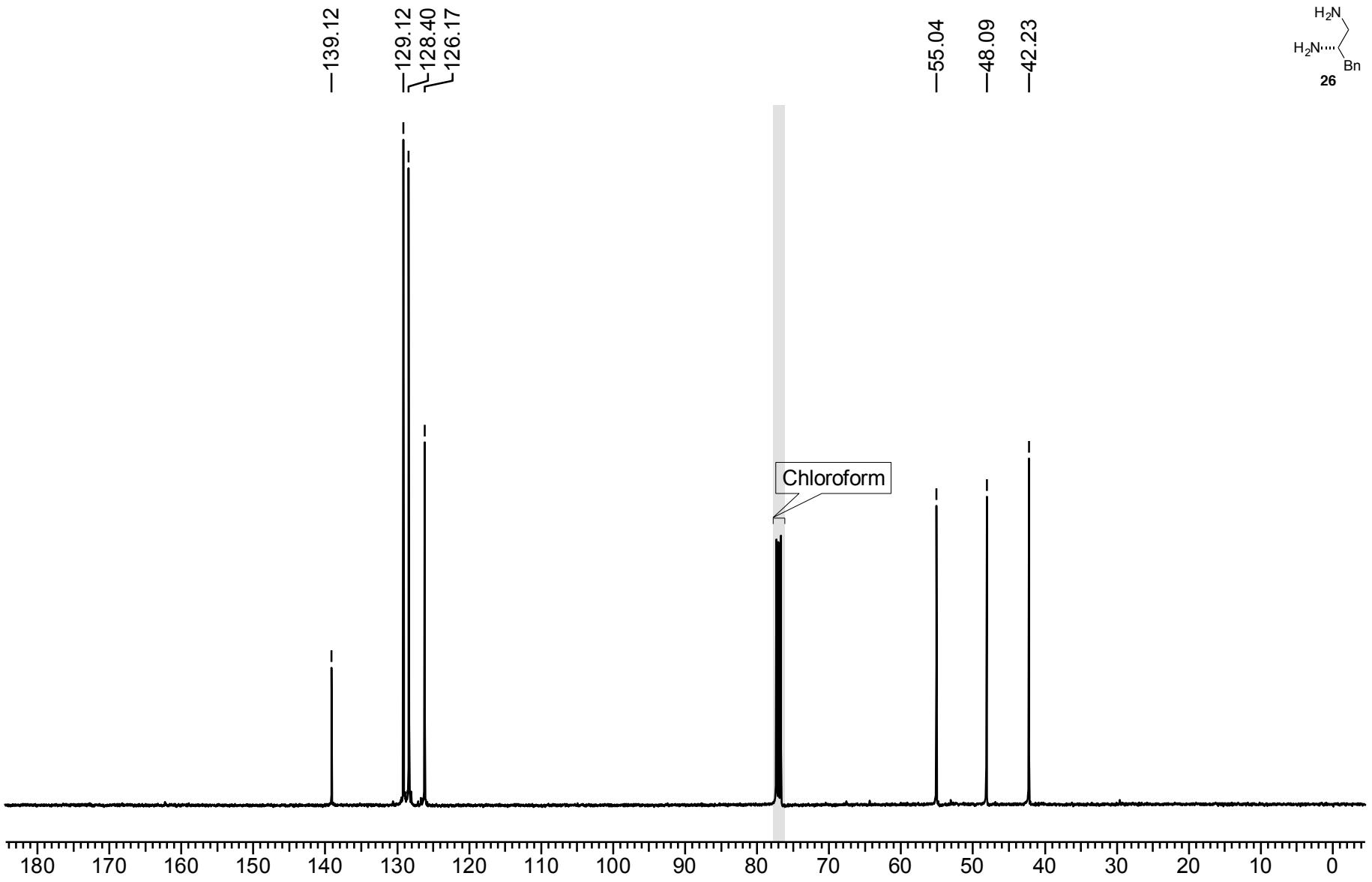

Figure S182. ^{13}C NMR (100 MHz, $CDCl_3$) spectrum of **26**.

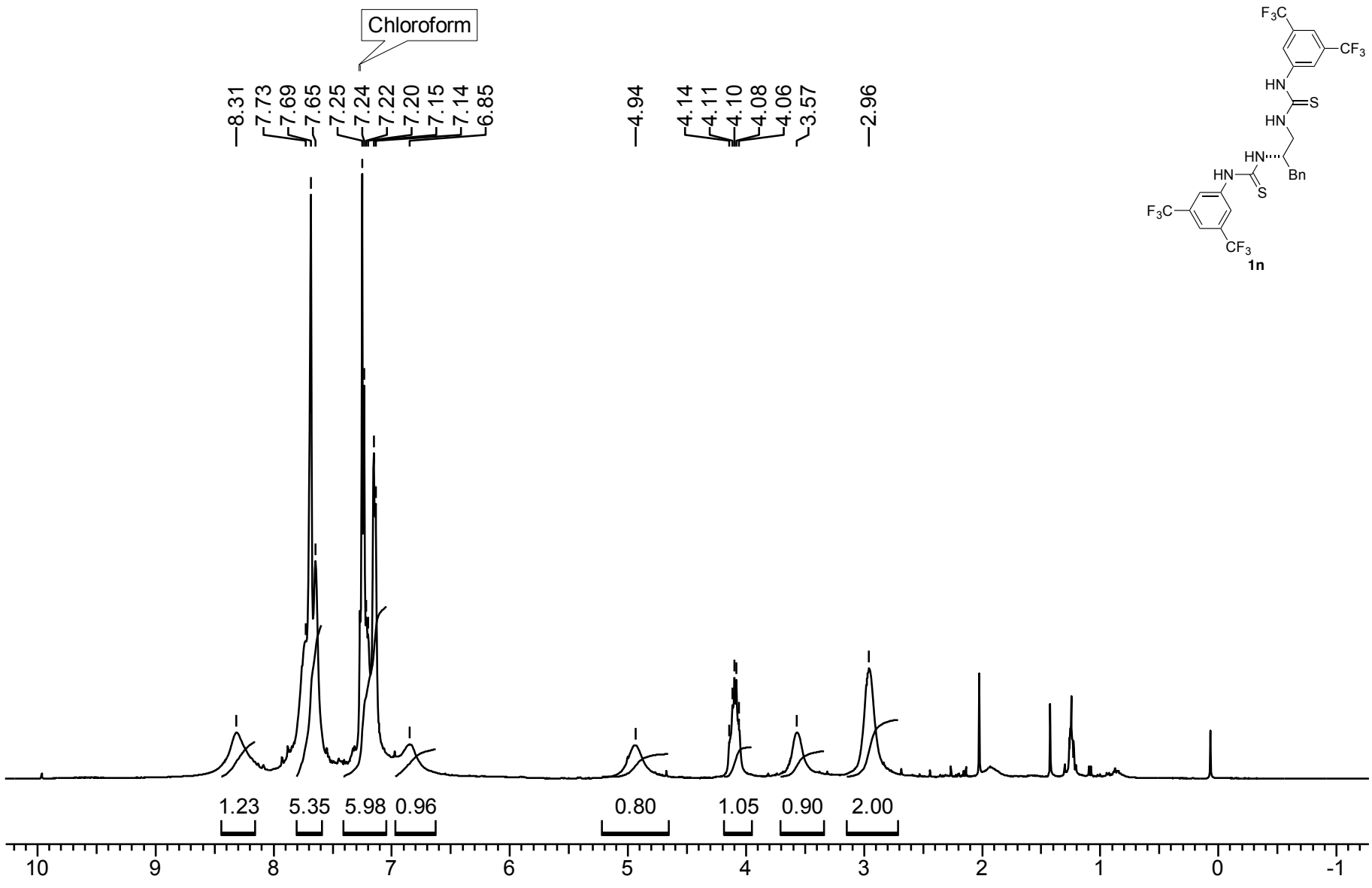

Figure S183. ^{1}H NMR (400 MHz, $CDCl_3$) spectrum of **1n**.

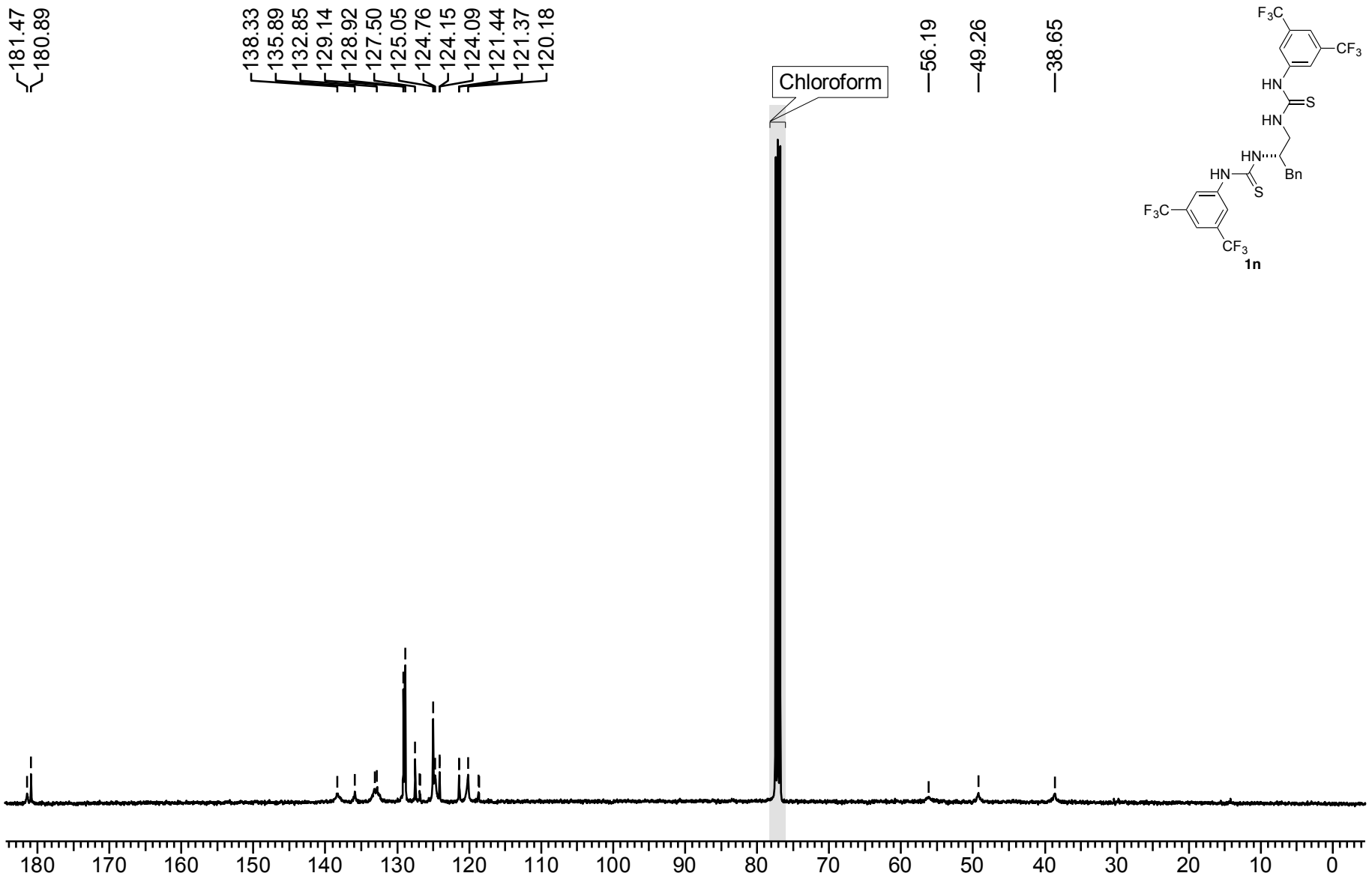

Figure S184. ^{13}C NMR (100 MHz, $CDCl_3$) spectrum of **1n**.

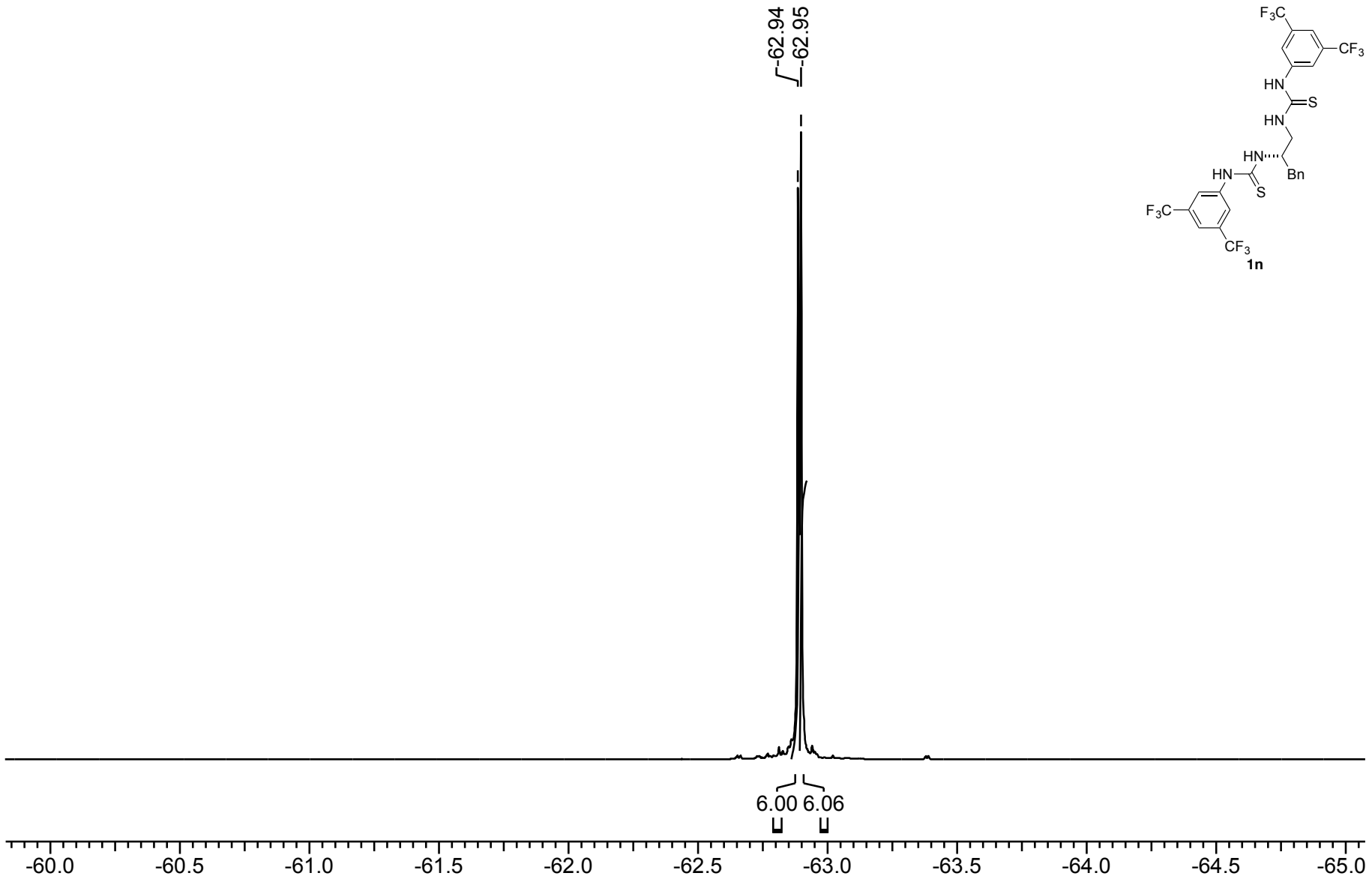

Figure S185. ^{19}F NMR (376 MHz, $CDCl_3$) spectrum of **1n**.

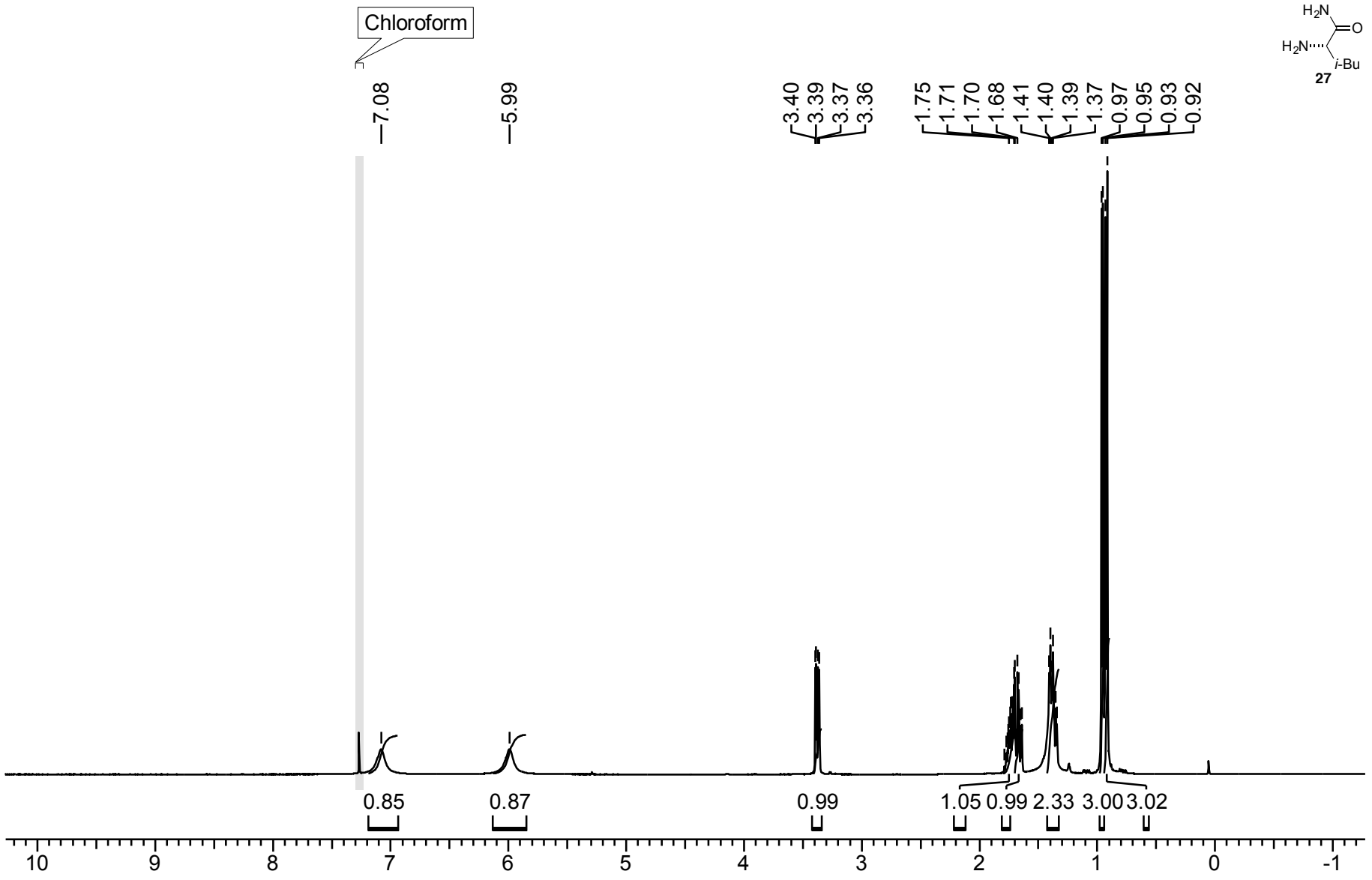

Figure S186. ^{1}H NMR (400 MHz, $CDCl_3$) spectrum of **27**.

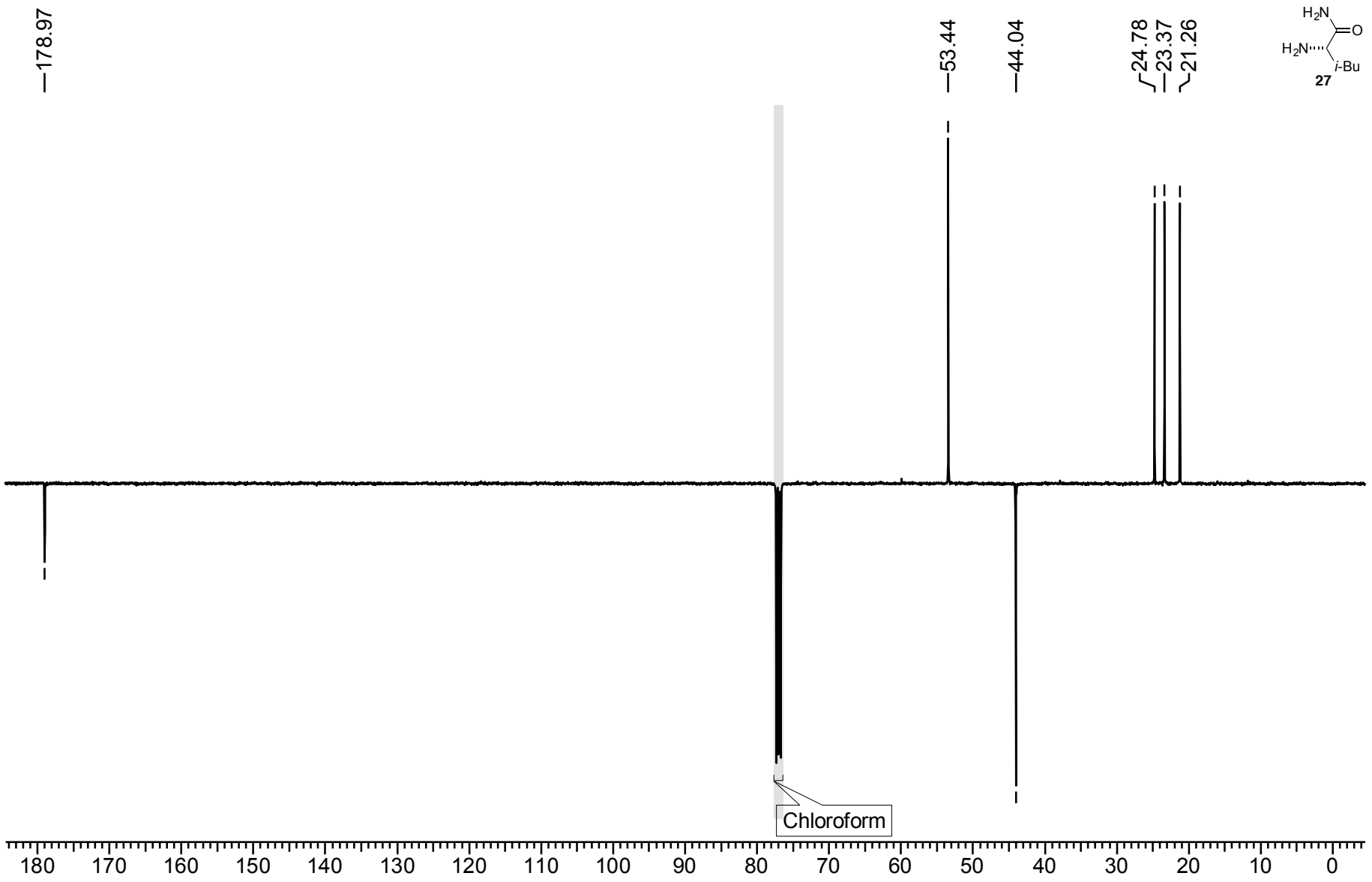

Figure S187. ^{13}C NMR (100 MHz, $CDCl_3$) spectrum of **27**.

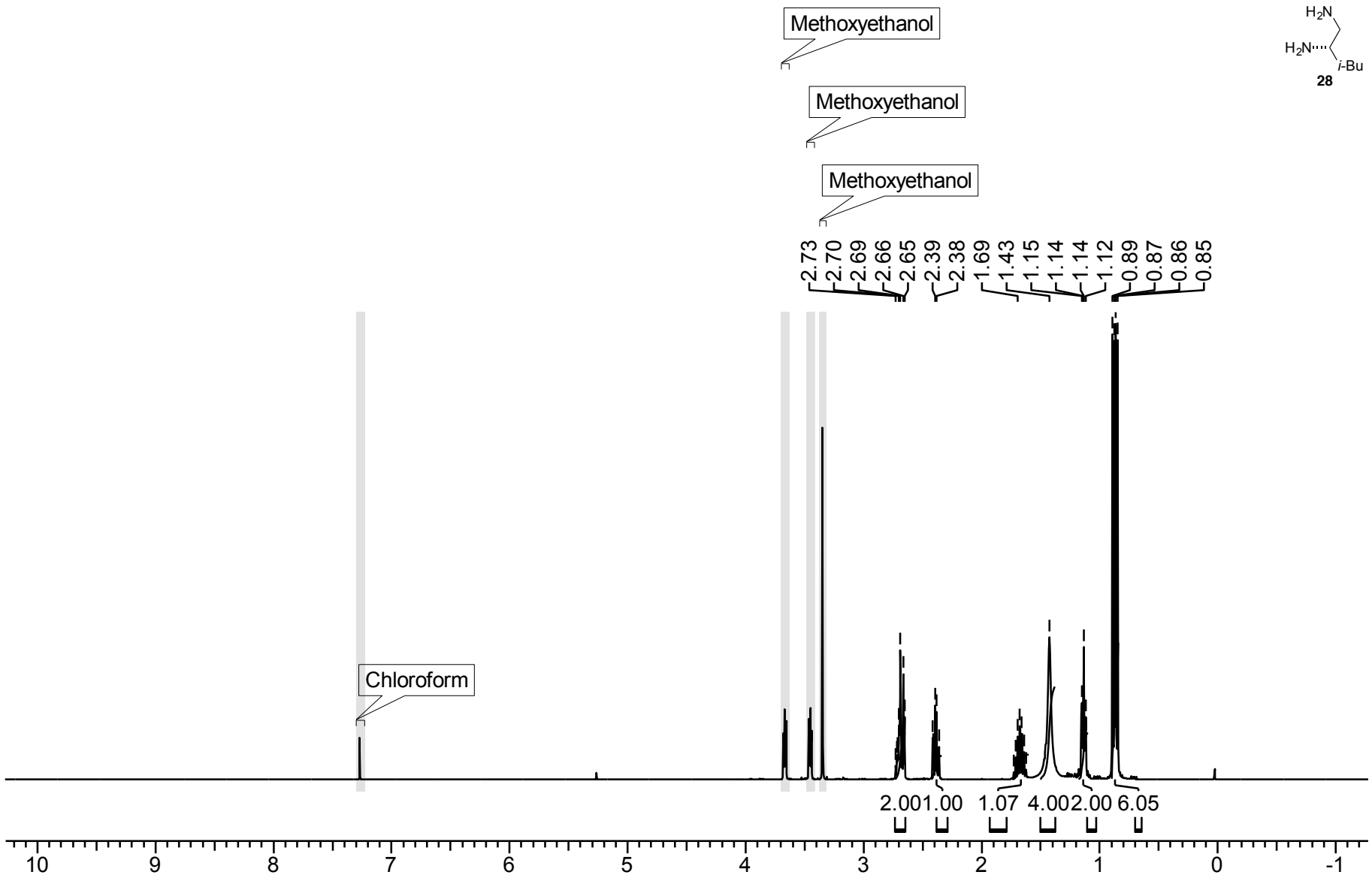

Figure S188. ^{1}H NMR (400 MHz, $CDCl_3$) spectrum of **28**.

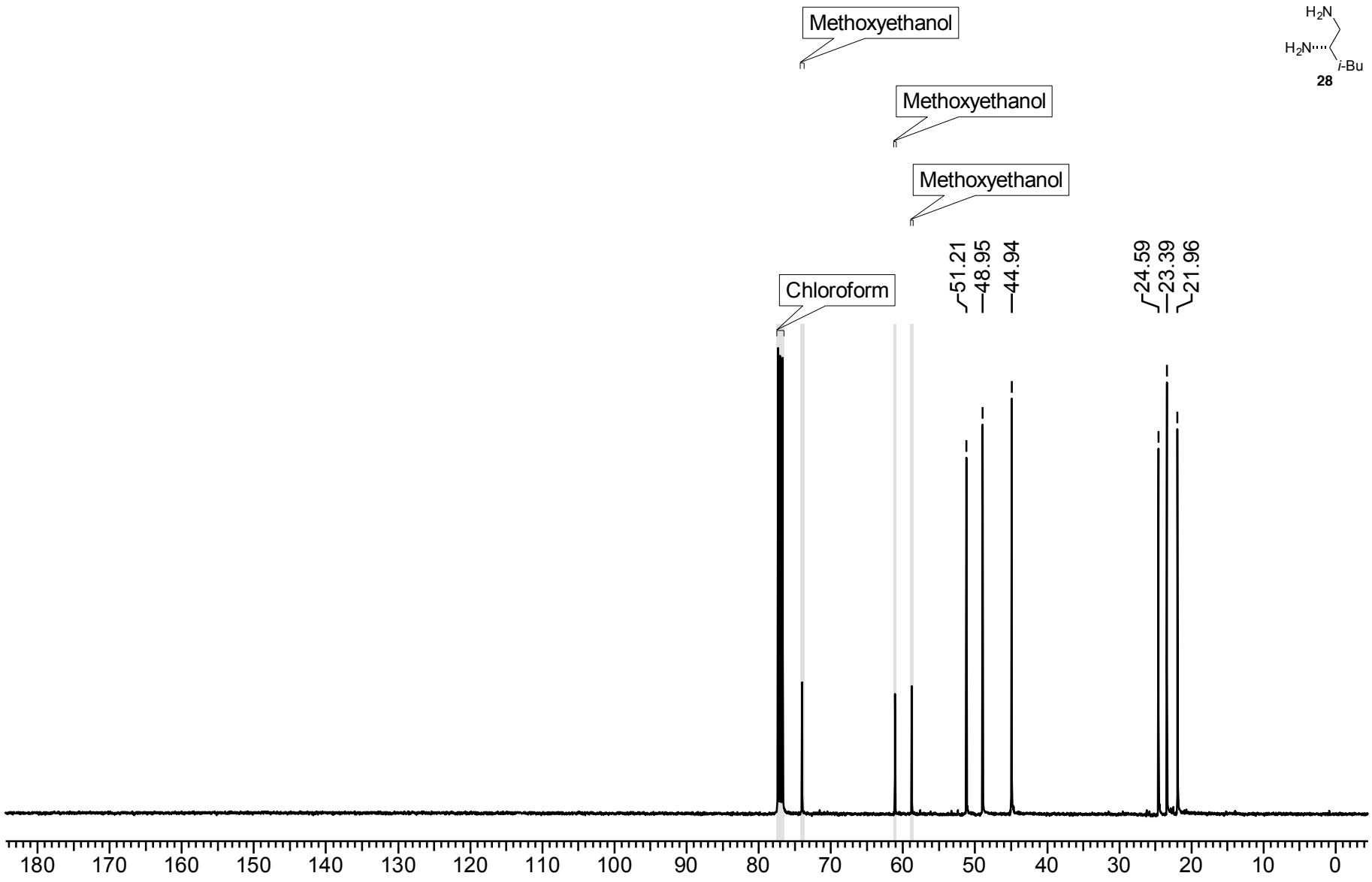

Figure S189. ^{13}C NMR (100 MHz, $CDCl_3$) spectrum of **28**.

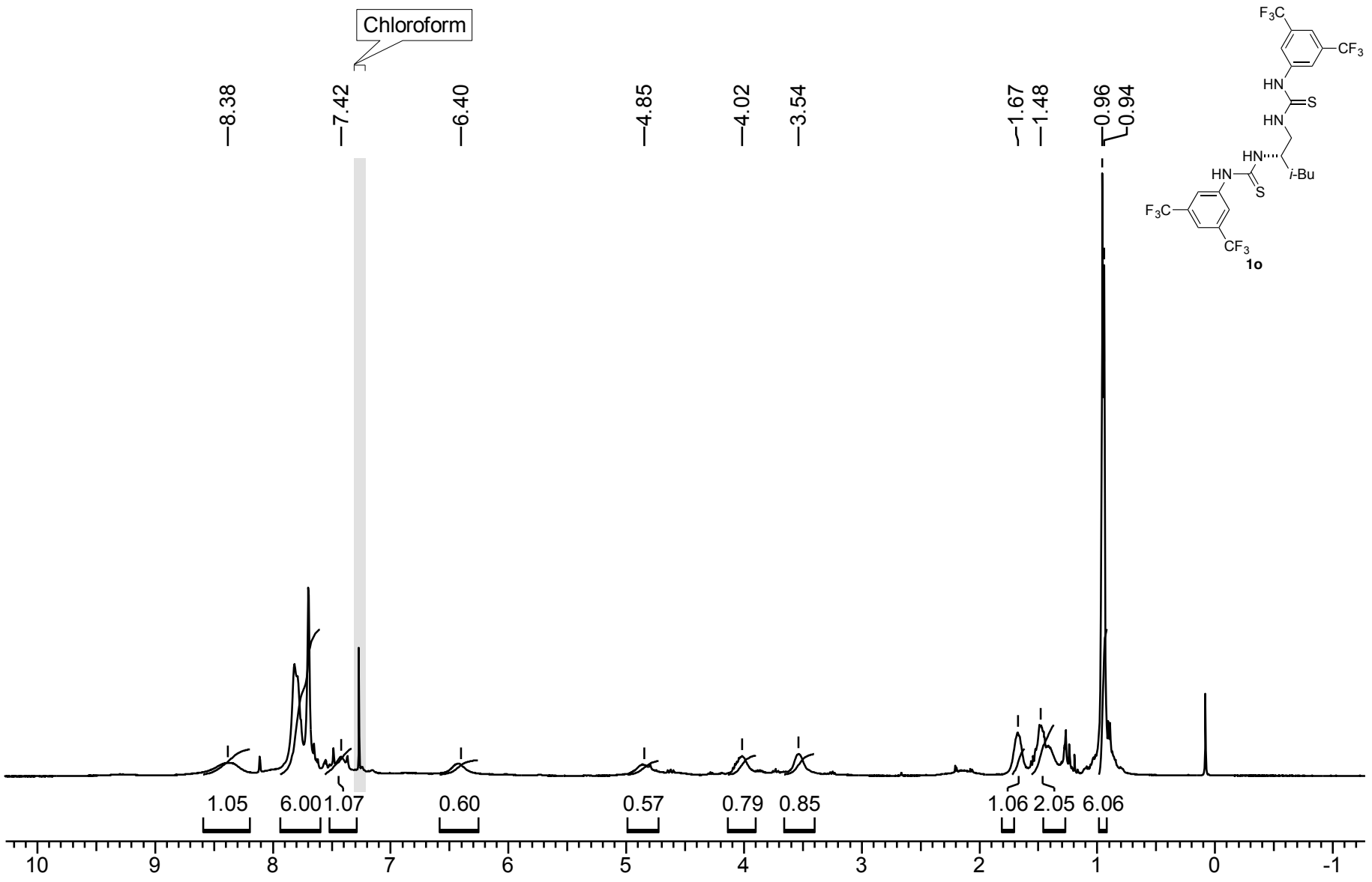

Figure S190. ^{1}H NMR (400 MHz, $CDCl_3$) spectrum of **1o**.

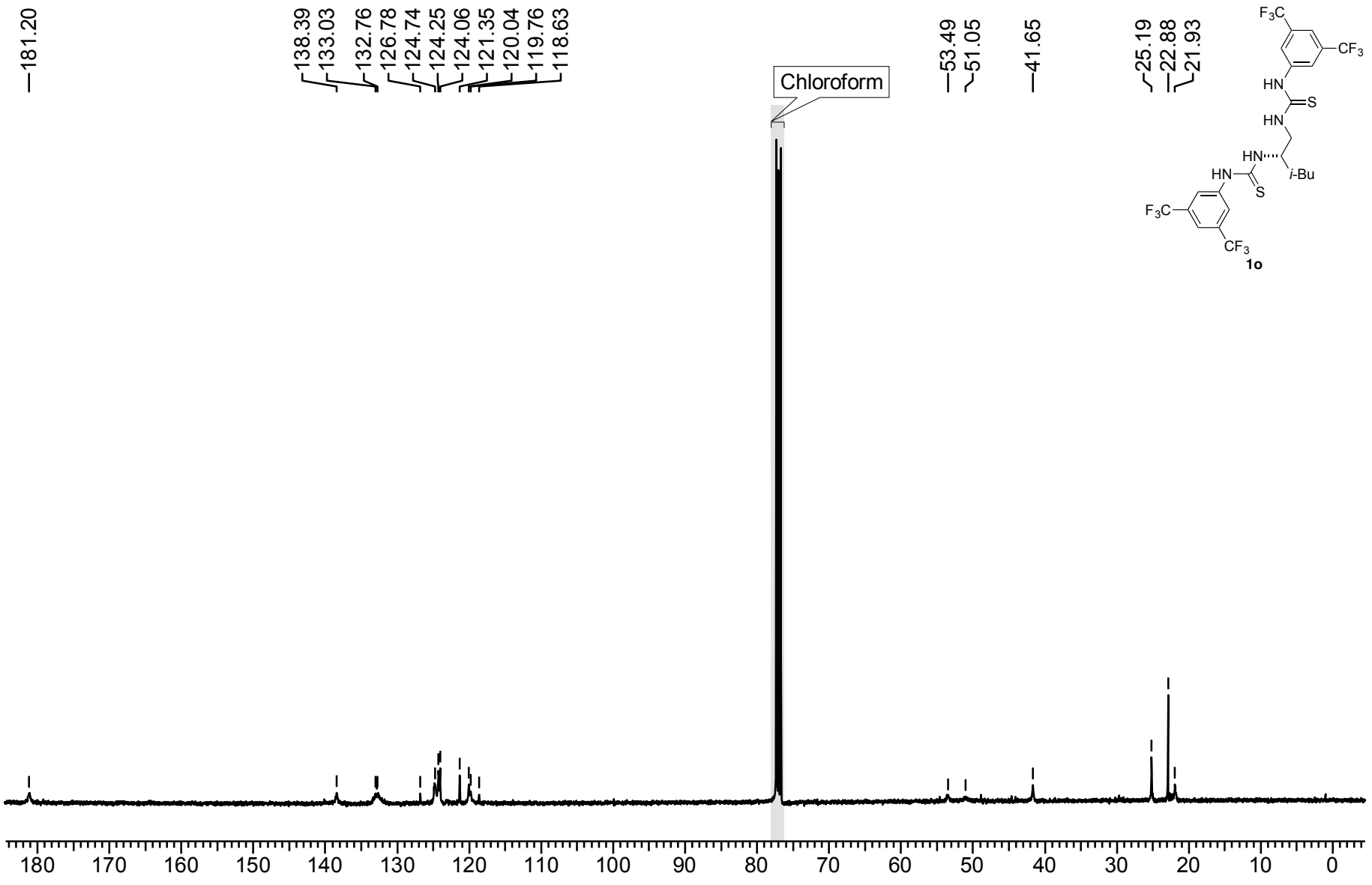

Figure S191. ^{13}C NMR (100 MHz, $CDCl_3$) spectrum of **1o**.

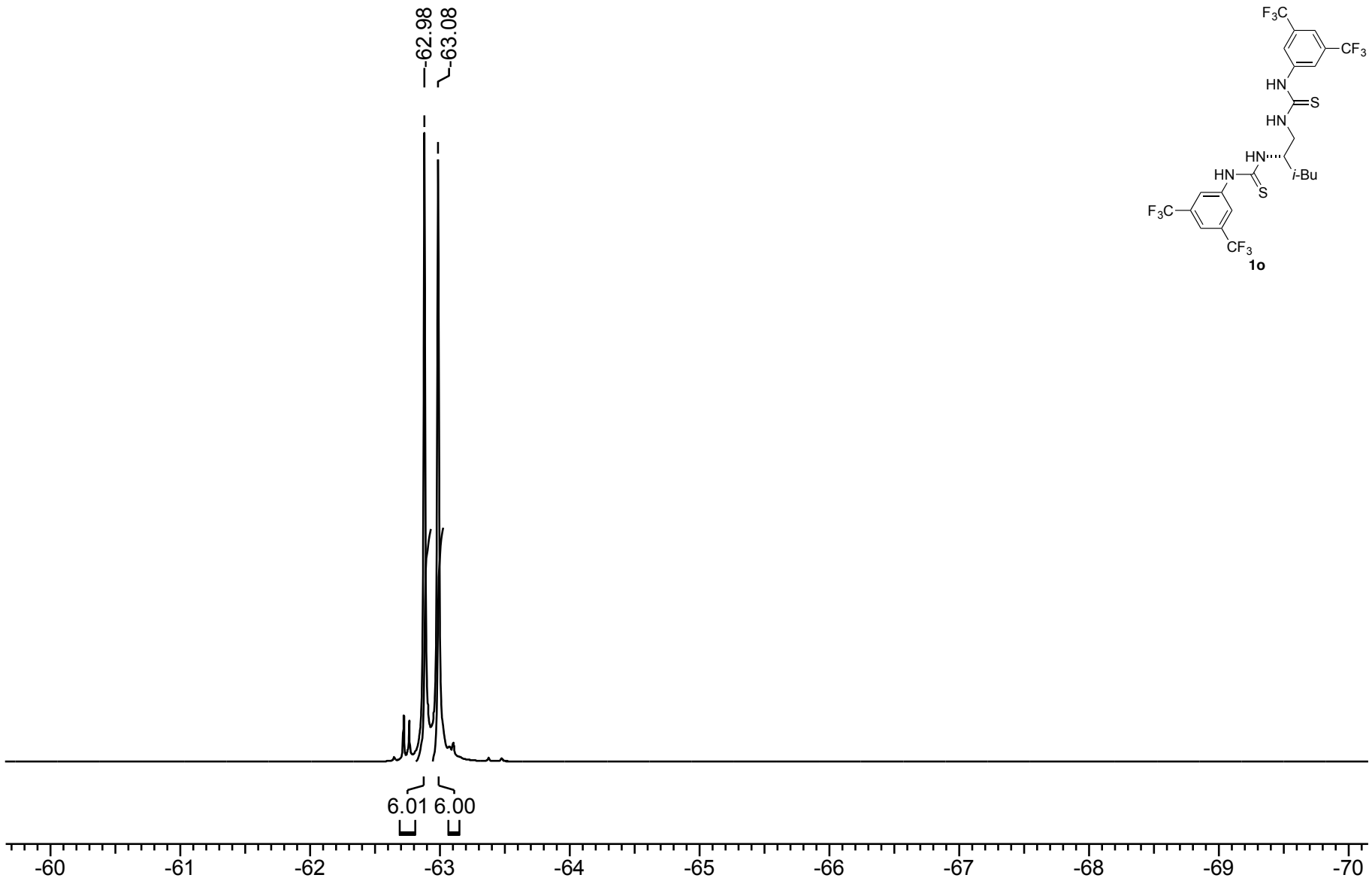

Figure S192. ^{19}F NMR (376 MHz, $CDCl_3$) spectrum of **1o**.

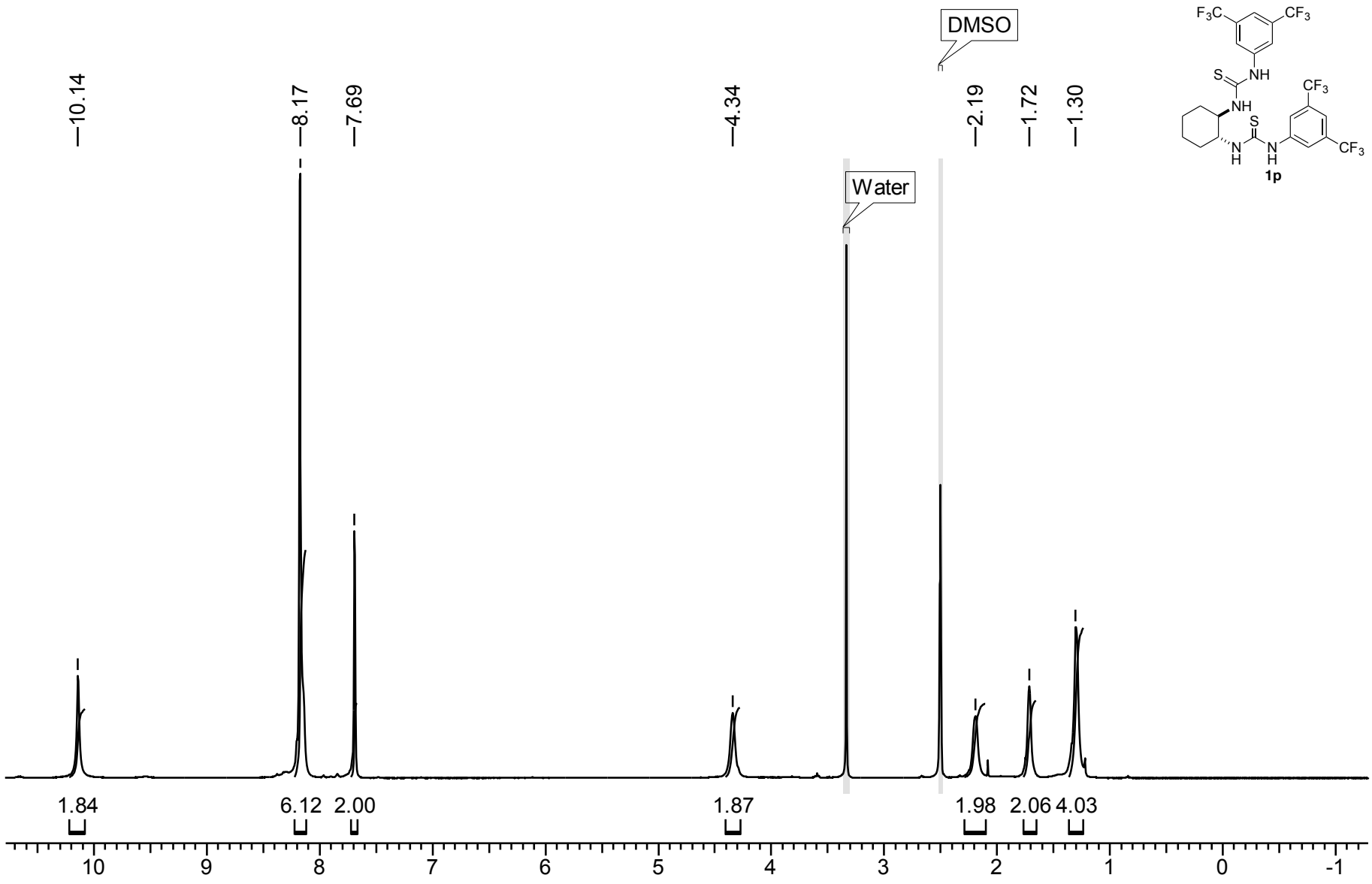

Figure S193. ^{1}H NMR (400 MHz, DMSO-d_6) spectrum of **1p**.

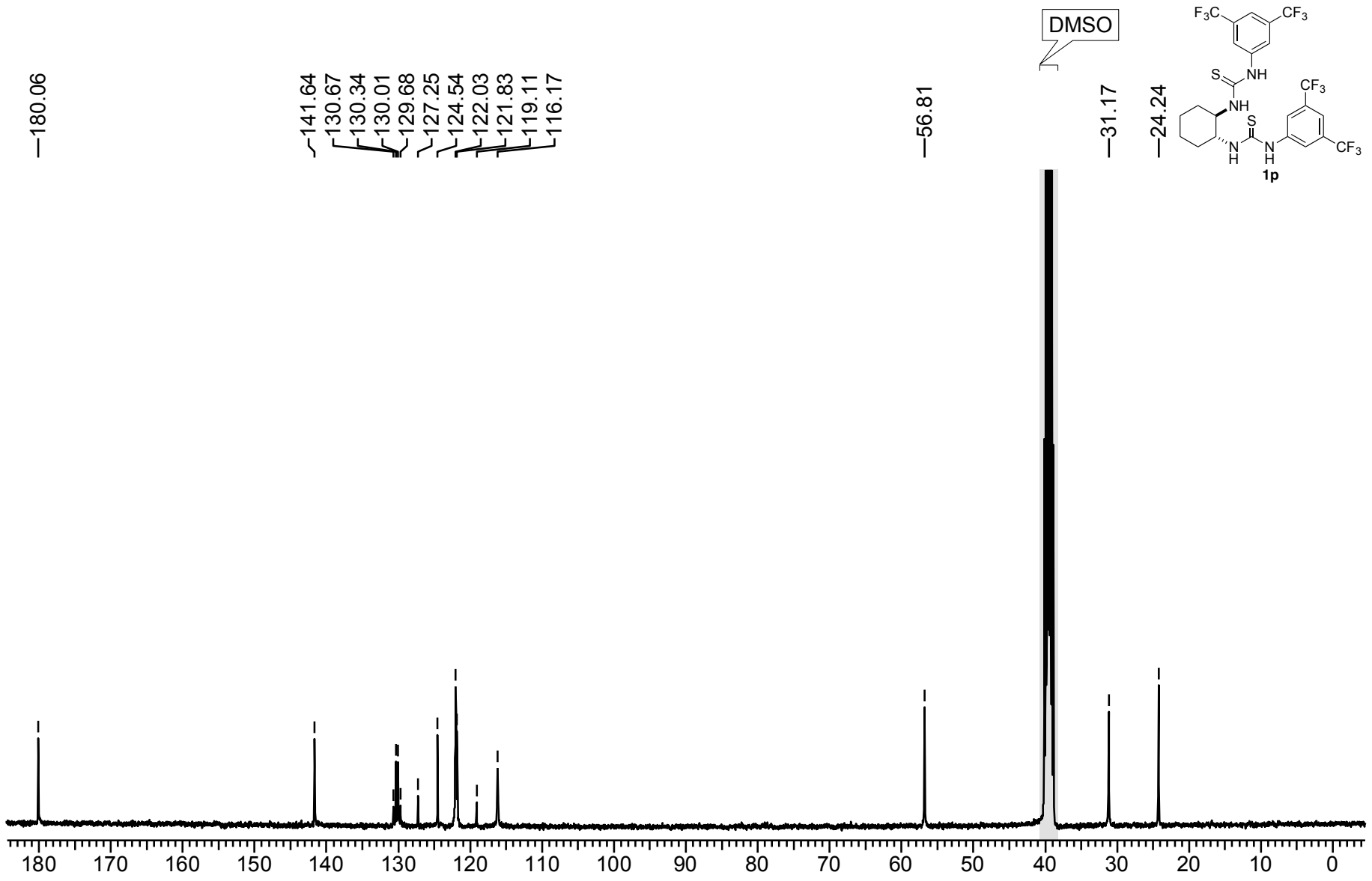

Figure S194. ^{13}C NMR (100 MHz, DMSO-d_6) spectrum of **1p**.

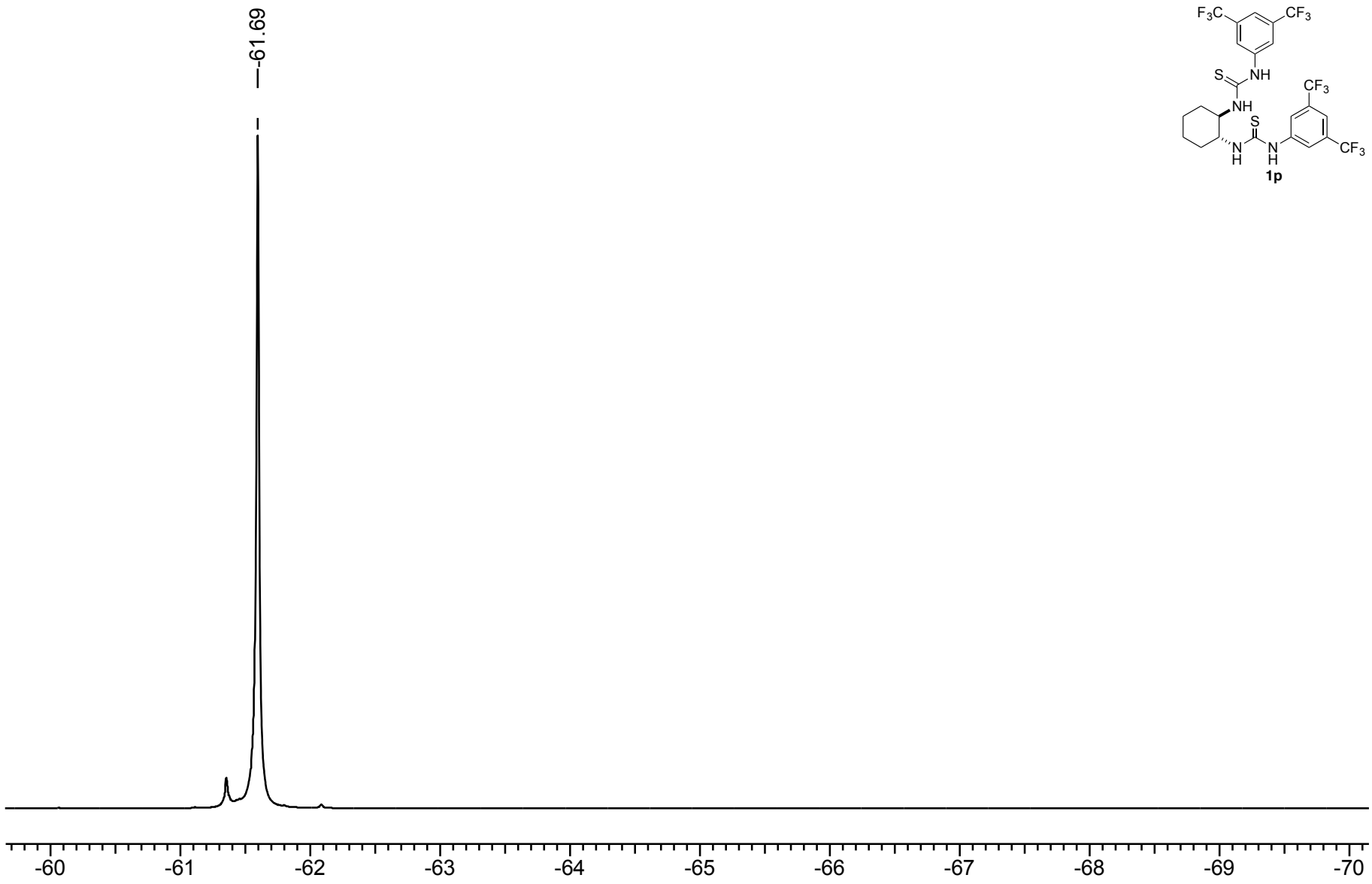

Figure S195. ^{19}F NMR (376 MHz, DMSO-d_6) spectrum of **1p**.

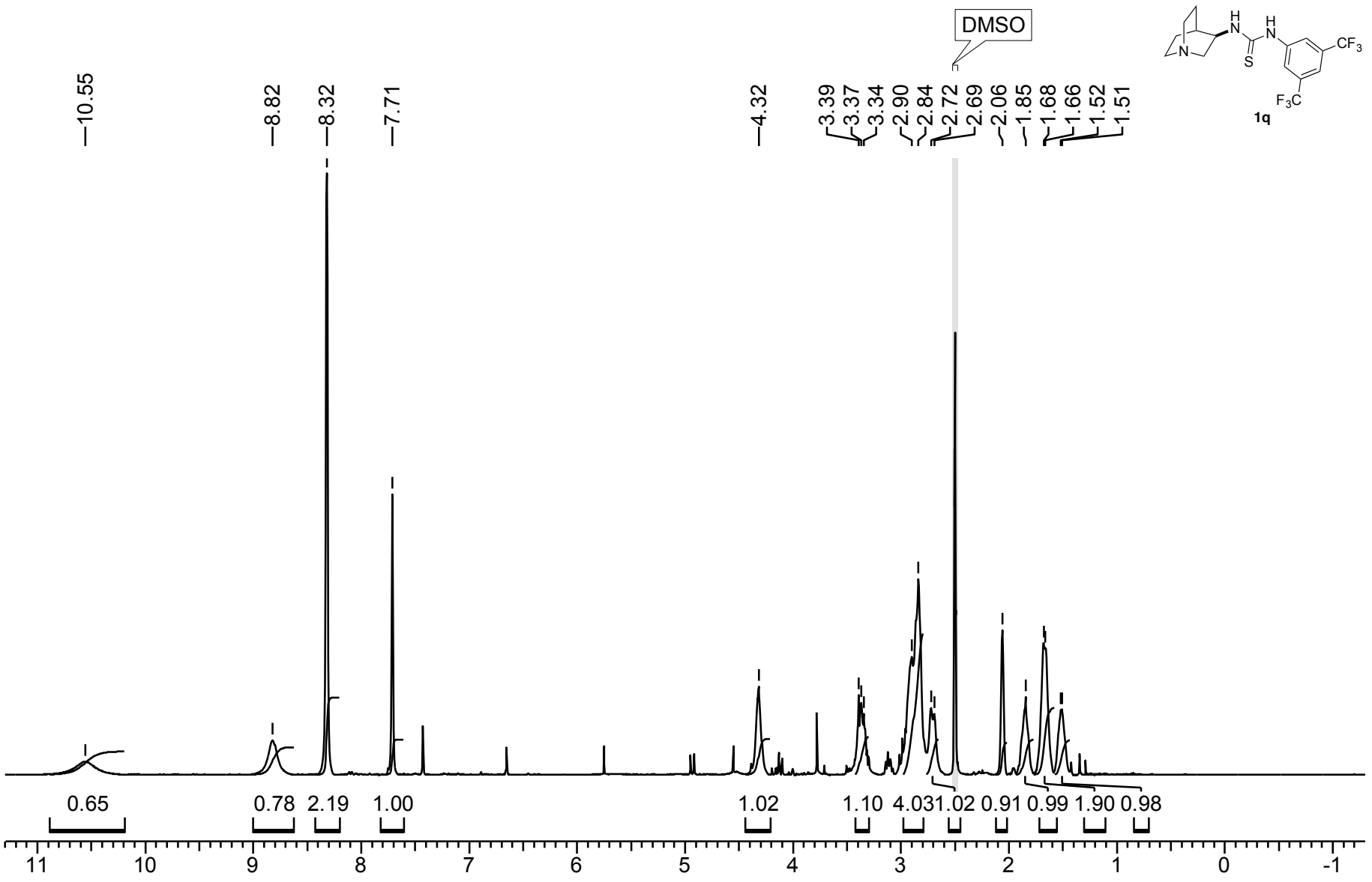

Figure S196. ^{1}H NMR (400 MHz, DMSO-d_6) spectrum of **1q**.

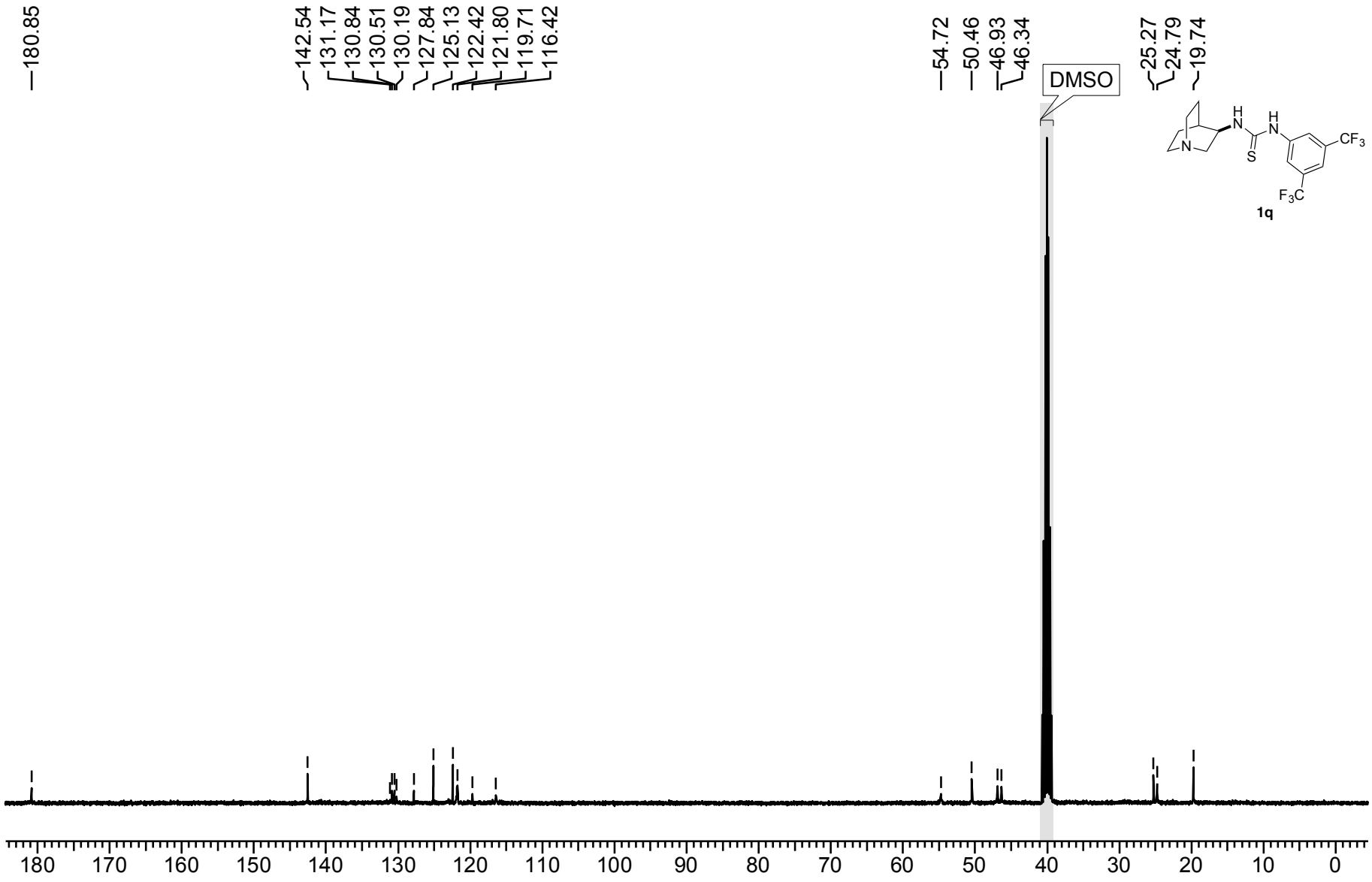

Figure S197. ^{13}C NMR (100 MHz, DMSO-d_6) spectrum of **1q**.

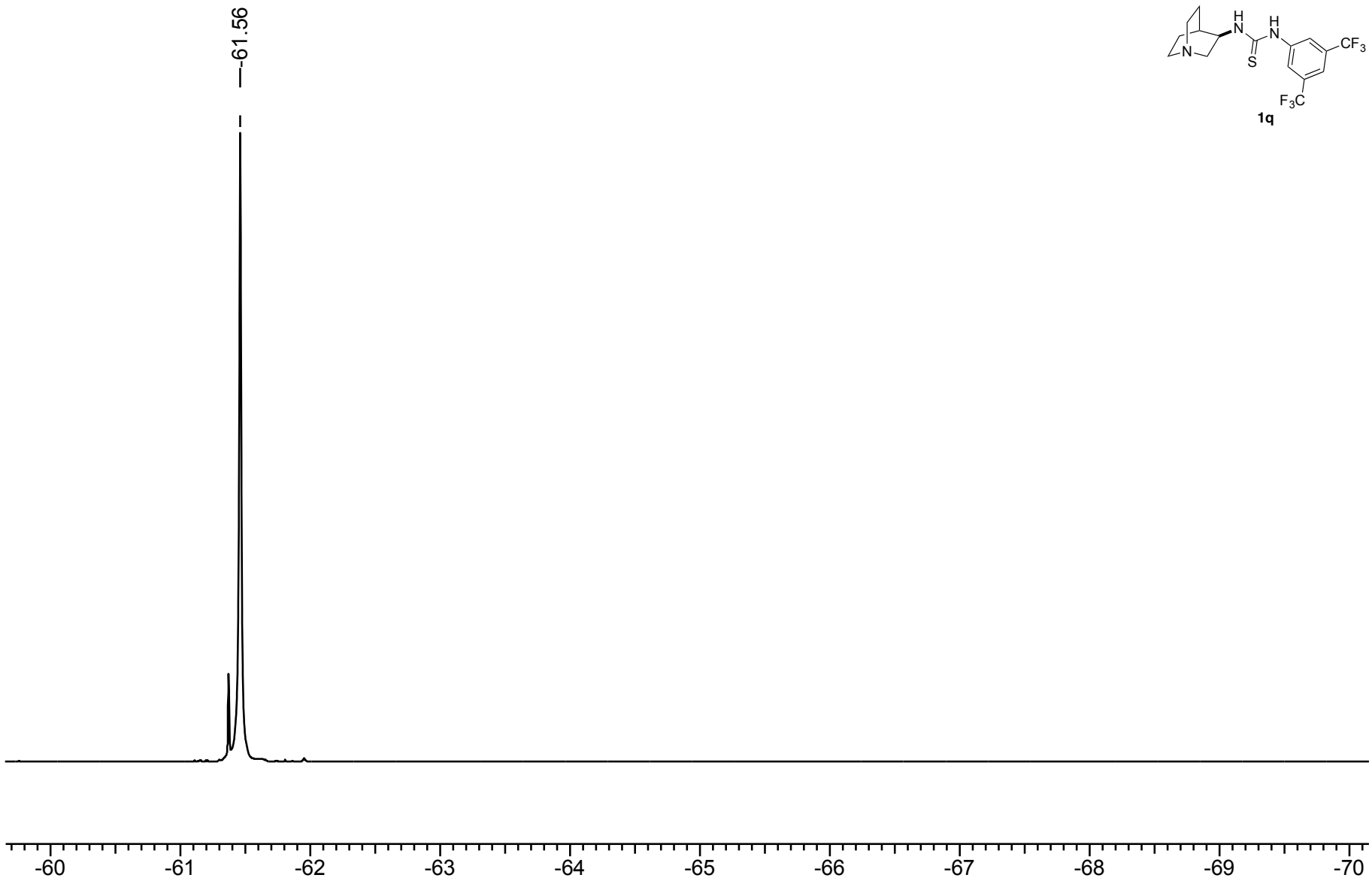

Figure S198. ^{19}F NMR (376 MHz, DMSO-d_6) spectrum of **1q**.

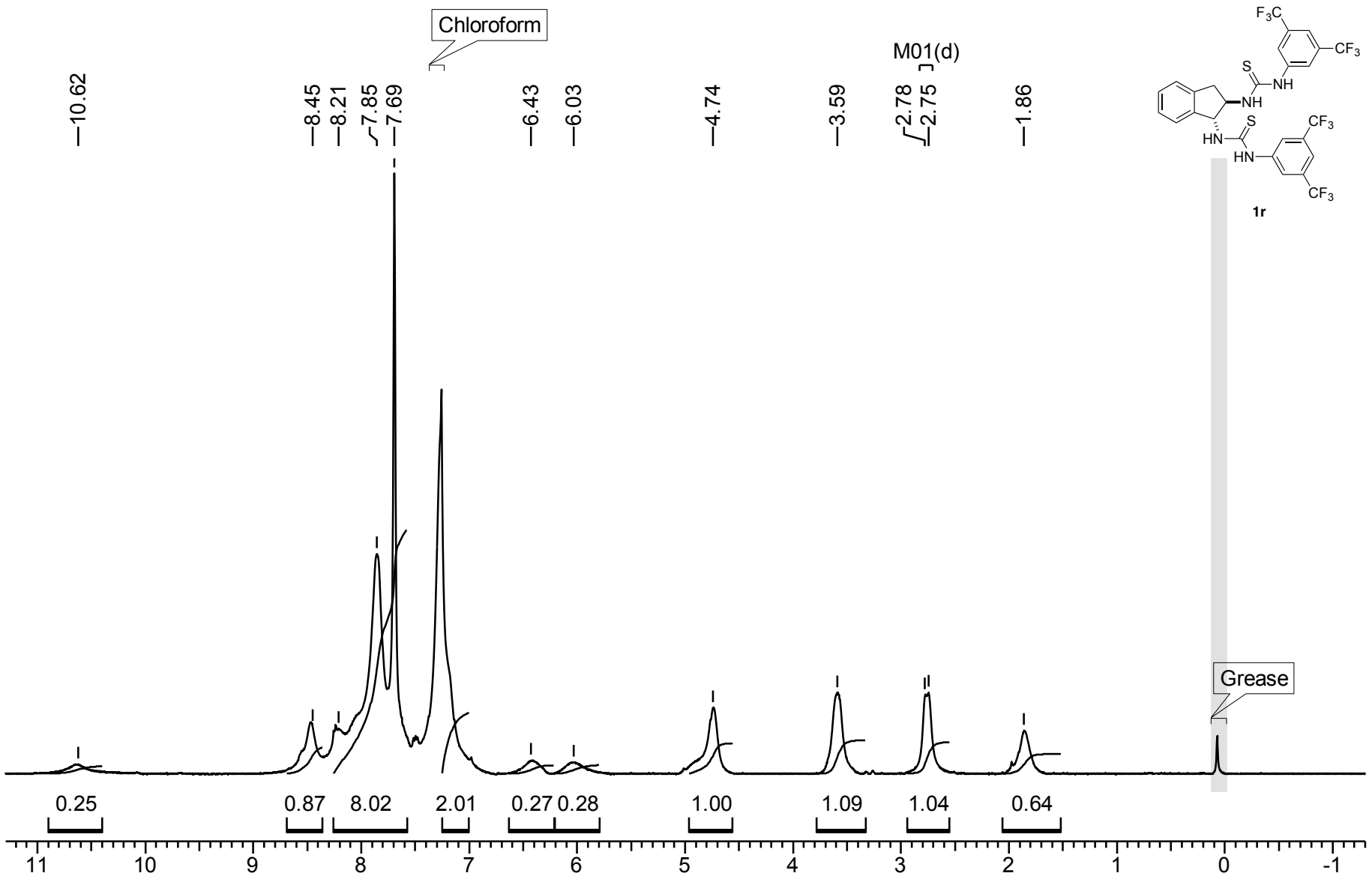

Figure S199. ^{1}H NMR (400 MHz, $CDCl_3$) spectrum of **1r**.

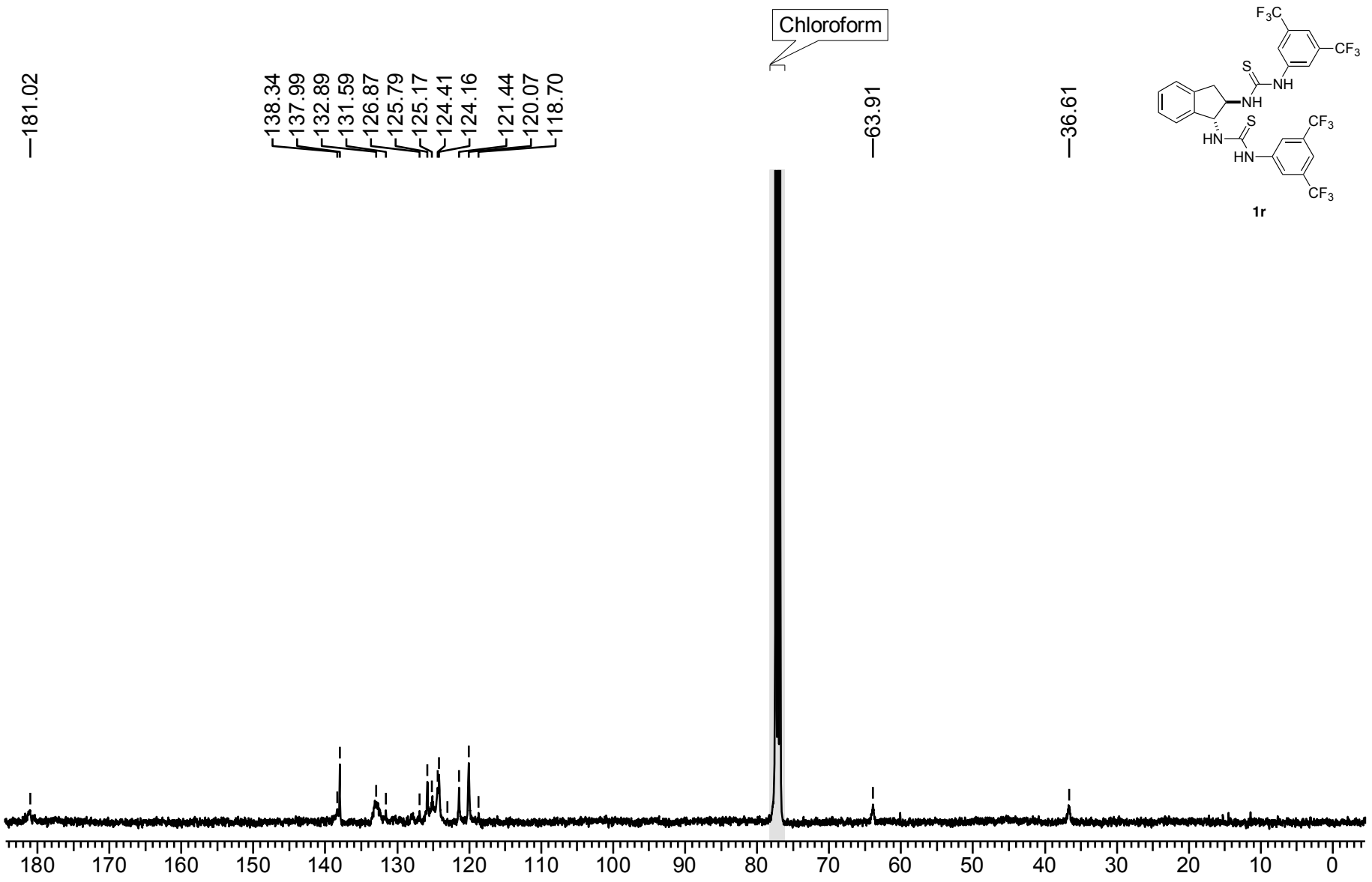

Figure S200. ^{13}C NMR (100 MHz, $CDCl_3$) spectrum of **1r**.

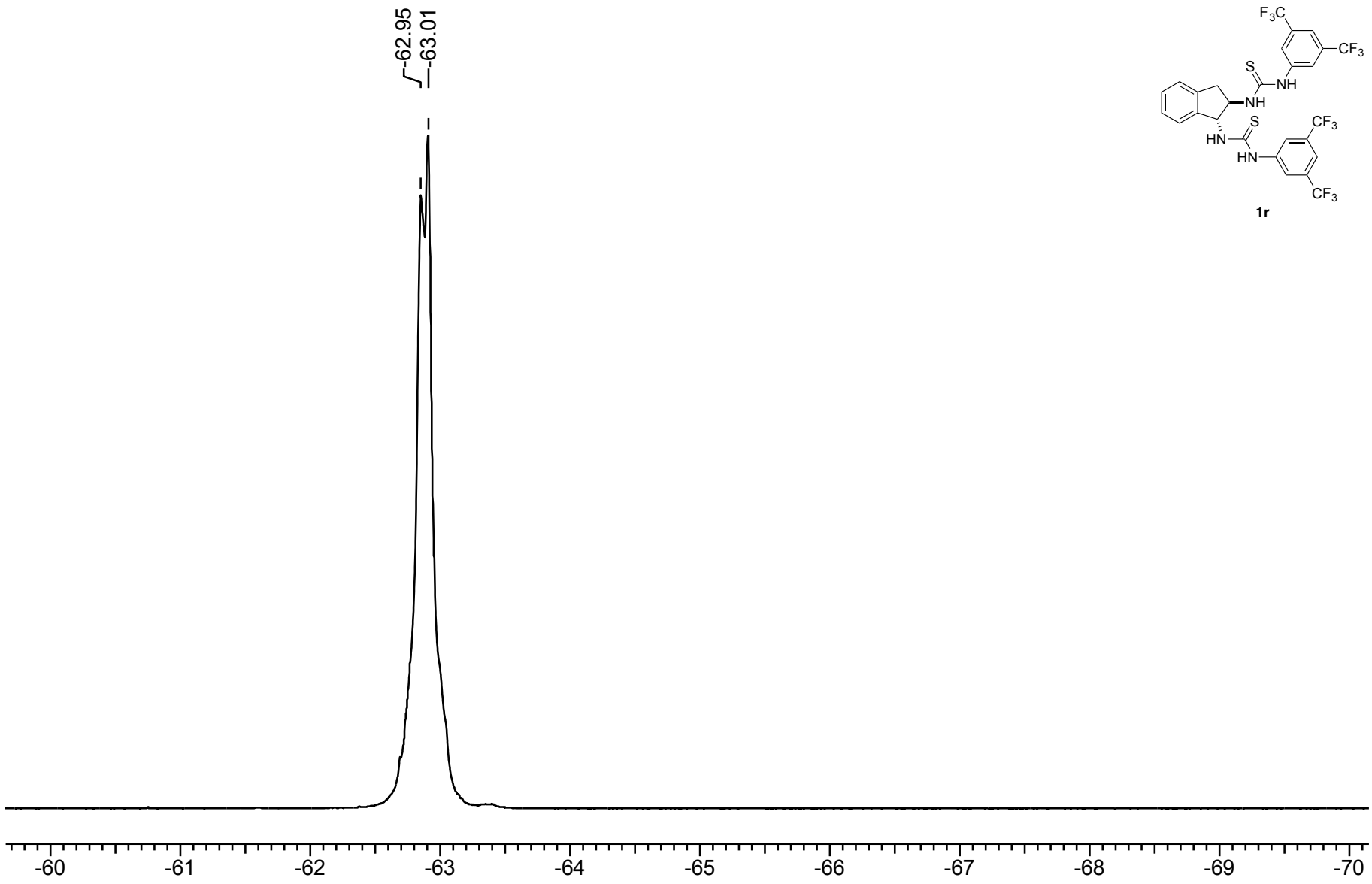

Figure S201. ^{19}F NMR (376 MHz, $CDCl_3$) spectrum of **1r**.

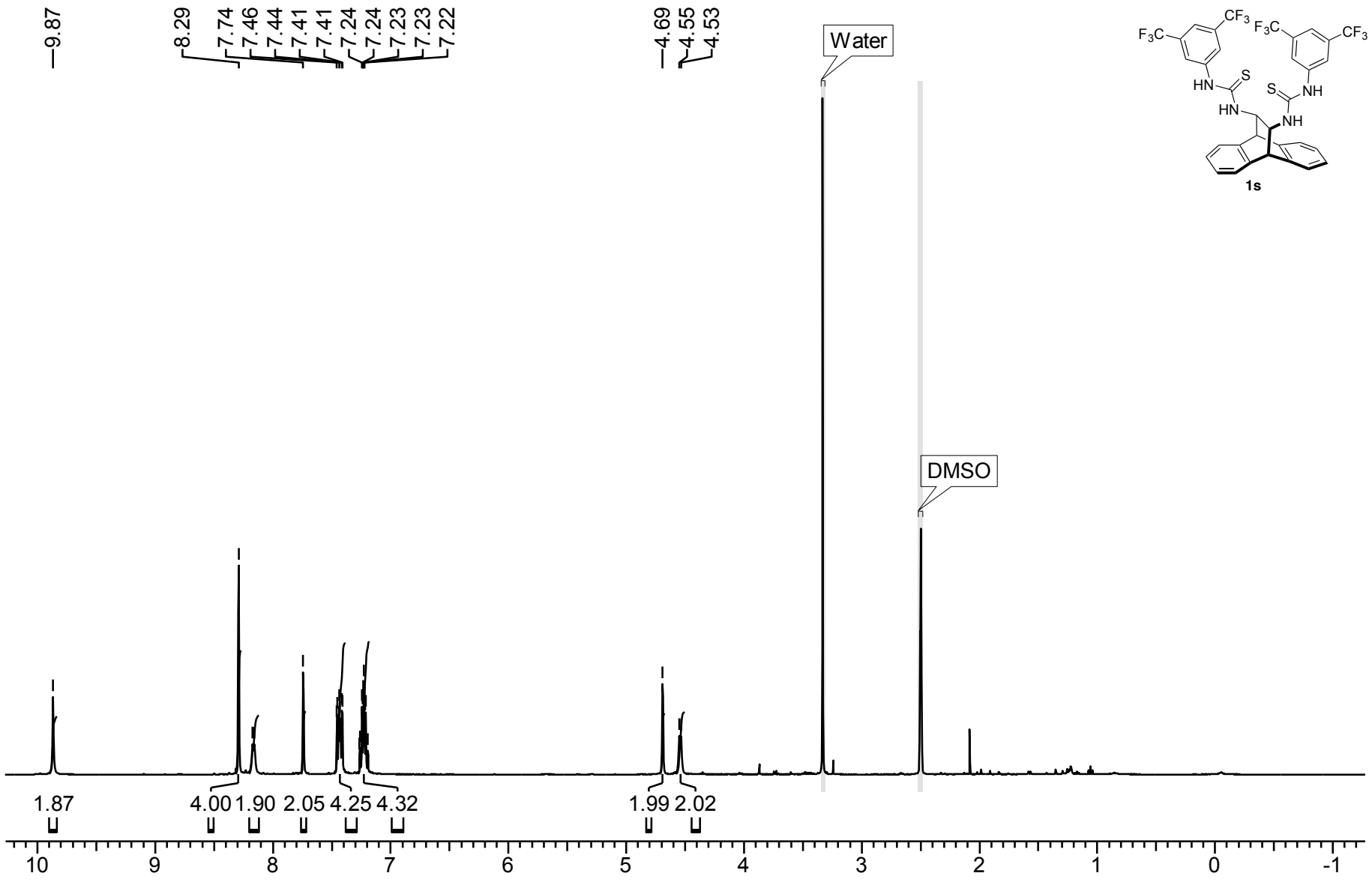

Figure S202. ^{1}H NMR (400 MHz, DMSO-d_6) spectrum of **1s**.

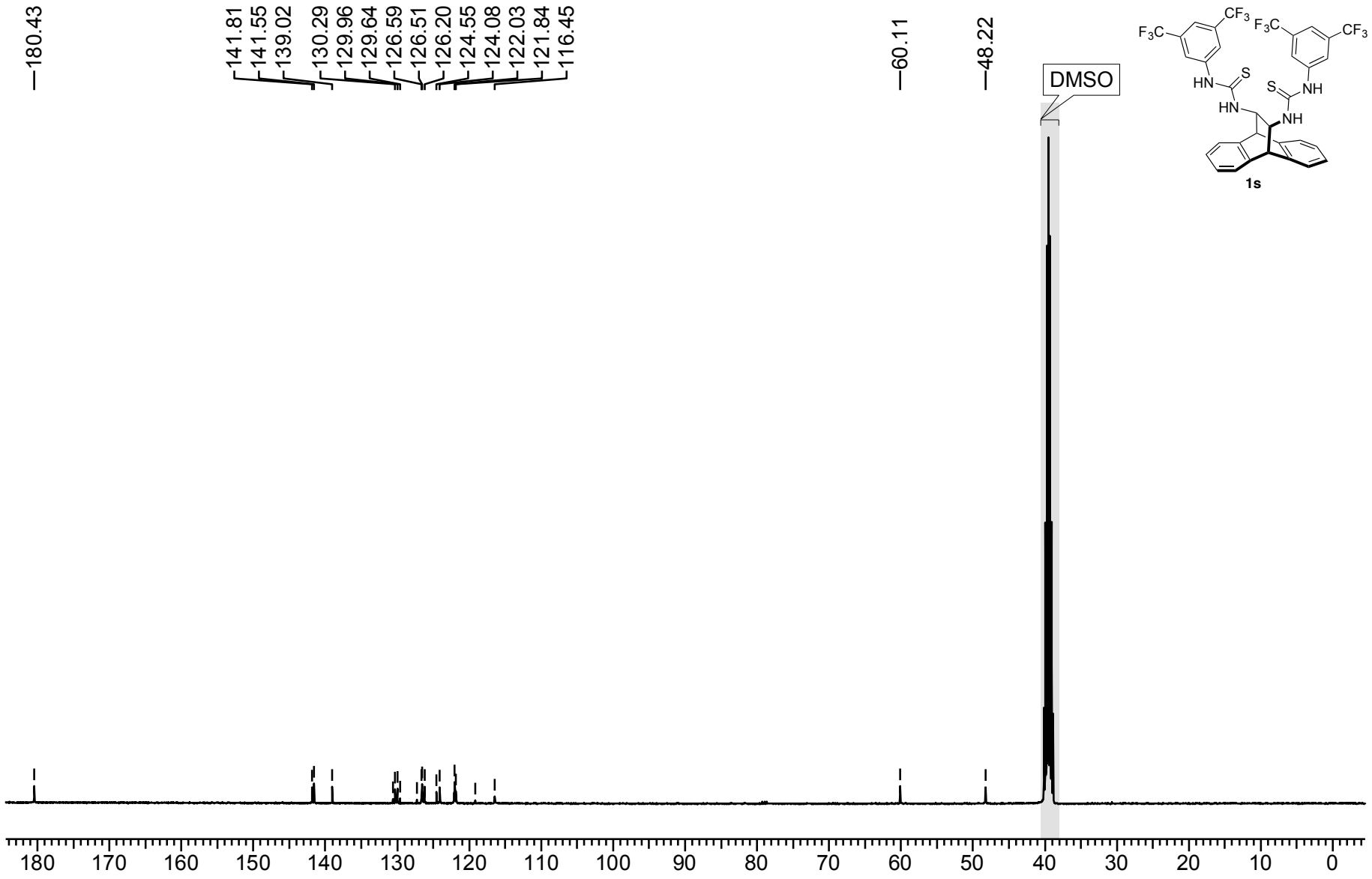

Figure S203. ^{13}C NMR (100 MHz, DMSO-d_6) spectrum of **1s**.

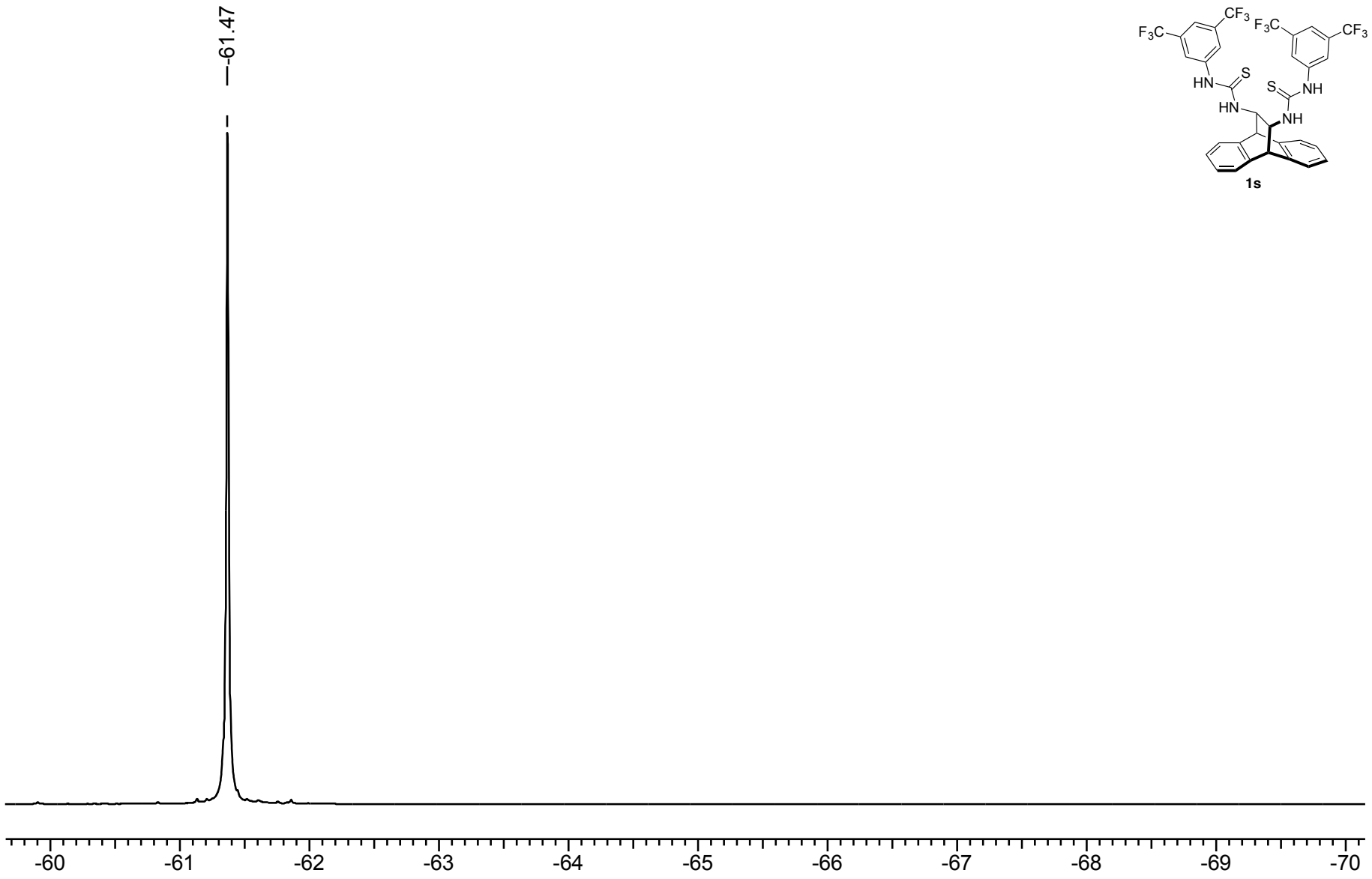

1s

Figure S204. ^{19}F NMR (376 MHz, DMSO-d_6) spectrum of **1s**.

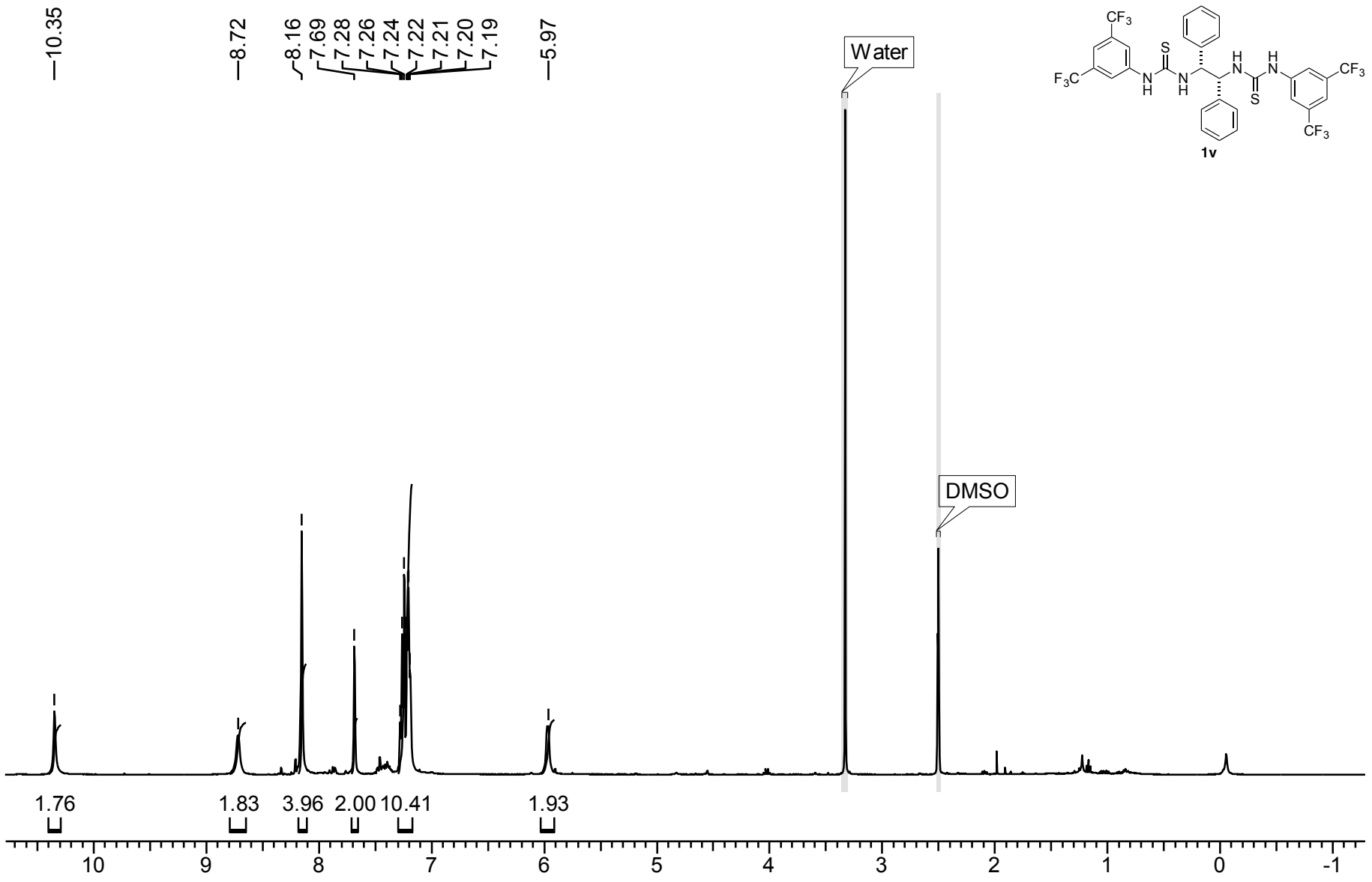

Figure S205. ^{1}H NMR (400 MHz, DMSO-d_6) spectrum of **1v**.

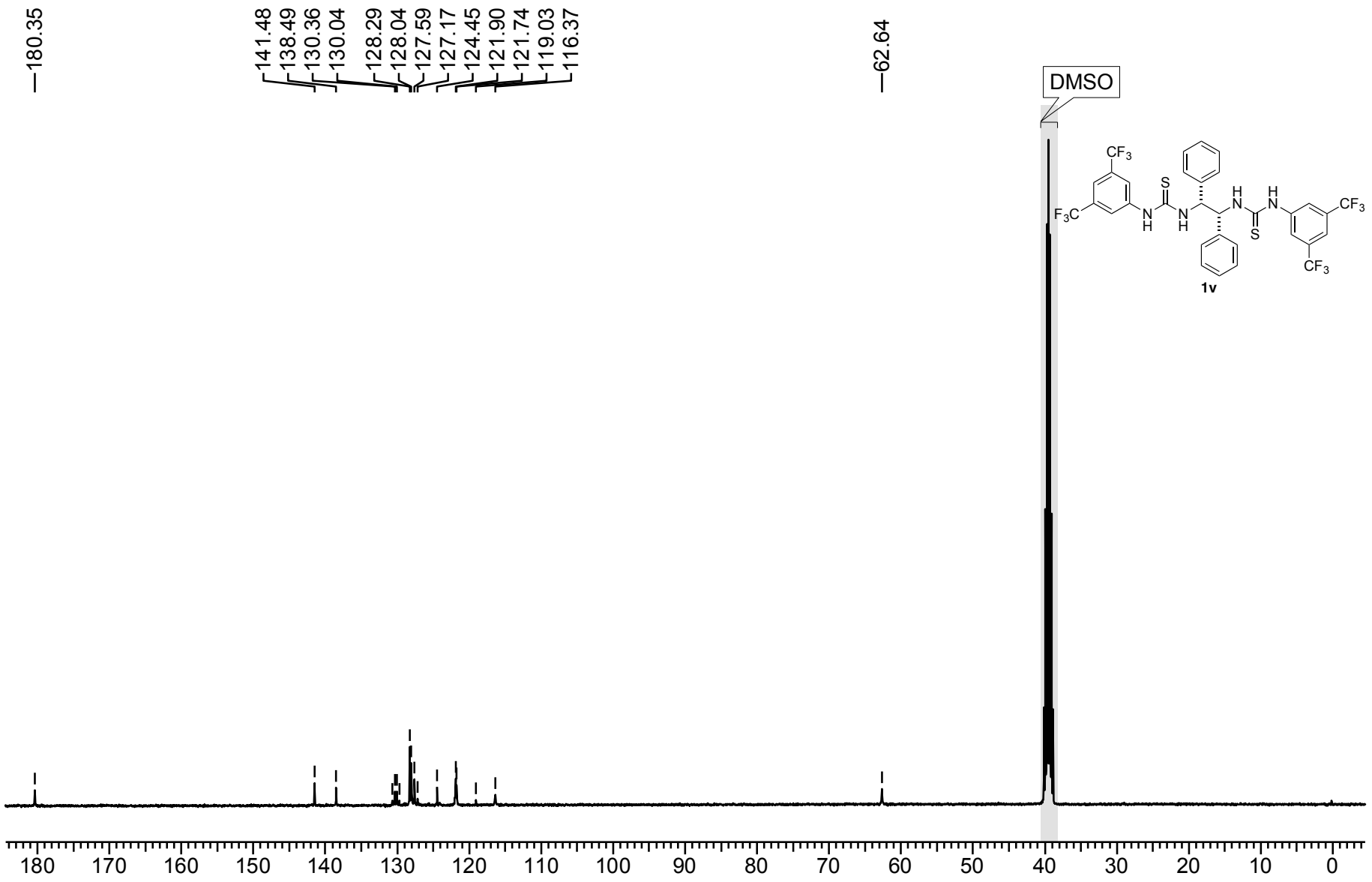

Figure S206. ^{13}C NMR (100 MHz, DMSO-d_6) spectrum of **1v**.

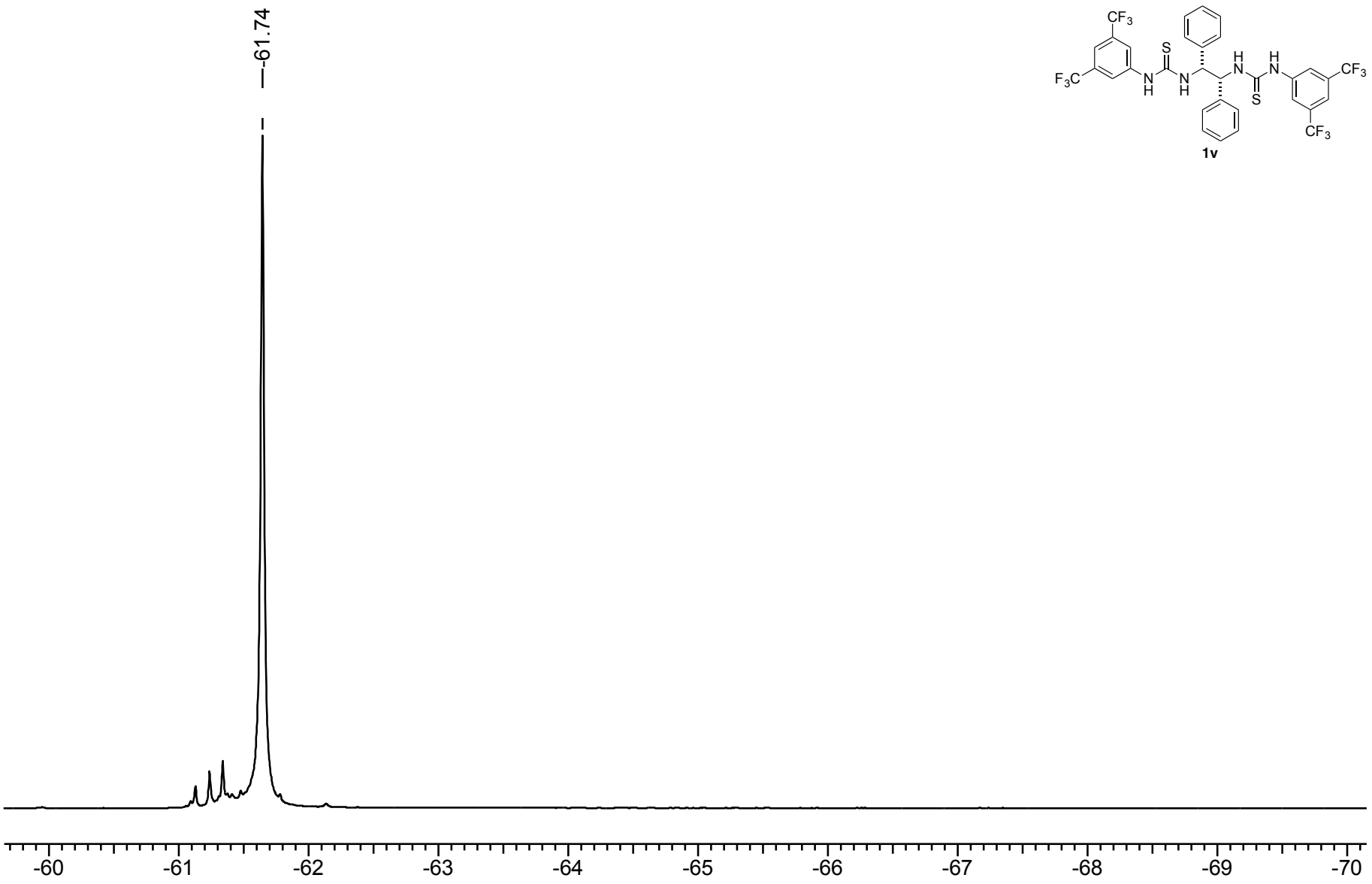

1v

Figure S207. ^{19}F NMR (376 MHz, DMSO-d_6) spectrum of **1v**.

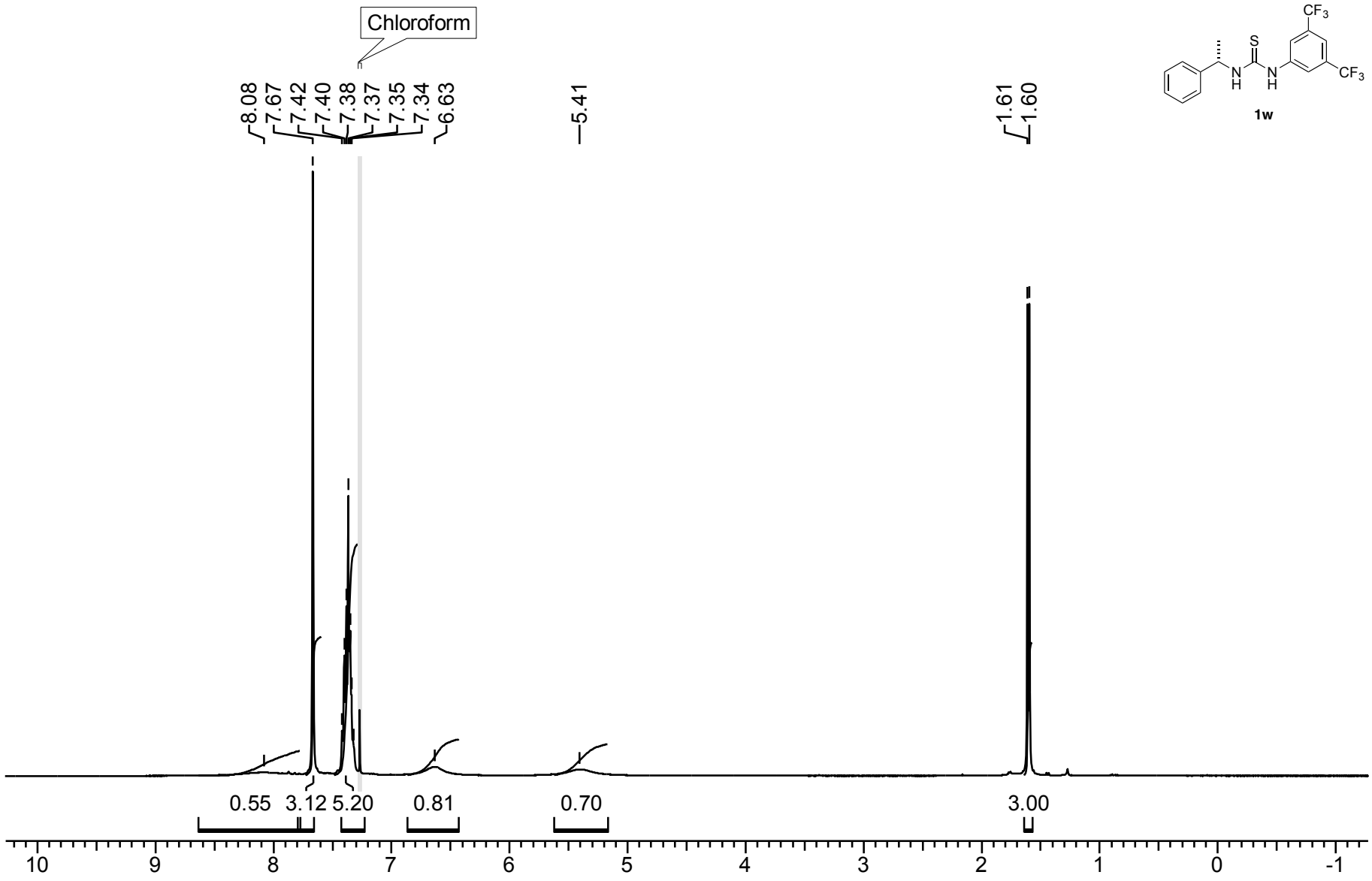

Figure S208. ^{1}H NMR (400 MHz, $CDCl_3$) spectrum of **1w**.

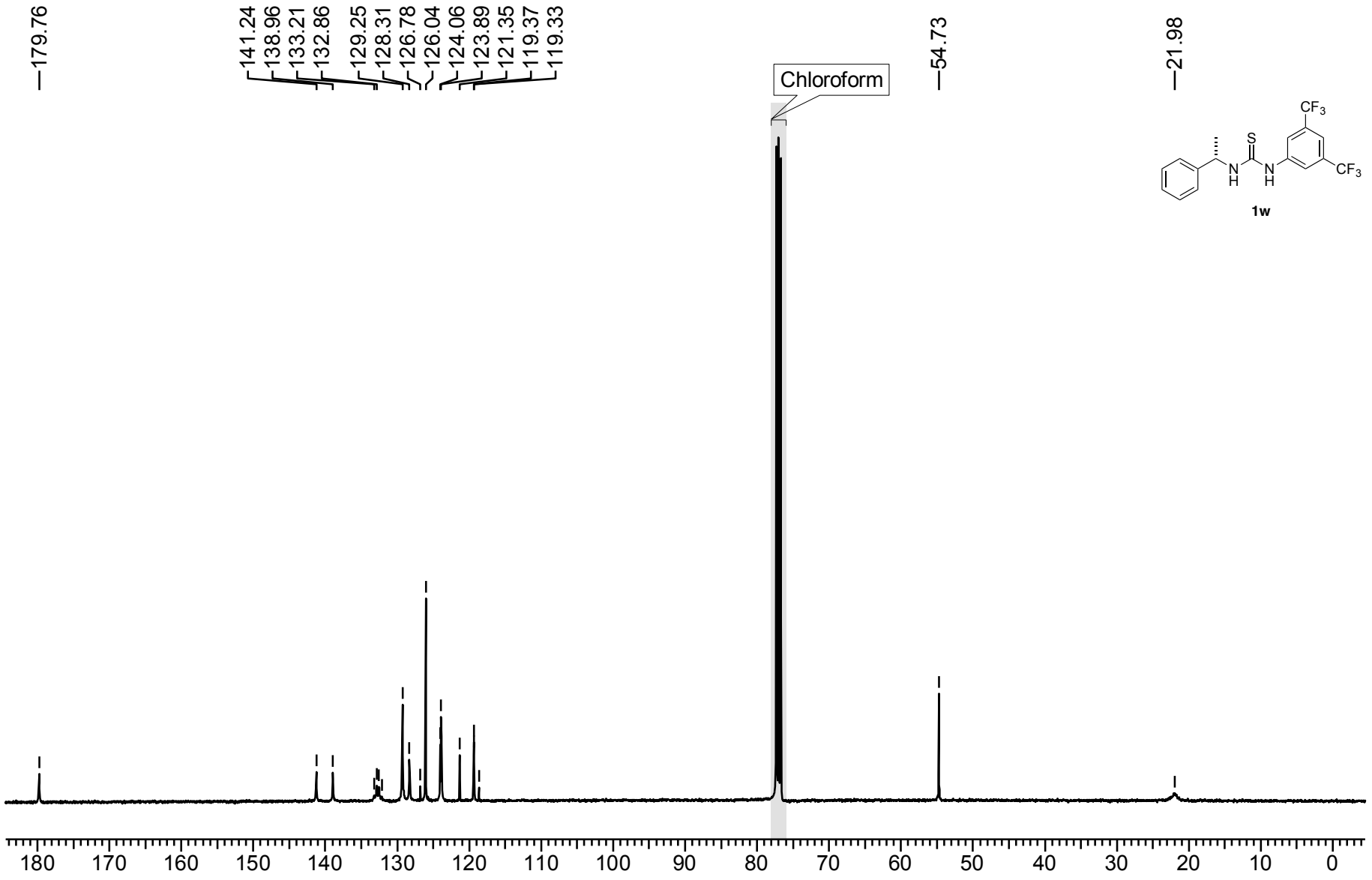

Figure S209. ^{13}C NMR (100 MHz, $CDCl_3$) spectrum of **1w**.

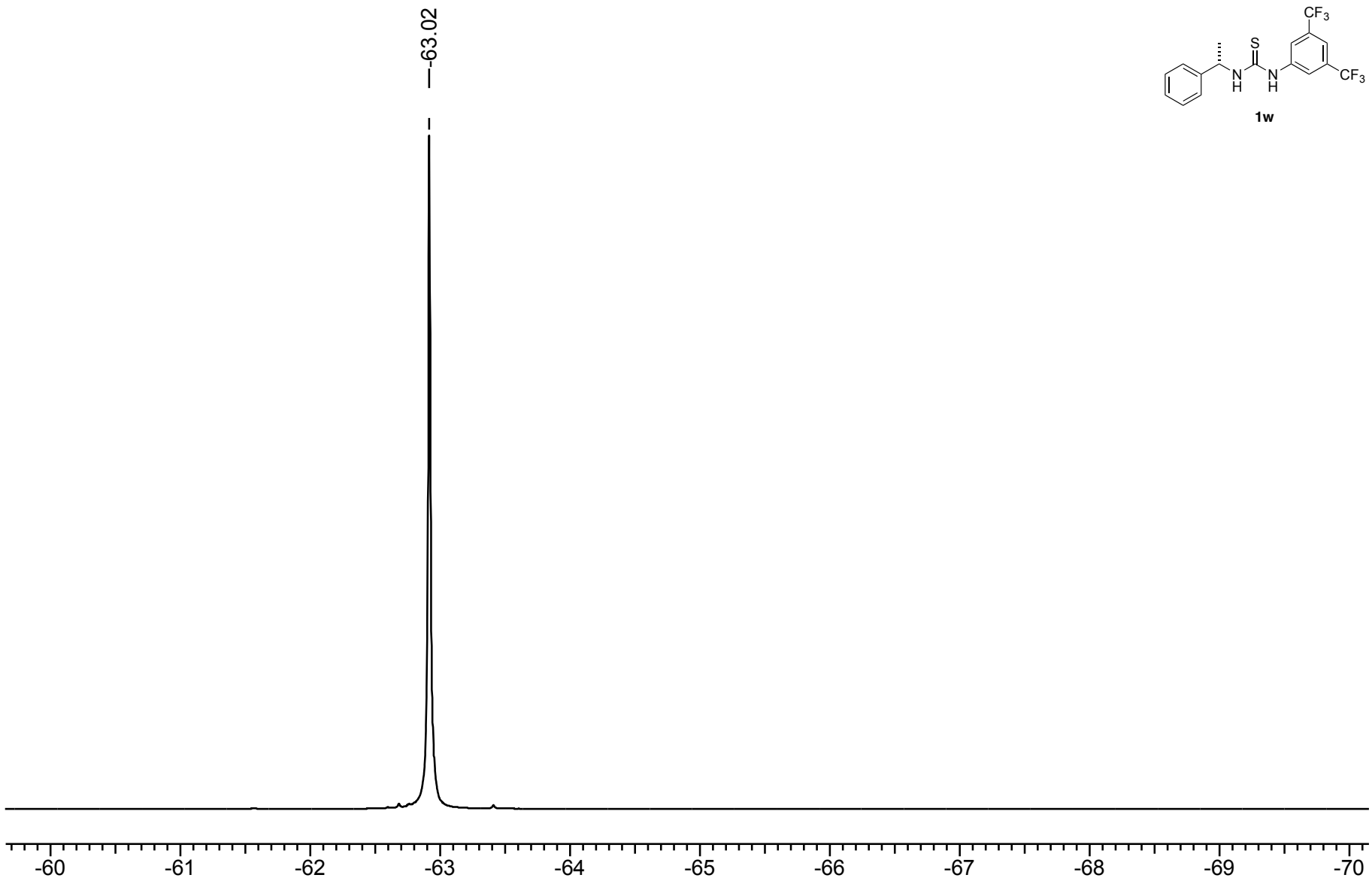

Figure S210. ^{19}F NMR (376 MHz, $CDCl_3$) spectrum of **1w**.

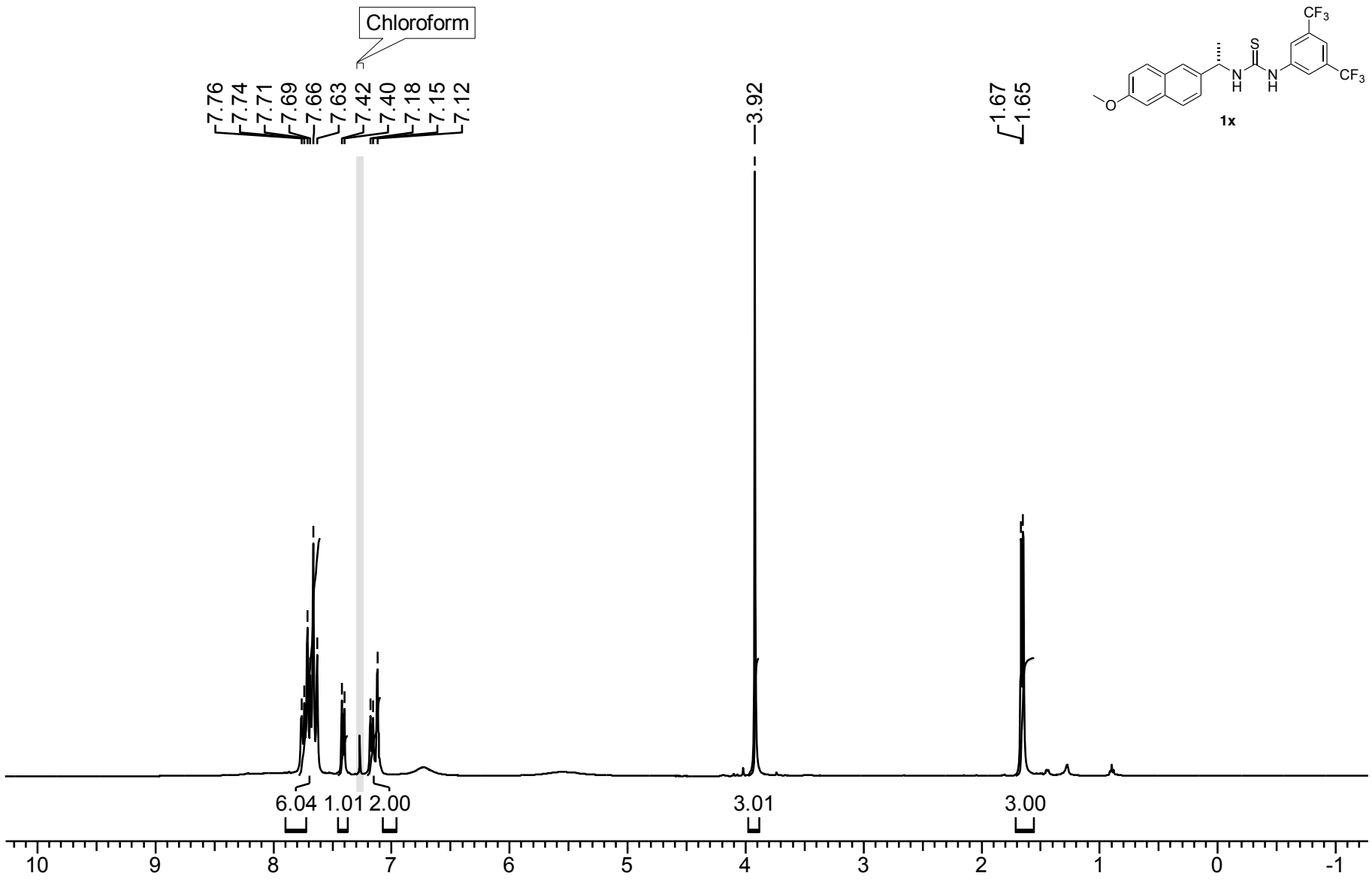

Figure S211. ^{1}H NMR (400 MHz, $CDCl_3$) spectrum of **1x**.

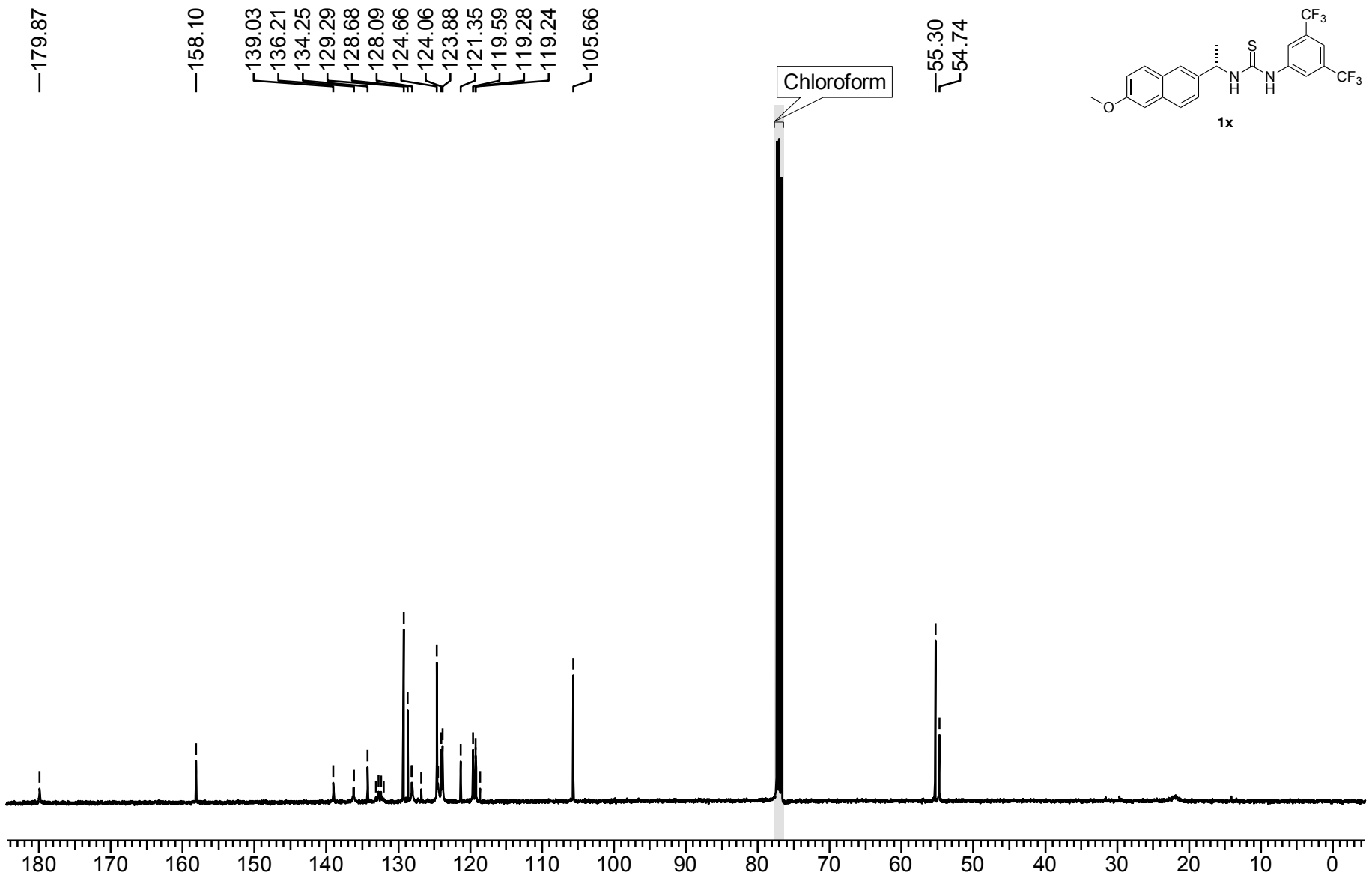

Figure S212. ^{13}C NMR (100 MHz, $CDCl_3$) spectrum of **1x**.

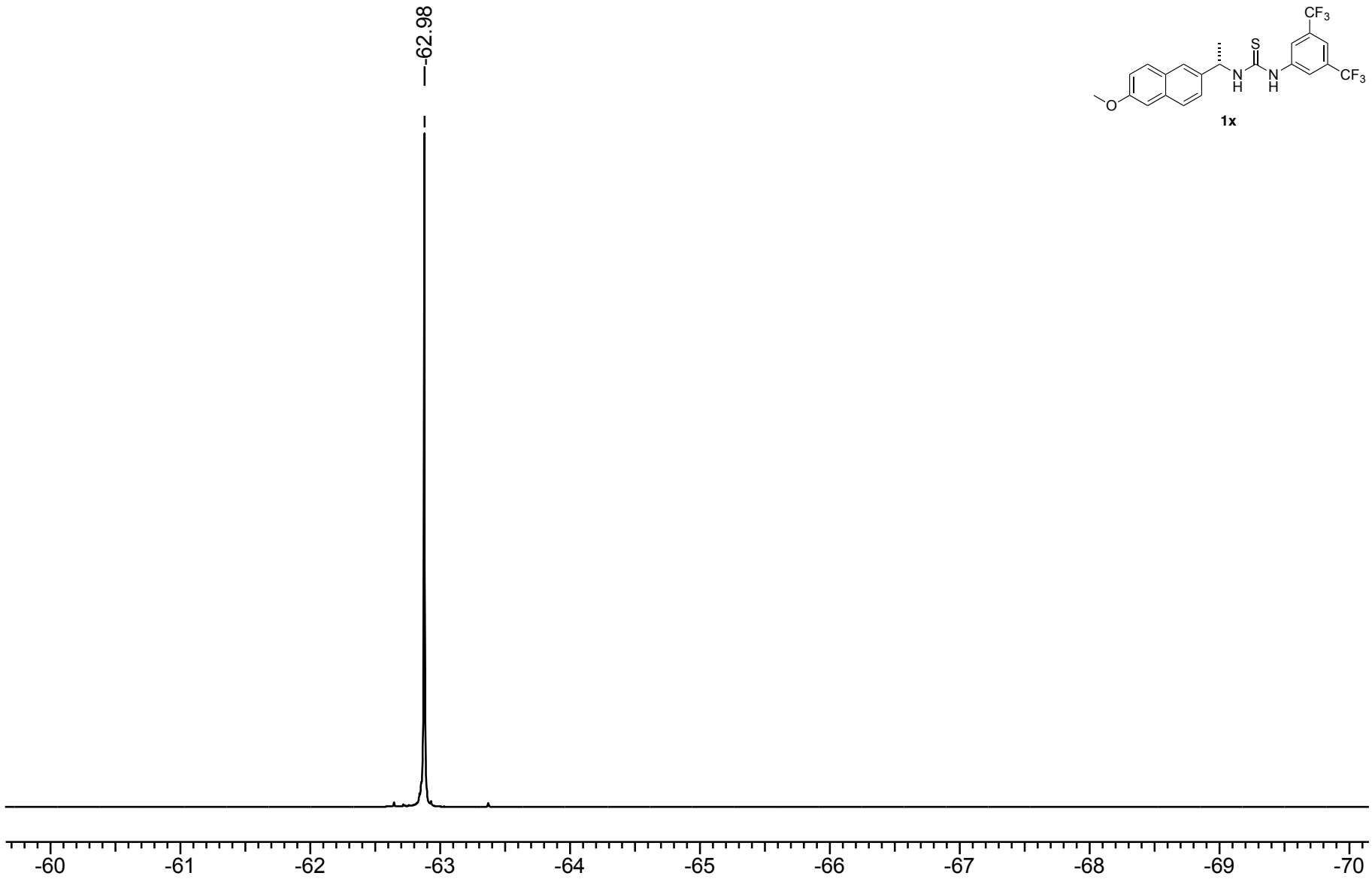

Figure S213. ^{19}F NMR (376 MHz, $CDCl_3$) spectrum of **1x**.

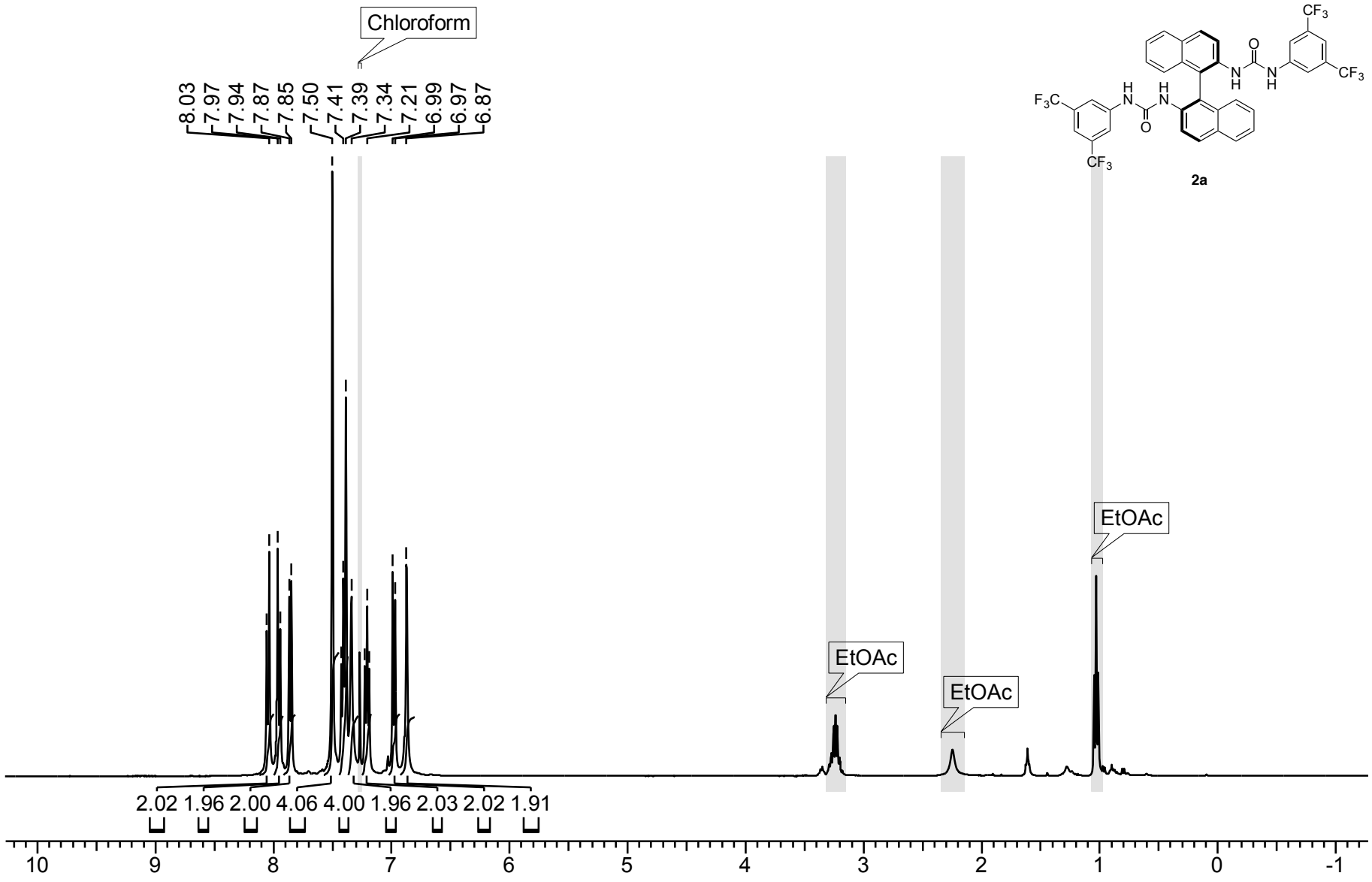

Figure S214. ^{1}H NMR (400 MHz, $CDCl_3$) spectrum of **2a**.

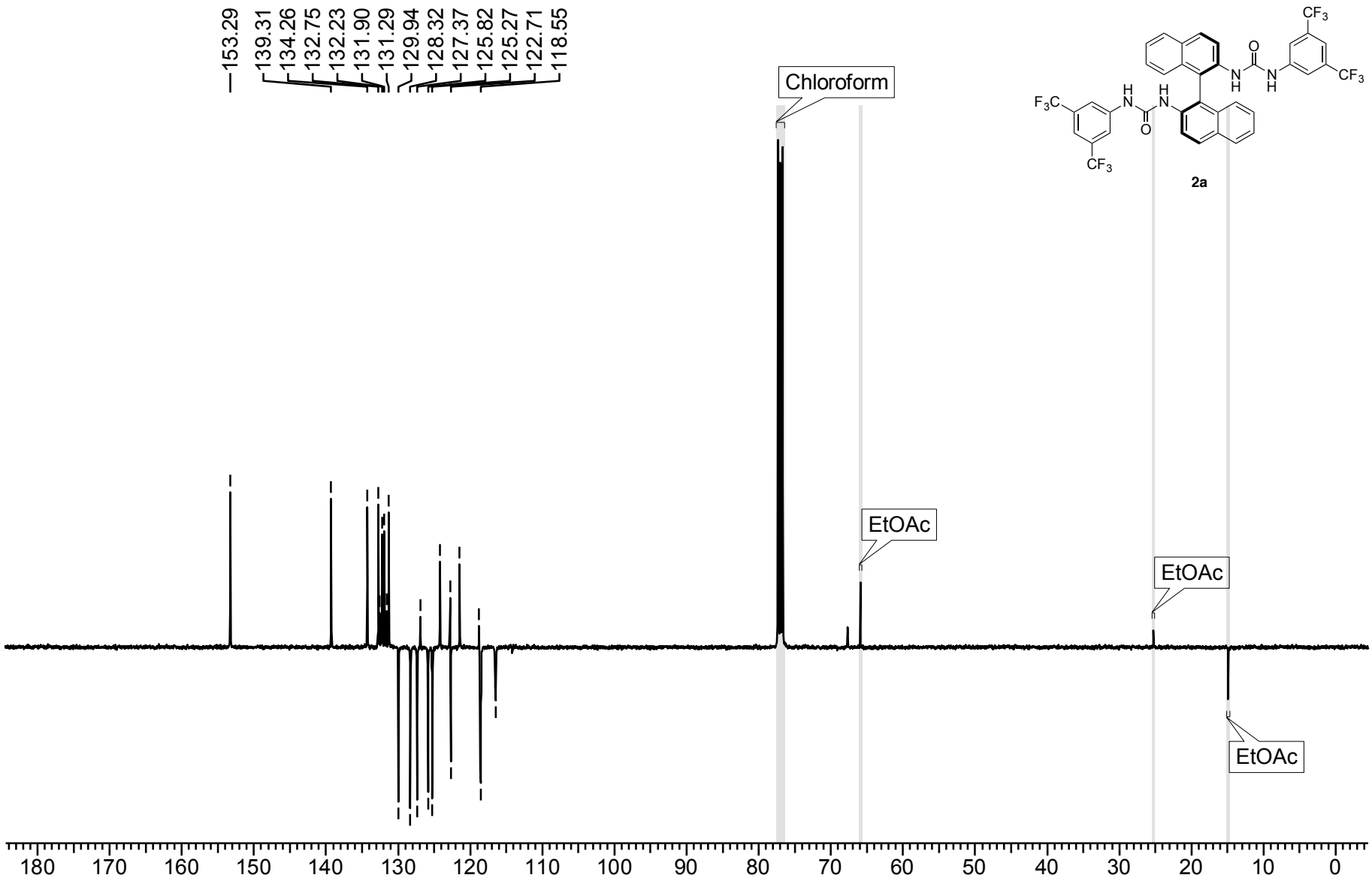

Figure S215. ^{13}C NMR APT (100 MHz, $CDCl_3$) spectrum of **2a**.

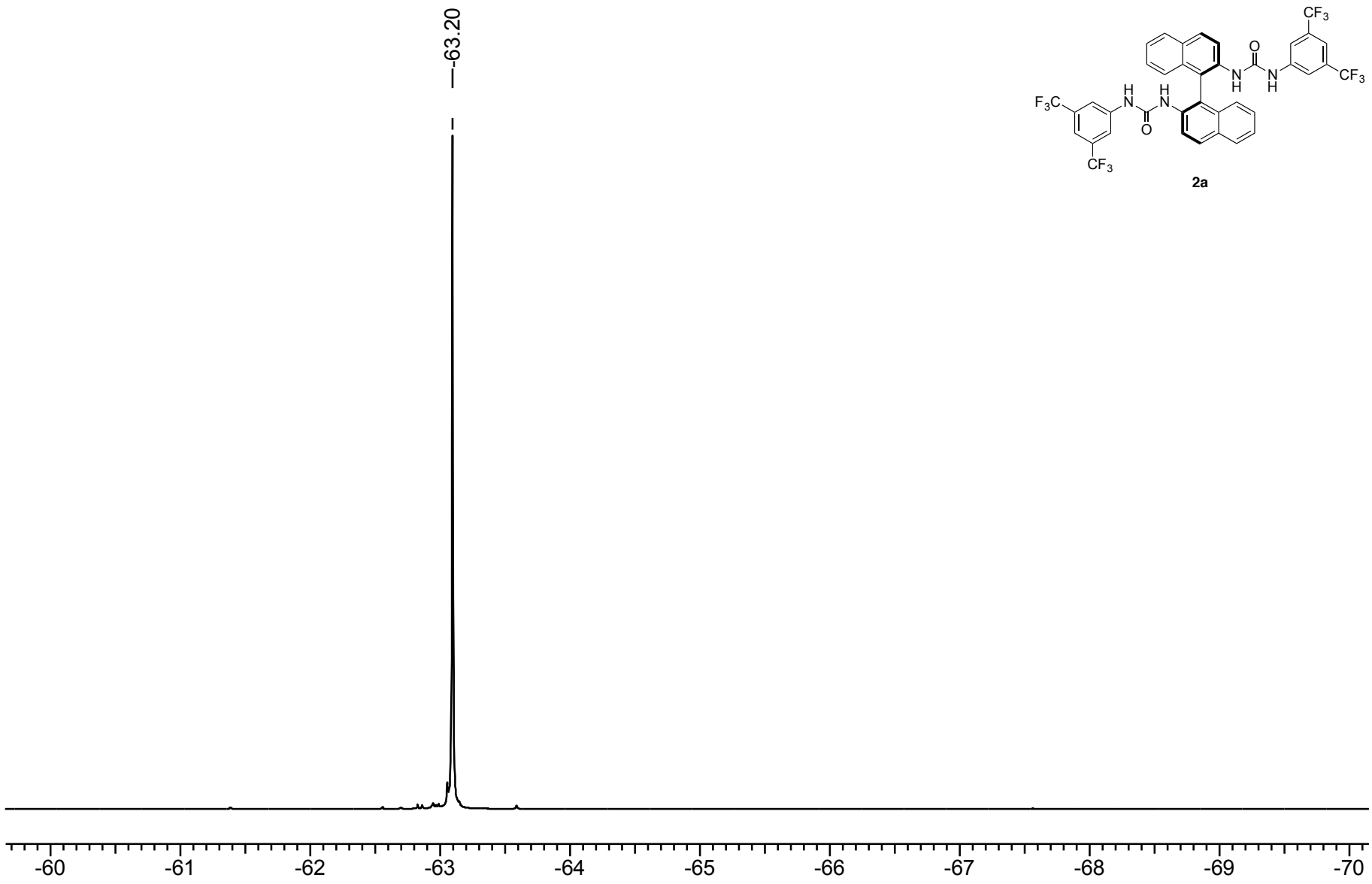

2a

Figure S216. ^{19}F NMR (376 MHz, $CDCl_3$) spectrum of **2a**.

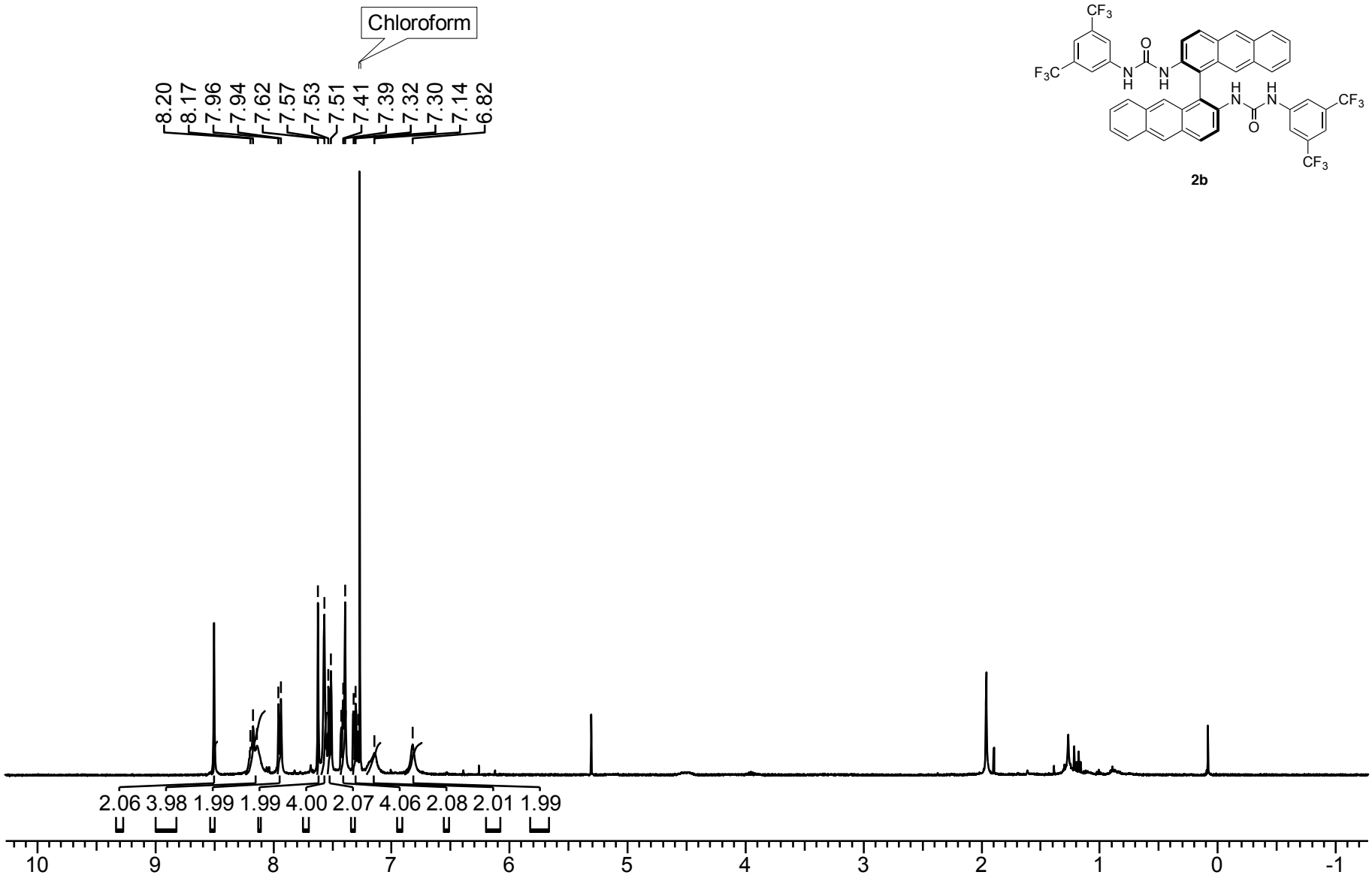

Figure S217. ^{1}H NMR (400 MHz, $CDCl_3$) spectrum of **2b**.

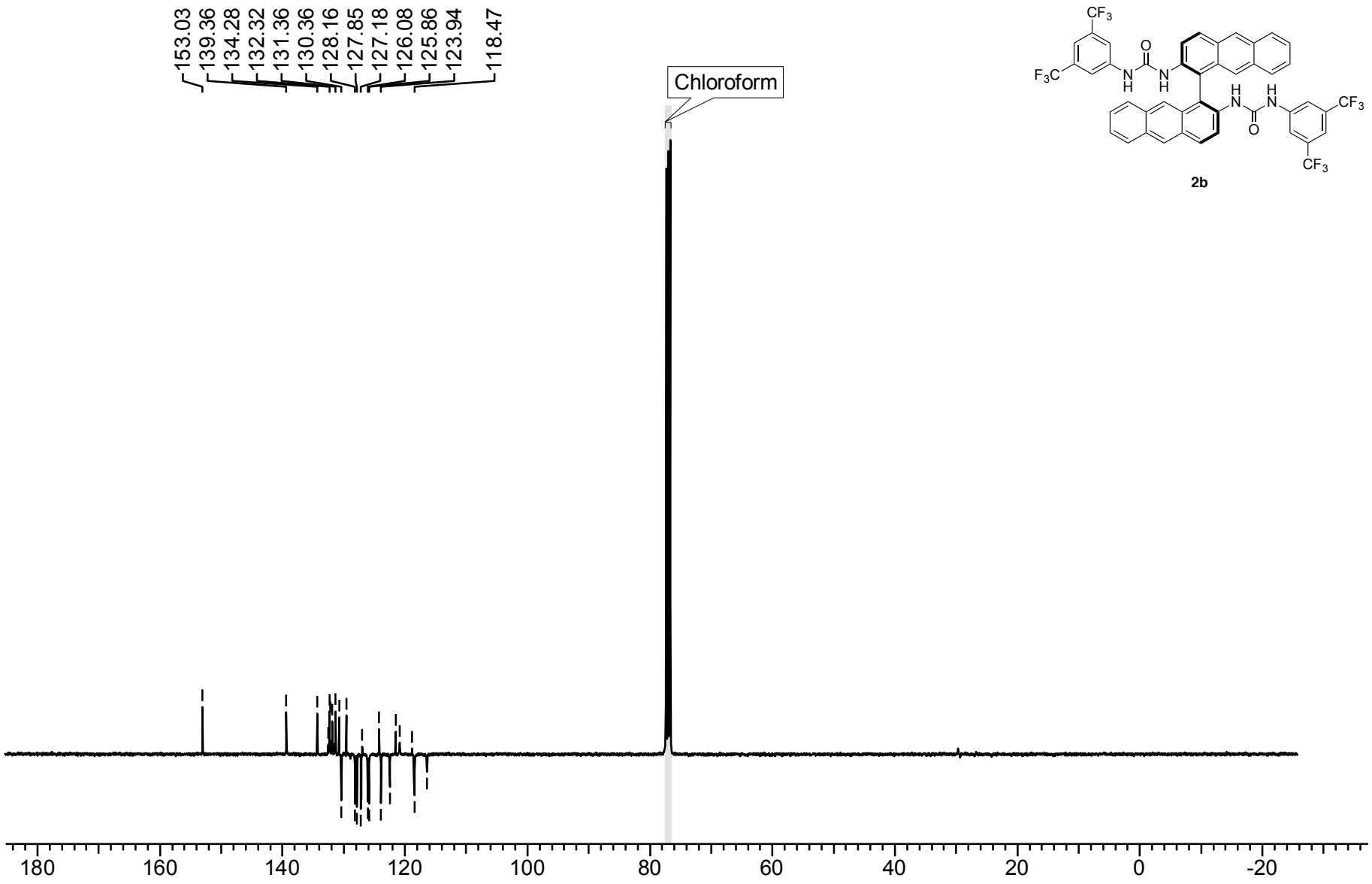

Figure S218. ^{13}C NMR APT (100 MHz, $CDCl_3$) spectrum of **2b**.

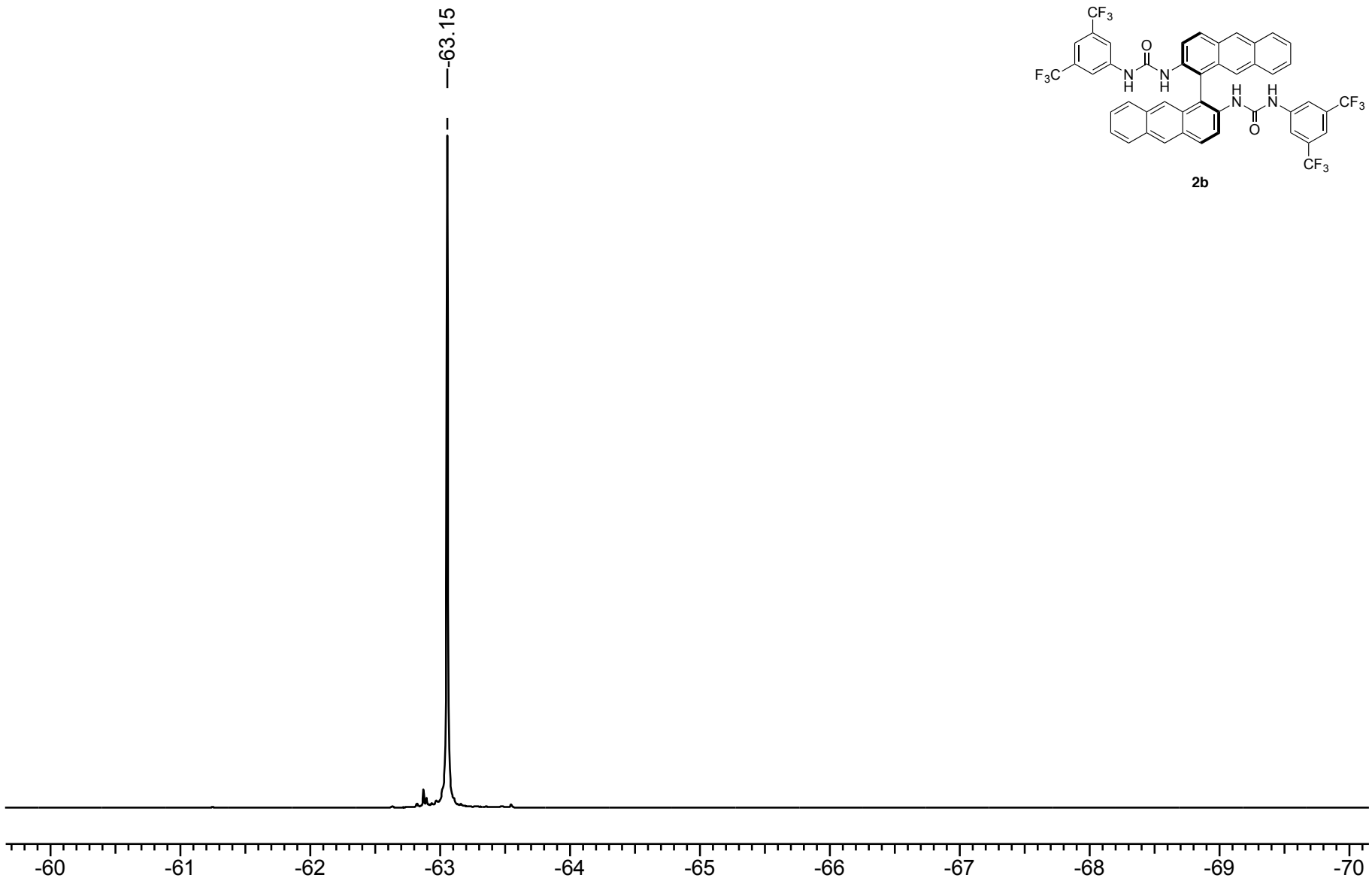

2b

Figure S219. ^{19}F NMR (376 MHz, $CDCl_3$) spectrum of **2b**.

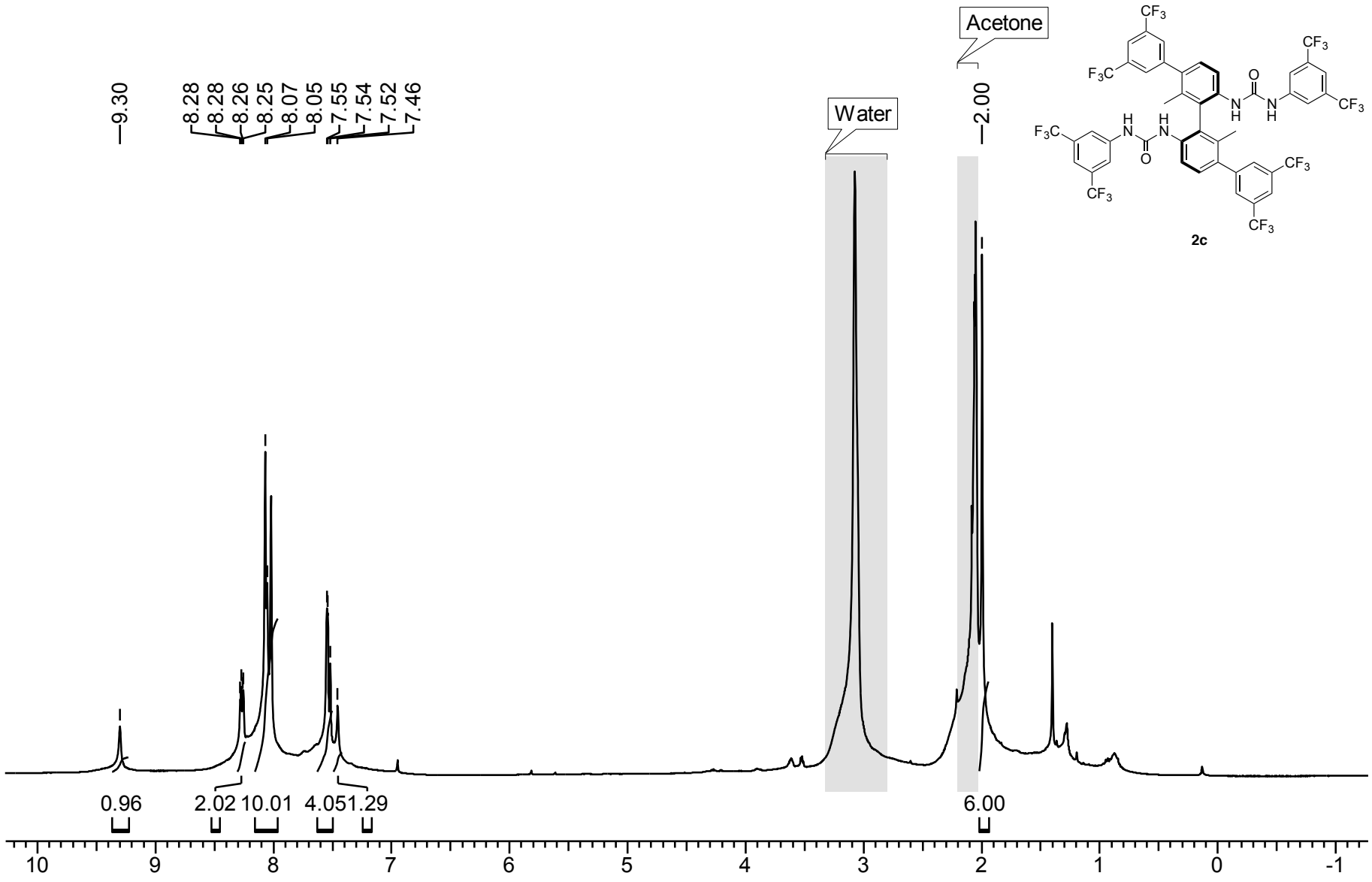

Figure S220. ^{1}H NMR (400 MHz, acetone-d_6) spectrum of **2c**.

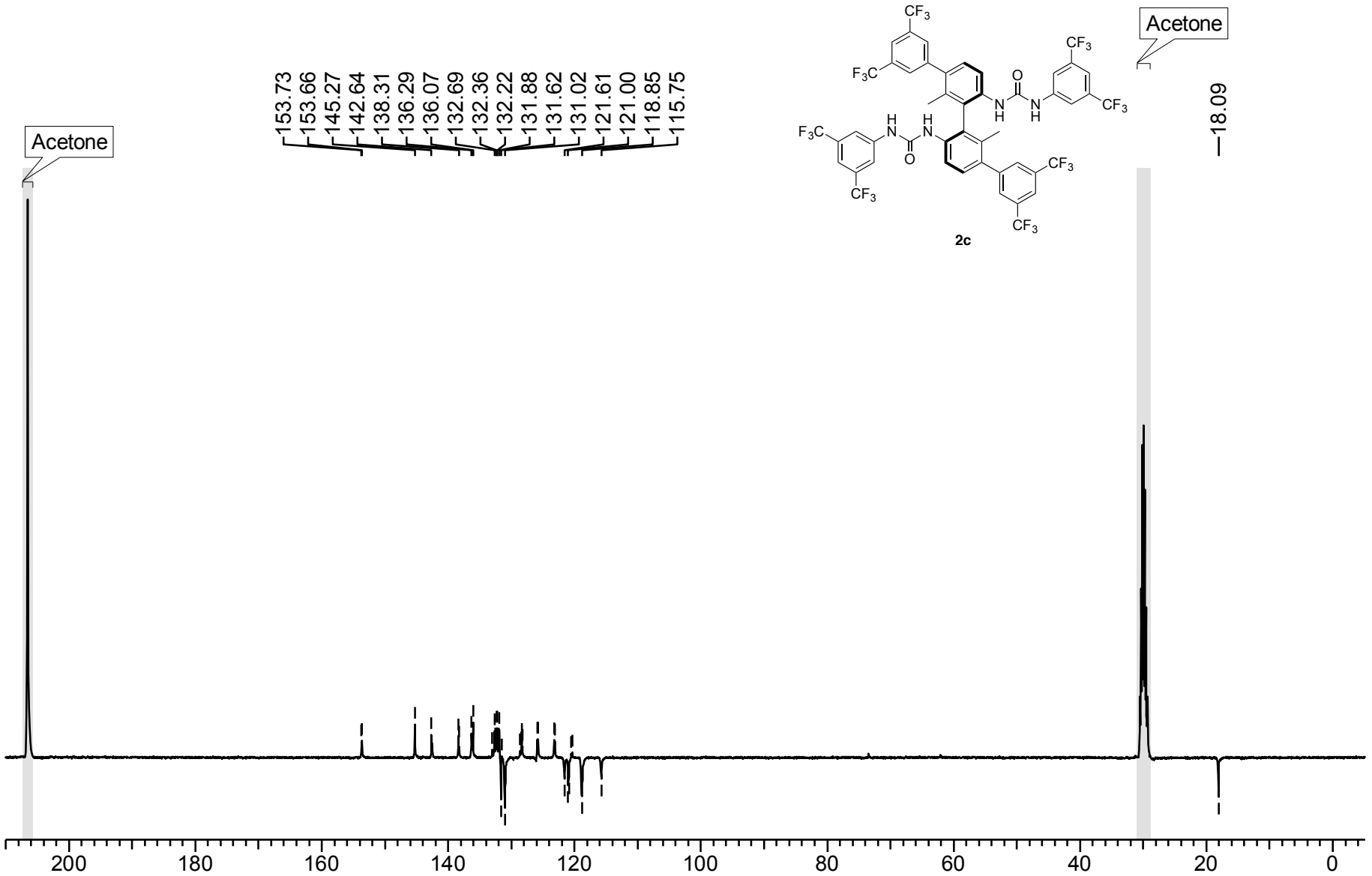

Figure S221. ^{13}C NMR APT (100 MHz, acetone-d_6) spectrum of **2c**.

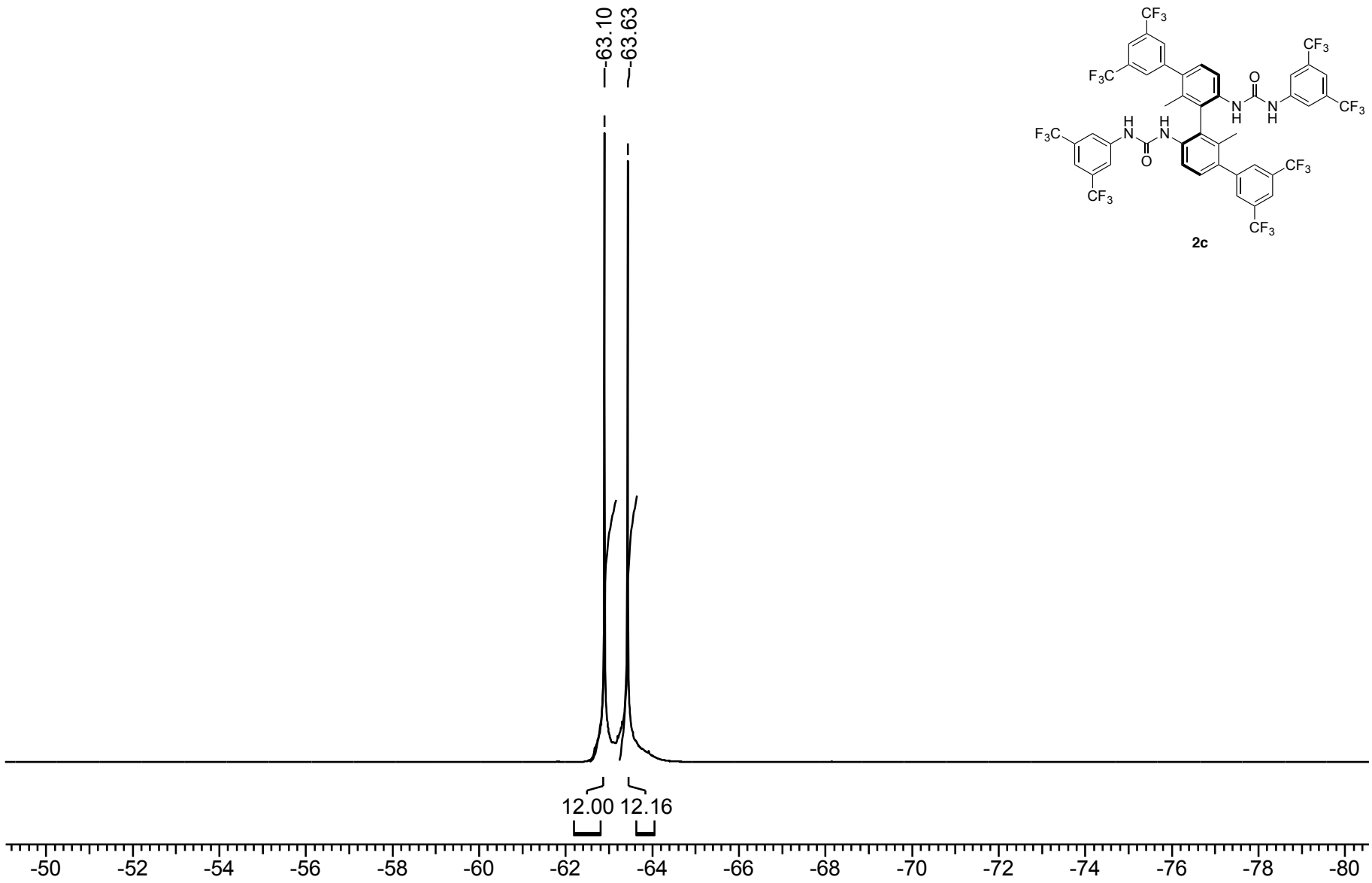

Figure S222. ^{19}F NMR (376 MHz, acetone-d_6) spectrum of **2c**.

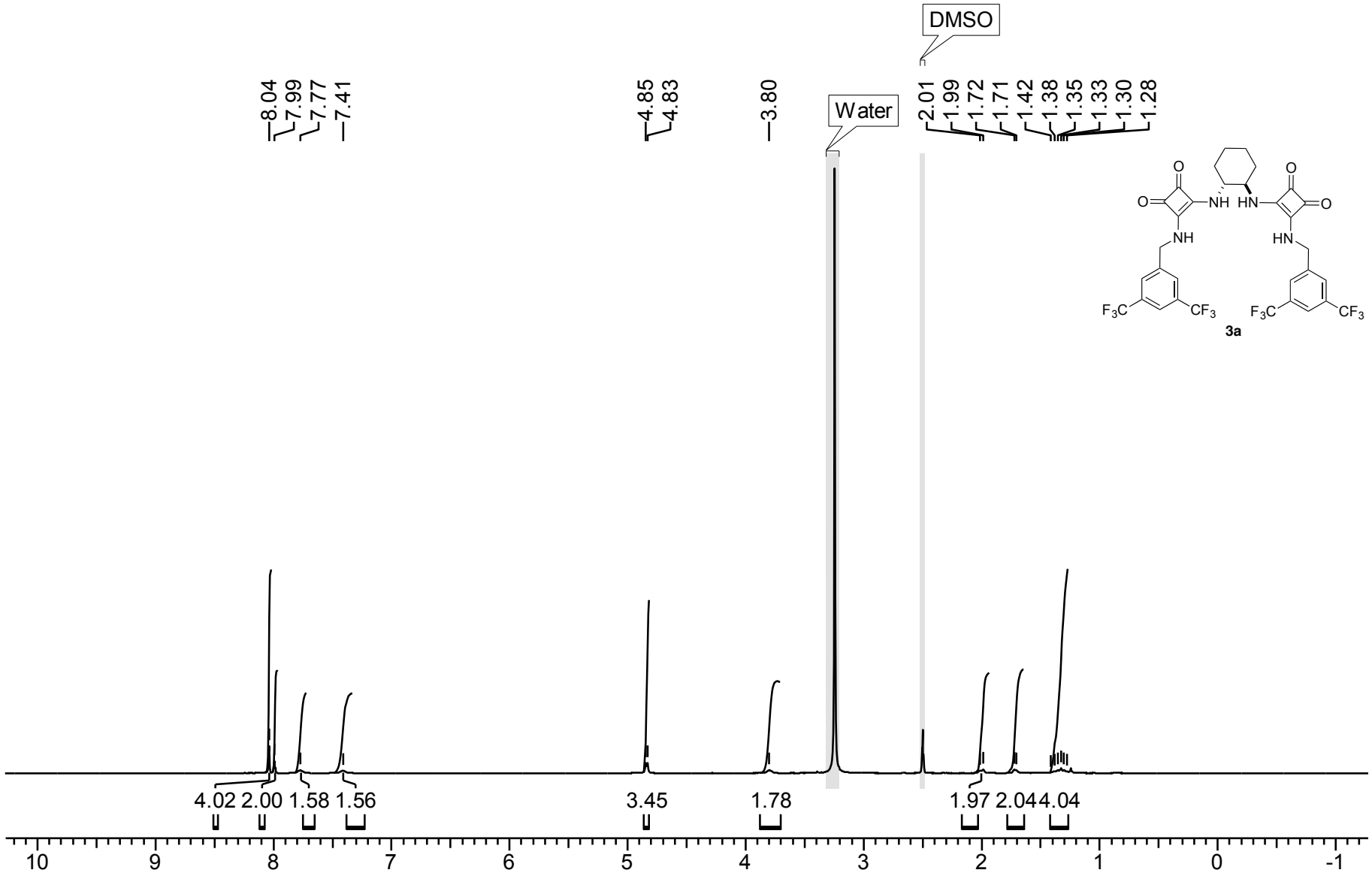

Figure S223. ^{1}H NMR (400 MHz, DMSO-d_6) spectrum of **3a**.

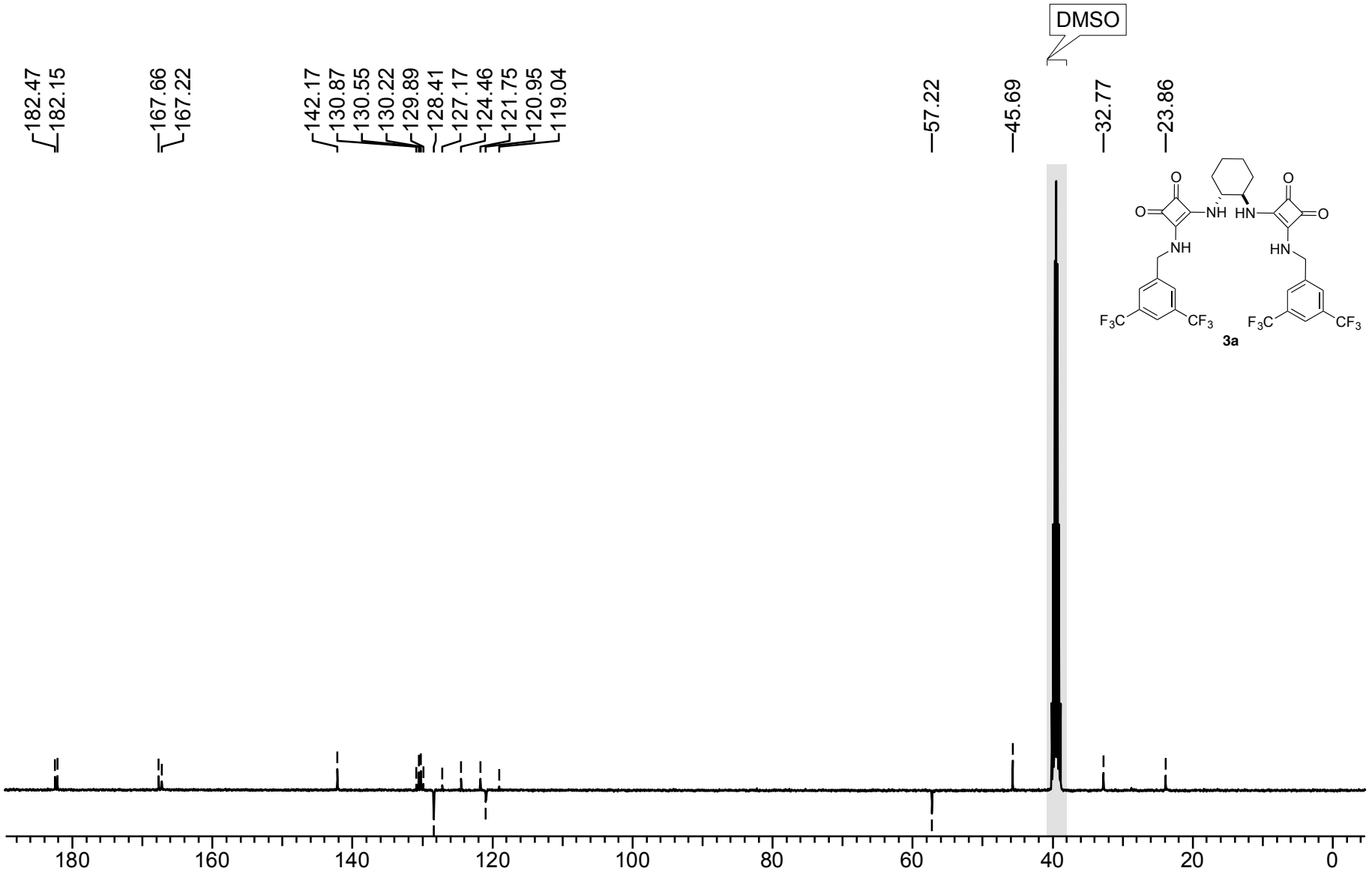

Figure S224. ^{13}C NMR APT (100 MHz, DMSO-d_6) spectrum of **3a**.

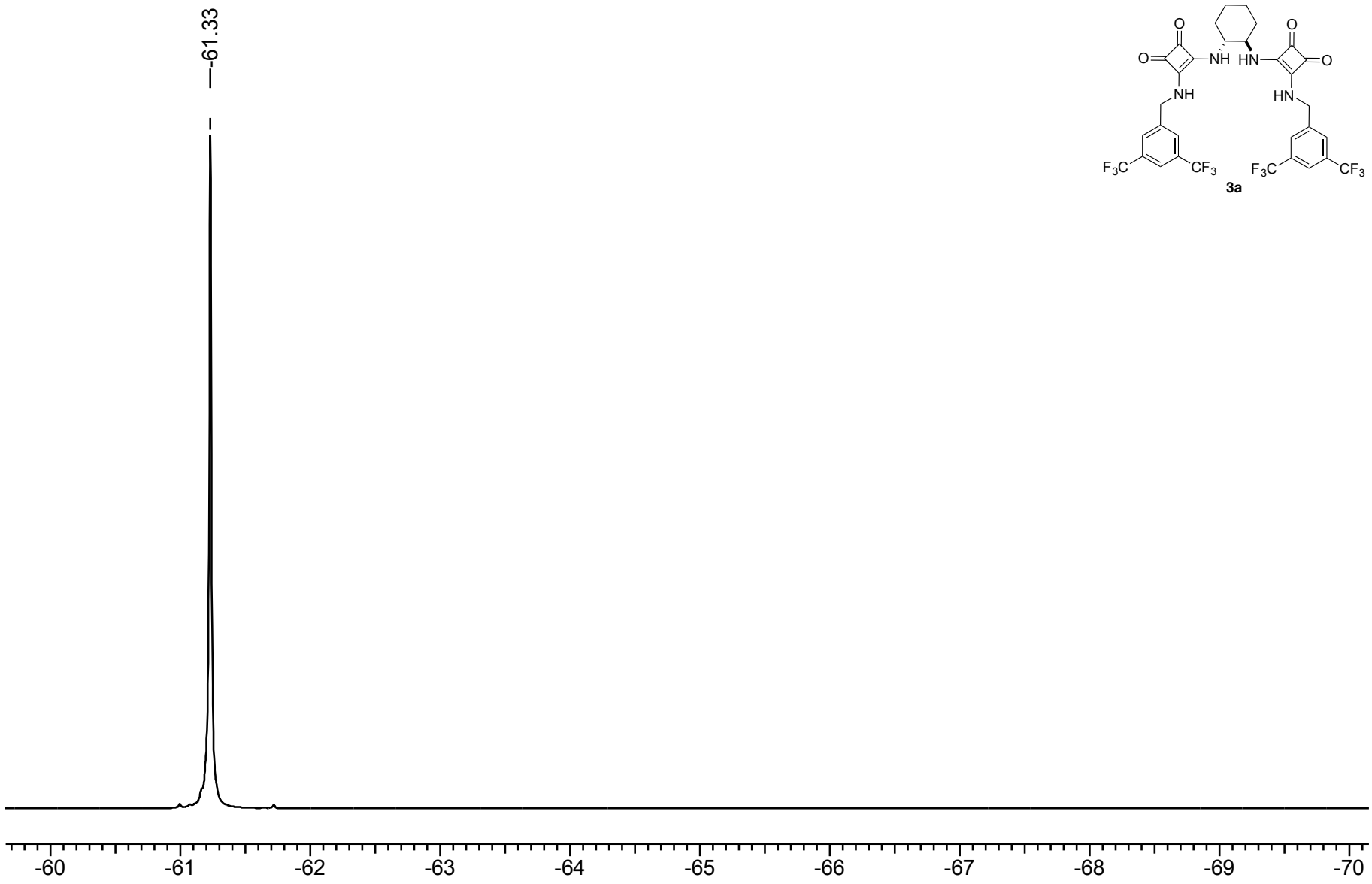

3a

Figure S225. ^{19}F NMR (376 MHz, DMSO-d_6) spectrum of **3a**.

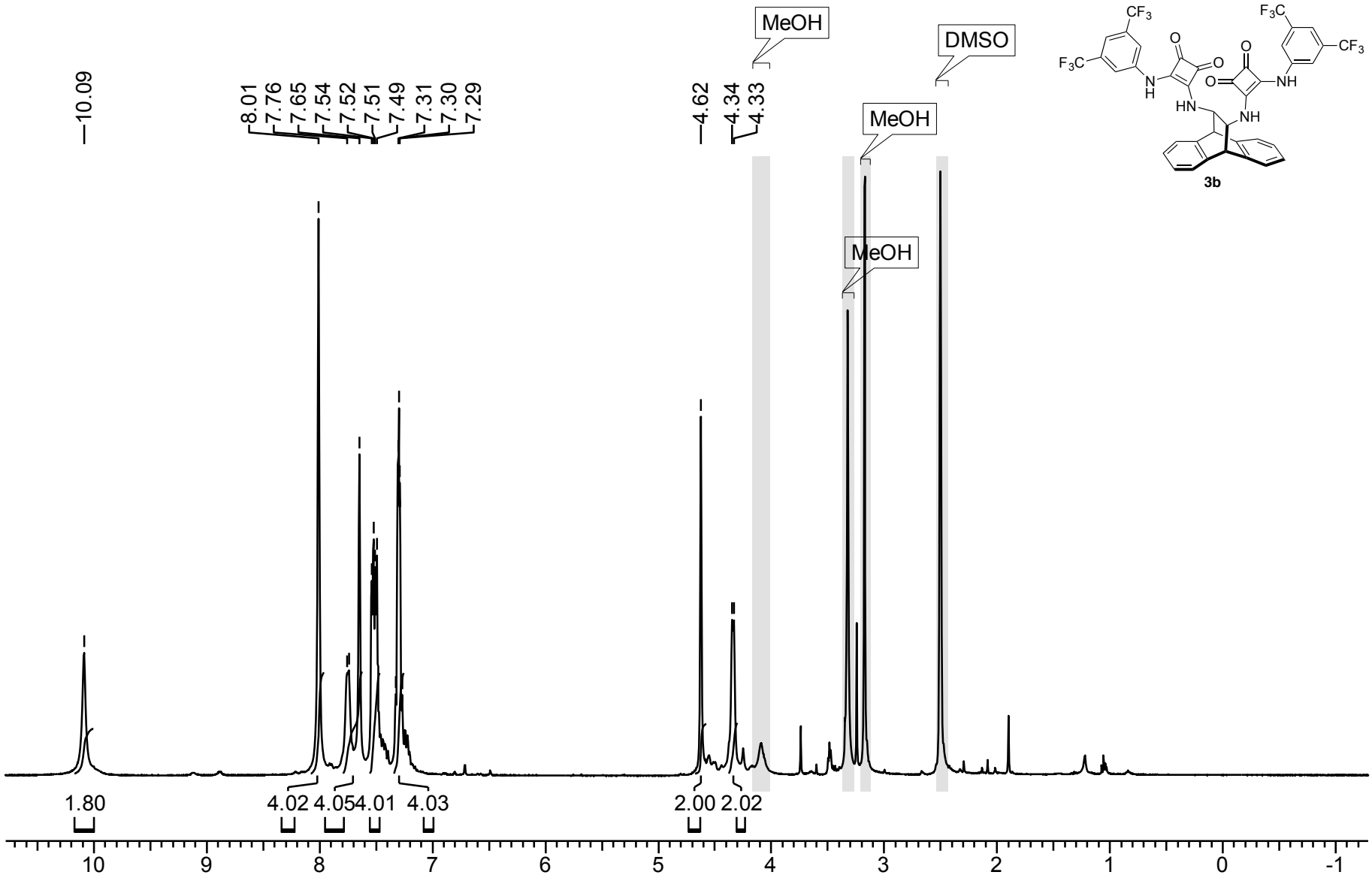

Figure S226. ^{1}H NMR (400 MHz, DMSO-d_6) spectrum of **3b**.

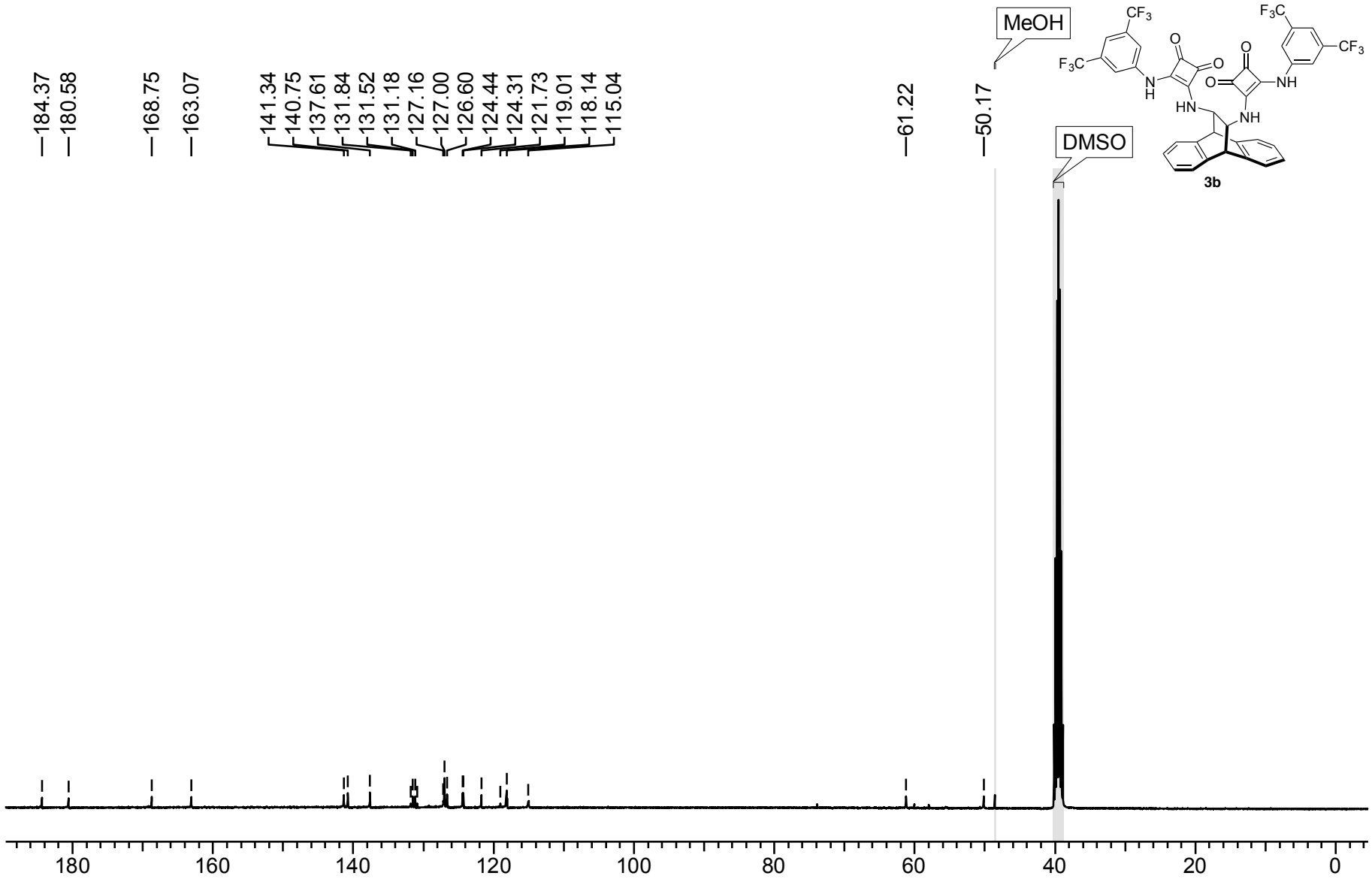

Figure S227. ^{13}C NMR (100 MHz, DMSO-d_6) spectrum of **3b**.

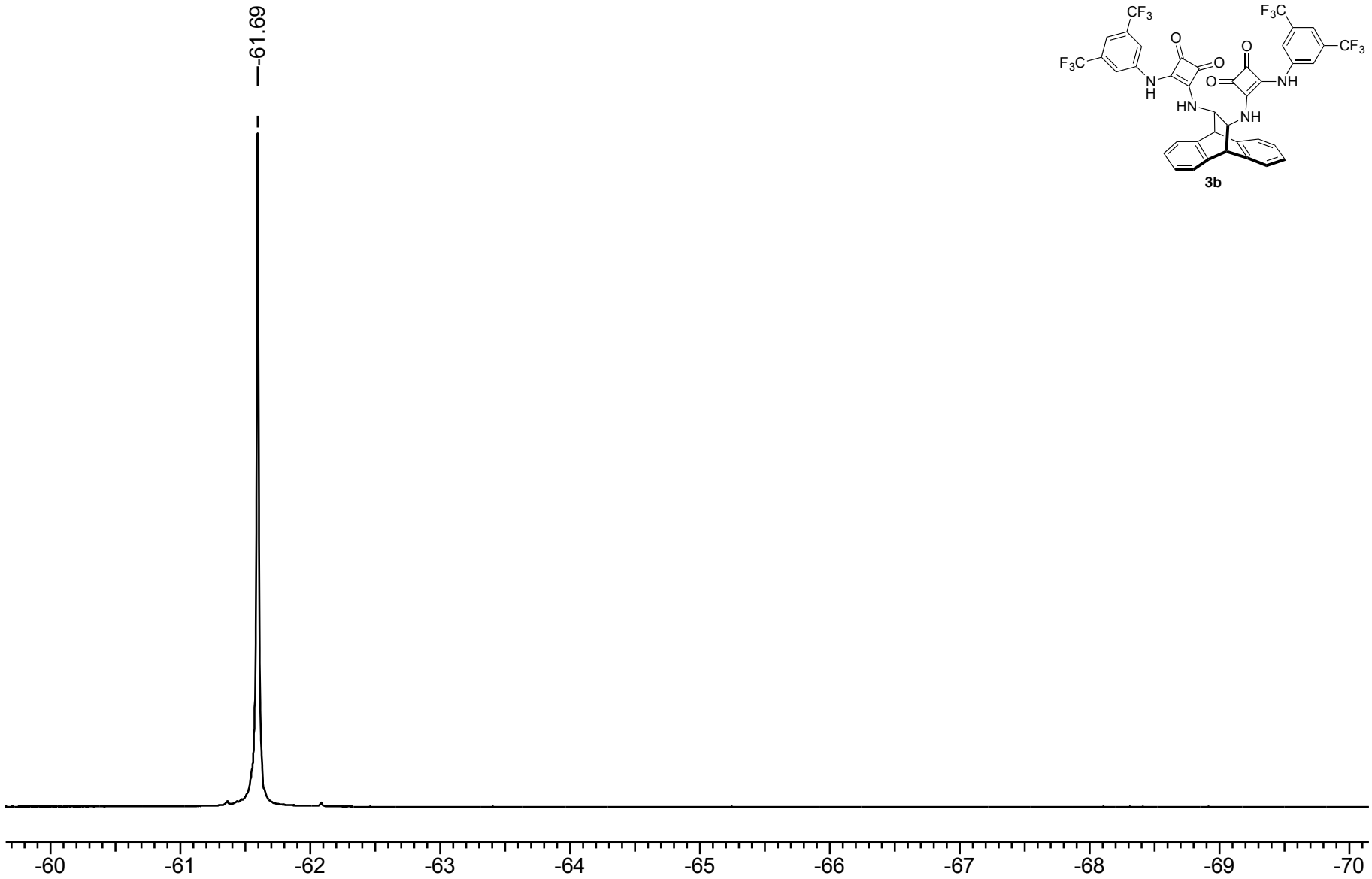

3b

Figure S228. ^{19}F NMR (376 MHz, DMSO-d_6) spectrum of **3b**.

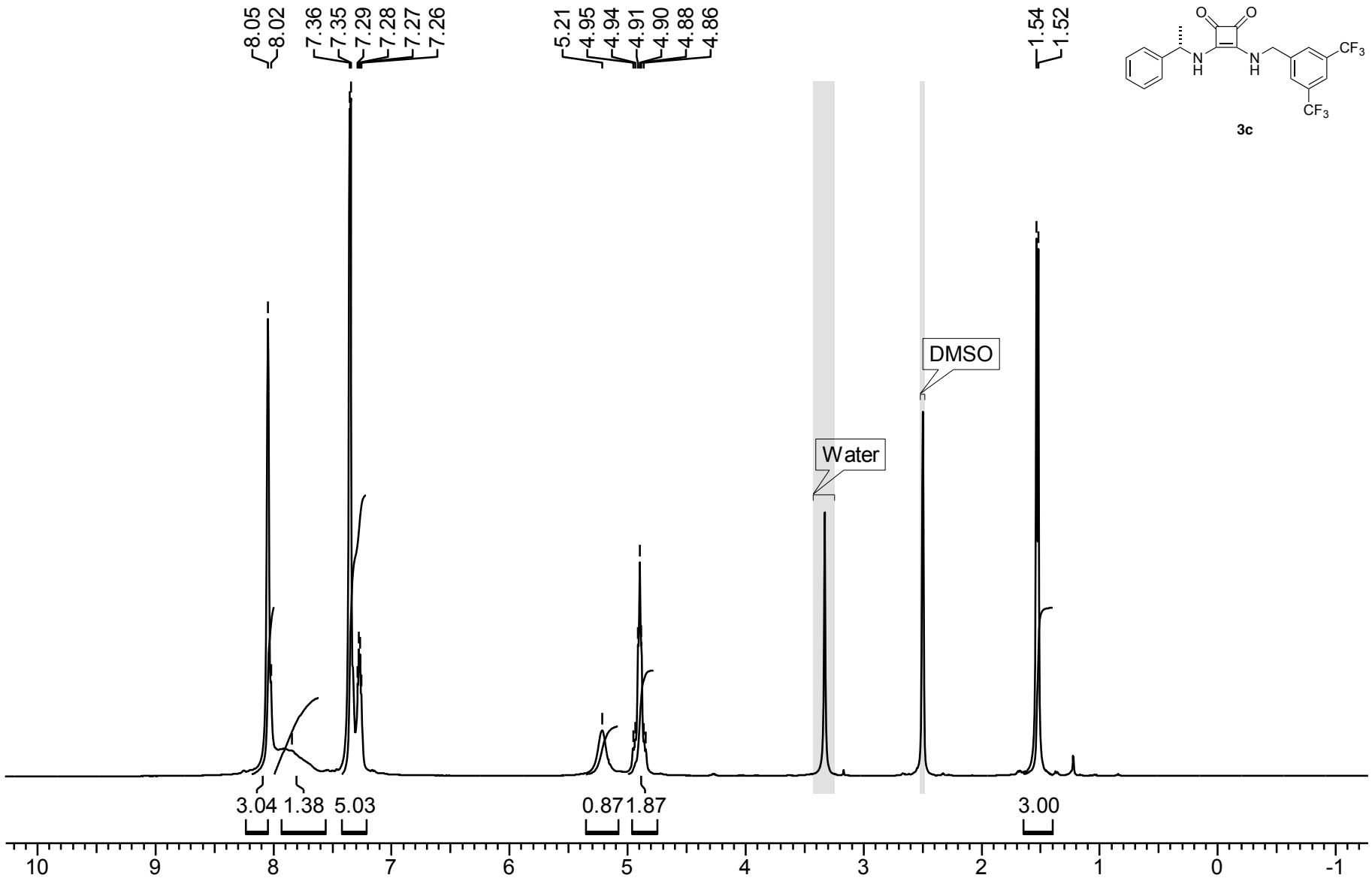

Figure S229. ^{1}H NMR (400 MHz, DMSO-d_6) spectrum of **3c**.

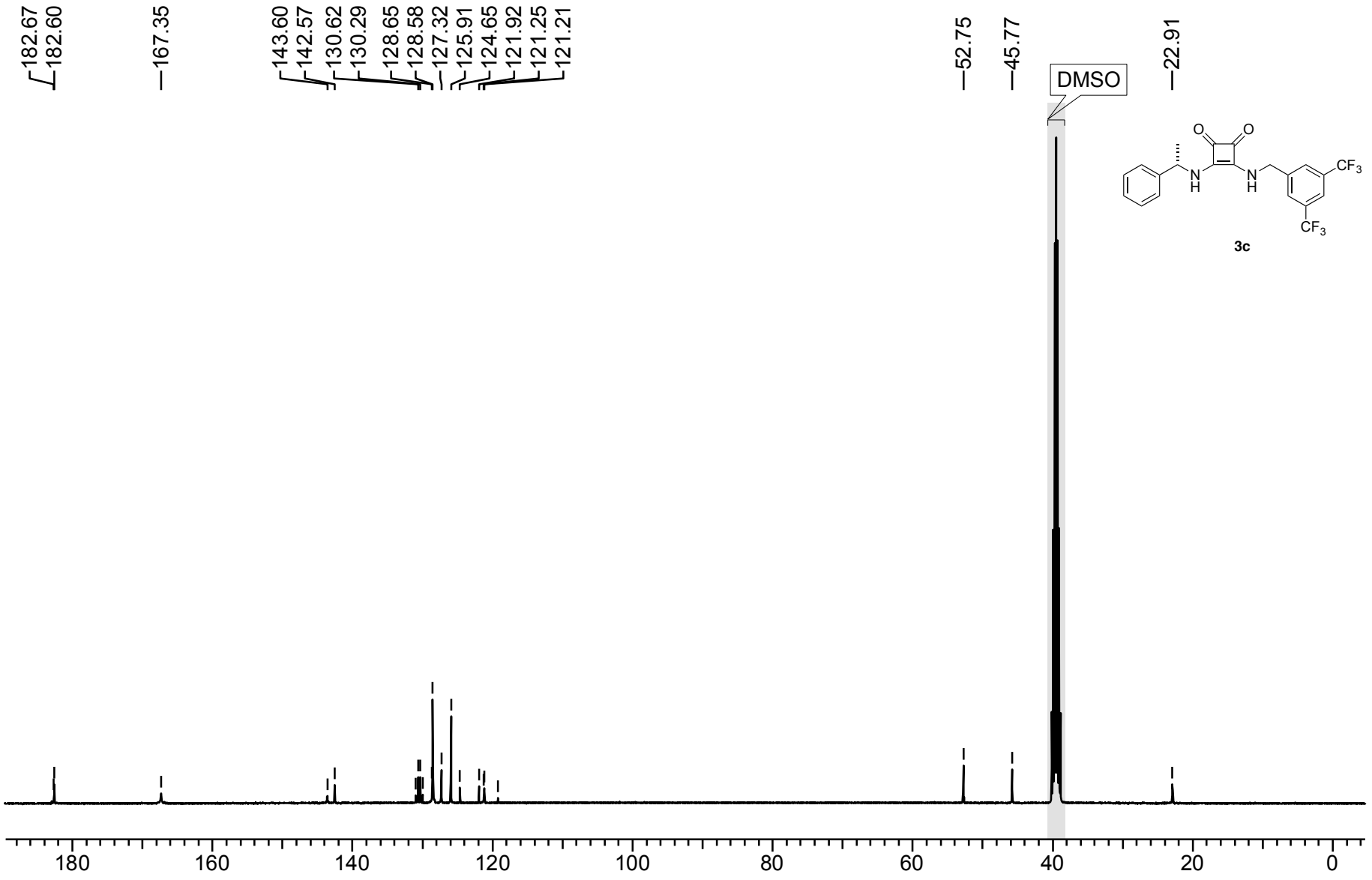

Figure S230. ^{13}C NMR (100 MHz, DMSO-d_6) spectrum of **3c**.

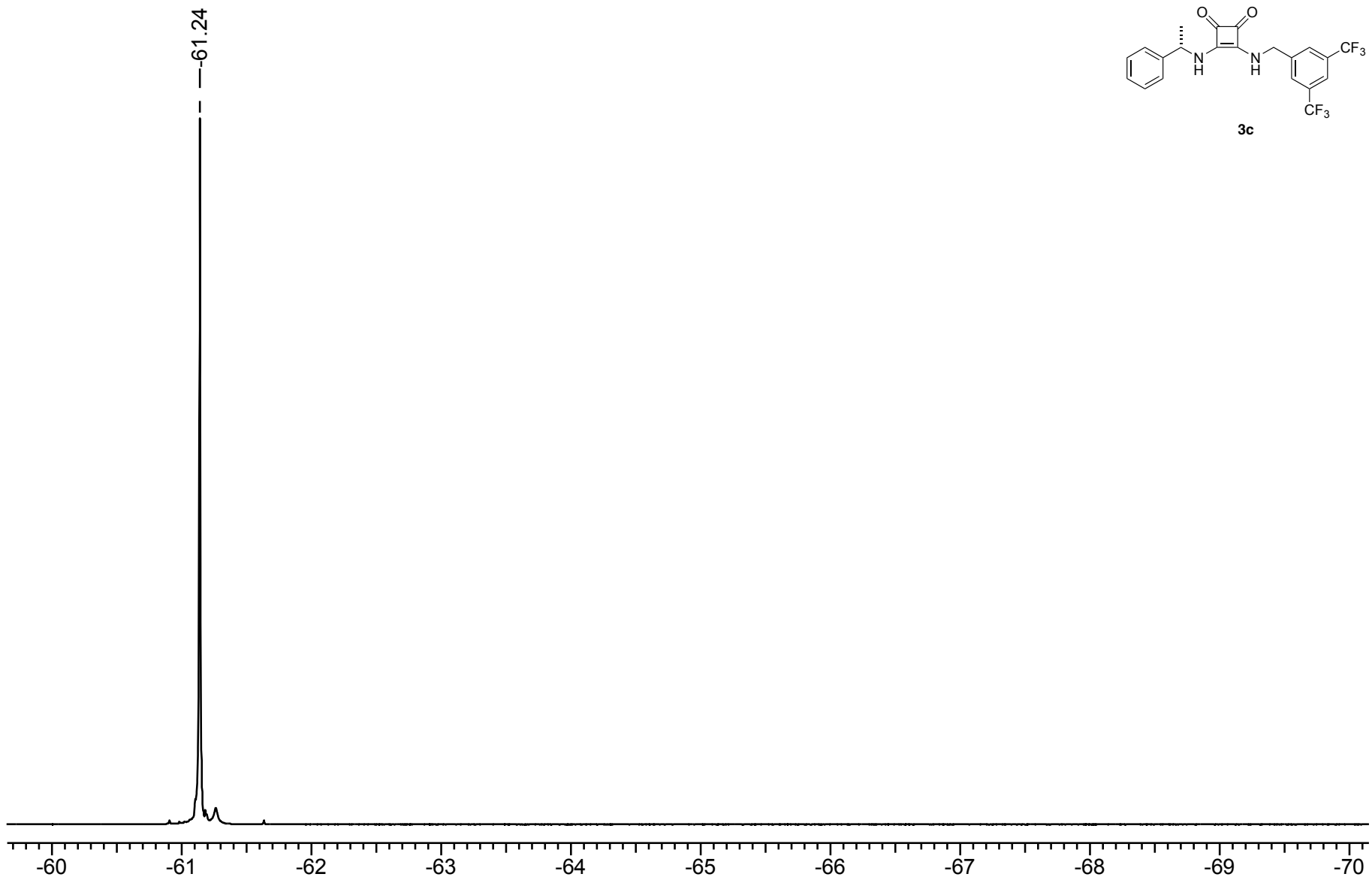

Figure S231. ^{19}F NMR (376 MHz, DMSO-d_6) spectrum of **3c**.

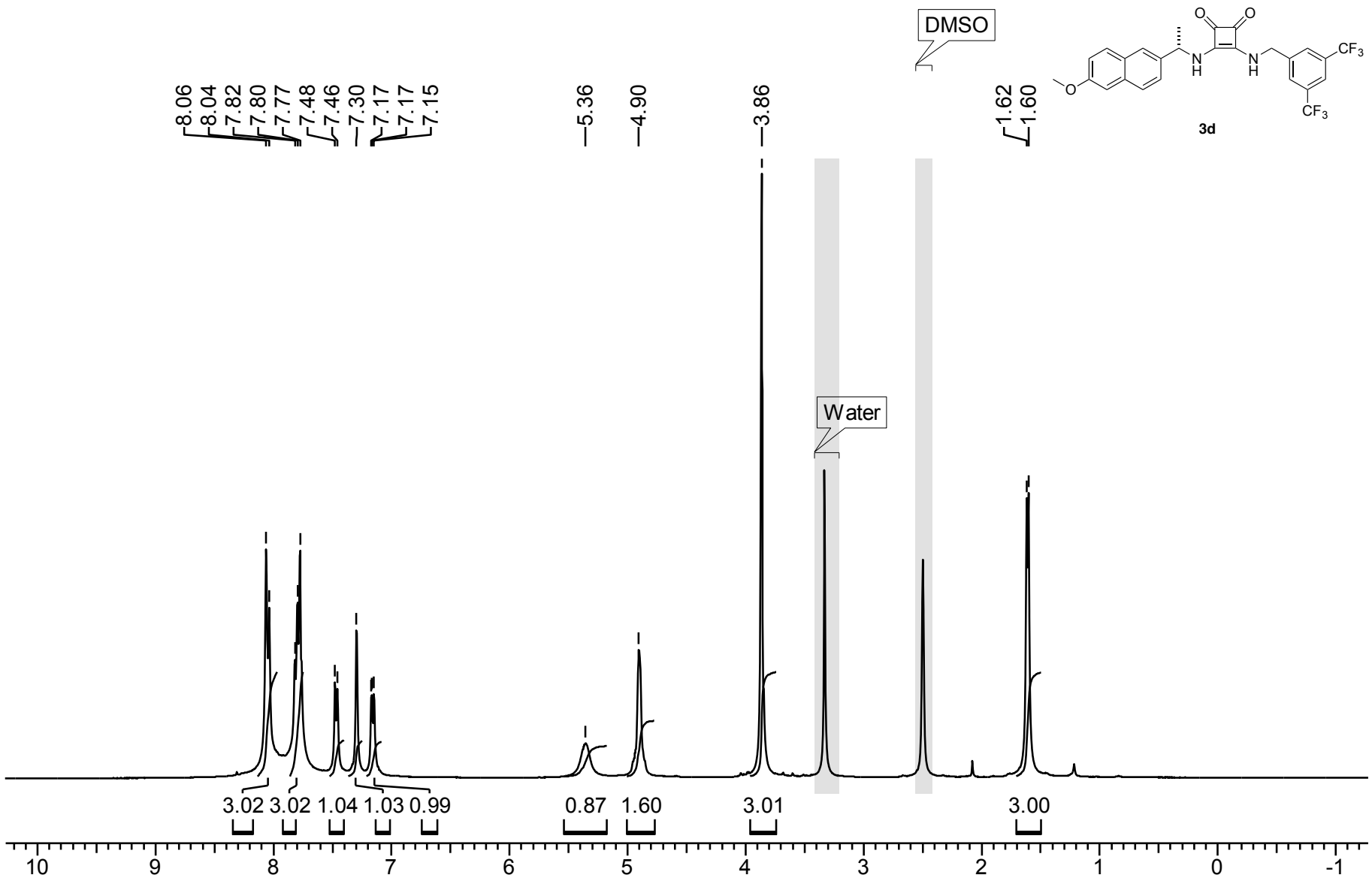

Figure S232. ^{1}H NMR (400 MHz, DMSO-d_6) spectrum of **3d**.

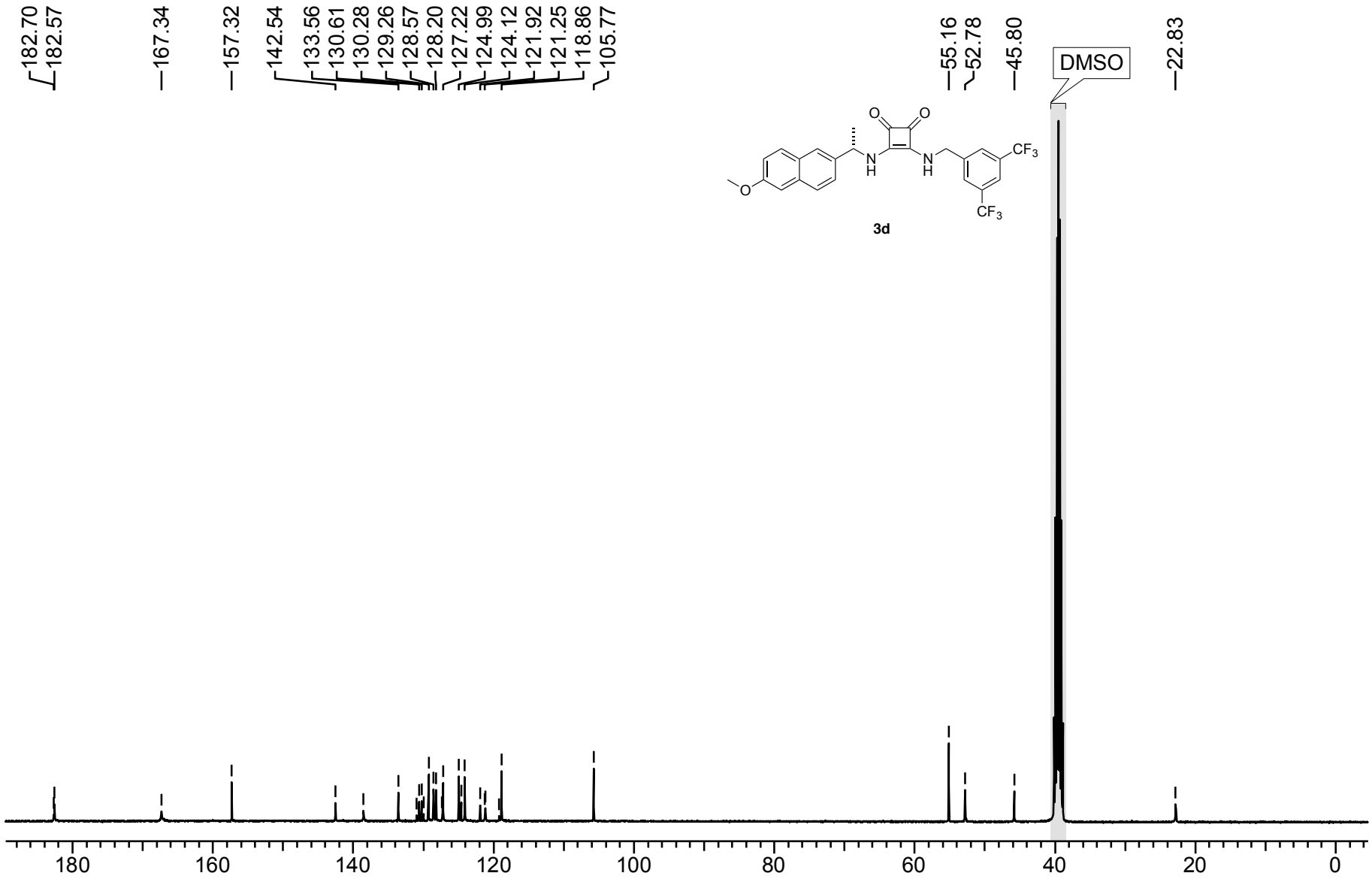

Figure S233. ^{13}C NMR (100 MHz, DMSO-d_6) spectrum of **3d**.

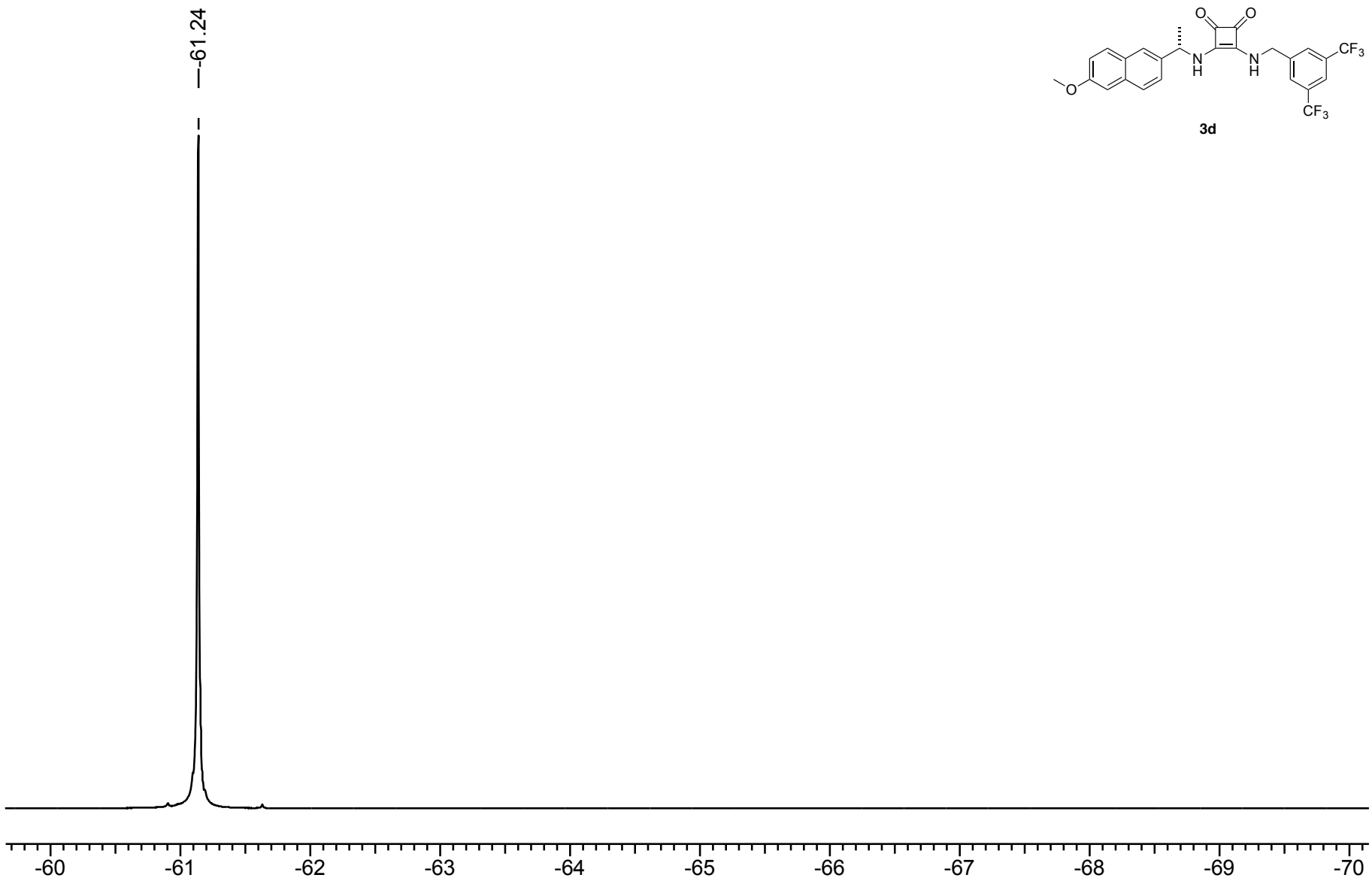

Figure S234. ^{19}F NMR (376 MHz, DMSO-d_6) spectrum of **3d**.

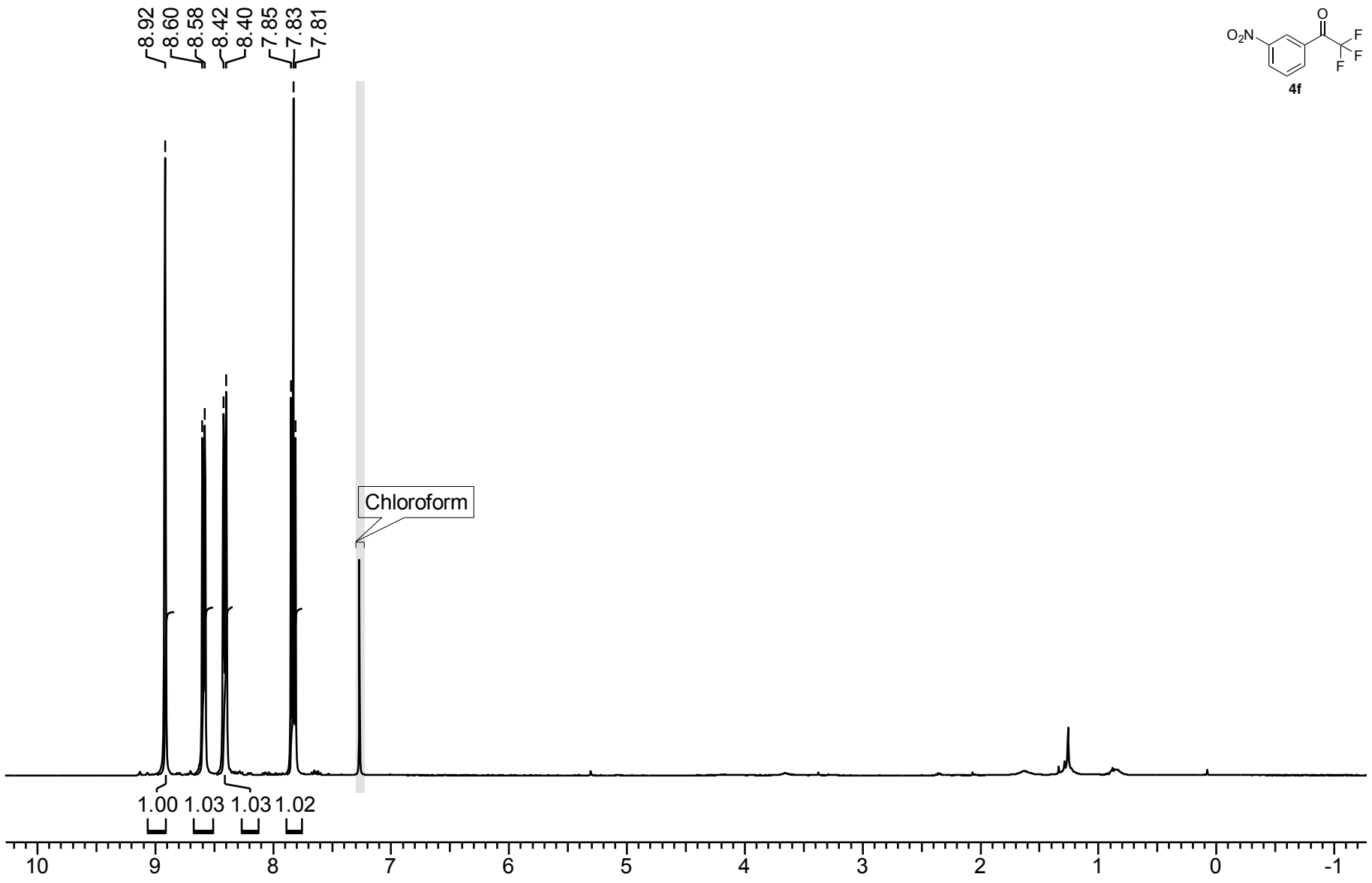

Figure S235. ^{1}H NMR (400 MHz, $CDCl_3$) spectrum of **4f.**

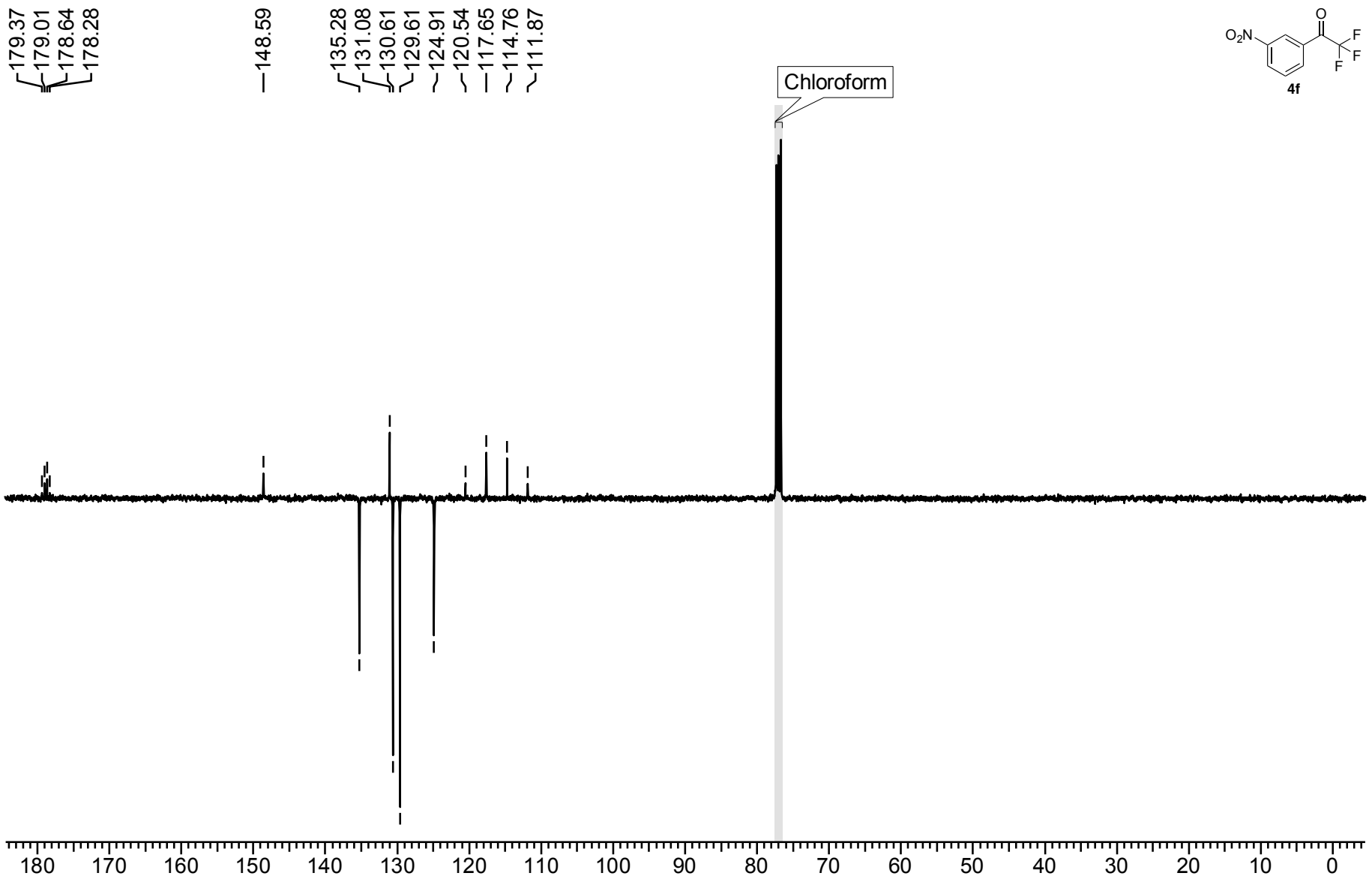

Figure S236. ^{13}C NMR APT (100 MHz, $CDCl_3$) spectrum of **4f**.

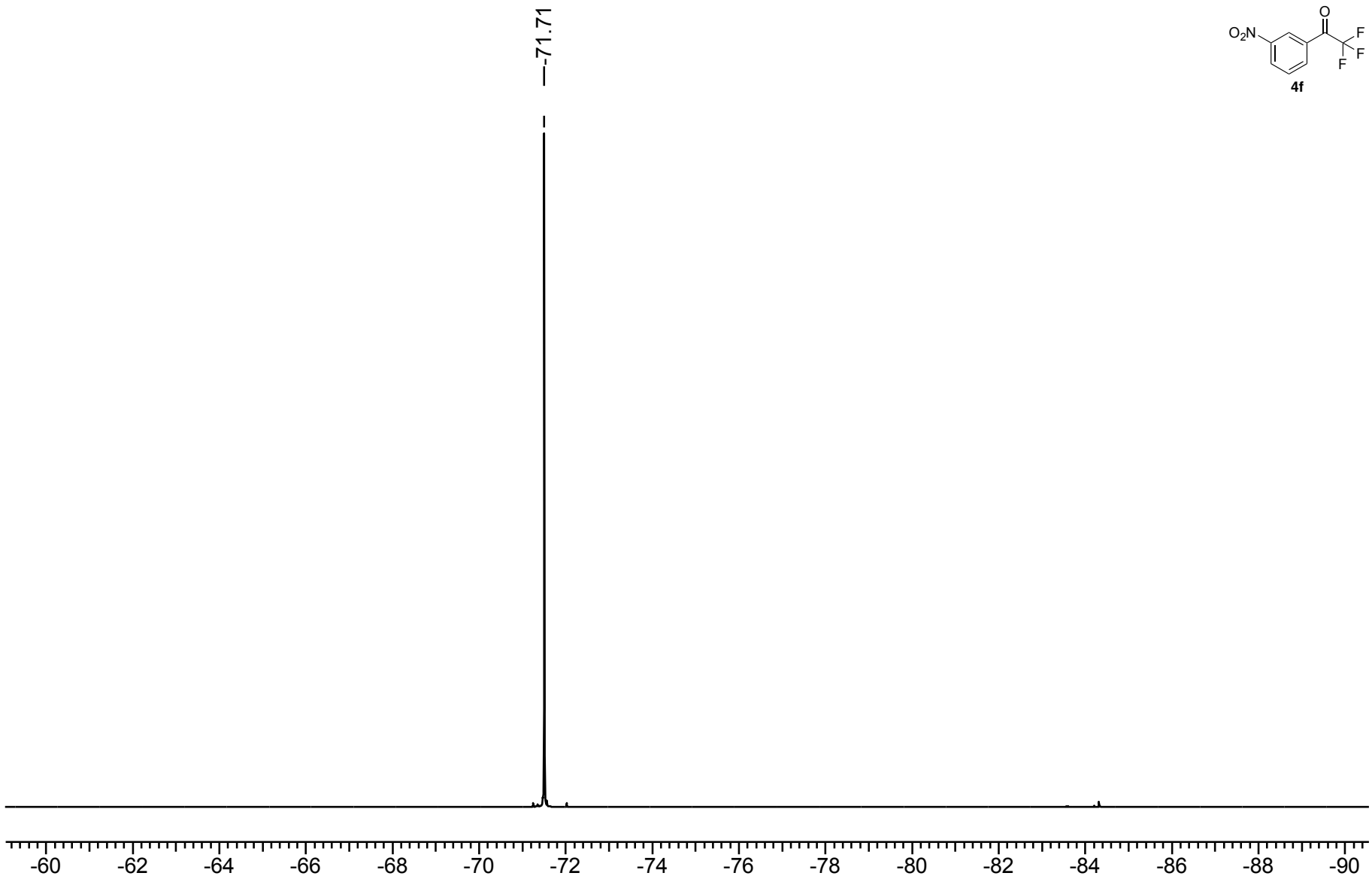

Figure S237. ^{19}F NMR (376 MHz, $CDCl_3$) spectrum of **4f**.

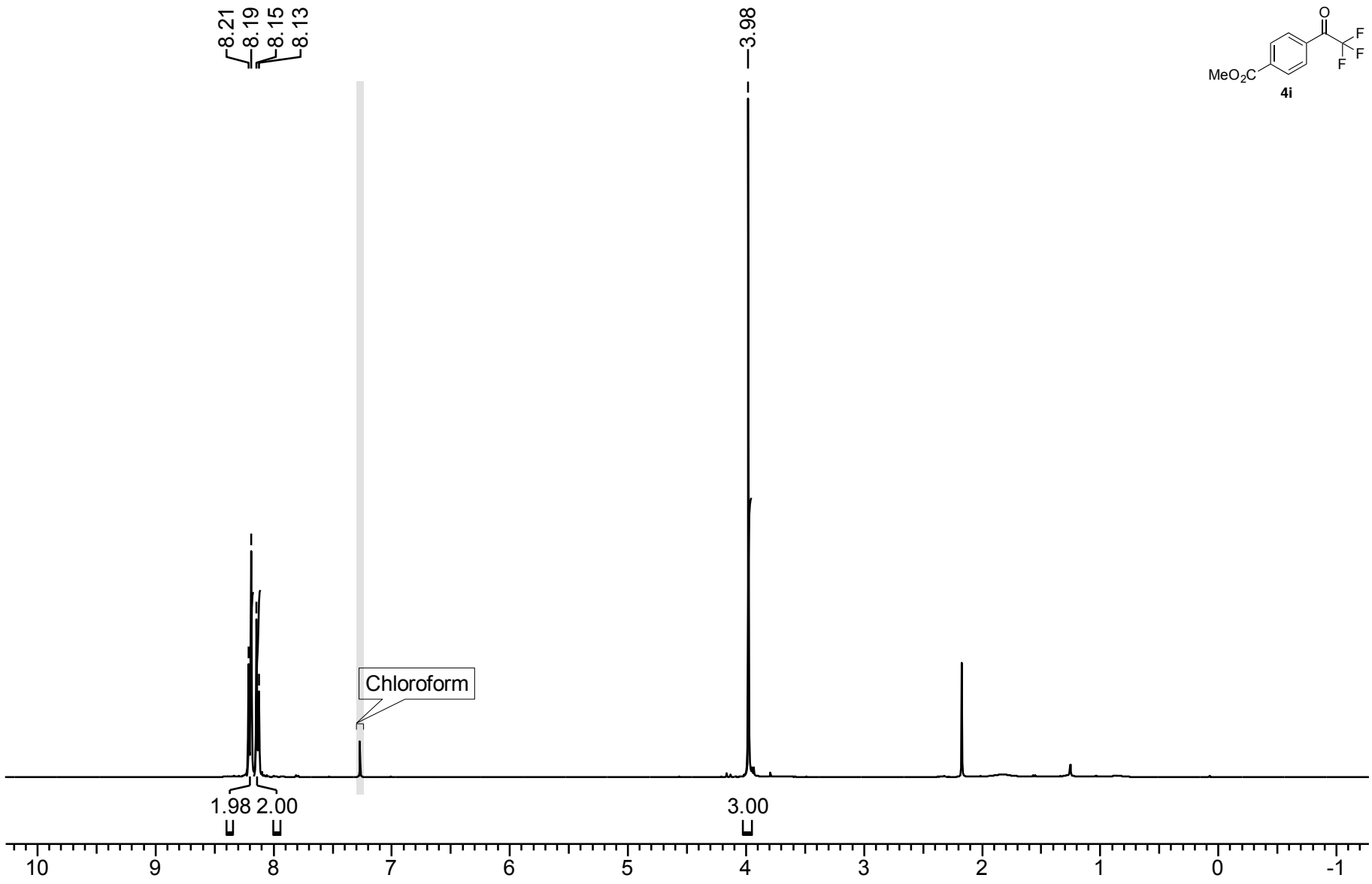

Figure S238. ^{1}H NMR (400 MHz, $CDCl_3$) spectrum of **4i**.

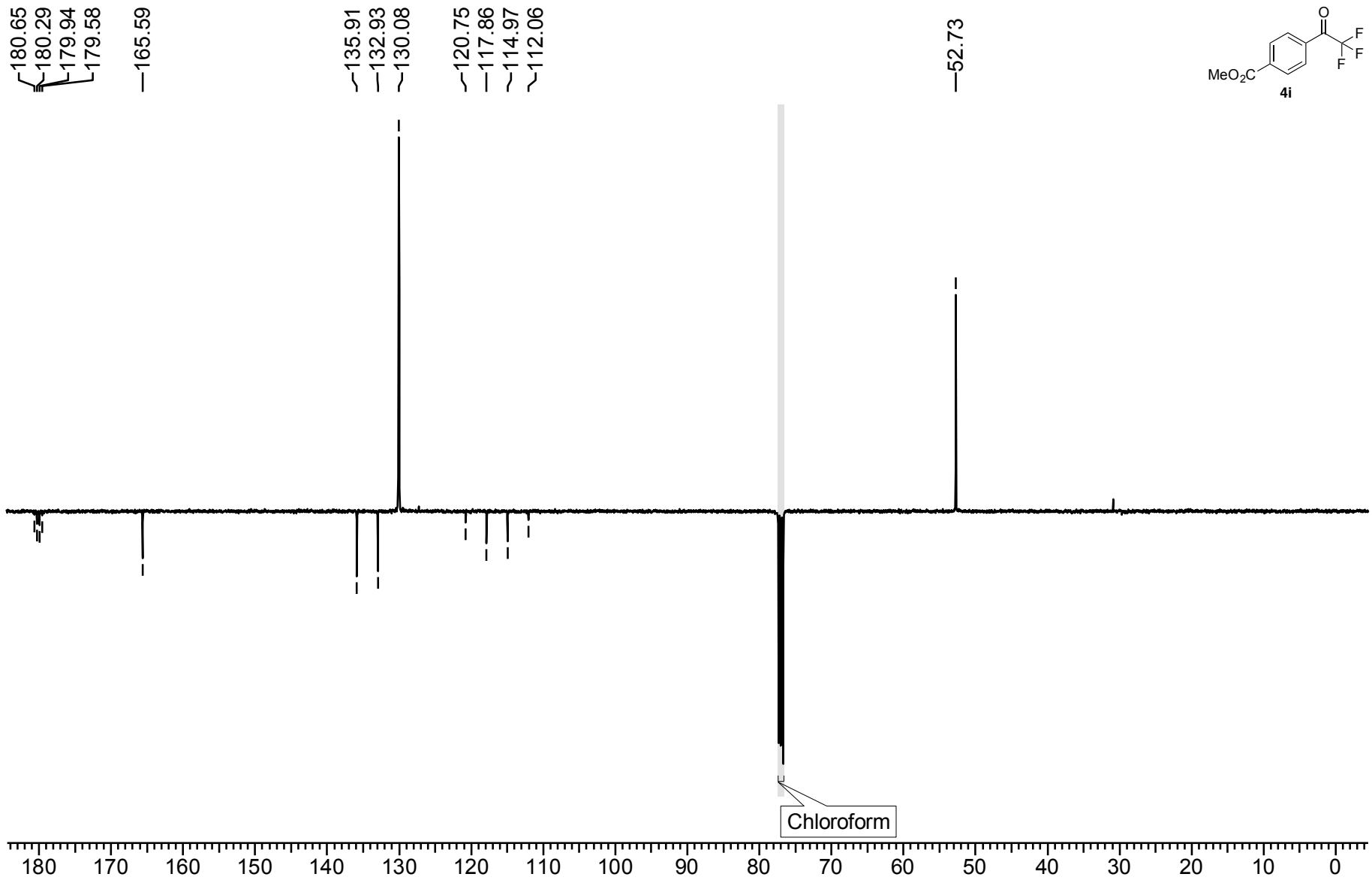

Figure S239. ^{13}C NMR APT (100 MHz, $CDCl_3$) spectrum of **4i**.

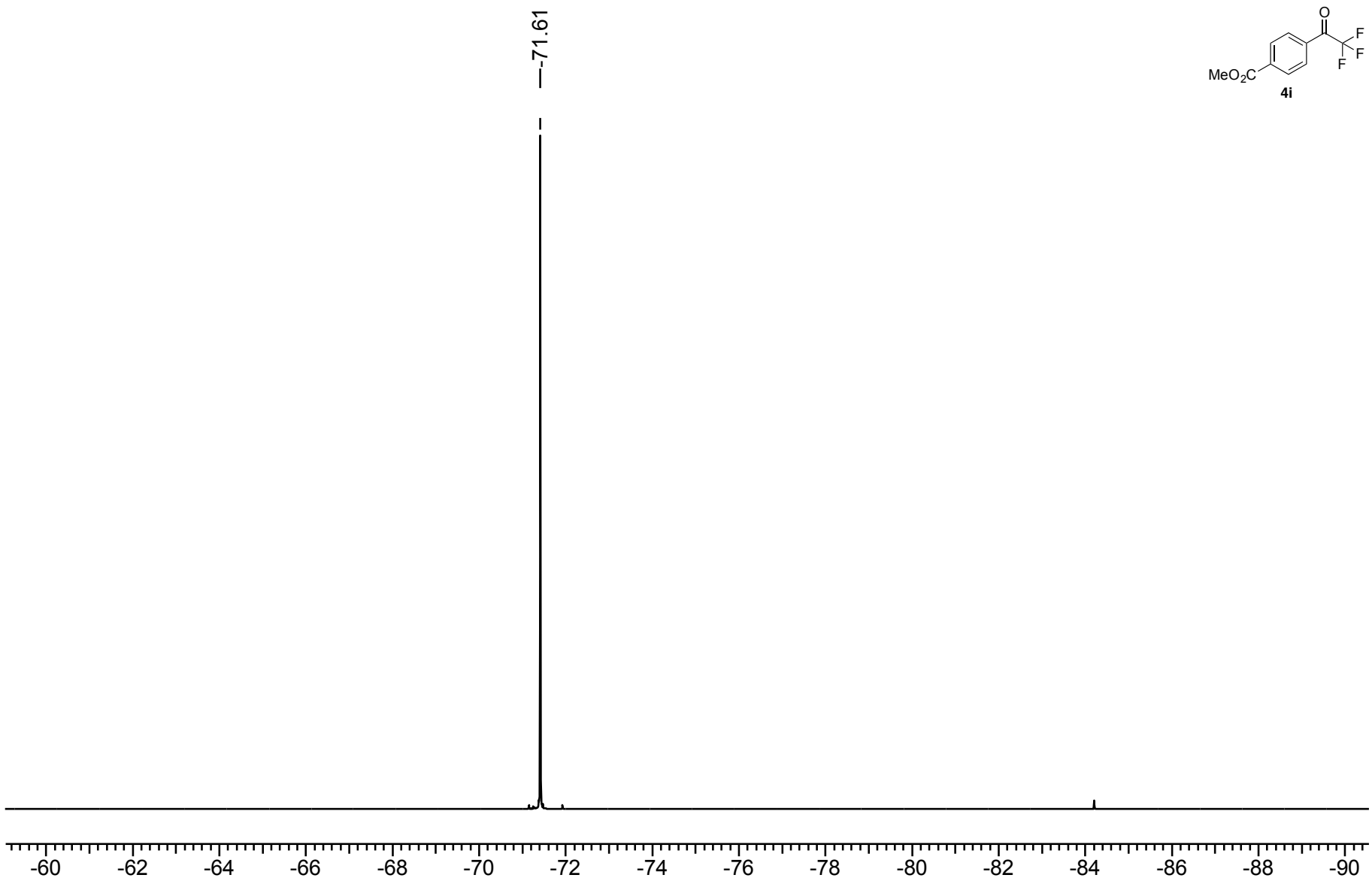

Figure S240. ^{19}F NMR (376 MHz, $CDCl_3$) spectrum of **4i**.

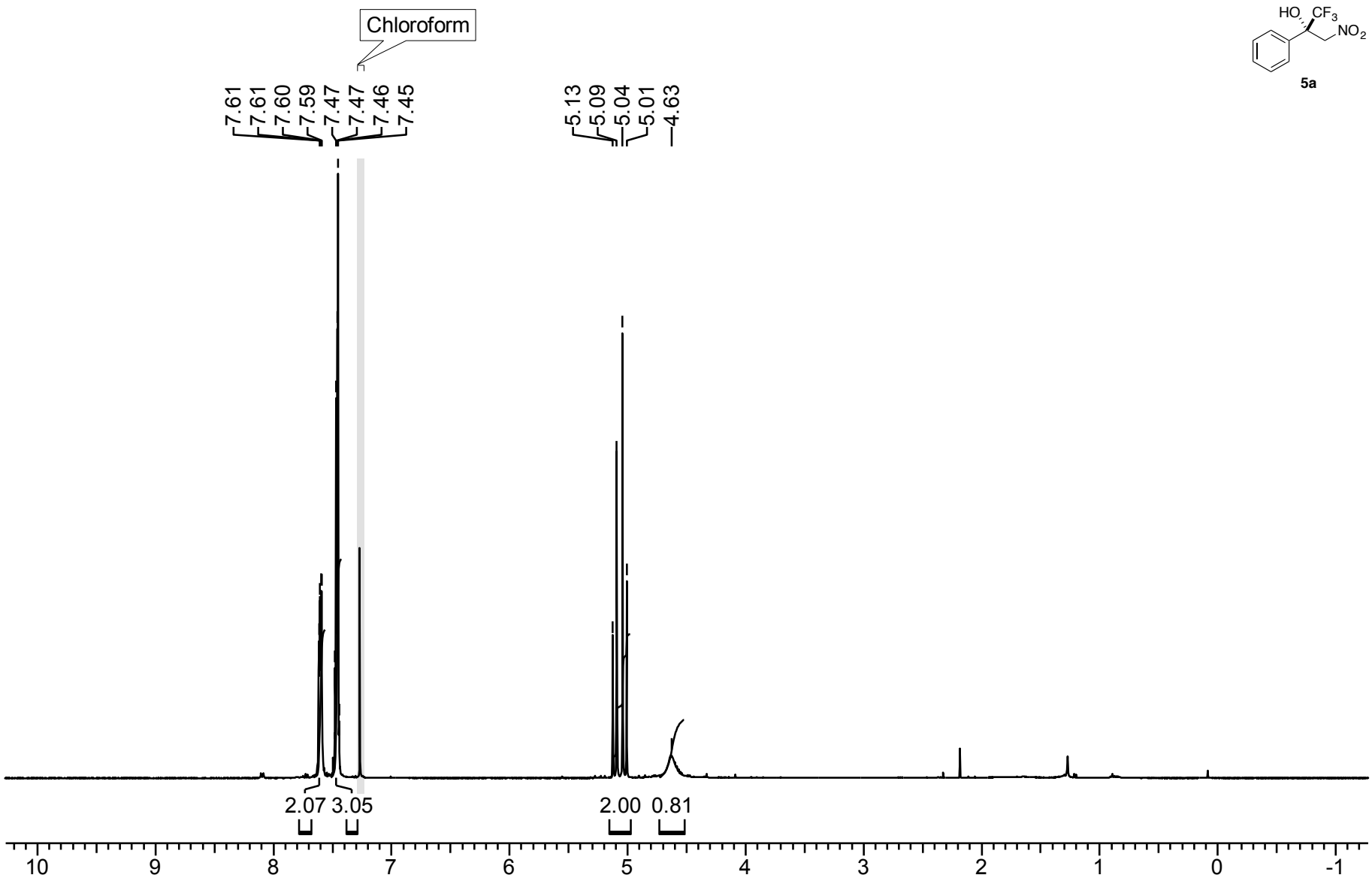

Figure S241. ^{1}H NMR (400 MHz, $CDCl_3$) spectrum of **5a**.

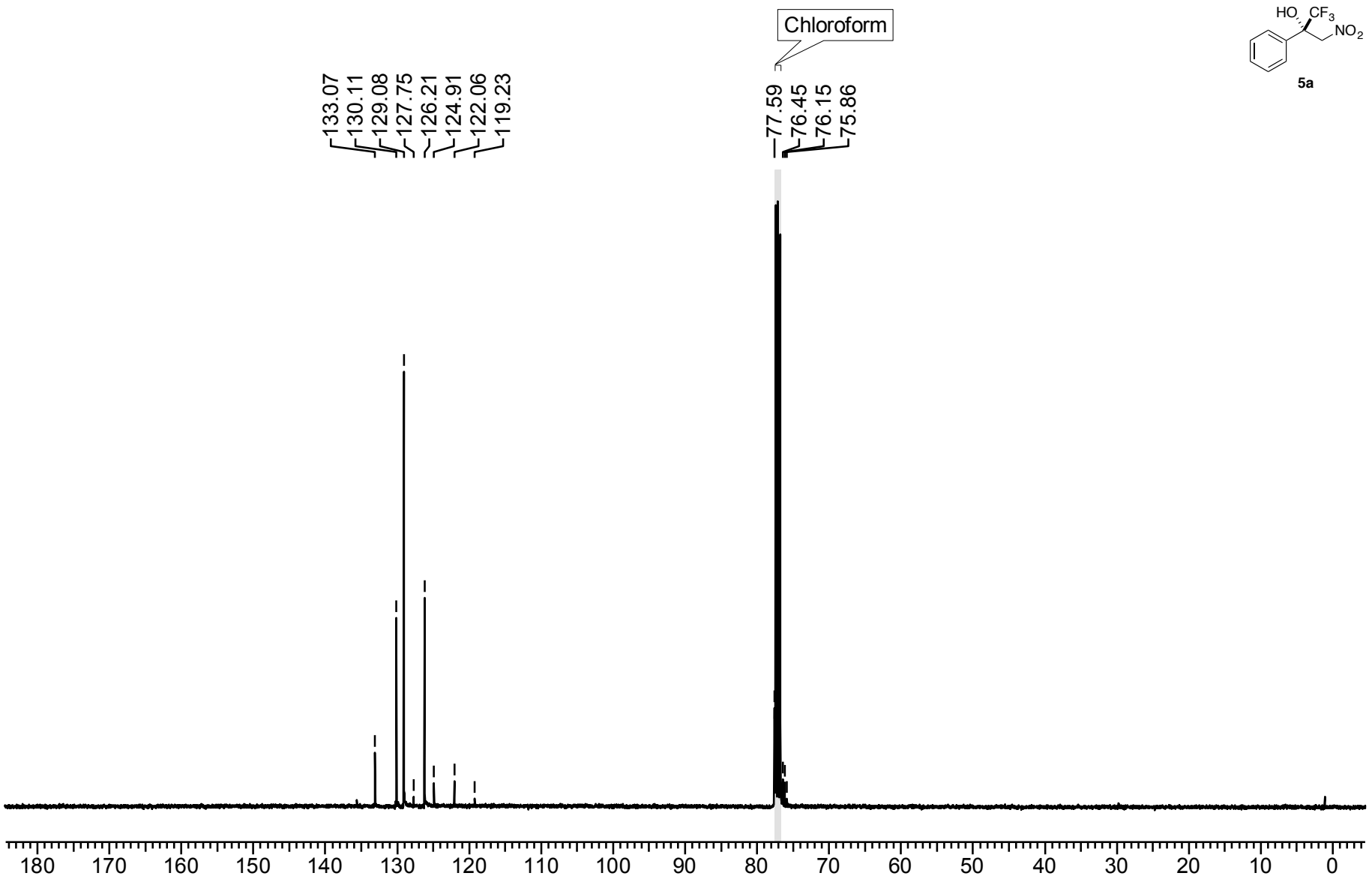

Figure S242. ^{13}C NMR (100 MHz, $CDCl_3$) spectrum of **5a**.

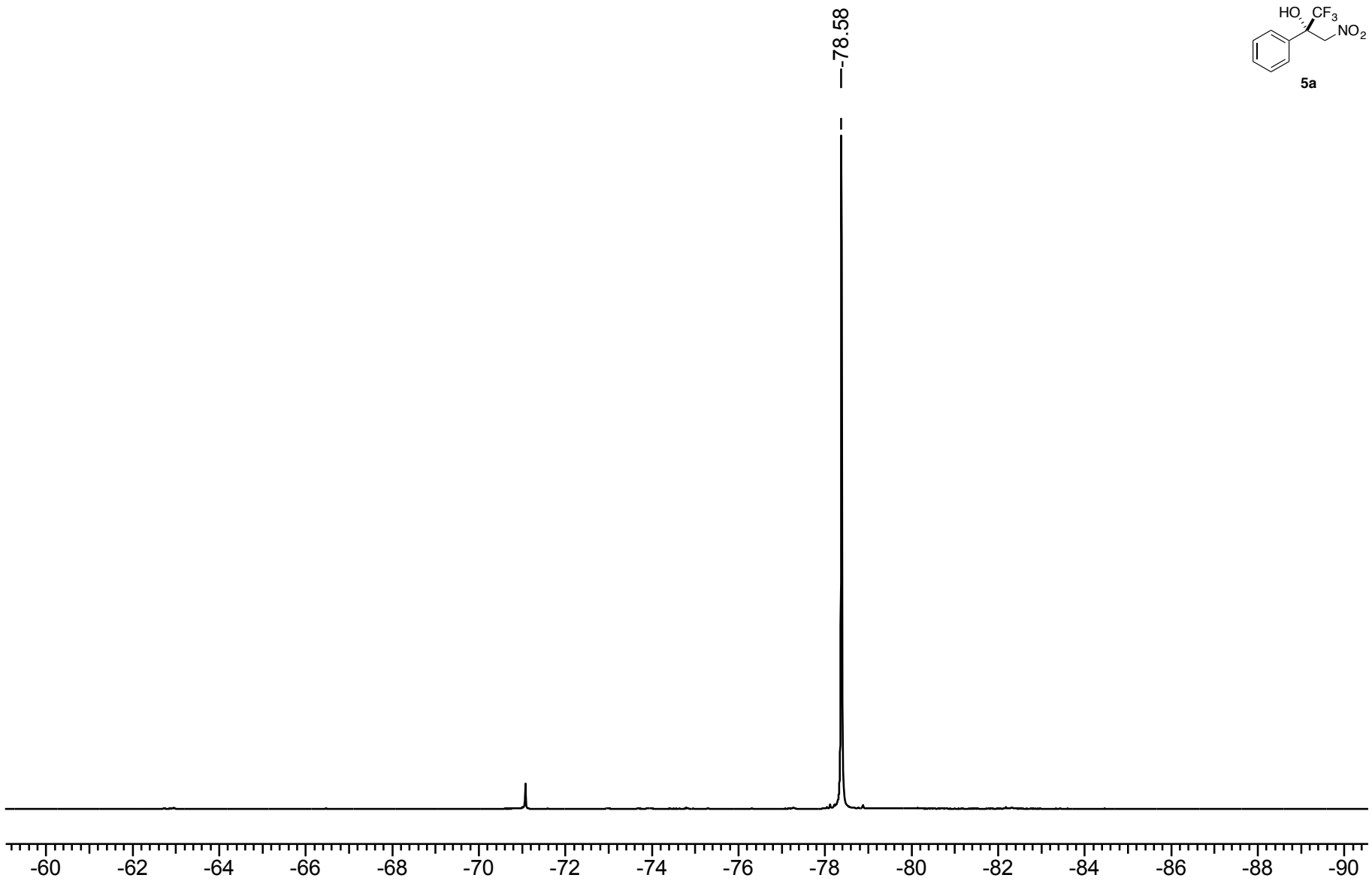

Figure S243. ^{19}F NMR (376 MHz, $CDCl_3$) spectrum of **5a**.

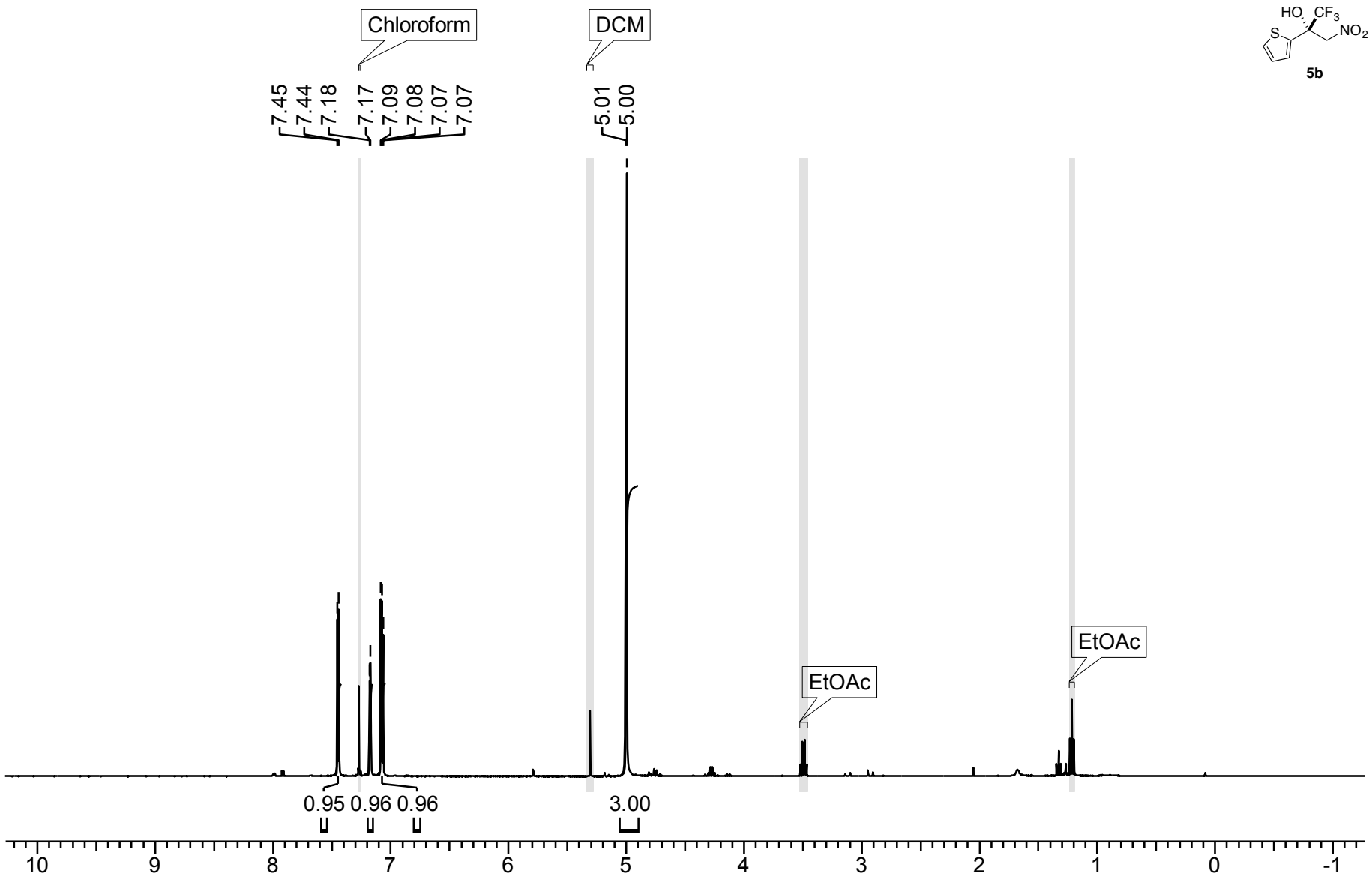

Figure S244. ^{1}H NMR (400 MHz, $CDCl_3$) spectrum of **5b**.

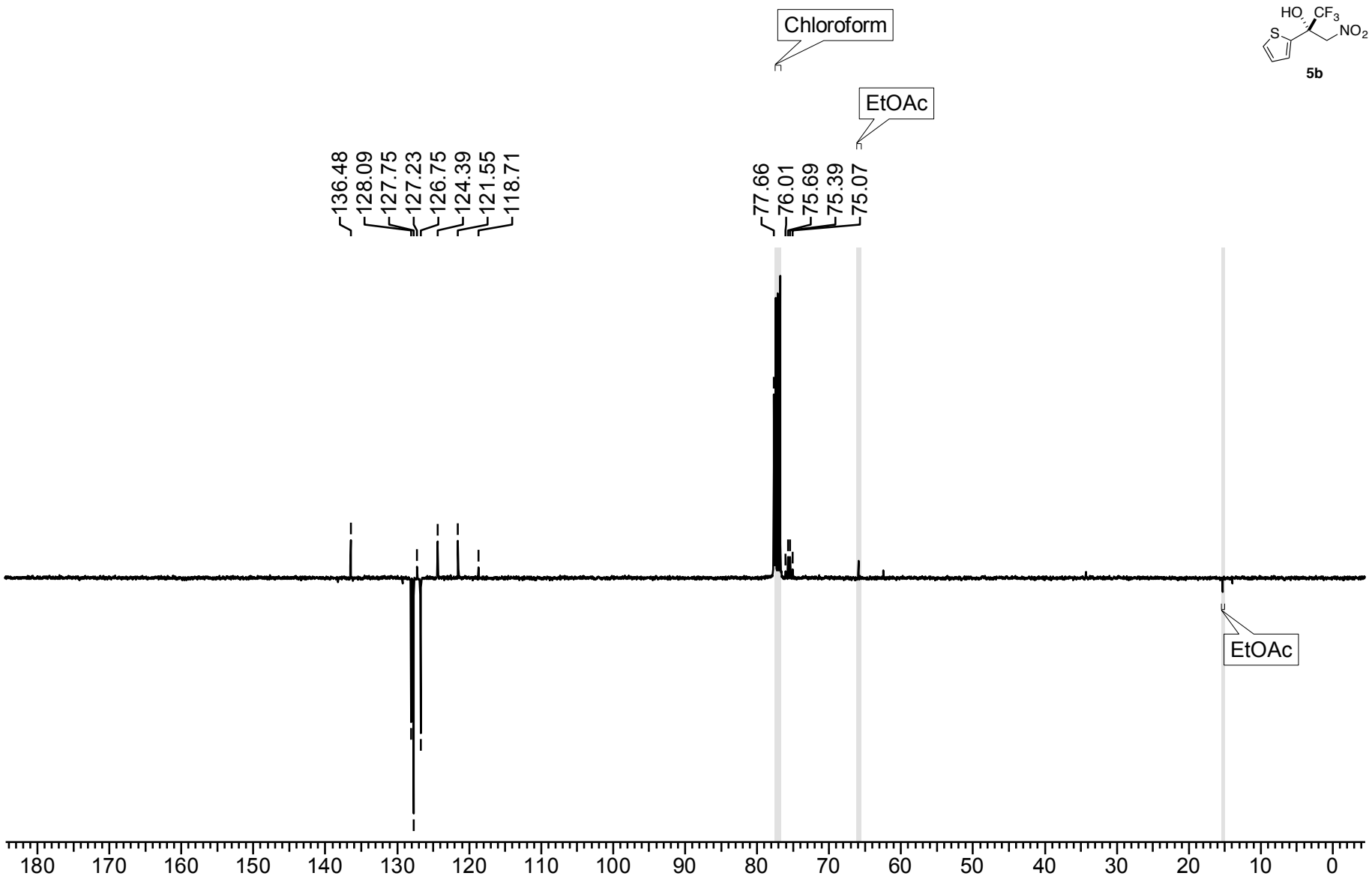

Figure S245. ^{13}C NMR APT (100 MHz, $CDCl_3$) spectrum of **5b**.

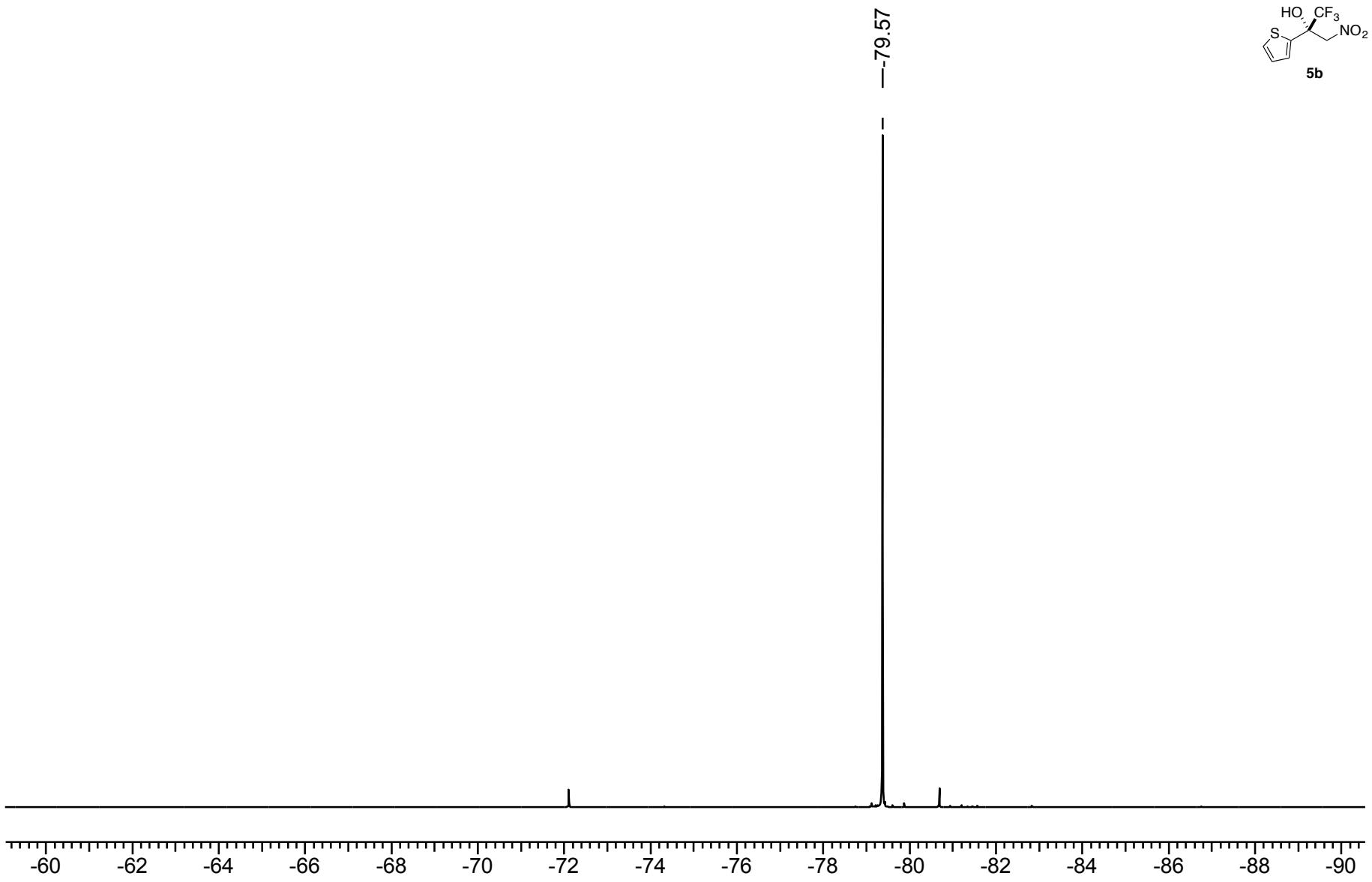

Figure S246. ^{19}F NMR (376 MHz, $CDCl_3$) spectrum of **5b**.

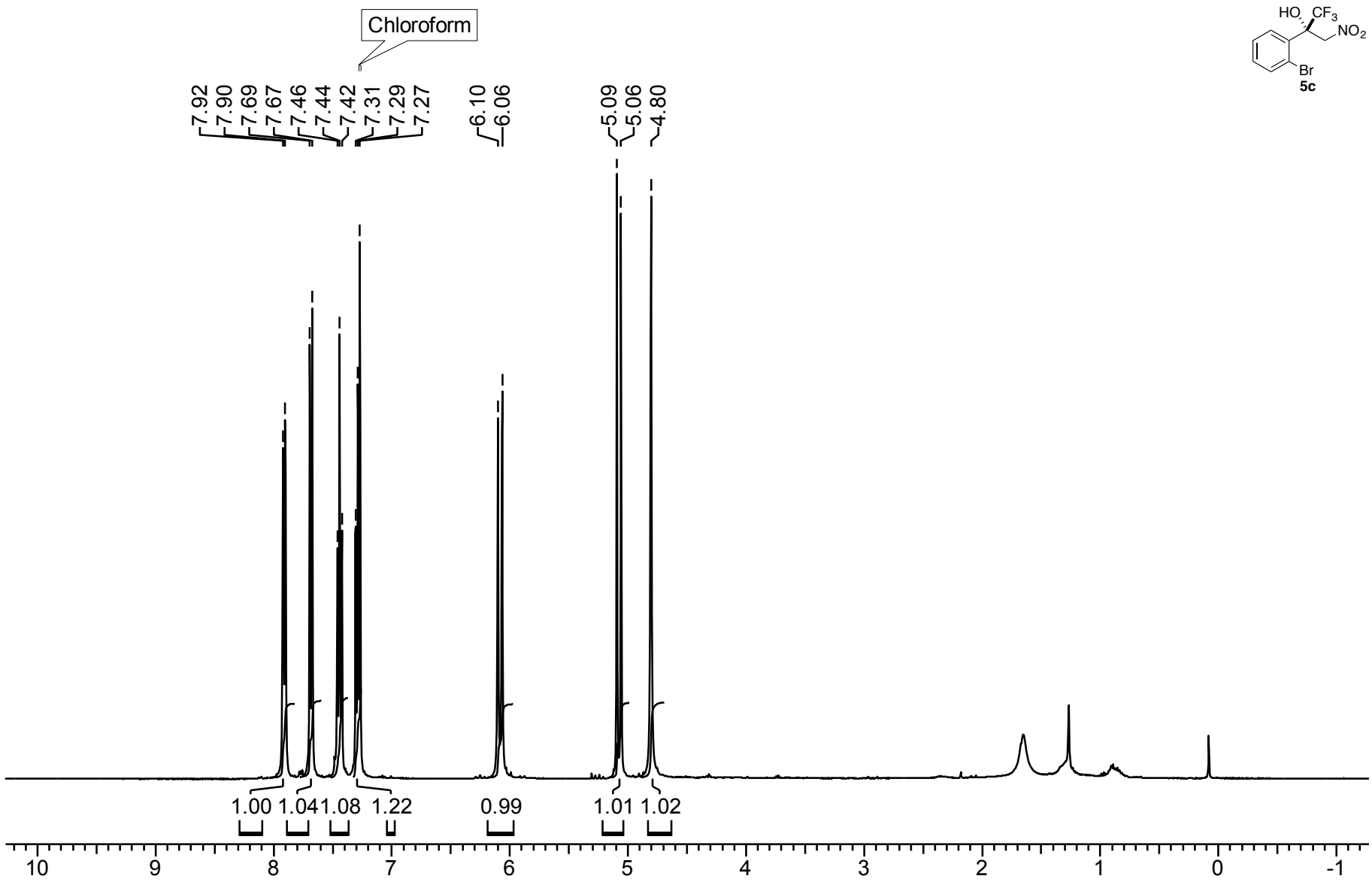

Figure S247. ^{1}H NMR (400 MHz, $CDCl_3$) spectrum of **5c**.

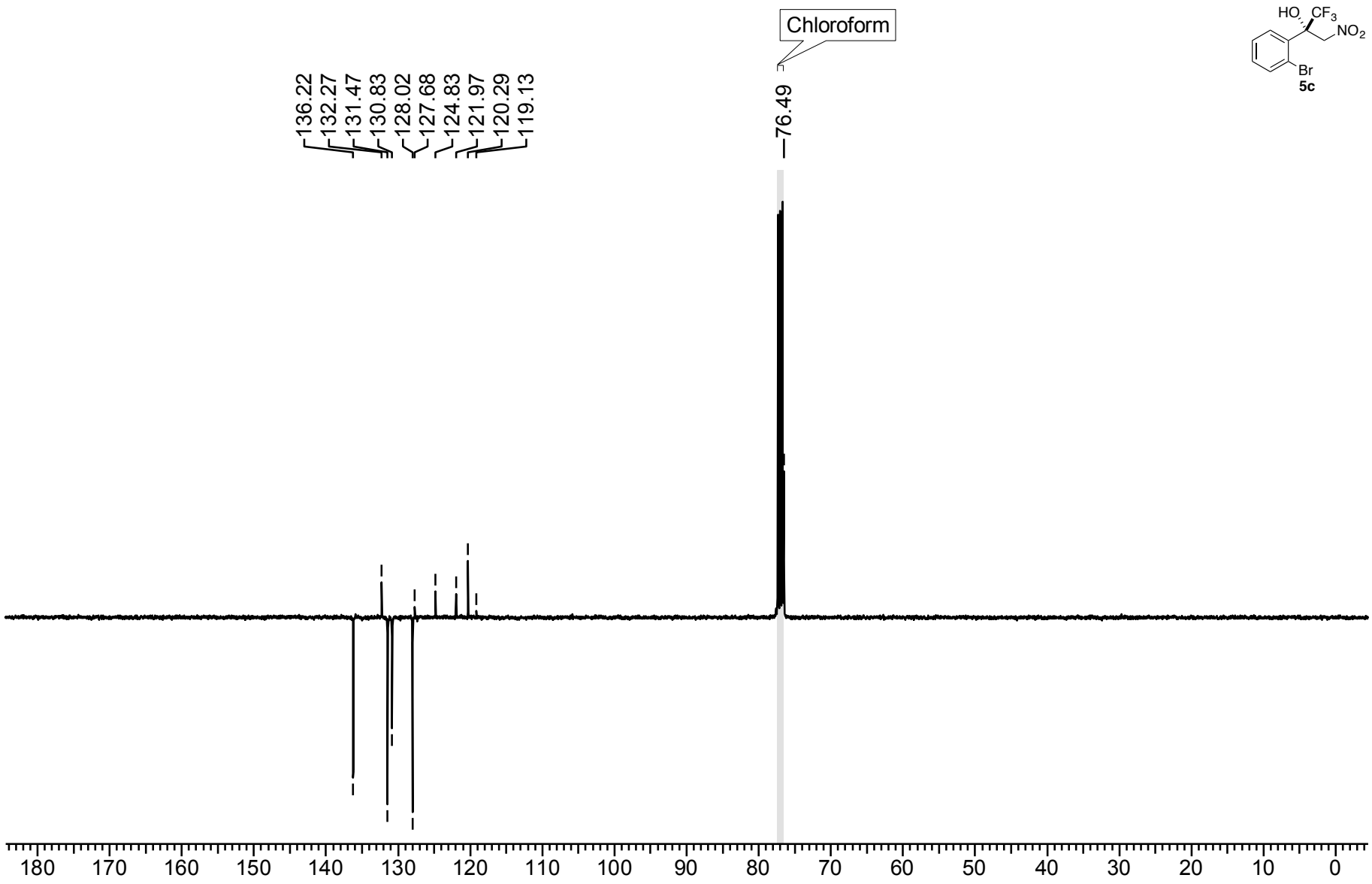

Figure S248. ^{13}C NMR APT (100 MHz, $CDCl_3$) spectrum of **5c**.

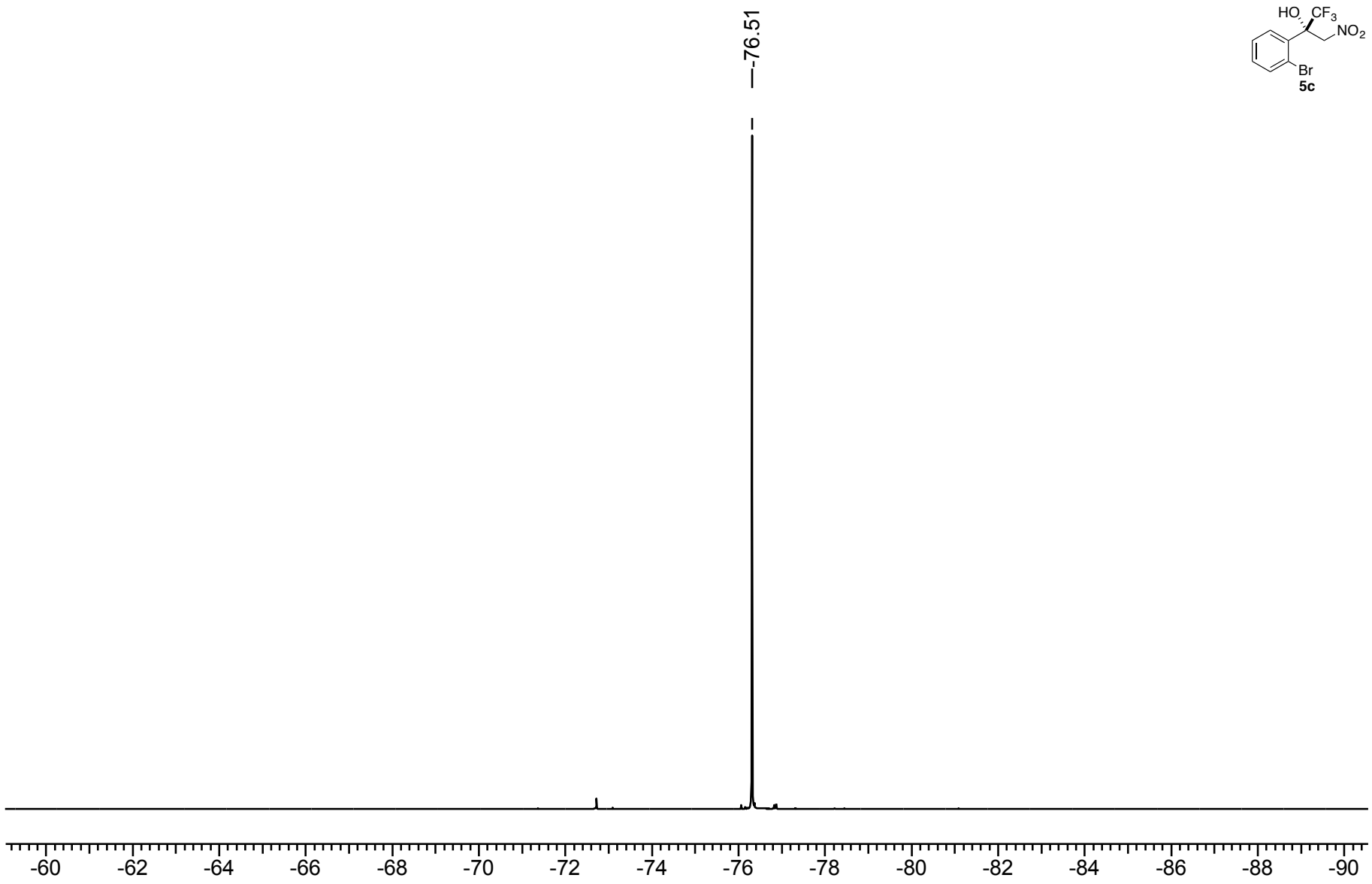

Figure S249. ^{19}F NMR (376 MHz, $CDCl_3$) spectrum of **5c**.

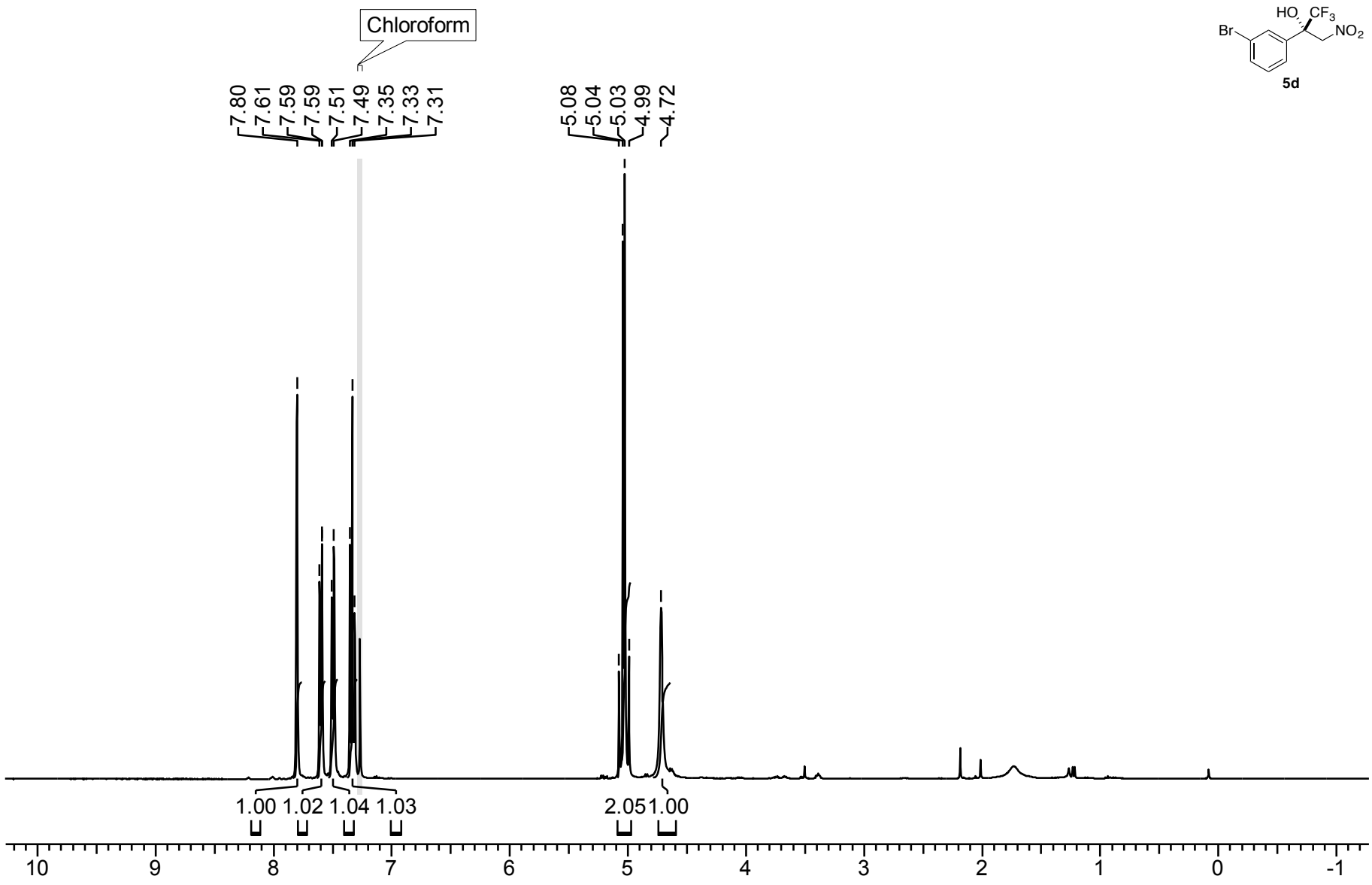

Figure S250. ^{1}H NMR (400 MHz, $CDCl_3$) spectrum of **5d**.

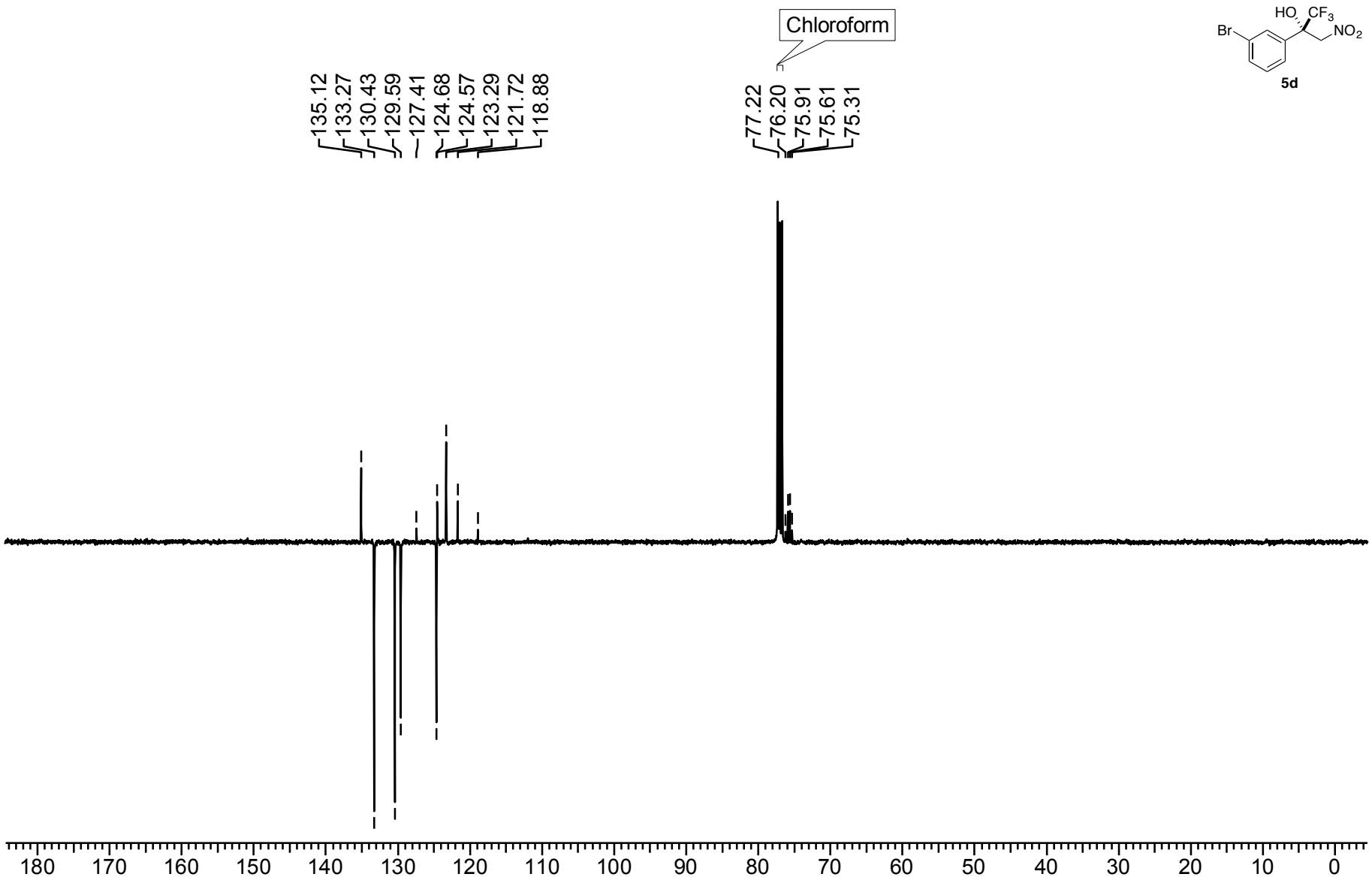

Figure S251. ^{13}C NMR APT (100 MHz, $CDCl_3$) spectrum of **5d**.

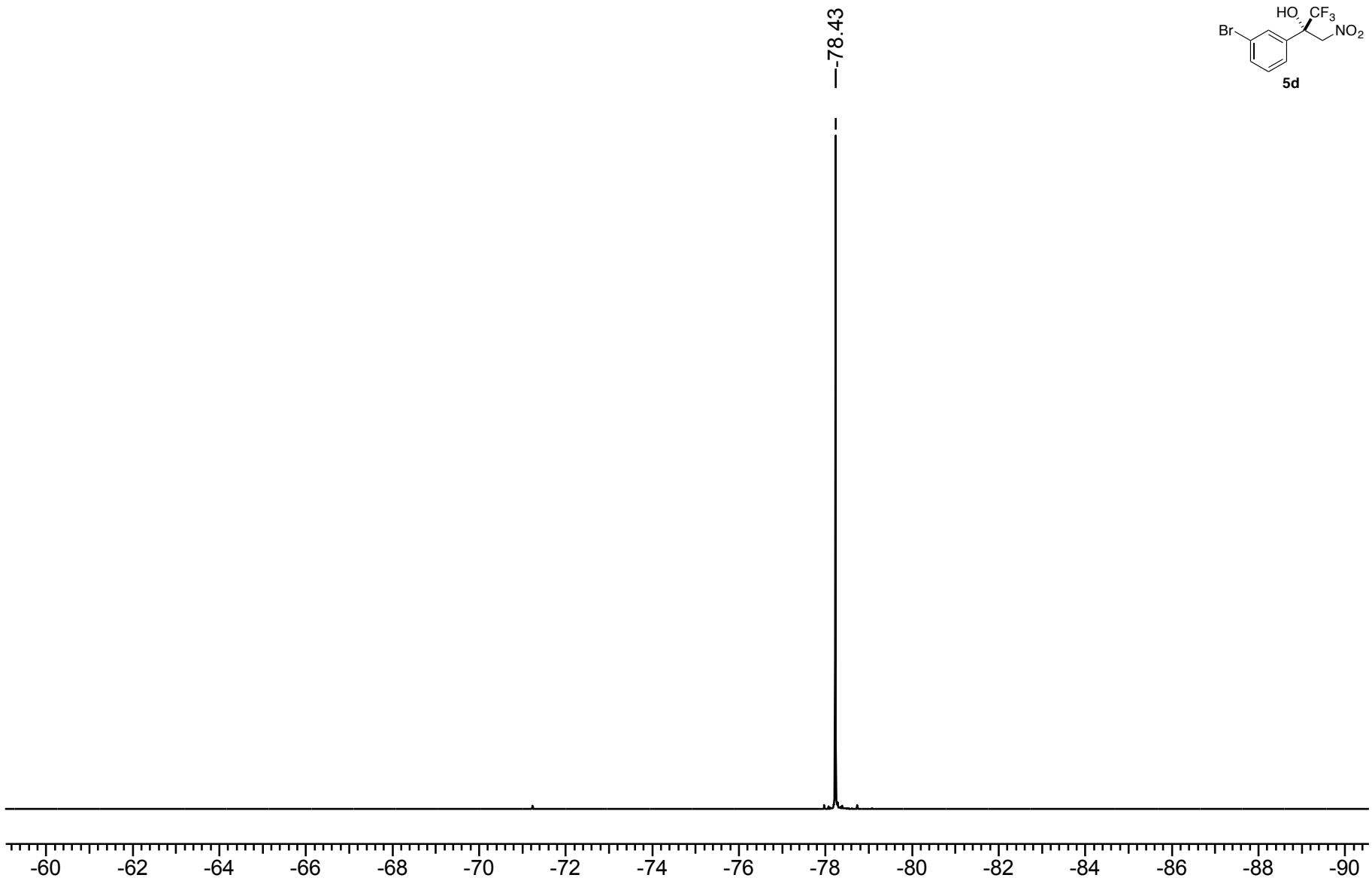

Figure S252. ^{19}F NMR (376 MHz, $CDCl_3$) spectrum of **5d**.

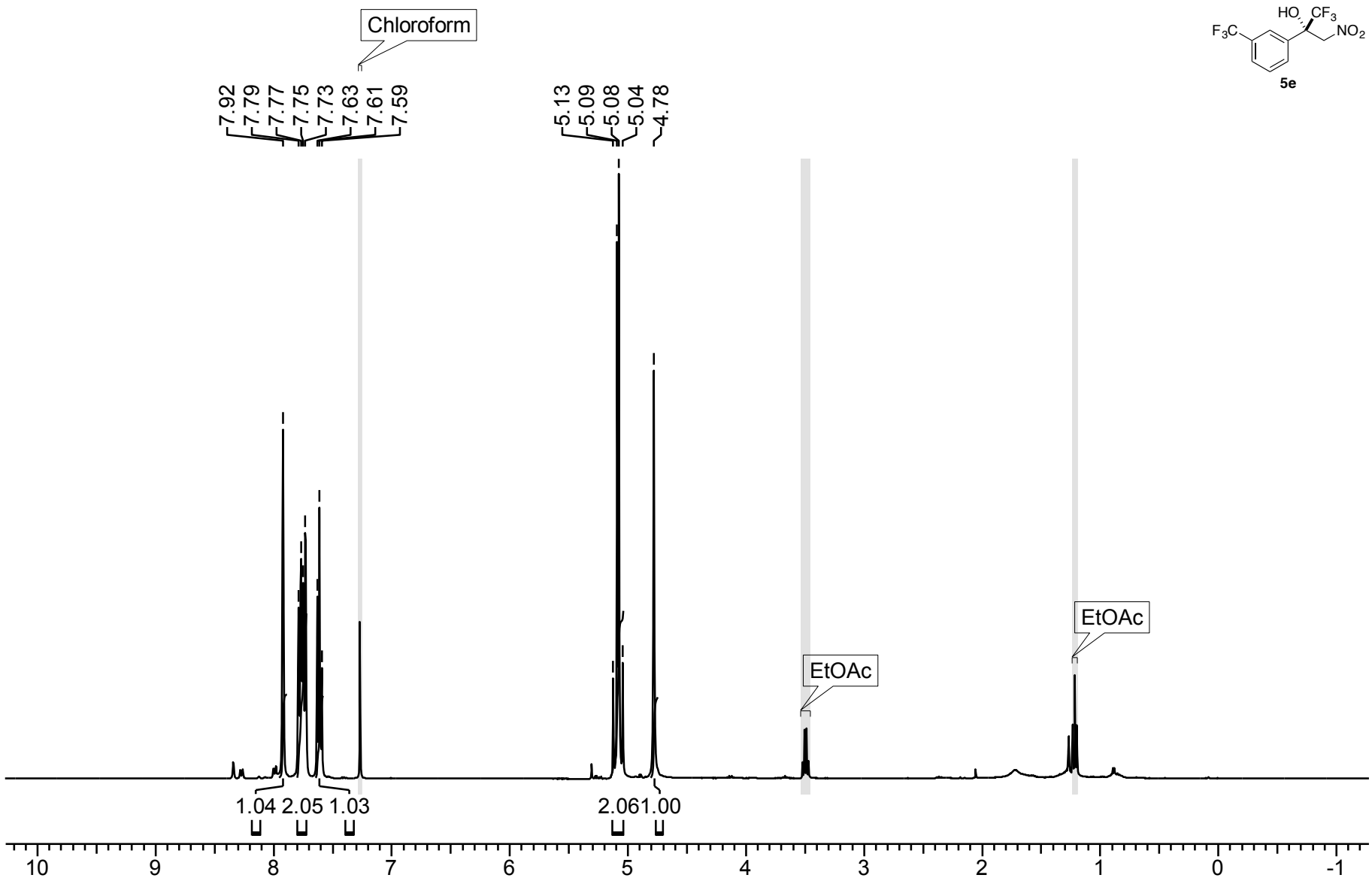

Figure S253. ^{1}H NMR (400 MHz, $CDCl_3$) spectrum of **5e**.

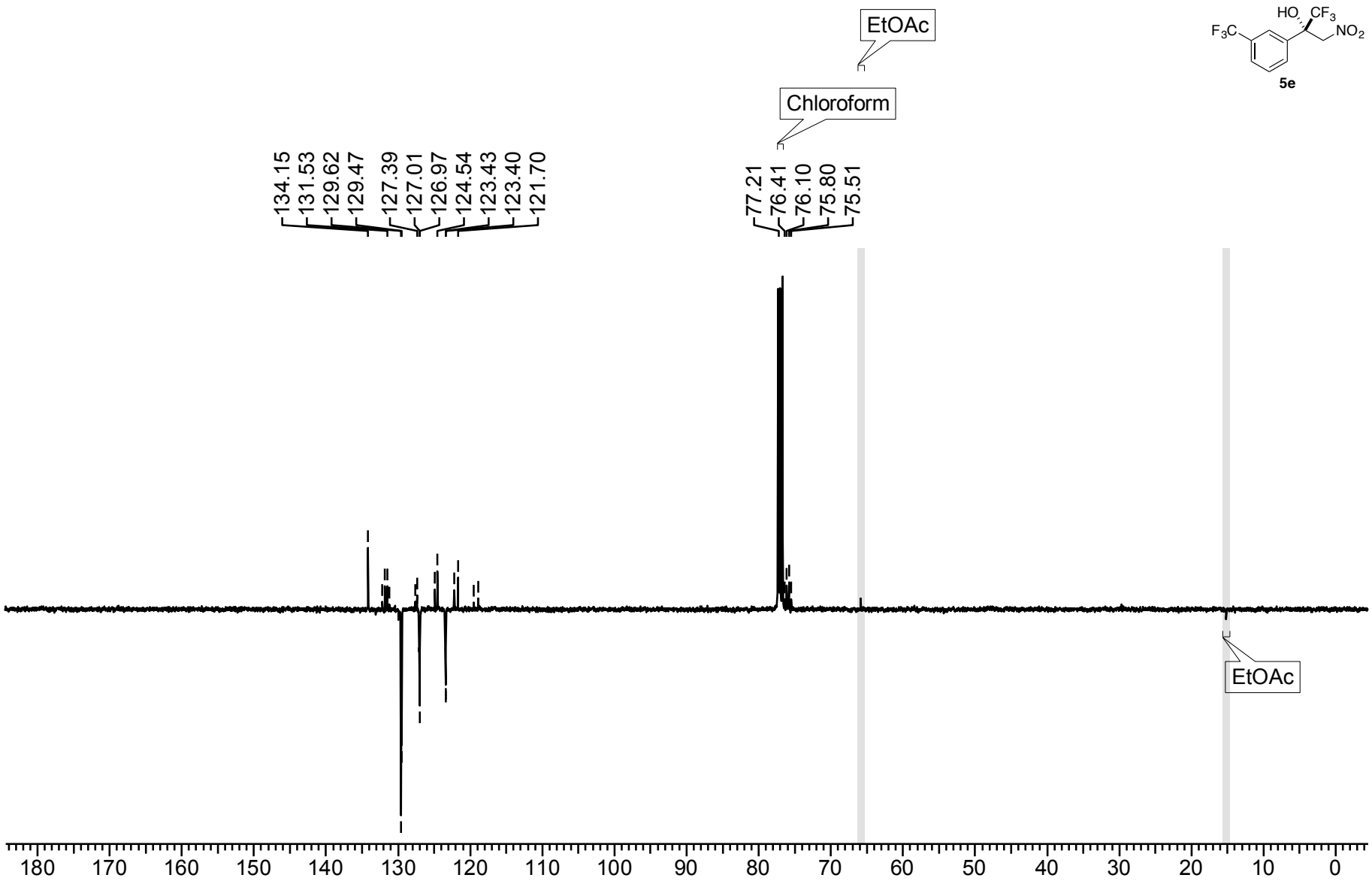

Figure S254. ^{13}C NMR APT (100 MHz, $CDCl_3$) spectrum of **5e**.

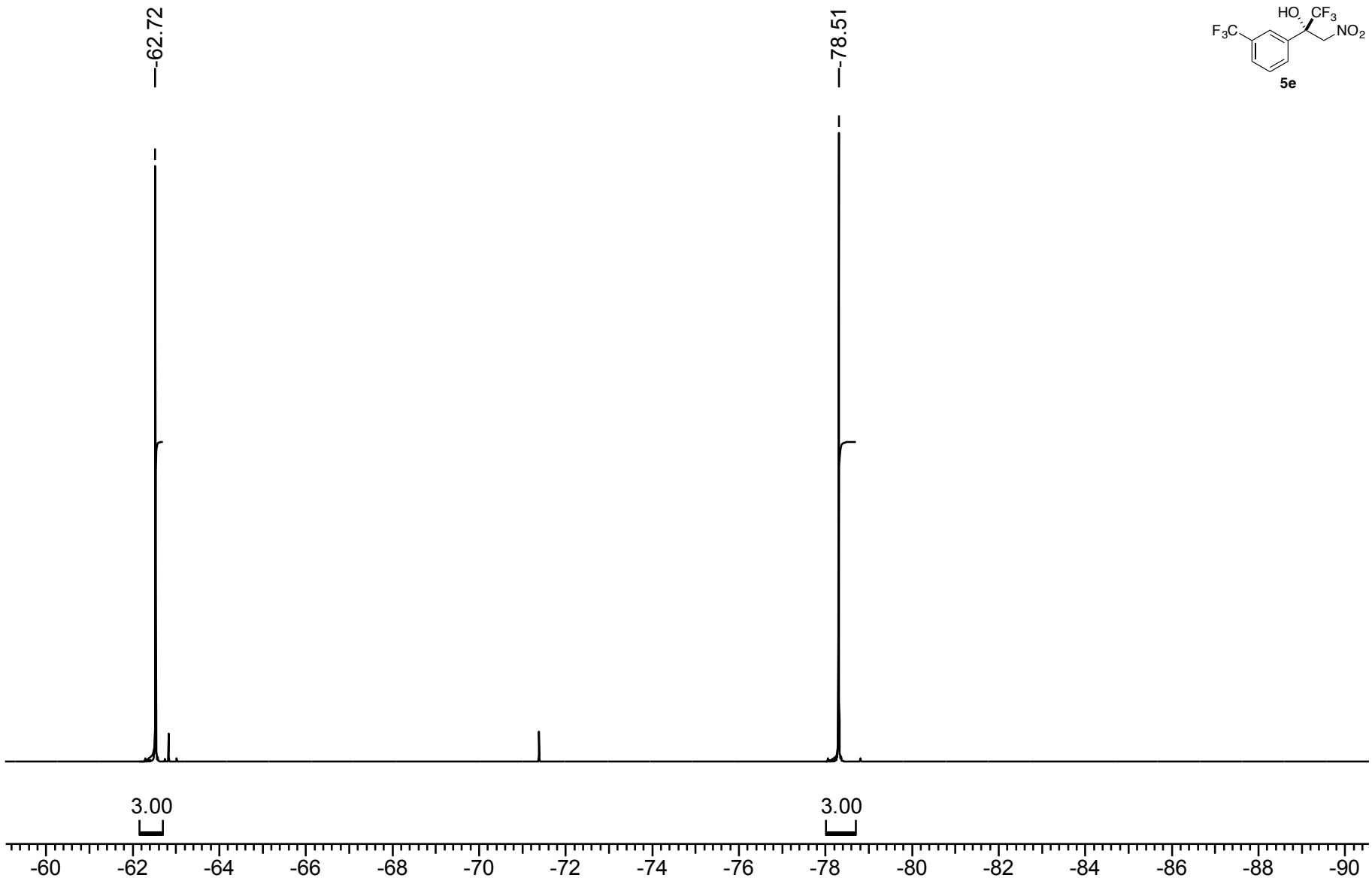

Figure S255. ^{19}F NMR (376 MHz, $CDCl_3$) spectrum of **5e**.

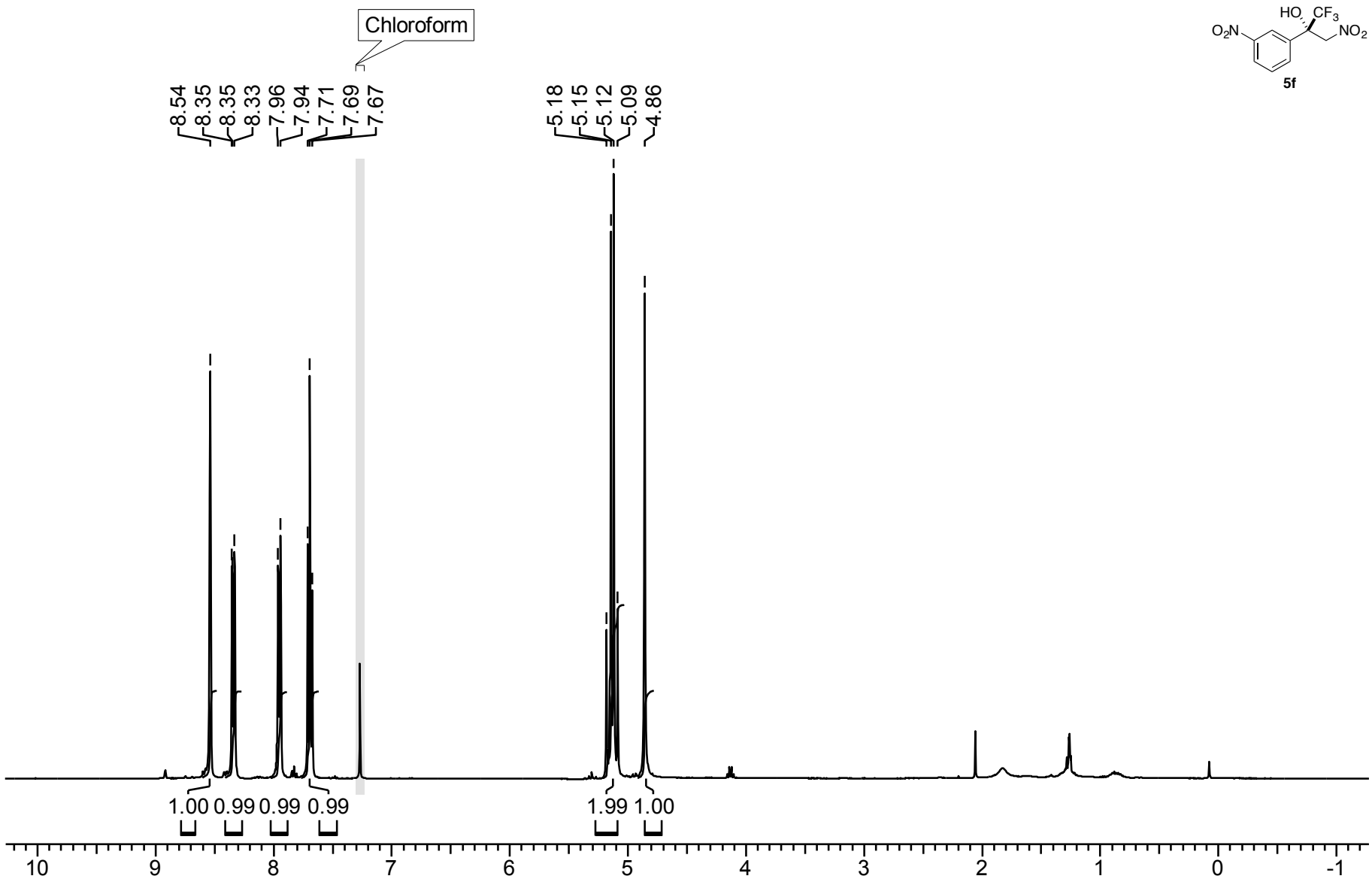

Figure S256. ^{1}H NMR (400 MHz, $CDCl_3$) spectrum of **5f**.

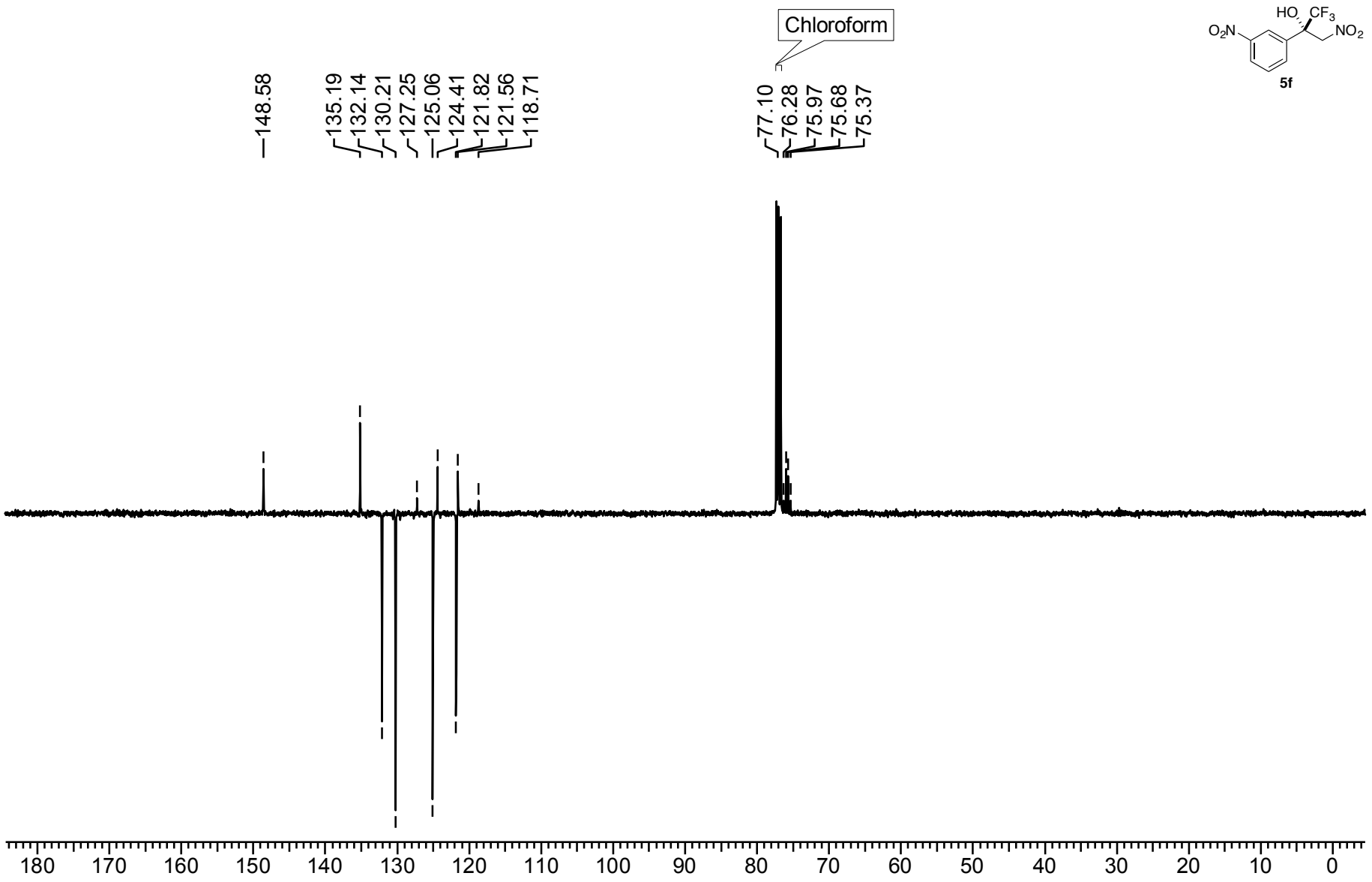

Figure S257. ^{13}C NMR APT (100 MHz, $CDCl_3$) spectrum of **5f**.

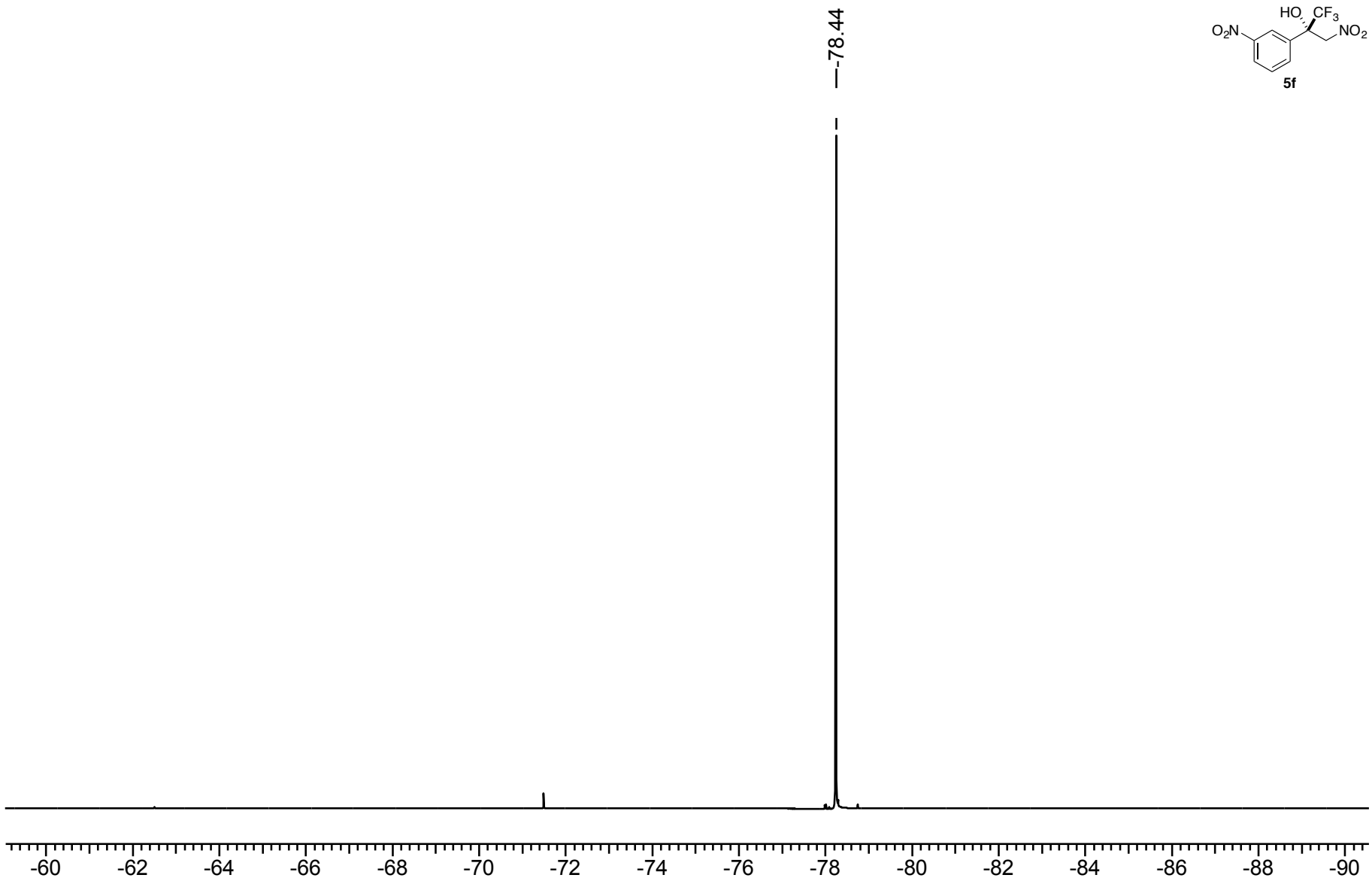

Figure S258. ^{19}F NMR (376 MHz, $CDCl_3$) spectrum of **5f**.

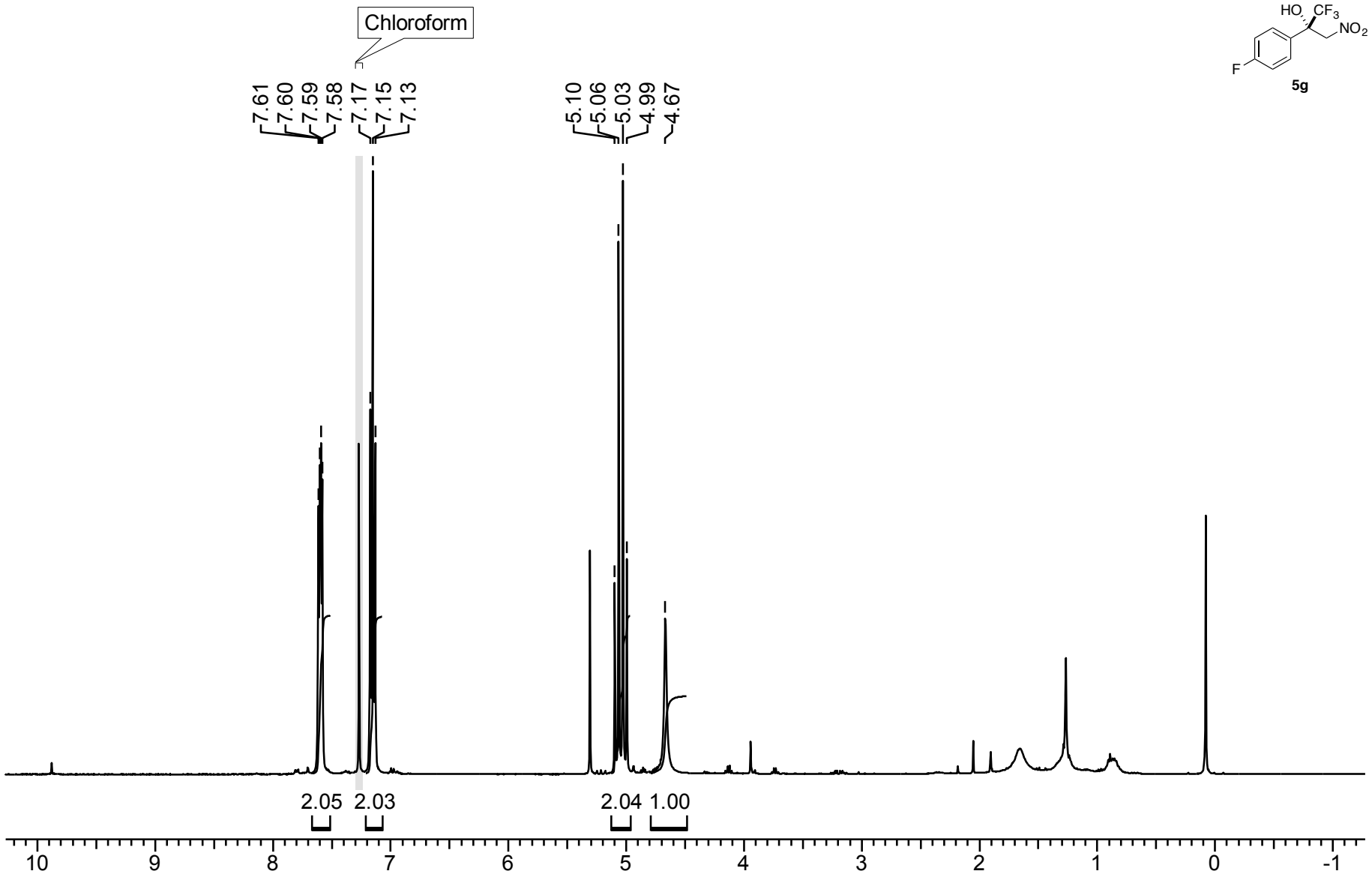

Figure S259. ^{1}H NMR (400 MHz, $CDCl_3$) spectrum of **5g**.

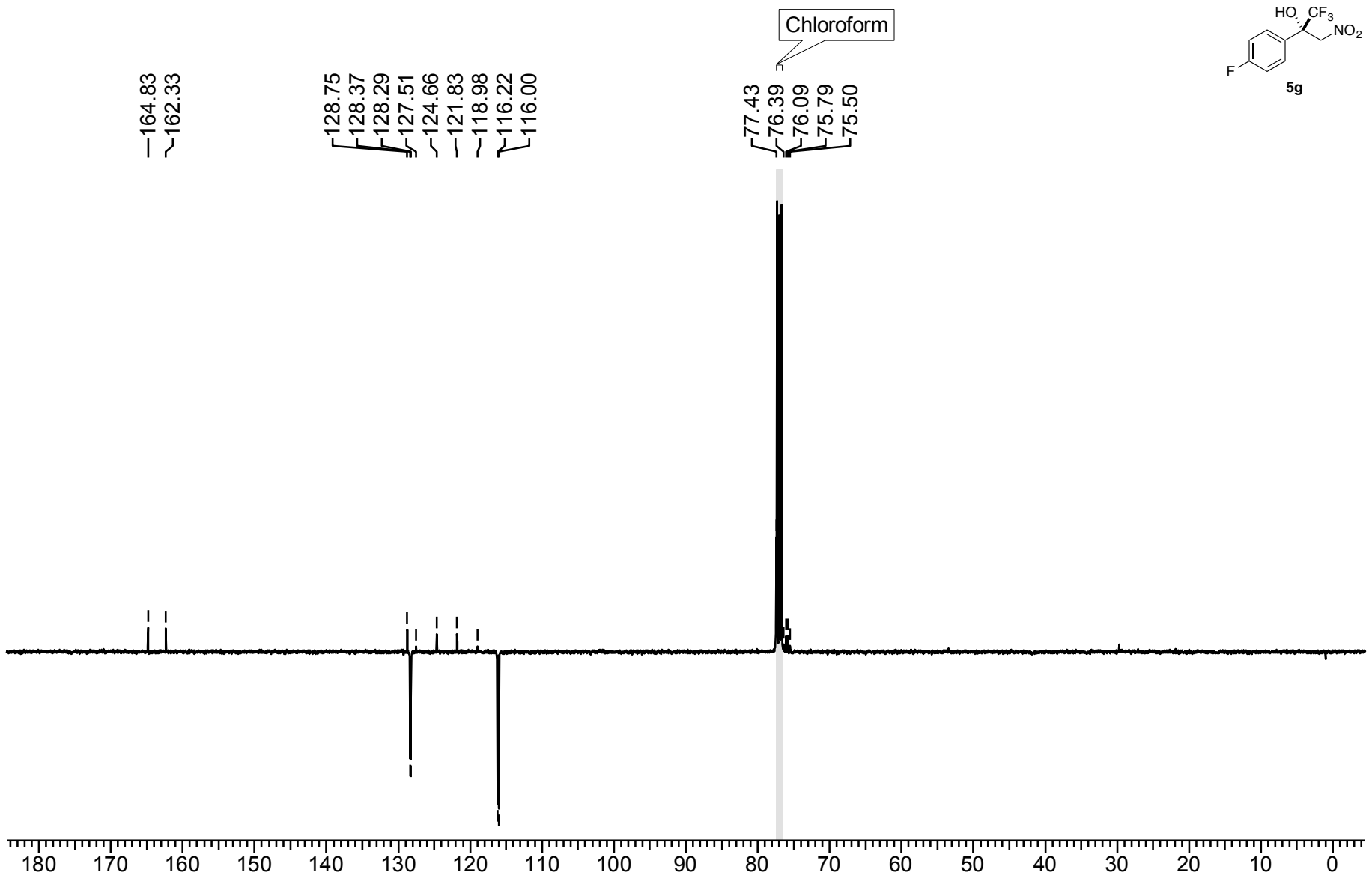

Figure S260. ^{13}C NMR APT (100 MHz, $CDCl_3$) spectrum of **5g**.

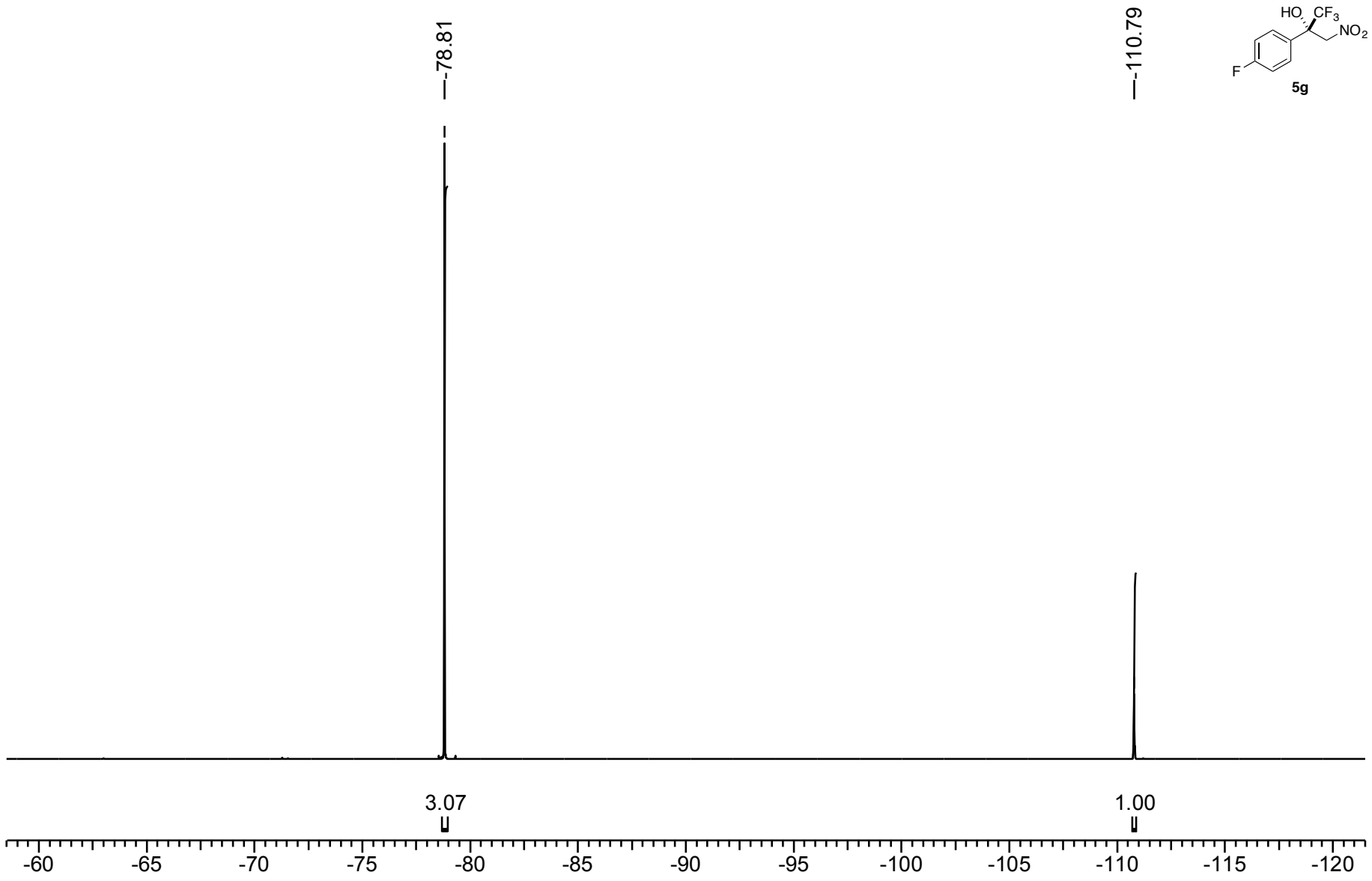

Figure S261. ^{19}F NMR (376 MHz, $CDCl_3$) spectrum of **5g**.

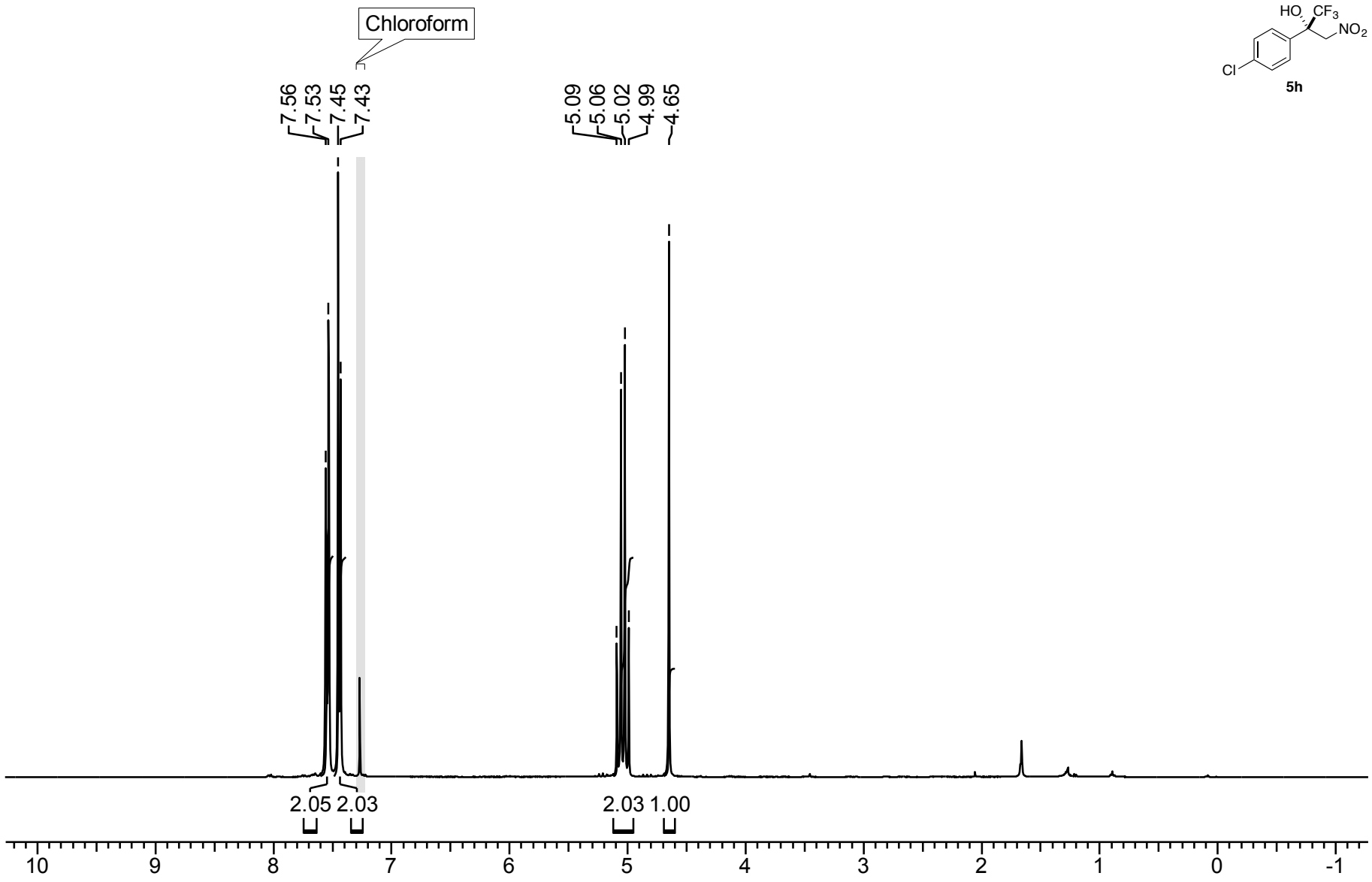

Figure S262. ^{1}H NMR (400 MHz, $CDCl_3$) spectrum of **5h**.

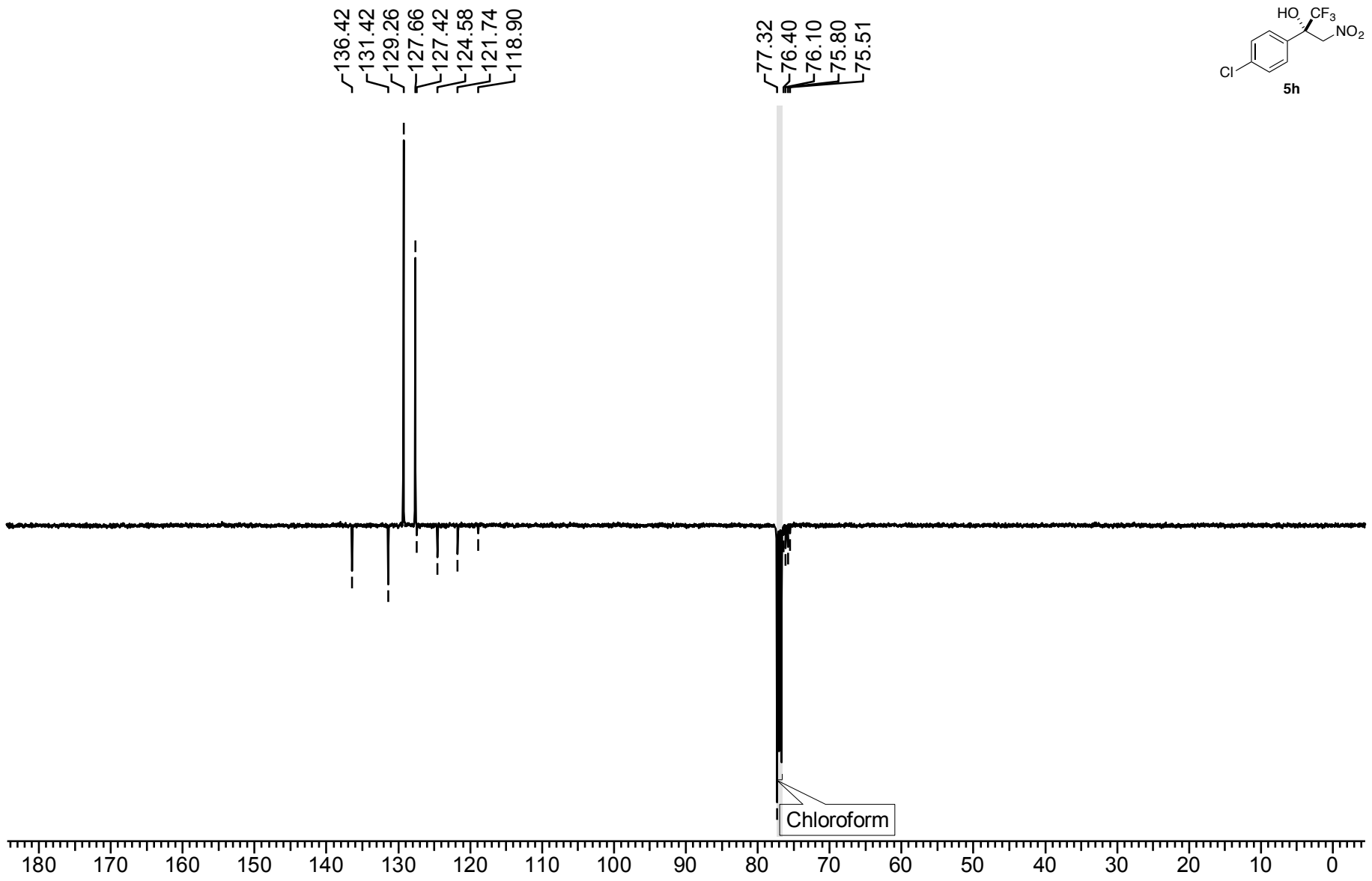

Figure S263. ^{13}C NMR (100 MHz, $CDCl_3$) spectrum of **5h**.

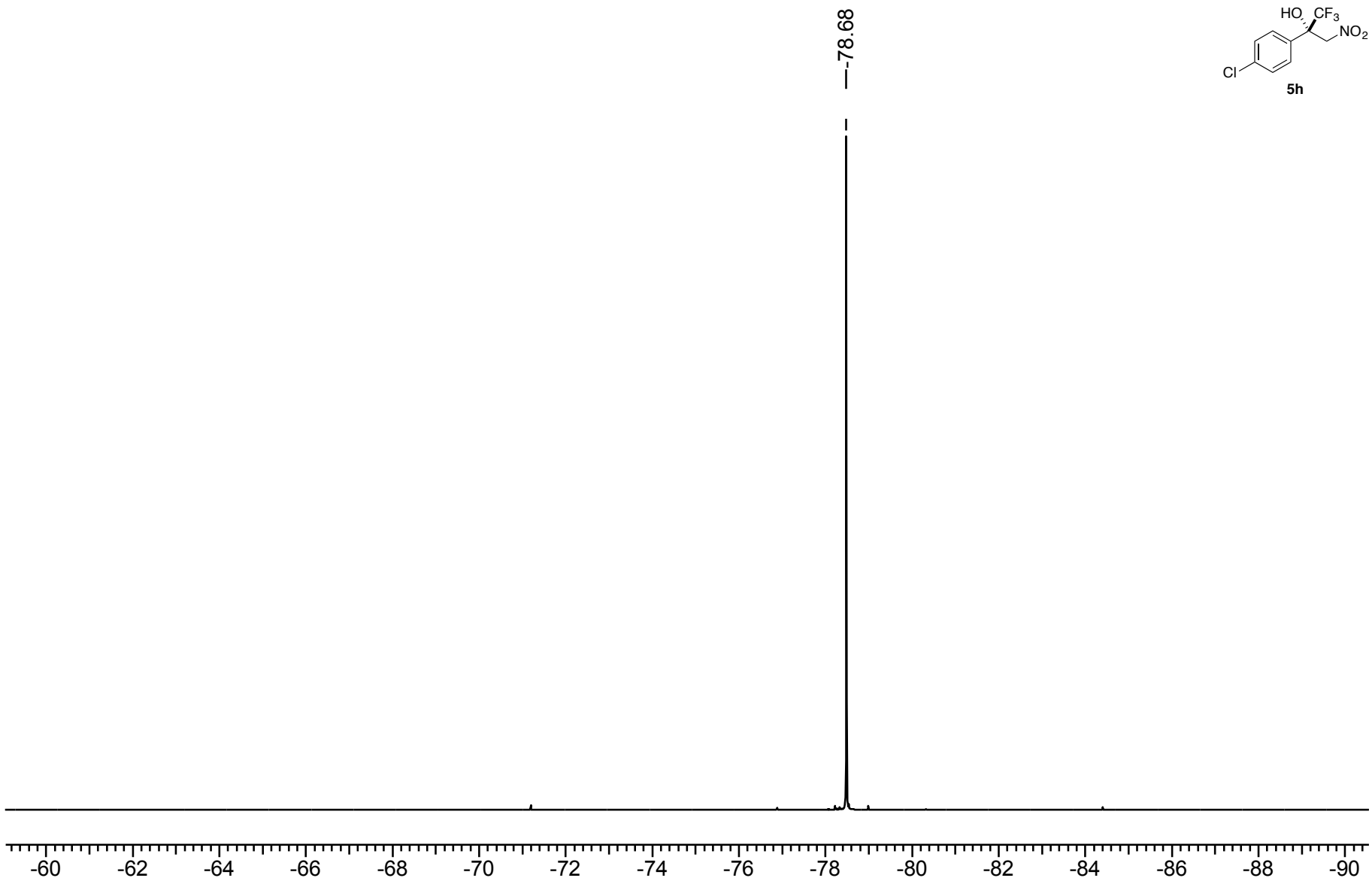

Figure S264. ^{19}F NMR (376 MHz, $CDCl_3$) spectrum of **5h**.

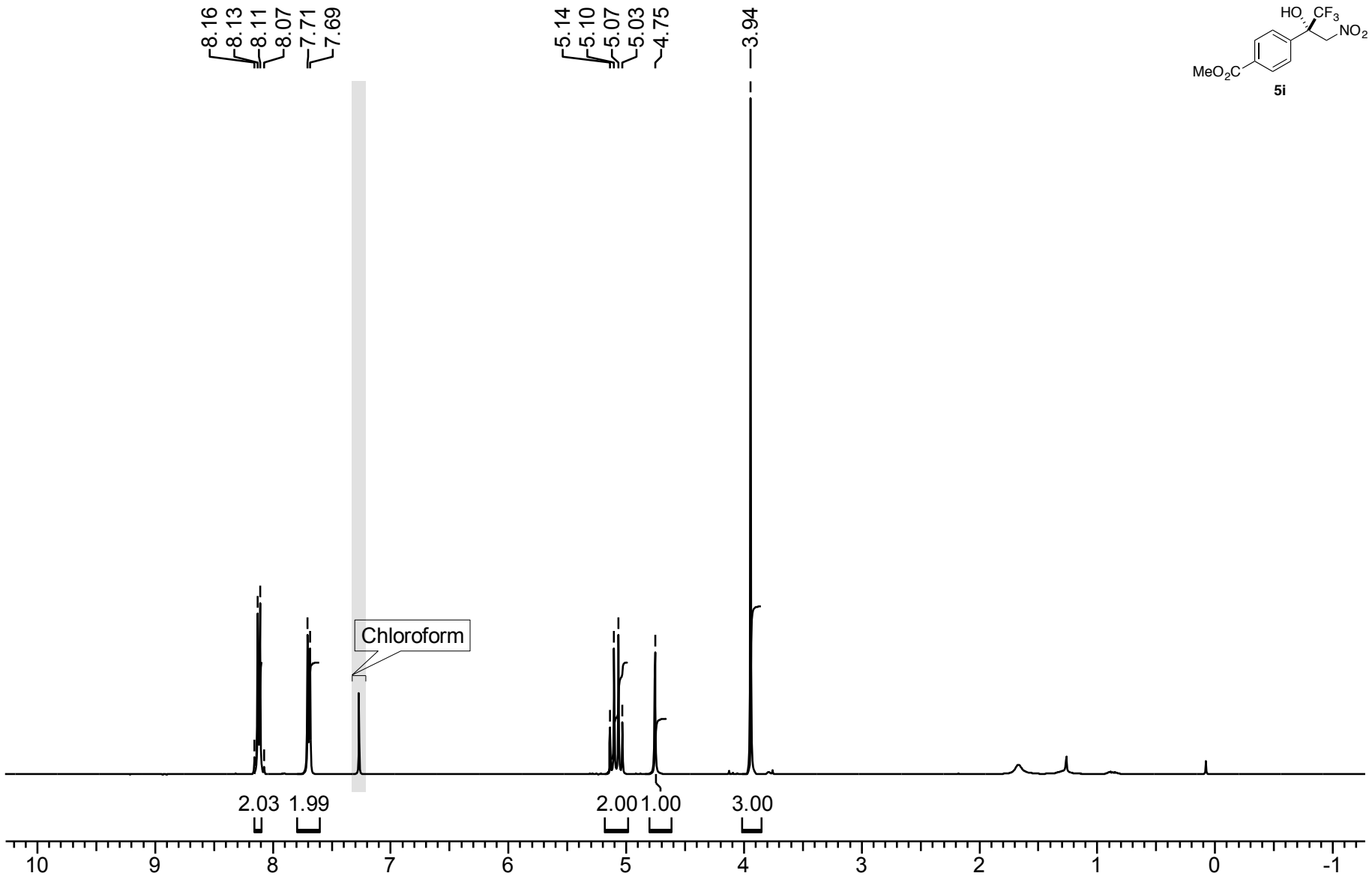

Figure S265. ^{1}H NMR (400 MHz, $CDCl_3$) spectrum of **5i**.

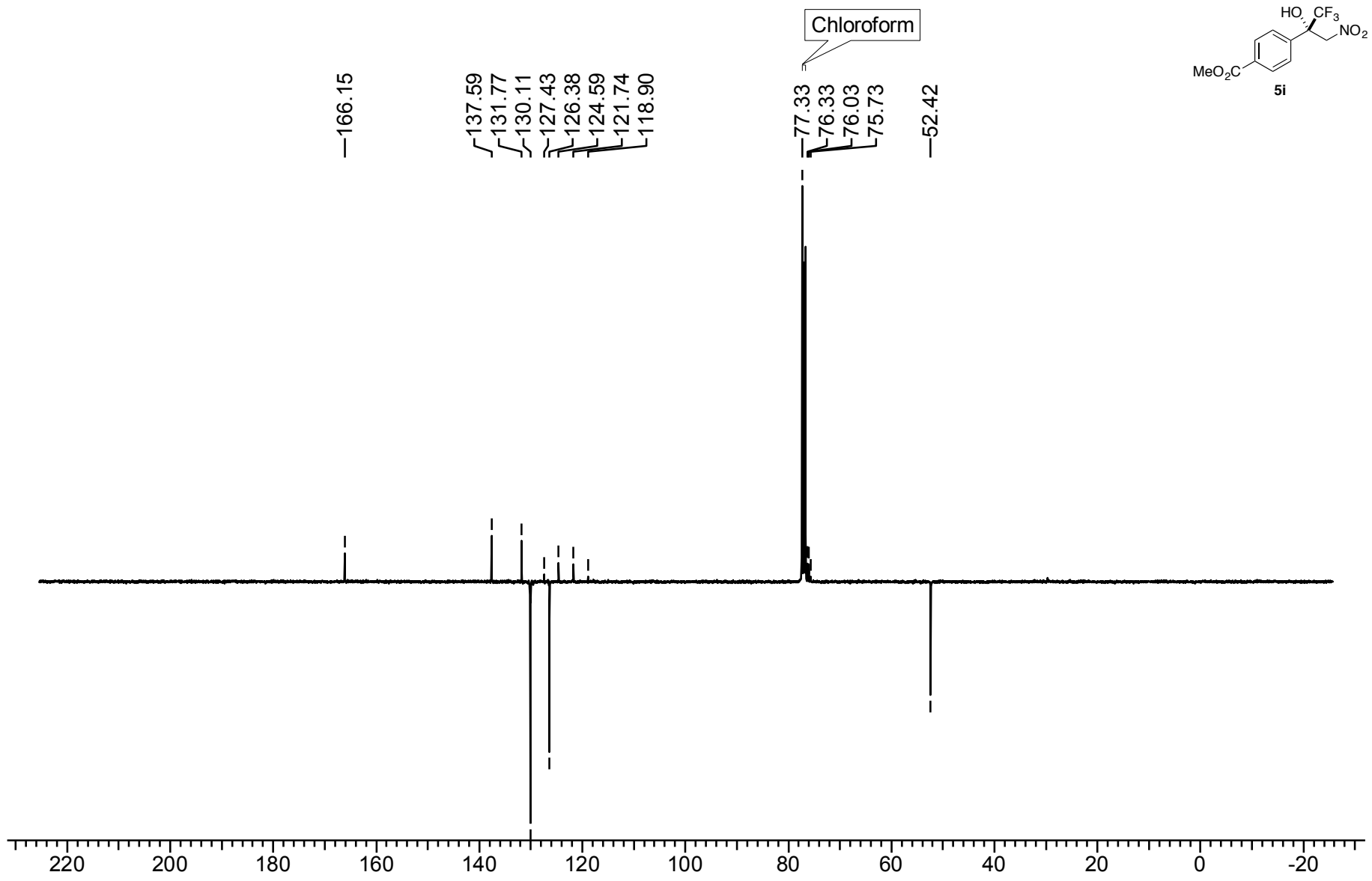

Figure S266. ^{13}C NMR APT (100 MHz, $CDCl_3$) spectrum of **5i**.

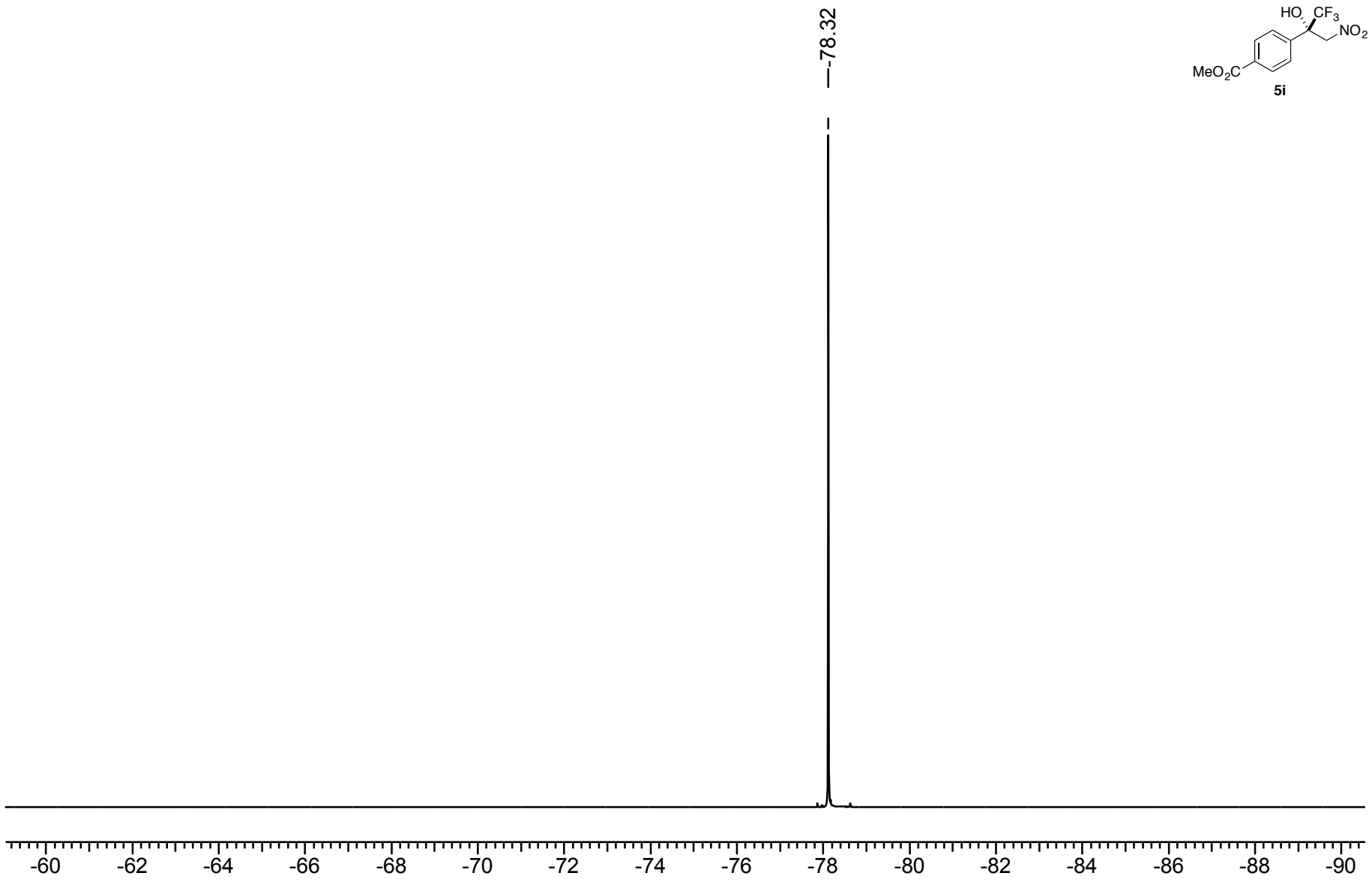

Figure S267. ^{19}F NMR (376 MHz, $CDCl_3$) spectrum of **5i**.

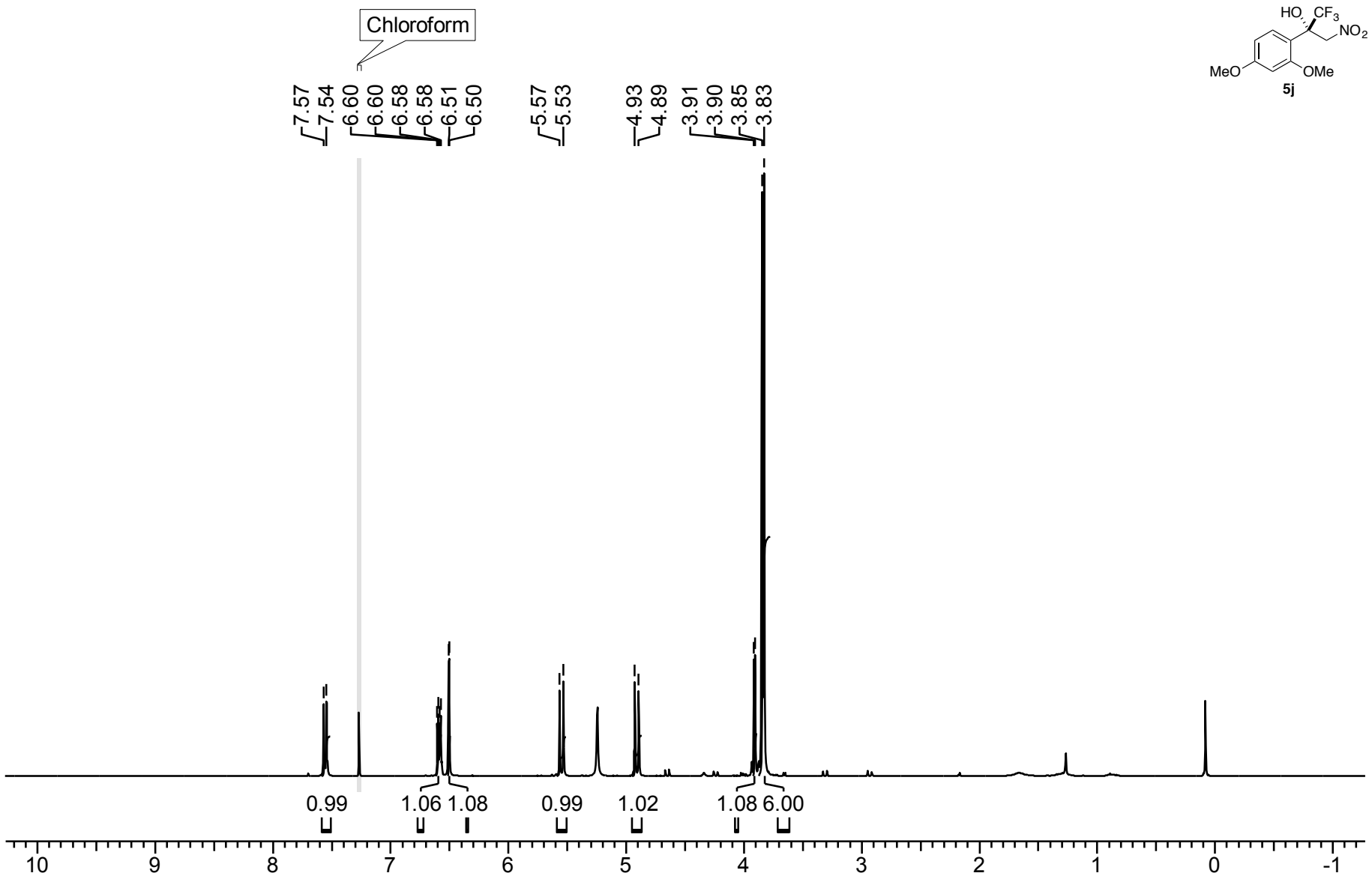

Figure S268. ^{1}H NMR (400 MHz, $CDCl_3$) spectrum of **5j**.

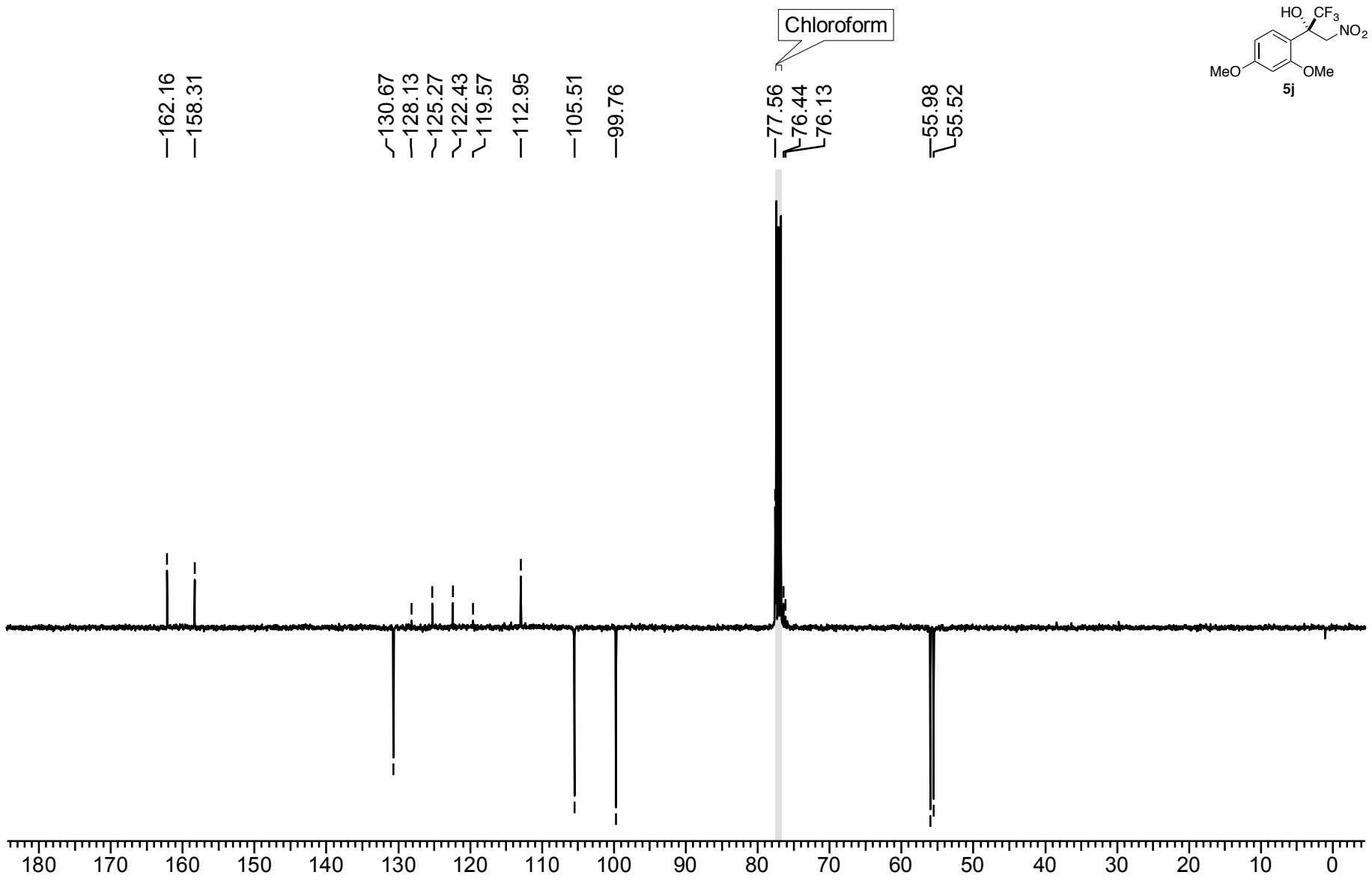

Figure S269. ^{13}C NMR APT (100 MHz, $CDCl_3$) spectrum of **5j**.

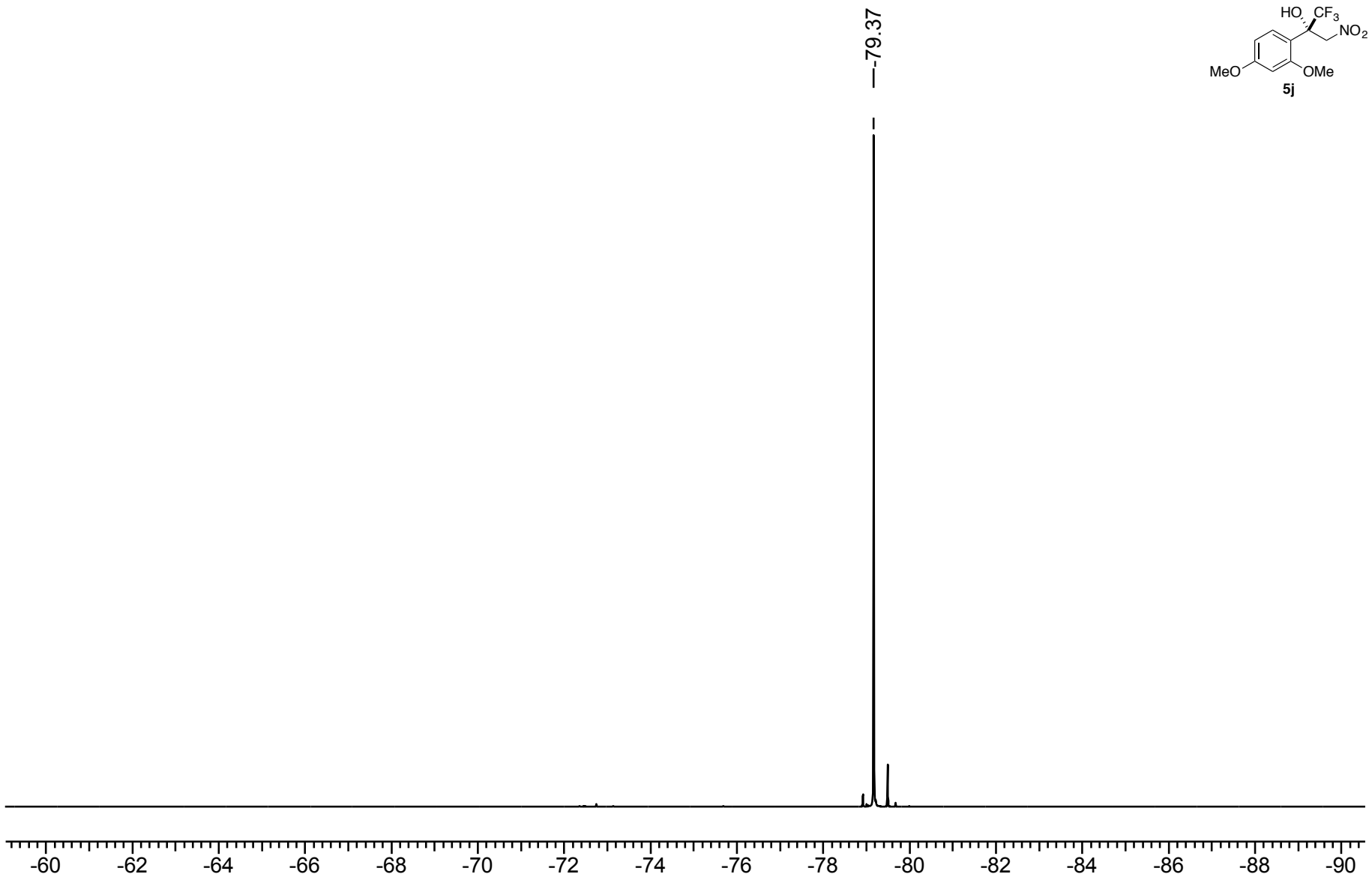

Figure S270. ^{19}F NMR (376 MHz, $CDCl_3$) spectrum of **5j**.

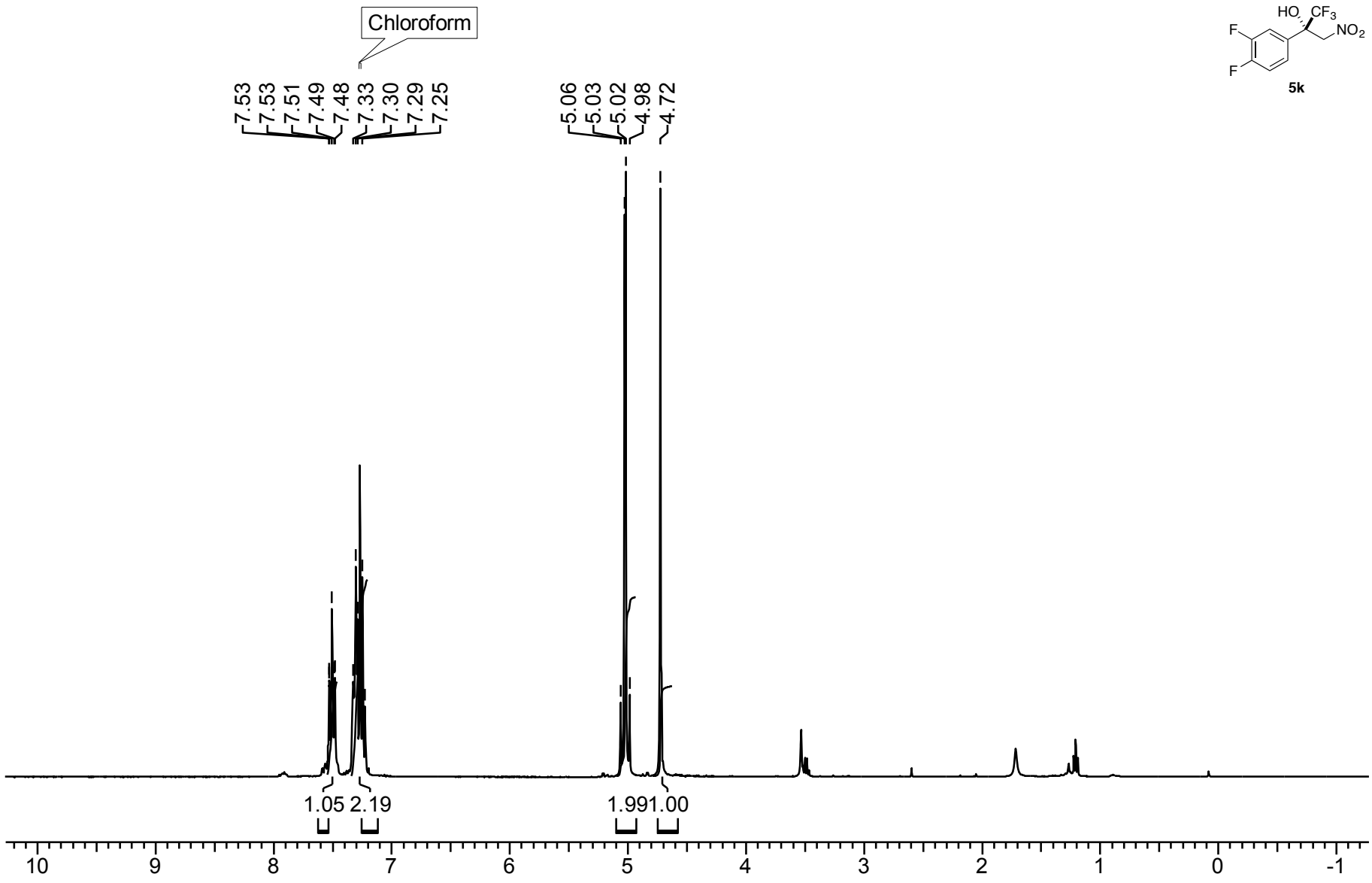

Figure S271. ^{1}H NMR (400 MHz, $CDCl_3$) spectrum of **5k**.

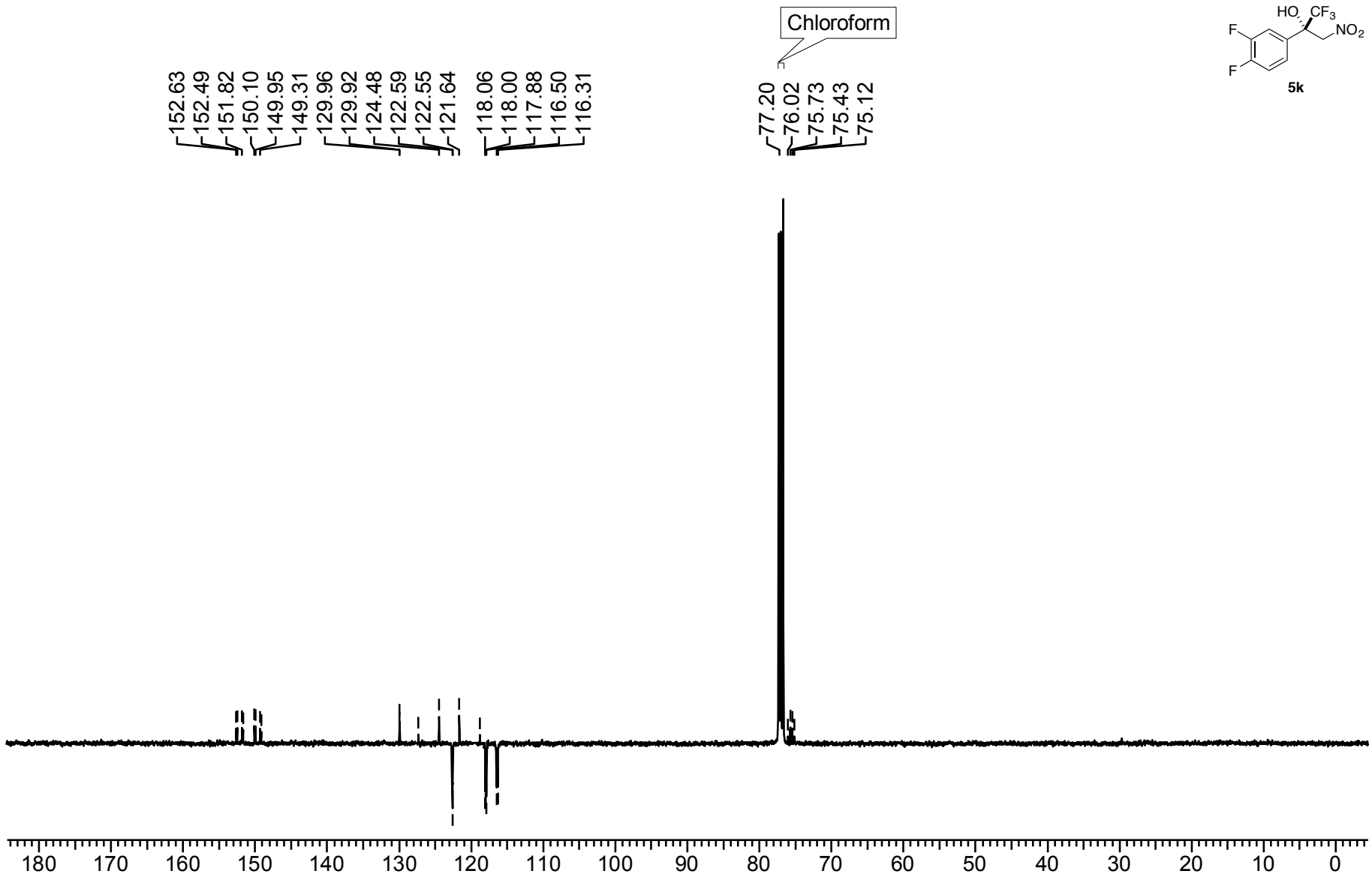

Figure S272. ^{13}C NMR APT (100 MHz, $CDCl_3$) spectrum of **5k**.

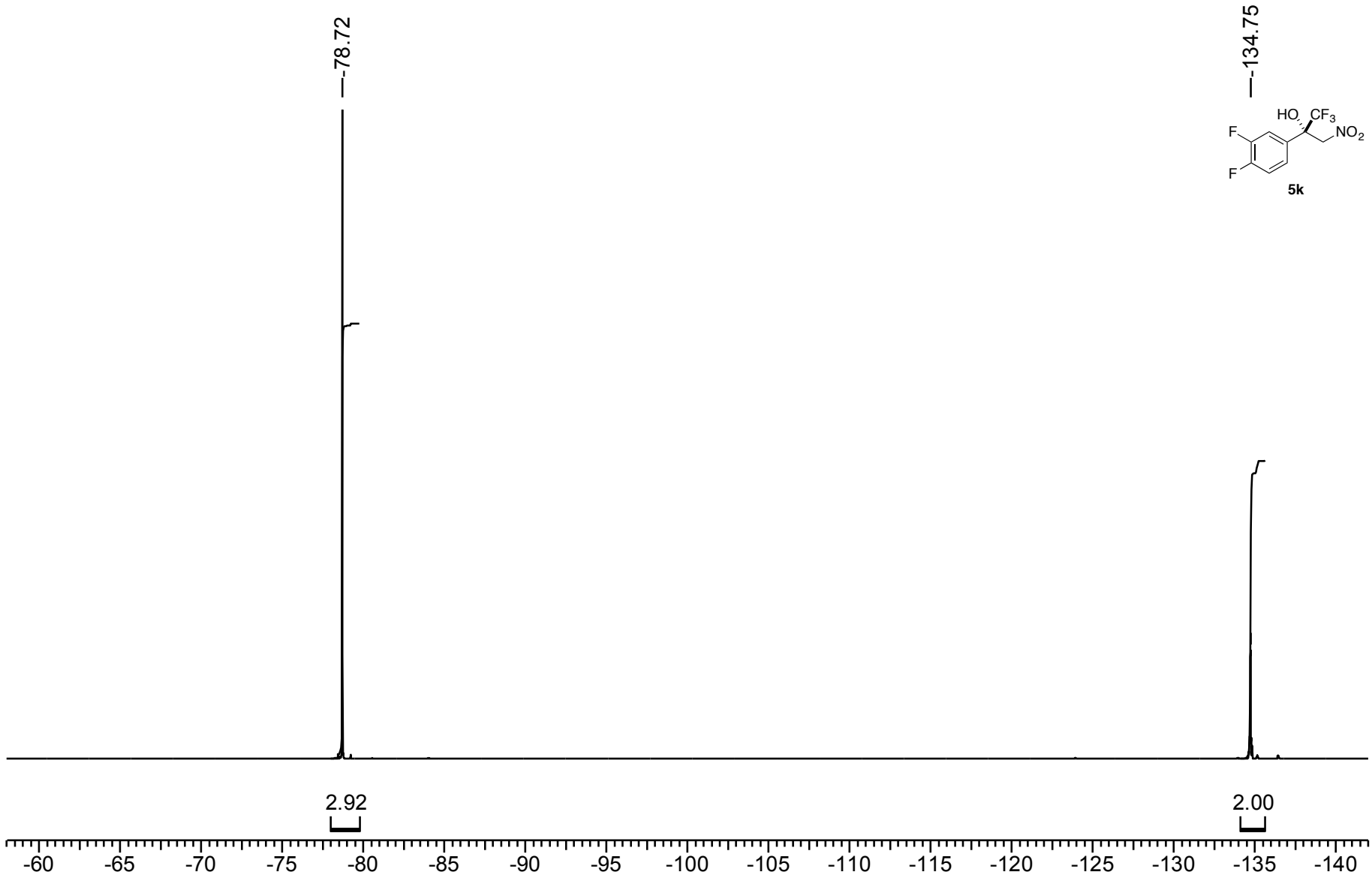

Figure S273. ^{19}F NMR (376 MHz, $CDCl_3$) spectrum of **5k**.

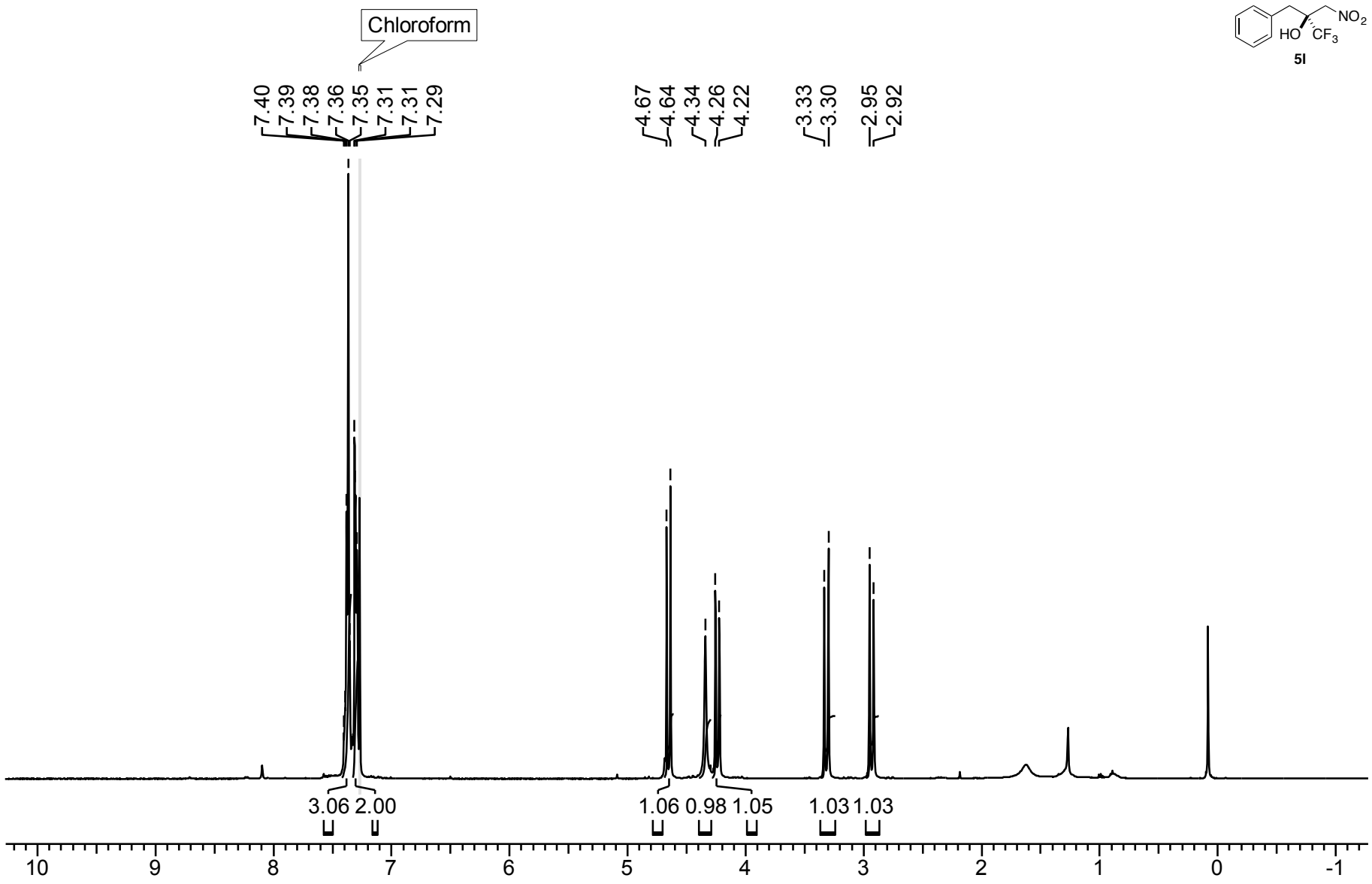

Figure S274. ^{1}H NMR (400 MHz, $CDCl_3$) spectrum of **5l**.

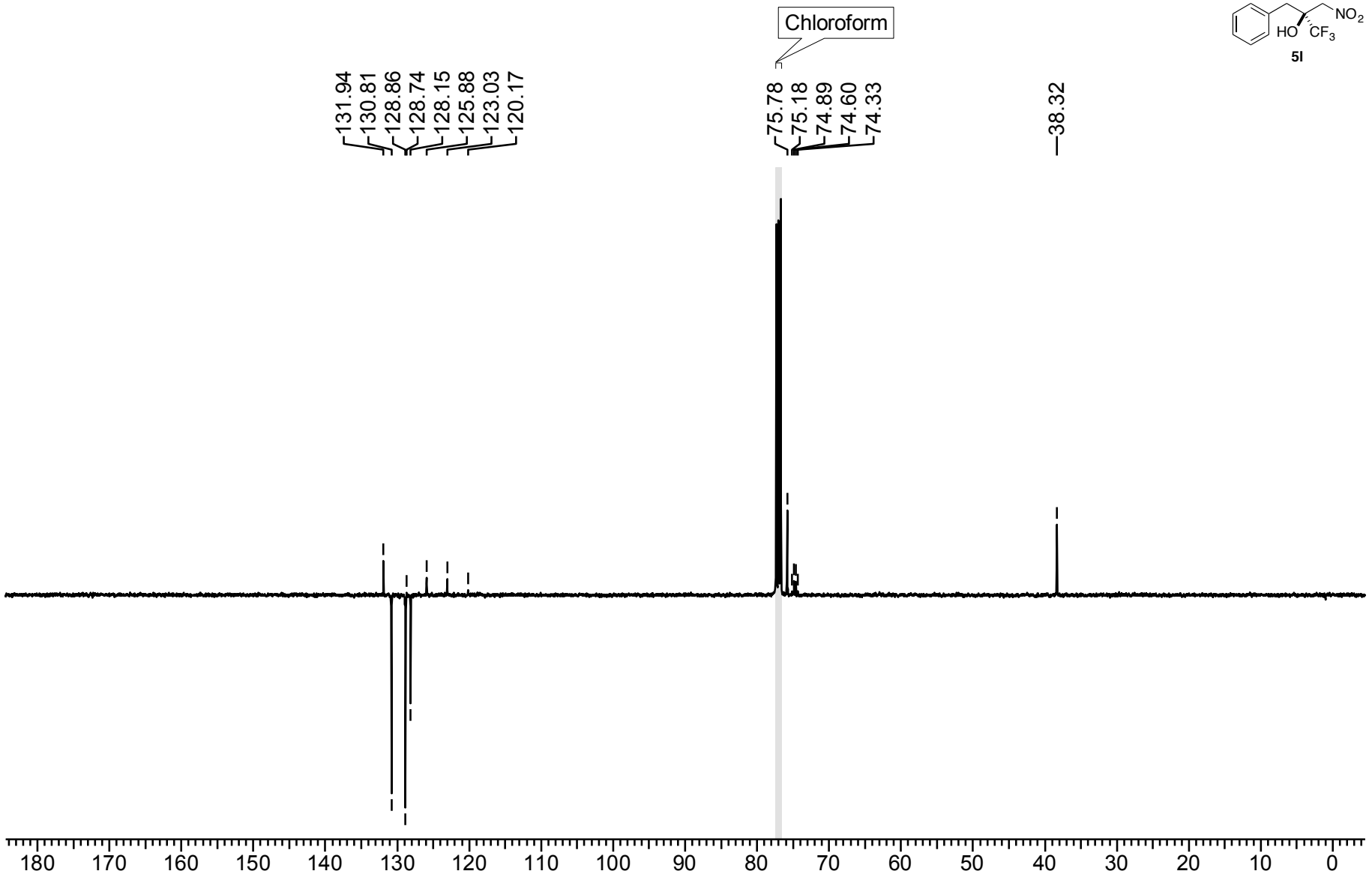

Figure S275. ^{13}C NMR APT (100 MHz, $CDCl_3$) spectrum of **5l**.

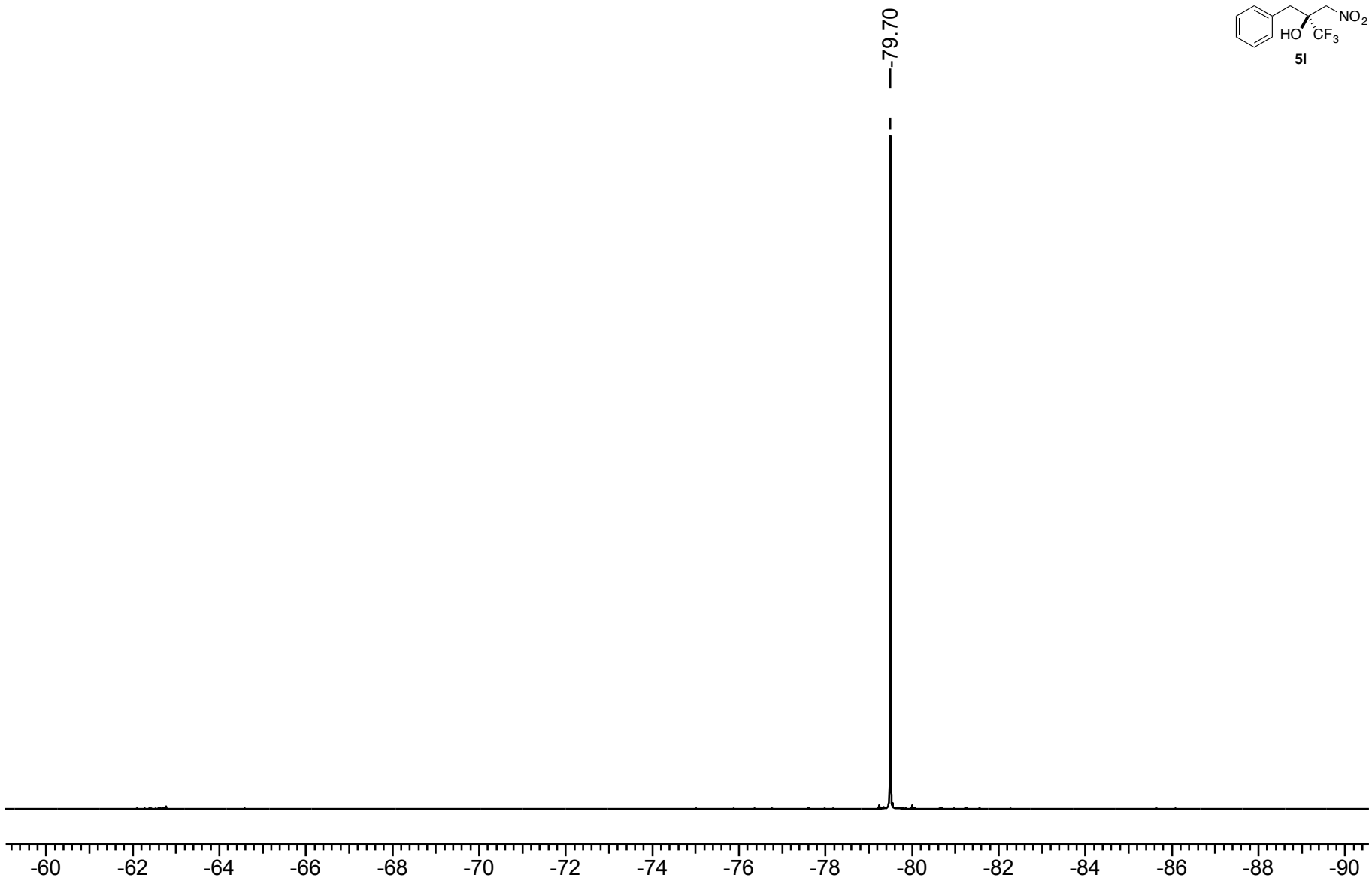

Figure S276. ^{19}F NMR (376 MHz, $CDCl_3$) spectrum of **5l**.

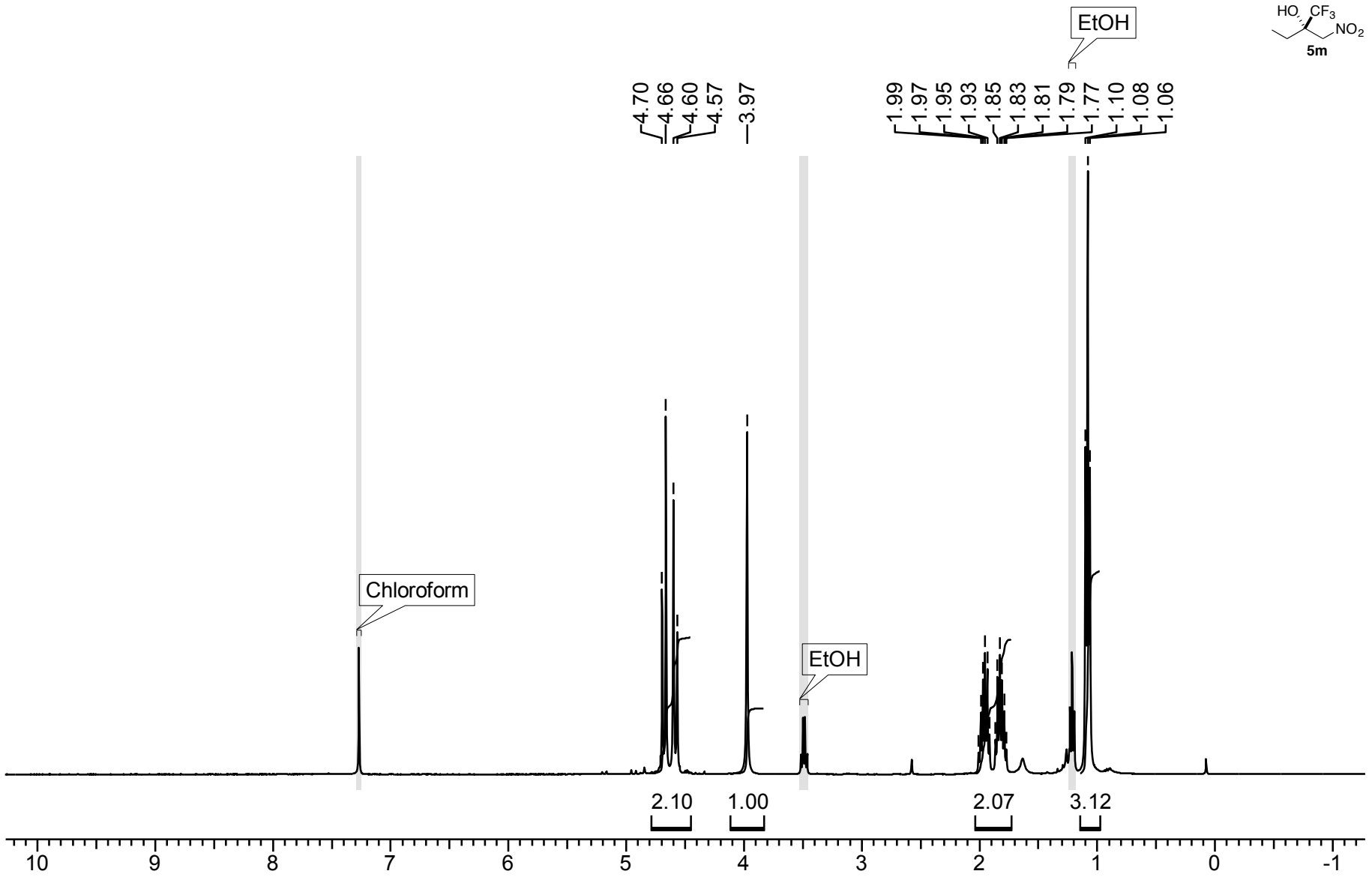

Figure S277. ^{1}H NMR (400 MHz, $CDCl_3$) spectrum of **5m**.

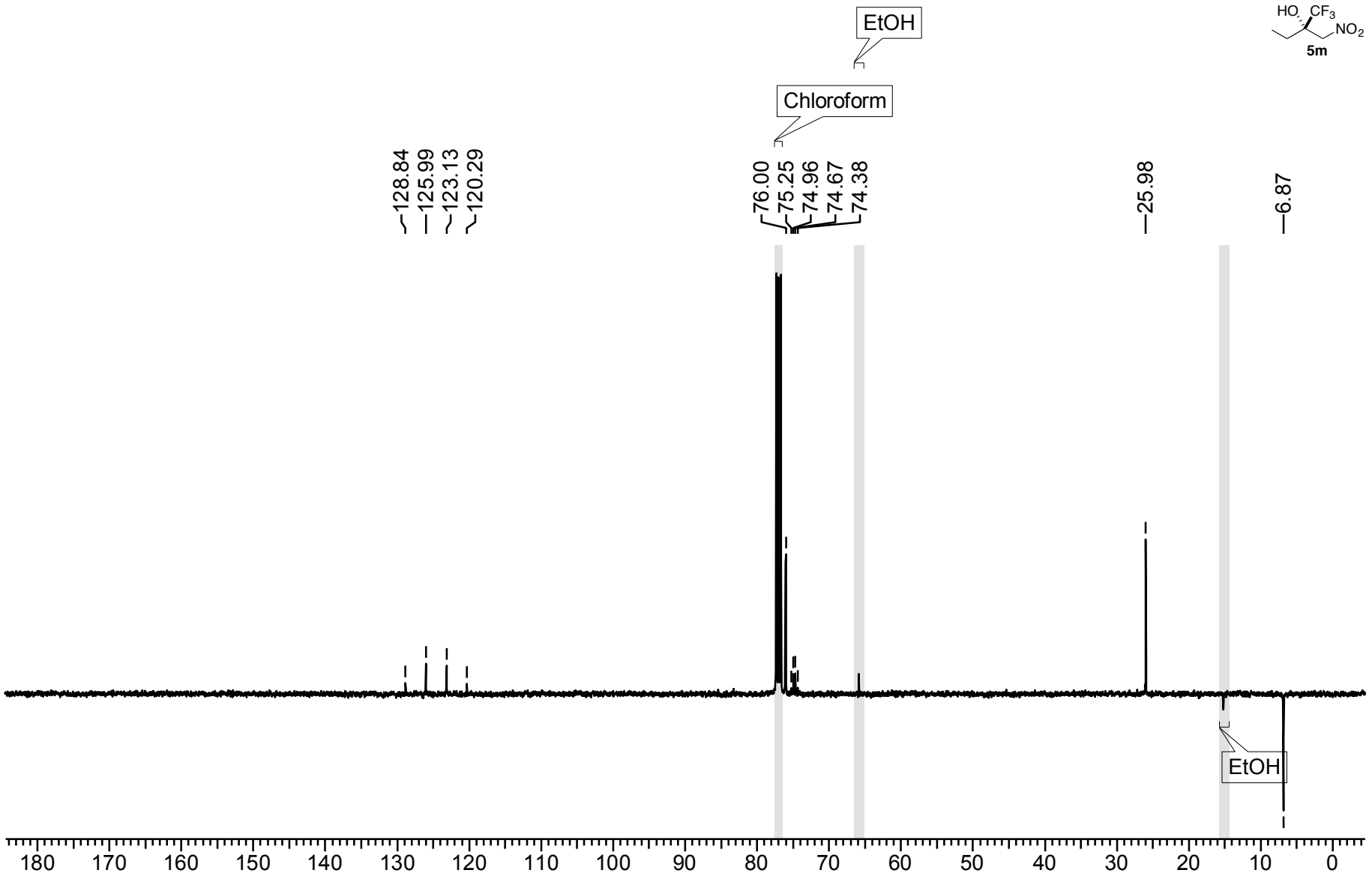

Figure S278. ^{13}C NMR APT (100 MHz, $CDCl_3$) spectrum of **5m**.

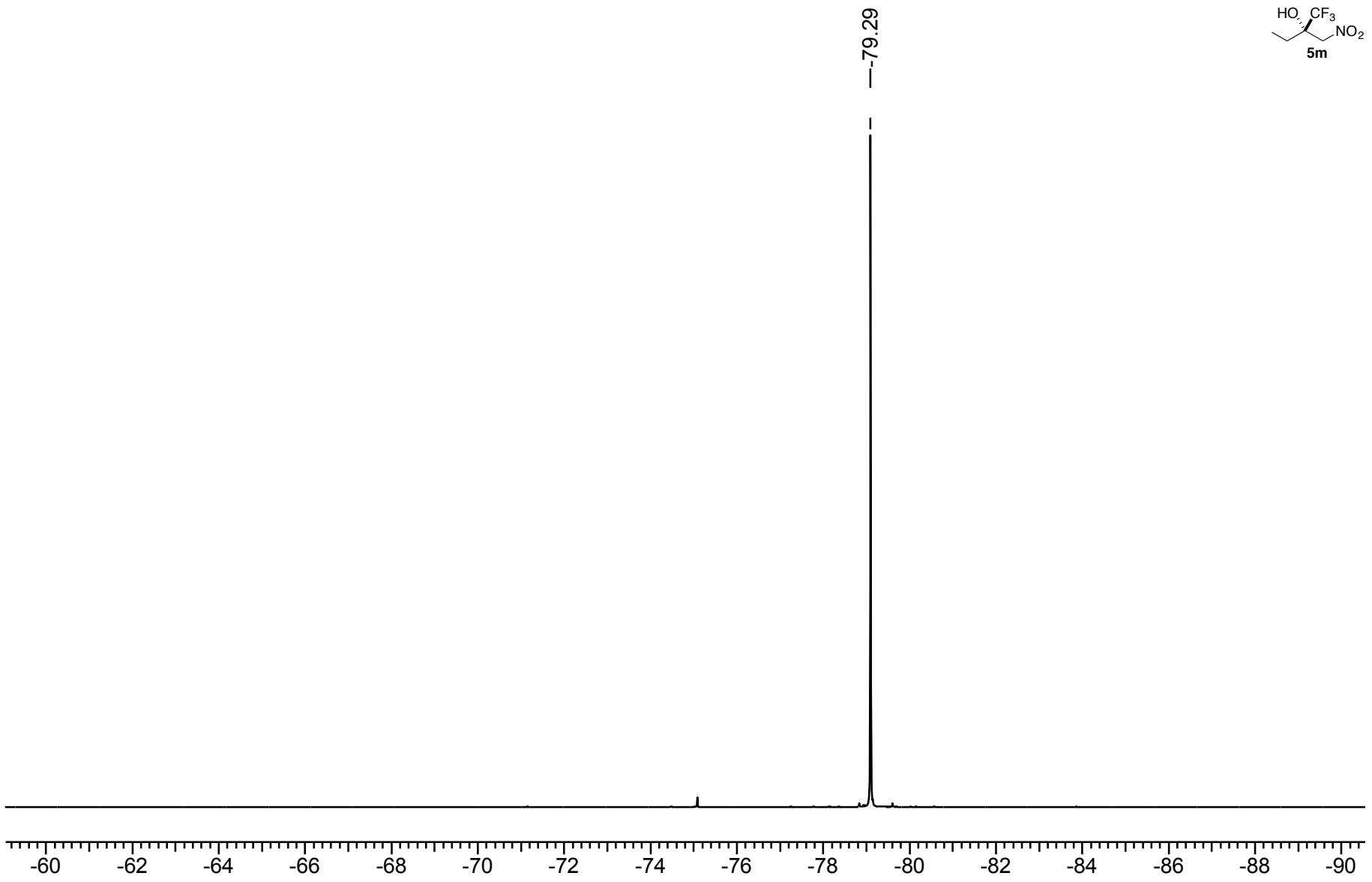

Figure S279. ^{19}F NMR (376 MHz, $CDCl_3$) spectrum of **5m**.

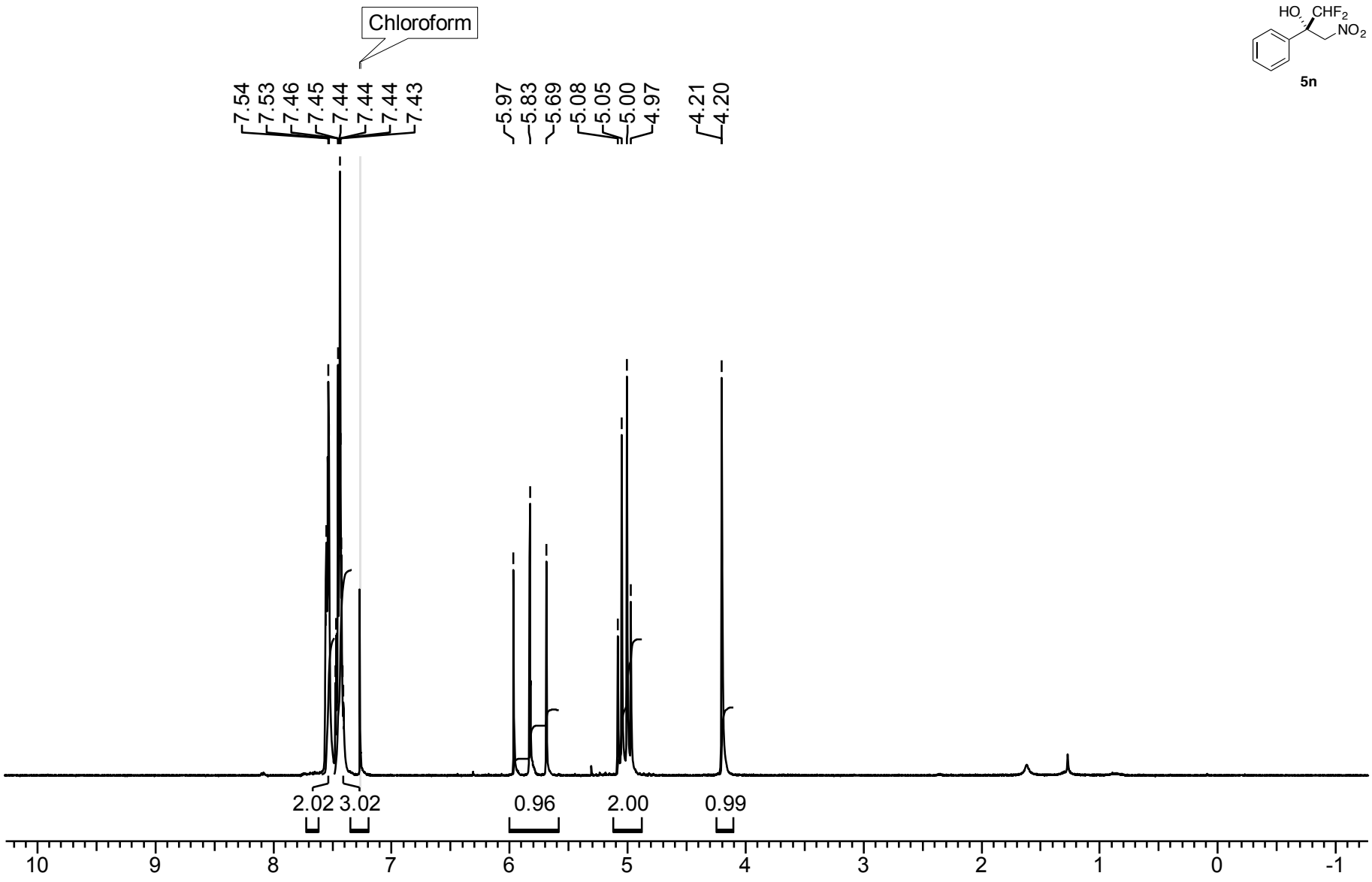

Figure S280. ^{1}H NMR (400 MHz, $CDCl_3$) spectrum of **5n**.

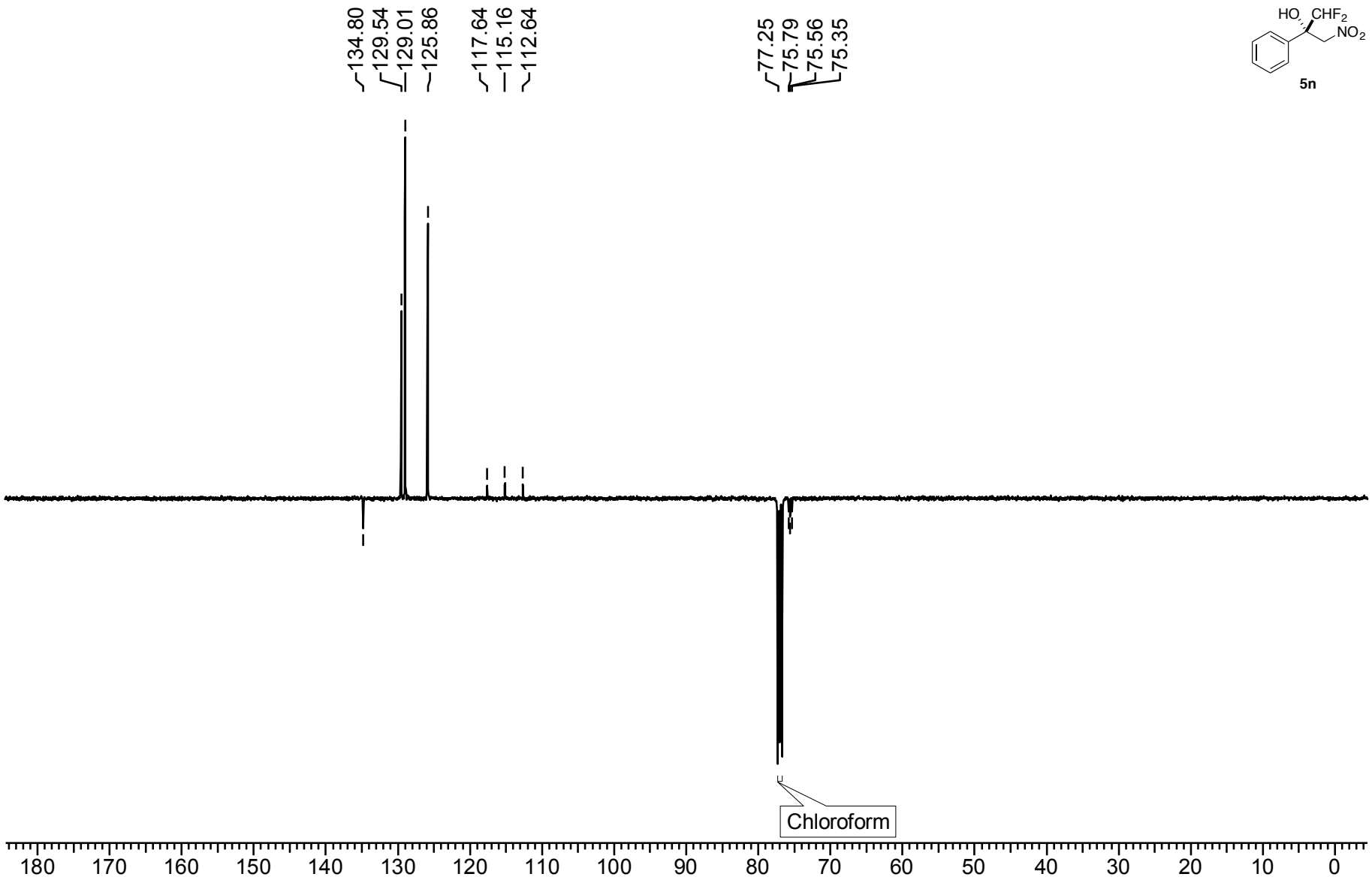

Figure S281. ^{13}C APT NMR (100 MHz, $CDCl_3$) spectrum of **5n**.

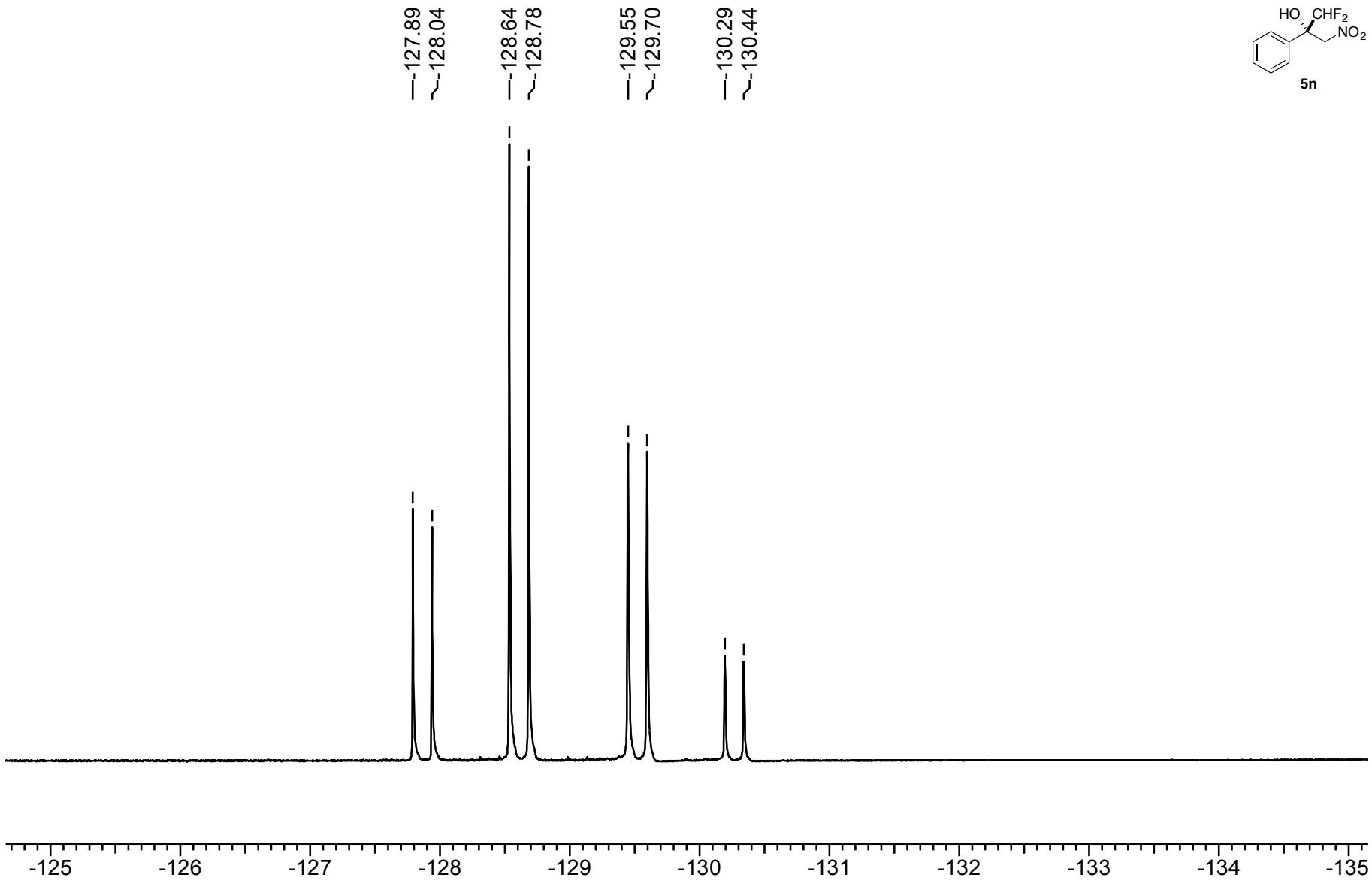

Figure S282. ^{19}F NMR (376 MHz, $CDCl_3$) spectrum of **5n**.

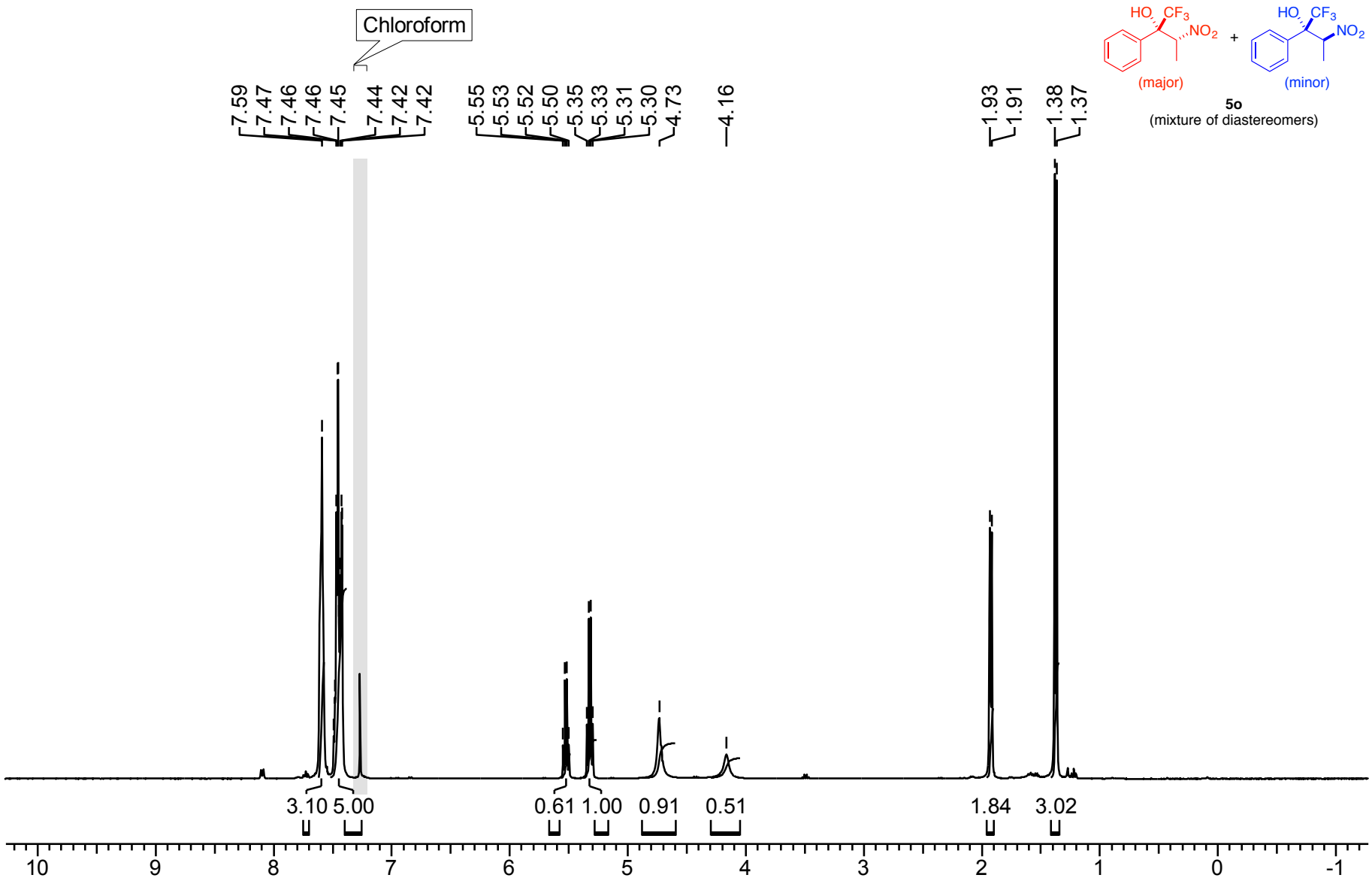

Figure S283. ^{1}H NMR (400 MHz, $CDCl_3$) spectrum of **5o**.

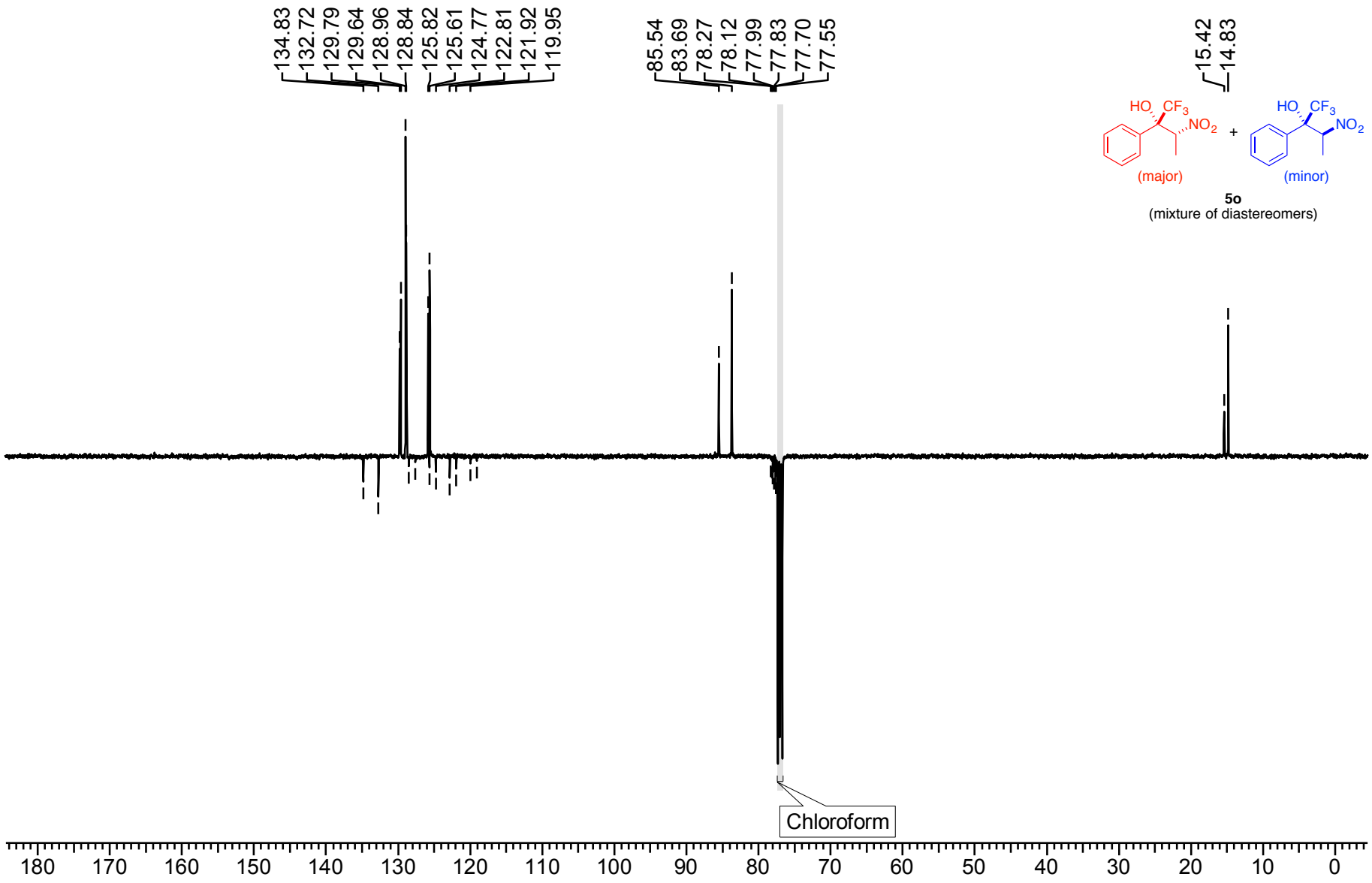

Figure S284. ^{13}C NMR APT (100 MHz, $CDCl_3$) spectrum of **5o**.

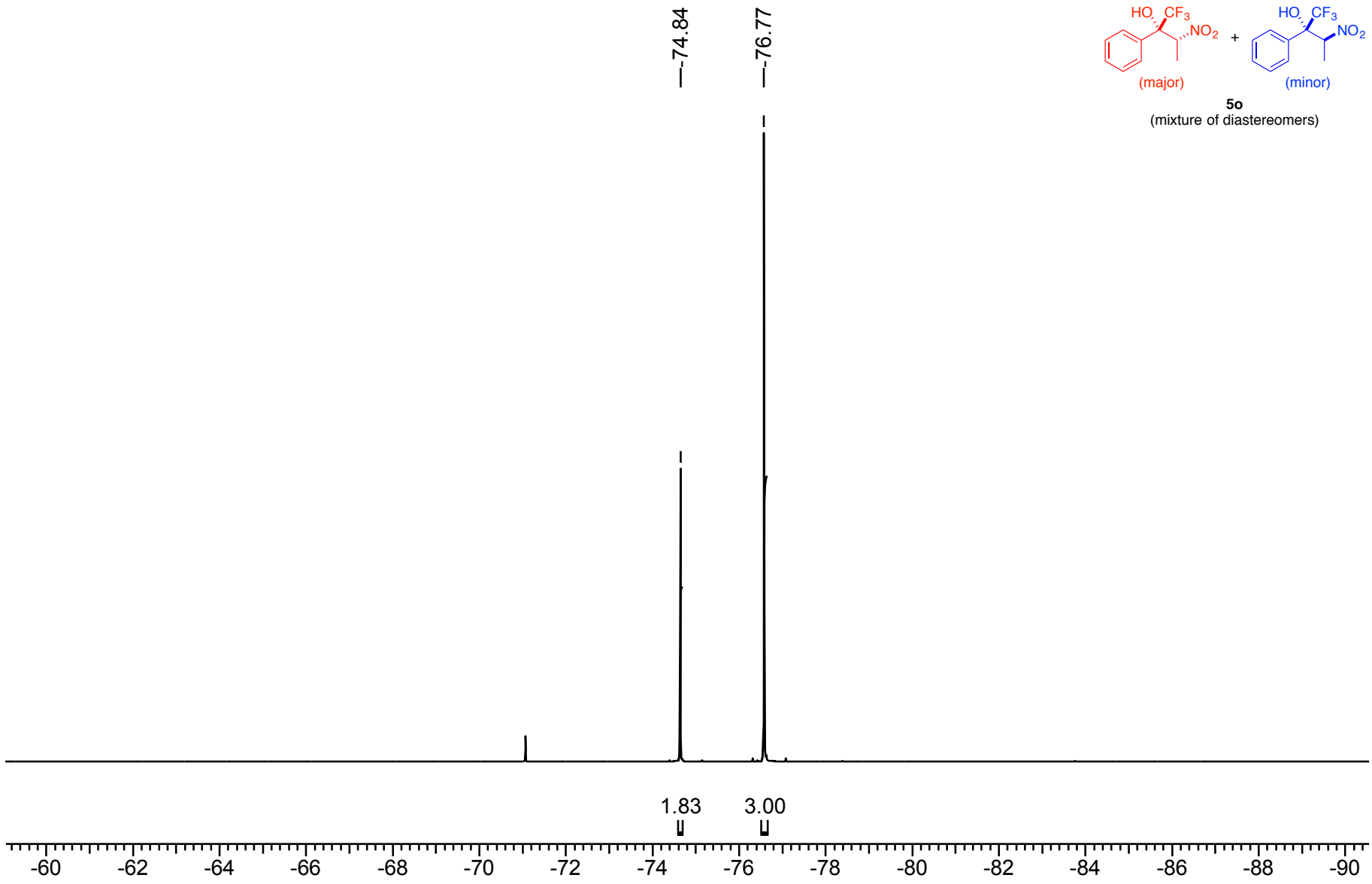

Figure S285. ^{19}F NMR (376 MHz, $CDCl_3$) spectrum of **5o**.

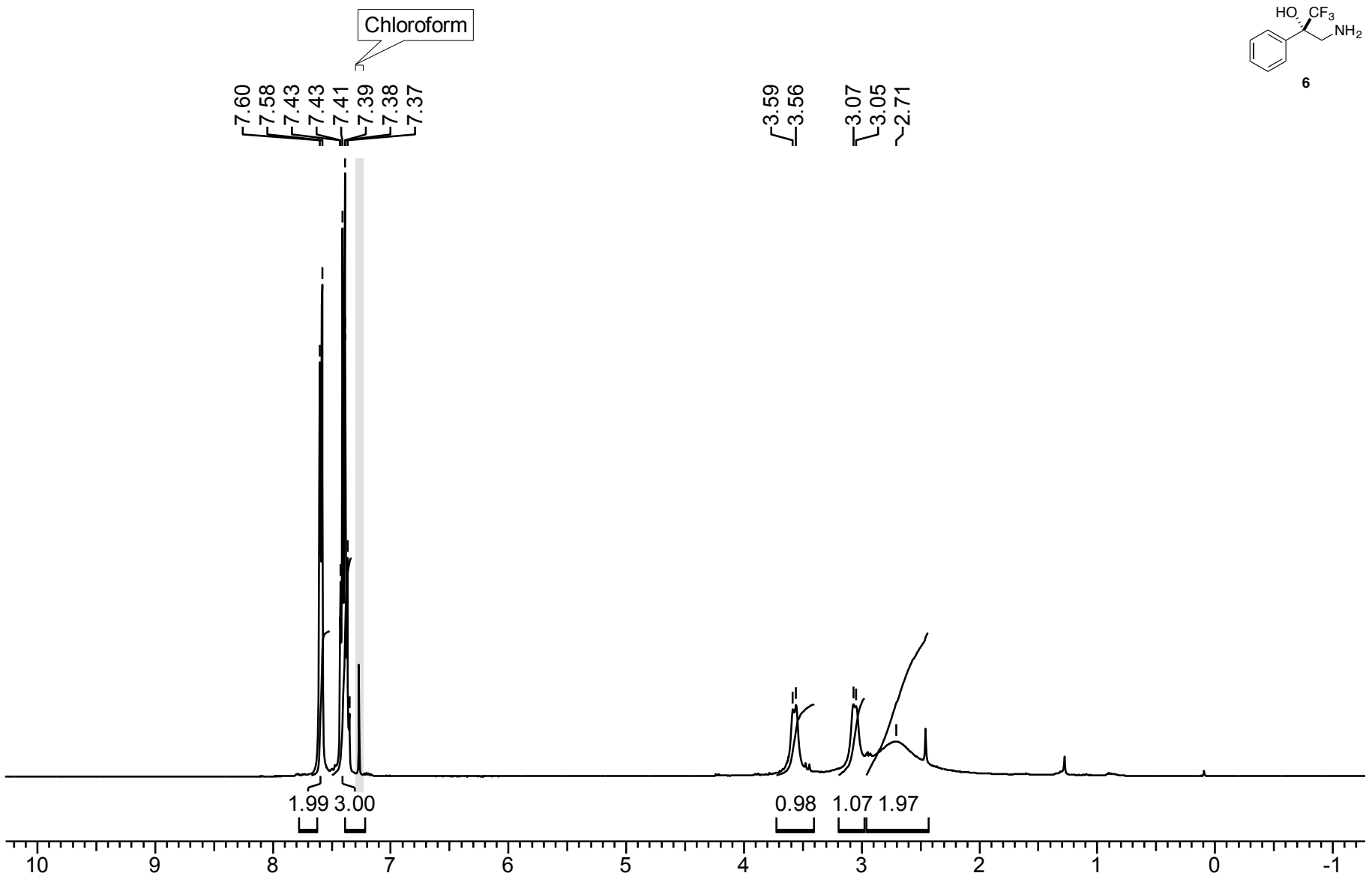

Figure S286. ^{1}H NMR (400 MHz, $CDCl_3$) spectrum of **6**.

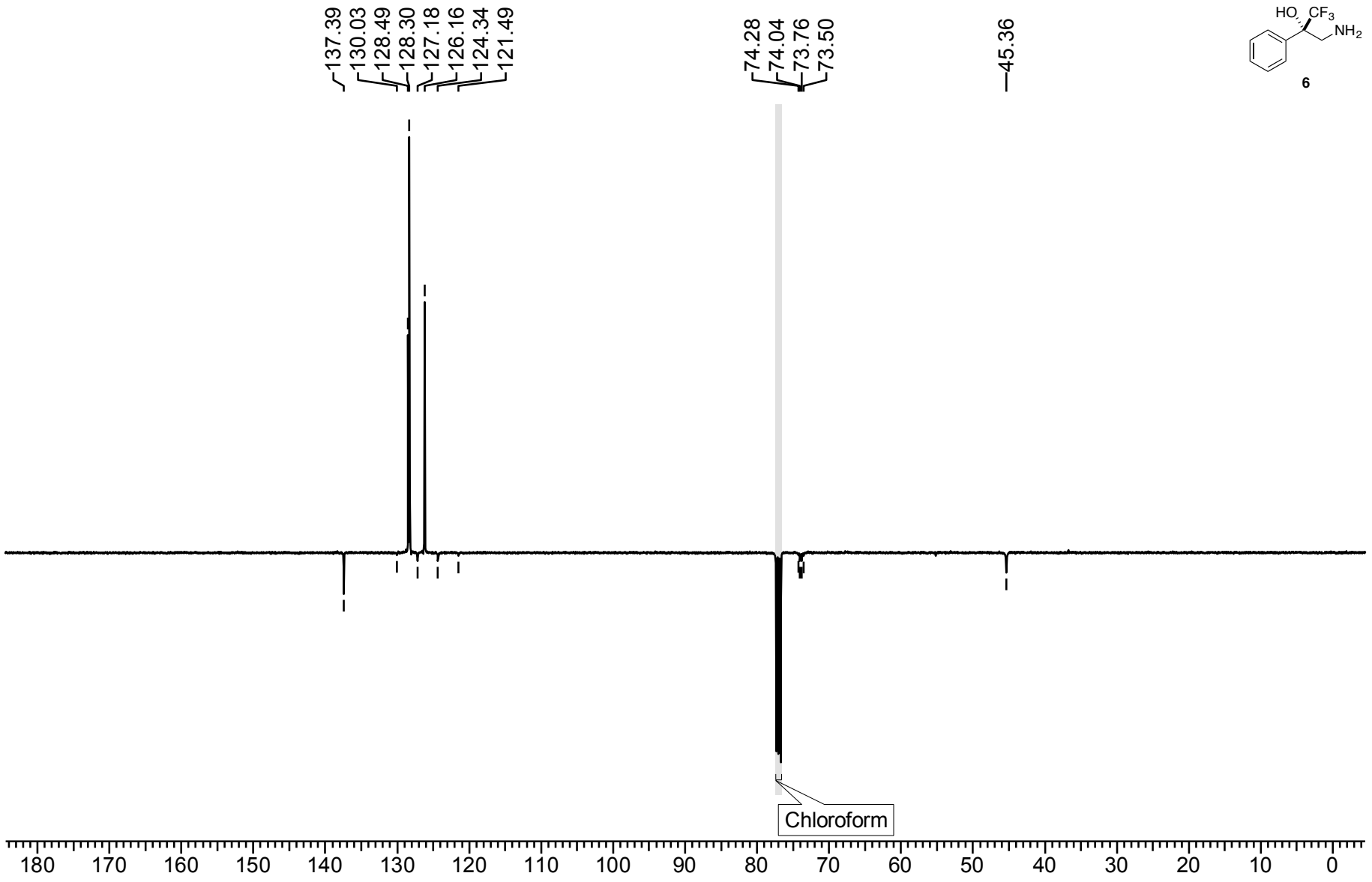

Figure S287. ^{13}C NMR APT (100 MHz, $CDCl_3$) spectrum of **6**.

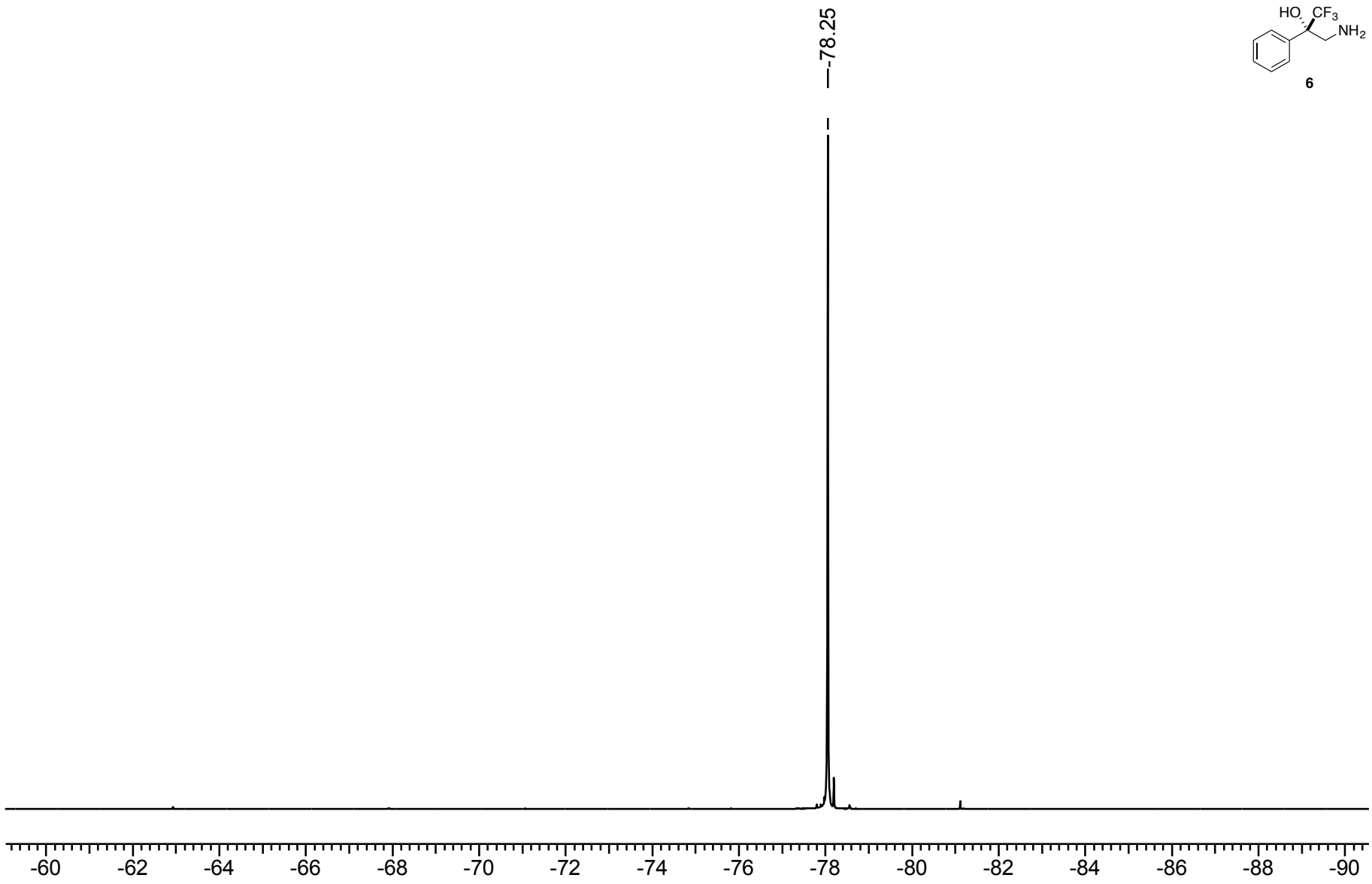

Figure S288. ^{19}F NMR (376 MHz, $CDCl_3$) spectrum of **6**.

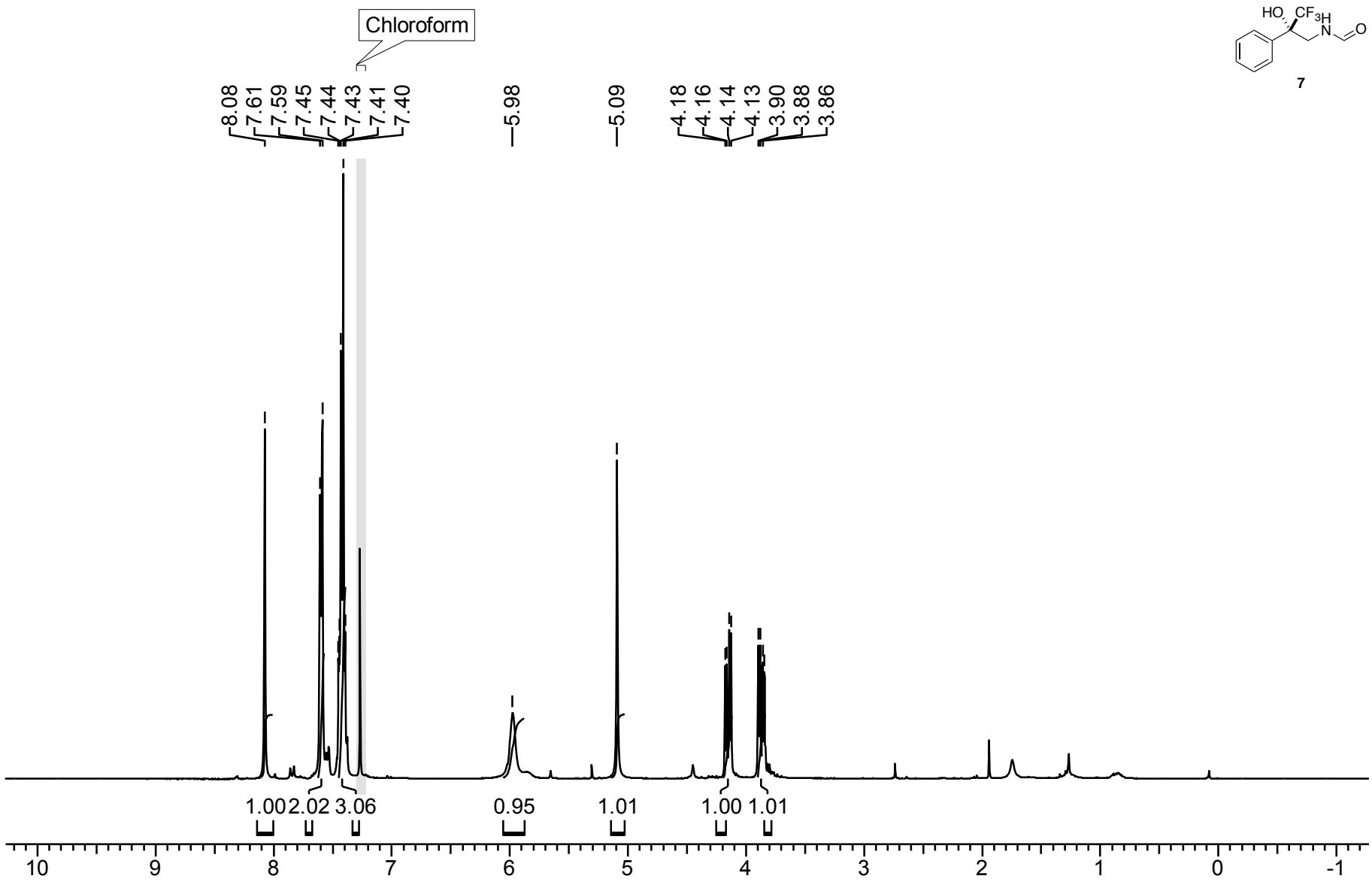

Figure S289. ^{1}H NMR (400 MHz, $CDCl_3$) spectrum of **7**.

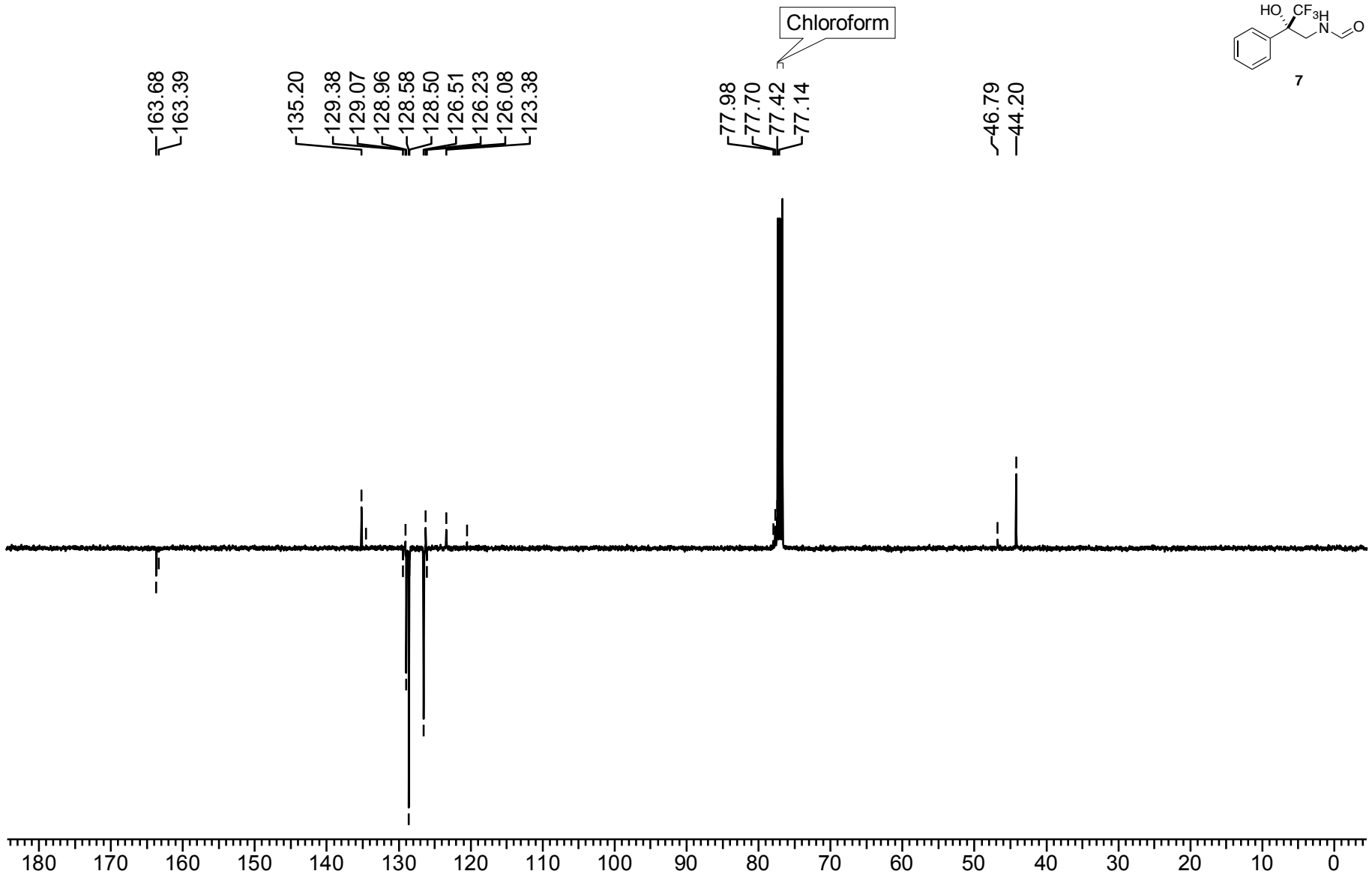

Figure S290. ^{13}C NMR APT (100 MHz, $CDCl_3$) spectrum of **7**.

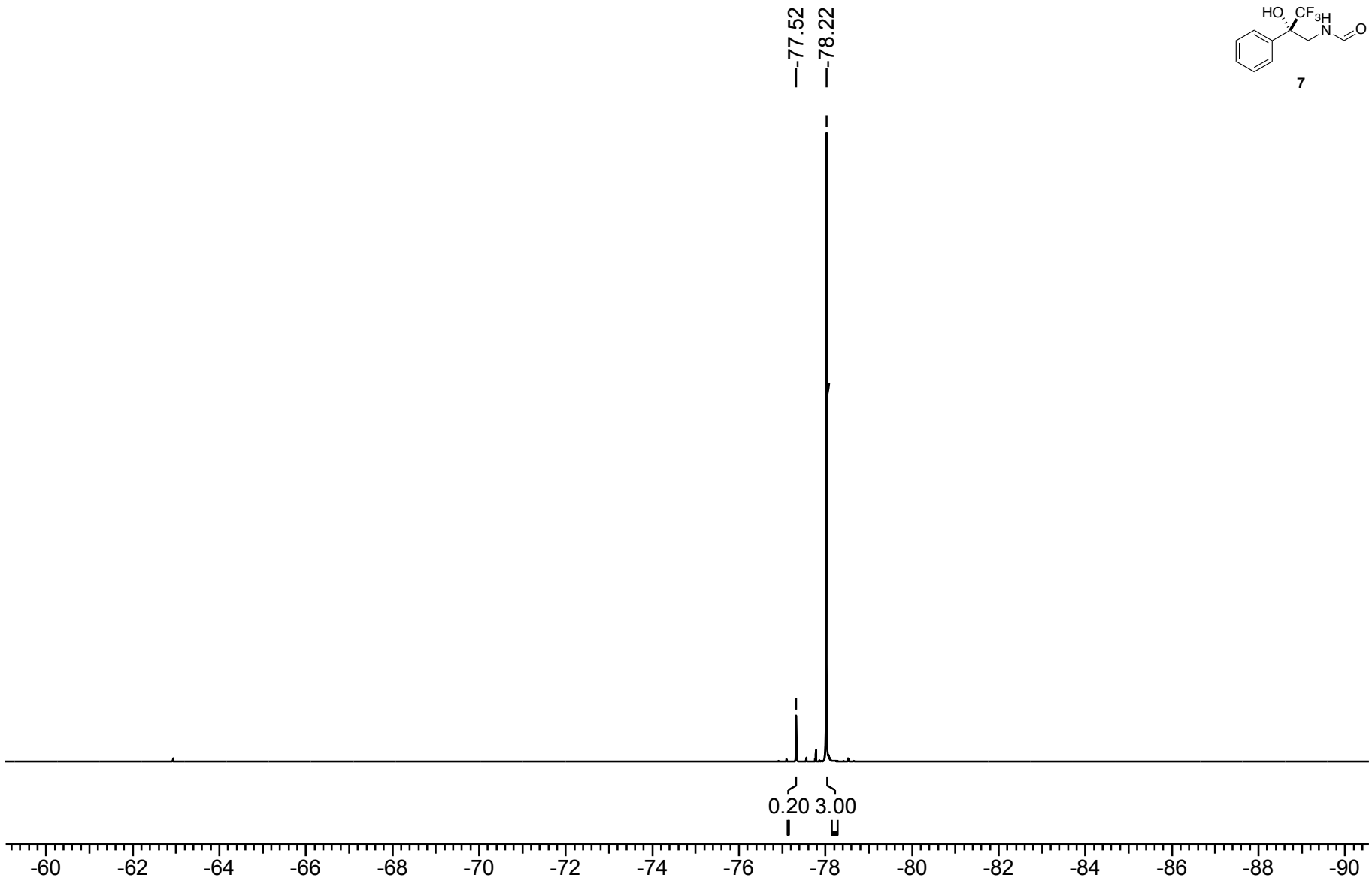

Figure S291. ^{19}F NMR (376 MHz, $CDCl_3$) spectrum of **7**.

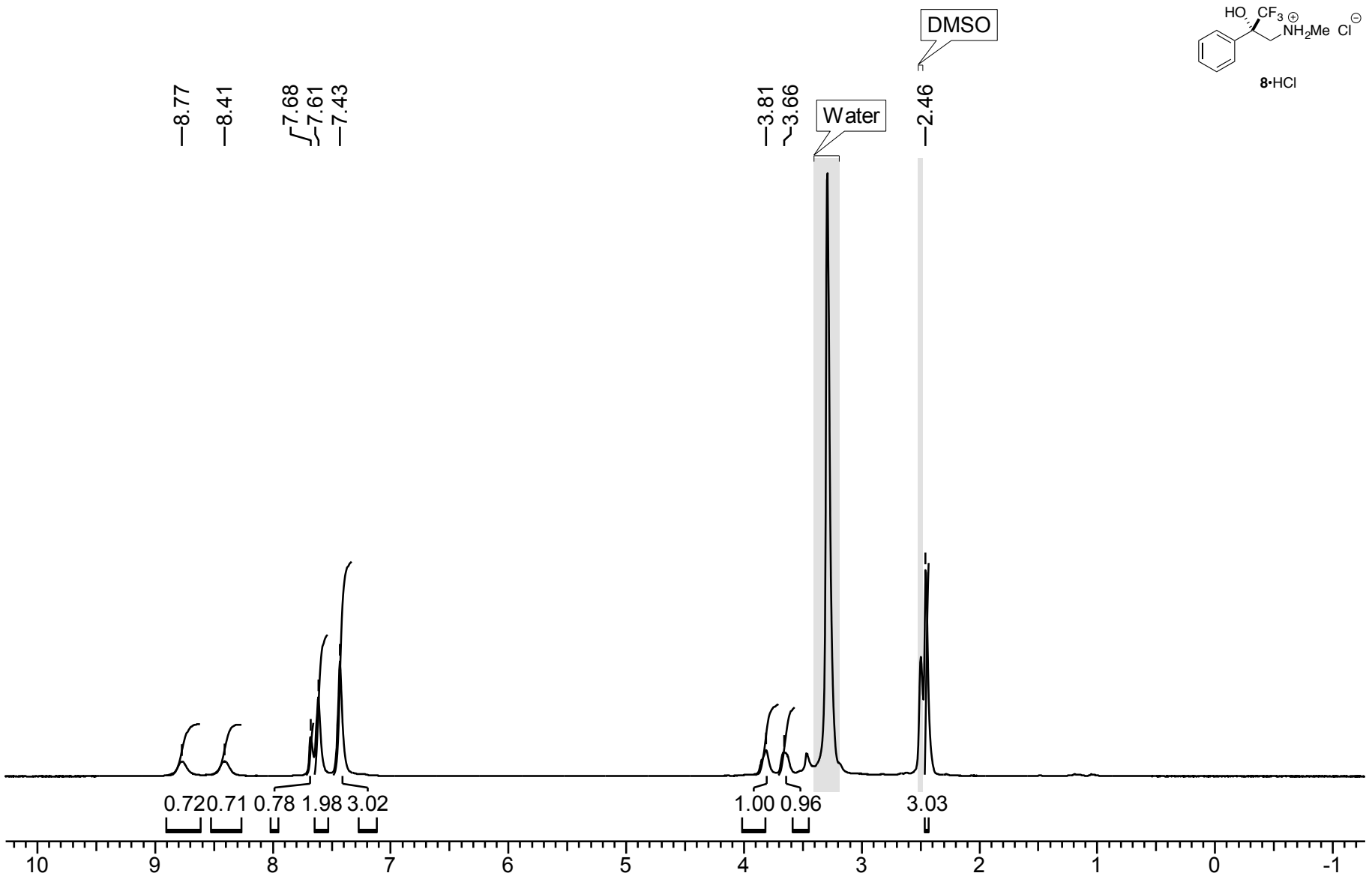

Figure S292. ^{1}H NMR (400 MHz, DMSO-d_6) spectrum of **8**·HCl.

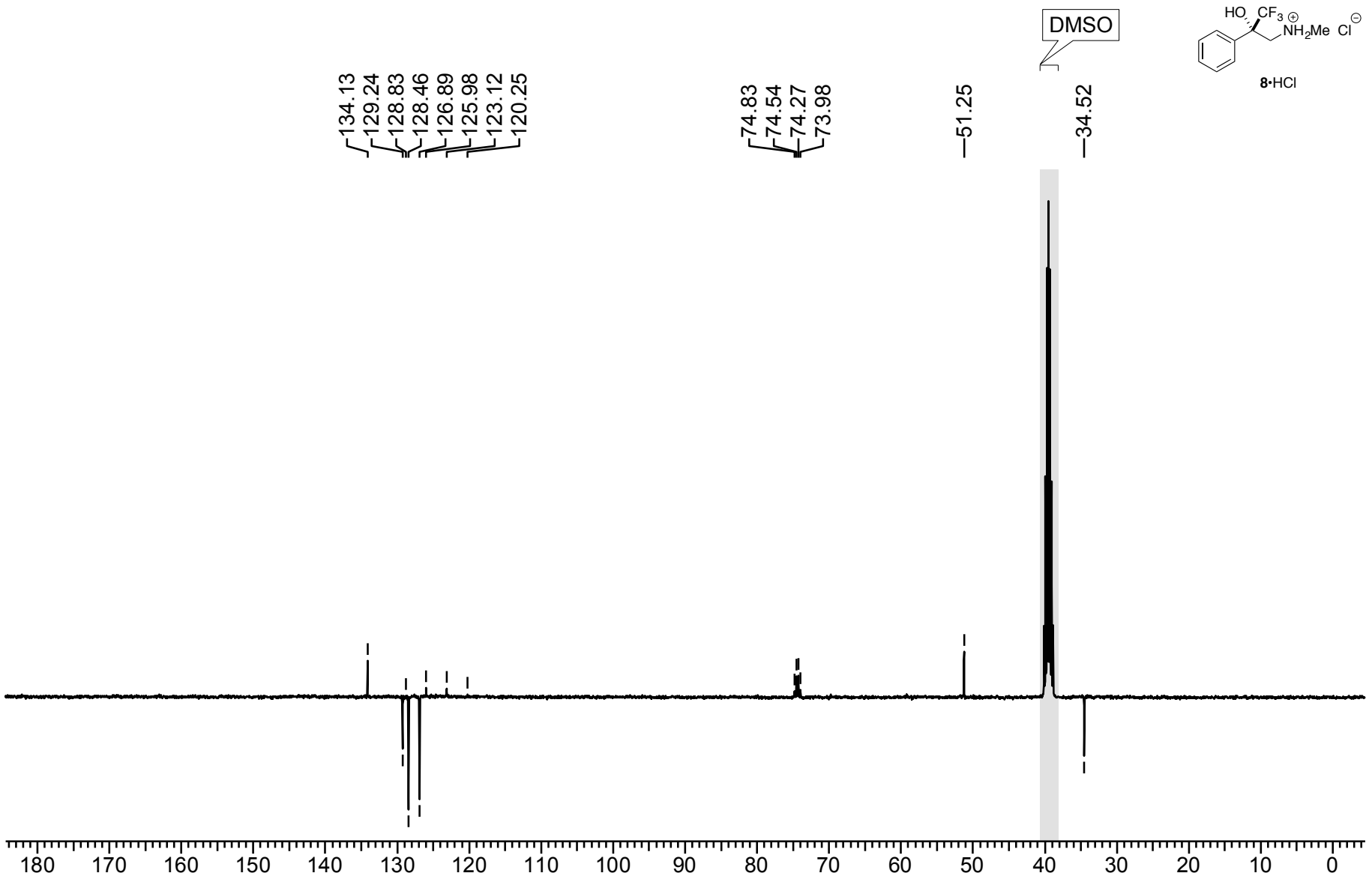

Figure S293. ^{13}C NMR (100 MHz, DMSO-d_6) spectrum of **8**·HCl.

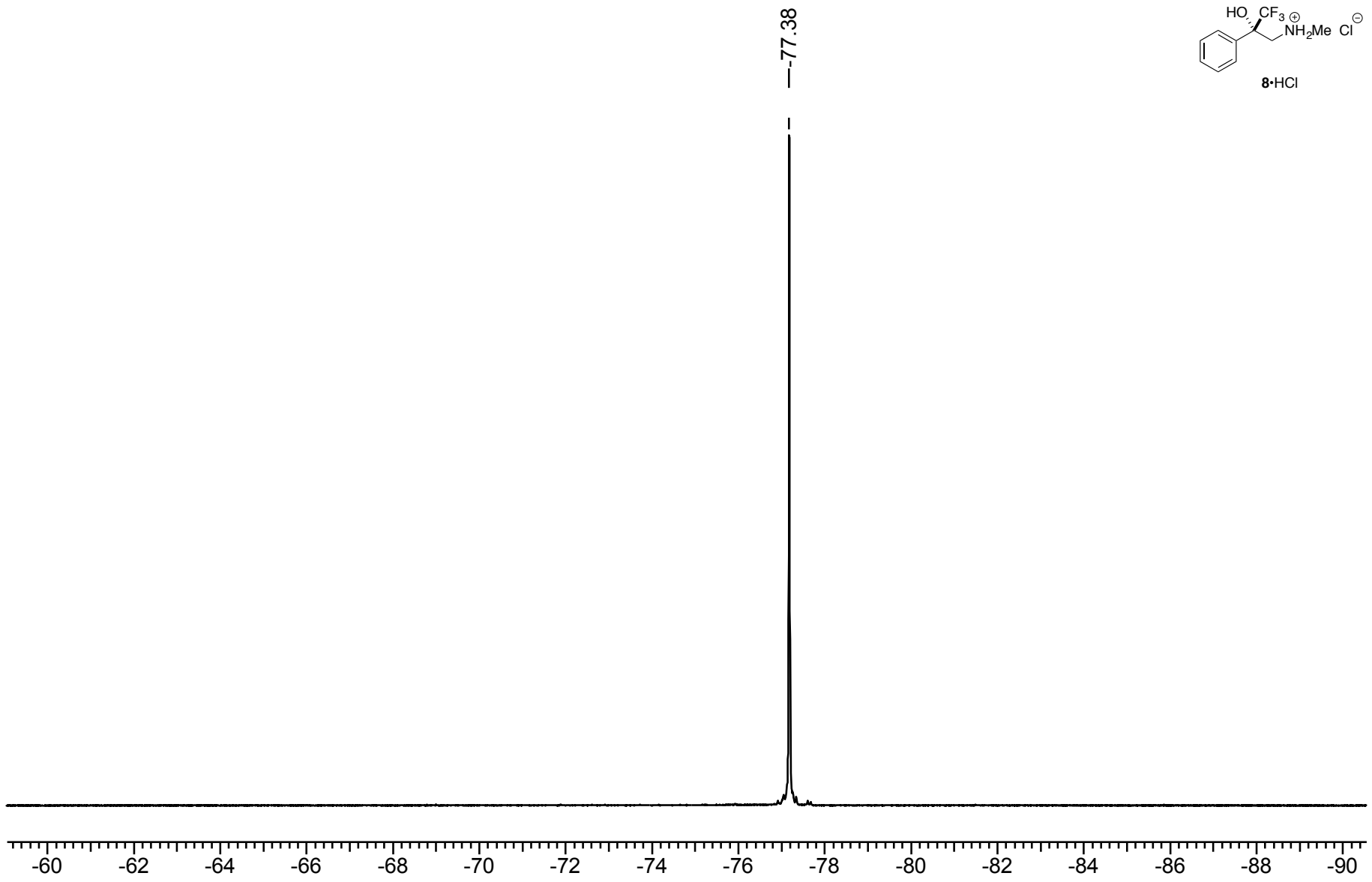

Figure S294. ^{19}F NMR (376 MHz, DMSO-d_6) spectrum of **8**·HCl.